Alma Mater Studiorum – Università di Bologna

DOTTORATO DI RICERCA IN

CHIMICA

Ciclo 35

Settore Concorsuale: 03/C1 – CHIMICA ORGANICA

Settore Scientifico Disciplinare: CHIM/06 – CHIMICA ORGANICA

Green approach to Palladium Cross-Coupling reactions and development of new methodologies based on highly abundant metals

Presentata da: Tommaso Fantoni

Coordinatore Dottorato

Luca Prodi

Supervisore

Walter Cabri

Co-supervisore

Pier Giorgio Cozzi

Esame finale anno 2023

Abstract

Transition metal catalyzed cross-coupling reactions represent one of the most employed and useful tools in organic synthesis for the carbon-carbon (C-C) bond formation and have a prominent role in both the academic and pharmaceutical segments. Among them, palladium catalyzed cross-coupling reactions, which were first discovered in the 1970s, are currently the most versatile. The main reasons behind the success of these reactions are the very high chemo- selectivity and flexibility in terms of substrates, solvents, catalysts, and reaction conditions. However, considering the increasing growth in the price of palladium during the last years, attempts to reduce its loading and to perform its recycling and recovering represent an inescapable necessity, especially if the final outlook is to apply reactions at industrial level. Nowadays, the development process must therefore respect principles of greenness and sustainability such as the selection of green solvents and reagents. Among the palladium-catalyzed cross-coupling methodologies, the Heck-Cassar-Sonogashira (HCS) coupling between terminal acetylenes and aryl/alkyl halides is one of the most useful reactions in the pharmaceutical segment and making it greener would offer notable productive advantages in terms of cost and sustainability. Solvents represent the main source of waste in chemical industrial processes and their selection is critical in Pd-catalyzed cross-couplings, because of their strong influence in the coordination sphere of the metals and their ability to stabilize the catalyst complexes. For this reason, the replacement of the most common used toxic solvents such as N,N-Dimethylformamide (DMF) and N-methylpyrrolidone (NMP) in the HCS cross-coupling reaction with greener alternatives represent an important challenge (Chapter 1).

Chapter 2 highlights how longer N-alkylpyrrolidones could offer novel opportunities since their metabolites are less toxic than formaldehyde and related compounds typically deriving from N-Me oxidation in DMF and NMP. Among them, 1-(2-Hydroxyethyl)-2-pyrrolidone (HEP) in combination with N,N,N,N-tetramethyl guanidine (TMG) as base showed the best performance in terms of reaction time and yield. HEP is a biogenic solvent that have very high affinity for water that allows a quantitative product extraction during work up using standard organic solvents.

In Chapter 3, the identification a sustainable protocol to recycle and recover the palladium catalyst in the HCS coupling was evaluated exploiting the solubility and polarity of HEP. The HCS protocol using HEP/water/TMG as green solvent/base mixture and sulfonated phosphine ligands, allowed to recycle the catalyst, always guaranteeing high yields and fast conversion under mild conditions, with aryl iodides, bromides, and triflates. No catalyst leakage or metal contamination of the final product were observed during the HCS recycling.

Chapter 4 discusses the Heck-Cassar and the Suzuki-Miyaura cross-coupling reactions on different unactivated aryl chlorides in the sustainable mixture HEP/water giving excellent results in terms of yield, TON, TOF and Process Mass Intensity (PMI), without any purification and nucleophile excess. The identification of the side reaction that generates the enyne derivatives byproducts with the copper-free Heck-Cassar protocol was limited by the simple control of the alkyne addition rate to optimize the stoichiometry.

Although its great success, the mechanism of the HCS coupling is still under discussion. In Chapter 5, to clarify the copper free HCS reaction mechanism, stoichiometric and catalytic reactions were carried out and monitored by $^{31}P/^{1}H$ NMR spectroscopy, HPLC, and GC chromatography. In particular, the role of the base was deeply investigated, highlighting the key role of the secondary amines that are able to strongly induce a fast reduction of the pre-catalyst and a decrease in the energy required for the alkyne coordination.

In Chapter 6 the development of a cross-coupling reaction to form aryldifluoronitriles in the presence of copper is discussed, highlighting the importance of inserting fluorine atoms within biological structures and the use of readily available metals such as copper as an alternative to palladium.

Table of Contents

Chapter 1:

Overview of Cross-Coupling reactions: from early discoveries to modern approaches

1.1 Introduction

Transition metal catalyzed reactions represent among the most versatile and useful tools in organic synthesis for the carbon-carbon (C-C) bond formation and have a prominent role in both the academic and pharmaceutical segments. The main reasons behind the success of these reactions consist largely in the fact that they have very high flexibility and selectivity in terms of substrates, solvents, catalysts, and reaction conditions, which allowed them to become increasingly popular within the scientific community.[1–5] Cross-coupling reactions represent one of the most important classes of metal catalyzed transformations in modern organic chemistry, providing a powerful tool for the construction of C–C and carbon–heteroatom (C–X) bonds. Among them, palladium-catalyzed cross-coupling reactions, which were first discovered in the 1970s, are currently the most versatile ones. The popularity of the field reached the pick in 2010 with Nobel Prizes in Chemistry to Professors Richard F. Heck (University of Delaware), Akira Suzuki (University of Hokkaido) and Ei-ichi Negishi (Purdue University) for their remarkable contributions within the Pd-catalyzed cross-coupling reactions.[6,7]

Generally, all these reactions need a transition metal to initiate the catalytic cycle. Although several metals have been used and developed, there is no doubt that palladium is the metal that has dominated the field for most of the years. Recently, attempts have been made to replace palladium, because of its cost and rarity, with cheaper and more abundant metals such as iron, cobalt, copper and nickel, but, because of its high reactivity and selectivity, it still remains the metal of choice, especially in the industrial segment.

Although the mechanisms for the various Pd catalyzed cross-coupling reactions differ in some details, the general accepted catalytic cycle is depicted in Figure 1.1.

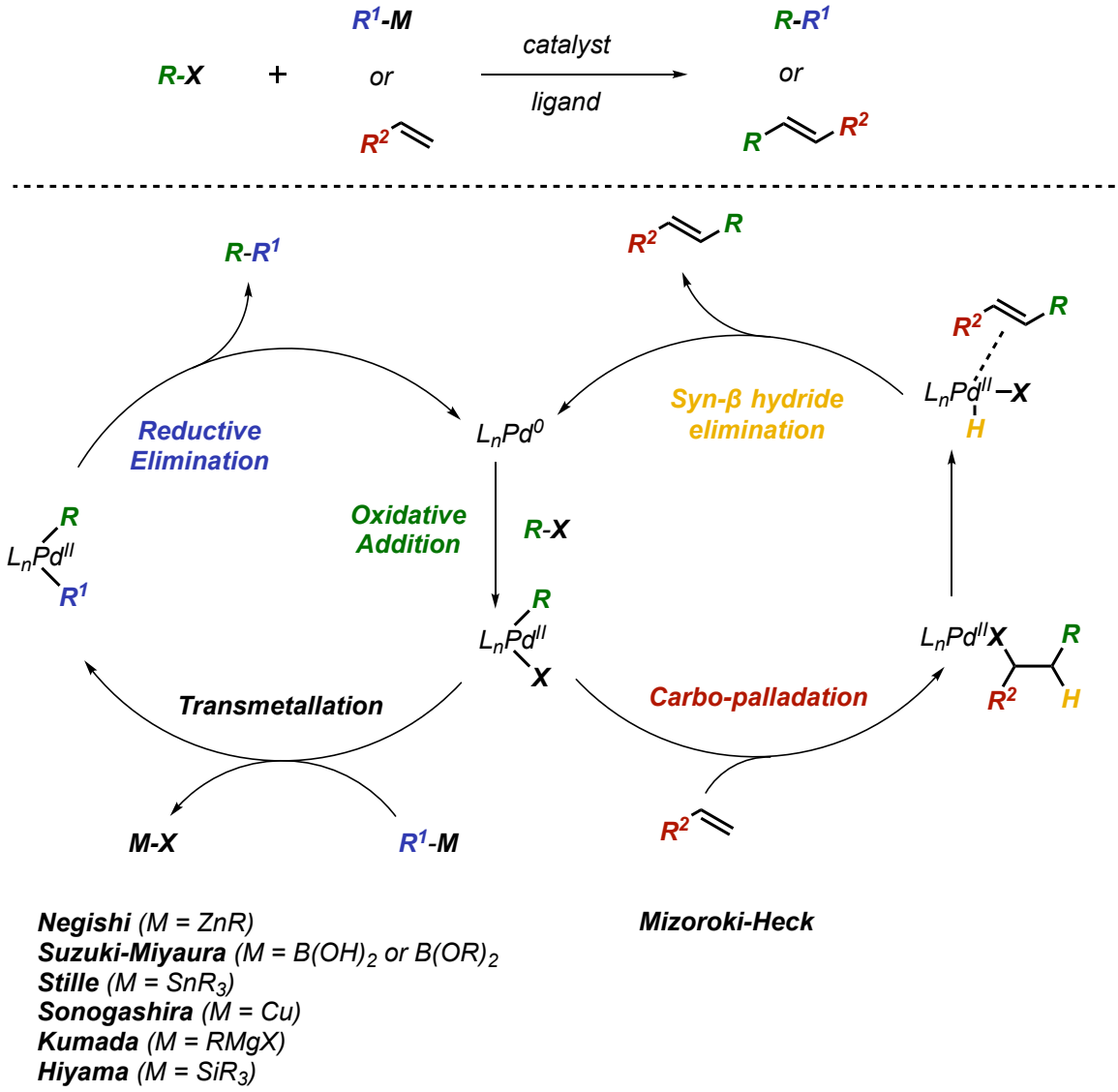

***Figure 1.1**: General catalytic cycle for Pd cross-coupling reaction*

The elementary steps involved in the mechanism are represented by the oxidative addition (OA), transmetallation (TM) and the reductive elimination (RE). The cycle starts with a Pd^0 species usually formed in situ from a Pd^{II} precursor that undergoes oxidative addition of aryl halides (or pseudohalides), affording the R-Pd^{II}-X intermediate. Usually, palladium (II) species are chosen as starting material because of their higher stability. Such compounds are then reduced in situ to palladium (0) active catalyst which initiates the catalytic cycle. The OA step of an aryl/alkyl halide to the Pd^0 complex is common to all type of cross coupling. At this point, if the reaction involves an organometallic partner (Figure 1.1, left), the TM step generates the Pd^{II} complex bearing two organic groups R-Pd^{II}-R^1.

The choice of the organometallic partner depends on the reaction typology. For example, organoboranes are used in the Suzuki coupling, organozinc compounds in the Negishi, organostannanes in the Stille, Grignard reagents in the Kumada, organosilicones in the Hiyama, and copper acetylides formed in situ in the Sonogashira cross-coupling. Finally, the RE step provides the product and the regeneration of the Pd^0 catalyst.

In the Mizoroki-Heck coupling a different catalytic cycle is involved (Figure 1.1, right). After the OA, the reaction proceeds with the alkene coordination to the R-Pd^{II}-X intermediate, followed by a syn migratory insertion. This step determinates the regioselectivity of the reaction, which depends on the nature of the alkene, the catalyst, and the reaction conditions. Then, the newly formed organopalladium species undergoes syn β-hydride elimination, to form the alkene product and the Pd^0 catalyst by a base-assisted elimination of HX.

These reactions have a very rich history that started in the 19th century. However, despite the positive characteristics of organometallic catalysis, a literature review of the main cross-coupling reactions reveals that it took decades before these methodologies became popular in the scientific community (Figure 1.2). [8–16]

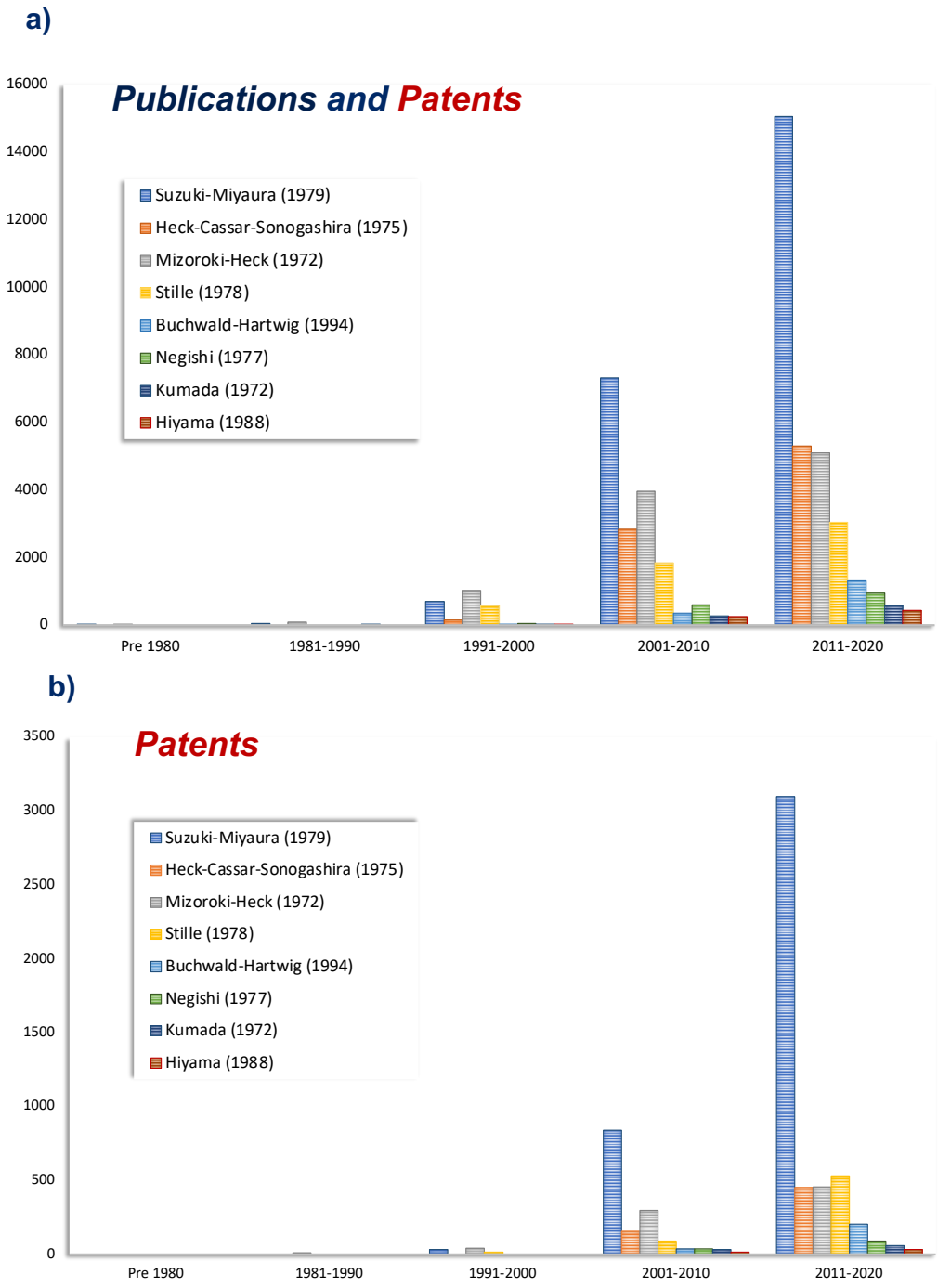

Figure 1.2: *Growth in publications and patents a) and only patents b) related to cross-coupling reactions*

The first discoveries were made by Ullmann and Glaser with the metal mediated homocoupling of two identical fragments. At that time, these discoveries inspired other chemists of the time to ponder the possibility to build up C-C compounds starting from different fragments. The 1970 was ripe of discoveries and innovations in the field of

transition metal catalyzed reactions with several contributions from Kharasch, Corriu, Kumada, Kochi, Murahashi, Sonogashira, Stille, Trost, Tsuji, and Yamamoto, Heck, Negishi, and Suzuki. These authors demonstrated that carbon atoms in all hybridization states can undergo C-C bond formation through palladium catalysis, initiating therefore a new era in organic chemistry. In addition, the increasing development of ligands, especially bulky electron rich trialkylphosphines, allowed to expand the scope to substrates, such as the less expensive but otherwise unreactive aryl chlorides, which up to that point had only rarely been used.[17] This led to the development of new molecular frames with a flexibility and a variability that is especially useful in medicinal chemistry and during drug discovery process design (Figure 1.3).[18]

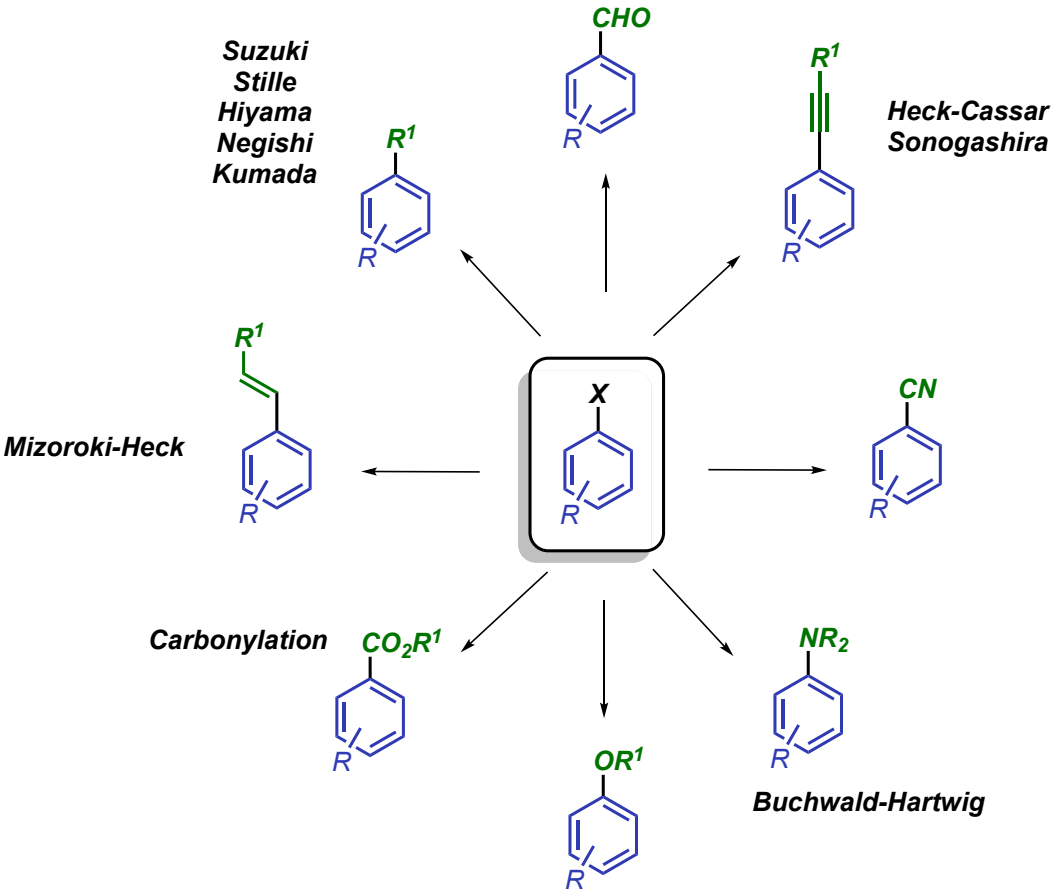

***Figure 1.3**: Examples of versatility of palladium catalyzed reactions*

As a consequence of these results, new cross-coupling reactions requiring milder conditions with lower Pd loadings were developed. In fact, due to the high price and low availability of palladium catalysts, efforts to reduce their loading and to perform their recycling became mandatory, especially if the aim is to transfer bench reaction protocols

to technologically advanced industrial processes. Indeed, the rapid increment of the palladium price in the last 10 years, from 29$/g to 84$/g (Figure 1.4), made the pharmaceutical industry the sector of choice for the application of palladium cross-coupling reactions. That, along with the limited earth abundance of the platinum group's metals, made palladium catalysis especially employed in those sectors that can afford an increase in the production process price, such as the drugs and fine chemicals manufacture.

***Figure 1.4**: Palladium prices trend in the last 10 years*
https://www.investing.com/commodities/palladium-streaming-chart

The purity of the final product plays also an important role for the application of palladium catalysis in the pharmaceutical industry. Regulation on residual metals in APIs are particularly strict and for palladium catalysis, according to ICH guidelines, the metal contamination in the final product must be lower than 10 ppm for orally administered drug, 1 ppm for parenteral drug, and 0.1 ppm for inhalation route of administration (Table 1.1). Hence, the development of catalytic processes with a high turnover number (TON), a low catalyst loading and a high catalyst recycling yield is beneficial not only from an economical point of view, but also to prevent metal contamination in the final product. For this reason, the study of a highly active catalytic system, which allows the use of mild conditions and

the recovery of the catalyst, without the need of environmentally and economically demanding purification steps, represents an increasingly active field of research.

***Table 1.1**: Permitted concentrations of metal impurities ICH Q3D(R1) Guideline*

element	class	oral concentration (μ/g)	parental concentration (μ/g)	inhalation concentration (μ/g)
Cd	1	0.5	0.2	0.3
Pb	1	0.5	0.5	0.5
As	1	1.5	1.5	0.2
Hg	1	3	0.3	0.1
Co	2A	5	0.5	0.3
V	2A	10	1	0.1
Ni	2A	20	2	0.5
Tl	2B	0.8	0.8	0.8
Au	2B	10	10	0.1
Pd	**2B**	**10**	**1**	**0.1**
Ir	2B	10	1	0.1
Os	2B	10	1	0.1
Rh	2B	10	1	0.1
Ru	2B	10	1	0.1
Se	2B	15	8	13
Ag	2B	15	1	0.7
Pt	2B	10	1	0.1
Li	3	55	25	2.5
Sb	3	120	9	2
Ba	3	140	70	30
Mo	3	300	150	1
Cu	3	300	30	3
Sn	3	600	60	6
Cr	3	1100	110	0.3

1.2 The Origins of Cross-Coupling Reactions

The discovery of cross-coupling reactions was facilitated by the observation in the 1940s that simple first-row transition metal salts, such as $CoCl_2$, $FeCl_3$, $NiCl_2$, $CuCl_2$, or $CrCl_2$, could be used as catalysts for the C-C bond formation.[19] Despite the simplicity of the reactions, the synthetic utility was quite limited before the 60s. Historically, the first discoveries in the field raised with organocopper chemistry through the homocoupling of metallic acetylides reported by Glaser in 1869.[20,21]

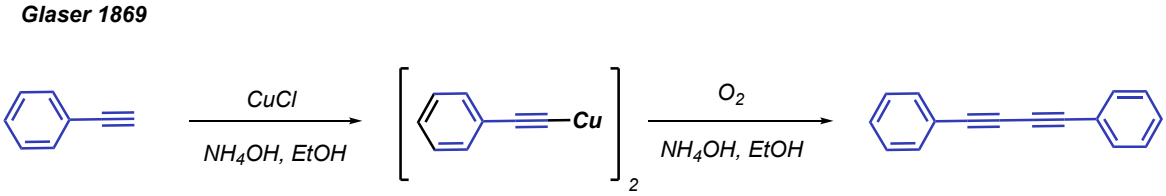

***Scheme 1.1**: The Glaser reaction*

In this study, Glaser described the oxidative dimerization of phenylacetylide to give diphenyldiacetylene through copper and silver catalysis (Scheme 1.1). These initial studies greatly attracted the scientific community and were considered valid approaches for the construction of new C-C bonds. After the development of C(sp)-C(sp) homocoupling, the copper protocol was extended to C(sp^2)-C(sp^2) bond formation. In 1901, Ullmann reported the dimerization of 2-halogen-nitrobenzene promoted by stoichiometric amount of copper (Scheme 1.2).[22]

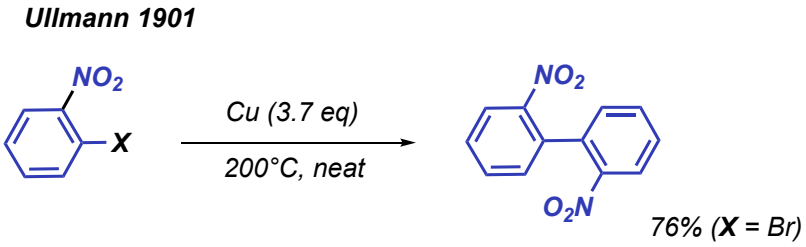

***Scheme 1.2**: The Ullmann reaction*

Since the Glaser and the Ullman organocopper reactions required harsh conditions, their development was rather limited. However, the Ullman coupling differentiated the Glaser one from one important aspect, that will be considered a must in cross-coupling reactions: the carbon dimerization in the presence of halogen groups instead of unfunctionalized carbon systems. This topic of using carbon atoms bearing halogens for coupling reactions opened the world to the areas of organo-magnesium (Grignard) and organo-sodium (Wurtz–Fittig) chemistry and later, of course to catalysis.[23–25] However, the development of alkyl and aryl halides, because of the drastic conditions, were limited and subjected to numerous side reactions. The first report using Grignard reagents to couple sp^2-sp^2 carbon bound is related to Bennet and Turner who described the dimerization of phenylmagnesium bromide through the use of stoichiometric quantities of chromium(III)

chloride[26] (Scheme 1.3) and a few years later by Krizewsky and Turner through a $CuCl_2$ promoted protocol.[27] Despite these important achievements, the early metal promoted cross coupling reactions were limited for several reasons, the most important of which regards the insolubility of these super stoichiometric reactants and the limited selectivity and applicability. In fact, the transformations were limited to homocoupling and often led to various side reactions and undesired byproducts.

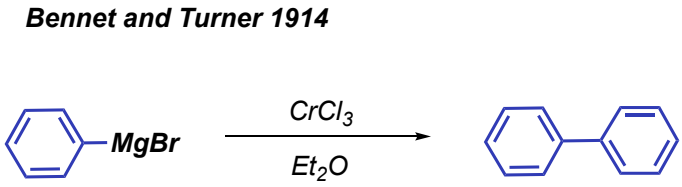

***Scheme 1.3**: Chromium chloride promoted dimerization of Grignard reagents*

The first example of transition-metal-catalyzed $C(sp^2)$-$C(sp^2)$ coupling was reported by Kharasch in 1941[28] with the cross-coupling between Grignard reagents and aryl halides, a reaction further described in general terms in his book on Grignard substrates.[19] In 1943,[29] and in subsequent studies, this protocol was applied to the cross-coupling of vinyl bromides with aryl organo-magnesium species using cobalt chloride as catalyst. These studies represent the earliest reports in which a metal was used for C-C bond formation between to different reaction partners (Scheme 1.4).

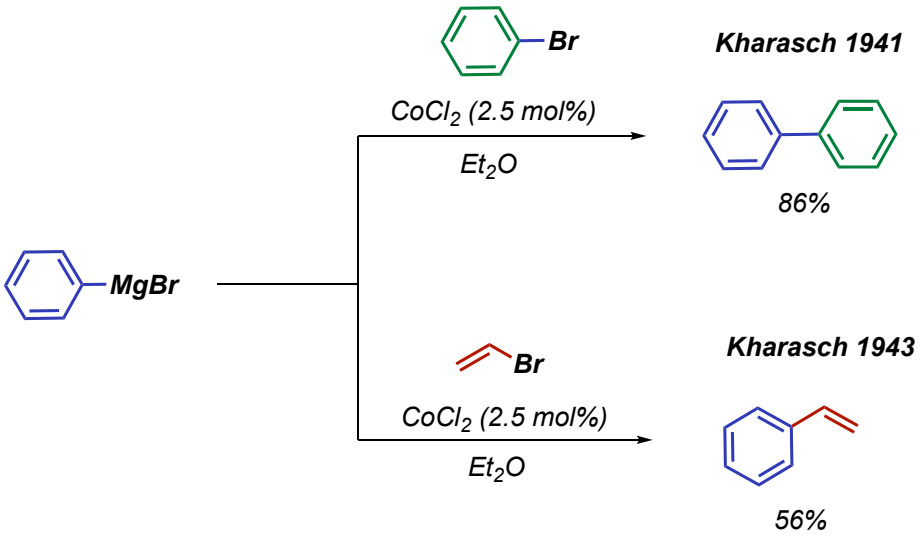

***Scheme 1.4**: The first examples of catalysis in couplings for C-C bond formation: Kharasch coupling*

In 1955, Cadiot and Chodkiewicz reported the copper-catalyzed coupling of alkynes with bromoalkynes,[30] followed by the Castro–Stephens reaction involving aryl or vinyl halides with alkynes derivatized as copper salts (Scheme 1.5).[31]

From this point in time there was a turning point in the development of cross coupling reactions. In the broadest sense, all coupling procedure required three components to achieve a selective reaction: 1) an organohalide, usually aryl or alkynyl, as a coupling partner; 2) a stoichiometric organometallic partner to avoid the halide homocoupling side reaction; 3) a transition metal, in stoichiometric or catalytic quantities to perform the C-C coupling. These components would represent a constant in coupling chemistry throughout the next 50 years.

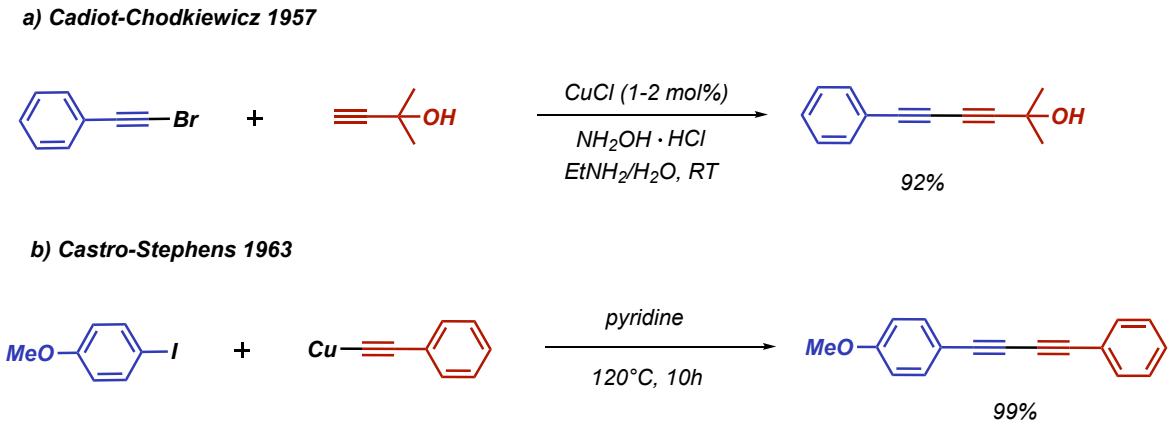

***Scheme 1.5**: The Cadiot–Chodkiewicz and the Castro–Stephens reactions*

The introduction of palladium represented a breakthrough in the history of cross-coupling reactions. In 1968 Richard Heck reported for the first time the use of palladium as catalyst for the arylations of alkenes by using an organomercury nucleophile reagent (Scheme 1.6a).[32] A modification of this reaction was reported by Moritani and Fujiwara who demonstrated the possibility to couple directly arenes with alkenes with catalytic amounts of palladium.[33] This represented an important discovery because, up to that moment, all the cross-coupling reactions involved the use of pre-functionalized coupling partners in terms of organometallic reagents as nucleophiles and aryl halides as electrophiles. In rapid succession, the independent and almost concurrent discoveries by Mizoroki [34,35] and Heck[36,37] reported the coupling reactions of aryl halides and alkenes with catalytic amounts

of palladium catalyst, introducing then what will be called as Mizoroki-Heck reaction (Scheme 1.6b-c). Over the following decades, a vast number of groups demonstrated the high functional group tolerance and wide applicability of this reaction protocol. With this reaction they introduced a new reaction system, opening the future of palladium as an important metal for catalysis. Mechanistically, the Mizoroki–Heck reaction differs from most of the previously reported cross-coupling reactions on one crucial point: the lack of an obligatory preformed organometallic species as one of the coupling partners.

However, together with the discoveries of Heck and Mizoroki, protocols that still involved the use of Grignard reagents continued to improve and develop, to allow selective aryl–aryl bond formation through this reaction system.

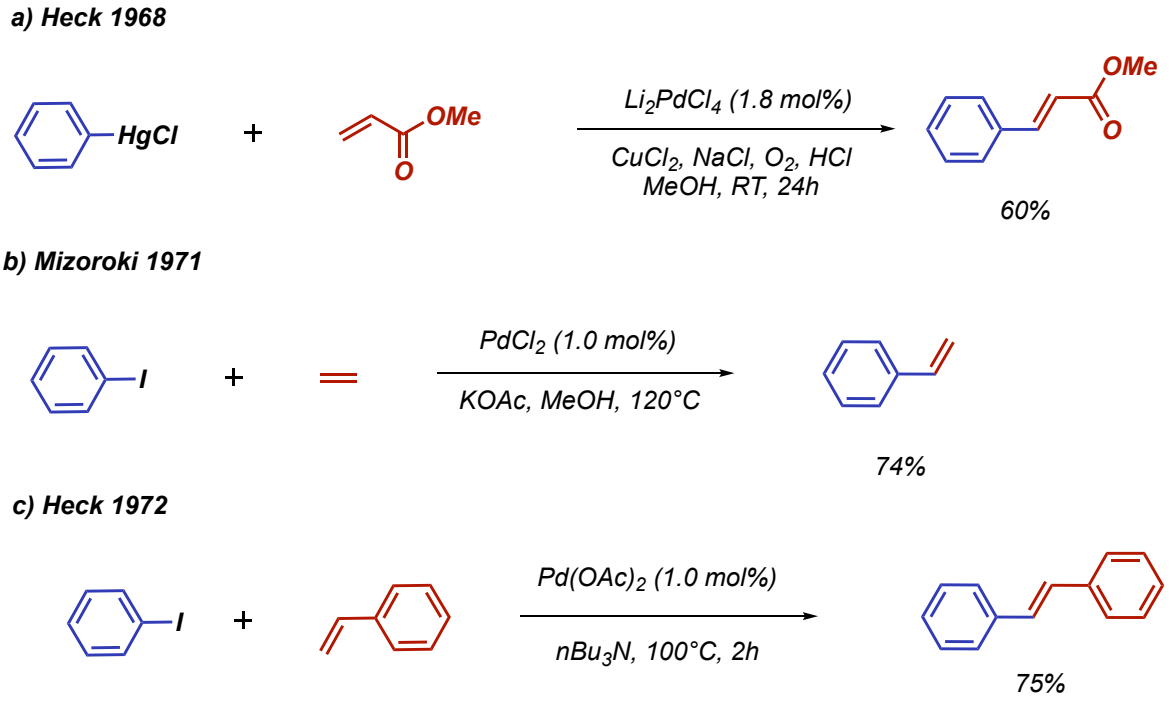

***Scheme 1.6**: The first palladium(II)-catalyzed cross-coupling reactions*

In 1972, Kumada[38,39] and Corriu[40] independently reported the nickel catalyzed coupling of Grignard reagents with alkenyl and aryl halides partners (Scheme 1.7). These works represented a remarkable development from Kharasch's coupling in which selectivity problems and homocoupling byproducts prevailed. Significantly, Kumada introduced the use of phosphine ligands to modulate the reactivity of the metal, a result that would initiate a continuing and powerful trend in future cross-coupling research.

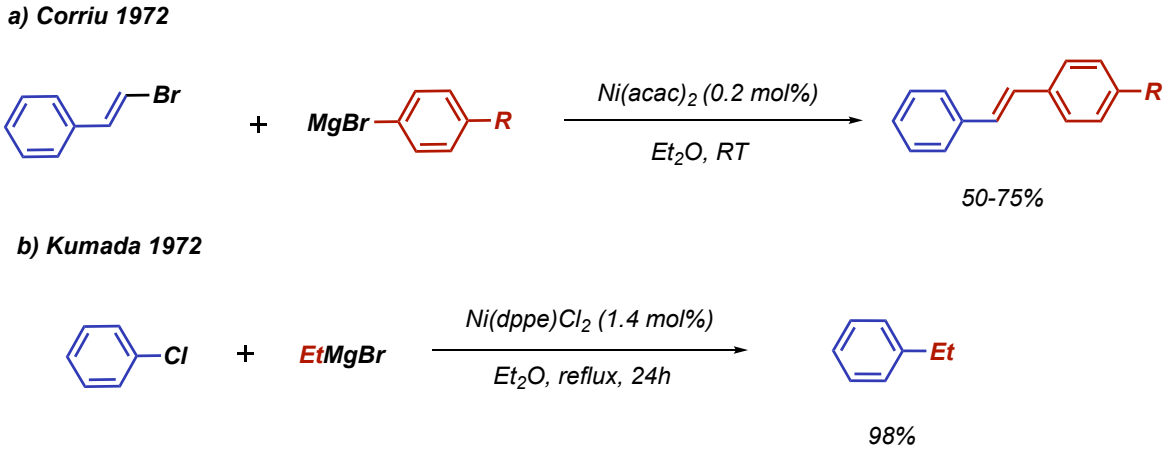

***Scheme 1.7**: The Corriu–Kumada reaction*

Until the 1970s, cross-coupling reactions had been dominated by three main metals, copper for coupling with acetylenes, nickel for solving the selectivity problems associated with the use of Grignards, and palladium for coming powerfully onto the scene thanks to the new system developed by the Mizoroki-Heck coupling. In the following years, palladium's role in coupling reactions will grow exponentially, becoming the absolute "master" of the field despite the other two metals.

The use of palladium in the reaction of aryl halides and acetylenes was reported independently by three different research groups in 1975: Cassar,[8] Heck[9] and Sonogashira.[11] The protocol presented by Sonogashira had the advantage of making the reaction condition milder than Cassar and Heck thanks to the use of a catalytic amount of copper as cocatalyst (Scheme 1.8). This system represents a remarkable development from the coupling described by Castro-Stephens, who performed the reaction between acetylenes and aryl bromides with stoichiometric amount of copper, high temperature and therefore a notable formation of Glaser-Hay byproduct.

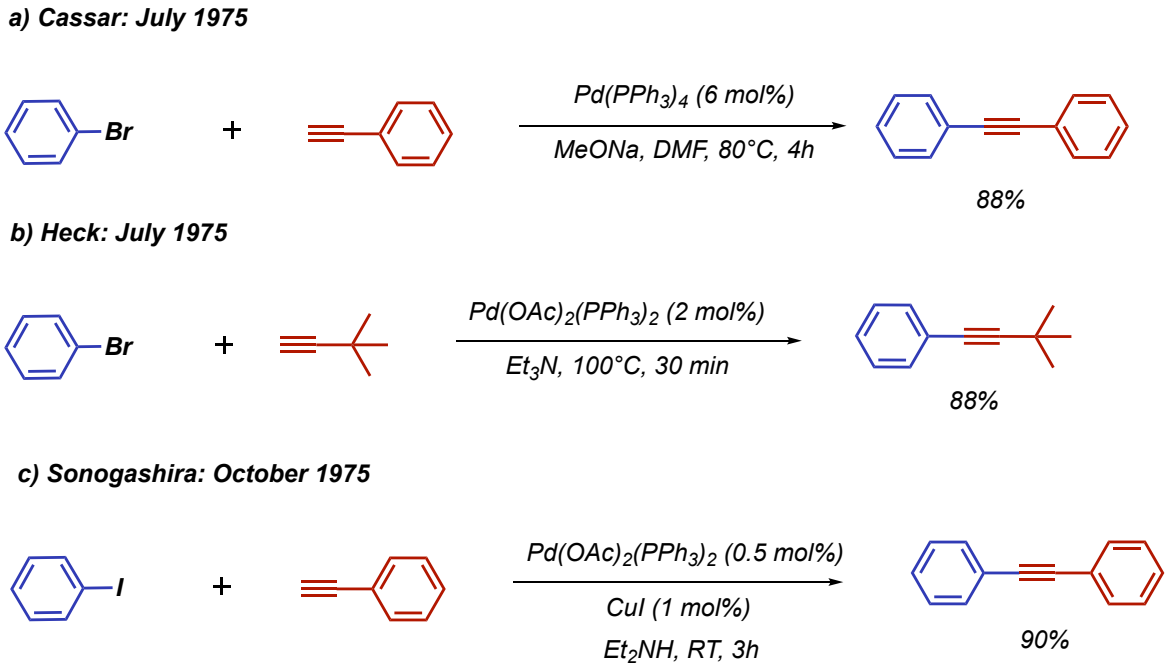

Scheme 1.8: *The Heck-Cassar-Sonogashira coupling*

The disclosure of the palladium-catalyzed Sonogashira reaction opened the world to C(sp^2)-C(sp) coupling reactions. The advantageous effects of palladium catalysis became increasingly recognized by the scientific community and transferring these benefits to protocols previously established through nickel catalyzed processes became an attractive prospect. Contributions by Murahashi[41,42] and Jutand[43] demonstrated how palladium chemistry could be applied to the previous reported nickel Corriu-Kumada coupling showing a stronger selectivity and a broader substrate scope (Scheme 1.9).

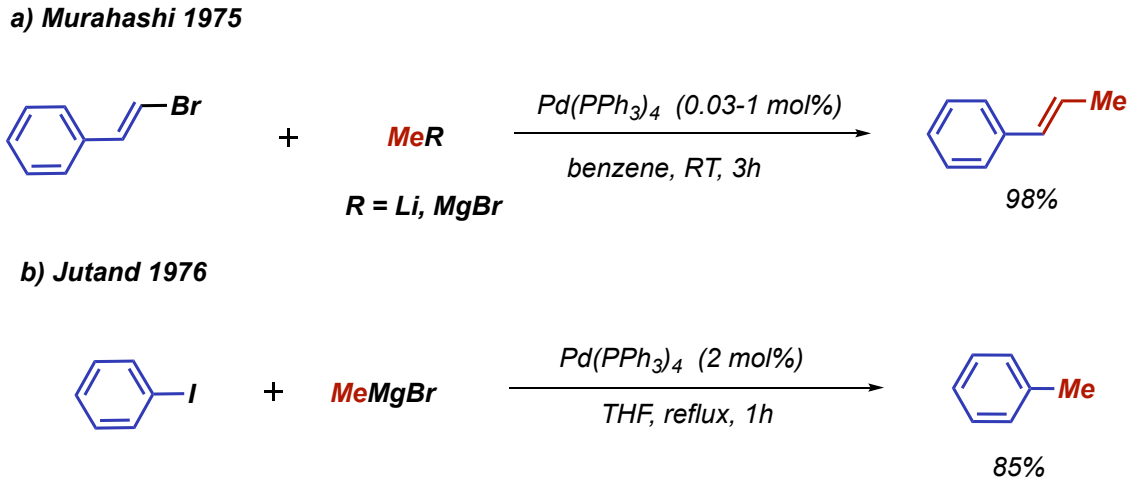

Scheme 1.9*: The palladium-catalyzed Corriu–Kumada cross-coupling reaction*

Until 1976, the development of cross-coupling reactions had focused on the use of magnesium-based Grignard reagents as nucleophiles, with the exceptions of the discoveries of Mizoroki, Heck, Cassar and Sonogashira. However, in 1976, Negishi showed that other organometallic reagents could be used as coupling partners. First by a nickel and palladium coupling performed with organoaluminium reagents as nucleophiles (Scheme 1.10a),[44,45] followed by the use of arylzinc reagents in the so-called Negishi reaction (Scheme 1.10b).[14] In this context, Negishi demonstrated the possibility of arylaluminum and arylzinc species to substitute the previously used arylmagnesium and aryllithium nucleophiles to perform the transmetalation of the cross-coupling process. Moreover, Negishi created a library to identify other possible organometallic reagents as coupling partners.[46] In the hands of Negishi and his students, the field of palladium- and nickel-catalyzed coupling reactions of unsaturated organic halides with organozinc reagents evolved into a general reaction which now stands out as a mild route with impressive functional-group compatibility.

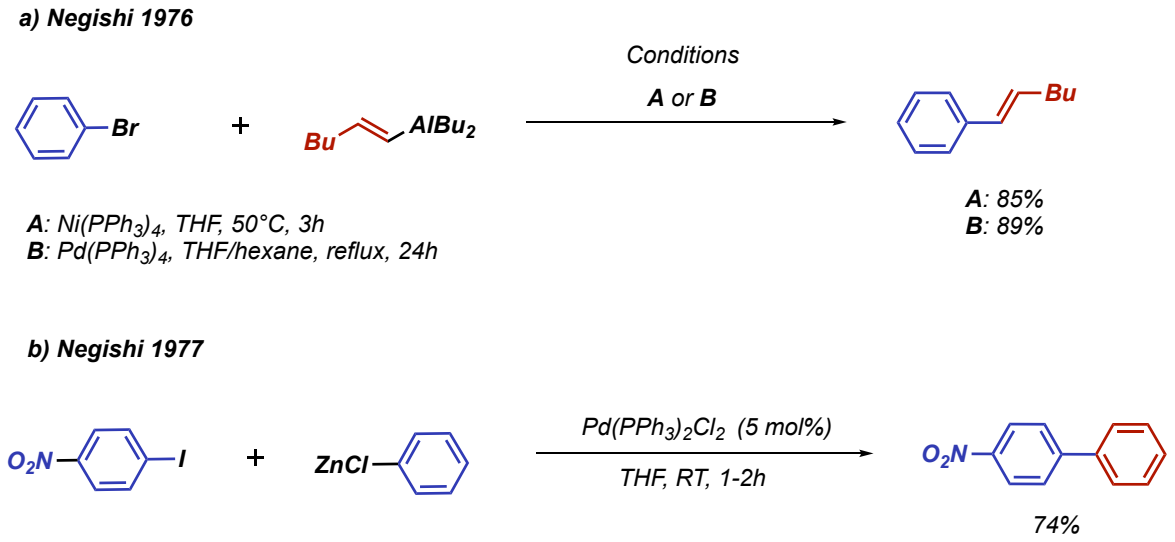

***Scheme 1.10**: The Negishi cross-coupling*

In 1976, Eaborn published the first palladium cross-coupling reaction of organodistannane reagents with aryl iodides (Scheme 1.11a),[47] followed by Migita and Kosugi who reported the coupling of organotin reagents with aryl bromides (Scheme 1.11b).[48,49] Subsequently, Stille and Milstein performed, in 1978, the synthesis of ketones by the coupling of aroyl

chlorides with organostannanes[16] applying milder conditions than those previously reported by Migita and Kosugi (Scheme 1.11c).

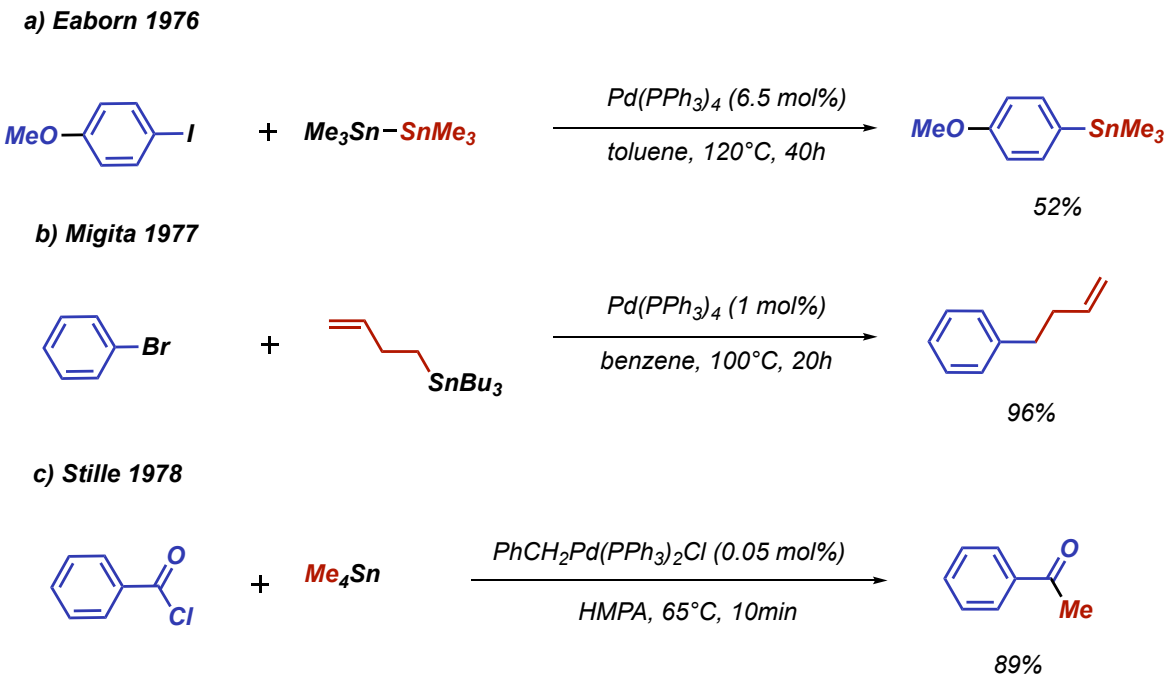

***Scheme 1.11**: The discoveries of stannane cross-coupling reactions*

In 1979 Suzuki reported the palladium-catalyzed cross-coupling between 1-alkenylboranes and aryl halides (Scheme 1.12a).[50] The Suzuki–Miyaura coupling developed into an extremely powerful and general method for the formation of C-C bonds, displaying several advantageous features: 1) easily handled and usually air stable organoboron starting materials; 2) mild and convenient reaction conditions and 3) the facile removal of less-toxic inorganic byproducts. These aspects made the Suzuki–Miyaura coupling reaction especially useful for the industrial segment and, as the date reported in Figure 2 demonstrate, the most widely used cross-coupling reaction over the years.

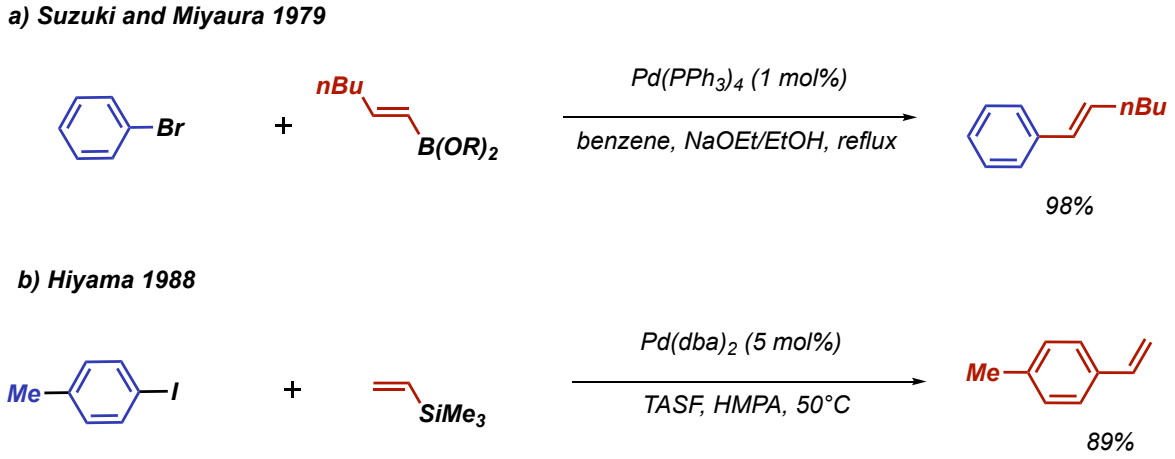

***Scheme 1.12**: Suzuki and Hiyama C-C bond formation couplings*

After the introduction of organoboron reagents as cross-coupling partners, in 1988 Hiyama reported efficient cross-coupling reactions of arylsilanes using fluoride additives (Scheme 1.12b).[51] By 1989, it was already possible to achieve C–C bond formation through cross-coupling reactions using a wide variety of organometallic reagents. Although in 1983 Migita and co-workers disclosed the first palladium-catalyzed formation of C-N bonds through a protocol requiring the use of stoichiometric amounts of a heat- and moisture-sensitive tributyltin amide reagent,[52] the real breakthrough came with the independent discoveries by Buchwald and Hartwig. They claimed that C–N bond formation could also be efficiently accomplished through palladium-catalyzed cross-coupling reactions of free amines with aryl halides (Scheme 1.13).[53–55]

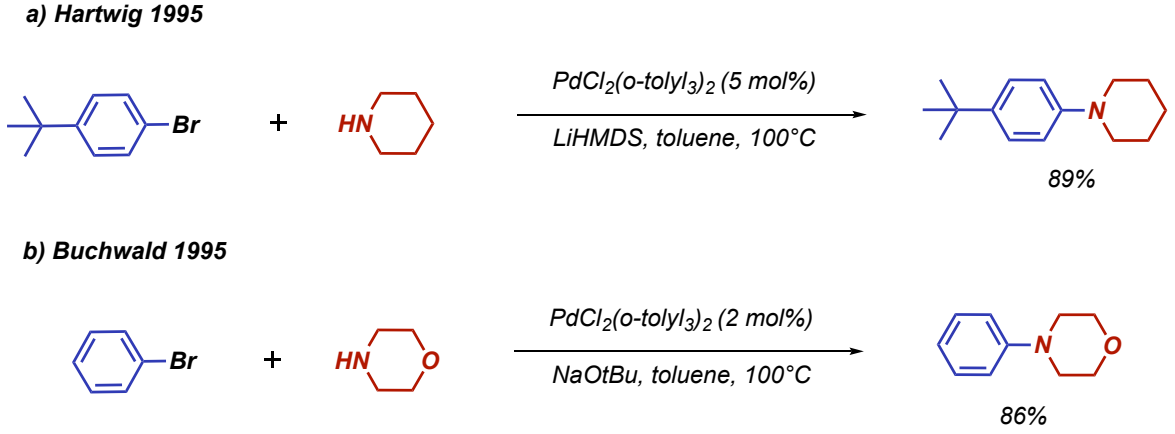

***Scheme 1.13**: The Buchwald-Hartwig amination cross-coupling*

Despite the many significant discoveries and developments since the first reports of cross-coupling reactions, enormous progresses have been made in the field during the last 30 years trying to make these reactions even more efficient, mild and sustainable. This signed the beginning of a new period called the 3rd wave of cross-coupling resulting in the continuous improvement and extension of each reaction type through ligand variation, expanding the substrate scope, by reaction optimization and fine tuning.

1.3 Recent advances in Cross-Coupling Reactions

Even though cross-coupling reactions now represent a mature technology, there is still a significant amount of research in this area that aims to improve the scope of these reactions, develop more efficient catalysts and make reactions more practical.

Since the palladium catalyzed cross-coupling find their application principally in the industrial segment, small improvements in catalyst efficiency can lead to significant economic advantages.[56–59] For this reason, there is always the necessity for the development of new and efficient catalysts, especially in the fine chemical industries. In addition, for both industrial and academic applications, it is useful to have catalytic systems that are not air sensitive and can easily be handled. Surprisingly, despite the extensive research on palladium catalyzed cross-coupling, there is still a variety of sp^2 and bulky substrates that are difficult to couple and require drastic conditions to have good yields.

Over the last 20 years, the development and the focus have been on expanding the scope of substrates and make the reaction more general, for example using less activated sp^2 electrophiles such as amide or esters[60–62] as well as sp^3 hybridized substrates.[63,64] Usually, in these reactions, palladium is replaced by more abundant and cheaper metals such as nickel, copper and iron and other more available first-raw transition metals.[65–71] Finally, traditional cross-coupling reactions have directly inspired more modern types of reactions, such as cross-electrophile coupling,[72–75] conjunctive coupling,[76] and metallaphotoredox chemistry,[77] which still requires time to be fully optimized.

In the following section we describe recent advances that are designed to solve some of the problems associated with palladium catalyzed reactions and the optimization of new methods for cross coupling.

1.3.1 Development of new ligands

One of the greatest advances in palladium catalyzed cross-coupling reactions over the last years, was the development of specialized classes of ligands to improve the reactivity of the elementary steps of the catalytic cycle. Especially, phosphines were found to have beneficial effect on the stability of palladium complexes together with steric and electronic properties that enhance the activity of the catalyst. Historically, the most common used ligands in the cross-coupling reactions were represented by triphenylphosphines, but seminal works reported by several research groups showed that more sterically bulky phosphine ligands generated catalytic systems with increased efficiency and substrate tolerance.[78] At the turn of the century, the development of new phosphines ligands with unprecedented properties that enabled a facile activation of difficult substrates such as aryl chlorides, tosylates and mesylates, were introduced by Beller,[79] Buchwald,[80,81] Fu[82] and Hartwig[83] (Figure 1.5). These new classes of ligands with a variable backbone that allows the tuning of the properties of the catalyst complex, could be applied to numerous cross-coupling reactions.[84]

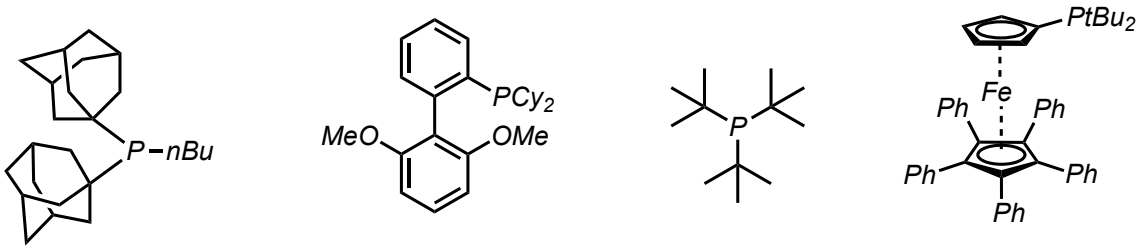

***Figure 1.5**: Phosphines introduced by Beller, Buchwald, Fu and Hartwig*

The dialkylbiarylphosphine ligands of Buchwald, for example, enabled the development of mild reaction conditions such as Suzuki-Miyaura coupling at room temperature with inactivated aryl chlorides[85] and new efficient Buchwald Hartwig amination couplings.[86] Currently a wide number of Buchwald ligands are commercially available and the general design principle to improve the elementary steps such as oxidative addition and reductive elimination is well known. It was demonstrated, in addition, by Buchwald and coworkers, that even minimal modifications of the properties of the ligand could lead to major

improvement in the catalytic activities for conversion of specific classes of substrates.[87,88] It is also possible now to predict which type and class of ligand fits perfectly and is more efficient for each type of cross coupling reaction (Figure 1.6).

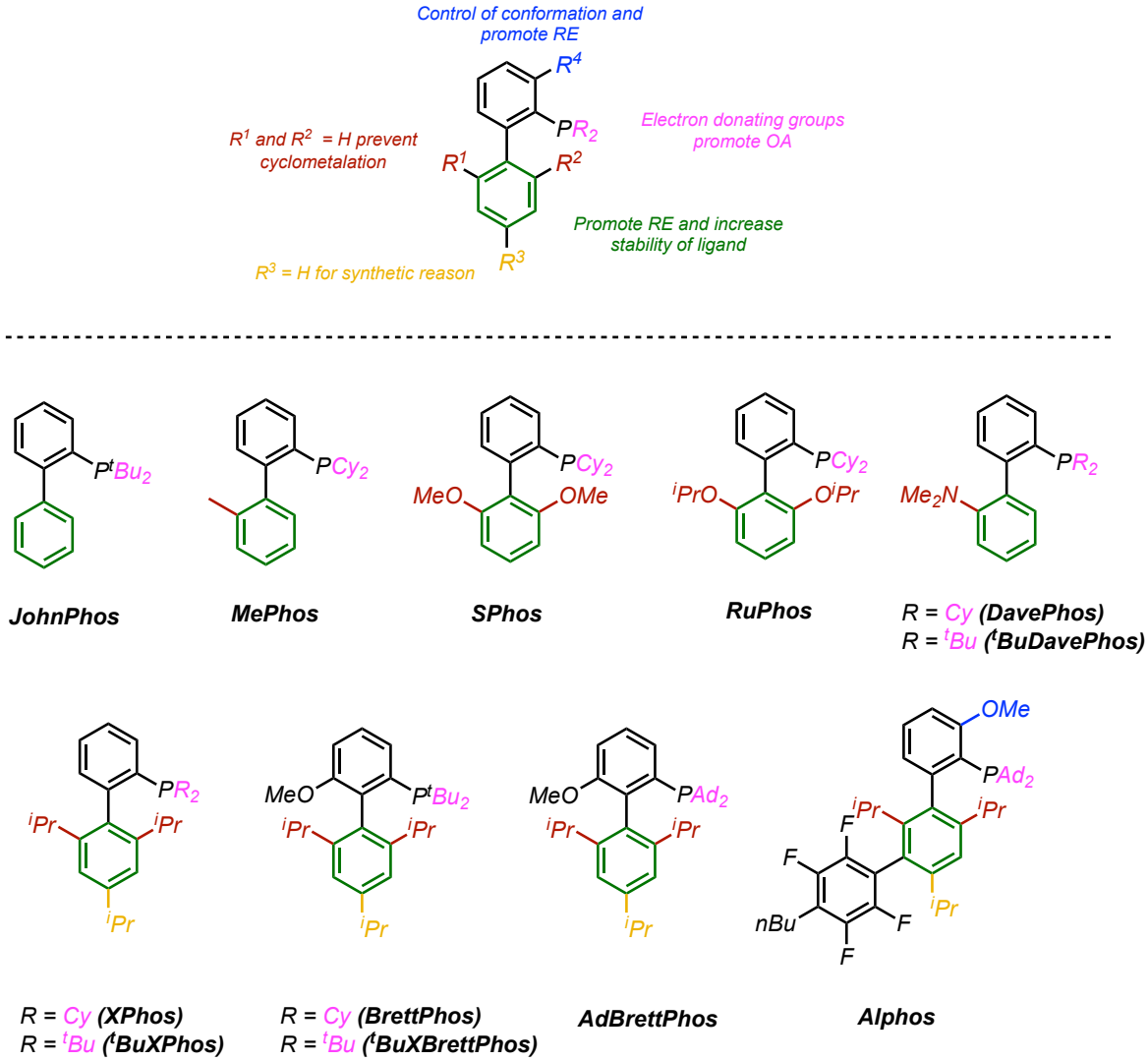

***Figure 1.6**: Generic advantages and design principles of Buchwald-type dialkylbiarylphosphine ligands*

Distinct effect of the ligands was noted for the oxidative addition, the reductive elimination and the stabilization of the catalyst.

The active catalyst species for the OA in the case of bulky phosphines was recently reported to be PdL_1.[89] In fact, the bulkiness of a ligand is supposed to shift the equilibrium PdL_2 = $PdL_1 + L_1$ to the right side, increasing the concentration of the monoligated active species. For this reason, the ratio between Pd and the ligand is very important in order to have

effective cross-coupling reactions: Fu noted that more than 1.5 eq of $PdtBu_3$ led to a significant decrease in the Suzuki coupling.[90] However, Brown and Jutand reported that the OA with less bulky phosphines (such as Cy_2PtBu, or PPh_3) is performed with a PdL_2 complex generating a four coordinated intermediate that is not formed with bulky phosphines. Indeed, the question of which of the two active species PdL_2 or PdL_1 is acting in the OA depends on the nature of the ligand and the reaction conditions.[91]

Subsequently, Hartwig reported a study claiming that the number of ligands coordinated to a phosphine depends more on the halide leaving group than on the nature of the phosphine.[92] When the OA occurs with Ph-I, the active catalyst is always $Pd(PR_3)_2$ in all cases. The reaction is zero order in added ligands ($PtBu_3$, $AdPtBu_2$, $CyPtBu_2$) with $Pd(PR_3)_2$, but it is negative order for ligand $Pd(PCy_3)_3$ and added PCy_3. For Ph-Cl, the step of the OA occurs with the monoligated $PdPR_3$, as demonstrated by an inverse dependence of the rate constant on the concentration of added ligand while with Ph-Br there is a competition of the two pathways depending on the reaction conditions.

The importance of electron-rich phosphines consists also in their ability to stabilize the active catalyst by a strong binding and preventing the formation of palladium black precipitate.[93] Consequently, the use of more equivalents of ligand enhances the stability of the Pd^0 catalyst. On the contrary, as written above, depending on the reaction conditions, an excess of phosphine can decrease the activity of the catalyst. For this reason, the ideal balance between enough ligand to stabilize the catalyst on one side and an equilibrium favoring the formation of the active species PdL_1 or PdL_2 on the other side is crucial to have an efficient cross-coupling reaction and is different for each phosphine and reaction condition.

Regarding the RE step, Hartwig summarized the effect of the steric and electronic properties of the ligands to make the process effective.[94] It is not surprising that a major steric hindrance of the phosphine ligand slows down the energy barrier of the RE step in contrast to less hindered phosphines. Nonetheless, another study demonstrated that electron-rich phosphines, that have a beneficial effect on the OA, are responsible to make the RE step slower than with electron-deficient ones.[95]

In general, the improvement of reactions through ligands in recent years has been minimal, in the sense that there are now ligands that are so efficient that only small improvements

can be made. Probably the most efficient improvement that can be made from now on is to develop more stable and less expensive ligands with the same catalytic activities.

Over the past decade, N-heterocyclic carbene (NHC) ligands have become increasingly popular in cross-coupling reactions.[96–98] In general, NHC ligands were first viewed as phosphines mimics, but subsequently were discovered to have better sigma donating properties compared to phosphines. For this reason, they could be useful for bulky and challenging substrates. The simples NHC ligands developed are represented by IMes and IPr,[96,97] but other more complicated ligands were rapidly synthetized[98] (Figure 1.7). In general, these types of ligands are more commonly used with cross coupling reaction with copper where, the OA is more challenging. Unfortunately, at the moment there is often relatively little understanding about whether a phosphine or NHC ligand would be more effective for a particular reaction, and experimental testing is generally required.

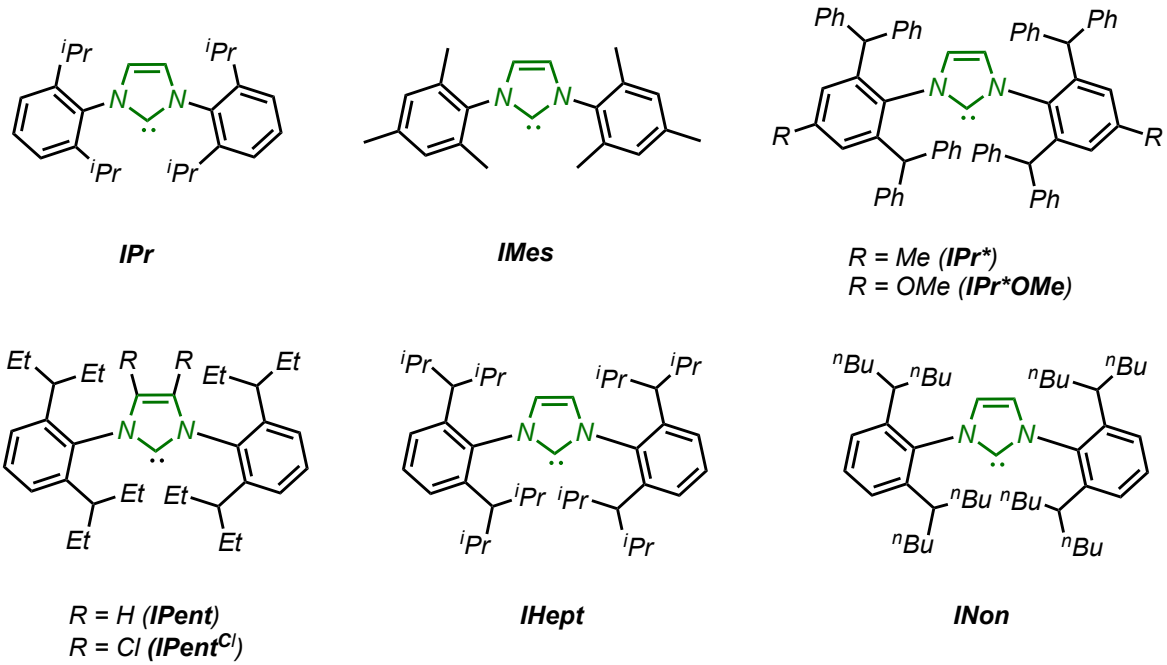

***Figure 1.7**: NHC ligands commonly used in cross-coupling reactions*

1.3.2 Introduction of alternative metals

Palladium based cross-coupling reactions are widely used in the industrial processes involving reaction with sp^2 hybridized carbon because of their high and well-known reactivity and stability. However, the use of palladium as catalyst can also present some

limitations: palladium is not an abundant metal in nature and therefore, for both environmental and economic reasons it would be desirable to find alternatives, particularly for large-scale transformations. In addition, the International Conference of Harmonization Guidelines Q3D (ICH Q3D) set very low limits for elemental impurities in medicines[99] and the quantity of palladium that is permissible in drugs must be tightly controlled at low (ppm) levels. It can be expensive to reduce the amount of palladium to such levels, especially if the coupling is used at a late stage in the synthesis of an active pharmaceutical ingredient. To avoid these problems, recently, cross-coupling reaction with new earth-abundant first raw metals have been developed. Studies about first-row transition metal complexes has focused primarily on iron, nickel, and copper systems, although recently cobalt-based catalysts have also been developed. [65–71] Although new systems have been developed recently, these first-row protocols generally give lower activity than palladium for traditional cross-coupling reactions and require significantly higher catalyst loadings and more drastic reaction conditions. The difference in reactivity between palladium and first raw transition metals can be exploited by using these abundant metals in reactions where the use of palladium catalysis is more challenging and differ therefore from the common sp^2 cross-coupling. It is difficult to say now if first raw transition metals are going to replace palladium, what is sure is that palladium is still very used both at industrial and academic level. The reason of that is also because palladium catalysis has been studied for more than 50 years and during all these years several improvements have been done, such as development of new ligands and new pre catalysts. If the first raw transition metal has to substitute palladium as catalyst, many of the same improvements that have occurred for palladium systems, would be required. Finally, given the high efficiency of palladium-based systems and the opportunity to recycle and recover the catalyst at the end of reactions, it could be advantageous to focus the research on developing new methodologies using systems based on earth-abundant metals rather than replacing palladium in conventional reactions.

1.3.3 The development of new substrates for Cross-Coupling reactions

The extension to other types of cross-coupling substrates different from the traditional sp^2 electrophiles has represented a new trend in metal catalysis in recent years. The aim of this

type of research was to develop more versatile, atom efficient and sustainable cross-coupling reactions by extending the range of potential substrates. Recent articles and the latest research have shown that for these kinds of substrates, palladium chemistry is not the most suitable and therefore the use and experimentation of new metals with different properties could offer novel opportunities to make these reactions more efficient.

Cross-Coupling Reactions using sp^3 -hybridized substrates

For many years the field of cross-coupling has been dominated by the sp^2 hybridized substrates. Although sp^2-sp^2 carbon bonds are quite common in nature, it is a fact that there is an even larger percentage of natural substances that contain sp^3-sp^3 bonds. [63,64] For this reason, the coupling between sp^3-sp^3 represent a very important discovery for transition metal catalysis. The main challenge for this coupling is represented by the β-hydride elimination and the slow oxidative addition that occurs with alkyl electrophiles (Scheme 1.14).

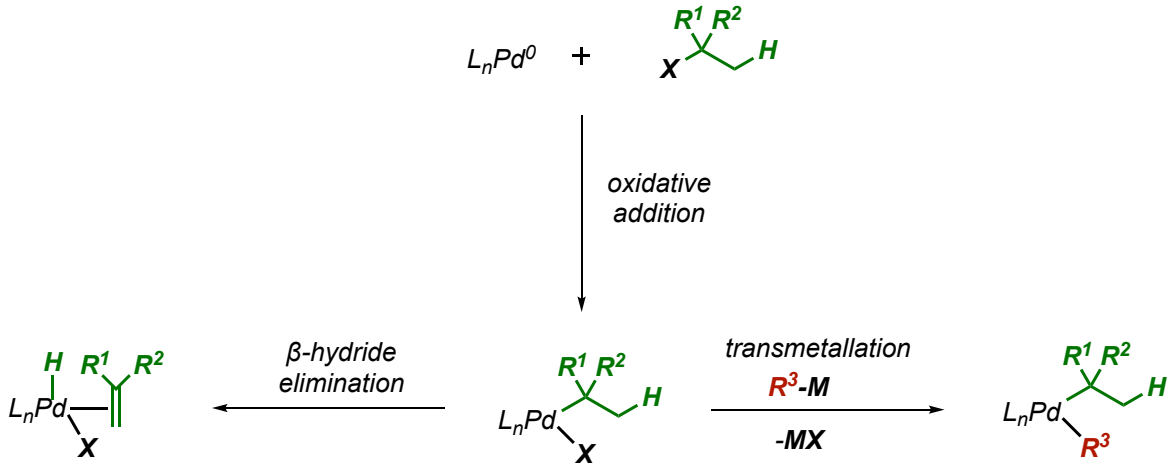

***Scheme 1.14**: Competition between β-hydride elimination and transmetallation in cross-coupling with sp^3-hybridized substrates*

One of the earliest works in this area is represented by Fu, who reported a paper in 2001 performing a room temperature palladium-catalyzed alkyl−alkyl Suzuki−Miyaura reaction using alkyl bromides as electrophile.[100] The importance of this work was represented by the fact that the β-elimination side reaction was suppressed, in contrast to most of the already reported sp^3 couplings. In addition, previous cross-couplings required drastic

conditions and toxic nucleophiles, whereas in this case the reaction was carried out at room temperature and using organoboranes (Scheme 1.15).

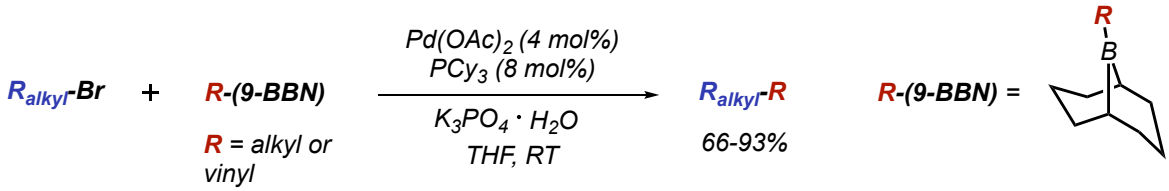

***Scheme 1.15**: Palladium-catalyzed alkyl–alkyl Suzuki–Miyaura reported by Fu*

As mentioned previously, for this new type of cross-coupling reaction, another metal began to take over the scene: nickel is more likely to undergo one-electron redox reactions compared to palladium because of its lower ligand field splitting, which for square-planar nickel(II) complexes means that it is easier to add an electron to the antibonding $d_{x^2-y^2}$ orbital or move to a tetrahedral geometry. A consequence of the greater tendency for one-electron chemistry is that nickel catalysts more readily undergo oxidative addition via a radical pathway than analogous palladium systems. Inspired by the work of Knochel on primary alkyl halide electrophiles,[101,102] Fu developed a nickel-based Negishi and Suzuki–Miyaura reaction involving secondary alkyl halide electrophiles.[103,104]

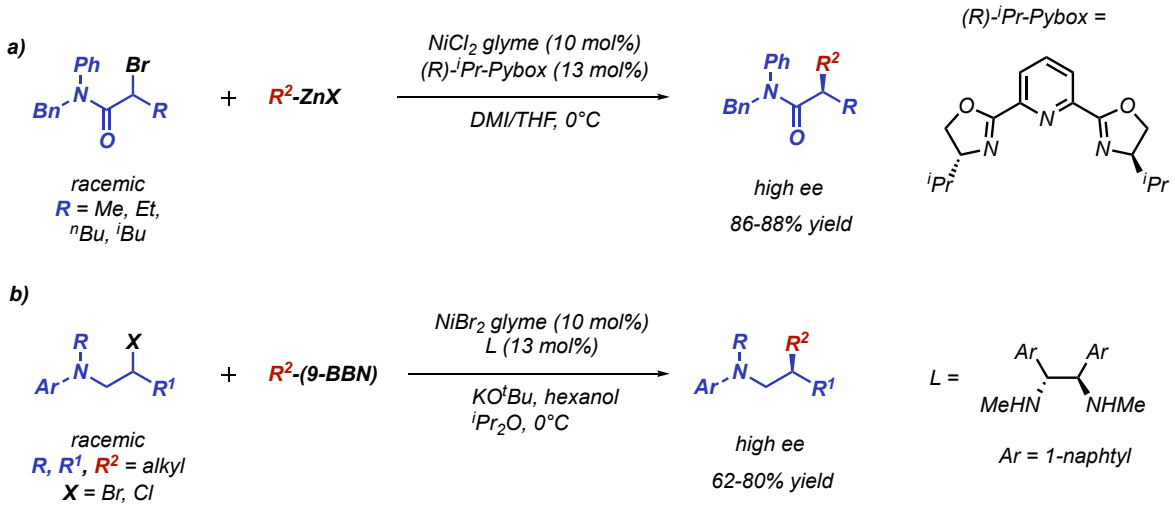

***Scheme 1.16**: Enantioselective Negishi a) and Suzuki–Miyaura b) reactions using racemic alkyl electrophiles*

Reactions employing secondary alkyl substrate opened the world also to enantioselective sp^3-sp^3 cross coupling reactions. The use of a chiral nickel catalyst makes it possible to generate a single enantiomer of the product starting from a racemic starting material (Scheme 1.16)[105,106]. Even if tertiary radicals are more stable than the respective primary and secondary ones, the number of examples of cross-coupling reactions utilizing tertiary alkyl electrophiles to generate quaternary carbon centers is much lower. A rare example was reported in 2013, when unactivated tertiary alkylbromides were used in the nickel-catalyzed Suzuki–Miyaura[107] (Scheme 1.17).

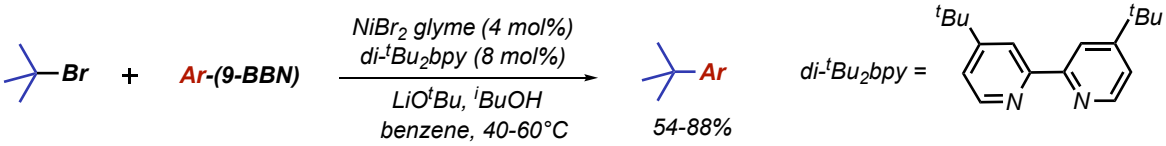

Scheme 1.17: *Nickel-catalyzed Suzuki–Miyaura coupling with tertiary alkyl bromides*

In general, there is still room to optimized cross coupling reaction with sp^3 hybridized electrophiles. The functional group tolerance of these reaction is much lower than the variety of different substrates that can be used for sp^2 coupling reactions. This challenge needs to be addressed to make these reactions more synthetically valuable.

Cross-Coupling Reactions Using Phenol Derivatives.

Although halides are most commonly employed as electrophilic coupling partners in these transformations, the use of phenolic derivatives, or "pseudohalides", provides a versatile alternative. Phenol containing moieties are intermediates in many target-oriented syntheses and can easily be used as coupling partners when traditional halides would be difficult to access.[108] While the reactivity of the most common used aryl sulfonates (triflates, tosylates and mesylates) in cross coupling reaction is well established, the development of efficient reactions for less reactive pseudohalide such as sulfamates, carbamates, esters, and ethers are less understood (Figure 1.8).

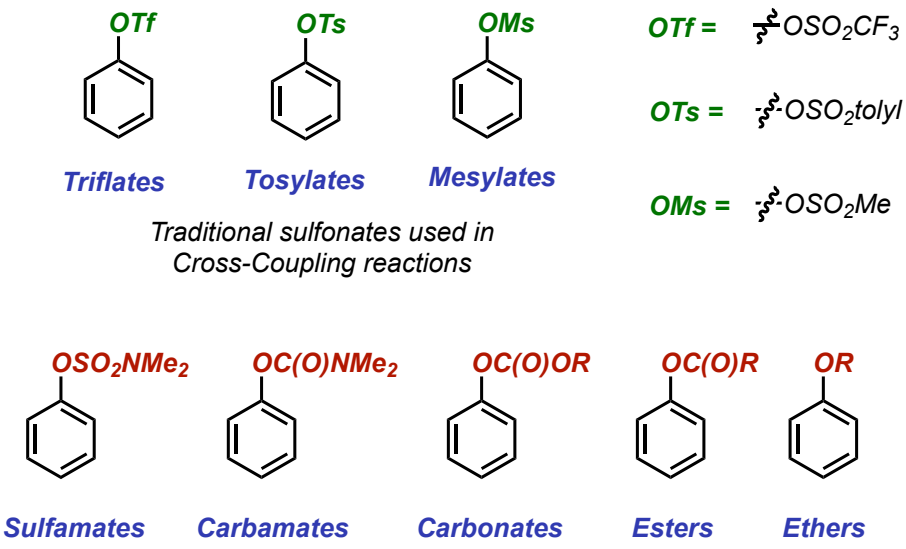

***Figure 1.8**: Phenol derivatives that are used as electrophiles in cross-coupling*

Garg reported in 2009 the nickel catalyzed Suzuki coupling of aryl carbamates and monodentate phosphine ligands[109] (Scheme 1.18). This seminal work was found very attractive because aryl carbamates can also be used as directing group in nickel catalysis, in contrast to the traditional aryl sulfonates. The same conditions were demonstrated to be effective to couple also aryl sulfamates and carbonates. Mechanistic studies suggest a traditional catalytic cycle involving oxidative addition of the sulfamate, carbamate, or carbonate, followed by transmetallation and reductive elimination to give the final product. Initially these reactions necessitated harsh conditions such as high temperature to allow OA and high catalyst loadings. Subsequently, the reaction had been optimized and could be performed at room temperature and with low amount of catalyst and generalizing the method also to other cross coupling reactions such as the Buchwald Hartwig amination using NHC ligands.[110,111]

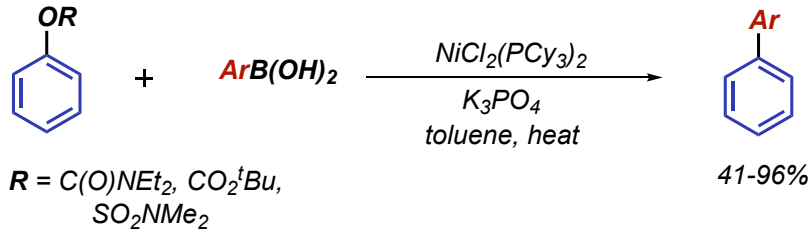

***Scheme 1.18**: Nickel catalyzed cross-coupling involving carbamates, carbonates and sulfamates*

Unactivated aryl esters area also valuable substrates for cross coupling reaction because they can readily be synthetized from aryl phenols[112] or carboxylic acids,[113] are bench stable and common substrates in organic synthesis. When aryl esters are used as electrophiles three different mechanism can occur depending on the reaction conditions: the cleavage of the C(aryl)-O or C(acyl)-O bonds and the activation of the C(acyl)-O followed by the decarbonylation (Scheme 1.19). Catalysts that are selective for all three possible reactions are known, and there is some mechanistic understanding about the factors that are important in promoting one pathway over another.[61,62,114] In general, major challenges that still need to be addressed are represented by the limited scope of substrates of these reactions and the difficulties to couple unactivated C(sp^3)-O(alkyl) bonds. A better understanding of the mechanism of this reaction system is necessary in order to expand the substrate tolerance and to use milder conditions.

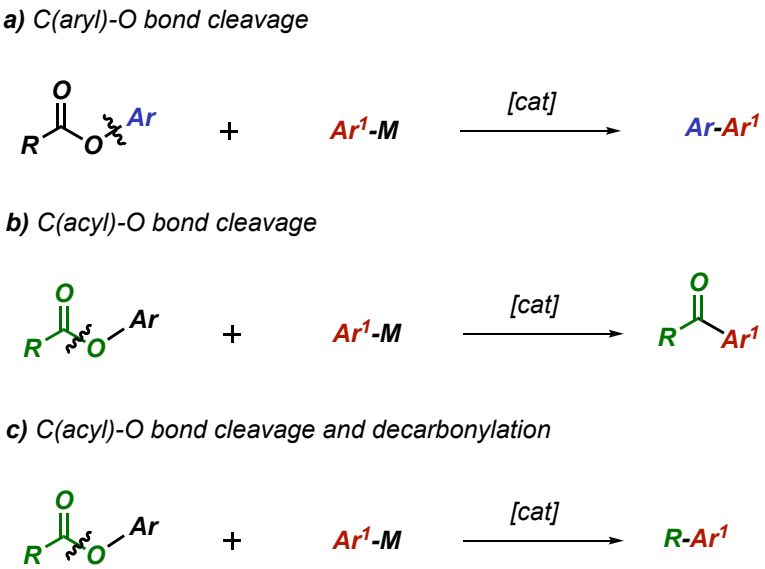

***Scheme 1.19:** Generic representations of the different types of cross-coupling reactions involving aryl ester electrophiles*

Cross-Coupling Reactions Using Amides, Aziridines and Nitroarenes

Amides are common functional groups in organic chemistry and their use as electrophiles can bring notable advantages. Traditionally, the use of amides was limited because the N-C bond activation and cleavage required harsh conditions as consequence of its high stability. Strong acids or bases and pyrophoric reagents are sometimes necessary to perform the rupture of the bond. In 2015, Garg and co-workers reported the first coupling reaction of amides involving both alkyl and aryl amides as electrophiles[115] (Scheme 1.20a). Methods for the C-C bond formation after the cleavage of the C-N bond have also been reported. Initially, Garg and co-workers described nickel-catalyzed Suzuki–Miyaura reactions of Boc-protected amides to furnish ketones in high yields[116] (Scheme 1.20b). Subsequently, other groups reported the same reaction with palladium catalyst demonstrating that also palladium is suitable for this type of chemistry.[117,118]

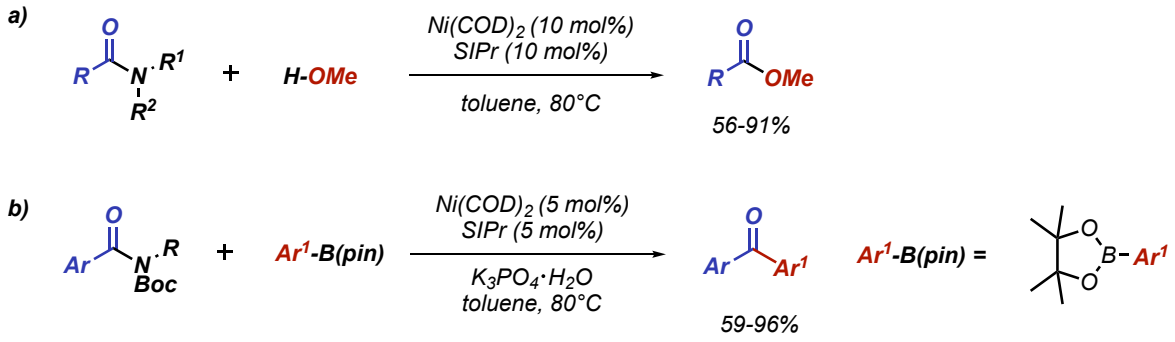

***Scheme 1.20**: Cross-coupling reactions involving alkyl and aryl amides*

Other electrophiles that are beginning to be used are represented by aziridines[119,120] and nitroarenes[121,122] (Scheme 1.21). Aziridines electrophiles represent a valuable pathway for the preparation of β-substituted amines while the coupling of nitroarenes is quite interesting because they are commonly used to prepare aryl halides and therefore their direct coupling could reduce waste and increase overall atom efficiency.

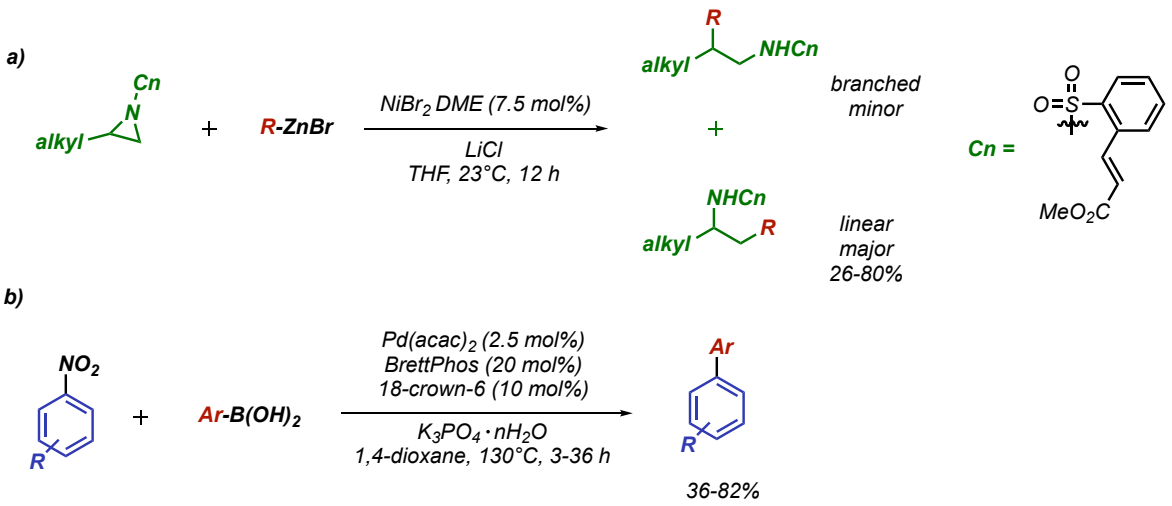

***Scheme 1.21**: Examples of coupling reactions involving aziridines a) and nitroarenes b)*

1.4 Application of Green protocols to Cross-Coupling Reactions

Even though in recent years, the development and use of less expensive and more abundant metals such as copper, cobalt, iron, and nickel has significantly grown, due to its high activity, improved selectivity and ability to enable conversion of less reactive substrates, palladium still represents the metal of choice. However, considering the increasing growth in the price during the last years, attempts to reduce its loading and to perform its recycling and recovering represent an inescapable necessity, especially if the final outlook is to apply reactions at industrial level. Nowadays, the development process must therefore respect principles of greenness and sustainability such as the selection of green solvents and reagents. The twelve principles of green chemistry[123] (Figure 1.9) were developed to inspire the creation of new processes and methodologies for active pharmaceutical ingredients (API) synthesis. In particular, the principles highlighted the necessity of safe, cheap and environmentally friendly methodologies, that can be translated into fast, selective, flexible and mild reaction conditions using sustainable and cheap chemicals.[124] The pharmaceutical industry was among the first sectors to integrate the practice of green chemistry, with the adoption of new tools and training, and the creation of green chemistry teams.[125]

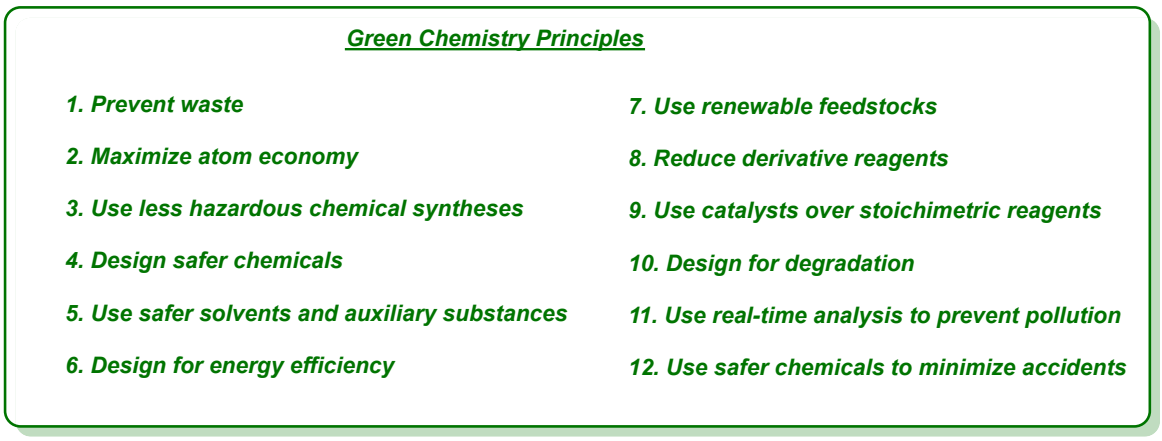

***Figure 1.9**: Twelve Principle of Green Chemistry*

Furthermore, in order to share the same vision of a more sustainable synthesis of APIs, pharmaceutical and biotechnology companies created, in 2005, the American Chemical Society's Green Chemistry Institute Pharmaceutical Roundtable (ACS GCIPR), with the mission of encouraging innovation and the integration of green engineering in the pharmaceutical industry.[126]

Palladium catalysed cross coupling reactions can easily satisfy some of these green principles and, for this reason, it would result in a huge waste not exploiting the enormous potential of this metal to create green and sustainable methodologies. In this context, the ninth principle of green chemistry recommends the use of catalysis as main alternative to classical stoichiometric chemistry for carbon-carbon bond formation in organic synthesis and for this reason represents an advantageous method to reduce waste and increment the efficiency of industrial and academic reactions. Chemical processes employing stoichiometric and mainly inorganic reagents, such as reductions with metal hydrides ($NaBH_4$, $LiAlH_4$) and metals (Na, Mg, Zn), or oxidations with permanganate and chromium (VI) reagents, as well as processes using stoichiometric Lewis acids and mineral acids have a very poor atom economy (AE), which is a parameter used to assess the production of waste in a process.[127,128]

Many important cross-coupling reactions are utilized in the pharmaceutical sector and among them, palladium-catalysed reactions are probably the most versatile ones. As described in the previous section, despite the actual popularity of palladium cross-coupling reactions, it took decades for these methodologies to become popular in the scientific

community. The reason for the slow development of cross-coupling reactions is particularly manifested in the industrial segment. In our opinion, this is also due to the fact that in the industrial sector the pharmaceutical industry is divided by users with entirely different aims: the medicinal chemist and the process development chemist. The medicinal chemist is focused on identifying the molecular space in order to optimize the interactions with the biological target.[129] For this reason, the synthetic methods should be simple to use and flexible to allow a rapid development in the molecular diversity. In contrast, the process chemist, focused on the chemical space, is interested in the synthesis of pure and high-quality products in the shortest time possible and with the lowest costs, not caring about the greenness of the process. Only in the late stage of the clinical development, aspects related to the environmental impact are fully established. As a result, Roger Sheldon in 2017 complained the poor attention to green chemistry principles in the industrial process development and called on the entire scientific community to pay more attention as it is now representing an inescapable necessity.[130] Our research group proposed a translation of the twelve green chemistry principles (Figure 1.10) into practical suggestions for the implementation of catalytic methods to facilitate the development of pharmaceutical-industry synthetic methodologies that will be presented in the following section starting from the explanation of the main green metrics to respect in order to develop a sustainable and efficient reaction process.

Figure 1.10: *Translation guide of the Twelve Principle of Green Chemistry for Cross-Coupling reactions*

1.4.1 Green metrics

Many green metrics have been introduced starting from the seminal work on the Environmental Factor (E-Factor) by Sheldon.[131,132] In our opinion, the most useful one for the optimization of a methodology is the Process Mass Intensity (PMI) that is the sum of all the chemical used to produce 1 kg of final product and comprises water and solvents (Figure 1.11a). However, the evaluation of the recovery of all the possible chemicals is critical to define the bottom line of raw material cost (RMC) at industrial level. Therefore, the PMI recalculated after recovery of all the chemicals (PMIr), that has a direct impact on the production costs, is the best metrics for methodology evaluation (Figure 1.11b). A strong impact on the final increase of the PMI is given by the protection and deprotection steps in a chemical process. Since the palladium catalyzed cross-coupling reactions are highly chemoselective, efficient and tolerate several functional groups, they can be considered advantageous in the chemical process design without a significant deviation from the ideality score reported by Baran (Figure 1.11d).

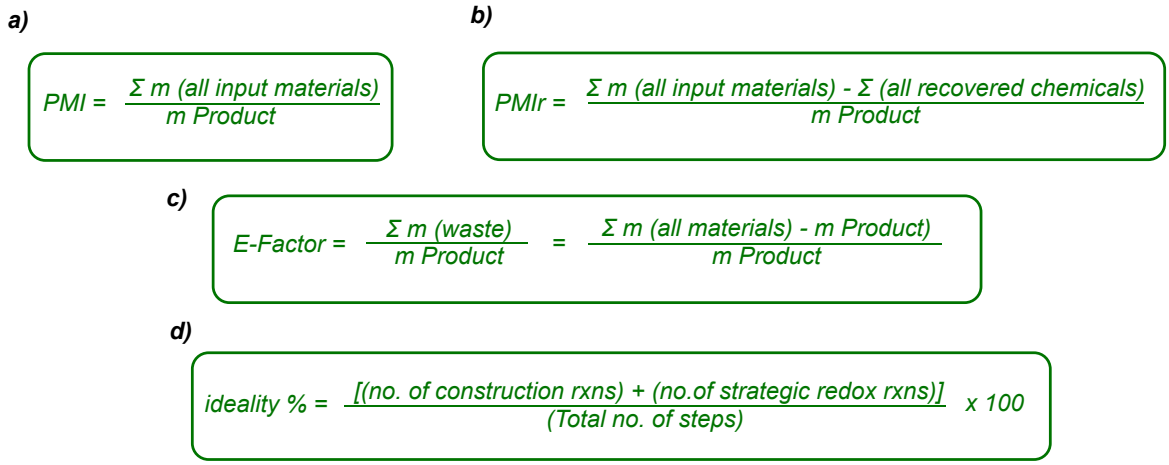

***Figure 1.11**: Green metrics that must be considered to develop efficient metal-catalyzed reactions*

Lipshutz highlighted that the recycling and recovery of precious metals catalysts like palladium, considering its relatively low abundancy, is fundamental for the process sustainability.[133] Therefore, for the development of a new methodology inspired by the twelve principles of green chemistry the key parameters to be considered are: i) PMIr that considers the recovery of chemicals comprising the metal catalyst; ii) reaction time and

temperature; iii) catalyst performances using the turn over number (TON) and turnover frequency (TOF) (Figure 1.12a-b).

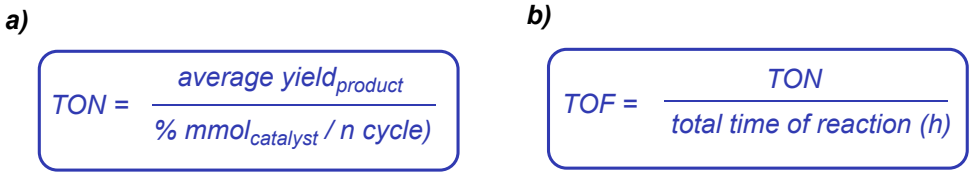

***Figure 1.12**: Parameters that evaluate the efficiency of a reaction*

1.4.2 The Twelve Green Principles Translation Guide for Catalytic Reactions

The twelve principles of green chemistry should inspire the chemists during the development of new processes or methodologies for API synthesis and, in fact, all the critical aspects of sustainability have been considered by Anastas and Wagner, namely environment (No. 1,2,3,5,7,8,10), health (No. 3,4,5), safety (No. 5,11,12) and energy optimization (n. 6). In addition, the overall synthetic strategy (No. 3) and the product design (No. 4) have been considered while the only methodology taken into consideration was catalysis (No. 9). Regarding principle No. 9 concerning catalysis, in our opinion, the efficiency of the reaction and the possibility to recycle and recover the catalyst is a crucial parameter for industrial applications and green methodologies. In this context, TON and TOF are standard parameters that should be increased during the process development in order to enhance the efficiency of the reaction. Therefore, a translation guide of the twelve principles could be useful to inspire the development of efficient and sustainable catalytic protocols applicable at industrial level (Table 1.2). Palladium catalyzed cross coupling reactions fits perfectly in this context: the high selectivity and the stoichiometry allow to control the atom economy (No. 2), catalytic transformations are generally based on the use of less hazardous technologies (No. 3) and high chemoselectivity allows to reduce functional groups manipulation and protective groups (No. 8). All the other principles should guide the methodology design and development. In particular, the solvent and auxiliaries' selection, while maintaining the catalyst efficiency, is a key target.

***Table 1.2**: The Twelve Principles of Green Chemistry: a translation guide for cross coupling reactions*

THE TWELWE PRINCIPLES OF GREEN CHEMISTRY	A TRANSLATION GUIDE FOR CATALYSIS
1. **Prevention.** It is better to prevent waste than to treat or clean up waste after it has been created.	Low PMI and PMIr are preferable. The catalytic reaction should be performed at very high concentration and the recovery of solvent, chemicals and catalysts should be one of the targets of the process design.
2. **Atom Economy.** Synthetic methods should be designed to maximize incorporation of all materials used in the process into the final product.	The catalytic reaction should be optimized by a fine tuning of the reaction conditions to minimize reagents excess and to get high chemo-regio and stereoselectivity.
3. **Less Hazardous Chemical Synthesis.** Wherever practicable, synthetic methods should be designed to use and generate substances that possess little or no toxicity to human health and to the environment.	Catalytic reactions should be chosen to design syntheses based on nontoxic and unreactive substrates. High reactivity is generally associated with high toxicity.
4. **Designing safer chemicals.** Chemical products should be designed to preserve efficacy of function while reducing toxicity.	Catalysts, solvents, starting materials and auxiliaries should be designed and combined in order to get high reaction performances while minimizing their toxicity.
5. **Safer Solvents & Auxiliary.** The use of auxiliary substances (e.g., solvents, separation agents, etc.) should be made unnecessary wherever possible and, innocuous when used.	Catalytic reactions should be performed using green and when possible biogenic sustainable solvents and auxiliaries.
6. **Design for Energy Efficiency.** Energy requirements should be recognized for their environmental and economic impacts and should be minimized. Synthetic methods should be conducted at ambient temperature and pressure.	The best energy efficiency should be achieved by the use of highly reactive catalysts to get fast reactions under mild conditions. The reaction temperature should be always <100°C.
7. **Use of Renewable Feedstocks.** A raw material or feedstock should be renewable rather than depleting whenever technically and economically practicable.	Use of renewable and/or biogenic materials should be the preferred choice. For what concern metal catalyst, the recovery is a must to guarantee sustainability for precious metals.
8. **Reduce Derivatives.** Unnecessary derivatization (use of blocking groups, protection/deprotection, temporary modification of physical/chemical processes) should be minimized or avoided if possible, because such steps require additional reagents and can generate waste.	The reaction should be highly chemoselective in order to avoid the introduction of stable and/or temporary protective groups or functional group manipulation.
9. **Catalysis.** Catalytic reagents (as selective as possible) are superior to stoichiometric reagents.	The catalytic reaction must be efficient and score high TON and TOF using only a relatively small amount (ppm) of catalyst.

10.**Design for Degradation.** Chemical products should be designed so that at the end of their function they break down into innocuous degradation products and do not persist in the environment.	Chemicals used in the catalytic reaction should not accumulate in the environment generating nontoxic metabolites.
11. **Real time analysis for pollution prevention.** Analytical methodologies need to be further developed to allow for real-time, in-process monitoring and control prior to the formation of hazardous substances.	The real time monitoring to control the formation of hazardous substances is based on the complete understanding of the mechanism and side product formation of the catalytic reaction.
12.**Inherently Safer Chemistry for Accident Prevention.** Substances and the form of a substance used in a chemical process should be chosen to minimize the potential for chemical accidents, including releases, explosions, and fires.	The catalytic reaction should be focused on the use of mild conditions avoiding the use of solvents with high flash point and sensitive to oxygen.

1.4.3 The development of green solvents

Solvents represent the main source of waste in chemical industrial processes, constituting 80−90% of the total process mass.[134] Recently, several legislative restrictions tried to reduce the usage of solvents in the chemical industry such as the Clean Air Act of 1990 and the European Union Solvents Emission Directive 1999/13/EC or regulate the use of damaging chemical substances through the Registration, Evaluation, Authorization and Restriction of Chemicals (REACH).[135] However, most of the chemical processes still use harmful and toxic solvents and some developing countries have increased their production because of the high availability and low prices. In addition, it was estimated that solvents constitute 50% of greenhouse gas emissions of pharmaceutical manufacture.[136] Therefore, both the solvent selection and the concentration of the reaction have a great impact on the overall greenness of an industrial catalytic process.[137] Furthermore, in a cross-coupling reaction, different types of reactants are involved, and the reaction medium must be able to dissolve lipophilic reactants, as well as organometallics, inorganic metal complexes, and sometimes salts.[138] These requirements make polar aprotic solvents the solvents of choice for metal-catalyzed cross-coupling reactions. However, the safety and environmental hazards of this solvent class have long been known, with N,N-Dimethylformamide (DMF)[139] and other aprotic polar solvents such as N-Methyl-2-pyrrolidone (NMP) and N-N dimethylacetamide (DMAc) being classified as substances of very high concern for authorization (SVHC), due to their reproductive toxicity.[140] From a pharmaceutical point of

view, the use of solvents such as DMF must be avoided for even more reasons, since it can be the source of N-dimethylnitrosamine (NDMA), which have been detected in several drugs.[141] N-nitrosamine, and particularly NDMA, are considered to be highly genotoxic and cancerogenic to humans, and their established daily limit of exposure is very low,[142] in the range of ppb (Table 1.3). For this reason, their detection and regulation are an active problem in the pharmaceutical manufacture.

***Table 1.3**: Limits established for some N-nitrosamines. Those limits are applicable only if a finished product contains a single N-nitrosamine (EMA/369136/2020)*

N-Nitrosamine	ng/day
N-dimethylnitrosamine (NDMA)	96.0
N-diethylnitrosamine (NDEA)	26.5
N-ethyl-isopropylnitrosamine (EIPNA)	26.5
N-diisopropylnitrosamine (DIPNA)	26.5
N-methylnitrosamine butanoic acid (NMBA)	96.0
N-nitrosomethylpiperazine (MeNP)	26.5
N-dibuthylnitrosamine (NDBA)	26.5

Generally, the formation of N-nitrosamines is possible in the presence of a secondary or tertiary amine and nitrite, and under acidic reaction conditions (Figure 1.13). NDMA derives from dimethylamine (DMA), which is formed from the decomposition of DMF at high temperature. It can be present as an impurity in DMF, since it is a precursor in the industrial synthesis of DMF or can be a degradation product formed during the storage of the solvent.[143]

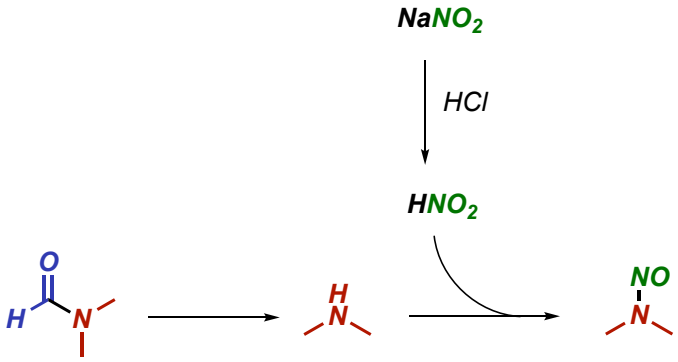

***Figure 1.13**: Formation of NDMA from DMF*

Other solvents commonly employed in cross-coupling reactions have also serious safety and environmental drawbacks. Ethereal and aromatic solvents, such as 1,4-dioxane, methyl tert-butyl ether (MTBE), 1,2-dimethoxyethane (DME) are classified as hazardous in many solvent guides, including the one realized in 2014 by the Innovative Medicines Initiative (IMI)-Chem21 comparing the data of several already published guides, while tetrahydrofuran (THF), 2-methyl-tetrahydrofuran (2-MeTHF) and toluene, are classified either as problematic, or problematic or hazardous. The majority of the already discussed aprotic polar solvents are instead classified as Hazardous (DMF, DMAc, NMP), with only dimethyl sulfoxide (DMSO) and acetonitrile (ACN) classified as problematic. (Figure 1.14).[144]

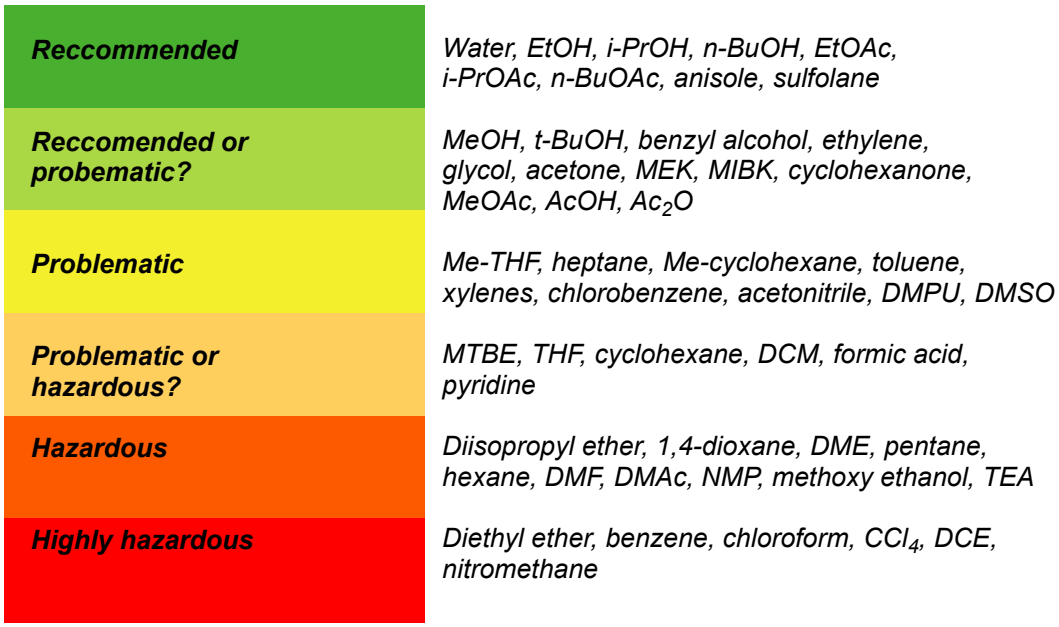

***Figure 1.14**: Classification of some of the most commonly used solvents*

Therefore, the replacement of these toxic solvents with greener alternatives in the industrial process have represented an important challenge in the last decades. The introduction of the green principles has inspired the chemists worldwide to develop reaction conditions that can be used in combination with green solvents.

With the aim to reduce the usage of organic solvents, ionic liquids have been introduced as a more sustainable alternative.[145,146] Several works where ionic liquids have been used efficiently in cross-coupling reactions instead of common organic solvents have been

reported.[146,147] Also supercritical CO_2 offers a more sustainable alternative and offers advantages such as availability and low toxicity.[148,149] The supercritical CO_2 is commonly used as extraction solvent, but its use in cross-coupling reactions recently have attracted the scientific community.[150–152] Another alternative to traditional organic solvents in C-C catalyzed reactions is represented by Deep Eutectic Solvents (DES), a homogenous mixture of Lewis or Brønsted acids and bases, that have recently become extremely popular.[153,154] The employment of these solvents could be advantageous because of their high boiling point and low flashpoint. Water, being considered by many to be the least toxic solvent, has also been tested in metal-catalyzed cross-coupling.[155,156] One of the major limitations related to the use of water in cross-coupling is represented by the poor solubility of organic compounds in the reaction mixture. To get around the solubility problems, a technique that has become increasingly successful is micellar catalysis, in which reactants can be solubilized within the surrounding aqueous phase by the addition of surfactants.[157] One of the leading exponents of micellar catalysis in water, is certainly Lipshutz who utilized the amphiphile DL-α-tocopherol methoxypolyethylene glycol succinate (TPGS-750-M) surfactant in several cross-coupling reactions.[158–161]

Despite the efforts of the scientific community to avoid the use of organic solvents or reduce their quantities, there are still several reactions that need the presence of an organic solvent to be highly efficient. Bio-based solvents derived from biological sources have therefore been launched as alternatives to the classic organic dipolar aprotic solvents like DMF and THF[162–164] (Figure 1.15). Glycerol, for example, which has a high boiling point and is a product from biodiesel production, has been considered a valid alternative in the last decades.[165] The large availability, thanks to the high production of biodiesel worldwide and its non-toxic nature has enhanced the popularity of this solvent in organic synthesis. Ethyl lactate, which is traditionally made from carbohydrates[166,167] with a boiling point similar to DMF has become more and more attractive in the industrial and academic sector. In addition, 2-MeTHF, even though it has been classified as a potentially problematic solvent, has gained increasing popularity as a more sustainable alternative in metal catalyzed cross-coupling reactions.[168–170] In contrast to THF, the production of 2-MeTHF utilizes renewable lignocellulosic biomass, which is fundamental to decrease waste generation in chemical industry and pharmaceutical manufacturing.[171]

Another sustainable solvent that has recently been used to replace the most common polar aprotic ones such as DMF, DMAc and NMP in organometallic chemistry is γ-Valerolactone (GVL),[172–175] that is typically made by hydrogenation of lignocellulosic biomass derived levulinic acid.[176] It has been proven that GVL is not only a more sustainable, safer and non-toxic chemical, but has also some interesting properties that minimize metal leaching from a heterogeneous catalyst, enhancing the reactivity and recyclability in metal catalyzed reaction. Another potential replacement for toxic dipolar aprotic solvents is cyrene (dihydrolevoglucosenone), which is synthetized from a variety of biomass starting material that converge to levoglucosenone (LGO) and finally gives cyrene.[177] The properties of cyrene as biogenic solvent have increasingly intrigued the scientific community and it was finally used for the first time in a metal catalyzed reaction by Watson and coworker[178] in 2016 in a Sonogashira and Cacchi-type annulation reactions demonstrating the compatibility of the solvent in metal-catalyzed reactions. Even dialkyl carbonates such as dimethylcarbonate (DMC) and diethylcarbonate (DEC) has been used successfully as sustainable solvents for palladium catalyzed reactions.[179–181] Finally, also our research group contributed recently with the development of greener and more sustainable palladium cross-coupling reactions introducing a new category of solvents: N-alkyl-pyrrolidones.[182,183] They represent a valid alternative to NMP and DMF because they display a similar polarity profile but develop fewer toxic metabolites and could therefore represent a novel and more sustainable alternative.

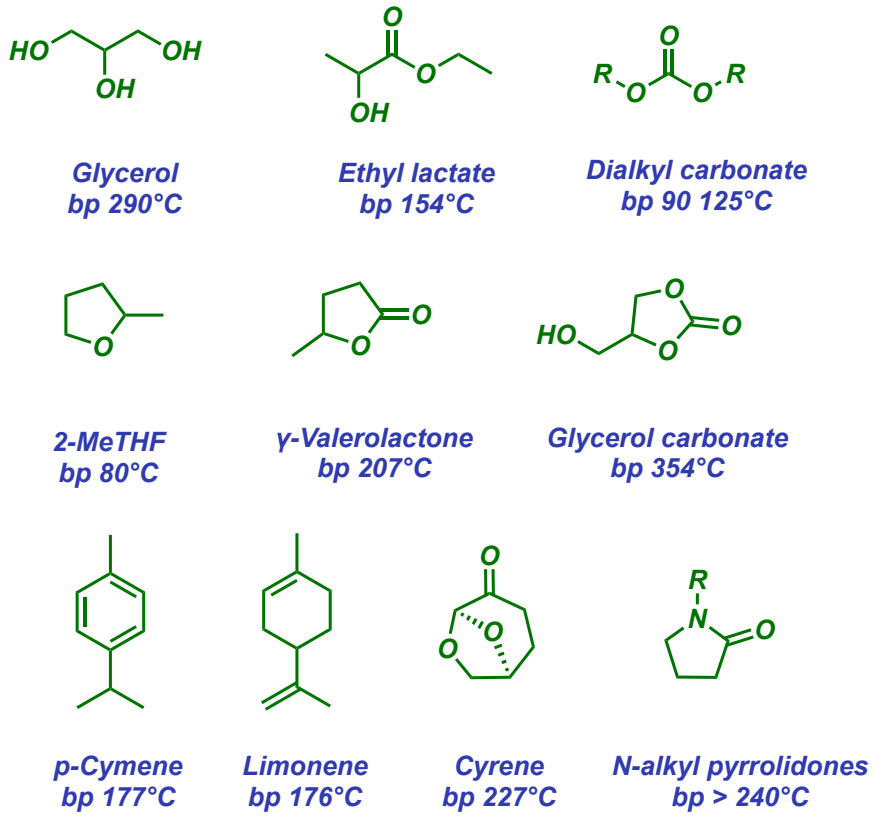

***Figure 1.15**: Examples of Bio-based solvents suitable for metal-catalyzed reactions*

1.5 Heck-Cassar-Sonogashira Cross-Coupling

Among the Palladium cross-coupling reactions, the coupling between an aryl halide and a terminal acetylide represents a powerful tool in organic synthesis because it is the most straightforward method for the construction of sp-sp^2 carbon-carbon bonds opening access to subsequent transformations.

The reaction was independently reported in 1975 by Heck[9] and Cassar[8] as a copper-free procedure.

Heck's procedure was based on the use of a phosphane-palladium complex as catalyst and triethylamine or piperidine as base and solvent, while Cassar used a phosphane-palladium catalyst with sodium methoxide as base and DMF as solvent. In both cases a high temperature was required. Their work was followed a few months later by Sonogashira and Hagihara,[11] who reported the realization of the same coupling reaction but using a Pd^0/Cu^I catalytic system and working at room temperature. Because of the milder reaction

conditions required, the Sonogashira protocol became the favorite procedure for the alkynylation of aryl or alkenyl halides.

Since then, the Heck−Cassar−Sonogashira (HCS) reaction was successfully applied for industrial production. Several studies have investigated the influence of leaving groups, palladium ligands, cocatalyst, and bases.[184,185] However, the addition of copper as cocatalyst, even if it has some beneficial effects in terms of reactivity, has also some drawbacks associated with the necessity to avoid completely the presence of oxygen to suppress the formation alkyne homocoupling side product through a copper-mediated Glaser/hay reaction. In addition, copper represents another environmentally unfriendly reagent, which is also difficult to separate from the palladium at the end of the reaction, complicating the recovery of the catalyst. To overcome these issues, the complete elimination of copper could represent a solution from both an environmental and a selectivity perspective.

Regarding the Pd/Cu Sonogashira mechanism, it is generally supposed to take place through two independent catalytic cycles (Figure 1.16). The Palladium cycle is the same as the classic C-C bond cross-coupling cycle in which the first step is the oxidative addition of an aryl/alkyl halide to the Pd^0 complex, which can be of PdL_2 specie or a low-ligated Pd^0 complex stabilized by weak ligands, including base and solvent molecules. This step highly depends on the characteristics of the Ar-X substrate, with its reactivity increasing in the order of ArI > ArBr > ArCl.[17] Furthermore, the presence of an electron-withdrawing group, reduces the electronic density on the C-X bond, thus facilitating the oxidative addition step. The formed $LnPd^{II}R^1X$ **B** intermediate in Figure 1.16a is then transformed into a $LnPd^{II}R^2CCR^1$ **C** complex after the transmetallation with a copper acetylide **F** formed in the copper-cycle. The copper is believed to assist the deprotonation step of the acetylene favoring the formation of a π complex **E**, which would make the alkyne terminal proton more acidic and make the transmetallation step more efficient. Although some specifics of the transmetallation step and the Cu cycle are not fully established, the mechanism of the Pd/Cu catalysed Sonogashira reaction is generally accepted in the scientific community.[186–189] Since the formation of the intermediate neutral copper acetylide **F** has never been proven, an alternative anionic mechanism for the Cu cycle (Figure 1.16b) was reported in 2017 following a computational study.[186] In this study, for the first time, it has been

proposed the anionic-coordinate Cu^{I} acetylide **G** as the active species of the Cu cycle, based on the observation that the formation of the anionic copper acetylide is more favorable, both kinetically and thermodynamically, than the neutral copper acetylide. Furthermore, this proposed mechanism explained the observed effect of the copper salt on the reactivity, with CuI > CuBr > CuCl, while the neutral mechanism is incapable.

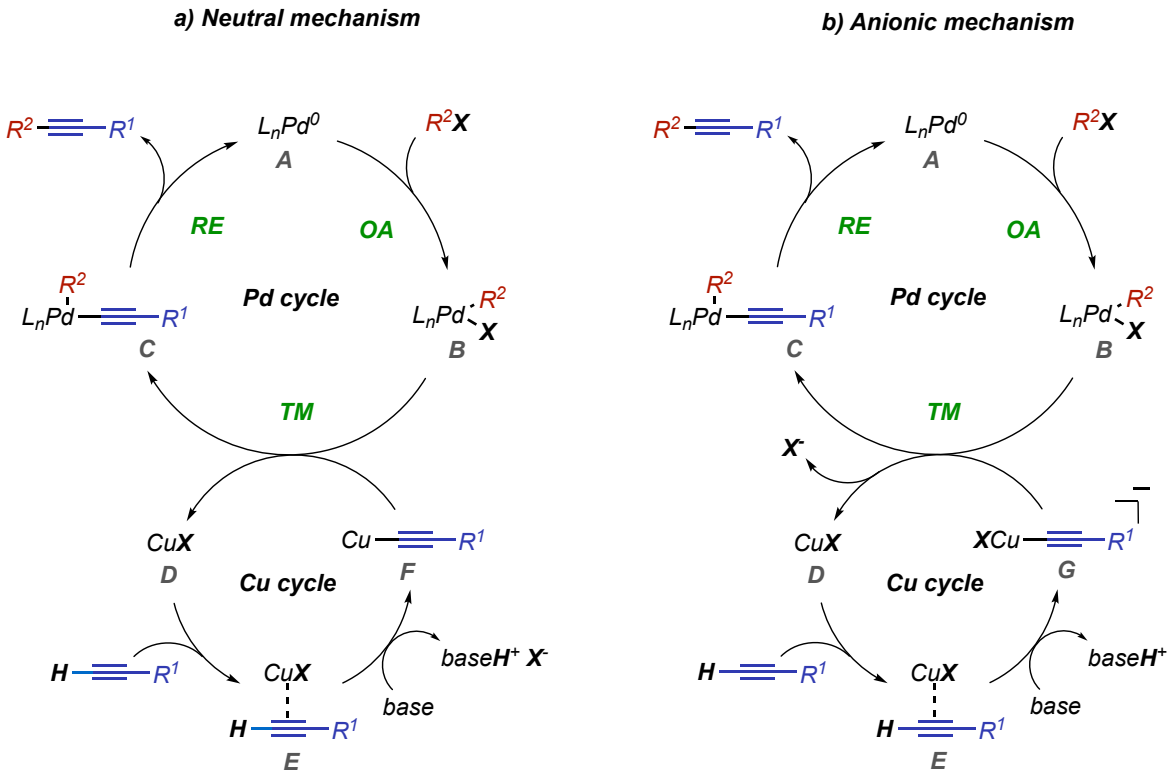

***Figure 1.16**: Pd/Cu Sonogashira catalytic cycle*

Although the copper free Sonogashira was reported for the first time more than 4 decades ago, the mechanism in absence of copper is still not clearly understood. Initially two different mechanisms had been proposed: the deprotonation step reported by Solehili[190] and the carbopalladation step by Heck[191] (Figure 1.17). Both mechanisms share the oxidative addition of the aryl halide to the Pd^{0} complex followed by the insertion of the acetylene that replaces one of the ligands forming complex **H**. The two mechanisms differ in the next steps to give the final product of the Sonogashira reaction. In mechanism 17a, the deprotonation of the acetylene and the coordination of the ligand brings to a square planar Pd complex **C** with the two organic groups in cis disposition, from which the coupled product is expelled by reductive elimination. On the other hand, in the carbopalladation

mechanism 17b, intermediate **H** undergoes the addition of the organic group R^2 to the terminal alkyne, followed by the coordination of the ligand L and subsequent base-mediated reductive elimination to give the coupling product.

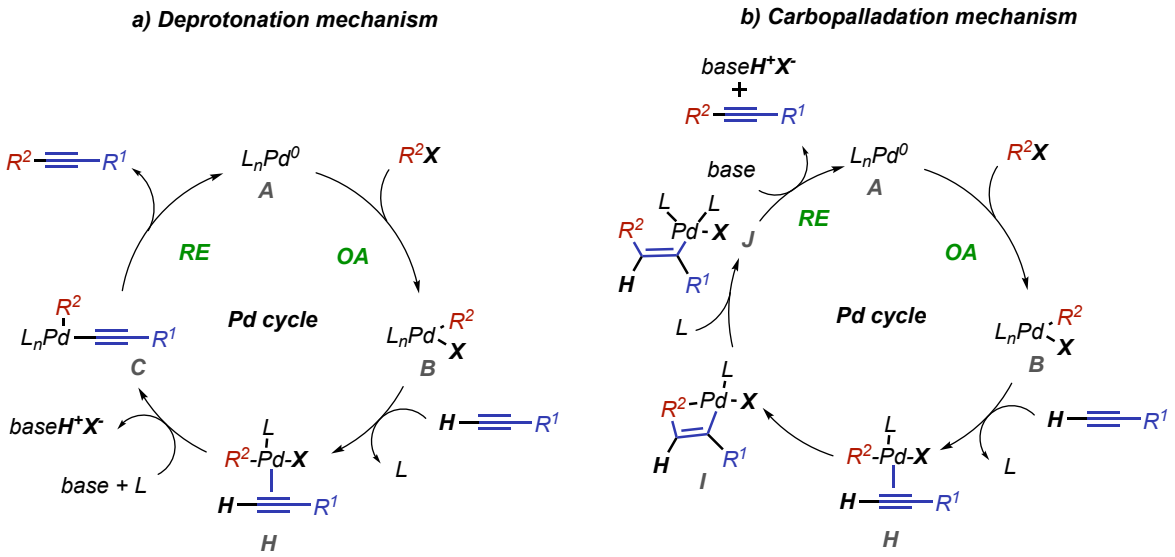

***Figure 1.17**: Proposed reaction mechanisms for the copper-free Sonogashira reaction: deprotonation a) and carbopalladation b) mechanisms*

Although a great effort has been undertaken in support of these mechanisms,[192–200] numerous questions are still open, and the copper free mechanism is not completely clear yet. A recent study by Jutand and coworkers, underlined the decelerating effect of alkynes in the oxidative addition[201] and the multiple roles of the base in the copper free reaction.[200] The base is not involved only in the deprotonation step but can also interfere in the oxidative addition complex increasing its reactivity by replacing one of the phosphine ligands. Depending on the rate of reactivity of the amine to substitute the ligand, another mechanism could also operate, together with the more classic one reported by Solehili in Figure 1.17a. The mechanism proposed in Figure 1.18 is preferred when the amine is a better ligand then the alkyne and replaces the phosphine in the Pd^{II} complex giving intermediate **K**. On the other hand, when the amine is a worst ligand then the alkyne, the insertion is performed on the classic Pd^{II} complex **B** reported in Figure 1.17a.

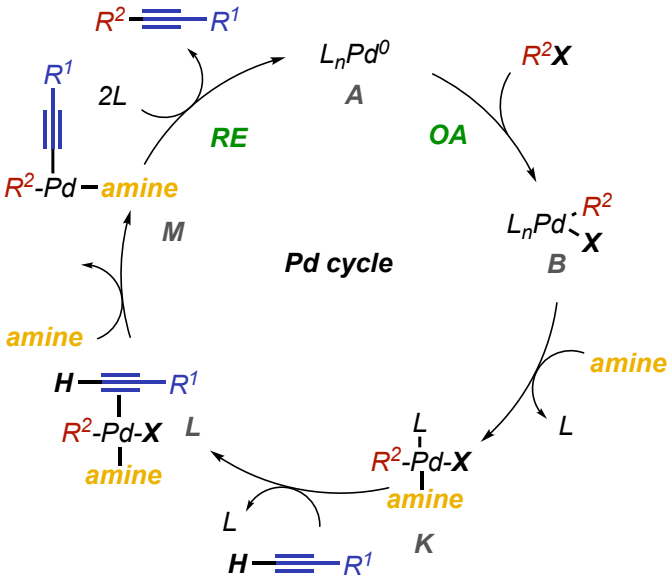

Figure 1.18: *Copper-free Sonogashira mechanism proposed by Jutand when the amine is a better ligand compared to the acetylene*

Subsequently, Martenson et al,[198] demonstrated experimentally that the carbopalladation pathway can be discarded and proposed two different alternatives mechanisms to the deprotonation one: a cationic and an anionic mechanism that differs only for the order in which the steps occur (Figure 1.19). In the cationic mechanism (Figure 1.19a), the halide group is substituted by the ligand in **H** giving the cationic intermediate **N**, which undergoes the deprotonation of the acetylene by an external base followed by the final reductive elimination. On the contrary, in the anionic mechanism (Figure 1.19b), the deprotonation of the acetylene occurs first giving the anionic intermediate **O** that undergoes the replacement of the halide by the ligand and then the reductive elimination to give the final product. The authors claimed that the choice of the mechanism depends on the nature of the different substituent groups on the alkyne. They suggested that the cationic pathway is favored with alkynes bearing electron donating groups (EDG) while electron withdrawing groups (EWG) accelerate the anionic mechanism.

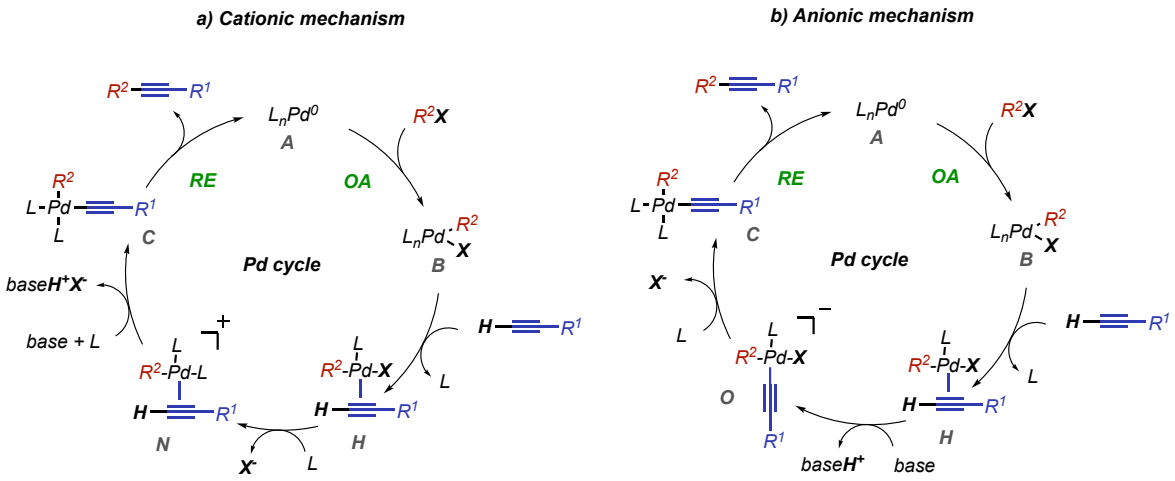

***Figure 1.19**: Cationic a) and anionic b) alternatives for the deprotonation mechanism*

An alternative mechanism recently proposed, hypothesized that the Heck-Cassar copper-free cross-coupling proceeds through a tandem Pd/Pd double-cycle (Figure 1.20).[202] This pathway is similar to the Pd/Cu catalyzed mechanism already discussed for the Sonogashira copper co-catalyzed reaction, but here the role of the copper co-catalyst is played by a Pd complex. The key step is the transmetallation between two palladium species: the product of the oxidative addition **B**, and the bisalkynylpalladium complex **P**. After the transmetallation step, the obtained compound **C** undergoes reductive elimination, releasing the desired product, while complex **P** is restored to close the Pd cycle II, by a reaction between **Q** and the base. The tandem Pd/Pd catalytic cycle was confirmed by the authors with experimental P^{31} studies and DFT (Density Functional Theory) calculations, emphasizing the importance of complex **P** in the transmetallation process.

Although several studies have gained insight to the Heck-Cassar-Sonogashira cross coupling, this reaction is still far from being clearly understood. All the papers reporting a critical study of the mechanism, underlined how it depends on the operating conditions including the solvent, the base, the ligand and the nature of the catalyst, suggesting that there is still room for further studies and developments.

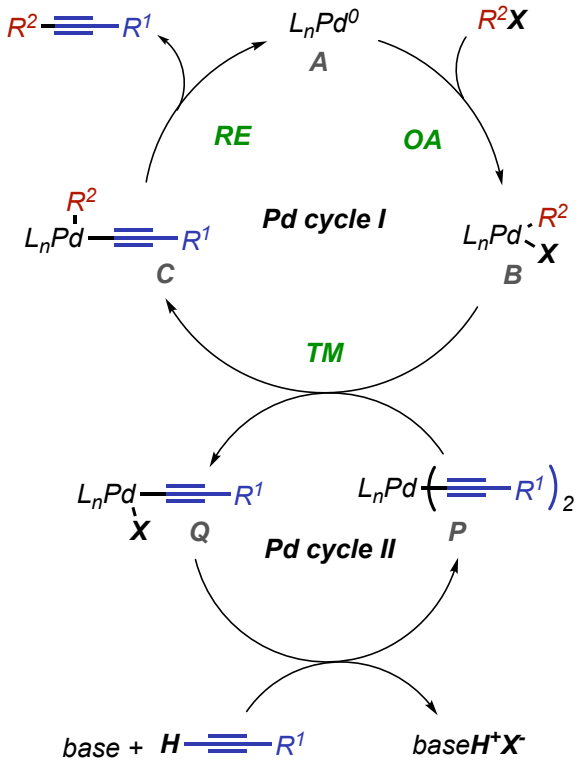

***Figure 1.20**: The tandem Pd/Pd mechanistic cycle proposed by Kosmrlj*

1.6 References

(1) Johansson Seechurn, C. C. C.; Kitching, M. O.; Colacot, T. J.; Snieckus, V. Palladium-Catalyzed Cross-Coupling: A Historical Contextual Perspective to the 2010 Nobel Prize. *Angew. Chem. Int. Ed*. May 21, 2012, pp 5062–5085. https://doi.org/10.1002/anie.201107017.

(2) Cabri, W. Catalysis: The Pharmaceutical Perspective. *Catal. Today* **2009**, *140* (1–2), 2–10. https://doi.org/10.1016/j.cattod.2008.07.014.

(3) Torborg, C.; Beller, M. Recent Applications of Palladium-Catalyzed Coupling Reactions in the Pharmaceutical, Agrochemical, and Fine Chemical Industries. *Adv. Synth. Catal*. December 2009, pp 3027–3043. https://doi.org/10.1002/adsc.200900587.

(4) Hayler, J. D.; Leahy, D. K.; Simmons, E. M. A Pharmaceutical Industry Perspective on Sustainable Metal Catalysis. *Organometallics* **2019**, *38* (1), 36–46. https://doi.org/10.1021/acs.organomet.8b00566.

(5) Campeau, L. C.; Hazari, N. Cross-Coupling and Related Reactions: Connecting Past Success to the Development of New Reactions for the Future. *Organometallics* **2019**, *38* (1), 3–35. https://doi.org/10.1021/acs.organomet.8b00720.

(6) Negishi, E. I. Magical Power of Transition Metals: Past, Present, and Future (Nobel Lecture). *Angew. Chem. Int. Ed*. **2011**, *50* (30), 6738–6764. https://doi.org/10.1002/anie.201101380.

(7) Suzuki, A. Cross-Coupling Reactions of Organoboranes: An Easy Way to Construct C-C Bonds (Nobel Lecture). *Angew. Chem. Int. Ed*. Wiley-VCH Verlag July 18, 2011, pp 6722–6737. https://doi.org/10.1002/anie.201101379.
(8) Cassar, L. Synthesis of Aryl- and Vinyl- Substituted Acetylene Derivatives by the Use of Nickel and Palladium Complexes; Elsevier Sequoia S-A, 1975; Vol. 93.
(9) Dieck, H. A.; Heck, F. R. *Palladium Catalyzed Synthesis of Aryl, Heterocyclic and Vinylic Acetylene Derivatives*; 1975; Vol. 93.
(10) Tidwell, J. H.; Buchwald, S. L.; Kosugi, M.; Kameyama, M.; Migita, T. Palladium-Catalyzed Aromatic Aminations with in Situ Generated Aminostannanes; 1994; Vol. 116. https://pubs.acs.org/sharingguidelines.
(11) Sonogashira, K.; Tohda, Y.; Hagihara, N. A Convenient Synthesis of Acetylenes: Catalytic Substitutions of Acetylenic Hydrogen with Bromo Alkanes and Bromopyridines; Pergamon Press. Frrnted m Great Britain, 1975.
(12) Hatanaka, Y.; Hiyama, T. Cross-Coupling of Organosilanes with Organic Halides Mediated by a Palladium Catalyst and Tris(Diethylamino)Sulfonium Difluorotrimethylsilicate. *J. Org. Chem.* **1988**, *53* (4), 918–920. https://doi.org/10.1021/jo00239a056.
(13) Tamao, K.; Sumitani, K.; Kumada, M. Selective Carbon-Carbon Bond Formation by Cross-Coupling of Grignard Reagents with Organic Halides. Catalysis by Nickel-Phosphine Complexes. *J. Am. Chem. Soc.* **1972**, *94* (12), 4374–4376. https://doi.org/10.1021/ja00767a075.
(14) Negishi, E.; King, A. O.; Okukado, N. Selective Carbon-Carbon Bond Formation via Transition Metal Catalysis. 3. A Highly Selective Synthesis of Unsymmetrical Biaryls and Diarylmethanes by the Nickel- or Palladium-Catalyzed Reaction of Aryl- and Benzylzinc Derivatives with Aryl Halides. *J. Org. Chem.* **1977**, *42* (10), 1821–1823. https://doi.org/10.1021/jo00430a041.
(15) Paul, F.; Patt, J.; Hartwig, J. F. Palladium-Catalyzed Formation of Carbon-Nitrogen Bonds. Reaction Intermediates and Catalyst Improvements in the Hetero Cross-Coupling of Aryl Halides and Tin Amides. *J. Am. Chem. Soc.* **1994**, *116* (13), 5969–5970. https://doi.org/10.1021/ja00092a058.
(16) Milstein, D.; Stille, J. K. A General, Selective, and Facile Method for Ketone Synthesis from Acid Chlorides and Organotin Compounds Catalyzed by Palladium. *J Am Chem Soc* **1978**, *100* (11), 3636–3638. https://doi.org/10.1021/ja00479a077.
(17) Barnard, C. Palladium-Catalysed C-C Coupling: Then and Now. *Platin. Met. Rev.* **2008**, *52* (1), 38–45. https://doi.org/10.1595/147106708X256634.
(18) Beller, M.; Zapf, A.; Mägerlein, W. Efficient Synthesis of Fine Chemicals and Organic Building Blocks Applying Palladium-Catalyzed Coupling Reactions. *Chem. Eng. Technol.* **2001**, *24* (6), 575–582. https://doi.org/10.1002/1521-4125(200106)24:6<575::AID-CEAT575>3.0.CO;2-D.
(19) Kharasch, M. S. R. O. *Grignard Reactions of Nonmetallic Substances*; 1954.
(20) Glaser, C. *Ann. Chem. Pharm.* **1870**, 137–171.
(21) Glaser, C. Beiträge Zur Kenntniss Des Acetenyl Benzols. *Berichte der deutschen chemischen Gesellschaft* **1869**, *2* (1), 422–424. https://doi.org/10.1002/cber.186900201183.

(22) Ullmann, F.; Bielecki, J. Ueber Synthesen in Der Biphenylreihe. *Berichte der deutschen chemischen Gesellschaft* **1901**, *34* (2), 2174–2185. https://doi.org/10.1002/cber.190103402141.
(23) Wurtz, A. Ueber Eine Neue Klasse Organischer Radicale. *Annalen der Chemie und Pharmacie* **1855**, *96* (3), 364–375. https://doi.org/10.1002/jlac.18550960310.
(24) Wurtz, A. *A. Ann. Chim. Phys.* **1855**, *44*, 275–312.
(25) Fittig, R. *Justus Liebigs Ann. Chem* **1862**, *121*, 361–365.
(26) Bennett, G. M.; Turner, E. E. CII.—The Action of Chromic Chloride on the Grignard Reagent. *J. Chem. Soc. Trans.* **1914**, *105* (0), 1057–1062. https://doi.org/10.1039/CT9140501057.
(27) Krizewsky, J.; Turner, E. *J. Chem. Soc* **1919**, *115* (559 – 561).
(28) Kharasch, M. S.; Fields, E. K. Factors Determining the Course and Mechanisms of Grignard Reactions. IV. The Effect of Metallic Halides on the Reaction of Aryl Grignard Reagents and Organic Halides. *J. Am. Chem. Soc.* **1941**, *63* (9), 2316–2320. https://doi.org/10.1021/ja01854a006.
(29) Kharasch M. S. Factors Influencing the Course and Mechanisms of Grignard Reactions. XI. The Effect of Metallic Halides on the Reaction of Grignard Reagents with Vinyl Halides and Substituted Vinyl Halides. *J. Am. Chem. Soc.* **1943**, *65*, 504–507.
(30) Chodkiewicz. W.; Cadiot. P.; Hebd. C. R. *Seances. Acad. Sci* **1955**, *241*, 1055–1057.
(31) Stephens, R. D.; Castro, C. E. The Substitution of Aryl Iodides with Cuprous Acetylides. A Synthesis of Tolanes and Heterocyclics. *J. Org. Chem.* **1963**, *28* (12), 3313–3315. https://doi.org/10.1021/jo01047a008.
(32) Heck, R. F. Acylation, Methylation, and Carboxyalkylation of Olefins by Group VIII Metal Derivatives. *J. Am. Chem. Soc.* **1968**, *90* (20), 5518–5526. https://doi.org/10.1021/ja01022a034.
(33) Fujiwara, Y.; Moritani, I.; Danno, S.; Asano, R.; Teranishi, S. Aromatic Substitution of Olefins. VI. Arylation of Olefins with Palladium(II) Acetate. *J Am Chem Soc* **1969**, *91* (25), 7166–7169. https://doi.org/10.1021/ja01053a047.
(34) Mizoroki, T.; Mori, K.; Ozaki, A. *Bull. Chem. Soc. Jpn.* **1971**, *44*, 581.
(35) Mori, K.; Mizoroki, T.; Ozaki, A. Arylation of Olefin with Iodobenzene Catalyzed by Palladium. *Bull. Chem. Soc. Jpn.* **1973**, *46* (5), 1505–1508. https://doi.org/10.1246/bcsj.46.1505.
(36) Dieck, H. A.; Heck, R. F. Organophosphinepalladium Complexes as Catalysts for Vinylic Hydrogen Substitution Reactions. *J. Am. Chem. Soc.* **1974**, *96* (4), 1133–1136. https://doi.org/10.1021/ja00811a029.
(37) Heck, R. F.; Nolley, J. P. Palladium-Catalyzed Vinylic Hydrogen Substitution Reactions with Aryl, Benzyl, and Styryl Halides. *J. Org. Chem.* **1972**, *37* (14), 2320–2322. https://doi.org/10.1021/jo00979a024.
(38) Tamao, K.; Kiso, Y.; Sumitani, K.; Kumada, M. Alkyl Group Isomerization in the Cross-Coupling Reaction of Secondary Alkyl Grignard Reagents with Organic Halides in the Presence of Nickel-Phosphine Complexes as Catalysts. *J. Am. Chem. Soc.* **1972**, *94* (26), 9268–9269. https://doi.org/10.1021/ja00781a070.
(39) Tamao, K.; Sumitani, K.; Kumada, M. Selective Carbon-Carbon Bond Formation by Cross-Coupling of Grignard Reagents with Organic Halides. Catalysis by Nickel-

Phosphine Complexes. *J. Am. Chem. Soc.* **1972**, *94* (12), 4374–4376. https://doi.org/10.1021/ja00767a075.

(40) Corriu, R. J. P.; Masse, J. P. Activation of Grignard Reagents by Transition-Metal Complexes. A New and Simple Synthesis of Trans-Stilbenes and Polyphenyls. *J. Chem. Soc. Chem. Commun.* **1972**, No. 3, 144a. https://doi.org/10.1039/c3972000144a.

(41) Yamamura, M.; Moritani, I.; Murahashi, S.-I. The Reaction of σ-Vinylpalladium Complexes with Alkyllithiums. Stereospecific Syntheses of Olefins from Vinyl Halides and Alkyllithiums. *J. Organomet. Chem.* **1975**, *91* (2), C39–C42. https://doi.org/10.1016/S0022-328X(00)89636-9.

(42) Murahashi, S.; Yamamura, M.; Yanagisawa, K.; Mita, N.; Kondo, K. Stereoselective Synthesis of Alkenes and Alkenyl Sulfides from Alkenyl Halides Using Palladium and Ruthenium Catalysts. *J. Org. Chem.* **1979**, *44* (14), 2408–2417. https://doi.org/10.1021/jo01328a016.

(43) Fauvarque J. F.; Jutand A. *Bull. Soc. Chim. Fr.* **1976**, 765–770.

(44) Baba, S.; Negishi, E. A Novel Stereospecific Alkenyl-Alkenyl Cross-Coupling by a Palladium- or Nickel-Catalyzed Reaction of Alkenylalanes with Alkenyl Halides. *J. Am. Chem. Soc.* **1976**, *98* (21), 6729–6731. https://doi.org/10.1021/ja00437a067.

(45) Negishi, E.; Baba, S. Novel Stereoselective Alkenyl–Aryl Coupling via Nickel-Catalysed Reaction of Alkenylanes with Aryl Halides. *J. Chem. Soc. Chem. Commun.* **1976**, No. 15, 596b–597b. https://doi.org/10.1039/C3976000596B.

(46) Negishi, E. Palladium- or Nickel-Catalyzed Cross Coupling. A New Selective Method for Carbon-Carbon Bond Formation. *Acc. Chem. Res.* **1982**, *15* (11), 340–348. https://doi.org/10.1021/ar00083a001.

(47) Azarian, D.; Dua, S. S.; Eaborn, C.; Walton, D. R. M. Reactions of Organic Halides with R3 MMR3 Compounds (M = Si, Ge, Sn) in the Presence of Tetrakis(Triarylphosphine)Palladium. *J. Organomet. Chem.* **1976**, *117* (3), C55–C57. https://doi.org/10.1016/S0022-328X(00)91902-8.

(48) Kosugi, M.; Sasazawa, K.; Shimizu, T.; Migita, T. Reactions of Allyltin Compounds. III. Allylation of Aromatic Halides with Allyltributyltin in the Presence of Tetrakis(Triphenylphosphine)Palladium(0). *Chem. Lett* **1977**, 301–302.

(49) Kosugi, M.; Shimizu, Y.; Migita, T. Reaction of Allyltin Compounds. *J Organomet Chem* **1977**, *129* (2), C36–C38. https://doi.org/10.1016/S0022-328X(00)92505-1.

(50) Miyaura, N.; Suzuki, A. Stereoselective Synthesis of Arylated (E)-Alkenes by the Reaction of Alk-1-Enylboranes with Aryl Halides in the Presence of Palladium Catalyst. *J. Chem. Soc. Chem. Commun.* **1979**, No. 19, 866. https://doi.org/10.1039/c39790000866.

(51) Hatanaka, Y.; Hiyama, T. Cross-Coupling of Organosilanes with Organic Halides Mediated by a Palladium Catalyst and Tris(Diethylamino)Sulfonium Difluorotrimethylsilicate. *J. Org. Chem.* **1988**, *53* (4), 918–920. https://doi.org/10.1021/jo00239a056.

(52) Kosugi, M.; Kameyama, M.; Migita, T. Palladium-Catalyzed Aromatic Amination of Aryl Bromides with N,N-Diethylamino-Tributylin. *Chem. Lett.* **1983**, *12* (6), 927–928. https://doi.org/10.1246/cl.1983.927.

(53) Guram, A. S.; Rennels, R. A.; Buchwald, S. L. A Simple Catalytic Method for the Conversion of Aryl Bromides to Arylamines. *Angew. Chem. Int. Ed*. **1995**, *34* (12), 1348–1350. https://doi.org/10.1002/anie.199513481.

(54) Guram, A. S.; Rennels, R. A.; Buchwald, S. L. A Simple Catalytic Method for the Conversion of Aryl Bromides to Arylamines. *Angew. Chem. Int. Ed*.**1995**, *34* (12), 1348–1350. https://doi.org/10.1002/anie.199513481.

(55) Louie, J.; Hartwig, J. F. Palladium-Catalyzed Synthesis of Arylamines from Aryl Halides. Mechanistic Studies Lead to Coupling in the Absence of Tin Reagents. *Tetrahedron Lett.* **1995**, *36* (21), 3609–3612. https://doi.org/10.1016/0040-4039(95)00605-C.

(56) Nicolaou, K. C.; Bulger, P. G.; Sarlah, D. Palladium-Catalyzed Cross-Coupling Reactions in Total Synthesis. *Angew. Chem. Int. Ed*. **2005**, *44* (29), 4442–4489. https://doi.org/10.1002/anie.200500368.

(57) Corbet, J.-P.; Mignani, G. Selected Patented Cross-Coupling Reaction Technologies. *Chem. Rev.* **2006**, *106* (7), 2651–2710. https://doi.org/10.1021/cr0505268.

(58) Magano, J.; Dunetz, J. R. Large-Scale Applications of Transition Metal-Catalyzed Couplings for the Synthesis of Pharmaceuticals. *Chem. Rev.* **2011**, *111* (3), 2177–2250. https://doi.org/10.1021/cr100346g.

(59) Gildner, P. G.; Colacot, T. J. Reactions of the 21st Century: Two Decades of Innovative Catalyst Design for Palladium-Catalyzed Cross-Couplings. *Organometallics* **2015**, *34* (23), 5497–5508. https://doi.org/10.1021/acs.organomet.5b00567.

(60) Dander, J. E.; Garg, N. K. Breaking Amides Using Nickel Catalysis. *ACS. Catal.* **2017**, *7* (2), 1413–1423. https://doi.org/10.1021/acscatal.6b03277.

(61) Guo, L.; Rueping, M. Decarbonylative Cross-Couplings: Nickel Catalyzed Functional Group Interconversion Strategies for the Construction of Complex Organic Molecules. *Acc. Chem. Res.* **2018**, *51* (5), 1185–1195. https://doi.org/10.1021/acs.accounts.8b00023.

(62) Takise, R.; Muto, K.; Yamaguchi, J. Cross-Coupling of Aromatic Esters and Amides. *Chem. Soc. Rev.* **2017**, *46* (19), 5864–5888. https://doi.org/10.1039/C7CS00182G.

(63) Fu, G. C. Transition-Metal Catalysis of Nucleophilic Substitution Reactions: A Radical Alternative to S_N1 and S_N2 Processes. *ACS. Cent. Sci.* **2017**, *3* (7), 692–700. https://doi.org/10.1021/acscentsci.7b00212.

(64) Choi, J.; Fu, G. C. Transition Metal–Catalyzed Alkyl-Alkyl Bond Formation: Another Dimension in Cross-Coupling Chemistry. *Science (1979)* **2017**, *356* (6334). https://doi.org/10.1126/science.aaf7230.

(65) Beletskaya, I. P.; Cheprakov, A. v. The Complementary Competitors: Palladium and Copper in C–N Cross-Coupling Reactions. *Organometallics* **2012**, *31* (22), 7753–7808. https://doi.org/10.1021/om300683c.

(66) Bauer, I.; Knölker, H.-J. Iron Catalysis in Organic Synthesis. *Chem. Rev.* **2015**, *115* (9), 3170–3387. https://doi.org/10.1021/cr500425u.

(67) Bedford, R. B. How Low Does Iron Go? Chasing the Active Species in Fe-Catalyzed Cross-Coupling Reactions. *Acc. Chem. Res.* **2015**, *48* (5), 1485–1493. https://doi.org/10.1021/acs.accounts.5b00042.

(68) Cassani, C.; Bergonzini, G.; Wallentin, C.-J. Active Species and Mechanistic Pathways in Iron-Catalyzed C–C Bond-Forming Cross-Coupling Reactions. *ACS. Catal.* **2016**, *6* (3), 1640–1648. https://doi.org/10.1021/acscatal.5b02441.

(69) Fürstner, A. Iron Catalysis in Organic Synthesis: A Critical Assessment of What It Takes To Make This Base Metal a Multitasking Champion. *ACS. Cent. Sci.* **2016**, *2* (11), 778–789. https://doi.org/10.1021/acscentsci.6b00272.

(70) Neely, J. M.; Bezdek, M. J.; Chirik, P. J. Insight into Transmetalation Enables Cobalt-Catalyzed Suzuki–Miyaura Cross Coupling. *ACS. Cent. Sci.* **2016**, *2* (12), 935–942. https://doi.org/10.1021/acscentsci.6b00283.

(71) Bhunia, S.; Pawar, G. G.; Kumar, S. V.; Jiang, Y.; Ma, D. Selected Copper-Based Reactions for C−N, C−O, C−S, and C−C Bond Formation. *Angew. Chem. Int. Ed*. **2017**, *56* (51), 16136–16179. https://doi.org/10.1002/anie.201701690.

(72) Knappke, C. E. I.; Grupe, S.; Gärtner, D.; Corpet, M.; Gosmini, C.; Jacobi von Wangelin, A. Reductive Cross-Coupling Reactions between Two Electrophiles. *Chem. Eur. J.* **2014**, *20* (23), 6828–6842. https://doi.org/10.1002/chem.201402302.

(73) Everson, D. A.; Weix, D. J. Cross-Electrophile Coupling: Principles of Reactivity and Selectivity. *J. Org. Chem.* **2014**, *79* (11), 4793–4798. https://doi.org/10.1021/jo500507s.

(74) Weix, D. J. Methods and Mechanisms for Cross-Electrophile Coupling of Csp ^{2} Halides with Alkyl Electrophiles. *Acc. Chem. Res.* **2015**, *48* (6), 1767–1775. https://doi.org/10.1021/acs.accounts.5b00057.

(75) Gu, J.; Wang, X.; Xue, W.; Gong, H. Nickel-Catalyzed Reductive Coupling of Alkyl Halides with Other Electrophiles: Concept and Mechanistic Considerations. *Org. Chem. Front.* **2015**, *2* (10), 1411–1421. https://doi.org/10.1039/C5QO00224A.

(76) Zhang, L.; Lovinger, G. J.; Edelstein, E. K.; Szymaniak, A. A.; Chierchia, M. P.; Morken, J. P. Catalytic Conjunctive Cross-Coupling Enabled by Metal-Induced Metallate Rearrangement. *Science (1979)* **2016**, *351* (6268), 70–74. https://doi.org/10.1126/science.aad6080.

(77) Levin, M. D.; Kim, S.; Toste, F. D. Photoredox Catalysis Unlocks Single-Electron Elementary Steps in Transition Metal Catalyzed Cross-Coupling. *ACS Cent. Sci.* **2016**, *2* (5), 293–301. https://doi.org/10.1021/acscentsci.6b00090.

(78) Martin, R.; Buchwald, S. L. Palladium-Catalyzed Suzuki−Miyaura Cross-Coupling Reactions Employing Dialkylbiaryl Phosphine Ligands. *Acc. Chem. Res.* **2008**, *41* (11), 1461–1473. https://doi.org/10.1021/ar800036s.

(79) Zapf, A.; Ehrentraut, A.; Beller, M. A New Highly Efficient Catalyst System for the Coupling of Nonactivated and Deactivated Aryl Chlorides with Arylboronic Acids. *Angew. Chem. Int. Ed.* **2000**, *39* (22), 4153–4155. https://doi.org/10.1002/1521-3773(20001117)39:22<4153::AID-ANIE4153>3.0.CO;2-T.

(80) Wolfe, J. P.; Singer, R. A.; Yang, B. H.; Buchwald, S. L. Highly Active Palladium Catalysts for Suzuki Coupling Reactions. *J. Am. Chem. Soc.* **1999**, *121* (41), 9550–9561. https://doi.org/10.1021/ja992130h.

(81) Aranyos, A.; Old, D. W.; Kiyomori, A.; Wolfe, J. P.; Sadighi, J. P.; Buchwald, S. L. Novel Electron-Rich Bulky Phosphine Ligands Facilitate the Palladium-Catalyzed Preparation of Diaryl Ethers. *J. Am. Chem. Soc.* **1999**, *121* (18), 4369–4378. https://doi.org/10.1021/ja990324r.

(82) Littke, A. F.; Fu, G. C. Palladium-Catalyzed Coupling Reactions of Aryl Chlorides. *Angew. Chem. Int. Ed.* **2002**, *41* (22), 4176–4211. https://doi.org/10.1002/1521-3773(20021115)41:22<4176::AID-ANIE4176>3.0.CO;2-U.

(83) Hartwig, J. F.; Kawatsura, M.; Hauck, S. I.; Shaughnessy, K. H.; Alcazar-Roman, L. M. Room-Temperature Palladium-Catalyzed Amination of Aryl Bromides and Chlorides and Extended Scope of Aromatic C−N Bond Formation with a Commercial Ligand. *J. Org. Chem.* **1999**, *64* (15), 5575–5580. https://doi.org/10.1021/jo990408i.

(84) Farina, V. High-Turnover Palladium Catalysts in Cross-Coupling and Heck Chemistry: A Critical Overview. *Adv. Synth. Catal.* **2004**, *346* (13–15), 1553–1582. https://doi.org/10.1002/adsc.200404178.

(85) Barder, T. E.; Walker, S. D.; Martinelli, J. R.; Buchwald, S. L. Catalysts for Suzuki−Miyaura Coupling Processes: Scope and Studies of the Effect of Ligand Structure. *J. Am. Chem. Soc.* **2005**, *127* (13), 4685–4696. https://doi.org/10.1021/ja042491j.

(86) Ruiz-Castillo, P.; Buchwald, S. L. Applications of Palladium-Catalyzed C–N Cross-Coupling Reactions. *Chem. Rev.* **2016**, *116* (19), 12564–12649. https://doi.org/10.1021/acs.chemrev.6b00512.

(87) Willis, M. C. Palladium-Catalyzed Coupling of Ammonia and Hydroxide with Aryl Halides: The Direct Synthesis of Primary Anilines and Phenols. *Angew. Chem. Int. Ed.* **2007**, *46* (19), 3402–3404. https://doi.org/10.1002/anie.200605071.

(88) Miura, M. Rational Ligand Design in Constructing Efficient Catalyst Systems for Suzuki–Miyaura Coupling. *Angew. Chem. Int. Ed.* **2004**, *43* (17), 2201–2203. https://doi.org/10.1002/anie.200301753.

(89) Christmann, U.; Vilar, R. Monoligated Palladium Species as Catalysts in Cross-Coupling Reactions. *Angew. Chem. Int. Ed.* **2005**, *44* (3), 366–374. https://doi.org/10.1002/anie.200461189.

(90) Littke, A. F.; Dai, C.; Fu, G. C. Versatile Catalysts for the Suzuki Cross-Coupling of Arylboronic Acids with Aryl and Vinyl Halides and Triflates under Mild Conditions. *J. Am. Chem. Soc.* **2000**, *122* (17), 4020–4028. https://doi.org/10.1021/ja0002058.

(91) Galardon, E.; Ramdeehul, S.; Brown, J. M.; Cowley, A.; Hii, K. K. (Mimi); Jutand, A. Profound Steric Control of Reactivity in Aryl Halide Addition to Bisphosphane Palladium(0) Complexes. *Angew. Chem. Int. Ed.* **2002**, *41* (10), 1760–1763. https://doi.org/10.1002/1521-3773(20020517)41:10<1760::AID-ANIE1760>3.0.CO;2-3.

(92) Barrios-Landeros, F.; Carrow, B. P.; Hartwig, J. F. Effect of Ligand Steric Properties and Halide Identity on the Mechanism for Oxidative Addition of Haloarenes to Trialkylphosphine Pd(0) Complexes. *J. Am. Chem. Soc.* **2009**, *131* (23), 8141–8154. https://doi.org/10.1021/ja900798s.

(93) Wolfe, J. P.; Buchwald, S. L. A Highly Active Catalyst for the Room-Temperature Amination and Suzuki Coupling of Aryl Chlorides. *Angew. Chem. Int. Ed.* **1999**, *38* (16), 2413–2416. https://doi.org/10.1002/(SICI)1521-3773(19990816)38:16<2413::AID-ANIE2413>3.0.CO;2-H.

(94) Hartwig, J. F. Electronic Effects on Reductive Elimination To Form Carbon−Carbon and Carbon−Heteroatom Bonds from Palladium(II) Complexes. *Inorg. Chem.* **2007**, *46* (6), 1936–1947. https://doi.org/10.1021/ic061926w.

(95) Low, J. J.; Goddard, W. A. Theoretical Studies of Oxidative Addition and Reductive Elimination. 3. Carbon-Hydrogen and Carbon-Carbon Reductive Coupling from Palladium and Platinum Bis(Phosphine) Complexes. *J. Am. Chem. Soc.* **1986**, *108* (20), 6115–6128. https://doi.org/10.1021/ja00280a003.

(96) Marion, N.; Nolan, S. P. Well-Defined N-Heterocyclic Carbenes−Palladium(II) Precatalysts for Cross-Coupling Reactions. *Acc. Chem. Res.* **2008**, *41* (11), 1440–1449. https://doi.org/10.1021/ar800020y.

(97) Würtz, S.; Glorius, F. Surveying Sterically Demanding N-Heterocyclic Carbene Ligands with Restricted Flexibility for Palladium-Catalyzed Cross-Coupling Reactions. *Acc. Chem. Res.* **2008**, *41* (11), 1523–1533. https://doi.org/10.1021/ar8000876.

(98) Froese, R. D. J.; Lombardi, C.; Pompeo, M.; Rucker, R. P.; Organ, M. G. Designing Pd–N-Heterocyclic Carbene Complexes for High Reactivity *and* Selectivity for Cross-Coupling Applications. *Acc. Chem. Res.* **2017**, *50* (9), 2244–2253. https://doi.org/10.1021/acs.accounts.7b00249.

(99) Guideline for Elemental Impurities ICH Q3D (R1) . 2019.

(100) Netherton, M. R.; Dai, C.; Neuschütz, K.; Fu, G. C. Room-Temperature Alkyl−Alkyl Suzuki Cross-Coupling of Alkyl Bromides That Possess β Hydrogens. *J. Am. Chem. Soc.* **2001**, *123* (41), 10099–10100. https://doi.org/10.1021/ja011306o.

(101) Devasagayaraj, A.; Stüdemann, T.; Knochel, P. A New Nickel-Catalyzed Cross-Coupling Reaction between Sp3 Carbon Centers. *Angew. Chem. Int. Ed.* **1996**, *34* (2324), 2723–2725. https://doi.org/10.1002/anie.199527231.

(102) Jensen, A. E.; Knochel, P. Nickel-Catalyzed Cross-Coupling between Functionalized Primary or Secondary Alkylzinc Halides and Primary Alkyl Halides. *J. Org. Chem.* **2002**, *67* (1), 79–85. https://doi.org/10.1021/jo0105787.

(103) Zhou, J.; Fu, G. C. Cross-Couplings of Unactivated Secondary Alkyl Halides: Room-Temperature Nickel-Catalyzed Negishi Reactions of Alkyl Bromides and Iodides. *J. Am. Chem. Soc.* **2003**, *125* (48), 14726–14727. https://doi.org/10.1021/ja0389366.

(104) Saito, B.; Fu, G. C. Alkyl−Alkyl Suzuki Cross-Couplings of Unactivated Secondary Alkyl Halides at Room Temperature. *J. Am. Chem. Soc.* **2007**, *129* (31), 9602–9603. https://doi.org/10.1021/ja074008l.

(105) Owston, N. A.; Fu, G. C. Asymmetric Alkyl−Alkyl Cross-Couplings of Unactivated Secondary Alkyl Electrophiles: Stereoconvergent Suzuki Reactions of Racemic Acylated Halohydrins. *J. Am. Chem. Soc.* **2010**, *132* (34), 11908–11909. https://doi.org/10.1021/ja105924f.

(106) Fischer, C.; Fu, G. C. Asymmetric Nickel-Catalyzed Negishi Cross-Couplings of Secondary α-Bromo Amides with Organozinc Reagents. *J. Am. Chem. Soc.* **2005**, *127* (13), 4594–4595. https://doi.org/10.1021/ja0506509.

(107) Zultanski, S. L.; Fu, G. C. Nickel-Catalyzed Carbon–Carbon Bond-Forming Reactions of Unactivated Tertiary Alkyl Halides: Suzuki Arylations. *J. Am. Chem. Soc.* **2013**, *135* (2), 624–627. https://doi.org/10.1021/ja311669p.

(108) Molander, G. A.; Shin, I. Potassium Boc-Protected Secondary Aminomethyltrifluoroborates: Synthesis and Suzuki–Miyaura Cross-Coupling Reactions. *Org. Lett.* **2012**, *14* (17), 4458–4461. https://doi.org/10.1021/ol301955s.

(109) Quasdorf, K. W.; Riener, M.; Petrova, K. v.; Garg, N. K. Suzuki−Miyaura Coupling of Aryl Carbamates, Carbonates, and Sulfamates. *J. Am. Chem. Soc.* **2009**, *131* (49), 17748–17749. https://doi.org/10.1021/ja906477r.
(110) Ramgren, S. D.; Silberstein, A. L.; Yang, Y.; Garg, N. K. Nickel-Catalyzed Amination of Aryl Sulfamates. *Angew. Chem. Int. Ed.* **2011**, *50* (9), 2171–2173. https://doi.org/10.1002/anie.201007325.
(111) Mesganaw, T.; Silberstein, A. L.; Ramgren, S. D.; Nathel, N. F. F.; Hong, X.; Liu, P.; Garg, N. K. Nickel-Catalyzed Amination of Aryl Carbamates and Sequential Site-Selective Cross-Couplings. *Chem. Sci.* **2011**, *2* (9), 1766. https://doi.org/10.1039/c1sc00230a.
(112) Rappoport, Z. *The Chemistry of Phenols; Rappoport, Z., Ed.; John Wiley & Sons: Chichester, U.K., 2003*, Ed.John Wiley & Sons.; Chichester, U.K, 2003.
(113) Li, J. J.; Corey, E. J. *In Name Reactions for Functional Group Transformations*, Ed.John Wiley & Sons.; Hoboken, NJ, 2007.
(114) Guo, L.; Rueping, M. Transition-Metal-Catalyzed Decarbonylative Coupling Reactions: Concepts, Classifications, and Applications. *Chem. Eur. J.* **2018**, *24* (31), 7794–7809. https://doi.org/10.1002/chem.201704670.
(115) Hie, L.; Fine Nathel, N. F.; Shah, T. K.; Baker, E. L.; Hong, X.; Yang, Y.-F.; Liu, P.; Houk, K. N.; Garg, N. K. Conversion of Amides to Esters by the Nickel-Catalysed Activation of Amide C–N Bonds. *Nature* **2015**, *524* (7563), 79–83. https://doi.org/10.1038/nature14615.
(116) Weires, N. A.; Baker, E. L.; Garg, N. K. Nickel-Catalysed Suzuki–Miyaura Coupling of Amides. *Nat. Chem.* **2016**, *8* (1), 75–79. https://doi.org/10.1038/nchem.2388.
(117) Li, X.; Zou, G. Acylative Suzuki Coupling of Amides: Acyl-Nitrogen Activation via Synergy of Independently Modifiable Activating Groups. *Chem. Comm.* **2015**, *51* (24), 5089–5092. https://doi.org/10.1039/C5CC00430F.
(118) Meng, G.; Szostak, M. Sterically Controlled Pd-Catalyzed Chemoselective Ketone Synthesis via N–C Cleavage in Twisted Amides. *Org. Lett.* **2015**, *17* (17), 4364–4367. https://doi.org/10.1021/acs.orglett.5b02209.
(119) Jensen, K. L.; Standley, E. A.; Jamison, T. F. Highly Regioselective Nickel-Catalyzed Cross-Coupling of *N* -Tosylaziridines and Alkylzinc Reagents. *J. Am. Chem. Soc.* **2014**, *136* (31), 11145–11152. https://doi.org/10.1021/ja505823s.
(120) Lin, B. L.; Clough, C. R.; Hillhouse, G. L. Interactions of Aziridines with Nickel Complexes: Oxidative-Addition and Reductive-Elimination Reactions That Break and Make C−N Bonds. *J. Am. Chem. Soc.* **2002**, *124* (12), 2890–2891. https://doi.org/10.1021/ja017652n.
(121) Yadav, M. R.; Nagaoka, M.; Kashihara, M.; Zhong, R.-L.; Miyazaki, T.; Sakaki, S.; Nakao, Y. The Suzuki–Miyaura Coupling of Nitroarenes. *J. Am. Chem. Soc.* **2017**, *139* (28), 9423–9426. https://doi.org/10.1021/jacs.7b03159.
(122) Inoue, F.; Kashihara, M.; Yadav, M. R.; Nakao, Y. Buchwald–Hartwig Amination of Nitroarenes. *Angew. Chem. Int. Ed.* **2017**, *56* (43), 13307–13309. https://doi.org/10.1002/anie.201706982.
(123) Anastas, P. T.; Warner, J. C. *Green Chemistry: Theory and Practice*; 1998.
(124) Fantoni, T.; Tolomelli, A.; Cabri, W. A Translation of the Twelve Principles of Green Chemistry to Guide the Development of Cross-Coupling Reactions. *Catal. Today* **2022**, *397–399*, 265–271. https://doi.org/10.1016/j.cattod.2021.09.022.

(125) Veleva, V. R.; Cue, B. W.; Todorova, S. Benchmarking Green Chemistry Adoption by the Global Pharmaceutical Supply Chain. *ACS. Sustain. Chem. Eng.* **2018**, *6* (1), 2–14. https://doi.org/10.1021/acssuschemeng.7b02277.

(126) Braun, M.-G.; Diorazio, L.; Fraunhoffer, K.; Hayler, J.; Hickey, M.; Latham, J.; Lovelle, L. E.; McLaws, M.; Parsons, A. T.; Richardson, P.; Roiban, G.-D.; Roosen, P. C.; Steven, A.; Terrett, J. A.; White, T.; Yin, J. Green Chemistry Articles of Interest to the Pharmaceutical Industry. *Org. Process Res. Dev.* **2020**, *24* (3), 334–346. https://doi.org/10.1021/acs.oprd.0c00036.

(127) Sheldon, R. A. E Factors, Green Chemistry and Catalysis: An Odyssey. *Chem. Comm,* **2008**, No. 29, 3352. https://doi.org/10.1039/b803584a.

(128) Dunn, P. J. The Importance of Green Chemistry in Process Research and Development. *Chem. Soc. Rev.* **2012**, *41* (4), 1452–1461. https://doi.org/10.1039/C1CS15041C.

(129) Schnorrenberg, G. New Trends in Drug Discovery. In *Successful Drug Discovery*; Wiley-VCH Verlag GmbH & Co. KGaA: Weinheim, Germany, 2018; pp 1–39. https://doi.org/10.1002/9783527808694.ch1.

(130) Roschangar, F.; Colberg, J.; Dunn, P. J.; Gallou, F.; Hayler, J. D.; Koenig, S. G.; Kopach, M. E.; Leahy, D. K.; Mergelsberg, I.; Tucker, J. L.; Sheldon, R. A.; Senanayake, C. H. A Deeper Shade of Green: Inspiring Sustainable Drug Manufacturing. *Green Chem.* **2017**, *19* (1), 281–285. https://doi.org/10.1039/C6GC02901A.

(131) Roschangar, F.; Sheldon, R. A.; Senanayake, C. H. Overcoming Barriers to Green Chemistry in the Pharmaceutical Industry – the Green Aspiration Level^{TM} Concept. *Green Chem.* **2015**, *17* (2), 752–768. https://doi.org/10.1039/C4GC01563K.

(132) Roschangar, F.; Zhou, Y.; Constable, D. J. C.; Colberg, J.; Dickson, D. P.; Dunn, P. J.; Eastgate, M. D.; Gallou, F.; Hayler, J. D.; Koenig, S. G.; Kopach, M. E.; Leahy, D. K.; Mergelsberg, I.; Scholz, U.; Smith, A. G.; Henry, M.; Mulder, J.; Brandenburg, J.; Dehli, J. R.; Fandrick, D. R.; Fandrick, K. R.; Gnad-Badouin, F.; Zerban, G.; Groll, K.; Anastas, P. T.; Sheldon, R. A.; Senanayake, C. H. Inspiring Process Innovation *via* an Improved Green Manufacturing Metric: IGAL. *Green Chem.* **2018**, *20* (10), 2206–2211. https://doi.org/10.1039/C8GC00616D.

(133) Lipshutz, B. H.; Ghorai, S.; Cortes-Clerget, M. The Hydrophobic Effect Applied to Organic Synthesis: Recent Synthetic Chemistry "in Water." *Chem. Eur. J.* **2018**, *24* (26), 6672–6695. https://doi.org/10.1002/chem.201705499.

(134) Clarke, C. J.; Tu, W.-C.; Levers, O.; Bröhl, A.; Hallett, J. P. Green and Sustainable Solvents in Chemical Processes. *Chem. Rev.* **2018**, *118* (2), 747–800. https://doi.org/10.1021/acs.chemrev.7b00571.

(135) Kerton, F.; Marriott, R. Chapter 2. Green Solvents – Legislation and Certification; 2013; pp 31–50. https://doi.org/10.1039/9781849736824-00031.

(136) Sheldon, R. A. The E Factor 25 Years on: The Rise of Green Chemistry and Sustainability. *Green Chem.* **2017**, *19* (1), 18–43. https://doi.org/10.1039/C6GC02157C.

(137) Amelio, A.; Genduso, G.; Vreysen, S.; Luis, P.; van der Bruggen, B. Guidelines Based on Life Cycle Assessment for Solvent Selection during the Process Design and Evaluation of Treatment Alternatives. *Green Chem.* **2014**, *16* (6), 3045–3063. https://doi.org/10.1039/C3GC42513D.

(138) Sherwood, J.; Clark, J. H.; Fairlamb, I. J. S.; Slattery, J. M. Solvent Effects in Palladium Catalysed Cross-Coupling Reactions. *Green Chem.* **2019**, *21* (9), 2164–2213. https://doi.org/10.1039/C9GC00617F.

(139) Yang, Q.; Sheng, M.; Huang, Y. Potential Safety Hazards Associated with Using *N* , *N* -Dimethylformamide in Chemical Reactions. *Org. Process Res. Dev.* **2020**, *24* (9), 1586–1601. https://doi.org/10.1021/acs.oprd.0c00330.

(140) *https://echa.europa.eu/it/candidate-list-table*.

(141) Scherf-Clavel, O.; Kinzig, M.; Besa, A.; Schreiber, A.; Bidmon, C.; Abdel-Tawab, M.; Wohlfart, J.; Sörgel, F.; Holzgrabe, U. The Contamination of Valsartan and Other Sartans, Part 2: Untargeted Screening Reveals Contamination with Amides Additionally to Known Nitrosamine Impurities. *J. Pharm. Biomed. Anal.* **2019**, *172*, 278–284. https://doi.org/10.1016/j.jpba.2019.04.035.

(142) European Medicinal Agency (EMA): & Committee for Medicinal Products for Human Use (CHMP). Assessment Report: Nitrosamine Impurities in Human Medicinal Products. (2020).

(143) European Medicinal Agency (EMA), Committee for Medicinal Products for Human Use (CHMP). Assestment Report: Angiotensin-II-Receptor Antagonists (Sartans) Containing a Tetrazole Group. (2020).

(144) Prat, D.; Hayler, J.; Wells, A. A Survey of Solvent Selection Guides. *Green Chem.* **2014**, *16* (10), 4546–4551. https://doi.org/10.1039/C4GC01149J.

(145) Náray-Szabó, G.; Mika, L. T. Conservative Evolution and Industrial Metabolism in Green Chemistry. *Green Chem.* **2018**, *20* (10), 2171–2191. https://doi.org/10.1039/C8GC00514A.

(146) Chen, J.; Zhong, M.; Tao, L.; Liu, L.; Jayakumar, S.; Li, C.; Li, H.; Yang, Q. The Cooperation of Porphyrin-Based Porous Polymer and Thermal-Responsive Ionic Liquid for Efficient CO_2 Cycloaddition Reaction. *Green Chem.* **2018**, *20* (4), 903–911. https://doi.org/10.1039/C7GC03801A.

(147) Wei, J.-F.; Jiao, J.; Feng, J.-J.; Lv, J.; Zhang, X.-R.; Shi, X.-Y.; Chen, Z.-G. PdEDTA Held in an Ionic Liquid Brush as a Highly Efficient and Reusable Catalyst for Suzuki Reactions in Water. *J. Org. Chem.* **2009**, *74* (16), 6283–6286. https://doi.org/10.1021/jo900481y.

(148) Noyori, R. Supercritical Fluids: Introduction. *Chem. Rev.* **1999**, *99* (2), 353–354. https://doi.org/10.1021/cr980085a.

(149) Oakes, R. S.; Clifford, A. A.; Rayner, C. M. The Use of Supercritical Fluids in Synthetic Organic Chemistry. *J. Chem. Soc. Perkin.* **2001**, No. 9, 917–941. https://doi.org/10.1039/b101219n.

(150) Beckman, E. Supercritical and Near-Critical CO_2 in Green Chemical Synthesis and Processing. In *The Journal of supercritical fluids*; 2004; Vol. 28, pp 121–191.

(151) Beckman, E. J. Production of H_2O_2 in CO_2 and Its Use in the Direct Synthesis of Propylene Oxide. This Work Was Presented at the Green Solvents for Catalysis Meeting Held in Bruchsal, Germany, 13-16th October, 2002. *Green Chem.* **2003**, *5* (3), 332. https://doi.org/10.1039/b300387f.

(152) Danciu, T.; Beckman, E. J.; Hancu, D.; Cochran, R. N.; Grey, R.; Hajnik, D. M.; Jewson, J. Direct Synthesis of Propylene Oxide with CO_2 as the Solvent. *Angew. Chem. Int. Ed.* **2003**, *42* (10), 1140–1142. https://doi.org/10.1002/anie.200390299.

(153) Marset, X.; Khoshnood, A.; Sotorríos, L.; Gómez-Bengoa, E.; Alonso, D. A.; Ramón, D. J. Deep Eutectic Solvent Compatible Metallic Catalysts: Cationic Pyridiniophosphine Ligands in Palladium Catalyzed Cross-Coupling Reactions. *ChemCatChem* **2017**, *9* (7), 1269–1275. https://doi.org/10.1002/cctc.201601544.
(154) García-Álvarez, J. Deep Eutectic Mixtures: Promising Sustainable Solvents for Metal-Catalysed and Metal-Mediated Organic Reactions. *Eur. J. Inorg. Chem.* **2015**, *2015* (31), 5147–5157. https://doi.org/10.1002/ejic.201500892.
(155) Lindström, U. M. Stereoselective Organic Reactions in Water. *Chem. Rev.* **2002**, *102* (8), 2751–2772. https://doi.org/10.1021/cr010122p.
(156) Narayan, S.; Muldoon, J.; Finn, M. G.; Fokin, V. v.; Kolb, H. C.; Sharpless, K. B. "On Water": Unique Reactivity of Organic Compounds in Aqueous Suspension. *Angew. Chem. Int. Ed.* **2005**, *44* (21), 3275–3279. https://doi.org/10.1002/anie.200462883.
(157) Dwars, T.; Paetzold, E.; Oehme, G. Reactions in Micellar Systems. *Angew. Chem. Int. Ed.* **2005**, *44* (44), 7174–7199. https://doi.org/10.1002/anie.200501365.
(158) Landstrom, E. B.; Akporji, N.; Lee, N. R.; Gabriel, C. M.; Braga, F. C.; Lipshutz, B. H. One-Pot Synthesis of Indoles and Pyrazoles via Pd-Catalyzed Couplings/Cyclizations Enabled by Aqueous Micellar Catalysis. *Org. Lett.* **2020**, *22* (16), 6543–6546. https://doi.org/10.1021/acs.orglett.0c02315.
(159) Pang, H.; Hu, Y.; Yu, J.; Gallou, F.; Lipshutz, B. H. Water-Sculpting of a Heterogeneous Nanoparticle Precatalyst for Mizoroki–Heck Couplings under Aqueous Micellar Catalysis Conditions. *J. Am. Chem. Soc.* **2021**, *143* (9), 3373–3382. https://doi.org/10.1021/jacs.0c11484.
(160) Wood, A. B.; Plummer, S.; Robinson, R. I.; Smith, M.; Chang, J.; Gallou, F.; Lipshutz, B. H. Continuous Slurry Plug Flow Fe/Ppm Pd Nanoparticle-Catalyzed Suzuki–Miyaura Couplings in Water Utilizing Novel Solid Handling Equipment. *Green Chem.* **2021**, *23* (19), 7724–7730. https://doi.org/10.1039/D1GC02461B.
(161) Jin, B.; Gallou, F.; Reilly, J.; Lipshutz, B. H. Ppm Pd-Catalyzed, Cu-Free Sonogashira Couplings in Water Using Commercially Available Catalyst Precursors. *Chem. Sci.* **2019**, *10* (12), 3481–3485. https://doi.org/10.1039/C8SC05618H.
(162) Vaccaro, L.; Curini, M.; Ferlin, F.; Lanari, D.; Marrocchi, A.; Piermatti, O.; Trombettoni, V. Definition of Green Synthetic Tools Based on Safer Reaction Media, Heterogeneous Catalysis, and Flow Technology. *Pure and Applied Chemistry* **2018**, *90* (1), 21–33. https://doi.org/10.1515/pac-2017-0409.
(163) Sarmah, M.; Mondal, M.; Bora, U. Agro-Waste Extract Based Solvents: Emergence of Novel Green Solvent for the Design of Sustainable Processes in Catalysis and Organic Chemistry. *Chem. Sel.* **2017**, *2* (18), 5180–5188. https://doi.org/10.1002/slct.201700580.
(164) DeSimone, J. M. Practical Approaches to Green Solvents. *Science (1979)* **2002**, *297* (5582), 799–803. https://doi.org/10.1126/science.1069622.
(165) Diaz-Alvarez, A. E.; Francos, J.; Croche, P.; Cadierno, V. Recent Advances in the Use of Glycerol as Green Solvent for Organic Chemistrye. In *Current Green Chemistry*; 2014; Vol. 1, pp 51–65.
(166) Asthana, N.; Kolah, A.; Vu, D. T.; Lira, C. T.; Miller, D. J. A Continuous Reactive Separation Process for Ethyl Lactate Formation. *Org. Process Res. Dev.* **2005**, *9* (5), 599–607. https://doi.org/10.1021/op0500640.

(167) Mäki-Arvela, P.; Simakova, I. L.; Salmi, T.; Murzin, D. Yu. Production of Lactic Acid/Lactates from Biomass and Their Catalytic Transformations to Commodities. *Chem. Rev.* **2014**, *114* (3), 1909–1971. https://doi.org/10.1021/cr400203v.
(168) Bisz, E.; Szostak, M. 2-Methyltetrahydrofuran: A Green Solvent for Iron-Catalyzed Cross-Coupling Reactions. *ChemSusChem* **2018**, *11* (8), 1290–1294. https://doi.org/10.1002/cssc.201800142.
(169) Farrán, A.; Cai, C.; Sandoval, M.; Xu, Y.; Liu, J.; Hernáiz, M. J.; Linhardt, R. J. Green Solvents in Carbohydrate Chemistry: From Raw Materials to Fine Chemicals. *Chem. Rev.* **2015**, *115* (14), 6811–6853. https://doi.org/10.1021/cr500719h.
(170) Pace, V.; Hoyos, P.; Castoldi, L.; Domínguez de María, P.; Alcántara, A. R. 2-Methyltetrahydrofuran (2-MeTHF): A Biomass-Derived Solvent with Broad Application in Organic Chemistry. *ChemSusChem* **2012**, *5* (8), 1369–1379. https://doi.org/10.1002/cssc.201100780.
(171) Cai, C. M.; Zhang, T.; Kumar, R.; Wyman, C. E. Integrated Furfural Production as a Renewable Fuel and Chemical Platform from Lignocellulosic Biomass. *J. Chem. Technol. Biotechnol.* **2014**, *89* (1), 2–10. https://doi.org/10.1002/jctb.4168.
(172) Strappaveccia, G.; Luciani, L.; Bartollini, E.; Marrocchi, A.; Pizzo, F.; Vaccaro, L. γ-Valerolactone as an Alternative Biomass-Derived Medium for the Sonogashira Reaction. *Green Chemi.* **2015**, *17* (2), 1071–1076. https://doi.org/10.1039/C4GC01728E.
(173) Ismalaj, E.; Strappaveccia, G.; Ballerini, E.; Elisei, F.; Piermatti, O.; Gelman, D.; Vaccaro, L. γ-Valerolactone as a Renewable Dipolar Aprotic Solvent Deriving from Biomass Degradation for the Hiyama Reaction. *ACS Sustain. Chem. Eng.* **2014**, *2* (10), 2461–2464. https://doi.org/10.1021/sc5004727.
(174) Tian, X.; Yang, F.; Rasina, D.; Bauer, M.; Warratz, S.; Ferlin, F.; Vaccaro, L.; Ackermann, L. C–H Arylations of 1,2,3-Triazoles by Reusable Heterogeneous Palladium Catalysts in Biomass-Derived γ-Valerolactone. *Chem. Comm.* **2016**, *52* (63), 9777–9780. https://doi.org/10.1039/C6CC03468C.
(175) Ferlin, F.; Santoro, S.; Ackermann, L.; Vaccaro, L. Heterogeneous C–H Alkenylations in Continuous-Flow: Oxidative Palladium-Catalysis in a Biomass-Derived Reaction Medium. *Green Chem.* **2017**, *19* (11), 2510–2514. https://doi.org/10.1039/C7GC01103B.
(176) Ferlin, F.; Luciani, L.; Santoro, S.; Marrocchi, A.; Lanari, D.; Bechtoldt, A.; Ackermann, L.; Vaccaro, L. A Continuous Flow Approach for the C–H Functionalization of 1,2,3-Triazoles in γ-Valerolactone as a Biomass-Derived Medium. *Green Chem.* **2018**, *20* (12), 2888–2893. https://doi.org/10.1039/C8GC01115J.
(177) Camp, J. E. Bio-Available Solvent Cyrene: Synthesis, Derivatization, and Applications. *ChemSusChem* **2018**, *11* (18), 3048–3055. https://doi.org/10.1002/cssc.201801420.
(178) Wilson, K. L.; Kennedy, A. R.; Murray, J.; Greatrex, B.; Jamieson, C.; Watson, A. J. B. Scope and Limitations of a DMF Bio-Alternative within Sonogashira Cross-Coupling and Cacchi-Type Annulation. *Beilstein J. Org. Chem.* **2016**, *12*, 2005–2011. https://doi.org/10.3762/bjoc.12.187.

(179) Fischmeister, C.; Doucet, H. Greener Solvents for Ruthenium and Palladium-Catalysed Aromatic C–H Bond Functionalisation. *Green Chem.* **2011**, *13* (4), 741. https://doi.org/10.1039/c0gc00885k.
(180) Dong, J. J.; Roger, J.; Verrier, C.; Martin, T.; le Goff, R.; Hoarau, C.; Doucet, H. Carbonates: Eco-Friendly Solvents for Palladium-Catalysed Direct Arylation of Heteroaromatics. *Green Chem.* **2010**, *12* (11), 2053. https://doi.org/10.1039/c0gc00229a.
(181) Ismael, A.; Gevorgyan, A.; Skrydstrup, T.; Bayer, A. Renewable Solvents for Palladium-Catalyzed Carbonylation Reactions. *Org. Process Res. Dev.* **2020**, *24* (11), 2665–2675. https://doi.org/10.1021/acs.oprd.0c00325.
(182) Fantoni, T.; Bernardoni, S.; Mattellone, A.; Martelli, G.; Ferrazzano, L.; Cantelmi, P.; Corbisiero, D.; Tolomelli, A.; Cabri, W.; Vacondio, F.; Ferlenghi, F.; Mor, M.; Ricci, A. Palladium Catalyst Recycling for Heck-Cassar-Sonogashira Cross-Coupling Reactions in Green Solvent/Base Blend. *ChemSusChem* **2021**, *14* (12), 2591–2600. https://doi.org/10.1002/cssc.202100623.
(183) Ferrazzano, L.; Martelli, G.; Fantoni, T.; Daka, A.; Corbisiero, D.; Viola, A.; Ricci, A.; Cabri, W.; Tolomelli, A. Fast Heck-Cassar-Sonogashira (Hcs) Reactions in Green Solvents. *Org. Lett.* **2020**, *22* (10), 3969–3973. https://doi.org/10.1021/acs.orglett.0c01269.
(184) Schilz, M.; Plenio, H. A Guide to Sonogashira Cross-Coupling Reactions: The Influence of Substituents in Aryl Bromides, Acetylenes, and Phosphines. *J. Org. Chem.* **2012**, *77* (6), 2798–2807. https://doi.org/10.1021/jo202644g.
(185) Chinchilla, R.; Nájera, C. Recent Advances in Sonogashira Reactions. *Chem. Soc. Rev.* **2011**, *40* (10), 5084. https://doi.org/10.1039/c1cs15071e.
(186) Wang, X.; Song, Y.; Qu, J.; Luo, Y. Mechanistic Insights into the Copper-Cocatalyzed Sonogashira Cross-Coupling Reaction: Key Role of an Anion. *Organometallics* **2017**, *36* (5), 1042–1048. https://doi.org/10.1021/acs.organomet.7b00010.
(187) Karak, M.; Barbosa, L. C. A.; Hargaden, G. C. Recent Mechanistic Developments and next Generation Catalysts for the Sonogashira Coupling Reaction. *RSC Adv.* **2014**, *4* (96), 53442–53466. https://doi.org/10.1039/C4RA09105A.
(188) Thomas, A. M.; Sujatha, A.; Anilkumar, G. Recent Advances and Perspectives in Copper-Catalyzed Sonogashira Coupling Reactions. *RSC Adv.* **2014**, *4* (42), 21688–21698. https://doi.org/10.1039/C4RA02529F.
(189) Sonogashira, K. Development of Pd–Cu Catalyzed Cross-Coupling of Terminal Acetylenes with Sp2-Carbon Halides. *J. Organomet. Chem.* **2002**, *653* (1–2), 46–49. https://doi.org/10.1016/S0022-328X(02)01158-0.
(190) Soheili, A.; Albaneze-Walker, J.; Murry, J. A.; Dormer, P. G.; Hughes, D. L. Efficient and General Protocol for the Copper-Free Sonogashira Coupling of Aryl Bromides at Room Temperature. *Org. Lett.* **2003**, *5* (22), 4191–4194. https://doi.org/10.1021/ol035632f.
(191) Dieck, H. A.; Heck, F. R. Palladium Catalyzed Synthesis of Aryl, Heterocyclic and Vinylic Acetylene Derivatives. *J. Organomet. Chem.* **1975**, *93* (2), 259–263. https://doi.org/10.1016/S0022-328X(00)94049-X.
(192) Sperger, T.; Sanhueza, I. A.; Kalvet, I.; Schoenebeck, F. Computational Studies of Synthetically Relevant Homogeneous Organometallic Catalysis Involving Ni, Pd, Ir, and Rh: An Overview of Commonly Employed DFT Methods and Mechanistic

Insights. *Chem. Rev.* **2015**, *115* (17), 9532–9586. https://doi.org/10.1021/acs.chemrev.5b00163.

(193) Ahmadi, Z.; Yunker, L. P. E.; Oliver, A. G.; McIndoe, J. S. Mechanistic Features of the Copper-Free Sonogashira Reaction from ESI-MS. *Dalton Trans.* **2015**, *44* (47), 20367–20375. https://doi.org/10.1039/C5DT02889B.

(194) García-Melchor, M.; Braga, A. A. C.; Lledós, A.; Ujaque, G.; Maseras, F. Computational Perspective on Pd-Catalyzed C–C Cross-Coupling Reaction Mechanisms. *Acc. Chem. Res.* **2013**, *46* (11), 2626–2634. https://doi.org/10.1021/ar400080r.

(195) García-Melchor, M.; Pacheco, M. C.; Nájera, C.; Lledós, A.; Ujaque, G. Mechanistic Exploration of the Pd-Catalyzed Copper-Free Sonogashira Reaction. *ACS Catal* **2012**, *2* (1), 135–144. https://doi.org/10.1021/cs200526x.

(196) Sikk, L.; Tammiku-Taul, J.; Burk, P. Computational Study of Copper-Free Sonogashira Cross-Coupling Reaction. *Organometallics* **2011**, *30* (21), 5656–5664. https://doi.org/10.1021/om2004817.

(197) Vikse, K. L.; Ahmadi, Z.; Manning, C. C.; Harrington, D. A.; McIndoe, J. S. Powerful Insight into Catalytic Mechanisms through Simultaneous Monitoring of Reactants, Products, and Intermediates. *Angew. Chem., Int. Ed.* **2011**, *50* (36), 8304–8306. https://doi.org/10.1002/anie.201102630.

(198) Ljungdahl, T.; Bennur, T.; Dallas, A.; Emtenäs, H.; Mårtensson, J. Two Competing Mechanisms for the Copper-Free Sonogashira Cross-Coupling Reaction. *Organometallics* **2008**, *27* (11), 2490–2498. https://doi.org/10.1021/om800251s.

(199) Ljungdahl, T.; Pettersson, K.; Albinsson, B.; Mårtensson, J. Solvent and Base Dependence of Copper-Free Palladium-Catalyzed Cross-Couplings between Terminal Alkynes and Arylic Iodides: Development of Efficient Conditions for the Construction of Gold(III)/Free-Base Porphyrin Dimers. *J. Org. Chem.* **2006**, *71* (4), 1677–1687. https://doi.org/10.1021/jo052423v.

(200) Tougerti, A.; Negri, S.; Jutand, A. Mechanism of the Copper-Free Palladium-Catalyzed Sonagashira Reactions: Multiple Role of Amines. *Chem. Eur. J.* **2007**, *13* (2), 666–676. https://doi.org/10.1002/chem.200600574.

(201) Amatore, C.; Bensalem, S.; Ghalem, S.; Jutand, A.; Medjour, Y. Decelerating Effect of Alkynes in the Oxidative Addition of Phenyl Iodide to Palladium(0) Complexes in Palladium-Catalyzed Multicomponent Reactions and Sonogashira Reactions. *Eur. J. Org. Chem.* **2004**, *2004* (2), 366–371.

(202) Gazvoda, M.; Virant, M.; Pinter, B.; Košmrlj, J. Mechanism of Copper-Free Sonogashira Reaction Operates through Palladium-Palladium Transmetallation. *Nat. Commun.* **2018**, *9* (1), 4814. https://doi.org/10.1038/s41467-018-07081-5.

Chapter 2:

Fast Heck–Cassar–Sonogashira (HCS) Reactions in Green Solvents

2.1 Introduction

The wide applicability of the HCS cross-coupling reaction (Scheme 2.1) to complex and sensitive structures has increased its use in many relevant industrial protocols, especially in the multistep synthesis of active pharmaceutical ingredients (API).[1–9]

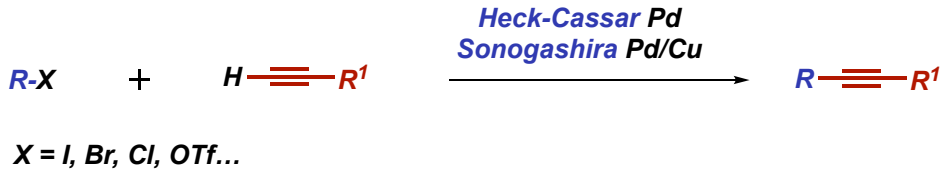

***Scheme 2.1**: General scheme for HCS cross-coupling*

The greenness of industrial processes to preserve the environment and to ensure health and safety of workers has evolved from an ethic approach to an inescapable necessity.[10] Since organic solvents and water represent the main source of waste in chemical industrial processes,[11–14] the identification of green and biogenic alternatives and the decrease of the Process Mass Intensity (PMI) are important drivers for the development of sustainable, efficient and mild protocols applied to palladium catalyzed industrial reactions.[15] In addition, the solvent selection is critical in Pd-catalyzed cross-couplings, because it can affect the stability of the catalyst, the equilibrium, the rate and selectivity of the process.[16] In particular, stable Pd^{II} precatalysts and ligands are necessary to guarantee high yields, high selectivity and design efficient synthetic strategies avoiding the use of protective groups. The reaction must also be efficient under mild conditions in order to decrease energy consumption and guarantee compatibility with complex and sensitive chemical structures. Concerning the palladium fate, there must be no leakage of the catalyst during the process to avoid product contamination,[17] and the metal must be fully recovered also for environmental reasons. The reaction protocol must guarantee a rapid, easy, and efficient scale up.

In the last decades, almost 40% of the published HCS reactions were performed in *N*,*N*-Dimethylformamide (DMF),[18] which is known to be a highly reprotoxic solvent.[19] In fact, it is classified as a substance of very high concern (SVHC) and is a potential source of genotoxic N-dimethylnitrosamines.[20] Other common solvents used in the HCS coupling are

tetrahydrofuran (THF), dimethylsulfoxide (DMSO), 1,4-dioxane, toluene, dimethoxyethane (DME), and amines,[21–24] but still not represent a real greener alternative as they share with DMF several drawbacks in terms of environmental health and safety (EHS).[25–28] The investigation of alcohols, water, ionic liquids, and bio-based solvents such as dimethylisosorbide, γ-valerolactone, and Cyrene were also reported.[14,29–33]

DMF has been successfully replaced in many processes by N-methylpyrrolidone (NMP), which displays a similar polarity profile. However, also NMP has limitations, because of the potential development of toxic metabolites, such as formaldehyde and oxidized derivatives.[34]

For this reason, longer N-alkylpyrrolidones could offer novel opportunities, since their metabolites are less toxic than formaldehyde and related compounds typically deriving from N-Me oxidation in DMF and NMP. Their lower toxicity allowed their use as surfactants and their addition in cosmetic formulations.[35]

Among them, N-butylpyrrolidone (NBP) has been already successfully used in Heck and Suzuki cross-coupling reactions,[36] while pyrrolidones with longer alkyl chains (N-octylpyrrolidone (NOP), N-benzylpyrrolidone (NBnP), N-cyclohexylpyrrolidone (NCP) and N-hydroxyethylpyrrolidone (HEP)) have not been extensively studied. In addition, anisole (An) and tert-butyl acetate (tBuOAc) have been included, since they are considered sustainable dipolar aprotic solvents.[37,38]

2.2 Results and discussion

The target of this study was to identify a versatile protocol able to perform fast and efficient HCS cross-coupling reactions under mild conditions using green and sustainable solvents. We selected the model reaction between iodobenzene **1a** and phenylacetylene **2a**, triethylamine (TEA) as base in the presence of $Pd(PPh_3)_2Cl_2$ as catalyst and CuI as co-catalyst, at 30°C to test the efficiency of new greener solvents, by screening several parameters such as acetylene equivalents, the amount of Cu co-catalyst and the role of the base (Table 2.1). A high-performance liquid chromatography ultraviolet (HPLC-UV) signal at 210 nm was used to follow the transformation of the reagents into diphenylacetylene **3a** product considering the Relative Response Factor (RRF) of the different compounds to evaluate the correct conversion. The reactions were stopped when no further evolution in

time was observed. Experiments with DMF and Cyrene were performed as reference reactions in order to have a comparison with the data available in literature.[33] Under the standard selected conditions, neither of the solvents reached a complete conversion (Table 2.1, entries 1–10).

***Table 2.1**: HCS model reaction screening in green solvents*

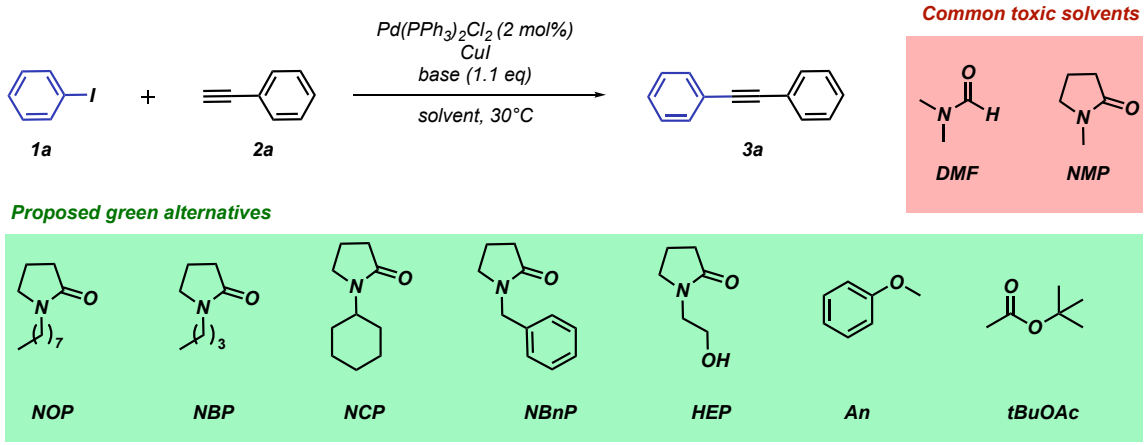

Entry[b]	solvent	**2a** equiv	base	CuI mol%	time h	conversion % (yield %)[a]
1	DMF	1.05	TEA	4	1	90
2	Cyrene	1.05	TEA	4	1	91
3	NMP	1.05	TEA	4	1	86
4	HEP	1.05	TEA	4	1	96 (90)
5	NBnP	1.05	TEA	4	1	83
6	NCP	1.05	TEA	4	1	66
7	NBP	1.05	TEA	4	1	65
8	NOP	1.05	TEA	4	1	72
9	An	1.05	TEA	4	1	86
10	tBuOAc	1.05	TEA	4	1	92
11	NOP	1.5	TEA	4	1	92
12	NOP	1.05	TMG	4	0.5	>99 (92)
13	NOP	1.05	TMG	1	0.5	>99 (93)
14	NBP	1.05	TMG	1	0.5	95 (90)
15	NBnP	1.05	TMG	1	0.5	>99 (90)
16	NCP	1.05	TMG	1	0.5	>99 (94)
17	HEP	1.05	TMG	1	0.5	>99 (97) [c]
18	An	1.5	TMG	1	0.5	>99 (94)
19	tBuOAc	1.5	TMG	1	0.5	>99 (95)
20	HEP	1.05	TEA	-	1	49
21	HEP	1.05	TMG	-	1	9

[a]Conversion monitored with HPLC-UV at 210 nm. The product was isolated only when the conversion was >95%. [b]All the reactions were performed with 0.5 mmol scale and a concentration of 0.5 M. [c]This reaction was performed in 10 mmol scale with similar results

One of the worst performing solvents, NOP, was selected to optimize the reaction conditions in further experiments. An excess of **2a** increased the conversion to 92% (Table 2.1, entry 11). Nevertheless, the strongest effect was observed when the reaction was performed by using N,N,N,N-tetramethyl guanidine (TMG) as base, in place of the most commonly used TEA. Under these conditions, the conversion was complete in 30 min, even in presence of 1 mol% of copper co-catalyst (Table 2.1, entries 12 and 13). Since the reaction was particularly efficient and performed in mild conditions, no excess of **2a** was required, and therefore no byproducts such as homocoupling coming from the Glaser-Hay side reaction or other enyne byproducts were detected. These conditions were successfully applied to all of the other green solvents (Table 2.1, entries 14−19) affording **3a** in 90%−95% isolated yield. Copper-free conditions were also attempted but did not reach satisfactory results at room temperature (Table 2.1, entries 20 and 21). The best results were achieved with HEP as solvent, allowing an easy recovery of product **3a** (97% isolated yield), because of the complete migration of the solvent in water during the workup. Finally, with the optimized conditions in hand, the model reaction between **1a** and **2a** in HEP was also performed on 10 mmol scale increasing the concentration from 0.5 M, used in the standard reaction, to 1 M, giving comparable results, in order to verify the recovery of HEP and to enhance the sustainability of the process. At the end of the process, distillation of the HEP/water phase was attempted, achieving the pyrrolidone in >90% yield. The PMIr of the overall process, considering also the solvents used for the work up, is around 20 while the E-Factor has a value of 3, comparable to the one achievable in DMF, as it does not consider the water used for extraction. HEP is a biogenic solvent that is already available in large quantities, being an intermediate for the synthesis of N-vinyl-pyrrolidone (Scheme 2.2).[39] Since it is considered only as an intermediate for synthesis, HEP is not included in any solvent database. However, we have used for its classification the CHEM21 selection guide for classical and less classical solvents (Table 2.2).[28] From an EHS point of view, this solvent has interesting properties, displaying a flash point close to 212°C and a rat oral LD50 > 14400 mg kg^{-1}.[40] Although HEP is a biogenic solvent with a good toxicological and ecotoxicological profile, it is penalized in the EHS criteria classification for green solvents by the fact that it has a boiling point > 200°C, which by definition increases also the cumulative energy demand (CED). Most of the recently reported biogenic solvents

such as cyrene, DES (that contain glycerol), dimethylisosorbide, and γ-valerolactone have boiling points > 200°C. However, in our opinion, with the actual distillation technologies, especially when the product does not require any rectification, the impact of the boiling point is mitigated at industrial level.[13]

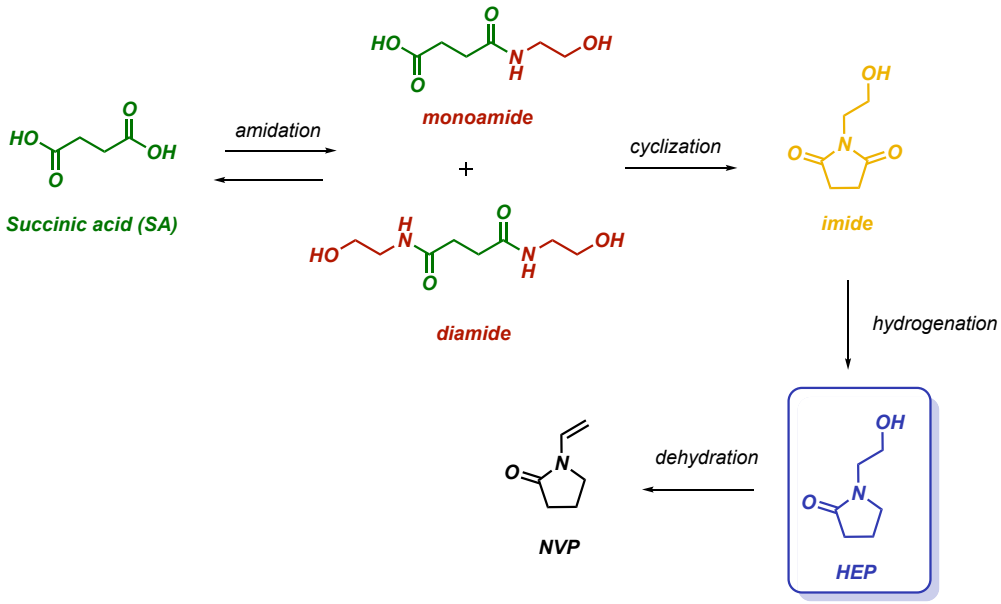

***Scheme 2.2**: Schematic process of the industrial synthesis of HEP*

Moreover, HEP is not genotoxic, not reprotoxic, and does not raise any environmental concern. The main concern on the use of DMF is related to workers exposure since it is reprotoxic, has a rat oral LD50 of 3010 mg kg^{-1}, and can lead to damages to various organs in humans, among which the liver is the primary target. [40,41]

***Table 2.2**: Solvents ranking according to CHEM21 selection guide*

Solvent	E	H	S
DMF	5	9	3
NMP	7	9	1
HEP	7	2	1

Since the metabolic fate of a solvent is a critical parameter to define its EHS impact and greenness, we decided to study this aspect that was not reported in literature for HEP. Therefore, the metabolism of HEP in comparison to the parent NMP (LD50 4100 mg kg^{-1}) was explored, since the hypothesis was that the lower LD50 of HEP could be related to a

different metabolic pathway.[42] Both in rat and human liver microsomes, HEP turned out to be more stable than NMP (Figure 2.1a). Under these in-vitro experimental conditions, NMP was converted by hydroxylation to 5-hydroxy-N-methyl-2-pyrrolidone (5-HNMP) and, barely, to 2-pyrrolidone (2-P) via N-demethylation (Figure 2.1b). In fact, 5-HNMP is a well-known biomarker of environmental exposure to NMP[43] and it is a major in-vivo urinary metabolite in rats[44,45] and humans,[46] while 2-P has been reported as a minor in-vivo metabolite both in rats and humans.[43,47]

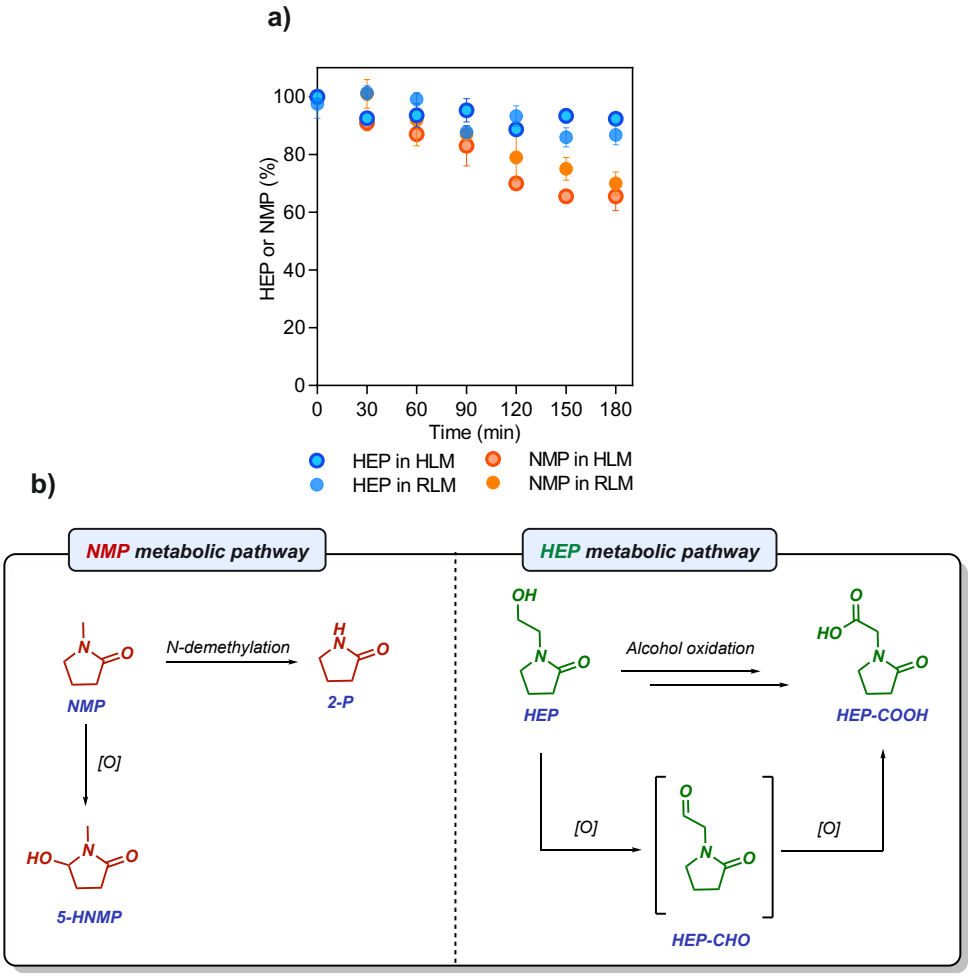

***Figure 2.1**: In vitro metabolism of NMP and HEP in rat (RLM) and human (HLM) liver microsomes. Comparison of metabolic stability under the same experimental conditions. Error bars correspond to one standard deviation a). Proposed metabolic pathways b)*

HEP revealed a different metabolic pathway from NMP, since it was converted into the corresponding acid (HEP-COOH) by oxidation of the hydroxy group on the N-hydroxyethyl side chain, via an aldehyde intermediate. The metabolites 5-HNMP, 2-P and HEP-COOH

were identified by comparison of their liquid chromatography and high-resolution mass spectrometry features with those of synthetic reference standards, and all the experimental data supporting these findings are available in the experimental section. Finally, not only HEP is more stable toward microsomal oxidation than NMP, but it also gives a polar acidic metabolite that can be easily eliminated by the kidneys. Therefore, HEP could represent a valid green, sustainable and non-toxic alternative to the dipolar solvents in organometallic catalysis. Our data clearly indicate that the primary metabolic oxidation site of HEP is the hydroxyethyl side chain. The glycine derivative can then undergo a further pyrrolidone ring degradation, generating a succinyl-glycine derivative in analogy with NMP ring oxidation/hydrolysis.

The reaction was then extended to substituted aryl iodides and acetylenes (Table 2.3). For each couple of substrates, the mildest conditions to reach complete conversion were investigated, starting from the best conditions identified in the model reaction between **1a** and **2a**. Thus, all of the reactions were performed in HEP, using $Pd(PPh_3)_2Cl_2$ (2 mol %) as precatalyst, CuI (1 mol %), and TMG (1.1 eq).

***Table 2.3**: Scope of the HCS reaction with substituted aryl iodides*

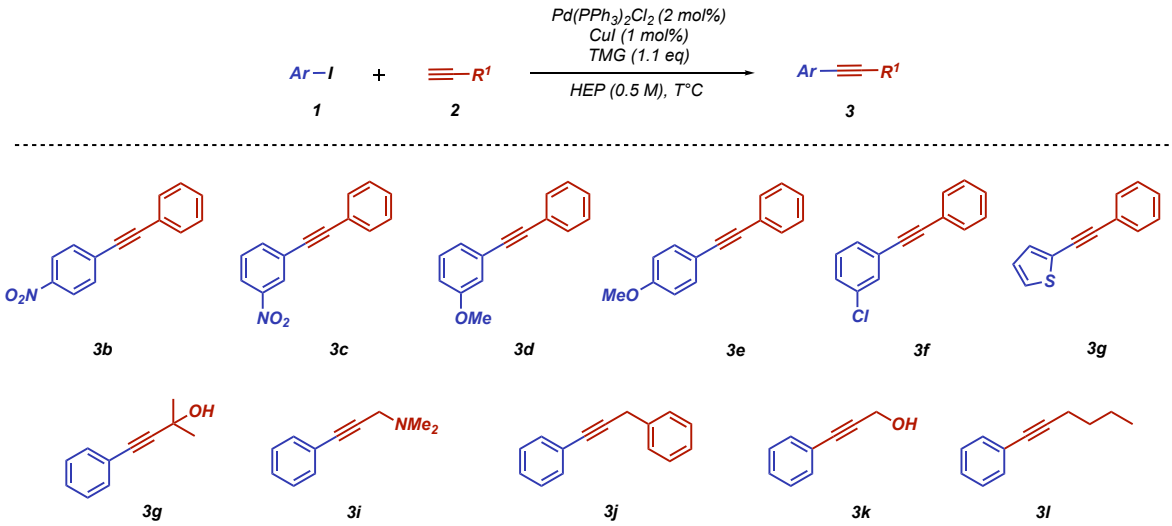

Entry	1	2	2 equiv	T °C	time h	conversion %[a] (yield %)	product
1	4-nitroiodobenzene, **1b**	phenylacetylene, **2a**	1.05	30	0.5	>99 (96)	**3b**
2	3-nitroiodobenzene, **1c**	phenylacetylene, **2a**	1.05	30	0.5	>99 (95)	**3c**
3	3-methoxyiodobenzene, **1d**	phenylacetylene, **2a**	1.05	30	0.5	>99 (98)	**3d**
4	4-methoxyiodobenzene, **1e**	phenylacetylene, **2a**	1.05	30	0.5	>99 (98)	**3e**
5	3-chloroiodobenzene, **1f**	phenylacetylene, **2a**	1.05	30	0.5	>99 (95)	**3f**
6	2-iodothiophene, **1g**	phenylacetylene, **2a**	1.05	30	0.5	>99 (98)	**3g**
7	iodobenzene, **1a**	2-methyl-3-butyn-2-ol, **2h**	1.05	30	1	>99 (94)	**3h**
8	iodobenzene, **1a**	3-dimethylamino-1-propyne, **2i**	1.5	30	1	>99 (96)	**3i**
9	iodobenzene, **1a**	3-phenyl-1-propyne, **2j**	1.5	30	1	>99 (98)	**3j**
10	iodobenzene, **1a**	propargyl alcohol, **2k**	1.5	50	0.5	>99 (95)	**3k**
11	iodobenzene, **1a**	1-hexyne, **2l**	1.5	50	1	>99 (95)	**3l**

[a]Conversion monitored with HPLC-UV at 210 nm

The presence of electron-withdrawing and electron-donating groups and the nature of the aromatic ring of the iodide (**1b–1g**) did not affect the reactivity, since all different reagents allowed complete conversions to **3b–3g** at 30 °C in 30 min (Table 2.3, entries 1–6).

In contrast, the transformation of differently substituted acetylenes required a modification of the reaction conditions, mainly as a consequence of a variable tendency to afford dimerization and because the electron-donating properties of the alkyl substituents make the acetylene less reactive through the transmetallation step. The cross-coupling of 2-methyl-3-butyn-2-ol **2h** with **1a** resulted in a complete conversion to **3h** under the standard conditions in 1 h (Table 2.3, entry 7). In a similar way, 3-dimethylamino-1-propyne **2i** and 3-phenyl-1-propyne **2j** reacted with **1a** at 30 °C to give **3i** and **3j** in 1 h and 30 min, respectively (Table 2.3, entries 8 and 9). In both cases, an excess of acetylene reagent (1.5 eq) was required to reach >99% conversion.

Propargyl alcohol **2k** and 1-hexyne **2l** showed a lower reactivity and the increase of reaction temperature to 50°C, together with an excess of reagent, was required. Under these conditions, products **3k** and **3l** were obtained in 30 min and 1h, respectively (Table 2.3, entries 10 and 11).

Moving from iodides to aryl bromides, stronger reaction conditions were needed because of the slower oxidative addition of the Ar-Br species. In fact, using the best protocol reported in Table 2.1 (entry 17), bromobenzene **4a** did not react with phenylacetylene **2a** (Table 2.4, entry 1). Satisfactory conversion was observed after 21h at 60°C with an excess of **2a** in the presence of copper (Table 2.4, entry 2), while the copper-free protocol allowed complete conversion to be attained within 14h always at 60°C highlighting the fact that at

higher temperatures and under more drastic conditions the presence of copper can have some drawbacks because it enhances the formation of byproducts (Table 2.4, entry 3). To increase the reaction speed and reach a more efficient protocol in terms of sustainability and turn over number, the inexpensive $Pd(PPh_3)_2Cl_2$ had to be replaced with better performative catalysts such as $Pd(ACN)_2Cl_2$/XPhos or $Pd(DPPF)Cl_2$.

Since its first use in HCS reactions in 2003 by Gelman and Buchwald,[48] Pd catalyst containing XPhos ligand has been reported to give extraordinary results in several applications because of its high electron-donating properties that enhance the rate of the oxidative addition step with more challenging substrates. Complete conversion of **4a** into **3a** was achieved within 2h with $Pd(ACN)_2Cl_2$/XPhos, with or without copper (Table 2.4, entries 4 and 5). The use of $Pd(DPPF)Cl_2$[49] did not produce comparable results, since 98% conversion was observed in the Heck-Cassar copper-free reaction only after 7 h (Table 2.4, entry 7), while the presence of the copper co-catalyst completely inhibited the reaction (Table 2.4, entry 6).[48]

***Table 2.4**: HCS reaction on aryl bromides*

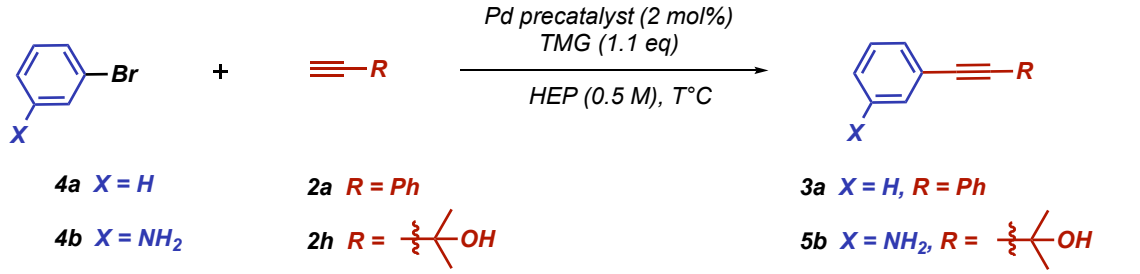

Entry	aryl bromide	alkyne (equiv)	Pd precatalyst	L	CuI mol%	T °C	time h	conversion %[a] (yield %)	product
1	**4a**	**2a** (1.05)	$Pd(PPh_3)_2Cl_2$	-	1	30	21	-	**3a**
2	**4a**	**2a** (3)	$Pd(PPh_3)_2Cl_2$	-	1	60	21	91	**3a**
3	**4a**	**2a** (3)	$Pd(PPh_3)_2Cl_2$	-	-	60	14	>99 (93)	**3a**
4	**4a**	**2a** (3)	$Pd(ACN)_2Cl_2$	XPhos	1	60	2	>99 (95)	**3a**
5	**4a**	**2a** (3)	$Pd(ACN)_2Cl_2$	XPhos	-	60	2	>99 (95)	**3a**
6	**4a**	**2a** (3)	$Pd(DPPF)Cl_2$	-	1	60	7	25	**3a**
7	**4a**	**2a** (3)	$Pd(DPPF)Cl_2$	-	-	60	7	98 (95)	**3a**
8	**4b**	**2h** (3)	$Pd(PPh_3)_2Cl_2$	-	1	60	22	50	**5b**
9	**4b**	**2h** (3)	$Pd(PPh_3)_2Cl_2$	-	-	60	22	95 (80)	**5b**
10	**4b**	**2h** (3)	$Pd(ACN)_2Cl_2$	XPhos	1	80	22	17	**5b**
11	**4b**	**2h** (3)	$Pd(ACN)_2Cl_2$	XPhos	-	60	14	>99 (85)	**5b**
12	**4b**	**2h** (3)	$Pd(DPPF)Cl_2$	-	1	80	22	86	**5b**
13	**4b**	**2h** (3)	$Pd(DPPF)Cl_2$	-	-	60	3	>99 (86)	**5b**

[a]Conversion monitored with HPLC-UV at 210 nm. The product was isolated only when conversion was >95%.
[b]Conversion was 94% after 7h. [c]Yield was calculated after telescoping transformation into **6b**

In order to have a further demonstration of the general applicability of the protocol, we selected an industrially relevant process requiring a Sonogashira reaction step. As an example, the synthesis of an intermediate of the pharmacologically active molecule Erlotinib resulted in being suitable for our scope. Erlotinib hydrochloride is an oral antitumor drug that acts by reversibly and selectively inhibiting epidermal growth factor receptor (EGFR)[50] type 1 tyrosine kinase activity in many types of human cancers affecting lung, pancreas, ovary, kidney, stomach, liver, and breast tissue.

The industrial process for its production (Scheme 2.3),[51–53] requires a HCS reaction to convert 3-bromoaniline **4b** to 3-ethynylaniline **6b**. Thus, the reaction between **4b** and 2-methyl-3-butyn-2-ol **2h** in HEP was studied. As reported in Table 2.4, the $Pd(ACN)_2Cl_2$/XPhos catalytic system allowed to achieve complete conversion into intermediate **5b** only after 14h through a Heck-Cassar copper-free protocol (Table 2.4, entry 11). The comparison of entries 5 and 11 in Table 2.4 shows a decreased efficiency of the Pd catalyst in giving the Erlotinib intermediate **5b** rather than product **3a** from the model reaction between bromobenzene **4a** and phenylacetylene **2a** that allowed a complete conversion in 2h in the same conditions. The reason lies in the fact that the free amine in compound **4b** interferes with the catalyst by decreasing its activity in the Sonogashira reaction.

The best catalytic system for the reaction of **4b** resulted in being $Pd(DPPF)Cl_2$ under copper-free HC conditions, which allowed complete conversion to be attained within 3h (Table 2.4, entry 13).

Finally, intermediate **5b** was not isolated and directly transformed under telescoping conditions with toluene/NaOH to afford product **6b** in 86% yield.

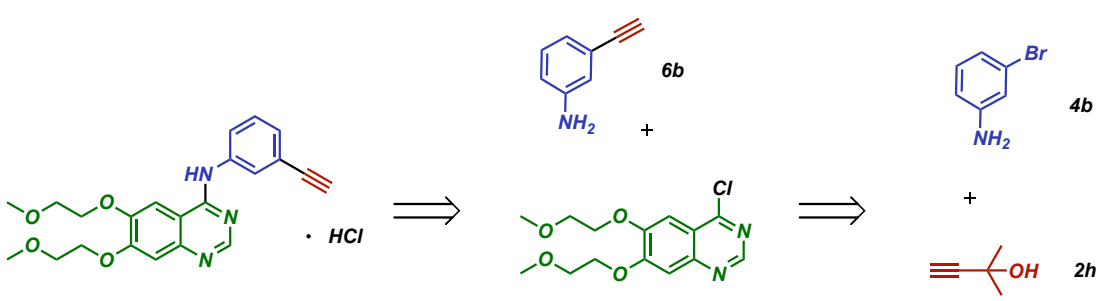

***Scheme 2.3**: Retrosynthetic Approach to the Synthesis of Erlotinib*

2.3 Conclusions

In summary, several green solvents have been tested to replace toxic DMF and NMP in the HCS cross-coupling between aryl halides and substituted acetylenes.

HEP has been shown to be the most suitable candidate, allowing to find mild conditions for poorly reactive alkynes and aryl bromides. The PMIr value of 20 encourages to exploit the solubility and the polarity of HEP to recycle and recover the catalyst and create a completely green and sustainable protocol. The versatility of the solvent is particularly important when complex molecules are synthesized via multistep procedures. The excellent results achieved in the synthesis of an intermediate of the drug Erlotinib encourage the application of HEP on a large scale and in industrial processes.

2.4 Experimental

General information

Commercial reagents (reagent grade, >99%) were used as received without additional purification. Solvents DMF, Cyrene, NBP, NBnP, HEP, NOP, NCP, An, tBuOAc are commercially available and were used after degasification.

^{1}H NMR and ^{13}C NMR spectra were recorded with an Agilent-Technologies-Varian INOVA 400 MHz and 100 MHz instrument $^{1}H/^{19}F/X$ 5 mm PFG ATB Broadband Probe, VT, single, double and triple resonance, z-axis pulsed field gradients, serves broadband probe and customized variable temperature – 5 mm Broadband probe. NMR multiplicities are abbreviated as follows: s = singlet, d = doublet, t = triplet, q = quartet, spt = septet, m = multiplet, bs = broad signal. Coupling constants *J* are given in Hz. All ^{1}H and ^{13}C chemical shifts are calibrated to residual protic-solvents.

HPLC-UV analysis were recorded with an Agilent 1260 InfinityLab instrument. Column: Zorbax® SB-C18; particle size 5 µm; pore size 100 Å; length 250 mm, internal diameter: 4.6 mm. Mobile phase A: H_2O, mobile phase B: ACN. Gradient (Time(min), %B): 0, 30; 8, 80; 22, 80; 24, 10; 30, 10; flow 0.5 mL min^{-1}column temperature 30°C; injection volume: 20 µL.

HPLC-UV analysis of Erlotinib product **5b**: Column:Hypersil BDS C18; particle size 5 µm; length 150 mm, internal diameter: 4.6 mm. Mobile phase A: ACN:MeOH 1:1; Mobile phase

B: H_2O:MeOH 1:1. Gradient (Time(min), %B): 0, 35; 40, 60; 50, 75; 51, 35; 60, 35; flow 1.0 mL min^{-1}; column temperature 25°C; injection volume: 10 µL.

GC-MS analysis were recorded with a Hewlett-Packard 5971 spectrometer with GC injection and EI ionization at 70 eV coupled with an Agilent Technologies MSD1100 single-quadrupole mass spectrometer, reported as: m/z (rel. intensity).

Mass Spectrometry analysis were recorded on a QTRAP 3200 mass spectrometer in ESI^+ mode.

*General procedure for the synthesis of **3a** from **1a***

To an oven-dried 10 mL schlenk purged under N_2 atmosphere, $Pd(PPh_3)_2Cl_2$ (7.0 mg, 0.01 mmol, 2%) and CuI (from 1% to 4%, see entries in Table 2.1), were dissolved in 1 mL of the desired degassed solvent (DMF, Cyrene, NBP, NBnP, HEP, NOP, NCP, An and tBuOAc), (see Table 2.1). The other reagents were then added in the following order: base (TEA or TMG, 0.55 mmol, 1.1 eq, see Table 2.1), iodobenzene **1a** (56 µL, 0.5 mmol, 1.0 eq) and phenylacetylene **2a** (from 1.05 to 1.5 eq, see Table 2.1). The reaction mixture was heated to 30°C with an oil bath and maintained at this temperature under stirring. Samples for HPLC monitoring were taken at set time intervals (30 min, 60 min), after a mini quenching with H_2O and dilution with CH_3CN. Conversions of limiting iodobenzene **1a** into diphenylacetylene **3a** were monitored at set time intervals (30 min, 60 min) through HPLC-UV analysis at 210 nm, after correction with the appropriate RRF (see following section on RRF calculation). In reactions with conversions >99%, after 1 h the mixture was quenched with H_2O (3 mL) and extracted with cyclohexane (3 x 5 mL). The collected organic phases were washed with brine, dried over anhydrous Na_2SO_4 and concentrated under reduced pressure to give a yellow oil, which was purified by flash chromatography (silica gel, 100% cyclohexane) to afford compound **3a** as a white solid (see Table 2.1).

The synthesis of **3a** was optimized using the following conditions: $Pd(PPh_3)_2Cl_2$ (7.0 mg, 0.5 mmol, 2%), CuI (1.0 mg, 0.005 mmol, 1%), TMG (69 µL, 0.55 mmol, 1.1 eq), iodobenzene **1a** (56 µL, 0.5 mmol, 1.0 eq), phenylacetylene **2a** (58 µL, 0.525 mmol, 1.05 eq), HEP (1 mL), 30°C, 30 min (see Entry 17, Table 2.1).

*General procedure for the synthesis of **3b-l** from **1b-l***

To an oven-dried 10 mL schlenk purged under N_2 atmosphere, $Pd(PPh_3)_2Cl_2$ (7.0 mg, 0.01 mmol, 2%) and CuI (1.0 mg, 0.005 mmol, 1%), were dissolved in 1 mL of degassed HEP. The other reagents were then added in the following order: TMG (69 µL, 0.55 mmol, 1.1 eq), aryl iodide (0.5 mmol, 1.0 eq, see entries in Table 2.3) and acetylene (from 1.05 to 1.5 eq, see entries in Table 2.3). The reaction mixture was heated to 30°C or 50°C (according to what reported in Table 2.3) with an oil bath and maintained at this temperature under stirring. Samples for HPLC monitoring were taken at set time intervals (30 min, 60 min), after a mini quenching with H_2O and dilution with CH_3CN. After 1 h, the mixture was quenched with H_2O (3 mL) and extracted with cyclohexane (3 x 5 mL). The collected organic phases were washed with brine, dried over anhydrous Na_2SO_4 and concentrated under reduced pressure to give a yellow oil, which was purified by flash chromatography to afford compounds **3b-l** (see Table 2.3).

*General procedure for the synthesis of **3a** and **5b** from **4a-b***

To an oven-dried 10 mL schlenk purged under N_2 atmosphere, Pd catalyst (0.01 mmol, 2%, see entries in Table 2.4), CuI (1.0 mg, 0.005 mmol, 1%, if specified in Table 2.4) and the desired ligand (0.02 mmol, 4%, if specified in Table 2.4) were dissolved in 1 mL of degassed HEP. The other reagents were then added in the following order: TMG (69 µL, 0.55 mmol, 1.1 eq), aryl bromide **4a** or **4b** (0.5 mmol, 1.0 eq, see entries in Table 2.4) and acetylene **2a** or **2h** (1.5 mmol, 3.0 eq, see entries in Table 2.4). The reaction mixture was heated (see temperatures in Table 2.4) with an oil bath and maintained at this temperature under stirring. Samples for HPLC monitoring were taken at set time intervals (see entries in Table 2.4), after a mini quenching with H_2O and dilution with CH_3CN.

Conversions of limiting bromobenzene **4a** into diphenylacetylene **3a** were monitored at set time intervals through HPLC-UV analysis at 210 nm, after correction with the appropriate RRF (see following section on RRF calculation). In reactions with conversions >99% (see times in Table 2.4), the mixture was quenched with H_2O (3 mL) and extracted with cyclohexane (3 x 5 mL). The collected organic phases were washed with brine, dried over

anhydrous Na_2SO_4 and concentrated under reduced pressure to give a yellow oil, which was purified by flash chromatography (silica gel, 100% cyclohexane) to afford compound **3a**.

Conversions of limiting 3-bromoaniline **4b** into 1-amino-3-ethynyl-benzene **5b** were monitored at set time intervals through HPLC-UV analysis at 210 nm. For reactions with conversions >99% (see Table 2.4), the work-up for compound **5b** was performed in toluene. The collected organic toluene layers were concentrated under reduced pressure to the final volume of 5 mL and NaOH (0.5 mmol, 20 mg) was added and the mixture was refluxed for 3h with an oil bath. The reaction was cooled to rt and washed with water. The organic phase was dried over anhydrous Na_2SO_4. After filtration, the solution was concentrated under reduced pressure to give 1- amino-3-ethynyl-benzene **6b** as a yellowish oil.

The synthesis of **3a** was optimized using the following conditions: $Pd(ACN)_2Cl_2$ (2.6 mg, 0.01 mmol, 2%), XPhos (10 mg, 0.02 mmol, 4%), TMG (69 µL, 0.55 mmol, 1.1 eq), bromobenzene **4a** (52 µL, 0.5 mmol, 1.0 eq), phenylacetylene **2a** (165 µL, 1.5 mmol, 3.0 eq), HEP (1 mL), 60°C, 2h (see Entry 4 Table 2.4).

The synthesis of **5b** was optimized using the following conditions: $Pd(DPPF)Cl_2{\cdot}CH_2Cl_2$ (8.1 mg, 0.01 mmol, 2%), TMG (69 µL, 0.55 mmol, 1.1 eq), 3-bromoaniline **4b** (54 µL, 0.5 mmol, 1.0 eq), 2-methyl-3-butyn-2-ol **2h** (145 µL, 1.5 mmol, 3.0 eq), HEP (1 mL), 60°C, 3h (see Entry 10, Table 2.4).

Compounds characterization

*1,2-diphenylethyne (**3a**)*

White solid (97% yield); Purification by flash chromatography (Cy 100%)

^{1}H NMR (400 MHz, $CDCl_3$) δ (ppm) 7.58 – 7.41 (m, 4H), 7.40 – 7.35 (m, 6H).

^{13}C NMR (100 MHz, $CDCl_3$) δ (ppm) 131.59, 128.33, 128.24, 123.27, 89.37.

Anal. Calcd. for $C_{14}H_{10}$: C, 94.34; H, 5.66; found: C, 94.68; H, 5.65;

GC-MS: m/z: 178 (100 %), 152 (13%), 126 (7%).

*1-nitro-4-(phenylethynyl)benzene (**3b**)*

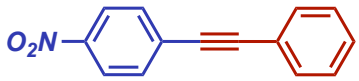

Yellow solid (96% yield); Purification by flash chromatography (Cy 100%)

^{1}H NMR (400 MHz, $CDCl_3$) δ (ppm) 8.19 – 8.17 (m, 2H), 7.64 – 7.62 (m, 2H), 7.56 – 7.53 (m, 2H), 7.38 – 7.36 (m, 3H).

^{13}C NMR (100 MHz, $CDCl_3$) δ (ppm) 146.95, 132.27, 131.84, 130.22, 129.28, 128.57, 123.58, 122.10, 94.75, 87.59.

Anal. Calcd. for $C_{14}H_9NO_2$: C, 75.33; H, 4.06; N, 6.27; found: C, 75.26; H, 4.06; N, 6.27

GC-MS: m/z: 223 (100%), 193 (33%), 176 (83%), 165 (40%), 151 (25%).

*1-nitro-3-(phenylethynyl)benzene (**3c**)*

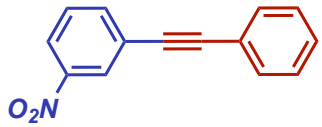

Yellow solid (95% yield); Purification by flash chromatography (Cy 100%)

^{1}H NMR (400 MHz, $CDCl_3$) δ (ppm) 8.36 – 8.35 (m, 1H), 8.17 – 8,15 (d, 1H, J = 8.2 Hz), 7.82 – 7.80 (d, 1H, J = 7.7 Hz), 7.53 – 7.49 (m, 3H), 7.40 – 7.38 (m, 3H).

^{13}C NMR (100 MHz, $CDCl_3$) δ (ppm) 148.11, 137.19, 131.77, 129.35, 129.06, 128.53, 126.28, 125.10, 122.84, 122.19, 91.92, 86.91.

Anal. Calcd. for $C_{14}H_9NO_2$: C, 75.33; H, 4.06; N, 6.27; found: C, 75.14; H, 4.06; N, 6.26.

GC-MS: m/z: 223 (100%), 176 (91%), 165 (10%), 151 (33%)

*1-methoxy-3-(phenylethynyl)benzene (**3d**)*

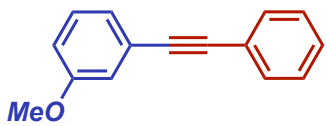

White solid (98% yield); Purification by flash chromatography (Cy/EtOAc = 95/5)

^{1}H NMR (400 MHz, $CDCl_3$) δ (ppm) 7.55 (m, 2H), 7.36 (m, 3H), 7.27 (m, 1H), 7.16 (m, 1H), 7.09 (m, 1H), 6.91 (m, 1H), 3.84 (s, 3H);

^{13}C NMR (100 MHz, CDCl3) δ (ppm) 159.6, 131.4, 129.3, 128.4, 128.3, 124.4, 124.2, 123.0, 116.3, 114.9, 89.3, 89.1.

Anal. Calcd. for $C_{15}H_{12}O$: C, 86.51; H, 5.81; found: C, 86.72; H, 5.81

GC-MS: m/z: 208 (100), 178 (34%), 165 (40%)

*1-methoxy-4-(phenylethynyl)benzene (**3e**)*

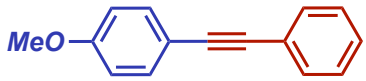

White solid (98% yield); Purification by flash chromatography (Cy/EtOAc = 95/5)

^{1}H NMR (400 MHz, $CDCl_3$) δ (ppm) 7.55 – 7.49 (m, 4H), 7.38 – 7.33 (m, 3H), 6.91 – 6.89 (m, 2H), 3.84 (s, 3H).

^{13}C NMR (100 MHz, $CDCl_3$) δ (ppm) 159.60, 133.03, 131.43, 128.28, 127.90, 123.59, 115.37, 113.98, 89.36, 88.06, 55.27.

Anal. Calcd. for $C_{15}H_{12}O$: C, 86.51; H, 5.81; found: C, 86.72; H, 5.81;

GC-MS: m/z: 208 (100%), 193 (55%), 165 (58%).

*1-chloro-3-(phenylethynyl)benzene (**3f**)*

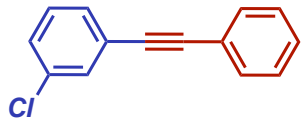

Colourless oil (95% yield); Purification by flash chromatography (Cy 100%)

^{1}H NMR (400 MHz, $CDCl_3$) δ (ppm) 7.55 (m, 3H), 7.42 (m, 1H), 7.37 (m, 3H), 7.30 (m, 2H);

^{13}C NMR (100 MHz, $CDCl_3$) δ (ppm) 134.2, 131.6, 131.3, 129.7, 129.5, 128.9, 128.6, 128.4, 125.0, 122.9, 91.0, 87.8.

Anal. Calcd. for $C_{14}H_9Cl$: C, 79.07; H, 4.27; found: C, 78.83; H, 4.27

GC-MS: m/z: 212 (100), 176 (45%), 151 (17%)

*2-(phenylethynyl)thiophene (**3g**)*

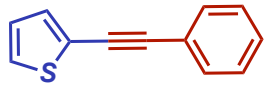

White solid (98% yield); Purification by flash chromatography (Cy/EtOAc = 95/5)

^{1}H NMR (400 MHz, $CDCl_3$) δ (ppm) 7.54 (m, 2H), 7.37 (m, 3H), 7.31 (m, 2H), 7.02 (m, 1H); ^{13}C NMR (100 MHz, $CDCl_3$) δ (ppm) 132.0, 131.1, 128.4, 128.3, 127.2, 127.0, 123.1, 123.0, 93.5, 82.4.

Anal. Calcd. for $C_{12}H_8S$: C, 78.22; H, 4.38; found: C, 78.31; H, 4.39

GC-MS: m/z: 184 (100%), 152 (13%), 139 (23%)

*2-methyl-4-phenylbut-3-yn-2-ol (**3h**)*

Yellow oil (94% yield); Purification by flash chromatography (Cy/EtOAc = 95/5)

^{1}H NMR (400 MHz, $CDCl_3$) δ (ppm) 7.40 (m, 2H), 7.30 (m, 3H), 2.01 (bs, 1H), 1.62 (s, 6H).

^{13}C NMR (100 MHz, $CDCl_3$) δ (ppm) 131.6, 128.3, 128.2, 122.7, 93.9, 82.0, 65.6, 31.4. Anal. Calcd. for $C_{11}H_{12}O$: C, 82.46; H, 7.55; found: C, 82.78; H, 7.54

GC-MS: m/z: 160 (22%), 145 (100%), 129 (10%), 115 (20%)

*N,N-dimethyl-3-phenylprop-2-yn-1-amine (**3i**)*

Colourless liquid (96% yield); Purification by flash chromatography (Cy/EtOAc = 95/5)

^{1}H NMR (400 MHz, $CDCl_3$) δ (ppm) 7.44 (m, 2H), 7.31 (m, 3H), 3.50 (s, 2H), 2.40 (s, 6H). ^{13}C NMR (100 MHz, $CDCl_3$) δ (ppm) 131.8, 128.3, 128.2, 128.1, 85.6, 84.3, 49.0, 44.3. Anal. Calcd. for $C_{11}H_{13}N$: C, 82.97; H, 8.23; N, 8.80; found: C, 82.99; H, 8.22; N, 8.77;

GC-MS: m/z: 159 (75%), 143 (9%), 115 (100%), 89 (15%), 82 (15%).

*prop-1-yne-1,3-diyldibenzene (**3j**)*

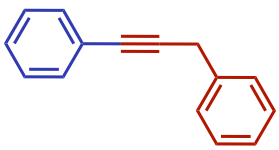

Yellow oil (98% yield); Purification by flash chromatography (Cy 100%)

^{1}H NMR (400 MHz, $CDCl_3$) δ (ppm) 7.45 (m, 4H), 7.31 (m, 6H), 3.84 (s, 2H);

^{13}C NMR (100 MHz, $CDCl_3$) δ (ppm) 136.8, 131.6, 128.7, 128.6, 128.4,128.2, 127.9, 126.4, 123.7, 88.0, 82.7, 25.4.

Anal. Calcd. for $C_{15}H_{12}$: C, 93.71; H, 6.29; found: C, 93.81; H, 6.27

GC-MS: rt 15.8 m/z: 192 (100%), 165 (30%), 115 (15%)

*3-phenylprop-2-yn-1-ol (**3k**)*

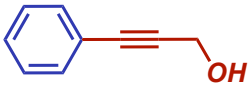

Yellow oil (95% yield); Purification by flash chromatography (Cy/EtOAc = 95/5)

^{1}H NMR (400 MHz, $CDCl_3$) δ (ppm) 7.43 (m, 2H), 7.33 (m, 3H), 4.50 (s, 2H), 1.84 (bs, 1H); ^{13}C NMR (100 MHz, $CDCl_3$) δ (ppm) 131.8, 128.7, 128.4, 122.7, 87.4, 85.6, 51.4.

Anal. Calcd. for C_9H_8O: C, 81.79; H, 6.10; found: C, 81.97; H, 6.09

GC-MS: m/z: 131 (100), 115 (20%), 103 (60%), 77 (53%)

*hex-1-yn-1-ylbenzene (**3l**)*

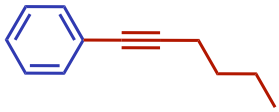

Yellow oil (75 mg, 95% yield);

^{1}H NMR (400 MHz, $CDCl_3$) δ (ppm) 7.39 (m, 2H), 7.26 (m, 3H), 2.41 (t, J = 7.0 Hz, 2H), 1.59 (m, 2H), 1.49 (m, 2H), 0.95 (t, J = 7.3 Hz, 3H);

^{13}C NMR (100 MHz, $CDCl_3$) δ (ppm) 131.5, 128.2, 127.8, 123.0, 89.9, 80.6, 30.6, 22.2, 20.9, 13.4.

Anal. Calcd. for $C_{12}H_{14}$: C, 91.08; H, 8.92; found: C, 91.22; H, 8.92

GC-MS: rt m/z: 158 (26%), 143 (41%), 129 (80%), 115 (100%)

*4-(3-aminophenyl)-2-methylbut-3-yn-2-ol (**5b**)*

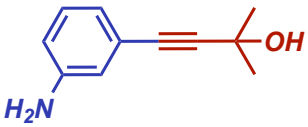

Pale yellow solid (96%); Purification by flash chromatography (Cy/EtOAc = 9/1)

^{1}H NMR (400 MHz, $CDCl_3$) δ (ppm) 7.08 (t, *J* = 7.8 Hz, 1H), 6.83 (d, *J* = 7.6 Hz, 1H), 6.75 (s, 1H), 6.64 (d, *J* = 8.0 Hz, 1H), 3.67 (s, NH_2), 2.21 (s, OH), 1.61 (s, 6H).

^{13}C NMR (100 MHz, $CDCl_3$) δ (ppm) 146.13, 129.15, 123.38, 122.03, 117.91, 115.28, 93.17, 82.26, 65.53, 31.47.

Anal. Calcd for $C_{11}H_{12}NO$: C, 75.40; H, 7.48; N, 7.99; found: C, 75.51; H, 7.42; N, 7.97;

GC-MS: m/z: 175 (65%), 160 (100%), 144 (9%), 132 (14%), 118 (31%).

*1-amino-3-ethynyl-benzene (**6d**)*

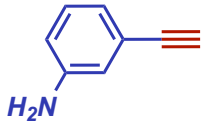

Yellow oil (99%, calculated on the deprotection step); Purification by flash chromatography (Cy/EtOAc = 95/5)

^{1}H NMR (400 MHz, $CDCl_3$) δ 7.11 (t, *J* = 7.8 Hz, 1H), 6.91 (d, *J* = 7.6 Hz, 1H), 6.82 (s, 1H), 6.68 (dd, *J* = 8.0, 1.1 Hz, 1H), 3.69 (s, NH_2), 3.03 (s, 1H).

^{13}C NMR (100 MHz, $CDCl_3$) δ 146.21, 129.23, 122.73, 122.46, 118.28, 115.77, 83.88.

Anal. Calcd for C_8H_7N: C, 82.02; H, 6.02; N, 11.96; found: C, 82.19; H, 6.00; N, 11.96;

GC-MS: 9.42 m/z: 117 (100%), 89 (53%), 74 (8%).

Calculation of the Relative Response Factor (RRF)

In HPLC with UV-DAD, the response of the detector is the absorbance of the compound at a fixed wavelength. Exploiting the Lambert-Beer law, it is possible to evaluate the RRF.

$$A = l \cdot c \cdot \varepsilon$$

Where:

- ε is the molar attenuation coefficient or absorptivity (corresponding to the absorbance of a 1M solution).
- *c* is expressed in molarity (mol/L).

The response factor, in analytical chemistry, is defined as the ratio between the molar concentration of a compound being analyzed and the response of the detector to that compound. In this way, the calculation of RRF is described below:

$$\text{Response Factor (RF)} = \frac{\text{Peak Area}}{\text{Concentration (M)}}$$

Thus, considering two substances in which one is the product (B) and the second is the reagent (A), the RRF is:

$$RF = \frac{RF_A}{RF_B} = \frac{\text{Peak Area}_A / \text{Concentration}_A}{\text{Peak Area}_B / \text{Concentration}_B} = \frac{\text{Peak Area}_A}{\text{Peak Area}_B} \cdot \frac{\text{Concentration}_A}{\text{Concentration}_B}$$

*RRF between iodobenzene **1a** and diphenylacetylene **3a***

***Table S2.1**: Calculation of iodobenzene RRF at several concentrations*

Concentration (M)	Iodobenzene area (mAu)	Diphenylacetylene (mAu)	RRF	Δ_{RRF}
0.0025	34305.7	84178.0	2.45	**3.05**
0.0005	7315.2	22370.1	2.06	
0.00025	3682.1	11189.9	3.04	
0.000025	365.5	1121.3	3.07	

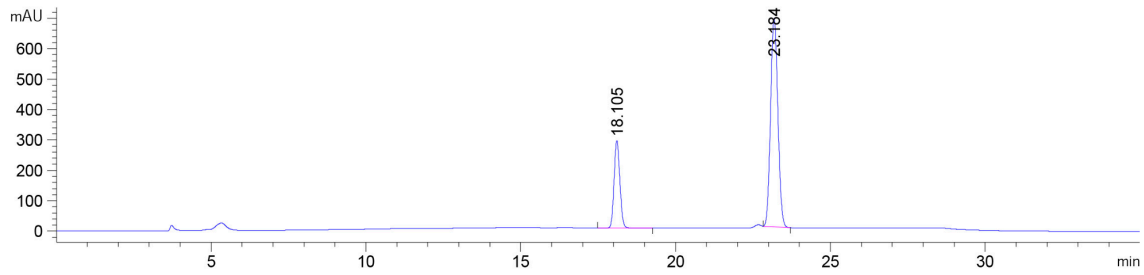

***Figure S2.1**: HPLC-UV spectrum of equimolar mixture of iodobenzene **1a** and diphenylacetylene **3a** at 0.0005 M concentration*

*RRF between bromobenzene **4a** and diphenylacetylene **3a***

***Table S2.2**: Calculation of bromobenzene RRF at several concentrations*

Concentration (M)	Bromobenzene area (mAu)	Diphenylacetylene (mAu)	RRF	Δ_{RRF}
0.0025	39286.7	8557.5	2.18	**2.68**
0.0005	8516.1	22536.4	2.65	
0.00025	4240.3	11310.3	2.67	
0.000025	418.1	1138.9	2.72	

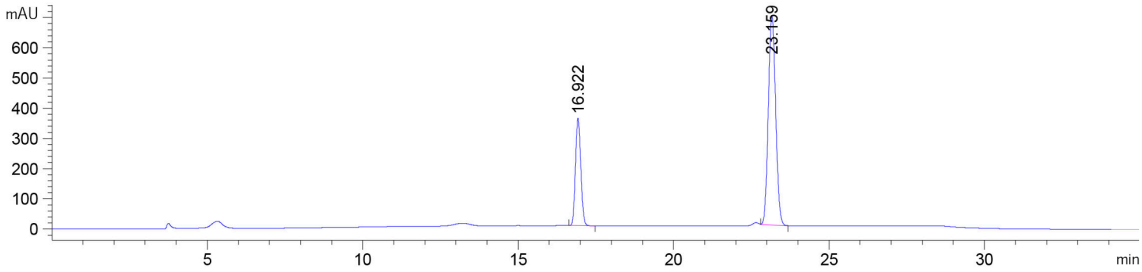

***Figure S2.2**: HPLC-UV spectrum of equimolar mixture of bromobenzene **4a** and diphenylacetylene **3a** at 0.0005 M concentration*

Calculation of PMI and E-Factor

The calculation of the green metrics (Chapter 1) parameters was performed on the model reaction between iodobenzene **1a** and phenylacetylene **2a** applying the optimized conditions described above with 10 mmol scale and considering 1M concentration. After the work up, HEP and cyclohexane were recovered through distillation giving crude product **3a**

***Table S2.3**: PMI and E-Factor calculations on the model reaction performed with 10 mmol scale*

Reagents	Quantities (g)[c]	Quantities with recovery (g)	Recovery %
Iodobenzene **1a**	2.0	2.0	-
Phenylacetylene **2a**	1.0	1.0	-
TMG	1.2	1.2	-
$Pd(PPh_3)_2Cl_2$	0.14	0.14	-
CuI	0.02	0.02	-
HEP	11.4	1.1	90
Water	30	30	-
Cyclohexane	23.3	1.2	95
Diphenylacetylene **3a**	1.75	1.75	-
PMI[a]	40	-	
PMIr[b]	-	21	
EF[b]	-	3.8	

[a]PMI calculated considering all the reagents used. [b]PMI and EF calculated considering the 90% of recovery of HEP and 95% of recovery of cyclohexane. [c]Reaction performed using 1M of concentration

In vitro metabolism of NMP and HEP

Reagents. Pooled Wistar rat liver microsomes (RLM, pooled from 50 donors) and Xtreme human liver microsomes (HLM, pooled from 200 donors) were purchased from Xenotech, LLC (Cambridge, USA). Glucose-6-phosphate, β-nicotinamide adenine dinucleotide phosphate ($NADP^+$), magnesium chloride, glucose-6-phosphate-dehydrogenase were purchased from Sigma-Aldrich (St. Louis, USA). 85% formic acid was provided by ACEF Spa (Piacenza, Italy); LC-grade acetonitrile (ACN) was supplied by Sigma Aldrich (Milan, Italy). Ultra-pure Millipore water was prepared by Milli-Q purification system (Millipore Corp., Bedford, MA, USA) and employed for LC mobile phase and sample preparations. All other chemicals and reagents were of analytical grade and commercially available.

LC-HRMS analytical conditions for NMP and HEP metabolite profiling. LC-HRMS analyses were carried out on a Thermo LTQ-Orbitrap mass spectrometer (Thermo, USA) interfaced to a Dionex Ultimate 3000 LC system (Thermo, USA) through an electrospray ionization (ESI) source. HILIC chromatographic separation occurred on a Waters BEH Amide column

(150 x 2.1 mm, 1.7 μm particle size). Mobile phases consisted of 0.2% formic acid in water (A) and acetonitrile (B) with a linear gradient as follows: 0 min 99%B, 0–10 min 99-90% B, 10–15 min 90–10% B, 15–20 min 10% B, 20-21 min 99% B, 21-30 min 99%B. The flow rate was 0.20 ml/min. ESI source was operated in positive and negative ion mode with the optimized source parameters as follows: capillary voltage 3.0 kV (ESI^+) 2.1 kV (ESI^-); capillary temperature 275°C; sheath gas (nitrogen gas) flow rate 20 arb; auxiliary gas (nitrogen gas) flow rate 5 arb. The data were obtained in the mass range of m/z 50–300 with resolution of 60,000 FWHM. The collision energy was set at 35 V for obtaining the MS/MS spectra. Xcalibur software (Version 2.3.1, Thermo Fisher Scientific, USA) was employed for instrument control and data acquisition and processing

LC-ESI-MS/MS analytical conditions for NMP and HEP metabolic stability assays. An Accela UHPLC system (Thermo, USA), equipped with a Phenomenex Luna HILIC column (2.0 x 100 mm, 3 μm; Phenomenex, USA) was employed for LC-ESI-MS/MS analysis in multiple reaction monitoring acquisition mode (MRM). Mobile phases A and B were acetonitrile and ultra-pure water respectively, both containing 0.1% v/v formic acid. The following gradient was applied for elution: 95% A between 0 and 0.5 min; linear gradient to 50% A to 7 min; returning to 95% A in 1 min with 7-min reconditioning time. Total run time: 16 min. The flow rate was maintained at 0.28 ml/min and injection volume was 10 μL. A TSQ Quantum Access Max Triple Quadrupole mass spectrometer (Thermo, USA), equipped with a heated electrospray (H-ESI) ion source, was employed for compound detection. All analyses were performed by setting ion source voltage at 4000 V and capillary temperature at 270 °C. Nitrogen served both as sheath and auxiliary gas at 35 psi and 15 psi, respectively; argon with a pressure of 1.5 mtorr was employed as collision gas. ESI ion source operated in positive ion mode (ESI^+). Tube lens voltages (TL) and collision energies (CE) for each parent-product ion transition were optimized by Flow Injection Analysis (FIA) of 10 μM solutions in MeOH. NMP: m/z = 100.1 $[M+H]^+ \rightarrow$ m/z = 69.3, 58.4, 41.6 [Tube Lens (TL) = 59 V; Collision Energies (CE) = 16, 22, 32 eV, respectively); HEP: m/z = 130.1 $[M+H]^+ \rightarrow$ m/z = 112.2, 84.3, 69.2 (TL = 52 V; CE = 8, 14, 15 eV). Xcalibur software version 2.2 (Thermo, USA) was employed for both data acquisition and processing.

Table S2.4: *NMP, HEP and their metabolites identified in rat (RLM) and human liver microsomes (HLM) by LC-HRMS.*

Compound ID	Formula	RT min	Ion	Calculated mass (m/z)	Observed mass (m/z)	Mass error (ppm)	MS/MS fragments	Metabolic pathway
NMP	$C_5H_{10}NO$	-	$[M+H]^+$	100.0757	100.0755	-1.6	82.0, 69.1, 71.2	-
5-HNMP	$C_5H_{10}NO_2$	3.33	$[M+H]^+$	116.0706	116.0704	-1.6	98.1, 85.1	hydroxylation
2-P	C_4H_8NO	3.41	$[M+H]^+$	86.0600	86.0599	-1.2	-	N-demethylation
HEP	$C_6H_{12}NO_2$	3.78	$[M+H]^+$	130.0863	130.0861	-1.1	112.1, 84.1, 69.1	-
HEP-COOH	$C_6H_{10}NO_3$	4.14	$[M+H]^+$	144.0655	144.0656	0.8	126.0, 88.0, 83.2	-OH→-COOH

2.5 References

(1) Huang, W.-S.; Metcalf, C. A.; Sundaramoorthi, R.; Wang, Y.; Zou, D.; Thomas, R. M.; Zhu, X.; Cai, L.; Wen, D.; Liu, S.; Romero, J.; Qi, J.; Chen, I.; Banda, G.; Lentini, S. P.; Das, S.; Xu, Q.; Keats, J.; Wang, F.; Wardwell, S.; Ning, Y.; Snodgrass, J. T.; Broudy, M. I.; Russian, K.; Zhou, T.; Commodore, L.; Narasimhan, N. I.; Mohemmad, Q. K.; Iuliucci, J.; Rivera, V. M.; Dalgarno, D. C.; Sawyer, T. K.; Clackson, T.; Shakespeare, W. C. Discovery of 3-[2-(Imidazo[1,2-]Pyridazin-3-Yl)Ethynyl]-4-Methyl -{4-[(4-Methylpiperazin-1-Yl)Methyl]-3-(Trifluoromethyl)Phenyl}benzamide (AP24534), a Potent, Orally Active Pan-Inhibitor of Breakpoint Cluster Region-Abelson (BCR-ABL) Kinase Including the T315I Gatekeeper Mutant. *J. Med. Chem.* **2010**, *53* (12), 4701–4719. https://doi.org/10.1021/jm100395q.

(2) Dong, Z.; Huang, W. S.; Thomas, R. M.; Romero, J. A. C.; Qi, J.; Wang, Y.; Zhu, X.; Shakespeare, W. C.; Sundaramoorthi, R.; Metcalf, C. A.; Dalgarno, D. A.; Awyer, T. K. Substituted Acetylenic Pyrazolo[1,5-a]Pyrimidines as Kinase Inhibitors. US9278971, 2016.

(3) Handa, S.; Jin, B.; Bora, P. P.; Wang, Y.; Zhang, X.; Gallou, F.; Reilly, J.; Lipshutz, B. H. Sonogashira Couplings Catalyzed by Fe Nanoparticles Containing Ppm Levels of Reusable Pd, under Mild Aqueous Micellar Conditions. *ACS Catal.* **2019**, *9* (3), 2423–2431. https://doi.org/10.1021/acscatal.9b00007.

(4) Cabri, W.; Oldani, E. Process for the Industrial Preparation of Aminoacetylenes. US5902902, 1999.

(5) Caporale, A.; Tartaggia, S.; Castellin, A.; de Lucchi, O. Practical Synthesis of Aryl-2-Methyl-3-Butyn-2-Ols from Aryl Bromides via Conventional and Decarboxylative Copper-Free Sonogashira Coupling Reactions. *Beilstein J. Org. Chem.* **2014**, *10*, 384–393. https://doi.org/10.3762/bjoc.10.36.

(6) Chandraratna, R. Disubstituted Acetylenes Bearing Heteroaromatic and Heterobicyclic Groups Having Retinoid like Activity. US5602130, 1997.

(7) Frigoli, S.; Fuganti, C.; Malpezzi, L.; Serra, S. A Practical and Efficient Process for the Preparation of Tazarotene. *Org. Process Res. Dev.* **2005**, *9* (5), 646–650. https://doi.org/10.1021/op050080x.

(8) Hughes, D. L. Patent Review of Manufacturing Routes to Recently Approved Oncology Drugs: Ibrutinib, Cobimetinib, and Alectinib. *Org. Process Res. Dev.* **2016**, *20* (11), 1855–1869. https://doi.org/10.1021/acs.oprd.6b00304.

(9) Cooke, J. W. B.; Bright, R.; Coleman, M. J.; Jenkins, K. P. Process Research and Development of a Dihydropyrimidine Dehydrogenase Inactivator: Large-Scale

Preparation of Eniluracil Using a Sonogashira Coupling. *Org. Process Res. Dev.* **2001**, *5* (4), 383–386. https://doi.org/10.1021/op0100100.

(10) Veleva, V. R.; Cue, B. W.; Todorova, S. Benchmarking Green Chemistry Adoption by the Global Pharmaceutical Supply Chain. *ACS Sustain. Chem. Eng.* **2018**, *6* (1), 2–14. https://doi.org/10.1021/acssuschemeng.7b02277.

(11) Clarke, C. J.; Tu, W.-C.; Levers, O.; Bröhl, A.; Hallett, J. P. Green and Sustainable Solvents in Chemical Processes. *Chem. Rev.* **2018**, *118* (2), 747–800. https://doi.org/10.1021/acs.chemrev.7b00571.

(12) Hooshmand, S. E.; Afshari, R.; Ramón, D. J.; Varma, R. S. Deep Eutectic Solvents: Cutting-Edge Applications in Cross-Coupling Reactions. *Green Chem.* **2020**, *22* (12), 3668–3692. https://doi.org/10.1039/D0GC01494J.

(13) Byrne, F. P.; Jin, S.; Paggiola, G.; Petchey, T. H. M.; Clark, J. H.; Farmer, T. J.; Hunt, A. J.; Robert McElroy, C.; Sherwood, J. Tools and Techniques for Solvent Selection: Green Solvent Selection Guides. *Sustain. Chem. Process.* **2016**, *4* (1), 7. https://doi.org/10.1186/s40508-016-0051-z.

(14) Cicco, L.; Dilauro, G.; Perna, F. M.; Vitale, P.; Capriati, V. Advances in Deep Eutectic Solvents and Water: Applications in Metal- and Biocatalyzed Processes, in the Synthesis of APIs, and Other Biologically Active Compounds. *Org. Biomol. Chem.* **2021**, *19* (12), 2558–2577. https://doi.org/10.1039/D0OB02491K.

(15) Dyson, P. J.; Jessop, P. G. Solvent Effects in Catalysis: Rational Improvements of Catalysts via Manipulation of Solvent Interactions. *Catal. Sci. Technol.* **2016**, *6* (10), 3302–3316. https://doi.org/10.1039/C5CY02197A.

(16) Sherwood, J.; Clark, J. H.; Fairlamb, I. J. S.; Slattery, J. M. Solvent Effects in Palladium Catalysed Cross-Coupling Reactions. *Green Chem.* **2019**, *21* (9), 2164–2213. https://doi.org/10.1039/C9GC00617F.

(17) Https://Database.Ich.Org/Sites/Default/Files/Q3D-R2_Guideline_Step4_2022_0308.

(18) Wilson, K. L.; Kennedy, A. R.; Murray, J.; Greatrex, B.; Jamieson, C.; Watson, A. J. B. Scope and Limitations of a DMF Bio-Alternative within Sonogashira Cross-Coupling and Cacchi-Type Annulation. *Beilstein J. Org. Chem.* **2016**, *12*, 2005–2011. https://doi.org/10.3762/bjoc.12.187.

(19) Kim, T. H.; Kim, S. G. Clinical Outcomes of Occupational Exposure to N,N-Dimethylformamide: Perspectives from Experimental Toxicology. *Saf. Health Work* **2011**, *2* (2), 97–104. https://doi.org/10.5491/SHAW.2011.2.2.97.

(20) European Medicinal Agency (EMA): & Committee for Medicinal Products for Human Use (CHMP). Assessment Report: Nitrosamine Impurities in Human Medicinal Products. (2020).

(21) Schilz, M.; Plenio, H. A Guide to Sonogashira Cross-Coupling Reactions: The Influence of Substituents in Aryl Bromides, Acetylenes, and Phosphines. *J. Org. Chem.* **2012**, *77* (6), 2798–2807. https://doi.org/10.1021/jo202644g.

(22) Chinchilla, R.; Nájera, C. The Sonogashira Reaction: A Booming Methodology in Synthetic Organic Chemistry. *Chem. Rev.* **2007**, *107* (3), 874–922. https://doi.org/10.1021/cr050992x.

(23) Chinchilla, R.; Nájera, C. Recent Advances in Sonogashira Reactions. *Chem Soc Rev* **2011**, *40* (10), 5084. https://doi.org/10.1039/c1cs15071e.

(24) Alonso, D.; Baeza, A.; Chinchilla, R.; Gómez, C.; Guillena, G.; Pastor, I.; Ramón, D. Solid-Supported Palladium Catalysts in Sonogashira Reactions: Recent Developments. *Catalysts* **2018**, *8* (5), 202. https://doi.org/10.3390/catal8050202.

(25) Amelio, A.; Genduso, G.; Vreysen, S.; Luis, P.; van der Bruggen, B. Guidelines Based on Life Cycle Assessment for Solvent Selection during the Process Design and Evaluation of Treatment Alternatives. *Green Chem.* **2014**, *16* (6), 3045–3063. https://doi.org/10.1039/C3GC42513D.

(26) Benazzouz, A.; Moity, L.; Pierlot, C.; Sergent, M.; Molinier, V.; Aubry, J.-M. Selection of a Greener Set of Solvents Evenly Spread in the Hansen Space by Space-Filling Design. *Ind. Eng. Chem. Res.* **2013**, *52* (47), 16585–16597. https://doi.org/10.1021/ie402410w.

(27) Prat, D.; Pardigon, O.; Flemming, H.-W.; Letestu, S.; Ducandas, V.; Isnard, P.; Guntrum, E.; Senac, T.; Ruisseau, S.; Cruciani, P.; Hosek, P. Sanofi's Solvent Selection Guide: A Step Toward More Sustainable Processes. *Org. Process Res. Dev.* **2013**, *17* (12), 1517–1525. https://doi.org/10.1021/op4002565.

(28) Prat, D.; Hayler, J.; Wells, A. A Survey of Solvent Selection Guides. *Green Chem.* **2014**, *16* (10), 4546–4551. https://doi.org/10.1039/C4GC01149J.

(29) Srinivas Reddy, A.; Laali, K. K. Sonogashira Cross-Coupling in a Designer Ionic Liquid (IL) without Copper, External Base, or Additive, and with Recycling and Reuse of the IL. *Tetrahedron Lett.* **2015**, *56* (33), 4807–4810. https://doi.org/10.1016/j.tetlet.2015.06.067.

(30) Hervé, G.; Len, C. Heck and Sonogashira Couplings in Aqueous Media – Application to Unprotected Nucleosides and Nucleotides. *Sustain. Chem. Process.* **2015**, *3* (1), 3. https://doi.org/10.1186/s40508-015-0029-2.

(31) Wilson, K.; Murray, J.; Sneddon, H.; Jamieson, C.; Watson, A. Dimethylisosorbide (DMI) as a Bio-Derived Solvent for Pd-Catalyzed Cross-Coupling Reactions. *Synlett* **2018**, *29* (17), 2293–2297. https://doi.org/10.1055/s-0037-1611054.

(32) Strappaveccia, G.; Luciani, L.; Bartollini, E.; Marrocchi, A.; Pizzo, F.; Vaccaro, L. γ-Valerolactone as an Alternative Biomass-Derived Medium for the Sonogashira Reaction. *Green Chem.* **2015**, *17* (2), 1071–1076. https://doi.org/10.1039/C4GC01728E.

(33) Camp, J. E. Bio-Available Solvent Cyrene: Synthesis, Derivatization, and Applications. *ChemSusChem* **2018**, *11* (18), 3048–3055. https://doi.org/10.1002/cssc.201801420.

(34) *https://echa.europa.eu/it/*.

(35) Yoneto, K.; Ghanem, A.; Higuchi, W. I.; Peck, K. D.; Kevin Li, S. Mechanistic Studies of the 1-Alkyl-2-pyrrolidones as Skin Permeation Enhancers. *J. Pharm. Sci.* **1995**, *84* (3), 312–317. https://doi.org/10.1002/jps.2600840310.

(36) Sherwood, J.; Parker, H. L.; Moonen, K.; Farmer, T. J.; Hunt, A. J. N-Butylpyrrolidinone as a Dipolar Aprotic Solvent for Organic Synthesis. *Green Chem.* **2016**, *18* (14), 3990–3996. https://doi.org/10.1039/C6GC00932H.

(37) Ferrazzano, L.; Corbisiero, D.; Martelli, G.; Tolomelli, A.; Viola, A.; Ricci, A.; Cabri, W. Green Solvent Mixtures for Solid-Phase Peptide Synthesis: A Dimethylformamide-Free Highly Efficient Synthesis of Pharmaceutical-Grade Peptides. *ACS Sustain. Chem. Eng.* **2019**, *7* (15), 12867–12877. https://doi.org/10.1021/acssuschemeng.9b01766.

(38) Alder, C. M.; Hayler, J. D.; Henderson, R. K.; Redman, A. M.; Shukla, L.; Shuster, L. E.; Sneddon, H. F. Updating and Further Expanding GSK's Solvent Sustainability Guide. *Green Chem.* **2016**, *18* (13), 3879–3890. https://doi.org/10.1039/C6GC00611F.

(39) Haus, M. O.; Louven, Y.; Palkovits, R. Extending the Chemical Product Tree: A Novel Value Chain for the Production of N-Vinyl-2-Pyrrolidones from Biogenic Acids. *Green Chem.* **2019**, *21* (23), 6268–6276. https://doi.org/10.1039/C9GC01488H.
(40) *https://echa.europa.eu/it/registration-dossi- er/-/registered-dossier/13179*.
(41) Kim, T. H.; Kim, S. G. Clinical Outcomes of Occupational Exposure to N,N-Dimethylformamide: Perspectives from Experimental Toxicology. *Saf. Health Work* **2011**, *2* (2), 97–104. https://doi.org/10.5491/SHAW.2011.2.2.97.
(42) *https://echa.europa.eu/it/registration-dossi- er/-/registered-dossier/13179*.
(43) Carnerup, M. A.; Spanne, M.; Jönsson, B. A. G. Levels of N-Methyl-2-Pyrrolidone (NMP) and Its Metabolites in Plasma and Urine from Volunteers after Experimental Exposure to NMP in Dry and Humid Air. *Toxicol. Lett.* **2006**, *162* (2–3), 139–145. https://doi.org/10.1016/j.toxlet.2005.09.035.
(44) Wells, D. A.; Digenis, G. A. Disposition and Metabolism of Double-Labeled [3H and 14C] N-Methyl-2-Pyrrolidinone in the Rat. *Drug Metab. Dispos.* **1988**, *16* (2), 243–249.
(45) Wells, D. A.; Hawi, A. A.; Digenis, G. A. Isolation and Identification of the Major Urinary Metabolite of N-Methylpyrrolidinone in the Rat. *Drug Metab.Dispos.* **1992**, *20*, 124–126.
(46) Akesson, B.; Jönsson, B. A. Major Metabolic Pathway for N-Methyl-2-Pyrrolidone in Humans. *Drug Metab. Dispos.* **1997**, *25* (2), 267–269.
(47) Carnerup, M. A.; Saillenfait, A. M.; Jönsson, B. A. G. Concentrations of N-Methyl-2-Pyrrolidone (NMP) and Its Metabolites in Plasma and Urine Following Oral Administration of NMP to Rats. *Food Chem. Toxicol.* **2005**, *43* (9), 1441–1447. https://doi.org/10.1016/j.fct.2005.04.007.
(48) Gelman, D.; Buchwald, S. L. Efficient Palladium-Catalyzed Coupling of Aryl Chlorides and Tosylates with Terminal Alkynes: Use of a Copper Cocatalyst Inhibits the Reaction. *Angew. Chem., Int. Ed.* **2003**, *42* (48), 5993–5996. https://doi.org/10.1002/anie.200353015.
(49) Moon, J.; Jeong, M.; Nam, H.; Ju, J.; Moon, J. H.; Jung, H. M.; Lee, S. One-Pot Synthesis of Diarylalkynes Using Palladium-Catalyzed Sonogashira Reaction and Decarboxylative Coupling of Sp Carbon and sp^2 Carbon. *Org. Lett.* **2008**, *10* (5), 945–948. https://doi.org/10.1021/ol703130y.
(50) Ling, Y.-H.; Li, T.; Yuan, Z.; Haigentz, M.; Weber, T. K.; Perez-Soler, R. Erlotinib, an Effective Epidermal Growth Factor Receptor Tyrosine Kinase Inhibitor, Induces P27KIP1 up-Regulation and Nuclear Translocation in Association with Cell Growth Inhibition and G1/S Phase Arrest in Human Non-Small-Cell Lung Cancer Cell Lines. *Mol. Pharmacol.* **2007**, *72* (2), 248–258. https://doi.org/10.1124/mol.107.034827.
(51) Tucker, C. E.; de Vries, J. G. *Homogeneous Catalysis for the Production of Fine Chemicals. Palladium-and Nickel-Catalysed Aromatic Carbon-Carbon Bond Formation*; 2002; Vol. 19.
(52) Caporale, A.; Tartaggia, S.; Castellin, A.; de Lucchi, O. Practical Synthesis of Aryl-2-Methyl-3-Butyn-2-Ols from Aryl Bromides via Conventional and Decarboxylative Copper-Free Sonogashira Coupling Reactions. *Beilstein J. Org. Chem.* **2014**, *10*, 384–393. https://doi.org/10.3762/bjoc.10.36.
(53) Cabri, W.; Oldani, E. U.S. Patent No. 5,902,902, 1999.

Chapter 3:

Palladium Catalyst Recycling for Heck-Cassar-Sonogashira Cross-Coupling in Green Solvent/Base Blend

3.1 Introduction

Catalysis has been listed by the fathers of green chemistry as a fundamental tool to shift the paradigm of chemical processes from classical to sustainable methodologies.[1,2] Green metrics parameters can rapidly reveal that the use of stoichiometric technologies and large volume of solvents are the primary source of concern regarding waste output (Chapter 1.4). We have already contributed with our preliminary results on the use of several green solvents for the HCS coupling, namely, N-octylpyrrolidone (NOP), N-benzylpyrrolidone (NBnP), N-cyclohexylpyrrolidone (NCP), N-hydroxyethylpyrrolidone (HEP), anisole (An), and tert-butyl acetate (tBuOAc).[3] However, with the exception of Lipshutz's micellar approach in water [Turnover number (TON) of 1740; Turnover frequency (TOF) of 217 h^{-1}; Process mass intensity (PMI) of 15],[4] the amount of catalyst used in green alternative solvents, the reaction conditions, yields and PMI are not in line with the design of versatile, efficient, green, sustainable, and low-cost reactions.[5–10] In addition, the metal must be readily separated and removed from the product, especially for pharmaceutical applications, since the International Conference of Harmonization Guidelines Q3D (ICH Q3D) set very low limits for elemental impurities in medicines.[11] Consequently, there is a need for a user-friendly, sustainable, efficient, and flexible protocol for the Heck-Cassar-Sonogashira (HCS) cross-coupling that could be easily used by chemists and easily optimized to design an industrial process. Finally, the identification of recycling and recovering conditions for the palladium catalysts remains a key goal to decrease costs while increasing reaction greenness and industrial potential.[12]

The target of this study was the identification of a flexible and sustainable procedure that can be applied in parallel synthesis for drug discovery and that allows to easily optimize the reaction conditions in order to achieve high yields, high TON/TOF values and competitive PMI recalculated considering solvent, base, and palladium recovery.

3.2 Results and discussion

In Chapter 2, an efficient HCS protocol based on the use of 2 mol% of $Pd(PPh_3)_2Cl_2$ as pre-catalyst, 1 mol% of CuI as co-catalyst, and N,N,N,N-tetramethyl guanidine (TMG)[13] as base in several green and biogenic solvents was described.[3] Among them, HEP in combination with TMG showed the best performance in terms of reaction time and yield.

In order to create a completely green protocol, we decided to exploit the solubility and polarity of HEP to recycle and recover the catalyst in the HCS cross coupling process. It was seen in fact that, by adding a certain percentage of water, the solvent formed a perfect separation with various organic solvents. To achieve our purpose, we had to substitute the common $Pd(PPh_3)_2Cl_2$ catalyst and use phosphine ligands that could transfer the catalyst in the HEP/H_2O phase.

Hence, with the aim to identify the best reaction conditions to recycle the catalyst with different substrates, the effect of water using simple and commercially available sulfonated phosphines as ligands was explored.[14] The model reaction between phenylacetylene **2** and aryl derivatives **1a–c** was performed in HEP using TMG as organic base, following both the Heck-Cassar and the Sonogashira protocols (Chapter 1.5) with Pd^{II} pre-catalysts. The beneficial effect of TMG to the HCS coupling can be ascribed to its very high pKa (15.2 in water and 23.3 in acetonitrile)[15] that favors a rapid rearrangement from a π to a σ complex between the alkyne and the metal, generating complex **C** (Figure 3.3, Pd cycle I) in the copper-free protocol and the suitable species for the transmetalation step in the Pd/Cu cycle (Chapter 1.5).

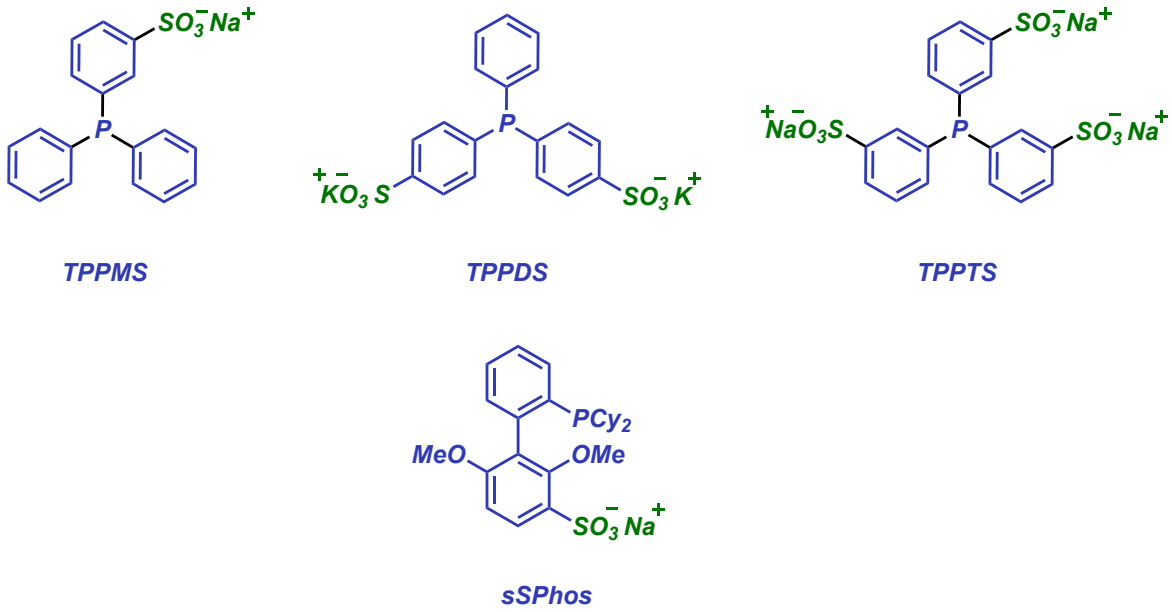

***Figure 3.2**: Sulfonated phosphines used in the HCS coupling*

The coupling between phenylacetylene **2** and **1a–c** was studied as a model reaction in order to identify the optimal conditions (concentration, cocatalyst, temperature, and stoichiometry) to be used in the recycling protocols. The results reported in Table 3.1 showed that using the Sonogashira conditions, the conversion was always complete within 1h, independently from the presence of water and from the nature of the phosphine (entries 1–5). The study was focused on readily available sulfonated ligands (Figure 3.2), namely sodium 3-(diphenylphosphino)benzenesulfonic acid sodium salt (TPPMS), 4,4'-(phenylphosphinidene)bis(benzenesulfonic acid) dipotassium salt hydrate (TPPDS), and 3,3',3''-phosphanetriyltris-(benzenesulfonic acid) trisodium salt (TPPTS). Since TPPTS is the cheapest and largely available water-soluble phosphine, being employed in the biphasic hydroformylation with rhodium catalysts (Ruhrchemie/Rhône-Poulenc process),[16,17] and it induces a faster conversion using only 5 % excess of **2** (entry 3), we did not consider TPPMS and TPPDS for further studies. Interestingly, the Sonogashira coupling still provided excellent results decreasing the CuI cocatalyst amount down to 0.1 mol% (entries 6 and 7). In addition, the reactions performed with CuI, CuBr, and CuCl gave comparable results (entries 6–9). The Pd^0/TPPTS catalyst proved to be efficient even in the absence of CuI, being able to smoothly generate diphenylacetylene **3** at 60°C in 1h (Entry 10) and at 30 °C in 14h (entry 11). However, the process can be accelerated by increasing the amount of acetylene (entry 12).

***Table 3.1**: Screening of HCS cross-coupling in HEP/TMG/H_2O system*

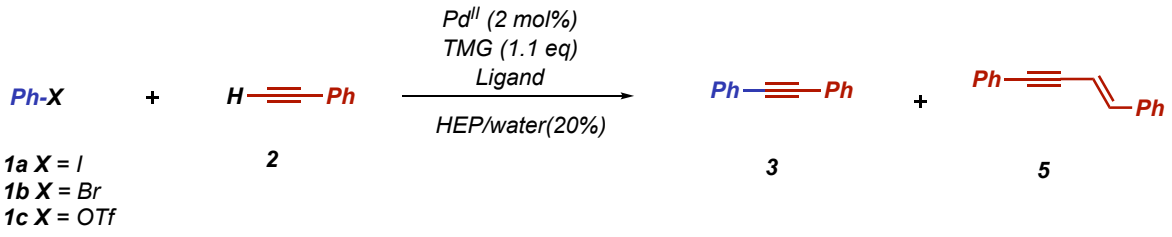

Entry	**1**	**2** equiv	Pd^{II}	Ligand (mol%)	CuX (mol%)	T °C	t h	Conv %[a] (yield %)[b]	**3**/**5**[a]
1	**1a**	1.05	$Pd(PPh_3)_2Cl_2$	-	CuI (1)	30	0.5	>99 (97)[c]	>99/1
2	**1a**	1.05	$Pd(PPh_3)_2Cl_2$	-	CuI (1)	30	0.5	>99 (95)	>99/1
3	**1a**	1.05	$Pd(ACN)_2Cl_2$	TPPTS (4)	CuI (1)	30	0.5	>99 (95)[d]	>99/1
4	**1a**	1.05	$Pd(ACN)_2Cl_2$	TPPMS (4)	CuI (1)	30	1	>99 (92)	>99/1
5	**1a**	1.5	$Pd(ACN)_2Cl_2$	TPPDS (4)	CuI (1)	30	1	>99 (95)	>99/1
6	**1a**	1.05	$Pd(ACN)_2Cl_2$	TPPTS (4)	CuI (0.25)	30	0.5	>99 (93)	>99/1
7	**1a**	1.05	$Pd(ACN)_2Cl_2$	TPPTS (4)	CuI (0.1)	30	1	>99 (95)	>99/1
8	**1a**	1.05	$Pd(ACN)_2Cl_2$	TPPTS (4)	CuBr (0.25)	30	0.5	>99 (95)	>99/1
9	**1a**	1.05	$Pd(ACN)_2Cl_2$	TPPTS (4)	CuCl (0.25)	30	0.5	>99 (92)	>99/1
10	**1a**	1.05	$Pd(ACN)_2Cl_2$	TPPTS (4)	-	60	1	>99 (95)	>99/1
11	**1a**	1.05	$Pd(ACN)_2Cl_2$	TPPTS (4)	-	30	14	>99 (97)	>99/1
12	**1a**	1.5	$Pd(ACN)_2Cl_2$	TPPTS (4)	-	30	3	>99 (94)	>99/1
13	**1b**	1.5	$Pd(ACN)_2Cl_2$	TPPTS (4)	-	60	4	>99 (91)	88/12
14	**1b**	1.2	$Pd(ACN)_2Cl_2$	TPPTS (4)	-	60	4	>99 (96)[e]	>99/1
15	**1b**	1.5	$Pd(ACN)_2Cl_2$	sSPhos (4)	-	60	2	>99 (95)	90/10
16	**1b**	1.05	$Pd(ACN)_2Cl_2$	sSPhos (4)	-	60	2	>99 (93)[e]	>99/1
17	**1b**	1.05	$Pd(ACN)_2Cl_2$	sSPhos (4)	-	30	24	80	>99/1
18	**1b**	1.05	$Pd(ACN)_2Cl_2$	sSPhos (4)	CuI (1)	30	2	>99 (94)	>99/1
19	**1b**	1.05	$Pd(ACN)_2Cl_2$	sSPhos (4)	CuI (0.1)	30	3	>99 (97)	>99/1
20	**1c**	1.2	$Pd(ACN)_2Cl_2$	sSPhos (4)	-	60	1	>99 (92)	90/10
21	**1c**	1.05	$Pd(ACN)_2Cl_2$	sSPhos (6)	-	60	3	>99 (92)[e]	>99/1
22	**1c**	1.05	$Pd(ACN)_2Cl_2$	sSPhos (6)	CuI (0.25)	30	4	>99 (95)	>99/1

[a]Determined by HPLC. [b]The products were isolated after cyclohexane extraction and purification by flash chromatography only if the conversion exceeds 90%. [c]The reaction was performed under anhydrous conditions. [d]The reaction was performed also using the recovered catalyst kept for one week under nitrogen, obtaining the same reaction yield. [e]Phenylacetylene **2** was added using a syringe pump over the reaction time

Moving to bromobenzene **1b**, the Pd^0/TPPTS catalyst was able to induce complete conversion at 60°C in 4h (entry 13) with a copper-free HC protocol. The homocoupling product **4** (Figure 3.4) was not detected, but, on the contrary, 12 % of [(E)-4-phenylbut-1-en-3-ynyl]benzene] **5** was found in the final reaction mixture. The side product was suppressed by a slow addition of phenylacetylene **2** in 4h (entry 14), which also allowed to decrease the need for alkyne excess. The catalyst generated with Buchwald's ligand, sodium 2'- dicyclohexylphosphino-2,6-dimethoxy-1,1'-biphenyl-3-sulfonate (sSPhos) (Figure 3.2),[18] afforded product **3** in high yield without copper at 60°C (entry 15). The formation of enyne **5** was again controlled by decreasing the excess of **2** and using the slow addition mode (entry 16).

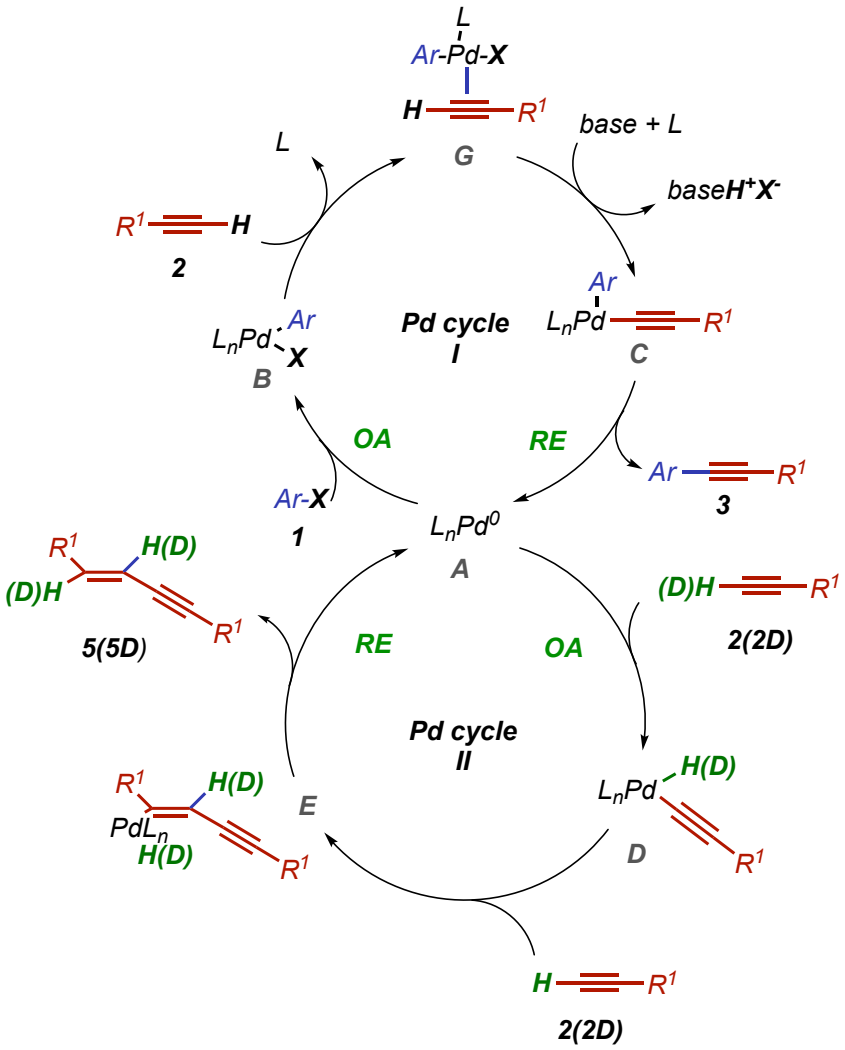

***Figure 3.2**: HC copper-free mechanism (Pd cycle I); Mechanism of the Pd^0 catalyzed self-hydroalkynylation of phenylacetylene **2** (Pd cycle II)*

Only the Sonogashira protocol could be successfully performed at 30°C and the reaction afforded selectively the coupling product **3** in a few hours even with 0.1 mol% of CuI (entries 17–19). Phenyl triflate **1c** behaved similarly to the corresponding bromide **1b**. In fact, the copper free reaction at 60 °C selectively afforded **3** in 1h with the rapid addition of **2** and in 3h with the slow addition of the acetylene to suppress the byproduct formation (entries 20 and 21), while with the Pd^0/Cu^I catalytic system the reaction was completed in 4h at 30°C (entry 22).

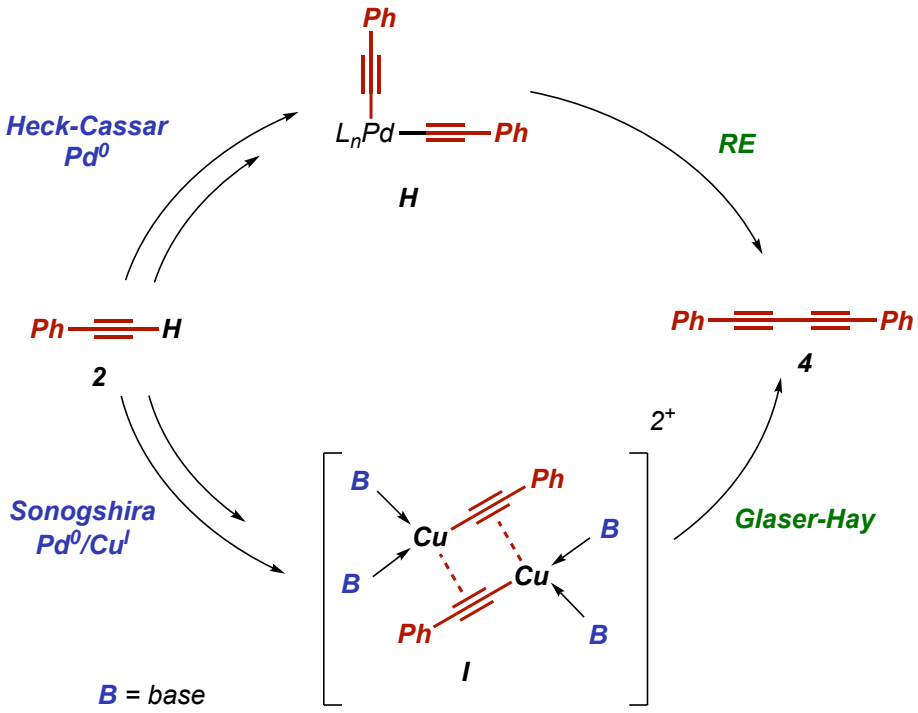

Figure 3.4**: Mechanisms for the formation of the homocoupling product **4

The formation of the homocoupling product **4** is considered the main side reaction of the HCS coupling reaction,[19] and it can be generated by both pathways described in Figure 3.4. Specifically, **4** could arise from the dimerization of complex **I** catalyzed by Cu^{I} salts (Glaser-Hay coupling) [20–23] or from a reductive elimination originated by Pd^{II} complex **H**. However, in our case, all the reactions were performed under nitrogen atmosphere with degassed solvents and the Glaser-Hay coupling, which would require oxidative conditions, was completely suppressed. On the other hand, when the copper-free HC coupling with HEP/water/TMG protocol was applied, the homocoupling byproduct **4** was never observed in the operative conditions with sulphonated phosphines. These observations are inconsistent with the mechanism proposed by Kosmrlj[24] who describes the copper-free reaction via a Pd-Pd transmetallation through complex **H** where the homocoupling **4** is the major byproduct (Chapter 1.5)

The different experimental evidence could be attributed to the matched effect of protic solvents, base and phosphine on the reaction mechanism. For this reason, the direct coordination of the acetylene on complex **B** in the copper-free protocol cannot be totally ruled out and requires further investigations.[25–27]

In a few reactions (entries 13, 15, 20), the presence of compound **5** was observed instead of the homocoupling product **4**, coming from self-hydroalkynylation of phenylacetylene **2** (Figure 3.3, Pd cycle II).[28,29] When the HCS coupling is inefficient and the reaction requires high temperature and a large excess of acetylene, the formation of enyne **5** can become a competitive process.[28,29]

This is observed only for coupling reactions performed using the Heck-Cassar protocol with bromides and triflates as leaving groups. The reaction outcome is related to the efficiency of the oxidative addition of the Pd^0 complex on the aryl halide **1** versus the one on the acetylene **2**. With iodide **1a** the HCS is fast and selective, while with less efficient **1b** and **1c,** where the OA is slow and probably the rate determining step of the reaction, the competition with alkyne **2** was emerging generating variable amount of enyne byproduct **5**. However, the simple slow addition of the acetylene allowed to suppress this side reaction and selectively afford diphenylacetylene **3** in high yield. When the reaction was performed using deuterated phenylacetylene **2D** in the absence of aryl halide and copper cocatalyst, the corresponding deuterated enyne **5D** was isolated, thus confirming that the vinylic hydrogens are coming exclusively from the acetylene moiety. In fact, enyne **5** is the first step toward acetylene oligomerization.[30]

It is also important to stress that the reactions of Table 3.1 (entries 10 and 16) carried out using 0.2 mol % of catalyst instead of 2 mol % under Heck-Cassar conditions did not reach complete conversion after 14 h. These observations supported the idea to recycle the catalyst using sulfonated phosphines with short reaction time, thus opening the possibility to increase the TON of the HCS reaction in HEP/water.

Since the HCS cross-coupling and, in general, Pd^0-catalyzed reactions are compatible with several functional groups on the aromatic ring, we decided to explore the substrate scope by performing the reaction on bromides and triflates bearing electron-donating substituents that could potentially decrease the efficiency of the oxidative addition step.

In addition, as highlighted by our recent results, the HCS outcome is mainly affected by the nature of the alkyne, and the attention was therefore focused on differently substituted acetylenes. The results reported in Table 3.2 show that the catalyst, generated in the HEP/water/TMG system, could be easily recycled independently from the leaving group, the electron-donating moiety on the aryl derivative, the sulfonated phosphine ligand and

the protocol used. The simple extraction with an immiscible solvent such as cyclohexane (Cy) allows to easily recover the final product, leaving the catalyst intact in the HEP/water phase. The catalyst solution was then used in the following reaction cycle by simply adding the two reagents and the TMG base (Figure 3.5). The recycling time was fixed (0.5, 1, 2, or 3h) according to the reaction rate, and the conversion, measured after each cycle workup, was > 95 % in all cases.

It is worth noting that the Sonogashira iterative protocol was stopped after 10 recycles with **1a** even if in many cases the catalyst was still active (Table 3.2, entries 1–8), whereas the copper-free protocol of the reaction between **2** and aryl iodide **1a** at 60°C was recycled 15 times (entry 9).

***Table 3.2**: HCS catalyst recycling: effect of ligand, leaving group and alkyne substitution*

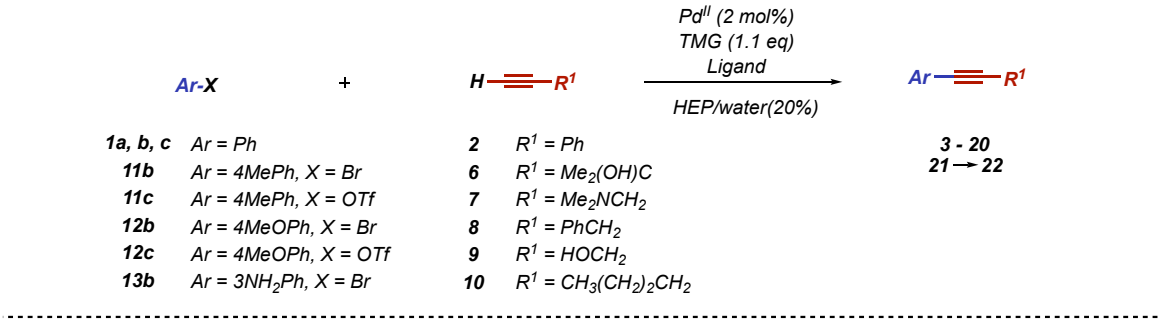

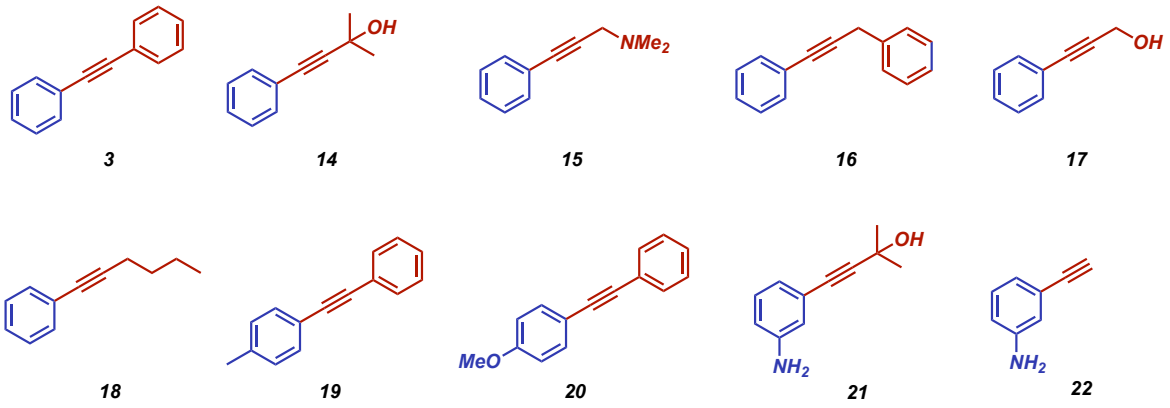

3 **14** **15** **16** **17**

18 **19** **20** **21** **22**

Entry[a]	Ar-X	Alkyne (eq)	Ligand (mol%)	CuI mol%	T °C	Cycle time h	Cycles	Alkyne addition	TON	Product (yield %)[b]
1	**1a**	**2** (1.05)	TPPTS (4)	0.5	30	0.5	10	rapid	470	**3** (94)[c]
2	**1a**	**2** (1.5)	TPPDS (4)	0.5	30	1	10	rapid	465	**3** (93)
3	**1a**	**2** (1.05)	TPPMS (4)	0.5	30	1	10	rapid	475	**3** (95)
4	**1a**	**6** (1.5)	TPPTS (4)	0.5	30	1	10	rapid	460	**14** (92)
5	**1a**	**7** (1.5)	TPPTS (4)	0.5	30	1	10	rapid	470	**15** (94)
6	**1a**	**8** (1.5)	TPPTS (4)	0.5	30	1	10	rapid	475	**16** (95)
7	**1a**	**9** (1.5)	TPPTS (4)	0.5	30	1	10	rapid	480	**17** (96)
8	**1a**	**10** (1.5)	TPPTS (4)	0.5	50	1	10	rapid	465	**18** (93)[d]
9	**1a**	**2** (1.05)	TPPTS (4)	-	60	1	15	rapid	705	**3** (94)[c]
10	**1b**	**2** (1.05)	sSphos (4)	-	60	2	10	2h	470	**3** (94)
11	**1b**	**2** (1.05)	sSphos (4)	0.5	30	2	7	rapid	330	**3** (94)
12	**11b**	**2** (1.05)	sSphos (4)	-	60	2	10	2h	460	**19** (92)
13	**12b**	**2** (1.05)	sSphos (4)	-	60	2	10	2h	475	**20** (95)
14	**1b**	**9** (1.5)	sSphos (4)	-	60	2	10	rapid	460	**17** (92)
15	**1b**	**10** (2)	sSphos (6)	-	60	2	5	rapid	238	**18** (95)[d]
16	**13b**	**6** (2)	sSphos (6)	-	60	3	8	rapid	376	**22** (94)[e]
17	**1c**	**2** (1.05)	sSphos (6)	-	60	3	10	3h	480	**3** (96)
18	**11c**	**2** (1.05)	sSphos (6)	-	60	3	10	3h	475	**19** (95)
19	**12c**	**2** (1.05)	sSphos (6)	-	60	3	10	3h	480	**20** (96)
20	**1c**	**7** (2)	sSphos (6)	-	60	2	10	rapid	460	**15** (92)
21	**1c**	**10** (2)	sSphos (6)	-	60	2	7	rapid	330	**18** (94)[d]

[a]All HCS couplings were carried out under nitrogen atmosphere. At the given time the reactions were cooled at rt, extracted with cyclohexane and the HEP/water phase containing the catalyst was recycled. [b]The combined cyclohexane extracts were distilled and the crude was subsequently purified by flash chromatography generating an average yield. [c]Entries 1 and 9 were carried out also using toluene, 2-MeTHF, MTBE, IBA as extraction solvents giving the same result. [d]Performed with 30% of water as cosolvent. [e]Deprotection of the intermediate **21** was directly performed by treatment with NaOH under reflux affording **22** in quantitative yield

Moving to aryl bromides and triflates **1b-c**, the catalyst was easily recycled more then 10 times in all cases excluding the reactions containing 1-hexyne **10** as starting alkyne (Table 3.2, entries 15 and 21). Moreover, in order to suppress the formation of the enynes and enhance the selectivity and the atom economy of the protocol, some reactions required the slow addition of the acetylene (entries 10, 12, 13, 17, 18, 19).

To further confirm the robustness of the procedure, the key intermediate for the synthesis of Erlotinib, **22**, was successfully isolated with an average yield of 94 % after 8 cycles and quantitative deprotection from **21** (entry 16). The HEP/water system allowed to completely recycle the catalyst avoiding any leakage. In fact, the combined crude materials coming from the reactions, obtained by extraction/solvent distillation, were analyzed by inductively coupled plasma optical emission spectrometry (ICP-OES) and contained < 0.25 ppm of palladium metal and < 0.02 ppm of copper when Sonogashira protocol was applied, hence satisfying an essential requirement for pharmaceutically industrial applications.

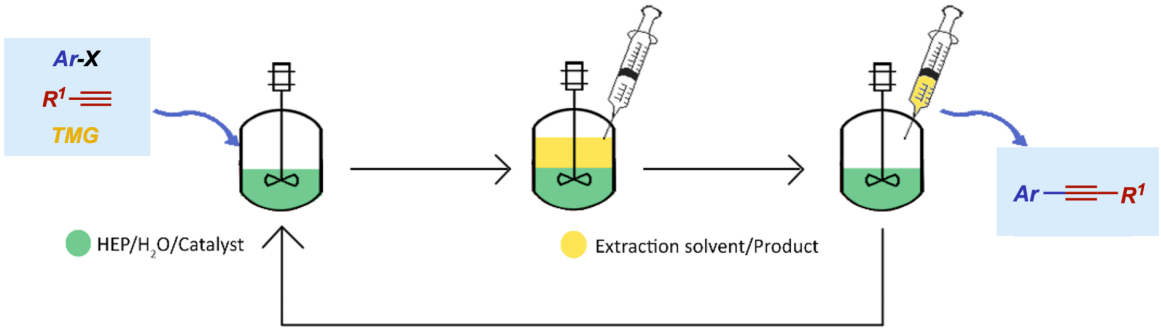

***Figure 3.4**: General recycling protocol*

The recycling sequence (10 cycles) normally took 2–3 days overall in the lab, and the catalyst solution in HEP/water was stored overnight at room temperature under nitrogen without any loss in the catalytic activity. Furthermore, in order to increase the flexibility of the protocol, alternative solvents for final product extraction were also tested, repeating the reaction reported in entries 1 and 9 of Table 3.2. Toluene, CH_2Cl_2, 2-methyl tetrahydrofuran (2-MeTHF), methyl tert-butyl ether (MTBE), ethyl acetate (EA), and the greener isobutyl acetate (IBA) were explored to test work-up efficiency. With the only exception of CH_2Cl_2 and EA, all the solvents were efficient in extracting the product from the reaction mixture and the possible organic solvent residue in the HEP/water phase did not affect the catalyst recycling. The extraction, phase separation and catalyst recycling can be easily scaled up in a continuous process at industrial level with currently available technologies. Finally, with the optimized conditions in hand, we scaled up 10 times the substrate amount reaching a 5 mmol scale and increased the reaction concentration from 1 to 2.5 M. The catalyst amount was decreased to 0.2 mol% still giving complete conversions in a few hours (3–4 h) independently from the leaving group and the protocol applied, allowing up to 5 recycles (Table 3.3). TON and TOF ranged between 1380–2375 and 110–158 h^{-1}, respectively, while the PMI ranged from 7 to 8.

Table 3.3: *HCS coupling with optimized condition: evaluation of TON, TOF, PMI and PMIr*

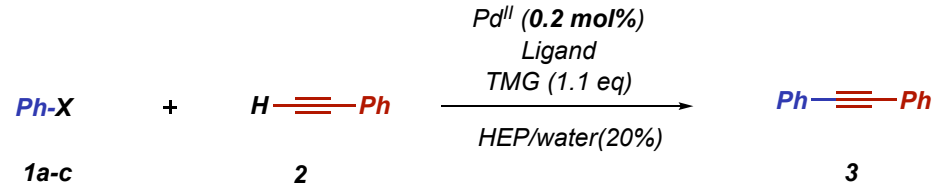

Entry[a]	Ph-X	Alkyne (eq)	Ligand (mol%)	CuI mol%	T °C	t h	Cycles	Yield[b] %	TON[c]	TOF[c]	PMI	PMIr[d]
1	**1a**	1.05	TPPTS (0.6)	0.05	30	3	5	95	2375	158	7.3	2.9
2	**1a**	1.05	TPPTS (0.4)	-	60	3	4	93	1860	155	7.6	3.0
3	**1b**	1.2	sSPhos (0.6)	0.05	60	4	3	90	1380	112	7.9	3.0
4	**1c**	1.2	sSPhos (0.6)	-	60	4	2	88	1760	110	8.2	3.4

[a]All reactions were carried out under a nitrogen atmosphere with a 2.5 M concentration; the conversions were measured by HPLC at the end of each cycle, being always higher than 90%. [b]The yield was obtained combining all the crude extracts. [c]TON and TOF were calculated considering the average yield and the overall reaction time. [d]The PMI was recalculated after recovery of cyclohexane (95%), TMG (95%), HEP (95%) and palladium (90%), see experimental for the detailed calculation.

In order to increase the sustainability, the spent catalyst solution was treated with sodium formate to generate palladium black that was filtered out with the aid of charcoal (90% palladium recovery). The remaining mixture was then treated with solid NaOH and distilled to recover TMG and HEP with a 95% yield. The PMI after recovery was close to 3 in all entries of Table 3.3.

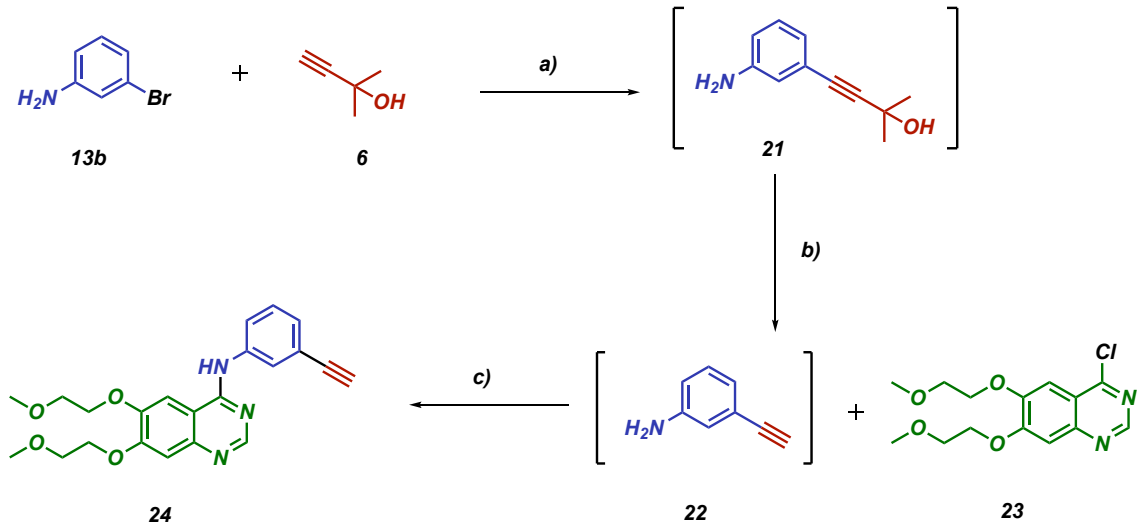

Scheme 3.1*: Erlotinib synthesis. Pd(ACN)$_2$Cl$_2$ (0.2 mol%), sSPhos (0.6 mol%),* ***6*** *(2 eq), HEP/H$_2$O/TMG, 80°C 10h; 3 recycles a) Toluene:NaOH (1.5 eq), 1h reflux b)* ***23*** *(0.9 eq), Toluene:IPA 1:1, 4h, 55°C, 75% yield c).*

The protocol was successfully applied to the telescoped synthesis of Erlotinib **24** (Scheme 3.1). The HCS was carried out following a procedure similar to the ones in Table 3.3 (3 recycles; TON: 1380; TOF: 46 h^{-1}) and using toluene for the extraction of **21** since it was the reaction solvent of step b).

The limited amount of recycles is related to the presence of the aniline moiety that interferes with the palladium catalyst. The toluene solution of intermediate **21** was treated with NaOH at reflux for 1 h to get **22**, washed with water, concentrated to 0.5 M solution, and immediately used in the coupling with **23** (toluene/isopropanol) to get Erlotinib **24** with a 75% overall yield from **13b**.

3.4 Conclusions

The palladium-catalyzed HCS cross-coupling using sulfonated phosphines in HEP/water as solvent mixture and TMG as base, proved to be applicable on aryl iodides, bromides, and triflates. The catalyst, being stable and perfectly soluble in HEP/water, could be recycled, and the product, after a simple extraction and solvent evaporation, recovered free from metal contamination.

The process was further optimized to drastically decrease the required amount of Pd catalyst and increase the TON and TOF up to 2375 and 158 h^{-1}, respectively.[31]

Palladium metal, TMG, and HEP were recovered from the exhausted catalyst solution, and the recalculated process mass intensity was close to 3 based on the crude mixture.

The identification of the side reaction that generates the enyne derivatives with the copper-free Heck-Cassar protocol was limited by the simple control of the alkyne addition rate to optimize the stoichiometry. Concerning the transmetalation process, HEP/water/TMG system plays an important role on the copper-free reaction mechanism; nevertheless, the occurrence of the alkyne direct coordination on the oxidative addition complex or the transmetallation process between two Pd^{II} complexes cannot be ascertained by our study and deserves further investigations. Tyrosine kinase inhibitor Erlotinib **24** was obtained in high yield from **13b** via a three-step telescoping process starting from a sustainable HCS coupling procedure.

3.5 Experimental

General information

Commercial reagents (reagent grade, >99%) were used as received without additional purification. Aryl triflates **11c** and **12c**[32] were synthesized as reported in literature, and phenylacetylene **2D**[33] as reported in literature.

Solvents (Cy, DCM, MTBE, HEP, toluene, 2-MeTHF, IBA, IPA) are commercially available and were used after degassing.

^{1}H NMR, ^{13}C NMR and ^{31}P NMR spectra were recorded with an Agilent-Technologies-Varian INOVA 400 MHz and 100 MHz instrument ^{1}H/^{19}F/X 5 mm PFG ATB Broadband Probe, VT, single, double and triple resonance, z-axis pulsed field gradients, serves broadband probe and customized variable temperature – 5 mm Broadband probe. NMR multiplicities are abbreviated as follows: s = singlet, d = doublet, t = triplet, q = quartet, spt = septet, m = multiplet, bs = broad signal. Coupling constants *J* are given in Hz. All ^{1}H and ^{13}C chemical shifts are calibrated to residual protic-solvents.

HPLC-UV analysis were recorded with an Agilent 1260 InfinityLab instrument. Column: Zorbax® SB-C18; particle size 5 µm; pore size 100 Å; length 250 mm, internal diameter: 4.6 mm. Mobile phase A: H_2O, mobile phase B: ACN. Gradient (Time(min), %B): 0, 30; 8, 80; 22, 80; 24, 10; 30, 10; flow 0.5 mL min^{-1}column temperature 30°C; injection volume: 20 µL.

HPLC-UV analysis of Erlotinib product **24**: Column:Hypersil BDS C18; particle size 5 µm; length 150 mm, internal diameter: 4.6 mm. Mobile phase A: ACN:MeOH 1:1; Mobile phase B: H_2O:MeOH 1:1. Gradient (Time(min), %B): 0, 35; 40, 60; 50, 75; 51, 35; 60, 35; flow 1.0 mL min^{-}1; column temperature 25°C; injection volume: 10 µL.

GC-MS analysis were recorded with a Hewlett-Packard 5971 spectrometer with GC injection and EI ionization at 70 eV coupled with an Agilent Technologies MSD1100 single-quadrupole mass spectrometer, reported as: m/z (rel. intensity).

Mass Spectrometry analysis were recorded on a QTRAP 3200 mass spectrometer in ESI^{+} mode.

Spectrometer ICP-OES AGILENT 5110 was used to determine the concentration of Pd and Cu in the solution. Power: 1200 W; Auxiliary gas: Argon (1.0 L min^{-1}); nebulizer gas: nitrogen (0.7 L min^{-1}); peristaltic pump speed: 12 rpm. Samples for ICP-OES were digested with 8 mL

HNO_3/HCl (1:3) using a microwave digestion system held at 175 °C for 10 minutes. The volume of the digests was then made up to 50 mL with de-ionized water before analysis by ICP-OES. Calibration standards for the quantification of the digested samples were prepared in 5% HNO_3. Palladium standards from FaggiEnrico and copper standards from Exaxol Italia.

Step c) of Erlotinib **24** synthesis and characterization (Scheme 3.1) performed with the collaboration of FKOL team in Gurgaon (India).

General procedure for Sonogashira cross-coupling

*Reaction with aryl iodides **1a***

To an oven-dried 10 mL Schlenk purged under N_2 atmosphere, palladium pre-catalyst (0.01 mmol, 2%, 2.6 mg), phosphine ligand (TPPTS, TPPDS, TPPMS, 0,02 mmol, 4%) and CuX co-catalyst (CuI, CuBr, CuCl, in different amounts: 1%, 0.5 %, 0.25%, 0.1%, see Table 3.1), were dissolved in 1 mL or 0.5 mL of HEP and water as co-solvent. The other reagents were then added in the following order: TMG (93 mg, 69 µL, 0.55 mmol, 1.1 eq), iodobenzene **1a** (102 mg, 56 µL, 0.5 mmol, 1.0 eq) and alkyne (from 1.05 to 1.5 eq, see Table 3.1). The reaction mixture was heated to 30°C with an oil bath and maintained at this temperature under stirring; the conversion was evaluated through HPLC-UV analysis at 210 nm considering the appropriate Relative Response Factor (RRF) (see Experimental section of Chapter 2 for RRF calculation). At reaction completion, the mixture was quenched with H_2O (3 mL) and extracted with an appropriate organic solvent (3x5 mL). The collected organic phases were washed with brine, dried over anhydrous Na_2SO_4 and concentrated under reduced pressure. The reaction crude was purified by flash chromatography (eluents and isolated yields specified below in Compound Characterization section).

*Reaction with aryl bromides **1b***

To an oven-dried 10 mL Schlenk purged under N_2 atmosphere, palladium pre-catalyst (0.01 mmol, 2%, 2.6 mg), TPPTS or sSPhos, (0.4% to 0.6%) and CuX co-catalyst (CuI, CuBr, CuCl, in different amounts: 1%, 0.5 %, 0.25%, 0.1%, see Table 3.1), were dissolved in HEP and water as co-solvent. The other reagents were then added in the following order: TMG (93

mg, 69 µL, 0.55 mmol, 1.1 eq), bromobenzene **1b** (102 mg, 56 µL, 0.5 mmol, 1.0 eq) and phenylacetylene **2** (from 1.05 to 1.5 eq, see Table 3.1). The reaction mixture was heated to 30°C with an oil bath and maintained at this temperature under stirring; the conversion was evaluated through HPLC-UV analysis at 210 nm considering the appropriate RRF (see Experimental section of Chapter 2 for RRF calculation). At reaction completion, the mixture was quenched with H_2O (3 mL) and extracted with an appropriate organic solvent (3x5 mL). The collected organic phases were washed with brine, dried over anhydrous Na_2SO_4 and concentrated under reduced pressure. The reaction crude was purified by flash chromatography (eluents and isolated yields specified below in Compound Characterization section).

*Reaction with aryl triflates **1c***

To an oven-dried 10 mL Schlenk purged under N_2 atmosphere, palladium pre-catalyst (0.01 mmol, 2%, 2.6 mg), sSPhos (from 4 to 6%) and CuI co-catalyst (from 0.25 to 1%), were dissolved in HEP and water as co-solvent. The other reagents were then added in the following order: TMG (93 mg, 69 µL, 0.55 mmol, 1.1 eq), phenyl trifluoromethanesulfonate **1c** (113 mg, 81 µL, 0.5 mmol, 1.0 eq) and phenylacetylene **2** (54 mg, 0.525 mmol, 1.05 eq). The reaction mixture was heated to 30°C with an oil bath and maintained at this temperature under stirring; the conversion was evaluated through HPLC-UV analysis at 210 nm considering the appropriate RRF (see Experimental section for RRF calculation). After reaction completion, the mixture was quenched with H_2O (3 mL) and extracted with an appropriate organic solvent (3x5 mL). The collected organic phases were washed with brine, dried over anhydrous Na_2SO_4 and concentrated under reduced pressure. The reaction crude was purified by flash chromatography (eluents and isolated yields specified below in Compound Characterization section).

General procedure for Heck-Cassar cross-coupling

The procedure for the Heck-Cassar protocol is analogue to that described for the Sonogashira cross-coupling, with the same classification for aryl iodide, bromide and triflate. Anyway, the reactions were conducted at 60°C or 30°C in absence of CuX as co-catalyst. An excess of alkyne was required to make the reaction faster, when necessary.

Slow addition of alkyne **2** was performed to completely supress the formation of by-product **5**.

Recycling protocol

After complete conversion of the desired reaction (monitored with HPLC-UV at 210 nm), the mixture was extracted three times under N_2 with an appropriate organic solvent, not miscible with the HEP/water solution. The organic layer was removed with a syringe, another portion of TMG, aryl halide and alkyne were added to the HEP/water phase and another catalytic cycle was performed at 30 or 60°C. The conversion of the new cycle of reaction was monitored by the previously mentioned analysis. The organic phases obtained from the different cycles were combined, distilled to recover the organic solvent, and the residue purified if necessary by flash chromatography (yields and recycles are reported in Table 3.2 and Table S3.1.

Table S3.1*: HCS catalyst recycle, TON and TOF of entries reported in Table 3.2*

Entry[a]	Ar-X	Alkyne (eq)	Ligand (mol%)	CuI mol%	T °C	Cycles	Product (yield %)[b]	TON	TOF	Pd[c] ppm	Cu[c] ppm
1	**1a**	**2** (1.05)	TPPTS (4)	0.5	30	10	**3** (94)	470	47	0.11	0.01
2	**1a**	**2** (1.5)	TPPDS (4)	0.5	30	10	**3** (93)	465	47	0.23	0.01
3	**1a**	**2** (1.05)	TPPMS (4)	0.5	30	10	**3** (95)	475	47	0.20	0.01
4	**1a**	**6** (1.5)	TPPTS (4)	0.5	30	10	**14** (92)	460	46	0.24	0.01
5	**1a**	**7** (1.5)	TPPTS (4)	0.5	30	10	**15** (94)	470	47	0.14	0.02
6	**1a**	**8** (1.5)	TPPTS (4)	0.5	30	10	**16** (95)	475	47	0.18	0.02
7	**1a**	**9** (1.5)	TPPTS (4)	0.5	30	10	**17** (96)	480	48	0.22	0.01
8	**1a**	**10** (1.5)	TPPTS (4)	0.5	50	10	**18** (93)	465	46	0.18	0.01
9	**1a**	**2** (1.05)	TPPTS (4)	-	60	15	**3** (94)	705	47	0.20	-
10	**1b**	**2** (1.05)	sSphos (4)	-	60	10	**3** (94)	470	23	0.22	-
11	**1b**	**2** (1.05)	sSphos (4)	0.5	30	7	**3** (94)	330	23	0.24	0.02
12	**11b**	**2** (1.05)	sSphos (4)	-	60	10	**19** (92)	460	23	0.17	-
13	**12b**	**2** (1.05)	sSphos (4)	-	60	10	**20** (95)	475	24	0.11	-
14	**1b**	**9** (1.5)	sSphos (4)	-	60	10	**17** (92)	460	23	0.18	-
15	**1b**	**10** (2)	sSphos (6)	-	60	5	**18** (95)	238	24	0.21	-
16	**13b**	**6** (2)	sSphos (6)	-	60	8	**22** (94)	376	16	0.22	-
17	**1c**	**2** (1.05)	sSphos (6)	-	60	10	**3** (96)	480	16	0.24	-
18	**11c**	**2** (1.05)	sSphos (6)	-	60	10	**19** (95)	475	16	0.19	-
19	**12c**	**2** (1.05)	sSphos (6)	-	60	10	**20** (96)	480	16	0.19	-
20	**1c**	**7** (2)	sSphos (6)	-	60	10	**15** (92)	460	23	0.20	-
21	**1c**	**10** (2)	sSphos (6)	-	60	7	**18** (94)	330	24	0.22	-

[a]All HCS couplings were carried out under nitrogen atmosphere. At the given time the reactions were cooled at rt, extracted with cyclohexane and the HEP/water phase containing the catalyst was recycled. [b]The combined cyclohexane extracts were distilled and the crude was subsequently purified by flash chromatography generating an average yield. [c]Determined on the reaction crude after distillation of the extraction solvent

Recovery of HEP, TMG and Pd

Protocol applied on the optimized reaction condition (Entries of Table 3.3)

At the given time, the reaction was cooled at rt, extracted with cyclohexane and the HEP/water phase containing the catalyst was recycled.

After the final cycle, product **3** was again extracted with cyclohexane and the combined organic extracts were distilled and the product could be recovered without further purification. It was also possible to distil the cyclohexane after each cycle. The reaction mixture, containing HEP/water, conjugated TMG acid and the catalyst complex, was treated with sodium formate (0.04 mmol, 2.8 mg) for 1h at 60°C in order to generate palladium black. At reaction completion, the mixture was filtered out with the aid of charcoal (60 mg) and the palladium metal was recovered. The filtrate was basified with NaOH (3.0 eq to the total amount of TMG) to achieve a pH around 13-14 and then distilled under reduced pressure to recover HEP and TMG with a 95% yield.

Table S3.2*: Example of PMI calculation on the optimized HCS reaction (Entry 1, Table 3.3)*

Reagents	Single run (mg)	5 cycles (mg)[a]	5 cycles and final recovery (mg)[b]	Recovery %
Iodobenzene **1a**	1020	5100	5100	-
Phenylacetylene **2a**	536	2680	2680	-
TMG	633	3165	158	95
$Pd(ACN)_2Cl_2$	2.6	2.6	0.26	90
TPPTS	17.1	17.1	17.1	-
CuI	0.5	0.5	0.5	95
HEP	1943	1943	97	-
Water	300	300	300	95
Sodium formate	-	-	2.8	-
NaOH	-	-	3000	-
Charcoal	-	-	60	-
Cyclohexane	3510	17550	877[c]	95
Diphenylacetylene **3a**[d]	875	4233	4233	-
PMI	9.0	-	-	-
PMI after Pd/TPPTS and HEP/water recycle	-	7.3	-	-
PMI after final recovery of Pd, HEP, TMG and Cy	-	-	2.9	-

[a]PMI calculated after 5 cycles and recycle of Pd complex and HEP/water. [b]PMI calculated after 5 cycles and recycle of Pd complex, HEP/water and final recovery of Pd metal, TMG, HEP and cyclohexane. [c]The organic phases obtained from the different cycles were combined and distilled to recover 95% of cyclohexane. It is possible to distill the cyclohexane also after each cycle. [d]Product **3a** obtained without purification.

***Table S3.3**: HCS catalyst recycle and TON, TOF and PMI calculations of entries reported in Table 3.3*

Entry[a]	Ar-X	Alkyne (eq)	Ligand (mol%)	CuI mol%	T °C	t h	Cycles	Yield[b] %	TON	TOF	PMI[c]	PMIr[c]	Pd[d] ppm	Cu[d] ppm
1	**1a**	1.05	TPPTS (0.6)	0.05	30	3	5	95	2375	158	7.3	2.9	0.14	0.01
2	**1a**	1.05	TPPTS (0.4)	-	60	3	4	93	1860	155	7.6	3.0	0.12	-
3	**1b**	1.2	sSPhos (0.6)	0.05	60	4	3	90	1380	112	7.9	3.0	0.12	0.02
4	**1c**	1.2	sSPhos (0.6)	-	60	4	2	88	1760	110	8.2	3.4	0.24	-

[a]All HCS couplings were carried out under nitrogen atmosphere. At the given time the reactions were cooled at rt, extracted with cyclohexane and the HEP/water phase containing the catalyst was recycled. [b]The combined cyclohexane extracts were distilled and the crude was subsequently purified by flash chromatography, when necessary, generating an average yield. It is possible to distil the cyclohexane also after each cycle. [c]PMI calculated on the crude product. [d]Determined on the combined reaction crude after solvent distillation.

*General procedure for the synthesis of **11c** and **12c***

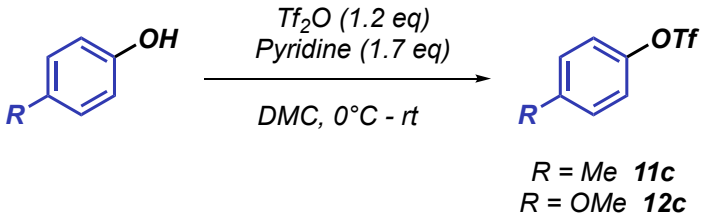

The preparation of **11c/12c** was adapted from literature.[32] To a solution of a general substituted phenol (4.0 mmol) and pyridine (1.7 eq, 6.8 mmol) in CH_2Cl_2 (6 ml), Tf_2O (1.2 eq, 4.8 mmol) was added dropwise at 0°C. After stirring for 2 h at room temperature, the reaction mixture was quenched with 10% aqueous HCl. The organic layer was washed with saturated aqueous $NaHCO_3$ and then with brine. The combined organic phases were dried over anhydrous Na_2SO_4 and filtered. The filtrate was concentrated under reduced pressure and the residue was purified with flash chromatography on silica gel) to give the desired product (eluents and isolated yields specified below in Compound Characterization section).

*Synthesis of Erlotinib **24***

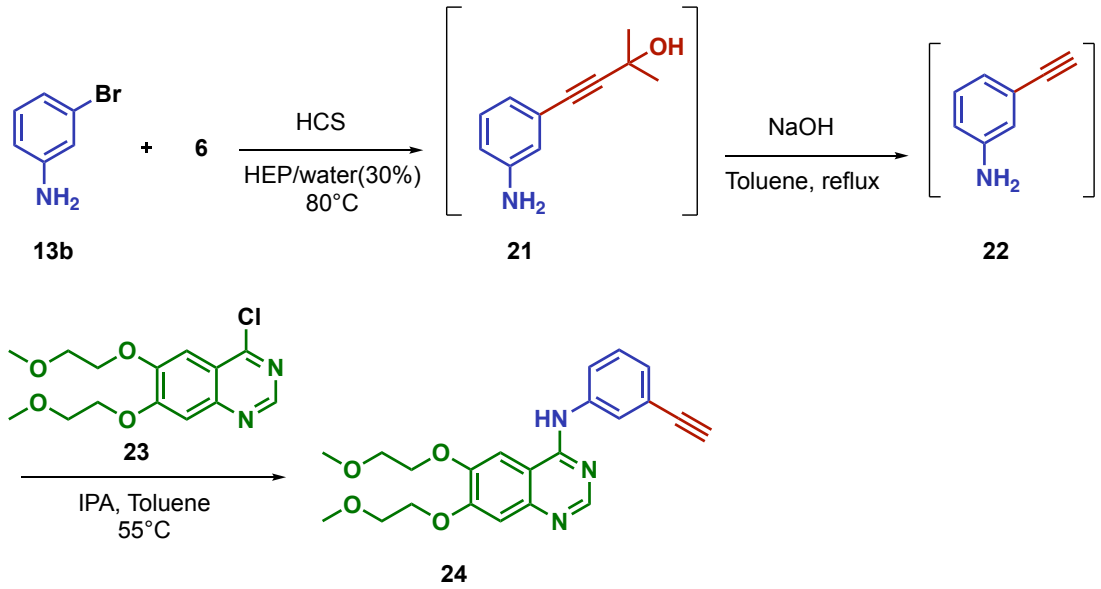

The intermediate **21** was prepared according to the general procedure for Heck-Cassar cross-coupling carried out in Table 3.3 (5 mmol scale) and using toluene as extraction solvent. After 3 recycles (10h for each cycle, 92% overall yield) the combined organic phases were transferred into a 100 mL round-bottom flask, and directly treated with NaOH (1.5 eq) to carry out the deprotection step of the masked acetylene.[34] The mixture was refluxed for 1h, and the acetone byproduct was removed periodically through a Dean-Stark trap. Upon completion, the reaction was cooled to 25°C, 10 mL of water was added and intermediate **22** was extracted with fresh toluene (3x20 mL) and transferred into 250 mL round-bottom flask. The volume of the mixture was then decreased to 30 mL after concentration under vacuum to reach a concentration 0.5 M. 4-chloro-6,7-bis(2-methoxyethoxy)quiniazoline **23** (0.9 eq) was dissolved in 30 mL of IPA and charged to the solution containing **22**. The reaction mixture was then stirred for 4h at 55°C. After reaction completion, monitored with TLC, the solution was cooled to room temperature and filtered to obtain product **24** with an overall yield of 75%.

Mechanistic studies

*Formation of byproduct **5** with aryl bromides (relative percentages are reported in Table 3.2)*

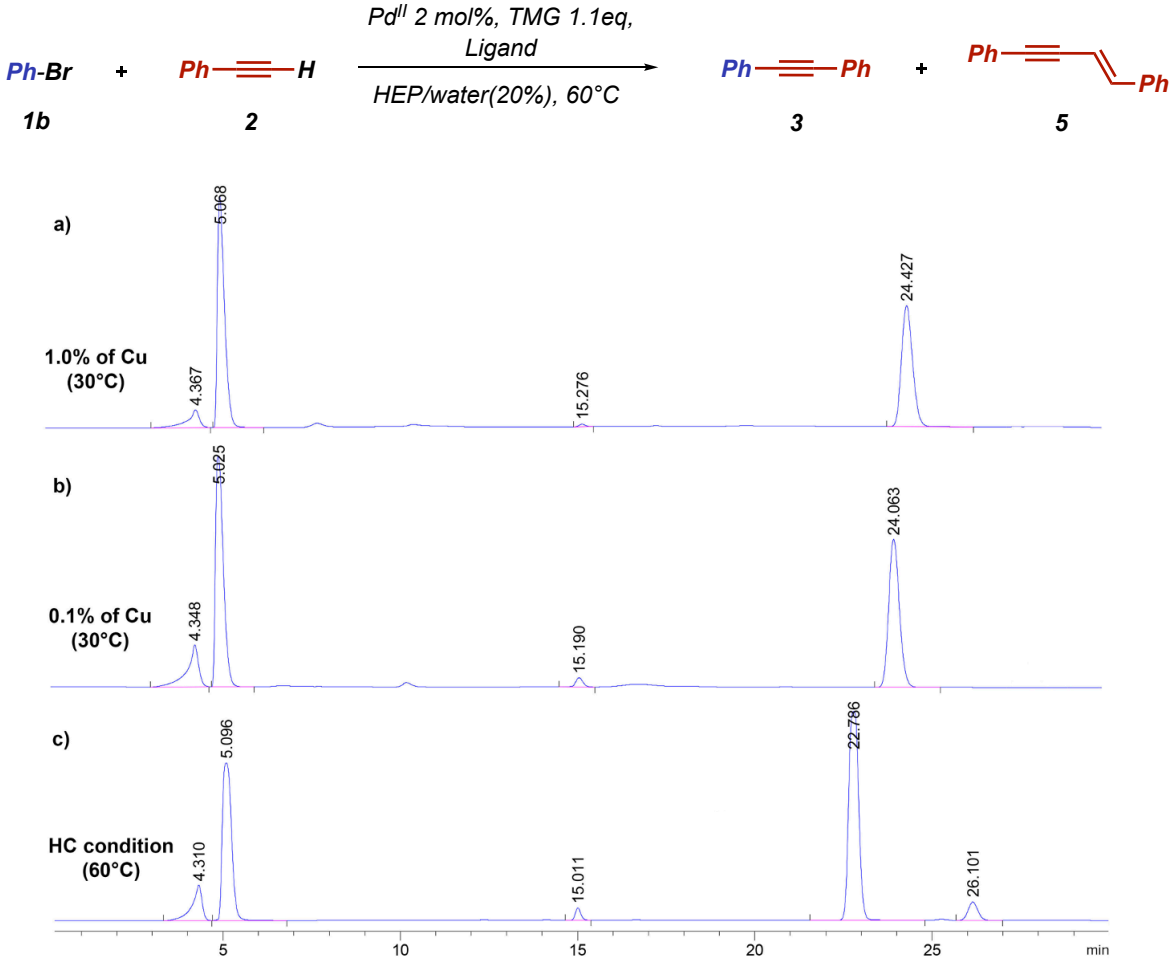

***Figure S3.1**: HPLC chromatogram of HCS cross-coupling (a, entry 18; b, entry 19; c, entry 15, Table 3.2). Diphenylacetylene product (**3**) at 24.427 min (a), 24.063 min (b), 22.786 min (c) and formation of byproduct **5** at 26.101 min (c). No trace of **5** in Sonogashira condition with 1.0% and 0.1% of copper salt at 30°C).*

*Formation of byproduct **5** with different aryl halides (relative percentages are reported in Table 3.2)*

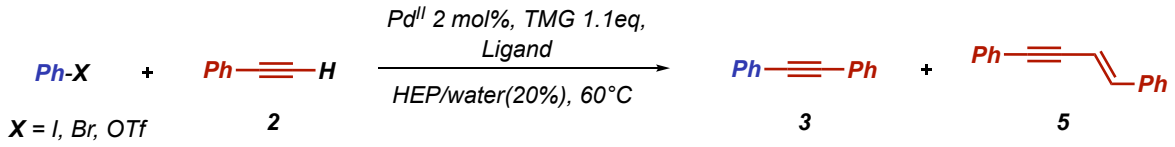

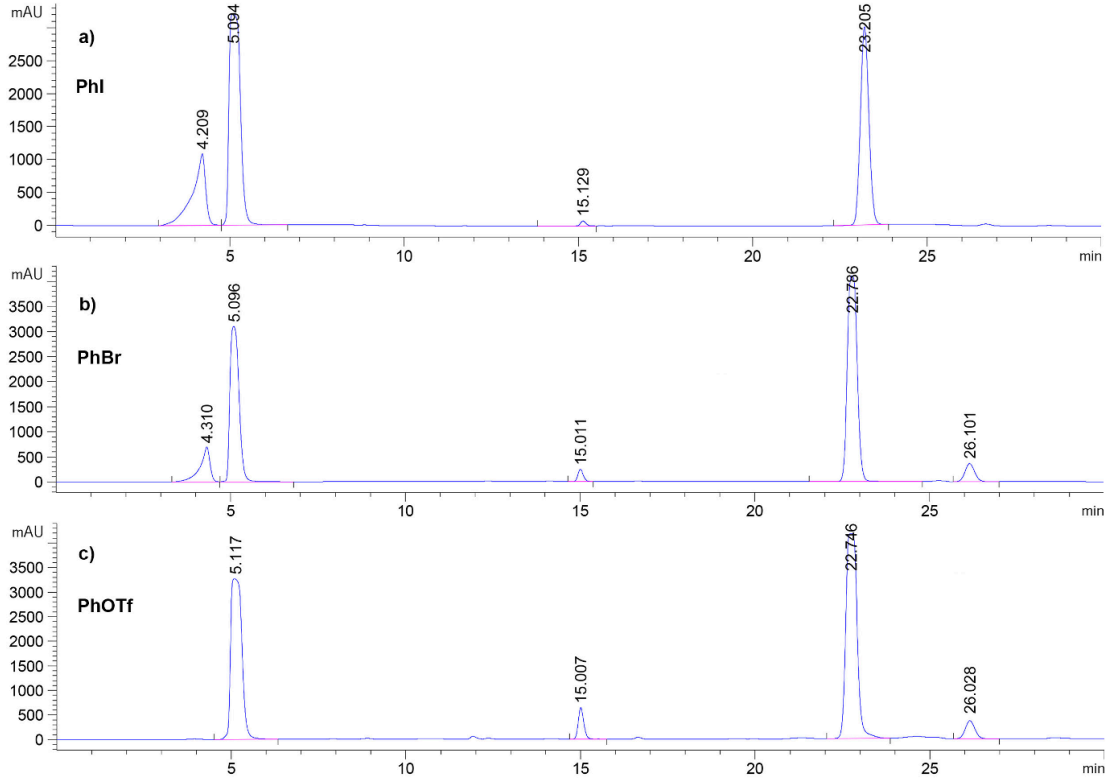

Figure S3.2: *HPLC chromatogram of HC cross-coupling reaction between aryl halides and phenylacetylene **2** in HEP/water solution at 60°C. a) peak at 15.129 min = residual phenylacetylene **2**; peak at 23.205 min = product **3** (entry 10, Table 3.2); b) peak at 15.011 min = residual phenylacetylene **2**; peak at 22.786 min = product **3**; peak at 26.101 min = byproduct **5** (entry 15, Table 3.2); c) peak at 15.007 min = residual phenylacetylene **2**; peak at 22.746 min = product **3**; peak at 26.028 = byproduct **5** (entry 20, Table 3.2).*

*Synthesis of byproduct **5***

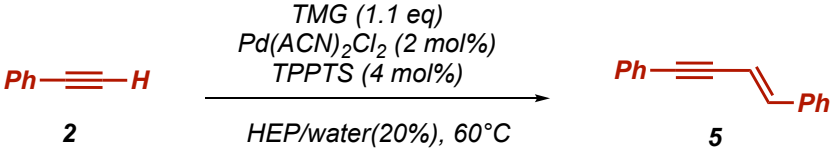

To an oven-dried 10 mL Schlenk purged under N_2 atmosphere, palladium pre-catalyst (0.01 mmol, 2%), TPPTS (0.02 mmol, 4%) (mmol calculated from the mmol of aryl halide in standard HCS cross-coupling) were dissolved in HEP and water as co-solvent. Then, the other reagents were added in the following order: TMG (93 mg, 69 µL, 0.55 mmol, 1.1 eq) and phenylacetylene **2** (153 mg, 164 µL eq, 1.5 mmol, 3.0 eq). The reaction mixture was heated to 60°C with an oil bath and maintained at this temperature under stirring for 14 h. The formation of **5** was monitored by HPLC-UV. The mixture was then quenched with H_2O (3 mL) and extracted with cyclohexane (3x5 mL). The collected organic phases were washed with brine, dried over anhydrous Na_2SO_4 and concentrated under reduced pressure. The reaction crude was purified by flash chromatography (eluent and isolated yield specified below in Compound Characterization section).

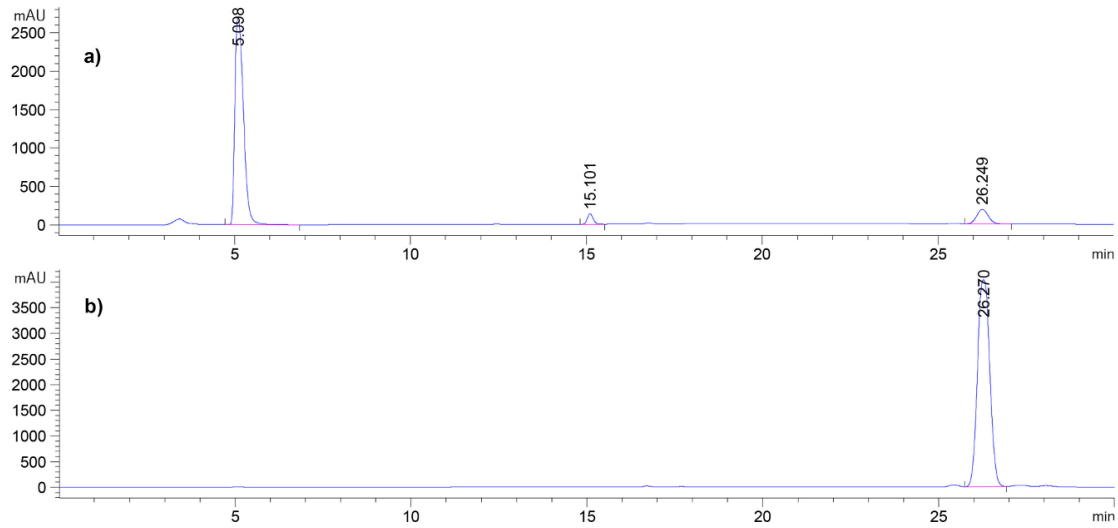

Figure S3.3: *a) HPLC chromatogram of the reaction of phenylacetylene **2** in HC condition in HEP/water: peak at 15.101 min = residual phenylacetylene **2**; peak at 26.249 = 1,4-diphenyl-1-buten-3-yne byproduct **5**; b) HPLC chromatogram of isolated byproduct **5**.*

*Synthesis of **2D***[33]

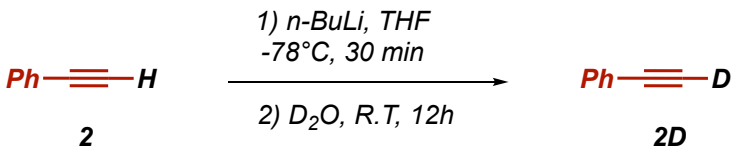

To a solution of phenylacetylene **2** (510 mg, 550 µL, 5.0 mmol) in dry THF (10 ml), n-BuLi (1.5 eq, 2.5 M in hexane solution) was added dropwise at −78˚C under N_2 atmosphere. The mixture was stirred at -78°C for 30 min, then warmed to room temperature. D_2O (2.5mL) was added under N_2 atmosphere, and the mixture was stirred at rt for 12 h. The organic layer was separated and the aqueous phase was extracted with CH_2Cl_2 (3x5 mL). The combined organic layers were washed with CH_2Cl_2 (3x20 mL), dried over anhydrous Na_2SO_4 and filtered. The filtrate was concentrated in vacuo to afford **2D** (490 mg, 95%, D% = 98%).

*Synthesis of **5D***[35,36]

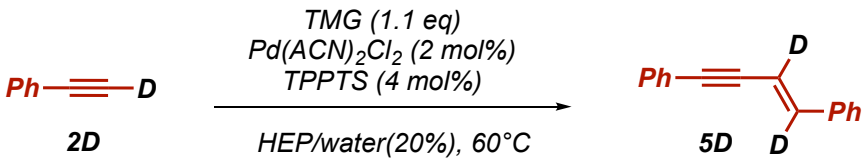

To an oven-dried 10 mL Schlenk purged under N_2 atmosphere, palladium pre-catalyst (0.01 mmol, 2%), and TPPTS (0,02 mmol, 4%) were dissolved in HEP/water mixture. Then, the other reagents were added in the following order: TMG (93 mg, 69 µL, 0.55 mmol, 1.1 eq) and **2D** (153 mg, 164 µL eq, 1.5 mmol, 3.0 eq). The reaction mixture was heated to 60°C with an oil bath and maintained at this temperature under stirring for 14h. The formation of **5D** was monitored by HPLC-UV. The mixture was then quenched with H_2O (3 mL) and extracted with cyclohexane (3x5 mL). The collected organic phases were washed with brine, dried over anhydrous Na_2SO_4 and concentrated under reduced pressure. The reaction crude was purified by flash chromatography (Cy 100%).

Compound characterization

The yields are calculated considering the single run of HCS reaction

*1,2-diphenylacetylene (**3**)*

White solid (98% yield); Purification by flash chromatography (Cy 100%)

^{1}H NMR (400 MHz, $CDCl_3$) δ (ppm) 7.58 – 7.41 (m, 4H), 7.40 – 7.35 (m, 6H).

^{13}C NMR (100 MHz, $CDCl_3$) δ (ppm) 131.59, 128.33, 128.24, 123.27, 89.37.

Anal. Calcd. for $C_{14}H_{10}$: C, 94.34; H, 5.66; found: C, 94.68; H, 5.65;

GC-MS: rt m/z: 178 (100 %), 152 (13%), 126 (7%).

*2-methyl-4-phenylbut-3-yn-2-ol (**14**)*

Yellow oil (94% yield); Purification by flash chromatography (Cy/EtOAc = 95/5)

^{1}H NMR (400 MHz, $CDCl_3$) δ (ppm) 7.42 – 7.39 (m, 2H), 7.28 – 7.26 (m, 3H), 2.50 (s, OH), 1.61 (s, 6H).

^{13}C NMR (100 MHz, $CDCl_3$) δ (ppm) 131.54, 128.15, 128.12, 122.68, 93.81, 82.01, 65.49, 31.40.

Anal. Calcd. for $C_{11}H_{12}O$: C, 82.46; H, 7.55; found: C, 82.78; H, 7.54;

GC-MS: rt 10.1, m/z: 160 (22%), 145 (100%), 129 (10%), 115 (20%).

*N,N-dimethyl-3-phenylprop-2-yn-1-amine (**15**)*

Colourless liquid (96% yield); Purification by flash chromatography (Cy/EtOAc = 95/5)

^{1}H NMR (400 MHz, $CDCl_3$) δ (ppm) 7.45 – 7.42 (m, 2H), 7.30 – 7.28 (m, 3H), 3.47 (s, 2H), 2.37 (s, 6H).

^{13}C NMR (100 MHz, $CDCl_3$) δ (ppm) 131.58, 128.13, 127.91, 123.12, 85.18, 84.45, 48.47, 44.13.

Anal. Calcd. for $C_{11}H_{13}N$: C, 82.97; H, 8.23; N, 8.80; found: C, 82.99; H, 8.22; N, 8.77;

GC-MS: rt 10.9 m/z: 159 (75%), 143 (9%), 115 (100%), 89 (15%), 82 (15%).

*Prop-1-yne-1,3-diyldibenzen (**16**)*

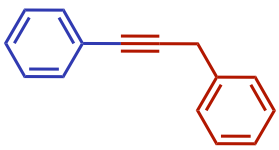

Yellow oil (98% yield); Purification by flash chromatography (Cy 100%)

^{1}H NMR (400 MHz, $CDCl_3$) δ (ppm) 7.48 – 7.43 (m, 4H), 7.38 – 7.27 (m, 6H), 3.86 (s, 2H).

^{13}C NMR (100 MHz, $CDCl_3$) δ (ppm) 136.73, 131.61, 128.52, 128.20, 127.93, 127.78, 126.61, 123.65, 87.49, 82.63, 25.73.

Anal. Calcd. for $C_{15}H_{12}$: C, 93.71; H, 6.29; found: C, 93.81; H, 6.27;

GC-MS: 15.8 m/z: 192 (100%), 165 (30%), 115 (15%).

*3-phenylprop-2-yn-1-ol (**17**)*

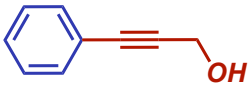

Yellow oil (97% yield); Purification by flash chromatography (Cy/EtOAc = 95/5)

^{1}H NMR (400 MHz, $CDCl_3$) δ (ppm) 7.44 – 7.41 (m, 2H), 7.31 – 7.28 (m, 3H), 4.48 (s, 2H), 2.45 (s, OH).

^{13}C NMR (100 MHz, $CDCl_3$) δ (ppm) 131.59, 128.38, 128.22, 122.47, 87.22, 85.52, 51.41.

Anal. Calcd. for C_9H_8O: C, 81.79; H, 6.10; found: C, 81.97; H, 6.09;

GC-MS: rt 10.4 m/z: 131 (100), 115 (20%), 103 (60%), 77 (53%).

*Hex-1-yn-1-ylbenzen (**18**)*

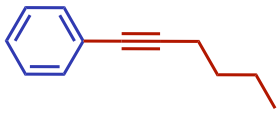

Yellow oil (95% yield); Purification by flash chromatography (Cy 100%)

^{1}H NMR (400 MHz, $CDCl_3$) δ (ppm) 7.43 – 7.41 (m, 2H), 7.31 – 7.27 (m, 3H), 2.43 (t, *J* = 7.0 Hz, 2H), 1.66 – 1.56 (m, 2H), 1.56 – 1.45 (m, 2H), 0.98 (t, *J* = 7.3 Hz, 3H).

^{13}C NMR (100 MHz, $CDCl_3$) δ (ppm) 131.50, 128.13, 127.40, 124.09, 90.37, 80.52, 30.84, 22.00, 19.08, 13.62.

Anal. Calcd. for $C_{12}H_{14}$: C, 91.08; H, 8.92; found: C, 91.22; H, 8.92;

GC-MS: rt m/z: 158 (26%), 143 (41%), 129 (80%), 115 (100%).

*1-methyl-4-(phenylethynyl)benzene (**19**)*

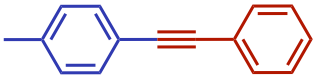

White solid (98% yield); Purification by flash chromatography (Cy 100%)

^{1}H NMR (400 MHz, $CDCl_3$) δ (ppm) 7.57 – 7.55 (m, 2H), 7.45 (d, *J* = 8.1 Hz, 2H), 7.40 – 7.33 (m, 3H), 7.17 (d, *J* = 7.9 Hz, 2H), 2.40 (s, 3H).

^{13}C NMR (100 MHz, $CDCl_3$) δ (ppm) 138.36, 131.53, 131.48, 129.09, 128.29, 128.04, 89.55, 88.71, 21.49.

Anal. Calcd. for $C_{15}H_{12}$: C, 93.79; H, 6.21; found: C, 93.57, H: 6.23;

GC-MS: rt 16.10 min m/z: 192 (100%), (165 (18%).

*1-methoxy-4-(phenylethynyl)benzene (**20**)*

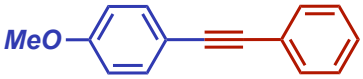

White solid (98% yield); Purification by flash chromatography (Cy/EtOAc = 95/5)

^{1}H NMR (400 MHz, $CDCl_3$) δ (ppm) 7.55 – 7.49 (m, 4H), 7.38 – 7.33 (m, 3H), 6.91 – 6.89 (m, 2H), 3.84 (s, 3H).

^{13}C NMR (100 MHz, $CDCl_3$) δ (ppm) 159.60, 133.03, 131.43, 128.28, 127.90, 123.59, 115.37, 113.98, 89.36, 88.06, 55.27.

Anal. Calcd. for $C_{15}H_{12}O$: C, 86.51; H, 5.81; found: C, 86.72; H, 5.81;

GC-MS: rt 17.8 min m/z: 208 (100%), 193 (55%), 165 (58%).

2-*Methyl-4-(3-aminophenyl)-3-butyn-2-ol (**21**)*

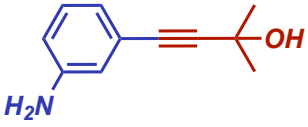

Pale yellow solid (96%); Purification by flash chromatography (Cy/EtOAc = 9/1)

^{1}H NMR (400 MHz, $CDCl_3$) δ (ppm) 7.08 (t, *J* = 7.8 Hz, 1H), 6.83 (d, *J* = 7.6 Hz, 1H), 6.75 (s, 1H), 6.64 (d, *J* = 8.0 Hz, 1H), 3.67 (s, NH_2), 2.21 (s, OH), 1.61 (s, 6H).

^{13}C NMR (100 MHz, $CDCl_3$) δ (ppm) 146.13, 129.15, 123.38, 122.03, 117.91, 115.28, 93.17, 82.26, 65.53, 31.47.

Anal. Calcd for $C_{11}H_{12}NO$: C, 75.40; H, 7.48; N, 7.99; found: C, 75.51; H, 7.42; N, 7.97;

GC-MS: rt 14.4 m/z: 175 (65%), 160 (100%), 144 (9%), 132 (14%), 118 (31%).

*1-amino-3-ethynyl-benzene (**22**)*

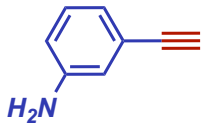

Yellow oil (99%, calculated on the deprotection step); Purification by flash chromatography (Cy/EtOAc = 95/5)

^{1}H NMR (400 MHz, $CDCl_3$) δ 7.11 (t, *J* = 7.8 Hz, 1H), 6.91 (d, *J* = 7.6 Hz, 1H), 6.82 (s, 1H), 6.68 (dd, *J* = 8.0, 1.1 Hz, 1H), 3.69 (s, NH_2), 3.03 (s, 1H).

^{13}C NMR (100 MHz, $CDCl_3$) δ 146.21, 129.23, 122.73, 122.46, 118.28, 115.77, 83.88.

Anal. Calcd for C_8H_7N: C, 82.02; H, 6.02; N, 11.96; found: C, 82.19; H, 6.00; N, 11.96;

GC-MS: rt 9.42 m/z: 117 (100%), 89 (53%), 74 (8%).

*N-(3-ethynylphenyl)-6,7-bis(2-methoxyethoxy)quinazolin-4-amine (**24**)*

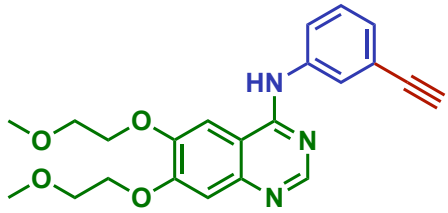

White solid (75% overall yield)

^{1}H NMR (400 MHz, DMSO-d_6) δ (ppm) 11.57 (s, NH), 8.84 (s, 1H), 8.46 (s, 1H), 7.88 (s, 1H), 7.78-7.81 (d, J = 8.8 Hz, 1H), 7.46-7.50 (t, 1H), 7.41 (s, 1H), 7.39 (d, *J* = 8.4 Hz, 1H), 4.30-4.33, 4.38-4.40 (t, 4H), 4.27 (s, 1H), 3.76-3.78 (t, 4H), 3.35 (s, 6H).

^{13}C NMR (400 MHz, DMSO-d_6) δ (ppm) 158.11, 155.64, 149.35, 148.63, 137.26, 135.43, 129.27, 129.08, 127.61, 125.31, 121.97, 107.34, 105.16, 100.58, 82.90, 81.28, 69.87, 69.74, 69.73, 69.07, 58.39, 58.34.

Anal. Calcd for $C_{22}H_{23}N_3O_4$: C, 67.16; H, 5.89; N, 10.78; O, 16.27; found: C, 66.82; H, 6.23; N, 10.60; O, 16.51

ESI^+: rt 11.20 m/z: 394 (100%), 416 (6%), 338 (5%).

*E-1,4-diphenyl-1-buten-3-yne (**5**)*

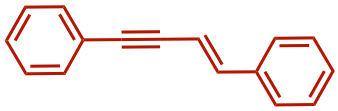

White solid (85% yield); Purification by flash chromatography (Cy 100%)

^{1}H NMR (400 MHz, $CDCl_3$) δ (ppm) 7.50-7.48 (m, 2H), 7.46-7.43 (m, 2H), 7.34 (dtd, *J* = 10.8, 8.5, 7.8 Hz, 6H), 6.64 (d, *J* = 8.0 Hz, 1H), 7.06 (d, *J* = 16.2 Hz, 1H), 6.40 (d, *J* = 16.2 Hz, 1H).

^{13}C NMR (100 MHz, $CDCl_3$) δ (ppm) 141.23, 136.30, 131.48, 128.70, 128.58, 128.30, 128.15, 126.27, 123.38, 108.10, 91.70, 88.84.

Anal. Calcd for $C_{16}H_{12}$: C, 94.08; H, 5.92; found: C, 94,11; H, 5.88;

GC-MS: rt 18.14 m/z: 204 (100%), 203 (94%), 202 (90%).

*4-Tolyl trifluoromethanesulfonate (**11c**)*

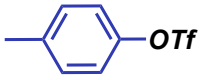

Colourless oil (91%). Purification by flash chromatography (Cy/EtOAc = 9/1)

^{1}H NMR (400 MHz, $CDCl_3$): δ (ppm) 7.26 – 7.23 (m, 2H), 7.19 – 7.14 (m, 2H), 2.39 (s, 3H).

^{13}C NMR (100 MHz, $CDCl_3$): δ (ppm) 147.55, 138.48, 130.64, 123.52, 120.94, 120.33, 117.15, 113.97, 20.78.

Anal. Calcd for C8H7F3O3S: C, 40.00; H, 2.94; found: C, 40.23; H, 2.99;

GC-MS: rt 7.02 m/z: 240 (51%), 77 (100%), 107 (96%), 69 (58%).

*4-Methoxyphenyl trifluoromethanesulfonate (**12c**)*

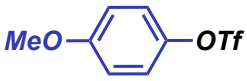

Colourless oil (93%). Purification by flash chromatography (Cy/EtOAc = 9/1)

^{1}H NMR (400 MHz, $CDCl_3$): δ (ppm) 7.26 – 7.12 (m, 2H), 7.02 – 6.83 (m, 2H), 3.83 (s, 3H).

^{13}C NMR (100 MHz, $CDCl_3$): δ (ppm) 159.09, 142.99, 123.53, 122.26, 120.34, 117.16, 114.97, 113.98, 55.55.

Anal. Calcd for C8H7F3O4S: C, 37.51; H, 2.75; found: C, 37.58; H, 2.71;

GC-MS: rt 9.16 m/z: 256 (28%), 123 (100%), 95 (40%); 69 (33%).

Calculation of the RRF

The RRF between iodobenzene **1a**, bromobenzene **1b** and diphenylacetylene **3** have already been discussed in the Experimental section of Chapter 2.

*RRF between aryl triflate **1c** and diphenylacetylene **3***

***Table S3.4**: RRF between **1c** and **3** at several concentrations*

Concentration (M)	Phenyl triflate (mAu)	Diphenylacetylene (mAu)	RRF	Δ_{RRF}
0.0025	18273.0	87537.6	4.79	**4.85**
0.0005	3767.6	18123.9	4.81	
0.00025	2249.5	11124.1	4.95	
0.000125	1141.0	5550.8	4.86	

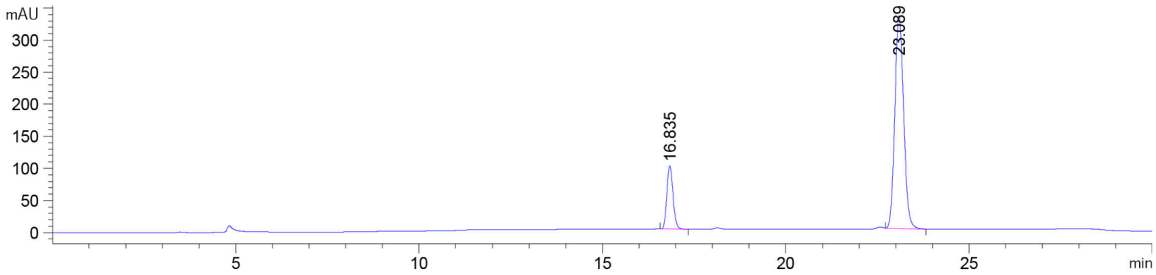

***Figure S3.4**: HPLC-UV spectrum of equimolar mixture of phenyl triflate **1c** and diphenylacetylene **3** at 0.0005 M.*

*RRF between diphenylacetylene **3** 1,4-diphenyl-1-buten-3-yne **5***

***Table S3.5**: RRF calculation between **3** and **5** at several concentrations*

Concentration (M)	Diphenylacetylene (mAu)	1,4-diphenyl-1-buten-3-yne (mAu)	RRF	Δ_{RRF}
0.0025	75423.4	59859.8	1.26	**1.24**
0.0005	17645.2	13573.2	1.30	
0.00025	7982.4	6597.0	1.21	
0.000025	3426.5	2879.4	1.19	

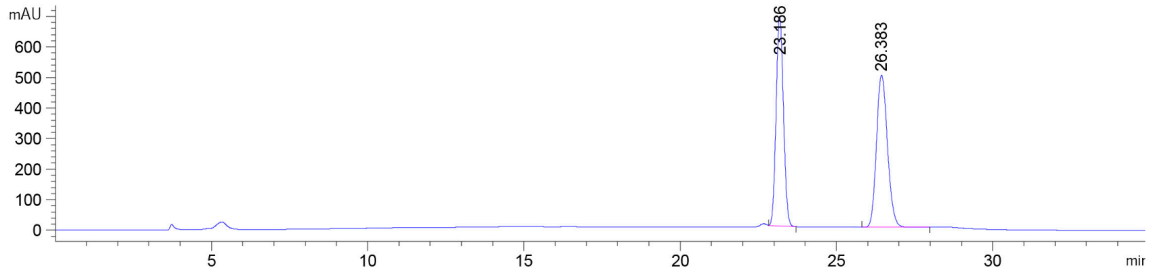

***Figure S3.5**: HPLC-UV spectrum of equimolar mixture of diphenylacetylene **3** and 1,4-diphenyl-1-buten-3-yne **5** at 0.0005 M concentration*

3.5 References

(1) Anastas, P. T.; Warner, J. C. *Green Chemistry: Theory and Practice*; 1998.

(2) Roschangar, F.; Sheldon, R. A.; Senanayake, C. H. Overcoming Barriers to Green Chemistry in the Pharmaceutical Industry – the Green Aspiration Level™ Concept. *Green Chem.* **2015**, *17* (2), 752–768. https://doi.org/10.1039/C4GC01563K.

(3) Ferrazzano, L.; Martelli, G.; Fantoni, T.; Daka, A.; Corbisiero, D.; Viola, A.; Ricci, A.; Cabri, W.; Tolomelli, A. Fast Heck-Cassar-Sonogashira (Hcs) Reactions in Green Solvents. *Org. Lett.* **2020**, *22* (10), 3969–3973. https://doi.org/10.1021/acs.orglett.0c01269.

(4) Jin, B.; Gallou, F.; Reilly, J.; Lipshutz, B. H. Ppm Pd-Catalyzed, Cu-Free Sonogashira Couplings in Water Using Commercially Available Catalyst Precursors. *Chem. Sci.* **2019**, *10* (12), 3481–3485. https://doi.org/10.1039/C8SC05618H.

(5) Schilz, M.; Plenio, H. A Guide to Sonogashira Cross-Coupling Reactions: The Influence of Substituents in Aryl Bromides, Acetylenes, and Phosphines. *J. Org. Chem.* **2012**, *77* (6), 2798–2807. https://doi.org/10.1021/jo202644g.

(6) Chinchilla, R.; Nájera, C. The Sonogashira Reaction: A Booming Methodology in Synthetic Organic Chemistry. *Chem. Rev.* **2007**, *107* (3), 874–922. https://doi.org/10.1021/cr050992x.

(7) Chinchilla, R.; Nájera, C. Recent Advances in Sonogashira Reactions. *Chem Soc Rev* **2011**, *40* (10), 5084. https://doi.org/10.1039/c1cs15071e.

(8) Köllhofer, A.; Plenio, H. A Convenient High Activity Catalyst for the Sonogashira Coupling of Aryl Bromides. *Adv. Synth. Catal.* **2005**, *347* (9), 1295–1300. https://doi.org/10.1002/adsc.200505095.

(9) Doucet, H.; Hierso, J.-C. Palladium-Based Catalytic Systems for the Synthesis of Conjugated Enynes by Sonogashira Reactions and Related Alkynylations. *Angew. Chem., Int. Ed.* **2007**, *46* (6), 834–871. https://doi.org/10.1002/anie.200602761.

(10) Martek, B. A.; Gazvoda, M.; Urankar, D.; Košmrlj, J. Designing Homogeneous Copper-Free Sonogashira Reaction through a Prism of Pd–Pd Transmetalation. *Org. Lett.* **2020**, *22* (13), 4938–4943. https://doi.org/10.1021/acs.orglett.0c01227.

(11) Guideline for Elemental Impurities ICH Q3D (R1) . 2019.

(12) Dumrath, A.; Lubbe, C.; Beller, M. *Palladium-Catalyzed Coupling Reactions: Practical Aspects and Future Developments*, Wiley-VCH.; Weinheim, 2013.

(13) Henderson, R. K.; Hill, A. P.; Redman, A. M.; Sneddon, H. F. Development of GSK's Acid and Base Selection Guides. *Green Chem.* **2015**, *17* (2), 945–949. https://doi.org/10.1039/C4GC01481B.
(14) Amatore, C.; Blart, E.; Genet, J. P.; Jutand, A.; Lemaire-Audoire, S.; Savignac, M. New Synthetic Applications of Water-Soluble Acetate Pd/TPPTS Catalyst Generated in Situ. Evidence for a True Pd(0) Species Intermediate. *J. Org. Chem.* **1995**, *60* (21), 6829–6839. https://doi.org/10.1021/jo00126a037.
(15) Ishikawa, T. *Superbases for Organic Synthesis: Guanidines, Amidines, Phosphazenes and Related Organocatalysts*, Wiley.; 2009.
(16) Kunz, E. G. FR2349562, 1976.
(17) Kohlpaintner, C. W.; Fischer, R. W.; Cornils, B. Aqueous Biphasic Catalysis: Ruhrchemie/Rhône-Poulenc Oxo Process. *Appl. Catal. A Gen.* **2001**, *221* (1–2), 219–225. https://doi.org/10.1016/S0926-860X(01)00791-8.
(18) Anderson, K. W.; Buchwald, S. L. General Catalysts for the Suzuki-Miyaura and Sonogashira Coupling Reactions of Aryl Chlorides and for the Coupling of Challenging Substrate Combinations in Water. *Angew. Chem., Int. Ed.* **2005**, *44* (38), 6173–6177. https://doi.org/10.1002/anie.200502017.
(19) Elangovan, A.; Wang, Y.-H.; Ho, T.-I. Sonogashira Coupling Reaction with Diminished Homocoupling. *Org. Lett.* **2003**, *5*, 1841–1844. https://doi.org/10.1021/ol034320.
(20) Jover, J.; Spuhler, P.; Zhao, L.; McArdle, C.; Maseras, F. Toward a Mechanistic Understanding of Oxidative Homocoupling: The Glaser–Hay Reaction. *Catal. Sci. Technol.* **2014**, *4* (12), 4200–4209. https://doi.org/10.1039/C4CY00322E.
(21) Siemsen, P.; Livingston, R. C.; Diederich, F. Acetylenic Coupling: A Powerful Tool in Molecular Construction. *Angew. Chem., Int. Ed.* **2000**, *39* (15), 2632–2657. https://doi.org/10.1002/1521-3773(20000804)39:15<2632::AID-ANIE2632>3.0.CO;2-F.
(22) Glaser, C. Beiträge Zur Kenntniss Des Acetenylbenzols. *Berichte der deutschen chemischen Gesellschaft* **1869**, *2* (1), 422–424. https://doi.org/10.1002/cber.186900201183.
(23) Hay, A. S. Oxidative Coupling of Acetylenes. *J. Org. Chem.* **1962**, *27* (9), 3320–3321. https://doi.org/10.1021/jo01056a511.
(24) Gazvoda, M.; Virant, M.; Pinter, B.; Košmrlj, J. Mechanism of Copper-Free Sonogashira Reaction Operates through Palladium-Palladium Transmetallation. *Nat. Commun.* **2018**, *9* (1), 4814. https://doi.org/10.1038/s41467-018-07081-5.
(25) Tougerti, A.; Negri, S.; Jutand, A. Mechanism of the Copper-Free Palladium-Catalyzed Sonagashira Reactions: Multiple Role of Amines. *Chem. Eur. J.* **2007**, *13* (2), 666–676. https://doi.org/10.1002/chem.200600574.
(26) García-Melchor, M.; Pacheco, M. C.; Nájera, C.; Lledós, A.; Ujaque, G. Mechanistic Exploration of the Pd-Catalyzed Copper-Free Sonogashira Reaction. *ACS Catal.* **2012**, *2* (1), 135–144. https://doi.org/10.1021/cs200526x.
(27) Soheili, A.; Albaneze-Walker, J.; Murry, J. A.; Dormer, P. G.; Hughes, D. L. Efficient and General Protocol for the Copper-Free Sonogashira Coupling of Aryl Bromides at Room Temperature. *Org. Lett.* **2003**, *5* (22), 4191–4194. https://doi.org/10.1021/ol035632f.
(28) Trost, B. M.; Sorum, M. T.; Chan, C.; Rühter, G. Palladium-Catalyzed Additions of Terminal Alkynes to Acceptor Alkynes. *J. Am. Chem. Soc.* **1997**, *119* (4), 698–708. https://doi.org/10.1021/ja9624937.

(29) Grünwald, A.; Heinemann, F. W.; Munz, D. Oxidative Addition of Water, Alcohols, and Amines in Palladium Catalysis. *Angew. Chem., Int. Ed***. 2020**, *59* (47), 21088–21095. https://doi.org/10.1002/anie.202008350.

(30) Wu, Y.-T.; Lin, W.-C.; Liu, C.-J.; Wu, C.-Y. Palladium-Catalyzed Trimerizations of Terminal Arylalkynes: Synthesis of 1,3-Diaryl-2-Arylethynyl-1,3-Butadienes. *Adv. Synth. Catal.* **2008**, *350* (11–12), 1841–1849. https://doi.org/10.1002/adsc.200800182.

(31) Huang, J.; Wang, W.; Li, H. Water–Medium Organic Reactions Catalyzed by Active and Reusable Pd/Y Heterobimetal–Organic Framework. *ACS Catal.* **2013**, *3* (7), 1526–1536. https://doi.org/10.1021/cs400094x.

(32) Yu, P.; Morandi, B. Nickel-Catalyzed Cyanation of Aryl Chlorides and Triflates Using Butyronitrile: Merging Retro-Hydrocyanation with Cross-Coupling. *Angew. Chem., Int. Ed.* **2017**, *56* (49), 15693–15697. https://doi.org/10.1002/anie.201707517.

(33) Zhu, X.; Guo, R.; Zhang, X.; Gao, Y.; Jia, Q.; Wang, Y. Iron-Promoted Domino Dehydrogenative Annulation of Deoxybenzoins and Alkynes Leading to B-Aryl-α-Naphthols. *Adv. Synth. Catal.* **2020**, *362* (15), 3190–3201. https://doi.org/10.1002/adsc.202000625.

(34) Castellin, A.; de Lucchi, O.; Caporale, A. Method for the Preparation of Erlotinib. US2012095228(A1), 2012.

(35) Zhuang, X.; Chen, J.-Y.; Yang, Z.; Jia, M.; Wu, C.; Liao, R.-Z.; Tung, C.-H.; Wang, W. Sequential Transformation of Terminal Alkynes to 1,3-Dienes by a Cooperative Cobalt Pyridonate Catalyst. *Organometallics* **2019**, *38* (19), 3752–3759. https://doi.org/10.1021/acs.organomet.9b00486.

(36) Pu, X.; Li, H.; Colacot, T. J. Heck Alkynylation (Copper-Free Sonogashira Coupling) of Aryl and Heteroaryl Chlorides, Using Pd Complexes of TBu2(p-NMe2C6H4)P: Understanding the Structure–Activity Relationships and Copper Effects. *J. Org. Chem.* **2013**, *78* (2), 568–581. https://doi.org/10.1021/jo302195y.

Chapter 4:

Heck-Cassar-Sonogashira and Suzuki reactions of Aryl chlorides: a sustainable approach

4.1 Introduction

The Heck-Cassar-Sonogashira (HCS) [1–3] and Suzuki-Miyaura (SM)[4] cross-coupling reactions, allowing the installation of a triple bond and a biaryl motif, are among the most powerful methods for the synthesis of active pharmaceutical ingredients (API).[5–17]

Compared to common precursors such as aryl iodides, bromides and triflates, aryl chlorides represent an interesting alternative as they are less active but more attractive due to their relatively low cost and broad availability. In this context, Plenio and co-workers were one of the first to report the coupling of aryl chlorides with alkynes using $Ad_2P(n\text{-}Bu)$ as ligand in presence of CuI as cocatalyst.[18] However, the state of the art in the area is still represented by the work of Buchwald that proposed a complete copper free HC coupling using XPhos in conjunction with $Pd(ACN)_2Cl_2$.[19] Even regarding the SM cross-coupling reaction, the breakthrough in the field was disclosed by Buchwald and coworkers in 1999, when they reported the coupling of different boronic compounds with aryl bromides and chlorides with ppm loadings of Pd catalyst.[20] From that moment, several studies have investigated the influence of leaving groups, palladium ligands, co-catalysts, solvents, and bases but, to date, only limited success has been achieved in the HCS cross-coupling of alkynes with aryl chlorides,[21,22] while several examples have been reported for SM.[23–28] For the SM reaction very high turnover number (TON) and turnover frequency (TOF) have been recently obtained with aromatic rings bearing electron withdrawing groups in water.[29] Although these methods are highly effective, there is still much room for improvement. In particular, most of the reactions require drastic conditions, toxic organic solvents, excessively long reaction times and a large excess of acetylene, in the case of HCS, which inevitably leads to the formation of by-products. In addition, there is a need to develop more robust and practical catalyst systems that allow to perform cross-coupling reactions with a large library of compounds. The target of this study was the identification of a flexible and sustainable procedure for HCS and SM cross-coupling reactions allowing selective high yield synthesis of a wide range of compounds, with the target to achieve high TON/TOF and competitive PMI values considering solvent and palladium recovery, avoiding product metal contamination. The minimization of the reagent excess is a critical item for the process mass intensity (PMI) and to limit the formation of side products in particular in the

HCS cross coupling. The easy recovery of the palladium metal is also a critical aspect that needs to be evaluated.

4.2 Results and discussion

Taking advantage of our experience in the HCS reaction using aryl iodides, bromides and triflates based on the use of a green protocols,[30,31] we explored the application of commercially available Buchwald's palladium ligand, sSPhos, in the N-hydroxyethylpyrrolidone (HEP)/water mixture for the HCS and SM coupling using aryl chlorides.

The coupling between phenylacetylene **2a** and chlorobenzene **1a** in a complete HC protocol was studied as a model reaction in order to identify the optimal conditions (concentration, temperature, stoichiometry and slow-addition) to perform fast cross-coupling reactions and to recycle the catalyst. The results reported in Table 4.1 demonstrate that applying the standard protocol starting from 2 mol% of Pd pre-catalyst, sSphos as ligand, N,N,N,N-tetramethyl guanidine (TMG) as base at 60°C with aryl chloride **1a**, the reaction is not complete (Entry 1). In addition, as for bromobenzene and triflate, the reaction with substrates that have a slow oxidative addition leads to the formation of an already characterized and studied by-product (E)-4-phenylbut-1-en-3-ynyl]benzene **4** in 77%, compared to the product **3a**, coming from self-hydroalkynylation of phenylacetylene **2a** (see Chapter 3), proving that it remains quite challenging to perform HC couplings in absence of copper on aryl chlorides. Even increasing the temperature, so as to facilitate the oxidative addition, it is noted that the presence of the by-product remains in the majority compared to the product (Entries 2-3). Our previous study showed that with aryl iodides the HCS is fast and selective, while with less efficient aryl bromides and triflates the competition with alkyne **2a** emerged, generating variable amount of enyne **4**. However, while with aryl bromides and triflates the simple slow addition of alkyne **2a** over the course of the reaction allowed to suppress the side-product formation and selectively affords diphenylacetylene **3a** in high yield, with aryl chloride **1a**, the detection of **4** was reduced, but remained however in a relevant percentage (Entries 4-5). Raising the temperature to 80°C and with a slow addition of 1.5 eq of phenylacetylene **2a** in 4h, the reaction reached complete conversion in 3h, but with 10% of enyne **4** still in solution (Entry 6).

Finally, combining the increase of temperature, concentration and slow addition, it was possible to find the ideal condition to transform efficiently aryl chloride **1a** in diphenylacetylene **3a** in 3-4h suppressing completely the side product and reducing the amount of acetylene from 1.5 eq to only 1.05, allowing a complete control of the reaction stoichiometry (Entries 7-8).

***Table 4.1**: Screening for the HCS in HEP/water/TMG system conditions*

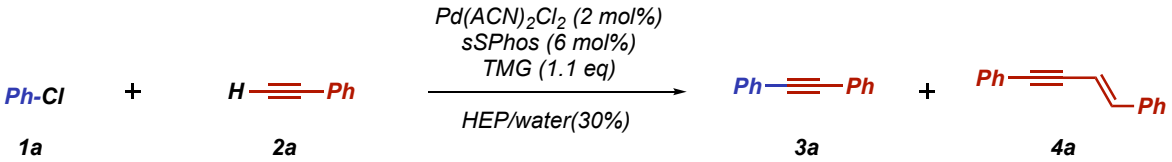

Entry[a]	Conc M	**2a** eq	T °C	t h	Alkyne addition	Conv[b] %	**3a/4a**[b]
1	0.5	2.0	60	3	rapid	20	23/77
2	0.5	2.0	70	3	rapid	25	32/68
3	0.5	2.0	80	3	rapid	45	35/65
4	1.0	1.5	60	3	4h	40	42/58
5	1,0	1.5	70	3	4h	80	77/23
6	1.0	1.5	80	3	4h	>99	90/10
7	1.0	1.05	80	4	4h	>99	99/1
8	1.0	1.05	90	3	3h	>99	99/1

[a]All HCS couplings were carried out under nitrogen atmosphere.
[b]Determined by HPLC

Since the goal of the study was to create a completely green and sustainable protocol, performing efficient and fast reactions under mild conditions even using a low percentage of palladium catalyst, we started from the optimal conditions just found to try to recycle the catalyst from 2 mol% and find exactly the TON and TOF to be able to perform the reaction directly with a lower amount of catalyst. After a complete conversion of aryl chloride **1a** in diphenylacetylene **3a**, the simple extraction with an immiscible solvent (see Chapter 3) allows to easily recover the final product, leaving the catalyst intact in the HEP/water phase. The catalyst solution was then used in the following reaction cycle by simply adding the two reagents and the TMG base. The results reported in Table 4.2 show that the catalyst, generated in the HEP/water/TMG system, could be easily recycled five times, always maintaining a conversion over 95% (Entry 1). It was also possible to perform the reaction in a termomorphic way exploiting the immiscibility of the HEP/water solution

at room temperature with organic solvents such as toluene and isobutyl acetate (IBA), while a homogeneous solution appears at higher temperatures. In this way, phenylacetylene **2a** is added slowly over the course of the reaction through toluene and when the reaction is complete, it is possible to remove directly toluene containing the product **3a** by syringe instead of adding an organic solvent at the end. The reaction was extended to substituted aryl chlorides and acetylenes to demonstrate the robustness of the protocol. For each couple of substrates, the mildest conditions to reach complete conversion were investigated, starting from the best conditions identified in the model reaction between **1a** and **2a**. While the presence of electron-withdrawing groups on the aromatic ring did not affect the reactivity (entries 2-4), the transformation of differently substituted acetylenes and electron-donating substrates required to apply different conditions, mainly as a consequence of a more complicated transmetallation in one case and stronger by-product competition in the other. In this case, raising the temperature to 90°C and slowing down the acetylene addition to 4h, it was still possible to get 3 recycles maintaining conversions higher than 95% and good yields (Entries 5-10).

***Table 4.2**: HC reaction scope and catalyst recycling*

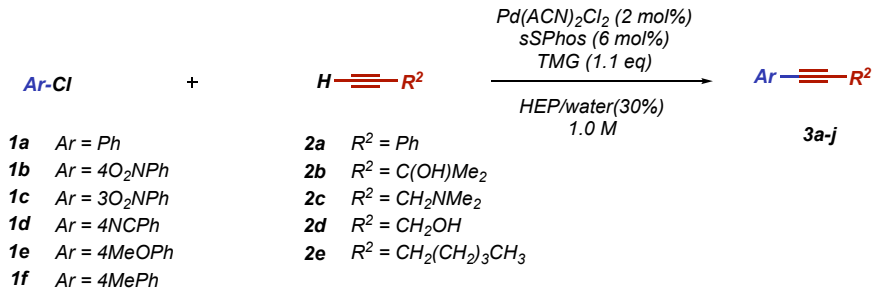

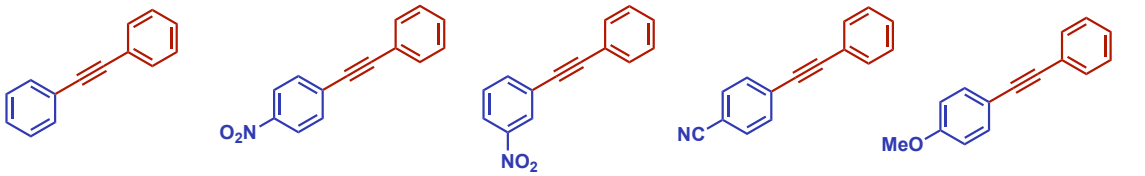

3a **3b** **3c** **3d** **3e**

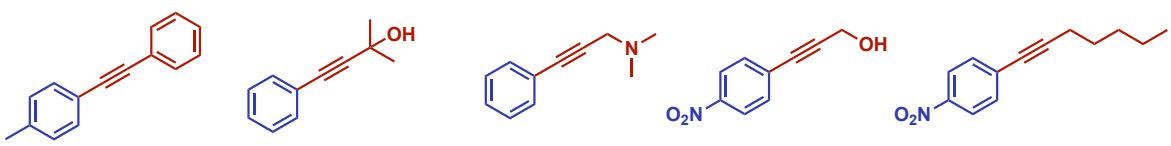

3f **3g** **3h** **3i** **3j**

Entry[a]	Ar-Cl	Alkyne	Alkyne[e] eq	T °C	Cycle time h	Cycles	TON	Product	Overall yield %[b]
1[c,d]	**1a**	**2a**	1.05	90	3	5	230	**3a**	90
2[c]	**1b**	**2a**	1.05	80	3	5	235	**3b**	94
3[c]	**1c**	**2a**	1.05	80	3	5	235	**3c**	94
4	**1d**	**2a**	1.05	80	3	5	233	**3d**	93
5	**1e**	**2a**	1.05	90	4	3	138	**3e**	92
6	**1f**	**2a**	1.05	90	4	3	138	**3f**	92
7	**1a**	**2b**	1.5	90	4	3	135	**3g**	90
8	**1a**	**2c**	1.5	90	4	3	132	**3h**	88
9	**1a**	**2d**	1.5	90	4	3	134	**3i**	89
10	**1a**	**2e**	1.5	90	4	3	129	**3j**	86

[a]All HCS couplings were carried out under nitrogen atmosphere. At the given time the reactions were cooled at rt, extracted with can immiscible organic solvent and the HEP/water phase containing the catalyst was recycled. [b]The combined extraction solvents were distilled and the crude was subsequently purified by flash chromatography, when necessary, generating an average yield. [c]Reaction time extended to 4h hours in the last two cycles. [d]Reaction performed also in a termomorphic way through slow addition of acetylene in toluene over the course of the reaction. [e]Alkyne added slowly over the course of the reaction.

With the optimized conditions in hand and finding the minimum amount of catalyst to be used directly, we performed the HC cross-coupling reaction with 0.4 mol% with the substrates able to make 5 cycles and 0.6 mol% with the less reactive substrates that only allowed 3 catalytic cycles. Aryl chlorides **1a** and **1e** were selected as model examples to assess the validity of the study. Unfortunately, applying the optimized protocol of Table 4.2, satisfactory conversions could not be achieved because of the decomposition of TMG over the course of the reaction (Table 4.3, Entries 1-2). However, it was sufficient to substitute TMG with Cs_2CO_3 as base to achieve complete conversions (Entries 3-4). The process was then further optimized to decrease the required amount of Pd catalyst, to enhance the TON and to decrease the PMI of the protocol by increasing the concentration from 1 to 2.5 M. The catalyst amount was therefore decreased to 0.2 mol% still giving conversion higher than 95% for the model reaction and for the substrates containing electron-withdrawing groups (Entries 5-8), while 0.4 mol% was necessary for the more difficult substrates (Entries 9-14).

***Table 4.3**: Direct HC reaction with decreased amount of catalyst*

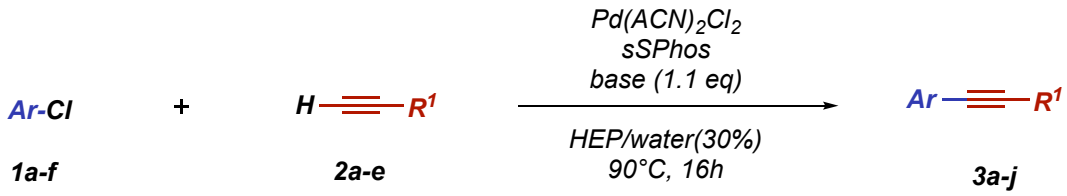

Entry[a]	Conc. M	Ar-X	Alkyne	Alkyne eq	$Pd(ACN)_2Cl_2$ mol%	Base	Yield %[b]	TON	Product
1	1.0	**1a**	**2a**	1.05	0.4	TMG	65	163	**3a**
2	1.0	**1e**	**2a**	1.05	0.6	TMG	56	140	**3e**
3	1.0	**1a**	**2a**	1.05	0.4	Cs_2CO_3	94	235	**3a**
4	1.0	**1e**	**2a**	1.05	0.6	Cs_2CO_3	92	150	**3e**
5	2.5	**1a**	**2a**	1.05	0.2	Cs_2CO_3	93	465	**3a**
6	2.5	**1b**	**2a**	1.05	0.2	Cs_2CO_3	94	470	**3b**
7	2.5	**1c**	**2a**	1.05	0.2	Cs_2CO_3	95	475	**3c**
8	2.5	**1d**	**2a**	1.05	0.2	Cs_2CO_3	93	465	**3d**
9	2.5	**1e**	**2a**	1.05	0.4	Cs_2CO_3	90	225	**3e**
10	2.5	**1f**	**2a**	1.05	0.4	Cs_2CO_3	91	228	**3f**
11	2.5	**1a**	**2b**	1.2	0.4	Cs_2CO_3	90	225	**3g**
12	2.5	**1a**	**2c**	1.2	0.4	Cs_2CO_3	91	228	**3h**
13	2.5	**1a**	**2d**	1.2	0.4	Cs_2CO_3	90	225	**3i**
14	2.5	**1a**	**2e**	1.2	0.4	Cs_2CO_3	90	225	**3j**

[a]All HCS couplings were carried out under nitrogen atmosphere. [b]The combined extraction solvents were distilled and the crude was subsequently purified by flash chromatography, when necessary, generating an average yield.

In order to demonstrate the versatility of the HEP/water system with sulphonated phosphines, we selected the Suzuki-Miyaura cross-coupling as a further proof. The main advantage of the SM reactions over other cross-coupling protocols is the use of boron-compounds as coupling partners, which are readily available, and provide high yields and good selectivity with a broad functional group tolerance.[32,33] For this reason, using our protocol to make it greener could offer several advantages in terms of cost and sustainability. Driven by the excellent results achieved with the HC protocol, the coupling reaction between phenylboronic acid **5a** and chlorobenzene **1a** was investigated. The reaction was performed in the HEP/water system with Cs_2CO_3 as base at 90°C starting from 0.05 mol% $Pd(ACN)_2Cl_2$ as catalyst loading (Table 4.4). As for the HC coupling reactions, also in this case, water has a crucial role as it not only increases the solubility of the sulphonated phosphines, but also speeds up the reaction. In our opinion and referring to studies available in literature,[34] the combination of base and water allow to convert rapidly the

boronic acid into the active "ate"-complex which can then easily perform the transmetallation step (Figure 4.1). Without the presence of a percentage of water, the base is not able to form the boronate complex and therefore the reaction is considerably slowed down (Table 4.4, Entry 1).

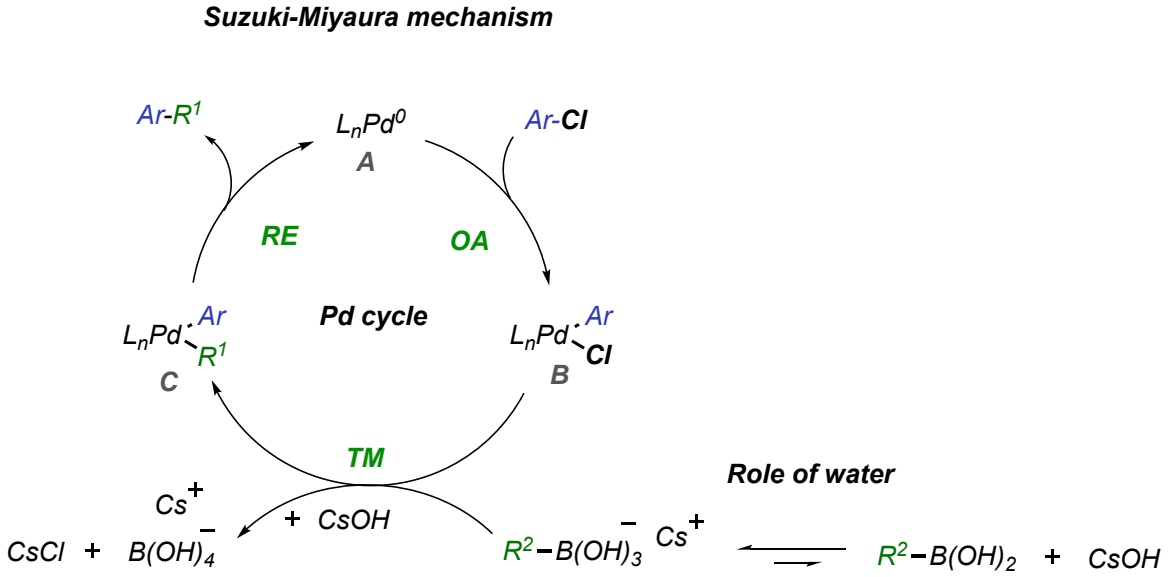

***Figure 4.1**: Mechanism of the Suzuki-Miyaura cross-coupling reaction in HEP/H_2O/Cs_2CO_3 system*

Although water is fundamental, the presence of an organic solvent is still essential to create a more flexible protocol and allow a complete solubilization of compounds that are not soluble in a pure water system. The results in Table 4.4 show that by adding 40% of water compared to the total volume of solvent, it was possible to reach a complete conversion in 4h with 0.05 mol% of catalyst achieving competitive TON and TOF values (Entry 2).

Using the optimized reaction conditions, we investigated the coupling with different substituents on both the aromatic rings. The reaction of phenylboronic acid **5a** with aryl chlorides bearing electron-donating substituents such as $–CH_3$ and $–OCH_3$ at the para position gave the desired products in excellent yields (Entry 3-4).

The reaction of aryl chlorides bearing electron-withdrawing groups such as $–NO_2$, was also tolerated in the cross-coupling reaction with phenylboronic acid **5a** and gave the desired products in good yields under the optimized reaction conditions (Entry 5-6). This catalyst protocol allowed also to perform the reaction with different substituted phenyl boronic acids allowing a complete conversion in all cases (Entry 7-9).

***Table 4.4**: SM optimization and reaction scope*

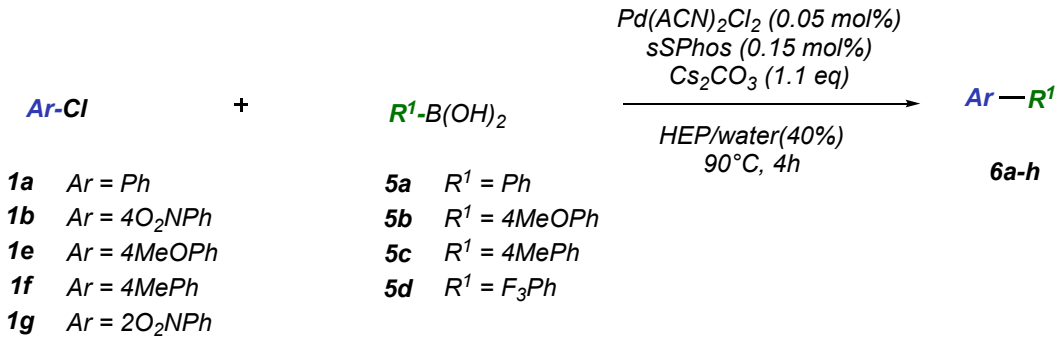

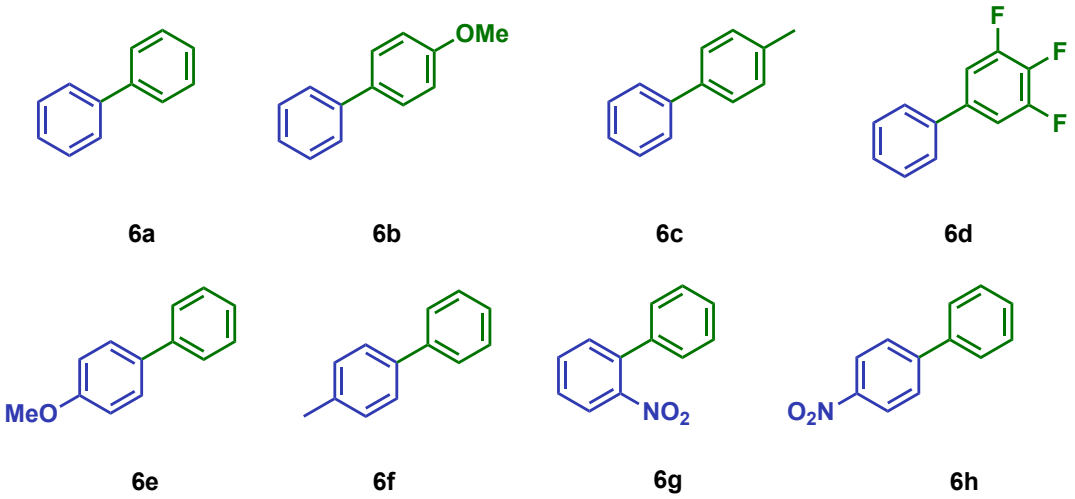

6a **6b** **6c** **6d**

6e **6f** **6g** **6h**

Entry[a]	1	5	Conv. %	Yield %	TON[b]	TOF[b]	Product
1	**1a**	**5a**	60	-	-	-	**6a**
2	**1a**	**5a**	>99	95	1900	475	**6a**
3	**1e**	**5a**	>99	92	1840	460	**6e**
4	**1f**	**5a**	>99	93	1860	465	**6f**
5	**1g**	**5a**	>99	95	1900	475	**6g**
6	**1b**	**5a**	>99	94	1880	470	**6h**
7	**1a**	**5b**	>99	90	1800	450	**6b**
8	**1a**	**5c**	>99	94	1880	470	**6c**
9	**1a**	**5d**	>99	92	1940	460	**6d**

[a]All SM couplings were carried out under nitrogen atmosphere at 1 M concentration and with no need of purification after extraction. [b]TON and TOF were calculated after work up and distillation of the extraction solvent

To validate the applicability of our methodology, the synthesis of the most commonly applied fungicides containing a biaryl-motive, namely Boscalid and Fluxapyroxad was

attempted. The industrial process for their production (Scheme 4.1), requires a SM reaction to convert **1g** in **6i** in one case and in **6j** in the other. Because of the high production volume of these compounds,[35,36] the development of greener methodologies, together with the reduction in Pd loading for their production, is highly desirable and would have a significant impact on the environment. The reaction between **1g** and **5d**/**5e** in HEP/water was studied and carried out following a procedure similar to the one described in Table 4.4 giving complete conversions in the desired product after 6h. In addition, ICP-OES studies demonstrated no metal contamination in the final product, satisfying an essential requirement for pharmaceutically industrial applications. Finally, in order to enhance the sustainability of both the HC and SM protocols, the recovery of the palladium metal and HEP solvent were performed, following the procedure of Chapter 3, achieving PMIr values of 3-4 for the Heck-Cassar coupling and 5 for the Suzuki-Miyaura (see Experimental section for PMI calculation).

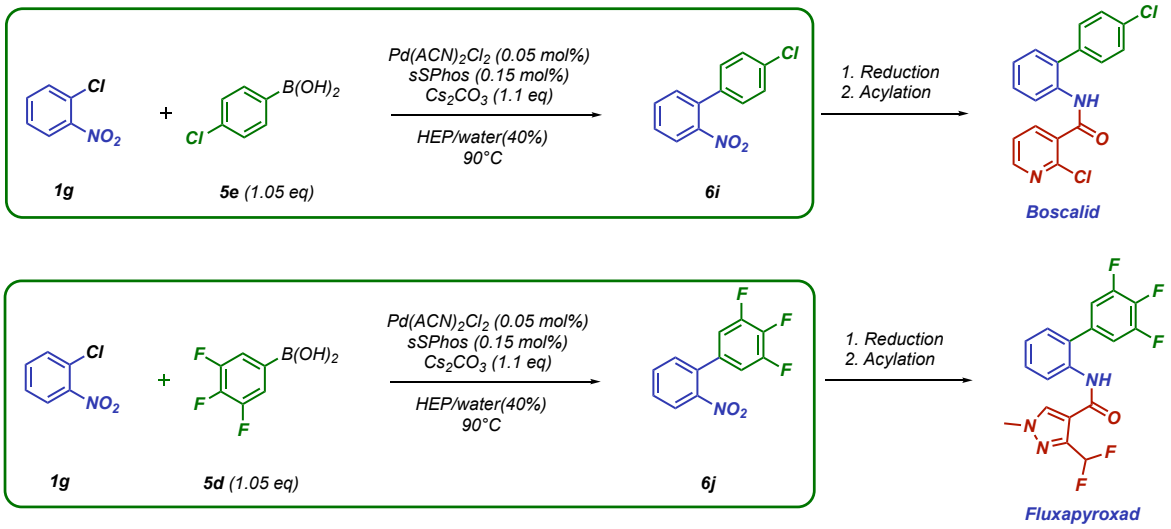

***Scheme 4.1**: General sequence for the industrial synthesis of Boscalid and Fluxapyroxad*

Selectivity tests: To have further evidence of the reaction efficiency, selectivity tests for the HC and the SM reactions were performed (Scheme 4.2). To achieve our purpose, we selected 1-cloro-3-iodobenzene **7** as model substrate and performed a one pot HC-HC reaction in one case (Scheme 4.2a) and a one pot HC-SM in the other (Scheme 4.2b), exploiting the different reactivity of the iodide leaving group in respect to the chloride. The reaction between **7** and alkyne **2b** with 2 mol% of palladium catalyst and TMG as

base afforded selectively product **8** with complete conversion in 2h. At this point, without the need of any work up, the direct slow addition of phenylacetylene **2a** together with TMG achieved pure product **9** without any purification procedure. The same thing can be done by adding in the second step, after achieving product **8**, phenyl boronic acid **5a** and Cs_2CO_3 instead of phenylacetylene **2a** and TMG, performing a one pot HC-SM cross-coupling reaction and affording product **10** with 99% of conversion and no need of further purification (Scheme 4.2b).

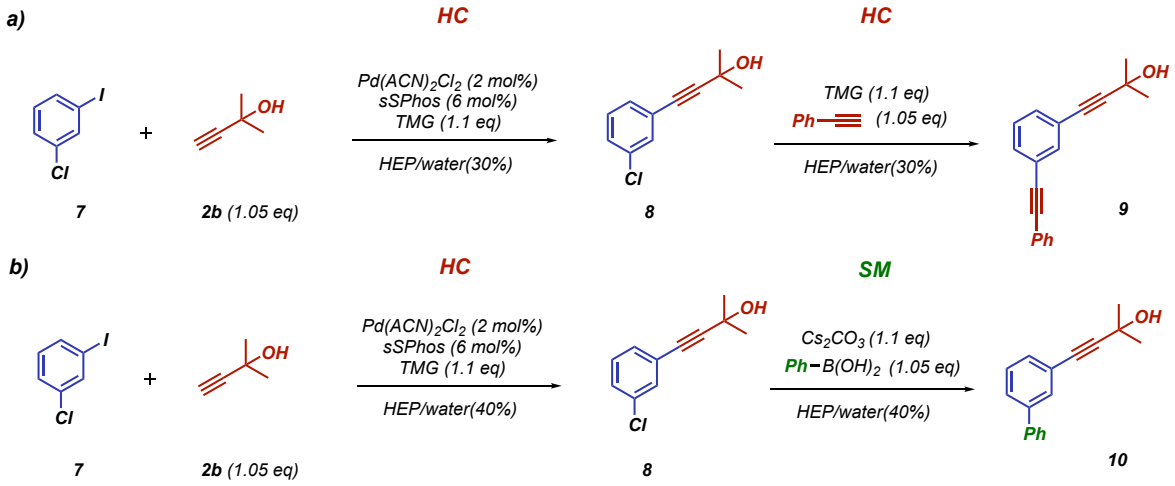

Scheme 4.2: *One-pot reactions: a) HC coupling to obtain **8** with 99% conversion in 2h. Direct slow-addition of phenylacetylene **2a** to achieve **9** with 99% conversion in 3h. b) HC coupling to obtain **8** with 99% conversion in 2h. Direct addition of phenylboronic acid **5a** to obtain **10** with 99% conversion in 1h.*

4.3 Conclusions

The Heck-Cassar and the Suzuki-Miyaura cross-coupling reactions on different aryl chlorides were performed in the sustainable mixture HEP/water giving excellent results in terms of yield, TON, TOF and PMI. The protocol proved to be suitable for activated and unactivated chlorides increasing the library of compounds to be used in these cross-coupling reactions. Both the HC and the SM are completely selective, achieving the product with high yield without any purification, avoiding an excess of nucleophile to be used. This concept is important if the final target is to use this protocol at industrial level, where the purification of the final product is one of the most problematic steps. Regarding the HC reactions, if sensitive substrates are used, the coupling can be

performed with 2 mol% in order to have fast reactions and the possibility to recycle and recover the catalyst at the end of the final cycle. On the other hand, it is also possible to perform the reaction directly with lower amount of catalyst achieving the product with high yield, but with longer reaction times. The SM protocol allowed to obtain pure products with 0.05 mol% of catalyst loading with fast and selective reactions. The applicability of this system was also demonstrated in the synthesis of agrochemical active ingredients such as Boscalid and Fluxapyroxad with excellent yields proving the efficacy and the flexibility of the protocol.

4.4 Experimental

General information

Commercial reagents (reagent grade, >99%) were used as received without additional purification.

Solvents (cyclohexane (Cy), dichloromethane (DCM), methyl-*tert*-butyl ether (MTBE), N-hydroxyethylpyrrolidone (HEP), toluene, 2-methyltetrahydrofuran (2-MeTHF), isobutylacetate (IBA), isopropyl alcohol (IPA)) are commercially available and were used after degassing.

^{1}H NMR and ^{13}C NMR spectra were recorded with an Agilent-Technologies-Varian INOVA 400 MHz and 100 MHz instrument $^{1}H/^{19}F/X$ 5 mm PFG ATB Broadband Probe, VT, single, double and triple resonance, z-axis pulsed field gradients, serves broadband probe and customized variable temperature – 5 mm Broadband probe. NMR multiplicities are abbreviated as follows: s = singlet, d = doublet, t = triplet, q = quartet, spt = septet, m = multiplet, bs = broad signal. Coupling constants *J* are given in Hz. All ^{1}H and ^{13}C chemical shifts are calibrated to residual protic-solvents.

HPLC-UV analysis were recorded with an Agilent 1260 InfinityLab instrument. Column: Zorbax® SB-C18; particle size 5 µm; pore size 100 Å; length 250 mm, internal diameter: 4.6 mm. Mobile phase A: H_2O, mobile phase B: ACN. Gradient (Time(min), %B): 0, 30; 8, 80; 22, 80; 24, 10; 30, 10; flow 0.5 mL min^{-1}column temperature 30°C; injection volume: 20 µL.

NE-1010 Higher Pressure Syringe Pump used to perform slow-addition of acetylenes in the Heck-Cassar-Sonogashira cross-coupling reactions.

Mass Spectrometry analysis were recorded on a QTRAP 3200 mass spectrometer in ESI^+ mode.

Spectrometer ICP-OES AGILENT 5110 was used to determine the concentration of Pd in the solution. Power: 1200 W; Auxiliary gas: Argon (1.0 L min^{-1}); nebulizer gas: nitrogen (0.7 L min^{-1}); peristaltic pump speed: 12 rpm. Samples for ICP-OES were digested with 8 mL HNO_3/HCl (1:3) using a microwave digestion system held at 175 °C for 10 minutes. The volume of the digests was then made up to 50 mL with de-ionized water before analysis by ICP-OES. Calibration standards for the quantification of the digested samples were prepared in 5% HNO_3. Palladium standards from FaggiEnrico and copper standards from Exaxol Italia.

General Procedures

General procedure for the HC coupling with aryl chlorides

*Heck-Cassar reactions with **2 mol%** of catalyst*

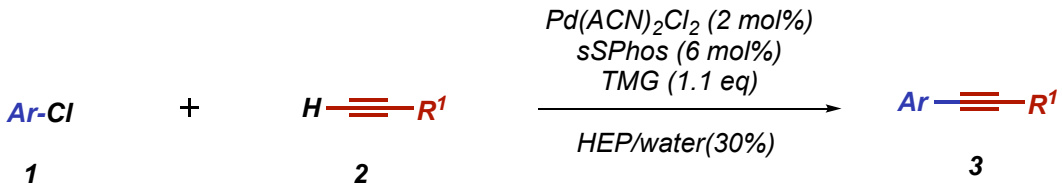

To an oven-dried 10 mL Schlenk purged under N_2 atmosphere, palladium pre-catalyst (0.02 mmol, 2 mol%, 5.2 mg), sSPhos, (0.06 mmol, 6 mol%, 30.8 mg) were dissolved in HEP and water as co-solvent. The other reagents were then added in the following order: TMG (126.9 mg, 138.0 µL, 1.1 mmol, 1.1 eq) and aryl chloride (1.0 mmol, 1.0 eq). The reaction mixture was heated to 80-90°C with an oil bath and alkyne (from 1.05 to 1.5 eq) was added slowly with a syringe pump over the course of the reaction; the conversion was evaluated through HPLC-UV analysis at 210 nm considering the appropriate Relative Response Factor (RRF) (see RRF calculation section). At reaction completion, the mixture was extracted with an appropriate organic solvent (3x1 mL) and the collected organic phases were concentrated under reduced pressure. The reaction crude was purified when necessary by

flash chromatography (eluents and isolated yields specified below in Compound Characterization section).

*Heck-Cassar reactions with **0.2-0.4 mol%** of catalyst*

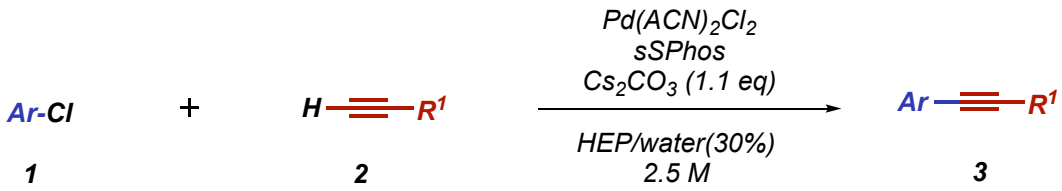

Preparation of stock solution of catalyst A

To an oven-dried 10 mL Schlenk purged under N_2 atmosphere, palladium pre-catalyst $Pd(ACN)_2Cl_2$ (0.04 mmol, 10.4 mg) and ligand sSPhos, (0.12 mmol, 61.6 mg) were dissolved in 4 mL of HEP/water(30%) solution. The mixture was stirred for 5 min at room temperature. A yellow-orange solution was obtained for subsequent HC reactions (stock solution is stable and can be used even after one week**)**

Procedure:

To an oven-dried 10 mL Schlenk purged under N_2 atmosphere, 200 - 400 µL of stock solution A (0.2-0.4 mol% of palladium catalyst) was added along with the amount of HEP/water(30%) solution needed to achieve the desired concentration. The other reagents were then added in the following order: Cs_2CO_3 (358 mg, 1.1 mmol, 1.1 eq) and aryl chloride (1.0 mmol, 1.0 eq). The reaction mixture was heated to 80-90°C with an oil bath and alkyne (1.05-1.2 eq) was added slowly with a syringe pump over the course of the reaction; the conversion was evaluated through HPLC-UV analysis at 210 nm considering the appropriate RRF. At reaction completion, the mixture was extracted with an appropriate organic solvent (3x1 mL). The collected organic phases were concentrated under reduced pressure. The reaction crude was purified when necessary by flash chromatography (eluents and isolated yields specified below in Compound Characterization section)

General procedure for Suzuki-Miyaura cross-coupling with aryl chlorides

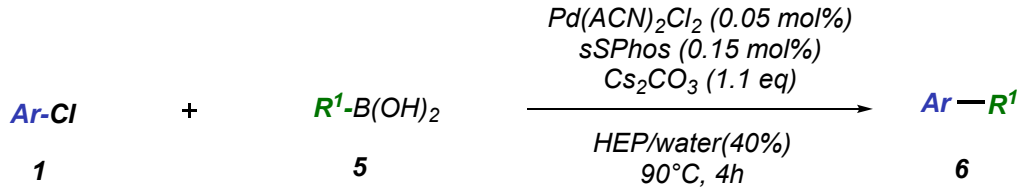

Preparation of stock solution of catalyst B

To an oven-dried 10 mL Schlenk purged under N_2 atmosphere, palladium pre-catalyst $Pd(ACN)_2Cl_2$ (0.04 mmol, 10.4 mg) and ligand sSPhos, (0.12 mmol, 61.6 mg) were dissolved in 4 mL of HEP/water(40%) solution. The mixture was stirred for 5 min at room temperature. A yellow-orange solution was obtained for subsequent SM reactions (stock solution is stable and can be used even after one week)

Procedure:

To an oven-dried 10 mL Schlenk purged under N_2 atmosphere, 50 µL of stock solution B (0.05 mol% of palladium catalyst) was added along with the amount of HEP/water(40%) solution needed to achieve the desired concentration. The other reagents were then added in the following order: Cs_2CO_3 (358 mg, 1.1 mmol, 1.1 eq), aryl chloride (1.0 mmol, 1.0 eq) and boronic acid (1.05 mmol, 1.05 eq). The reaction mixture was heated to 90°C with an oil bath and maintained at this temperature under stirring; the conversion was evaluated through HPLC-UV analysis at 210 nm considering the appropriate RRF. At reaction completion, the mixture was extracted with an appropriate organic solvent (3x1 mL). The collected organic phases were concentrated under reduced pressure. The product was isolated without need of purification (yields specified below in Compound Characterization section).

PMI calculation

Recovery of HEP and Pd in the HC cross-coupling with ***2 mol%***

At the given time, the reaction was cooled at rt, extracted with cyclohexane and the HEP/water phase containing the catalyst was recycled (see Chapter 3 for the recycling protocol).

After the final cycle, product **3a** was again extracted with cyclohexane and the combined organic extracts were distilled and the product could be recovered without further purification. The reaction mixture, containing HEP/water, conjugated TMG acid and the catalyst complex, was treated with sodium formate (0.03 mmol, 2.0 mg) for 1h at 60°C to generate palladium black. At reaction completion, the mixture was filtered out with the aid of charcoal (30 mg) and the palladium metal was recovered. The filtrate was distilled under reduced pressure to recover HEP in 95% yield

Table S4.1*: Example of PMI calculation on the optimized HC reaction (Entry 1, Table 4.2)*

Reagents	Single run (mg)	5 cycles (mg)[a]	5 cycles and final recovery (mg)[b]	Recovery %
Chlorobenzene **1a**	112.6	563	563	-
Phenylacetylene **2a**	107.2	536	536	-
TMG	126.7	633	633	-
$Pd(ACN)_2Cl_2$	5.1	5.1	0.5	90
sSPhos	30.8	30.8	30.8	-
HEP	800	800	40	95
Water	300	300	300	-
Sodium formate	-	-	2	-
Charcoal	-	-	30	-
Cyclohexane[c]	2337	11685	584	95
Diphenylacetylene **3a**[d]	174.6	802	802	-
PMI	21	-	-	-
PMI after Pd/sSPhos and HEP/water recycle	-	18.1	-	-
PMI after final recovery of Pd, HEP and Cy	-	-	3.3	-

[a]PMI calculated after 5 cycles and recycle of Pd complex and HEP/water [b]PMI calculated after 5 cycles and recycle of Pd complex, HEP/water and final recovery of Pd metal, HEP and cyclohexane. [c]The organic phases obtained from the different cycles were combined and distilled to recover 95% of cyclohexane. [d]Product **3a** obtained without need of purification.

*Recovery of HEP and Pd in the HC cross-coupling with **0.2 mol%***

At the given time, the reaction was cooled at rt, extracted with cyclohexane achieving product **3a** with 93% yield with no need of purification. The reaction mixture, containing HEP/water, conjugated Cs_2CO_3 acid and the catalyst complex, was treated with sodium formate (0.01 mmol, 1.0 mg) for 1h at 60°C in order to generate palladium black. At reaction completion, the mixture was filtered out with the aid of charcoal (6.0 mg) and the palladium metal was recovered. The filtrate was distilled under reduced pressure to recover HEP in 95% yield

***Table S4.2**: Example of PMI calculation on the direct HC reaction (Entry 5, Table 4.3)*

Reagents	Single run (mg)	Single run and final recovery (mg)[b]	Recovery %
Chlorobenzene **1a**	112.6	112.6	-
Phenylacetylene **2a**	107.2	107.2	-
Cs_2CO_3	358	358	-
$Pd(ACN)_2Cl_2$	0.5	0.05	90
sSPhos	3.0	3.0	-
HEP	320	16	95
Water	120	120	-
Sodium formate	-	1	-
Charcoal	-	6	-
Cyclohexane[c]	930	46	95
Diphenylacetylene **3a**[d]	174.6	165	-
PMI[a]	11.1	-	-
PMI after final recovery of Pd, HEP and Cy	-	4.6	-

[a]PMI calculated considering all the reagents used without recovery [b]PMI calculated after final recovery of Pd metal, HEP and cyclohexane. [c]The organic phases obtained from the different cycles were combined and distilled to recover 95% of cyclohexane. [d]Product **3a** obtained without need of purification.

*Recovery of HEP and Pd in the SM cross-coupling with **0.05 mol%***

At the given time, the reaction was cooled at rt, extracted with cyclohexane achieving product **6a** with 95% yield with no need of purification. The reaction mixture, containing HEP/water, conjugated Cs_2CO_3 acid and the catalyst complex, was treated with sodium

formate (0.01 mmol, 1.0 mg) for 1h at 60°C in order to generate palladium black. At reaction completion, the mixture was filtered out with the aid of charcoal (6.0 mg) and the palladium metal was recovered. The filtrate was distilled under reduced pressure to recover HEP in 95% yield

***Table S4.3**: Example of PMI calculation on the direct SM reaction of Scheme 4.1a*

Reagents	Single run (mg)	Single run and final recovery (mg)[b]	Recovery %
1g	157	157	-
5e	164	164	-
Cs_2CO_3	358	358	-
$Pd(ACN)_2Cl_2$	0.1	0.01	90
sSPhos	0.7	0.7	-
HEP	685	34	95
Water	400	400	-
Sodium formate	-	1	-
Charcoal	-	6	-
Cyclohexane[c]	2337	116	95
6i[d]	224	224	-
PMI[a]	18.1	-	-
PMI after final recovery of Pd, HEP and Cy	-	5.5	-

[a]PMI calculated considering all the reagents used without recovery [b]PMI calculated after final recovery of Pd metal, HEP and cyclohexane. [c]The organic phases obtained from the different cycles were combined and distilled to recover 95% of cyclohexane. [d]Product **6i** obtained without need of purification.

Selectivity studies

One-pot HC-HC cross-coupling reactions

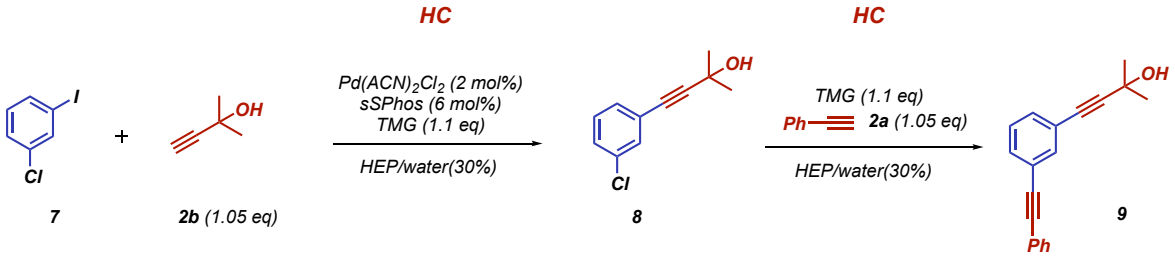

To an oven-dried 10 mL Schlenk purged under N_2 atmosphere, palladium pre-catalyst (0.02 mmol, 2 mol%, 5.2 mg), sSPhos, (0.06 mmol ,6 mol%, 30.4 mg) were dissolved in HEP and

water as co-solvent. The other reagents were then added in the following order: TMG (126.7 mg, 138.0 µL, 1.1 mmol, 1.1 eq), 1-chloro-3-iodobenzene **7** (238.4 mg, 123.8 µL, 1.0 mmol, 1.0 eq) and alkyne **2b** (92.5 mg, 106.6 µL, 1.1 mmol, 1,1 eq). The reaction mixture was heated to 70°C with an oil bath and the conversion was evaluated through HPLC-UV analysis at 210 nm. After 2h, intermediate **8** was achieved with a complete conversion and a selectivity >99%. The mixture was then heated to 90°C, TMG (1.1 eq) was directly added and phenylacetylene **2a** was added slowly in 4h with a syringe pump in order to achieve product **9** with 95% of conversion. The mixture was extracted with IBA (3x5 mL). The collected organic phases were concentrated under reduced pressure. The collected organic phases were concentrated under reduced pressure to achieve compound **9** without need of purification

One-pot HC-SM cross-coupling reactions

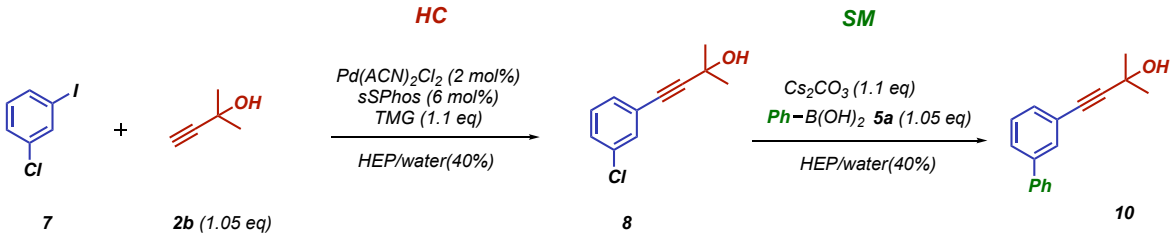

7 **2b** *(1.05 eq)* **8** **10**

To an oven-dried 10 mL Schlenk purged under N_2 atmosphere, palladium pre-catalyst (0.02 mmol, 2 mol%, 5.2 mg), sSPhos, (0.08 mmol ,8 mol%, 40.1 mg) were dissolved in HEP and water as co-solvent. The other reagents were then added in the following order: TMG (126.7 mg, 138.0 µL, 1.1 mmol, 1.1 eq), 1-chloro-3-iodobenzene **7** (238.4 mg, 123.8 µL, 1.0 mmol, 1.0 eq) and alkyne **2b** (92.5 mg, 106.6 µL, 1.1 mmol, 1,1 eq). The reaction mixture was heated to 70°C with an oil bath and the conversion was evaluated through HPLC-UV analysis at 210 nm. After 2h, intermediate **8** was achieved with a complete conversion and a selectivity >99%. The mixture was then heated to 90°C, Cs_2CO_3 (358.4 mg, 1.1 mmol, 1.1 eq) and phenyl boronic acid **5a** (128.0 mg, 1.05 mmol, 1.05 eq) were directly added to the solution. The reaction was complete in 2h giving product **10** with a complete conversion. The mixture was extracted with IBA (3x5 mL). The collected organic phases were concentrated under reduced pressure in order to achieve compound **10** without need of purification.

Compound characterization

The yields are calculated considering the single run of HC and SM reactions

*1,2-diphenylacetylene (**3a**)*

White solid (98% yield)

^{1}H NMR (400 MHz, $CDCl_3$) δ (ppm) 7.58 – 7.56 (m, 4H), 7.39 – 7.36 (m, 6H).

^{13}C NMR (100 MHz, $CDCl_3$) δ (ppm) 131.27, 128.00, 127.91, 122.94, 89.04.

Anal. Calcd. for $C_{14}H_{10}$: C, 94.33; H, 5.67; found: C, 94.62; H, 5.69.

*1-nitro-4-(phenylethynyl)benzene (**3b**)*

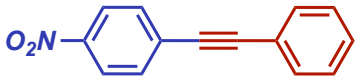

Yellow solid (97% yield)

^{1}H NMR (400 MHz, $CDCl_3$) δ (ppm) 8.19 – 8.17 (m, 2H), 7.64 – 7.62 (m, 2H), 7.56 – 7.53 (m, 2H), 7.38 – 7.36 (m, 3H).

^{13}C NMR (100 MHz, $CDCl_3$) δ (ppm) 146.95, 132.27, 131.84, 130.22, 129.28, 128.57, 123.58, 122.10, 94.75, 87.59.

Anal. Calcd. for $C_{14}H_9NO_2$: C, 75.33; H, 4.06; N, 6.27; found: C, 75.26; H, 4.06; N, 6.27.

*1-nitro-3-(phenylethynyl)benzene (**3c**)*

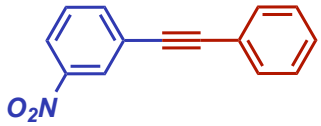

Yellow solid (96% yield)

^{1}H NMR (400 MHz, $CDCl_3$) δ (ppm) 8.36 – 8.35 (m, 1H), 8.17 – 8,15 (d, 1H, J = 8.2 Hz), 7.82 – 7.80 (d, 1H, J = 7.7 Hz), 7.53 – 7.49 (m, 3H), 7.40 – 7.38 (m, 3H).

^{13}C NMR (100 MHz, $CDCl_3$) δ (ppm) 148.11, 137.19, 131.77, 129.35, 129.06, 128.53, 126.28, 125.10, 122.84, 122.19, 91.92, 86.91.

Anal. Calcd. for $C_{14}H_9NO_2$: C, 75.33; H, 4.06; N, 6.27; found: C, 75.14; H, 4.06; N, 6.26.

*4-(phenylethynyl)benzonitrile (**3d**)*

Yellow solid (96% yield).

^{1}H NMR (400 MHz, $CDCl_3$) δ (ppm) 7.66– 7.61 (m, 4H), 7.57 – 7.55 (m, 2H), 7.40 – 7.38 (m, 3H).

^{13}C NMR (100 MHz, $CDCl_3$) δ (ppm) 132.05, 132.02, 131.77, 129.10, 128.49, 128.23, 122.21, 118.50, 111.45, 93.76, 87.70.

Anal. Calcd. for $C_{14}H_9N$: C, 88.64; H, 4.46; N, 6.89; found C, 88.69; H, 4.38; N, 6.92.

*1-methoxy-4-(phenylethynyl)benzene (**3e**)*

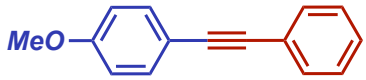

White solid (96% yield).

^{1}H NMR (400 MHz, $CDCl_3$) δ (ppm) 7.55 – 7.49 (m, 4H), 7.37 – 7.33 (m, 3H), 6.91 – 6.89 (m, 2H), 3.84 (s, 3H).

^{13}C NMR (100 MHz, $CDCl_3$) δ (ppm) 159.60, 133.02, 131.42, 128.28, 127.90, 123.58, 115.36, 113.98, 89.35, 88.05, 55.26.

Anal. Calcd. for $C_{15}H_{12}O$: C, 86.51; H, 5.81; found: C, 86.72; H, 5.81.

*1-methyl-4-(phenylethynyl)benzene (**3f**)*

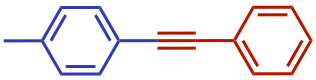

White solid (95% yield).

^{1}H NMR (400 MHz, $CDCl_3$) δ (ppm) 7.57 – 7.54 (m, 2H), 7.47 – 7.45 (d, *J* = 8.1 Hz, 2H), 7.38 – 7.34 (m, 3H), 7.19 – 7.17 (d, *J* = 7.9 Hz, 2H), 2.40 (s, 3H).

^{13}C NMR (100 MHz, $CDCl_3$) δ (ppm) 138.36, 131.53, 131.48, 129.09, 128.29, 128.04, 89.55, 88.71, 21.49.

Anal. Calcd. for $C_{15}H_{12}$: C, 93.79; H, 6.21; found: C, 93.57, H: 6.23.

*2-methyl-4-phenylbut-3-yn-2-ol (**3g**)*

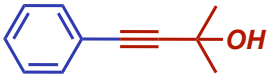

Yellow oil (93% yield); Purification by flash chromatography (Cy/EtOAc = 95/5).

^{1}H NMR (400 MHz, $CDCl_3$) δ (ppm) 7.44 – 7.42 (m, 2H), 7.31 – 7.29 (m, 3H), 2.53 (s, OH), 1.64 (s, 6H).

^{13}C NMR (100 MHz, $CDCl_3$) δ (ppm) 131.23, 127.83, 127.81, 122.37, 93.50, 81.69, 65.17, 31.08.

Anal. Calcd. for $C_{11}H_{12}O$: C, 82.46; H, 7.55; found: C, 82.78; H, 7.54.

*N,N-dimethyl-3-phenylprop-2-yn-1-amine (**3h**)*

Colourless liquid (94% yield); Purification by flash chromatography (Cy/EtOAc = 95/5).

^{1}H NMR (400 MHz, $CDCl_3$) δ (ppm) 7.45 – 7.43 (m, 2H), 7.30 – 7.28 (m, 3H), 3.47 (s, 2H), 2.37 (s, 6H).

^{13}C NMR (100 MHz, $CDCl_3$) δ (ppm) 131.27, 127.82, 127.59, 122.80, 84.86, 84.13, 48.15, 43.81.

Anal. Calcd. for $C_{11}H_{13}N$: C, 82.97; H, 8.23; N, 8.80; found: C, 82.99; H, 8.22; N, 8.77.

*3-(4-nitrophenyl)prop-2-yn-1-ol (**3i**)*

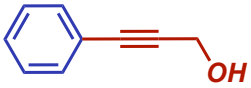

Yellow oil (95% yield); Purification by flash chromatography (Cy/EtOAc = 95/5).

^{1}H NMR (400 MHz, $CDCl_3$) δ (ppm) 8.21 – 8.18 (dd, J = 8.0, 4.0 Hz, 2H), 7.60 – 7.57 (dd, J = 8.0, 4.0 Hz, 2H), 4.55 (s, 2H).

^{13}C NMR (100 MHz, $CDCl_3$) δ (ppm) 147.25, 132.39, 129.41, 123.57, 92.46, 83.81, 51.49.

Anal. Calcd. for $C_9H_7NO_3$: C, 61.02; H, 3.98; N, 7.91; O, 27.09; found: C, 61.11; H, 3.95; N, 7.87; O, 28.1.

*1-(hept-1-yn-1-yl)-4-nitrobenzene (**3j**)*

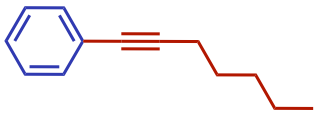

Yellow oil (94% yield); Purification by flash chromatography (Cy 100%).

^{1}H NMR (400 MHz, $CDCl_3$) δ (ppm) 8.16 – 8.14 (dd, J = 8.0, 4.0 Hz, 2H), 7.52 – 7.50 (dd, J = 8.0, 4.0 Hz, 2H), 2.46 – 2.43 (t, *J* = 12.0 Hz, 2H), 1.66 – 1.60 (m, 2H), 1.48 – 1.34 (m, 4H), 0.95 – 0.91 (t, *J* = 12.0 Hz, 3H).

^{13}C NMR (100 MHz, $CDCl_3$) δ (ppm) 146.53, 132.19, 131.20, 123.43, 96.79, 79.25, 31.08, 28.08, 22.16, 19.50, 13.93.

Anal. Calcd. for $C_{13}H_{15}NO_2$: C, 71.87; H, 6.96; N, 6.45; O, 14.73; found: C, 71.93; H, 6.92; N, 6.50; O, 14.69.

1,1'-biphenyl, **6a**

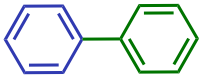

White solid (98% yield).

^{1}H NMR (400 MHz, $CDCl_3$) δ (ppm) 7.69 – 7.66 (m, 4H), 7.54 – 7.49 (m, 4H), 7.44 – 7.40 (m, 2H).

^{13}C NMR (100 MHz, $CDCl_3$) δ (ppm) 141.28, 128.80, 127.29, 127.21.

Anal. Calcd. for $C_{12}H_{10}$: C, 93.46; H, 6.54; found: C, 93.37; H, 6.62.

4-methoxy-1,1'-biphenyl, **6b-6e**

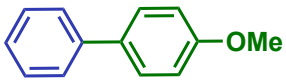

White solid (97% yield).

^{1}H NMR (400 MHz, $CDCl_3$) δ (ppm) 7.58 – 7.52 (m, 4H), 7.45 – 7.41 (m, 2H), 7.33 – 7.29 (m, 1H), 7.00 – 6.98 (m, 2H), 3.87 (s, 3H).

^{13}C NMR (100 MHz, $CDCl_3$) δ (ppm)159.11, 140.81, 133.76, 128.68, 128.12, 126.71, 126.62, 114.17, 55.32.

Anal. Calcd. for $C_{13}H_{12}O$: C, 84.75; H, 6.57; O, 8.68; found: C, 84.77; H, 6.51; O, 8.70.

4-methyl-1,1'-biphenyl, **6c-6f**

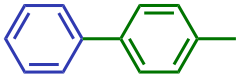

White solid (95% yield).

^{1}H NMR (400 MHz, $CDCl_3$) δ (ppm) 7.68 – 7.66 (m, 2H), 7.60 – 7.58 (m, 2H), 7.53 – 7.49 (m, 2H), 7.43 – 7.39 (m, 1H), 7.35 – 7.33 (d, J = 7.8 Hz, 2H).

^{13}C NMR (100 MHz, $CDCl_3$) δ (ppm) 141.22, 138.44, 137.06, 129.57, 128.79, 127.04, 127.02, 21.14.

Anal. Calcd. for $C_{13}H_{12}$: C, 92.81; H, 7.19; found: C, 92.75; H, 7.23.

3,4,5-trifluoro-1,1'-biphenyl, **6d**

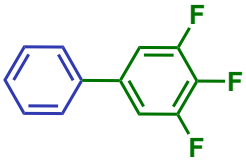

White solid (94% yield).

^{1}H NMR (400 MHz, $CDCl_3$) δ (ppm) 7.53 – 7.42 (m, 5H), 7.22 – 7.18 (m, 2H).

^{13}C NMR (100 MHz, $CDCl_3$) δ (ppm) 152.72 – 152.58 (dd, J^F = 9.9, 4.2 Hz), 150.25 – 150.11 (dd, J^F = 10.1, 4.4 Hz), 140.63 – 140.32 (t, J^F = 15.1 Hz), 138.17 – 137.43 (m), 137.45 – 137.25 (m), 129.06, 128.37, 126.81, 111.10 – 110.88 (dd, J^F = 16.1, 6.0 Hz).

Anal. Calcd. for $C_{12}H_7F_3$: C, 69.23; H, 3.39; F, 27.38; found: C, 69.20; H, 3.45; F, 27.44.

2-nitro-1,1'-biphenyl, **6g**

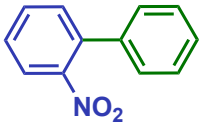

Yellow oil (96% yield).

^{1}H NMR (400 MHz, $CDCl_3$) δ (ppm) 7.89– 7.87 (dd, J = 8.0, 1.3 Hz, 1H), 7.65 – 7.61 (td, J = 7.6, 1.3 Hz, 1H), 7.52 – 7.44 (m, 5H), 7.38 – 7.35 (m, 2H).

^{13}C NMR (100 MHz, $CDCl_3$) δ (ppm) 149.32, 137.42, 136.32, 132.31, 131.97, 128.70, 128.24, 128.20, 127.91, 124.06.

Anal. Calcd. for $C_{12}H_9NO_2$: C, 72.35; H, 4.55; N, 7.03; O, 16.06; found: C, 72.39; H, 4.52; N, 7.01; O, 16.09.

4-nitro-1,1'-biphenyl, **6h**

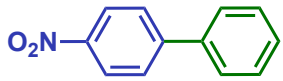

Yellow solid (94% yield).

^{1}H NMR (400 MHz, $CDCl_3$) δ (ppm) 8.32 – 8.30 (m, 2H), 7.76 – 7.74 (m, 2H), 7.65 (m, 2H), 7.54 – 7.46 (m, 3H).

^{13}C NMR (100 MHz, $CDCl_3$) δ (ppm) 147.61, 147.07, 138.75, 129.16, 128.89, 127.80, 127.36, 124.08.

Anal. Calcd. for $C_{12}H_{14}$: C, 72.35; H, 4.55; N, 7.03; O, 16.06; found: C, 72.25; H, 4.61; N, 7.07; O, 15.9.

4'-chloro-2-nitro-1,1'-biphenyl, **6i**

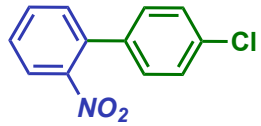

Yellow solid (97% yield).

^{1}H NMR (400 MHz, $CDCl_3$) δ (ppm) 7.90 – 7.87 (dd, J = 8.1, 1.3 Hz, 1H), 7.65 – 7.61 (td, J = 7.6, 1.3 Hz, 1H), 7.53 – 7.49 (m, 1H), 7.43 – 7.39 (m, 3H), 7.27 – 7.25 (m, 2H).

^{13}C NMR (100 MHz, $CDCl_3$) δ (ppm) 149.03, 135.95, 135.15, 134.41, 132.55, 131.85, 129.30, 128.89, 128.61, 124.25.

Anal. Calcd. for $C_{12}H_8ClNO_2$: C, 61.69; H, 3.45; Cl, 15.17; N, 5.99; O, 13.69; found: C, 61.74; H, 3.38; Cl, 15.13; N, 6.04; O, 13.74.

3',4',5'-trifluoro-2-nitro-1,1'-biphenyl, **6j**

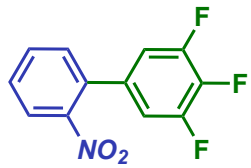

Yellow solid (95% yield).

^{1}H NMR (400 MHz, $CDCl_3$) δ (ppm) 7.96 – 7.93 (dd, J = 8.1, 1.3 Hz, 1H), 7.69 – 7.65 (td, J = 7.5, 1.3 Hz, 1H), 7.60 – 7.55 (dt, *J* = 7.8, 1.5 Hz, 1H), 7.41 – 7.39 (dd, J = 7.6, 1.5 Hz, 1H), 6.97 – 6.94 (m, 2H).

^{13}C NMR (100 MHz, $CDCl_3$) δ (ppm) 152.41 – 152.27 (dd, J^F = 10.3, 4.2 Hz), 149.92 – 149.77 (dd, J^F = 10.1, 4.4 Hz), 148.68, 141.19 – 140.89 (t, J^F = 15.1 Hz), 138.68 – 138.38 (t, J^F = 15.1 Hz), 133.51 – 133.46 (m), 132.79, 131.63, 129.37, 124.49, 112.68 – 112.46 (dd, J^F = 16.1, 6.0 Hz).

Anal. Calcd. for $C_{12}H_6F_3NO_2$: C, 56.93; H, 2.39; F, 22.51; N, 5.53; O, 12.64; found: C, 56.98; H, 2.35; F, 22.46; N, 5.61; O, 12.60.

2-methyl-4-(3-(phenylethynyl)phenyl)but-3-yn-2-ol, **9**

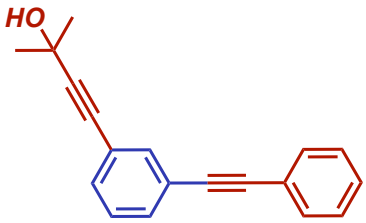

Yellow oil (92% yield).

^{1}H NMR (400 MHz, $CDCl_3$) δ (ppm) 7.63 (s, 1H), 7.56 – 7.53 (m, 2H), 7.49 – 7.47 (m, 1H), 7.40 – 7.30 (m, 5H), 1.65 (s, 6H).

^{13}C NMR (100 MHz, $CDCl_3$) δ (ppm) 134.68, 131.62, 131.29, 128.47, 128,37, 123.53, 123.08, 122.98, 94.39, 89.94, 88.47, 81.35, 65.58, 31.43.

Anal. Calcd. for $C_{19}H_{16}O$: C, 87.66; H, 6.20; O, 6.15; found: C, 87.61; H, 6.29; O, 6.14.

4-([1,1'-biphenyl]-3-yl)-2-methylbut-3-yn-2-ol, **10**

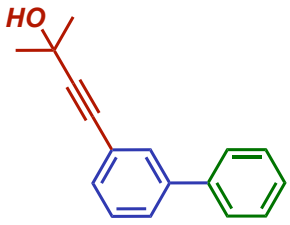

Yellow oil (96% yield).

^{1}H NMR (400 MHz, $CDCl_3$) δ (ppm) 7.72 – 7.55 (m, 4H), 7.49 – 7.38 (m, 5H), 1.70 (s, 6H).

^{13}C NMR (100 MHz, $CDCl_3$) δ (ppm) 141.34, 140.32, 130.45, 128.89, 128.79, 127.66, 127.11, 123.30, 94.13, 82.21, 65.70, 31.57.

Anal. Calcd. for $C_{17}H_{16}O$: C, 86.40; H, 6.82; O, 6.77; found: C, 86.44; H, 6.74; O, 6.81.

Calculation of the RRF

*RRF between chlorobenzene **1a** and diphenylacetylene **3a***

***Table S4.4**: RRF between **1a** and **3a** at several concentrations*

Concentration (M)	Chlorobenzene area (mAu)	Diphenylacetylene area (mAu)	RRF	Δ_{RRF}
0.0025	2142.2	5633.3	2.63	
0.0005	438.7	1126.4	2.57	**2.59**
0.00025	256.0	658.6	2.57	

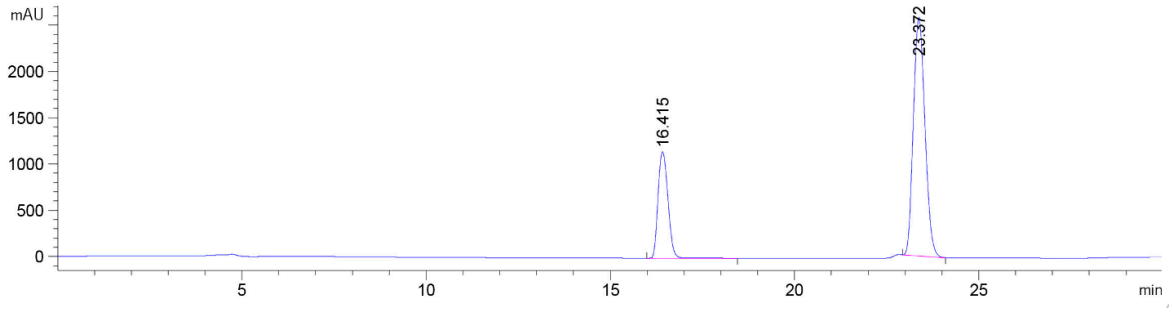

***Figure S4.1**: HPLC-UV spectrum of equimolar mixture of phenyl triflate **1a** and diphenylacetylene **3a** at 0.0005 M*

*RRF between chlorobenzene **1a** and biphenyl **6a***

***Table S4.5**: RRF calculation between **1a** and **6a** at several concentrations*

Concentration (M)	Chlorobenzene area (mAu)	Biphenyl area (mAu)	RRF	Δ_{RRF}
0.0025	1923.8	4230.5	2.19	
0.0005	496.3	1124.2	2.26	**2.23**
0.00025	351.0	790.1	2.25	

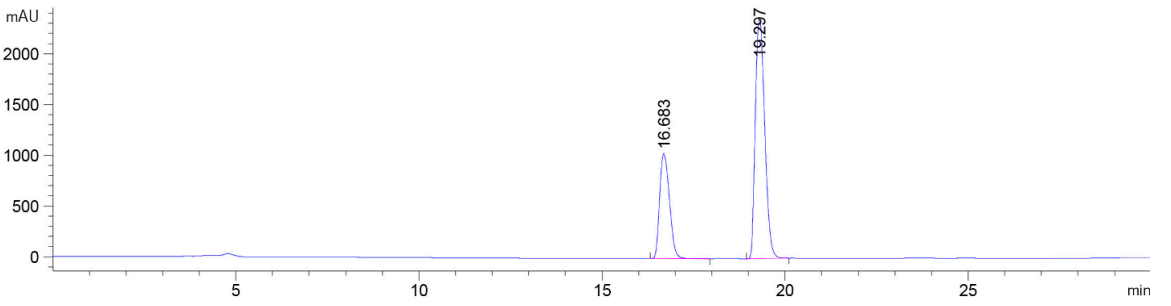

***Figure S4.2**: HPLC-UV spectrum of equimolar mixture of chlorobenzene **1a** and biphenyl **6a** at 0.0025 M concentration*

4.5 References

(1) Sonogashira, K.; Tohda, Y.; Hagihara, N. *A Convenient Synthesis of Acetylenes: Catalytic Substitutions of Acetylenic Hydrogen with Bromo Alkanes and Bromopyridines*; Pergamon Press. Frrnted m Great Britain, 1975.

(2) Dieck, H. A.; Heck, F. R. *Palladium Catalyzed Synthesis of Aryl, Heterocyclic and Vinylic Acetylene Derivatives*; 1975; Vol. 93.

(3) Cassar, L. *Synthesis of Aryl- and Vinyl- Substituted Acetylene Derivatives by the Use of Nickel and Palladium Complexes*; Elsevier Sequoia S-A, 1975; Vol. 93.

(4) Miyaura, N.; Suzuki, A. Stereoselective Synthesis of Arylated (E)-Alkenes by the Reaction of Alk-1-Enylboranes with Aryl Halides in the Presence of Palladium Catalyst. *J. Chem. Soc. Chem. Commun.* **1979**, No. 19, 866–867. https://doi.org/10.1039/C39790000866.

(5) Handa, S.; Jin, B.; Bora, P. P.; Wang, Y.; Zhang, X.; Gallou, F.; Reilly, J.; Lipshutz, B. H. Sonogashira Couplings Catalyzed by Fe Nanoparticles Containing Ppm Levels of Reusable Pd, under Mild Aqueous Micellar Conditions. *ACS Catal.* **2019**, *9* (3), 2423–2431. https://doi.org/10.1021/acscatal.9b00007.

(6) Cabri, W.; Oldani, E. Process for the Industrial Preparation of Aminoacetylenes. US5902902, 1999.

(7) Caporale, A.; Tartaggia, S.; Castellin, A.; de Lucchi, O. Practical Synthesis of Aryl-2-Methyl-3-Butyn-2-Ols from Aryl Bromides via Conventional and Decarboxylative Copper-Free Sonogashira Coupling Reactions. *Beilstein J. Org. Chem.* **2014**, *10*, 384–393. https://doi.org/10.3762/bjoc.10.36.

(8) Castellin, A.; de Lucchi, O.; Caporale, A. Method for the Preparation of Erlotinib. US2012095228(A1), 2012.

(9) Hughes, D. L. Patent Review of Manufacturing Routes to Recently Approved Oncology Drugs: Ibrutinib, Cobimetinib, and Alectinib. *Org. Process Res. Dev.* **2016**, *20* (11), 1855–1869. https://doi.org/10.1021/acs.oprd.6b00304.

(10) Miyaura, Norio.; Suzuki, Akira. Palladium-Catalyzed Cross-Coupling Reactions of Organoboron Compounds. *Chem. Rev.* **1995**, *95* (7), 2457–2483. https://doi.org/10.1021/cr00039a007.

(11) Littke, A. F.; Fu, G. C. Palladium-Catalyzed Coupling Reactions of Aryl Chlorides. *Angew. Chem., Int. Ed.* **2002**, *41* (22), 4176–4211. https://doi.org/10.1002/1521-3773(20021115)41:22<4176::AID-ANIE4176>3.0.CO;2-U.

(12) Alberico, D.; Scott, M. E.; Lautens, M. Aryl−Aryl Bond Formation by Transition-Metal-Catalyzed Direct Arylation. *Chem. Rev.* **2007**, *107* (1), 174–238. https://doi.org/10.1021/cr0509760.

(13) Shi, W.; Liu, C.; Lei, A. Transition-Metal Catalyzed Oxidative Cross-Coupling Reactions to Form C–C Bonds Involving Organometallic Reagents as Nucleophiles. *Chem. Soc. Rev.* **2011**, *40* (5), 2761. https://doi.org/10.1039/c0cs00125b.

(14) Kruger, A. W.; Rozema, M. J.; Chu-Kung, A.; Gandarilla, J.; Haight, A. R.; Kotecki, B. J.; Richter, S. M.; Schwartz, A. M.; Wang, Z. The Discovery and Development of a Safe, Practical Synthesis of ABT-869. *Org. Process Res. Dev.* **2009**, *13* (6), 1419–1425. https://doi.org/10.1021/op900208y.

(15) de Koning, P. D.; McAndrew, D.; Moore, R.; Moses, I. B.; Boyles, D. C.; Kissick, K.; Stanchina, C. L.; Cuthbertson, T.; Kamatani, A.; Rahman, L.; Rodriguez, R.; Urbina, A.; Sandoval (née Accacia), A.; Rose, P. R. Fit-for-Purpose Development of the Enabling Route

to Crizotinib (PF-02341066). *Org. Process Res. Dev.* **2011**, *15* (5), 1018–1026. https://doi.org/10.1021/op200131n.

(16) Taheri Kal Koshvandi, A.; Heravi, M. M.; Momeni, T. Current Applications of Suzuki–Miyaura Coupling Reaction in The Total Synthesis of Natural Products: An Update. *Appl. Organomet. Chem.* **2018**, *32* (3), e4210. https://doi.org/10.1002/aoc.4210.

(17) Rayadurgam, J.; Sana, S.; Sasikumar, M.; Gu, Q. Palladium Catalyzed C–C and C–N Bond Forming Reactions: An Update on the Synthesis of Pharmaceuticals from 2015–2020. *Org. Chem. Front.* **2021**, *8* (2), 384–414. https://doi.org/10.1039/D0QO01146K.

(18) Remmele, H.; Köllhofer, A.; Plenio, H. Recyclable Catalyst with Cationic Phase Tags for the Sonogashira Coupling of Aryl Bromides and Aryl Chlorides. *Organometallics* **2003**, *22* (20), 4098–4103. https://doi.org/10.1021/om030450a.

(19) Gelman, D.; Buchwald, S. L. Efficient Palladium-Catalyzed Coupling of Aryl Chlorides and Tosylates with Terminal Alkynes: Use of a Copper Cocatalyst Inhibits the Reaction. *Angew. Chem., Int. Ed.* **2003**, *42* (48), 5993–5996. https://doi.org/10.1002/anie.200353015.

(20) Wolfe, J. P.; Buchwald, S. L. A Highly Active Catalyst for the Room-Temperature Amination and Suzuki Coupling of Aryl Chlorides. *Angew. Chem., Int. Ed.* **1999**, *38* (16), 2413–2416. https://doi.org/10.1002/(SICI)1521-3773(19990816)38:16<2413::AID-ANIE2413>3.0.CO;2-H.

(21) Huang, H.; Liu, H.; Jiang, H.; Chen, K. Rapid and Efficient Pd-Catalyzed Sonogashira Coupling of Aryl Chlorides. *J. Org. Chem.* **2008**, *73* (15), 6037–6040. https://doi.org/10.1021/jo800994f.

(22) Yi, C.; Hua, R. Efficient Copper-Free $PdCl_2(PCy_3)_2$-Catalyzed Sonogashira Coupling of Aryl Chlorides with Terminal Alkynes. *J. Org. Chem.* **2006**, *71* (6), 2535–2537. https://doi.org/10.1021/jo0525175.

(23) Kirchhoff, J. H.; Dai, C.; Fu, G. C. A Method for Palladium-Catalyzed Cross-Couplings of Simple Alkyl Chlorides: Suzuki Reactions Catalyzed by $[Pd_2(Dba)_3]/PCy_3$. *Angew. Chem., Int. Ed.* **2002**, *41* (11), 1945. https://doi.org/10.1002/1521-3773(20020603)41:11<1945::AID-ANIE1945>3.0.CO;2-7.

(24) Kataoka, N.; Shelby, Q.; Stambuli, J. P.; Hartwig, J. F. Air Stable, Sterically Hindered Ferrocenyl Dialkylphosphines for Palladium-Catalyzed C−C, C−N, and C−O Bond-Forming Cross-Couplings. *J. Org. Chem.* **2002**, *67* (16), 5553–5566. https://doi.org/10.1021/jo025732j.

(25) Zapf, A.; Jackstell, R.; Rataboul, F.; Riermeier, T.; Monsees, A.; Fuhrmann, C.; Shaikh, N.; Dingerdissen, U.; Beller, M. Practical Synthesis of New and Highly Efficient Ligands for the Suzuki Reaction of Aryl Chlorides. *Chem. Comm.* **2004**, No. 1, 38. https://doi.org/10.1039/b311268n.

(26) Colacot, T. J.; Shea, H. A. Cp2Fe(PR2)2PdCl2 (R = i-Pr, TBu) Complexes as Air-Stable Catalysts for Challenging Suzuki Coupling Reactions. *Org. Lett.* **2004**, *6* (21), 3731–3734. https://doi.org/10.1021/ol048598t.

(27) Rajabi, F.; Thiel, W. R. An Efficient Palladium N-Heterocyclic Carbene Catalyst Allowing the Suzuki-Miyaura Cross-Coupling of Aryl Chlorides and Arylboronic Acids at Room Temperature in Aqueous Solution. *Adv. Synth. Catal.* **2014**, *356* (8), 1873–1877. https://doi.org/10.1002/adsc.201300841.

(28) Lee, J.-Y.; Ghosh, D.; Lee, J.-Y.; Wu, S.-S.; Hu, C.-H.; Liu, S.-D.; Lee, H. M. Zwitterionic Palladium Complexes: Room-Temperature Suzuki–Miyaura Cross-Coupling of Sterically

Hindered Substrates in an Aqueous Medium. *Organometallics* **2014**, *33* (22), 6481–6492. https://doi.org/10.1021/om500834y.

(29) Orecchia, P.; Petkova, D. S.; Goetz, R.; Rominger, F.; Hashmi, A. S. K.; Schaub, T. Pd-Catalysed Suzuki–Miyaura Cross-Coupling of Aryl Chlorides at Low Catalyst Loadings in Water for the Synthesis of Industrially Important Fungicides. *Green Chem.* **2021**, *23* (20), 8169–8180. https://doi.org/10.1039/D1GC02602J.

(30) Ferrazzano, L.; Martelli, G.; Fantoni, T.; Daka, A.; Corbisiero, D.; Viola, A.; Ricci, A.; Cabri, W.; Tolomelli, A. Fast Heck-Cassar-Sonogashira (HCS) Reactions in Green Solvents. *Org. Lett.* **2020**, *22* (10), 3969–3973. https://doi.org/10.1021/acs.orglett.0c01269.

(31) Fantoni, T.; Bernardoni, S.; Mattellone, A.; Martelli, G.; Ferrazzano, L.; Cantelmi, P.; Corbisiero, D.; Tolomelli, A.; Cabri, W.; Vacondio, F.; Ferlenghi, F.; Mor, M.; Ricci, A. Palladium Catalyst Recycling for Heck-Cassar-Sonogashira Cross-Coupling Reactions in Green Solvent/Base Blend. *ChemSusChem* **2021**, *14* (12), 2591–2600. https://doi.org/10.1002/cssc.202100623.

(32) Blakemore, D. *Synthetic Methods in Drug Discovery, Vol. 1*; Blakemore, D., Doyle, P. M., Eds.; 2016; Vol. 1.

(33) Miyaura, N. *Cross-Coupling Reactions*; Miyaura, N., Ed.; Heidelberg, 2002.

(34) Carrow, B. P.; Hartwig, J. F. Distinguishing Between Pathways for Transmetalation in Suzuki−Miyaura Reactions. *J. Am. Chem. Soc.* **2011**, *133* (7), 2116–2119. https://doi.org/10.1021/ja1108326.

(35) Mayer, H.; Golsch, D.; Isak, H.; Schroder, J. Method for Producing 2-Halogen-Pyridine-Carboxylic Acid Amides. US7241896 B2, 2007.

(36) Eiken, K.; Goetz, N.; Harreus, A.; Ammermann, E.; Lorenz, G.; Rang, H. Anilide Derivatives and Their Use for Combating Botrytis. US005589493, 1996.

Chapter 5:

New Mechanistic Insights into the Copper-free Heck–Cassar–Sonogashira cross-coupling reaction

5.1 Introduction

The general mechanism of the copper-free HC protocol is known (Chapter 1.5), but the coordination of the acetylene is still a matter of investigation for several research groups. The first step in the HCS reaction mechanism, as for all palladium cross-coupling reactions, is the oxidative addition of the Ar-X onto the Pd^0 complex. This step has been extensively studied by several research groups and for this reason it was not investigated in this study.[1–7] Harvey, Fu and Hartwig have reported studies in which they demonstrated that the active species in the Oxidative Addition (OA) step, depending on the ligand and the reaction conditions, could be Pd^0L or Pd^0L_2.[1,5,7] Moreover, the presence of anionic palladium species, postulated by Amatore and coworkers, such as $[Pd^0L_2X]^-$, can also play a role in the presence of halides.[3] Several hypothetical mechanisms have been proposed, passing through the carbopalladation mechanism reported by Heck in 1975,[8] the direct insertion protocol hypothesized by Soheili[9] and the cationic and anionic pathways of Mårtensson and coworkers[10,11] (Chapter 1.5).

Subsequently, scientific efforts devoted to understand the Heck–Cassar protocol mechanism were mainly centered on the nature of the π/σ switching, and, in addition to the anionic and cationic coordination-insertion process, an ionic pathway was also proposed (Figure 5.1).[12] On examination of the density functional theory (DFT) data, the energy barriers did not look very different considering the standard operational conditions in polar aprotic solvents at a temperature of >60°C. In addition, the different coordination–insertion processes appear to be a function of several factors, such as the nature of the leaving group, the pKa of the alkyne, the solvent, and the strength and nucleophilicity of the base. In 2018, Košmrlj and coworkers proposed a general mechanism for the Heck–Cassar protocol based on a second cycle of palladium, as shown in Figure 5.2.[13] Based on the Pd^{II}–Pd^{II} transmetallation (TM) in Figure 5.2, the main side product should be the homodimer **4** generated from complex **M** via a simple reductive elimination process. However, this hypothesis was not in line with our findings already described in Chapter 3 where the homocoupling product was never observed, even by GC-MS.[14]

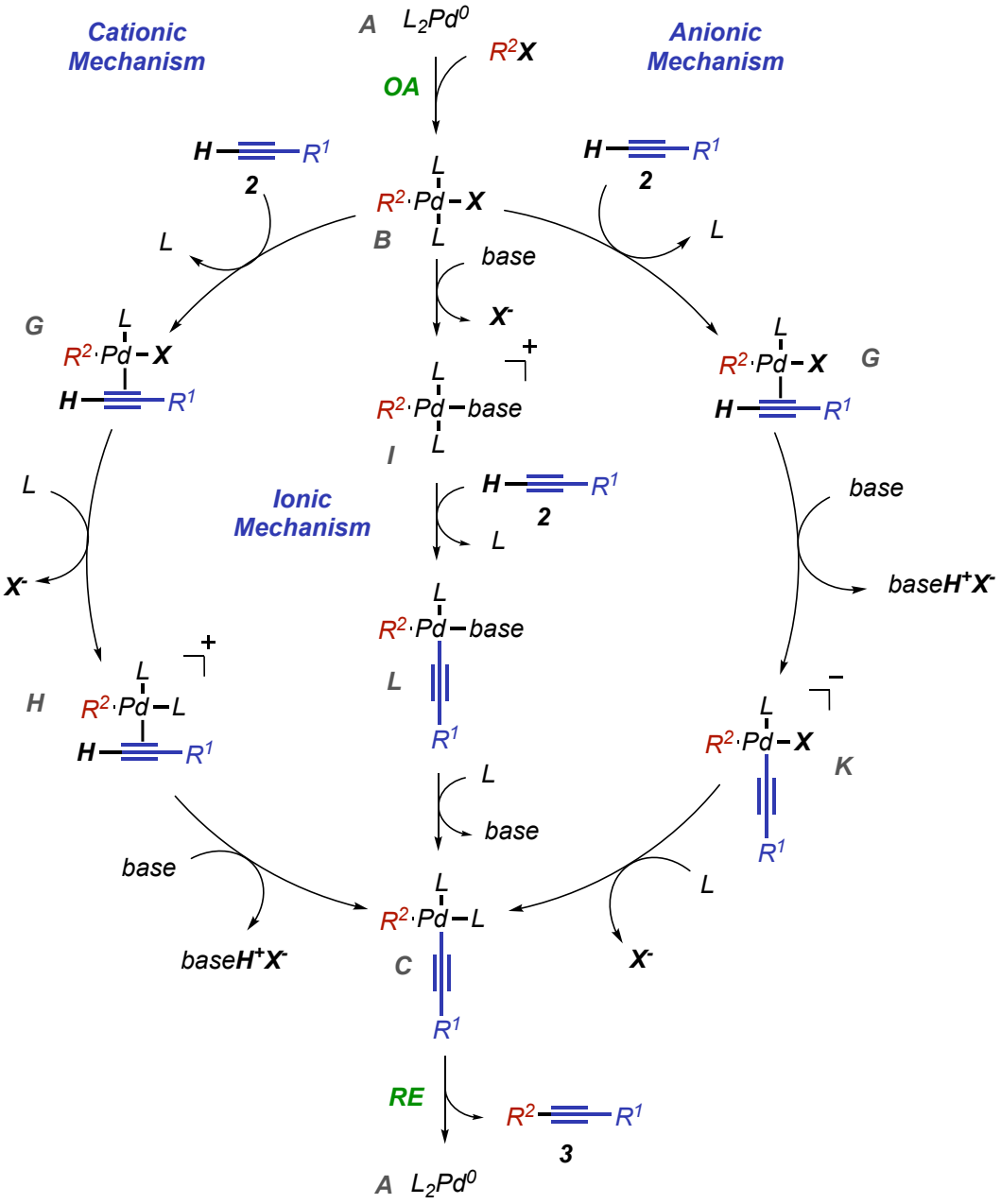

***Figure 5.1**: Heck–Cassar protocol based on direct coordination of alkyne, via cationic, anionic and ionic routes*

When the oxidative addition step to generate **B** was inefficient, the corresponding enyne originating from a self-hydroalkynylation was observed. However, the formation of this side product was easily controlled by the slow addition of the alkyne. These observations triggered this investigation on the Heck–Cassar protocol, which focuses the attention on the fate of the alkyne under both stoichiometric and catalytic conditions. Several parameters have to be considered in order to control the reaction, such as the ligand, base, solvent, leaving group, concentration, and temperature. The highly reactive palladium

species that are generated under the cross-coupling operative conditions can also promote parallel side reactions that could completely change the outcome. Monitoring the reaction through ^{31}P NMR, HPLC, GC and DFT calculations, the target of this study was to shed light on the Heck–Cassar protocol mechanism under operative conditions.

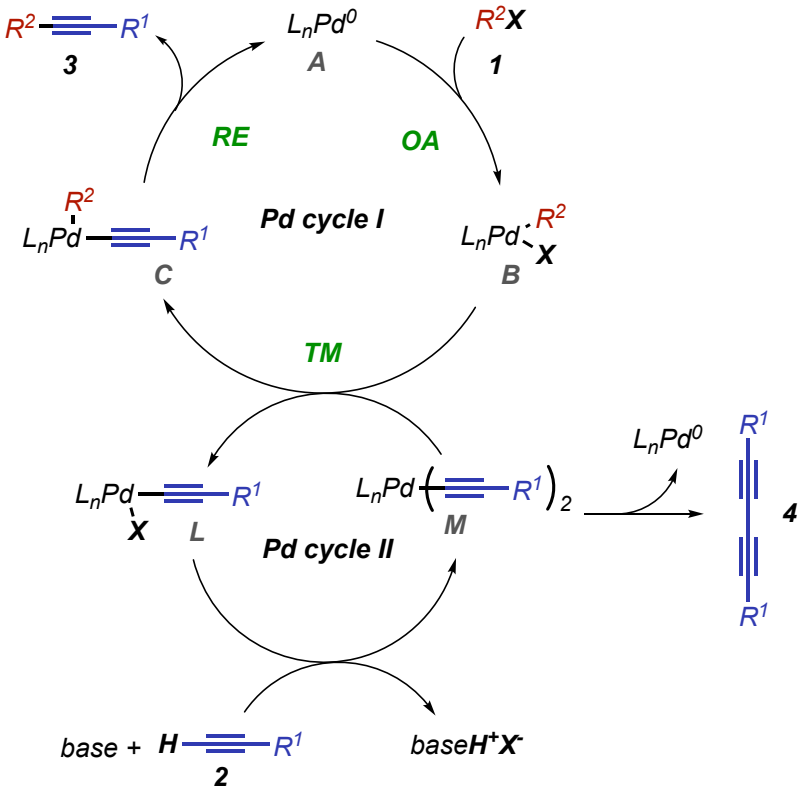

***Figure 5.2**: Heck–Cassar protocol based on Pd^{II}–Pd^{II} transmetalation mechanism*

5.2 Results and discussion

Pd^{II} Pre-catalyst Reduction. A rapid and complete pre-catalyst reduction is critical for an efficient process. Therefore, we investigated base, ligand and solvent effects on the reduction of $Pd(PPh_3)_2Cl_2$. The stoichiometry of the reaction requires one molecule of water and generates one molecule of triphenylphosphine oxide. Three bases used in the HCS reaction, i.e., N,N,N',N'-tetramethyl guanidine (TMG), pyrrolidine (PYR), and triethylamine (TEA), were tested in two different solvents, $CDCl_3$ and DMF-d_7 (Table 5.1).[15] PYR and TEA are standard bases for the HCS reaction, while TMG was introduced by Cabri et al. only in 1998.[16] Using ^{31}P NMR, we observed that the nature of the base affects the reduction process. TMG, with a high pKa (23.3 in acetonitrile),[17] was more efficient than PYR in

reducing the pre-catalyst (entries 1 and 2 versus entries 3 and 4, respectively, Table 5.1) at room temperature, while TEA was not able to reduce Pd^{II}. Interestingly, in the presence of an excess of PPh_3 for entries 1–4, the conversion of $Pd(PPh_3)_2Cl_2$ into Pd^0 complexes was completed in a few minutes. These experiments showed that the base affects the reduction process and probably increases the phosphine mobility, and when extra quantities of PPh_3 are present, the process is more efficient.

***Table 5.1**: Evaluation of base and ligand effect on $Pd(PPh_3)_2Cl_2$ reduction to Pd^0*

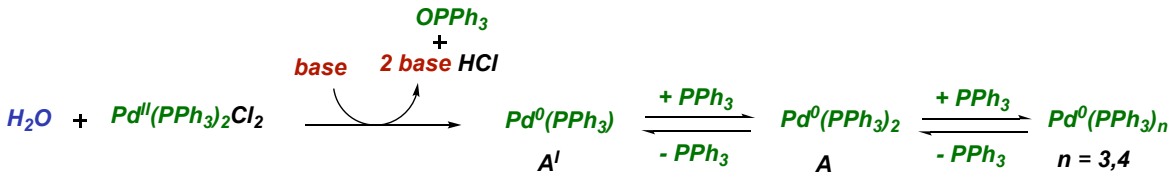

Entry[a]	Base	Solvent	Conv %	PPh_3 addition[b] Conv %
1	TMG	DMF-d_7	64	100
2	TMG	$CDCl_3$	85	100
3	PYR	DMF-d_7	31	100
4	PYR	$CDCl_3$	65	100
5	TEA	DMF-d_7	0	0
6	TEA	$CDCl_3$	0	0

[a]Reactions were carried out at rt with 0.013 mmol of pre-catalyst and 0.026 mol of base in 600 µl of solvent for 10 minutes. Conversions of Pd^{II} into Pd^0 were calculated by ^{31}P NMR. [b]Two equivalents of PPh_3 were added.

Alkyne Direct Coordination versus Pd^{II}-Pd^{II} Transmetalation: **Catalytic and Stoichiometric Reactions**. The Heck–Cassar copper-free reaction was studied using the model protocol: 4-NO_2PhX **1**, 1.1 eq of phenylacetylene **2a**, 2.0 eq of base and 20 mol% of pre-catalyst $Pd(PPh_3)_2Cl_2$. The presence of the electron-withdrawing (EWG) nitro substituent on the aromatic ring of aryl iodide **1** was chosen because of its capability to slow down the Reductive Elimination (RE) step and increases the chances to detect intermediate complexes of the catalytic cycle. The Pd^{II} complexes **B**, **C**, **M**, and **L** (Figure 5.2) were individually synthetized according to previously reported procedures.[13] For this purpose, only TMG and PYR were screened as base, while TEA was not tested, because of its inefficiency in generating Pd^0 species at room temperature. Independently from the bases

or solvents used, it is possible to observe the formation of a small amount of **M**. Nonetheless, with the addition of PPh_3, which accelerates the Pd^{II} reduction, complex **M** was not detected by ^{31}P NMR, regardless of the organic base (TMG, PYR) and solvent (DMF-d_7, $CDCl_3$) used (Figure 5.3b). In Figure 5.3, the ^{31}P NMR of the reaction with TMG as base in DMF-d_7, with and without additional quantities of PPh_3, is described. Complex **M** was formed and detected only when the reduction of the Pd^{II} pre-catalyst was inefficient (Figure 5.3a). Accordingly, when using palladium tetrakis triphenylphosphine as catalyst, **M** was never detected (see Experimental section). In addition, to evaluate the role of **M** in the transmetallation process, kinetic experiments were performed (Figure 5.4). Considering the stoichiometric reactions described in Figure 5.4, performed in $CDCl_3$ because of the scarce solubility of **M** in other solvents, it is possible to observe that the reaction carried out between **B** and **M** at room temperature in $CDCl_3$ (Figure 5.4, green dotted line) was slower than the coupling between **B** and **2a** (Figure 5.4, red dotted line). Complex **M** was able to promote the cross-coupling, but this pathway was significantly less efficient than the direct reaction between the oxidative addition complex **B** and the alkyne **2a**. The reaction between **B** and **2a** did not require the formation of complex **M**.

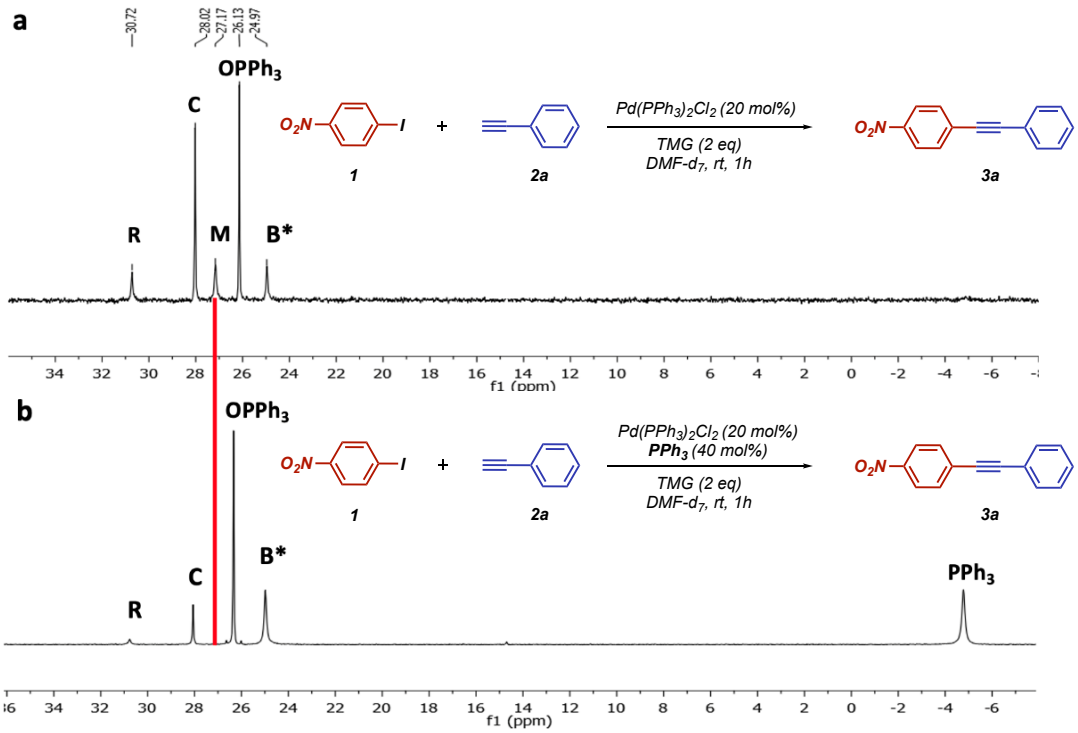

***Figure 5.3**: ^{31}P NMR of the HCS reaction carried out with TMG as base in $CDCl_3$. Complex **R** is the OA complex with TMG coordinated to palladium (see below)*

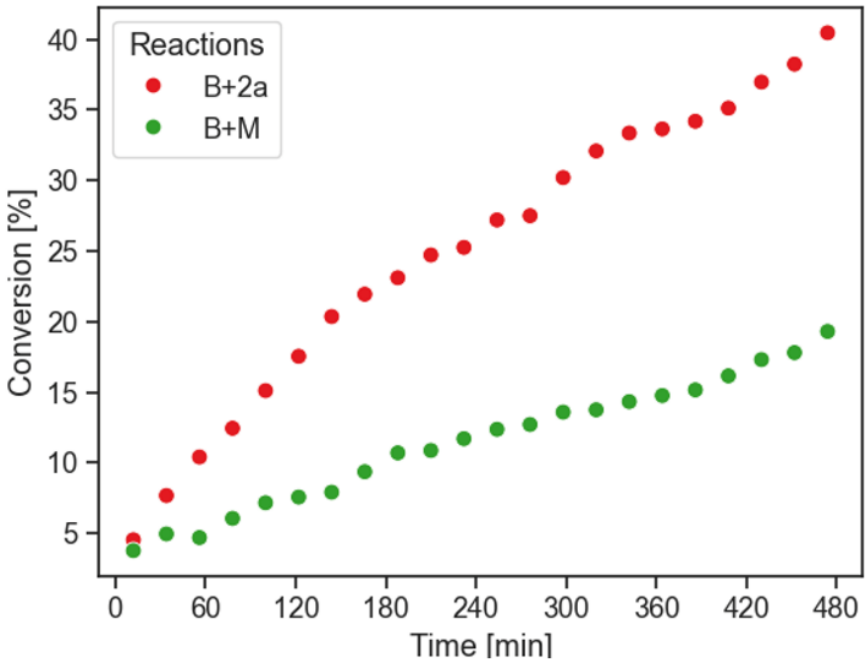

***Figure 5.4**: HCS reaction between the oxidative addition complex **B** with **2a** and with **M**. The formation of **3a** was monitored by ^{1}H NMR*

Parallel Side Reactions. A series of stoichiometric experiments were designed to clearly identify the palladium catalyzed side reactions that could interfere with the HCS cross-coupling process. In particular, the target was to evaluate the stability of the key intermediate Pd^{II} complexes, monitoring the formation of the coupling product **3a** and the homocoupling of the alkyne **4a** after 30 min, see Table 5.2. Complex **M** resulted very stable at room temperature at 25°C in $CDCl_3$ and in DMF-d_7 (entry 1 and 2). However, at 60°C in $CDCl_3$ (entry 3), complex **4a** was detected. It is worth noting that at 40°C, the conversion of **M** into **4a** in DMF-d_7, with concomitant formation of the Pd^0L_2 complex **A**, was completed within 30 min (entry 4). On the other hand, complex **B** in the presence of **M** in $CDCl_3$ generated only a small amount of cross-coupling product **3a** (entry 5) at 25°C, while at 60°C, 95% of **M** was transformed into the homocoupling product **4a** (entry 6). This data showed that at 60°C, the RE process of **M** to give Pd^0 and **4a** was much faster than the Pd^{II}-Pd^{II} TM step. On the contrary, the cross coupling between the oxidative addition complex **B** and **2a** generated the target product **3a** only.

***Table 5.2**: HCS side reactions and stoichiometric studies*

Entry[a]	Solvent	T°C	**B**	**2a**	**M**	Conv (%)	**3a/4a**[b]
1	$CDCl_3$	25	-	-	1	**M** (0)[b]	0/0
2	DMF-d_7	25	-	-	1	**M** (0)[b]	0/0
3	$CDCl_3$	60	-	-	1	**M** (30)[b]	0/100
4	DMF-d_7	40	-	-	1	**M** (100)[c]	0/100
5	$CDCl_3$	25	1	-	1	**B** (5)[b]	100/0
6	DMF-d_7	60	1	-	1	**M** (100)[c]	21/79[d]
7	$CDCl_3$	25	1	1	-	**B** (36)[b]	100/0
8	DMF-d_7	60	1	1	-	**B** (42)[b]	100/0

[a]All reactions were carried out for 30 min in deuterated solvents with 0.024 M. For entries 7 and 8, 1.1 eq of TMG were added. [b]The mixture was analyzed after 30 min by ^{1}H NMR. [c]The mixture was analyzed after 30 min and the conversion was calculated using ^{31}P NMR. [d]The ratio **3a/4a** was determined by HPLC.

Alkyne Direct Coordination versus Pd^{II}-Pd^{II} Transmetalation: Stoichiometric Competitive Reactions. The direct competition between the direct coordination process and the Pd^{II}–Pd^{II} transmetallation was studied at 60°C in DMF-d_7 with an equimolecular amount of the complexes **B**, **M** and 4-methyl-phenyl acetylene **2b** (Scheme 5.1). The different substituents on the aromatic rings allowed all potential products of the reaction to be distinguished. The only cross-coupling product found in the reaction mixture was **3b**, derived from the reaction between **B** and **2b**, while complex **M** generated the homocoupling product **4a** only. Compounds **3a**, **4b**, **4c**, **5a**, and **5b** were not detected. In fact, based on the results in Table 5.2, if complex **P** or **Q** were the key intermediates of the reaction mechanism, the homocoupling products **4b** and/or **4c** should have also been detected in the final mixture. These data support the direct coordination mechanism hypothesis, which deserves further investigation to establish the role of both the base and the leaving group in directing the reaction towards an anionic, cationic, or ionic mechanism (Figure 5.1). Finally, based on the data described, it is possible to exclude any contribution of the Pd^{II}–Pd^{II} transmetallation process to the out-come of the HCS reaction.

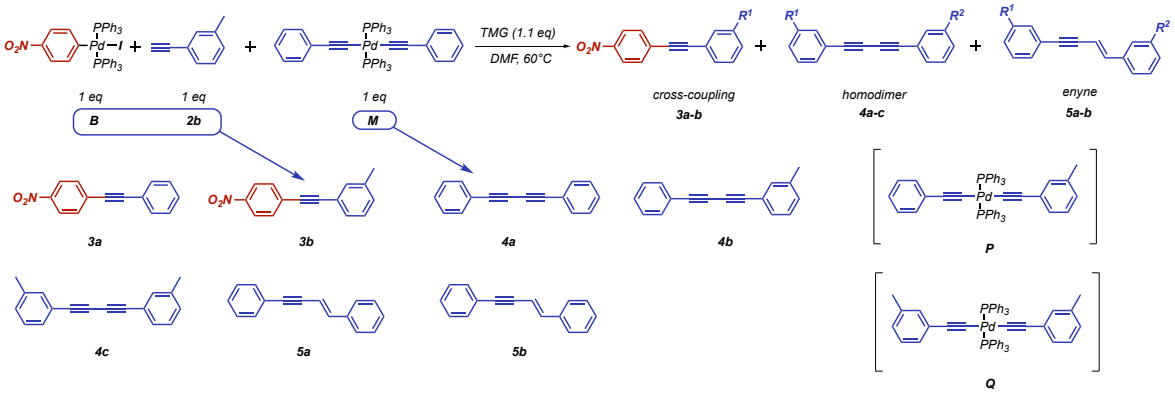

Scheme 5.1**: Competition between **M** and **2b** in reacting with oxidative addition complex **B

Oxidative Addition Complex B: Role of the Base. In order to understand the behavior of the different Pd^{II} complexes under operative conditions, we carried out ^{31}P analysis of the oxidative addition complexes **B** with several leaving groups X, namely, I, Br, Cl, or OTf, in the presence of TMG, PYR and TEA in DMF (Table 5.3). The base effect was studied using 50/20/10 equivalents of base with respect to the Pd^{II} complex **B** to reproduce the operative conditions. In fact, when using a 1 mol% concentration of the catalyst, the data showed the impact of 1.1 equivalents of base on the oxidative addition catalyst at different conversion (60, 90 and 99 %). The ^{31}P spectra clearly showed that complexes **R** were the dominant Pd^{II} species with TMG and PYR (entries 1–6), regardless of the excess of base, while the tertiary base TEA was not able to enter the metal coordination sphere (entries 7–9).

***Table 5.3**: Base effect on the oxidative addition complexes **B**, X = I, Br, Cl, OTf*

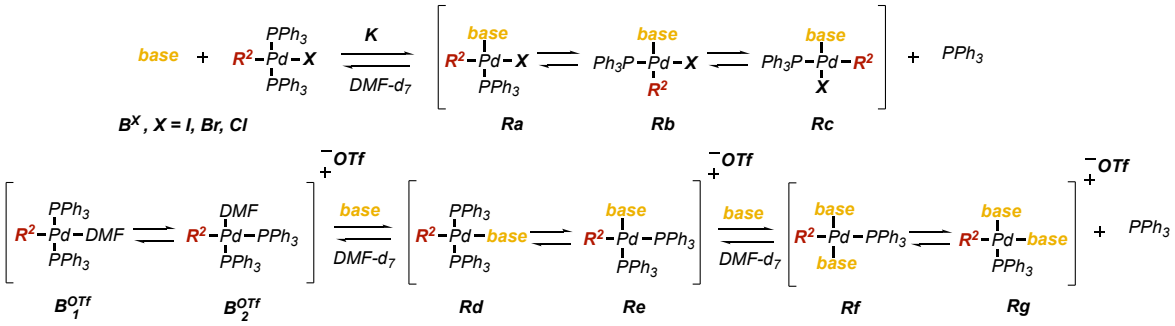

Entry[a]	**X**	R^2	base	R/B ratio			K
				50 eq	20eq	10 eq	
1	I	NO_2	Pyr	93/7	85/15	68/32	0.182
2	Br	NO_2	Pyr	91/9	78/22	68/32	0.099
3	Cl	NO_2	Pyr	93/7	82/18	70/30	0.134
4	I	NO_2	TMG	100/0	97/3	93/7	0.910
5	Br	NO_2	TMG	96/4	85/15	74/26	0.122
6	Cl	NO_2	TMG	87/13	71/29	63/37	0.074
7	I	NO_2	TEA	0/100	0/100	0/100	-
8	Br	NO_2	TEA	0/100	0/100	0/100	-
9	Cl	NO_2	TEA	0/100	0/100	0/100	-
10	I	OCH_3	TMG	>99/1	99/1	94/6	0.306
11	OTf	NO_2	TMG	100/0	100/0	100/0	-[b]

[a]Ratios of the complexes and equilibrium constants were calculated using ^{31}P NMR. [b]It was not possible to calculate K since the formation of the R^2 complex is efficient even with a low amount of base.

The value of the equilibrium constant K is generally low and in line with the studies of Jutand and coworkers.[18] It is clear that the presence of a large excess of base pushes the equilibrium toward the formation of the **R** complexes. Interestingly, with the exception of the chloride complex (entries 3 and 6), TMG was always more efficient than PYR in replacing PPh_3 in the Pd^{II} coordination sphere (entries 1,2 and 4,5). The introduction of a methoxy group at position 4 of the phenyl iodide favored the formation of complex **R** (entry 10). The results showed that the exchange between the base and the halide does not take place because the strength of the Pd^{II}–I,Br,Cl bonds is very high.[19,20] In fact, the formation of complexes **R** is perfectly balanced by the release of free PPh_3 in solution (see Figure 5.6a $\mathbf{B^{Br}}$ + 20 equivalents of TMG). With oxidative addition complexes coming from aryl halides, triphenylphosphine release begins upon the addition of the first equivalent of TMG or PYR into the mixture.

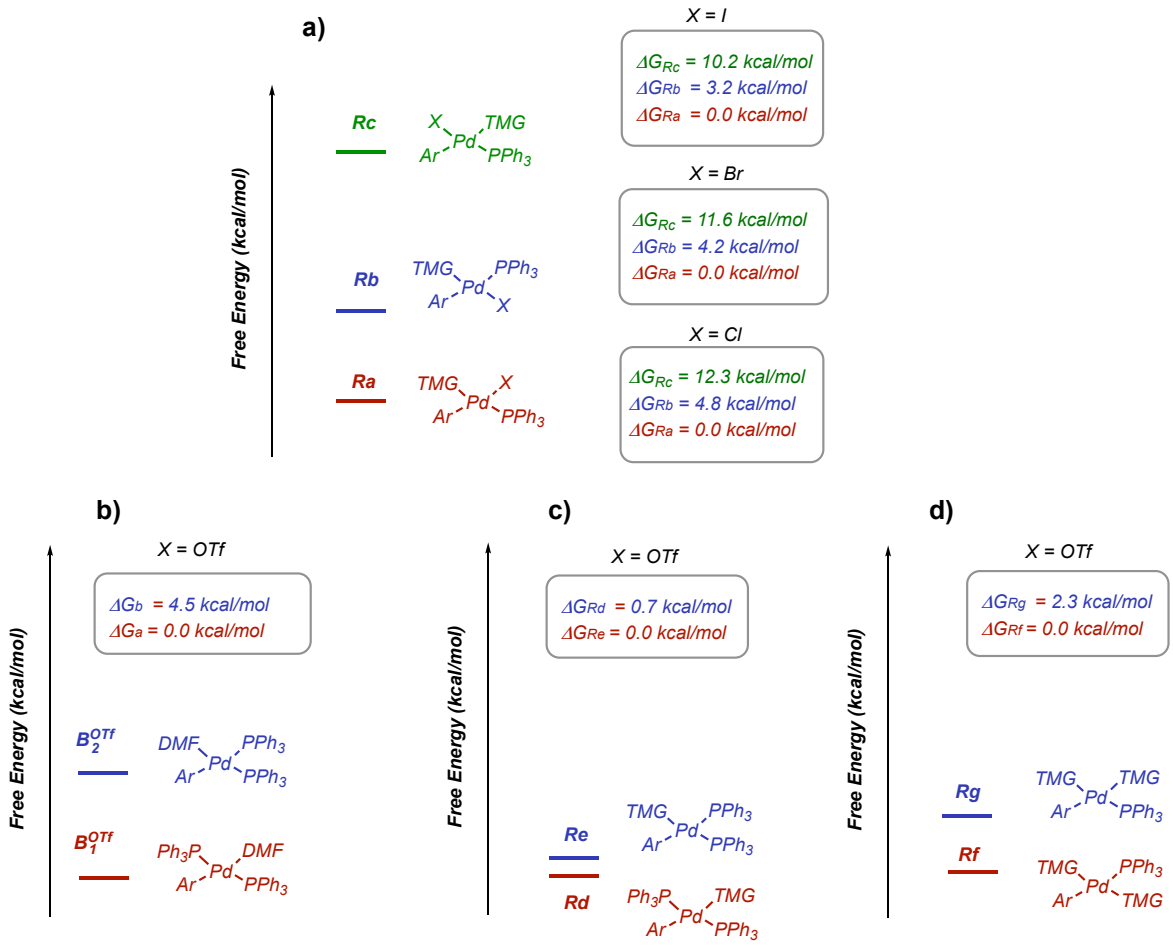

***Figure 5.5**: Gibbs energies (ΔG, kcal mol^{-1}) for isomers of complexes **B^{OTf}** and **R** at 298 K*

The ^{31}P NMR spectra showed two or three peaks related to complexes **Ra–c** (see the Experimental section). With aryl halides, we carried out DFT calculations with TMG as the base, and the data supported the hypothesis that among the different isomers, **Ra** was the most stable (Figure 5.5). However, the energy difference between **Ra** and **Rb** (3.2–4.8 kcal) is smaller than the one between **Rb** and **Rc** (7.0–7.5 kcal), independent of the halide (Figure 5.5a). Considering the oxidative addition complex generated with triflate as the counterion **B^{OTf}**, the formation of complexes **Rd–g** is even more efficient than the corresponding aryl halide (Figure 5.5b-d). Complex **B^{OTf}** is completely dissociated in DMF and with the addition of the first equivalent of TMG, the formation of two peaks was observed at 27.78 and 19.32 ppm in the ^{31}P NMR spectrum (Figure 5.6b). With the excess of base, only the peak at 27.78 ppm is detected along with the corresponding amount of PPh_3. The complex at 19.32 ppm has only one TMG attached to the palladium (**Rd,e**), while the complex at 27.78 ppm has two molecules of TMG (**Rf,g**). The cationic complexes **Rd,e** generated from **B^{OTf}** and one

TMG in the coordination sphere of the palladium had almost the same energy, while for those generated with two molecules of TMG, **Rf** was more stable than **Rg** by 2.3 kcal.

Alkyne coordination step. The intermediate complexes described in Table 5.3 and in Figure 5.5 support a coordination-insertion process of the alkyne that is very close to the one described by Jutand for the HCS and Cabri for the Heck-type reaction.[18,21] The reaction mechanism, via neutral (**Ra-c**) or cationic (**Rd-g**) complexes, is mainly related to the nature of the counterion in the oxidative addition complex **B**.

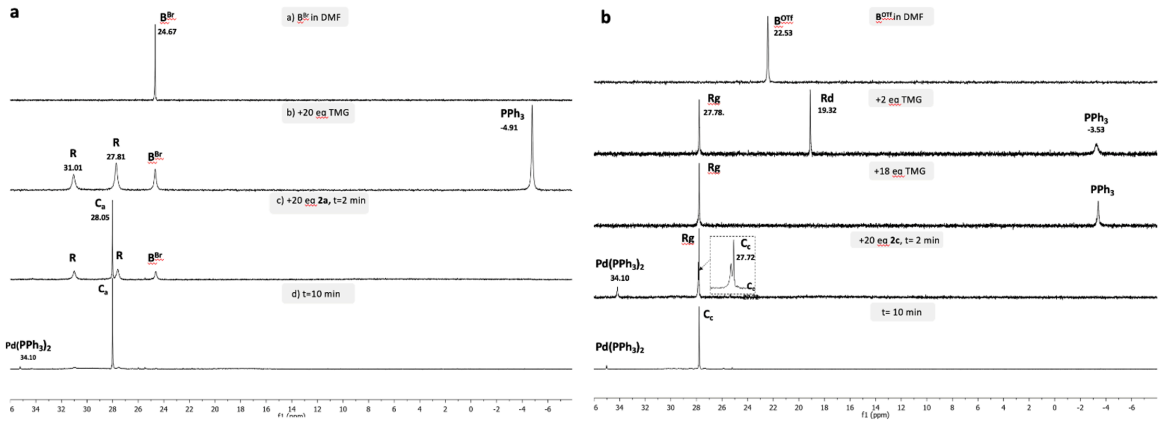

***Figure 5.6**: [31]P NMR spectra of the Heck–Cassar copper-free protocol at room temperature, starting from **B**^{Br} a) and **B**^{OTf} b)*

The coordination of the base and then the alkyne took place in a neutral complex with the halide counterion (**Ra-c**) and in a cationic complex with the triflate (**Rd-g**). To the reactions with 20 equivalents of base described in Table 5.3, 20 equivalents of **2a** were added. Regardless of the counterion, the formation of complex **C** that preceded the RE step is a fast process, see the Experimental section. In Figure 5.6a, the ^{31}P NMR spectra showed that starting from **B**^{Br}, the addition of the base generated a mixture of two main peaks at 27.71 and 31.03 ppm (**Ra-c**), which disappeared after 10 min from the addition of **2a**, forming only complex **C** at 28.03 ppm. Using the **B**^{Br} complex, we studied the effect of the alkyne on the reaction outcome. Complex **C** is rapidly generated after 10 minutes at room temperature (see Figure 5.6a) and, after 5h, complex **C** was not present anymore and the corresponding HCS products **3a-q** were detected by HPLC (Figure 5.7). These results further support the observation that the different excess of alkyne necessary to achieve complete

conversions under standard conditions is not determined by the alkyne reactivity in the HCS coupling. The alkyne coordination and the π/σ switching necessary to generate **C** is very fast, and we were unable to detect any intermediate. Therefore, the only possibility was to take advantage of DFT calculations.

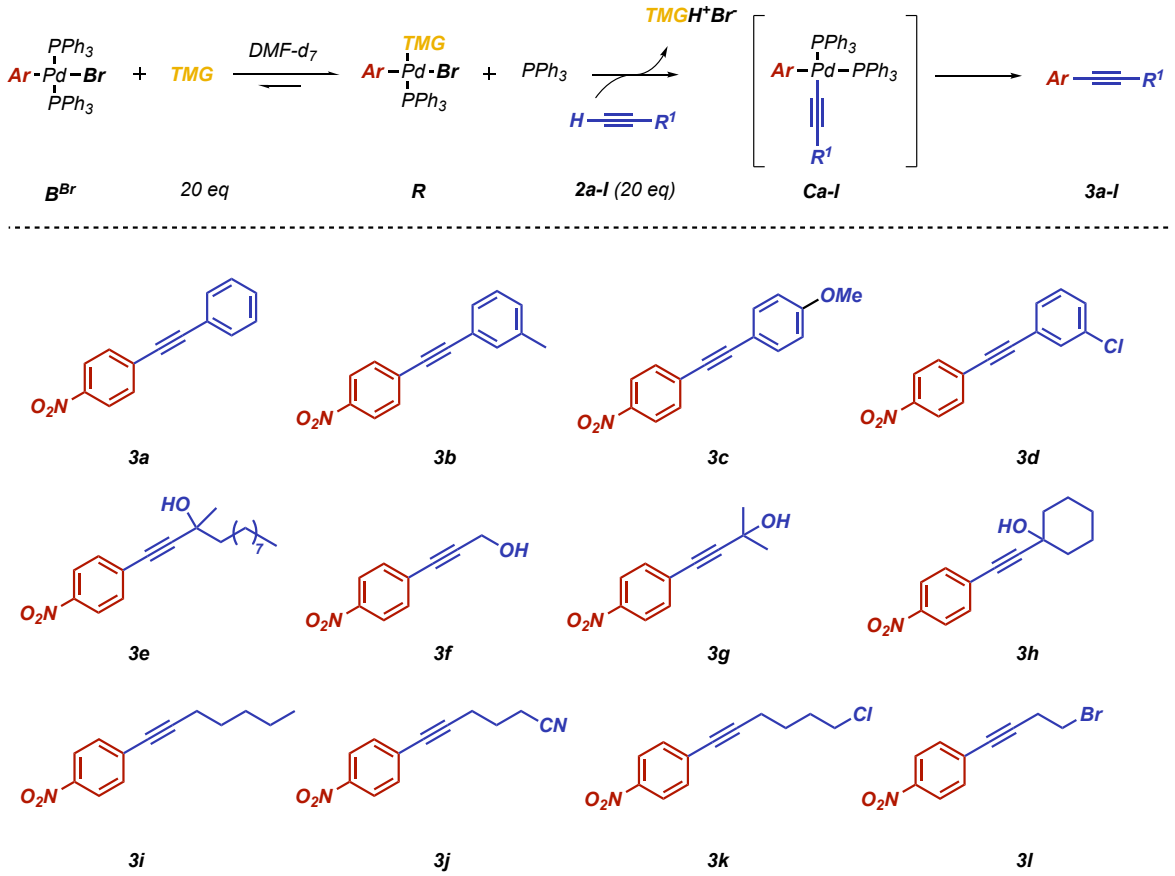

***Figure 5.7**: Alkyne insertion into complex **B**^{Br}*

DFT Calculations. Density functional theory calculations of the HC reaction coordinate were performed with PBE/def2-TZVP level of theory[22–25] starting from the oxidative addition complexes, namely **B**^{I} and **B**^{OTf}, phenylacetylene **2a**, and TMG as a model system to gain molecular-level insight into the mechanism of the alkyne insertion step.

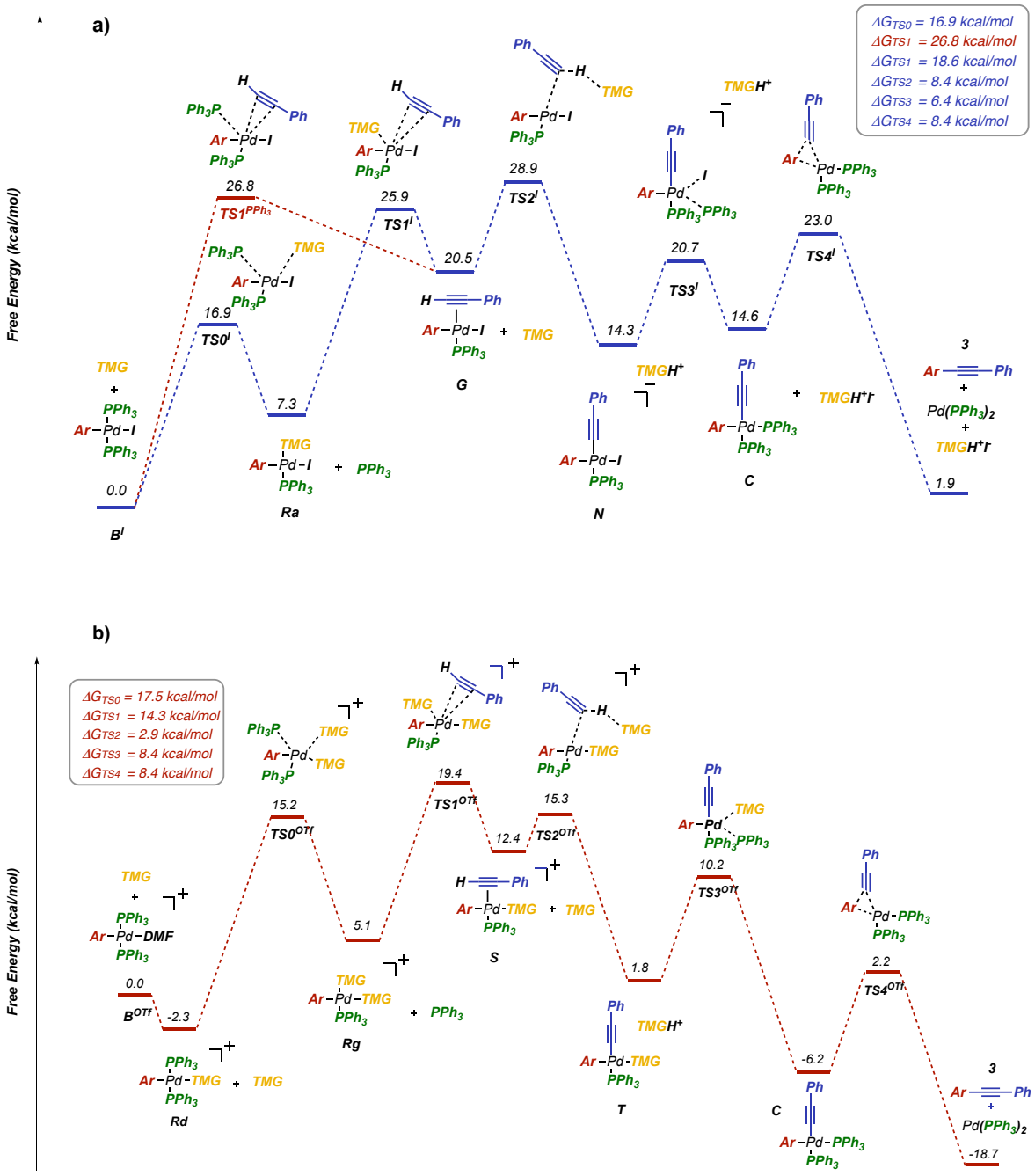

***Figure 5.8**: DFT-calculation-computed reaction profile and solution-state Gibbs free energies (ΔG, kcal mol-1) PBE/def2-TZVP level of theory at 298 K for stationary points of the Heck–Cassar protocol mechanism using aryl halides 5.8a and aryl triflates 5.8b*

According to the experimental data on the effect of the TMG base, two different mechanisms were studied using the iodide and the triflate as counterions: the neutral/anionic pathway via **Ra–c** for the halide species and the cationic/neutral pathway via **Rd–g** for the triflate as the leaving group (Figure 5.8). The computed Gibbs energy profile for the copper-free HCS reaction starting from the oxidative addition complex **B**^{I} is

shown in Figure 5.8a. The energy of the transition state of the direct insertion of the acetylene on complex **B^{I},** without passing through **TS0^{I}**, was found to be 26.8 kcal/mol (**TS1^{PPh3}**). This is the energy required for the mechanism involving tertiary amines. With secondary amines like TMG the key step of the process is the transformation of **B^{I}** into intermediate **Ra**, through the displacement of one equivalent of PPh_3 by the base. Our calculations found a barrier of 16.9 kcal/mol (**TS0^{I}**), a difference in energy offset by the excess base that is used in the process. The reaction coordinate was based on **Ra** because it was the most stable isomer, see Figure 5.5a. The ability of the secondary amine to enter in the coordination sphere of the metal is critical because it lowers the energy required for the acetylene insertion step. The energy required to go from **Ra** to **G** through **TS1^{I}** is only 18.6 kcal/mol, a process favored by 8.2 kcal over the direct passage from **TS1^{PPh3}**. The calculations reinforce therefore the concept that the insertion step is much faster when passing through complex **Ra**, instead of going directly from complex **B^{I}**. The step from **Ra** to **G** through **TS1^{I}** is the rate determining step of the alkyne insertion process. All subsequent energy barriers from **G** to **C** are lower than the previous transition state from **R** to **G**. The deprotonation of the acetylene is also favored because the base, having just left the complex to make room for the alkyne, remains near the intermediate, facilitating the formation of the anionic complex **N** with an energy barrier of 8.4 kcal/mol. The rupture of the Pd–I bond from the anionic complex **N** requires a lower activation energy and the replacement with PPh_3 is therefore very efficient. In fact, the ΔG between **N** and **TS3^{I}** is only 6.4 kcal/mol, affording the neutral complex **C** that rapidly undergoes reductive elimination with a free energy of 8.4 kcal/mol giving rise to the coupling product **3** and regenerating the catalyst.

In contrast to the neutral/anionic mechanism that occurs with halides as leaving group, the HC reaction with triflates is characterized by a cationic/neutral mechanism, see Figure 5.8b. Currently there are no data in literature on DFT calculations for aryl triflates in copper-free HCS reactions. The Pd–OTf bond is weaker than the Pd–I bond and easily dissociates even in the presence of a ligand such as DMF. For this reason, we started the Gibbs energy profile of the mechanism from **B$_1^{OTf}$** (more stable than the correspondent **B$_2^{OTf}$** isomer by 4.5 kcal/mol) with DMF instead of TfO- as the Pd^{II} ligand. Based on experimental ^{31}P NMR data, the key initial step was the formation of complex **Rg** with two TMGs coordinated to the metal. The coordination of the first TMG stabilized the cationic complex by −2.3 kcal/mol

(ΔG between $\mathbf{B_1^{OTf}}$ and **Rd**). Similar to the previous mechanism, the second TMG replaced one of the PPh_3 ligands, with a Gibbs free energy of 17.5 kcal/mol, to give isomer **Rg**, corresponding to the rate determining step of the process ($\mathbf{TS0^{OTf}}$). The insertion of the acetylene into **Rg** takes place with an energy barrier of 14.3 kcal/mol. This transition state energy barrier from **Rg** to $\mathbf{TS1^{OTf}}$ is consistently lower that the one previously calculated for the corresponding mechanism step from the iodide complex **Ra**. Interestingly, the average distance between the sp carbons of the alkyne and the palladium complex in $\mathbf{TS1^{I}}$ was 2.40–2.47 Å, while for $\mathbf{TS1^{OTf}}$ a distance of 2.62–2.92 Å was sufficient to activate the C–H bond, creating a lower stressful steric interaction. Analogous to mechanism outlined for the iodide, after $\mathbf{TS1^{OTf}}$, all the other reaction steps required very low activation energies: the TMG base, which had just come out of the coordination sphere in $\mathbf{TS1^{OTf}}$, deprotonates the acetylene favoring the switch from the π complex **S** to the σ complex **T** with an activation energy of only 2.9 kcal. This process is highly favored because it leads to the more stable complex **T** and subsequently to intermediate **C** through the displacement of TMG by the phosphine with ΔG energy of 8.4 kcal/mol.

Concerning the overall reaction rate determining step, with iodides the oxidative-addition and the coordination of the alkyne transition states have very similar energy requirements, around 15-17 kcal.[12,26] On the contrary, for bromides, chlorides and triflates the oxidative addition is by far the most demanding step, with an energy higher than 30 kcal[27] and higher than that of the acetylene insertion $\mathbf{TS1^{Br,\ Cl,\ OTf}}$, which in our calculations turns out to be just 14-18 kcal/mol.

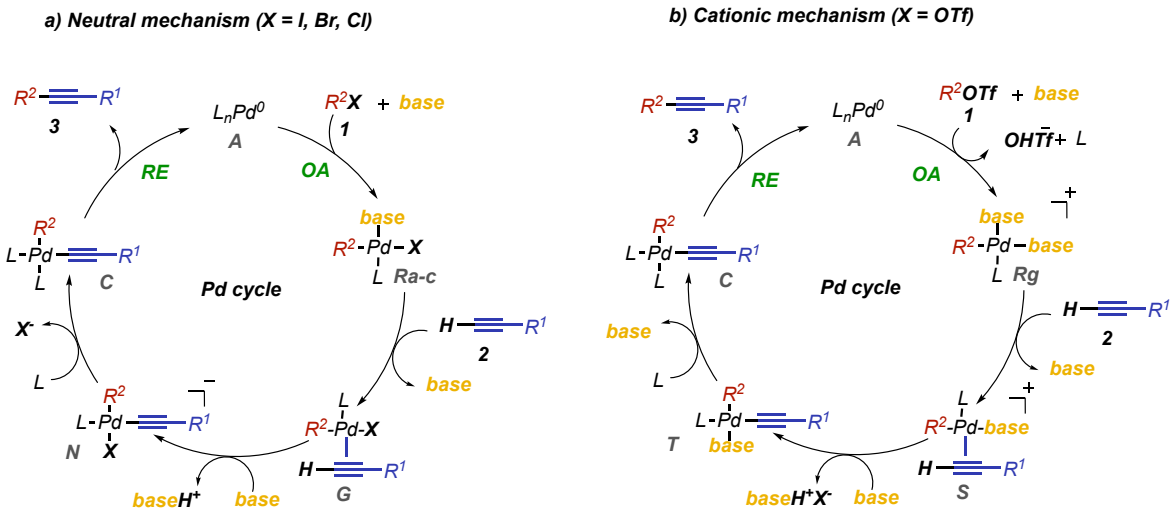

***Figure 5.9**: Heck–Cassar–Sonogashira reaction mechanisms according to neutral a) or cationic b) route*

5.3 Conclusions

A critical evaluation of the fate of the palladium complexes under real catalytic conditions was required, to have a clear understanding of the copper free HCS reaction mechanism. With highly reactive palladium species it is necessary to consider the contribution of side reactions that can completely change the outcome. In this work, we explored the fundamental role of the secondary organic amines in the Heck-Cassar copper free protocol, being able to promote the pre-catalyst reduction and enter in the coordination sphere of the metal. Under catalytic conditions, the large excess of the secondary amines respect to the palladium metal and the phosphine ligand is proved to affect the Pd^{II} complexes and their fate. Theoretical calculations together with experimental results pointed out the presence of two catalytic cycles based on the different counterions. With halides, the mechanism goes via dissociation of the ligand through a neutral π alkyne-Pd^{II} complex **G** that rapidly evolves into the negatively charged σ complex **N** and then to **C** (Figure 5.9a). Whereas, if the leaving group on the aromatic ring is the triflate, which is completely dissociated from the metal, two molecules of the secondary amine enter in the palladium coordination sphere favoring the formation of a cationic π alkyne-Pd^{II} complex **S** (Figure 5.9b). We have reported for the first time a DFT calculation on the aryl triflate reactivity in HCS coupling. This mechanism, which highlights the critical role of the counterion, resulted similar to the coordination-insertion step of the alkene in the Heck reaction.[21]

Further investigations are under way to evaluate the role of the secondary base complexes in other cross-coupling reaction mechanisms.

5.4 Experimental

General information

Commercially available reagents (reagent grade, >99%) were purchased from Sigma Aldrich, Fluorochem and TCI Chemicals and used without any further purification.

Solvents (dichloromethane (DCM), Tetrahydrofuran (THF), toluene, deuterated N,N-Dimethylformamide (DMF-d_7), deuterated chloroform ($CDCl_3$), are commercially available and were used after degassing.

Tetrakis(triphentlphosphine)palladium $Pd(PPh_3)_4$ and bis(triphenylphospine)palladium chloride $PdCl_2(PPh_3)_2$ from FaggiEnrico (Italy).

^1H NMR, ^{13}C NMR and ^{31}P NMR spectra were recorded on Varian 400-MR (400 MHz) (equipped with autoswitchable PFG probe) and Bruker Avance Neo 600 MHz (equipped with CryoProbe Prodigy Broadband 5mm) spectrometers. NMR multiplicities are abbreviated as follows: s = singlet, d = doublet, t =triplet, q = quartet, spt = septet, m = multiplet, bs = broad signal. Coupling constants *J* are given in Hz. All ^1H and ^{13}C chemical shifts are calibrated to residual protic-solvents and all ^{31}P chemical shifts are referenced to external 85% phosphoric acid (δ = 0 ppm).

HPLC-UV analysis were recorded with an Agilent 1260 InfinityLab instrument. Column: Zorbax® SB-C18; particle size 5 µm; pore size 100 Å; length 250 mm, internal diameter: 4.6 mm. Mobile phase A: H_2O, mobile phase B: ACN. Gradient (Time(min), %B): 0, 80; 25, 80; 28, 10; 30, 10; flow 0.5 mL min^{-1}column temperature 30°C; injection volume: 10 µL.

GC-MS analysis were recorded with a Hewlett-Packard 5971 spectrometer with GC injection and EI ionization at 70 eV coupled with an Agilent Technologies MSD1100 single-quadrupole mass spectrometer, reported as: m/z (rel. intensity).

HRMS spectra were obtained with a G2XS QTof mass spectrometer using either ESI.

Room temperature (rt) refers to the ambient temperature of the laboratory, ranging from 22 °C to 26 °C.

Chemical shift of Pd species

Entry	Compound	δ (ppm)	
		DMF-d_7	$CDCl_3$
1	$Pd(PPh_3)_4$	26.00	28.25
2	$Pd(PPh_3)_3$	24.84	23.85
3	$Pd(PPh_3)_2$	34.33	33.78
4	PPh_3	-4.83	-5.46
5	$OPPh_3$	26.00	29.70
6	$Pd(PPh_3)_2Cl_2$	24.85	23.86
7	complex **L**	24.06	23.43
8	complex **M**	27.19	26.56
9	complex **C**	28.05	27.53
10	complex $\mathbf{B^I}$	23.43	23.17
11	complex $\mathbf{B^{Br}}$	24.67	24.08
12	complex $\mathbf{B^{Cl}}$	24.93	24.18
13	complex $\mathbf{B^{OTf}}$	22.53	-
14	complex $\mathbf{B^I_{OMe}}$	23.79	24.15

Synthesis of palladium complexes

Synthesis of OA complex ***B^I***[28]

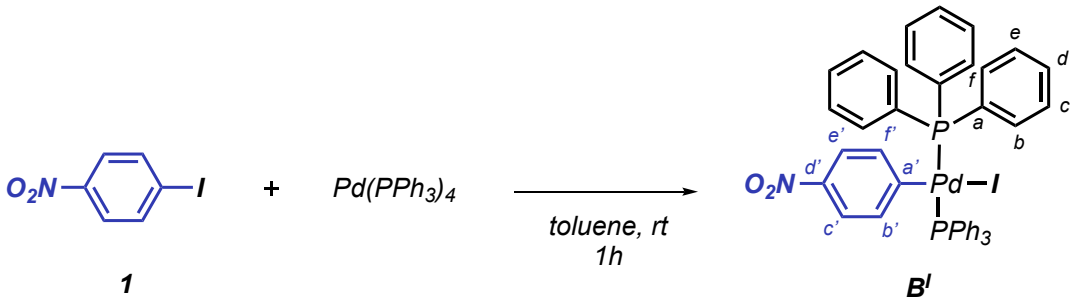

1 ***B^I***

To an oven-dried 20 mL Schlenk purged under argon atmosphere, a mixture of 1-Iodo-4-nitrobenzene **1** (423 mg, 1.7 mmol, 2.46 eq) and $Pd(PPh_3)_4$ (798 mg, 0.69 mmol, 1.0 eq) was stirred in degassed toluene (13 mL), in the dark for 1 h at room temperature. The reaction mixture was filtered out and the crude was washed with diethyl ether (Et_2O) to obtain the pure product (564 mg, 93 %) as a white solid.

^{1}H NMR (600 MHz, $CDCl_3$): δ 7.56-7.53 (m, 12H, Hb-Hf); 7.36-7.33 (m, 6H, Hd); 7.27-7.25 (m, 12H, Hc-He); 7.02-7.01 (d, J = 6 Hz 2H, Hc'-He'); 6.85-6.84 (m, 2H, Hb'-Hf')

^{13}C NMR (151.2 MHz, $CDCl_3$): δ 177.07 (s, Cd'); 143.84 (t, J=1.51 Hz, Ca'); 135.96 (t, J=4.53 Hz, Cb'-Cf'), 134.94 (t, 6.05 Hz, Cb-Cf), 131.49 (t, J=24.2 Hz, Ca), 130.37 (s, Cd), 128.10 (t, J=4.53, Cc-Ce), 120.95 (t, Cc'-Ce').

^{31}P NMR (242.4 MHz, $CDCl_3$): δ +23.17 (s)

Synthesis of OA complex $\boldsymbol{B^{I}_{OMe}}$[28]

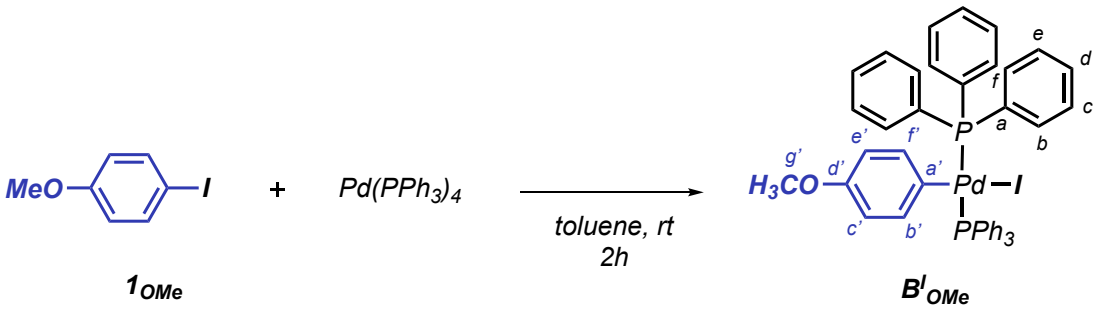

$\boldsymbol{1_{OMe}}$ $\boldsymbol{B^{I}_{OMe}}$

To an oven-dried 20 mL Schlenk purged under argon atmosphere, a mixture of 4-Iodoanisole $\mathbf{1_{OMe}}$ (397 mg, 1.7 mmol, 2.46 eq) and $Pd(PPh_3)_4$ (798 mg, 0.69 mmol, 1.0 eq) was stirred in degassed toluene (13 mL), in the dark for 2 h at room temperature. The reaction mixture was filtered out and the crude was washed with Et_2O to obtain the pure product (543 mg, 91 %) as a white solid.

^{1}H NMR (400 MHz, $CDCl_3$): δ 7.52-7.48 (m, 12H, Hb-Hf); 7.33-7.30 (m, 6H, Hd); 7.26-7.21 (m, 12H, Hc-He); 6.42-6.40 (d, J=4 Hz 2H, Hb'-Hf'); 6.08-6.07 (m, 2H, Hc'-He'); 1.92 (s, 3H, Hg').

^{13} C NMR (100.8 MHz, $CDCl_3$): δ 152.90 (s, Ca'); 135.59 (t, J=5.04 MHz, Cb'-Cf'); 135.04 (t, J=7.06 MHz, Cb-Cf); 132.33 (t, J=23.18 MHz, Ca); 131.08 (s, Cd'); 129.74 (s, Cd); 129.07 (s, Cc'-Ce'); 127.82 (t, J=5.04 MHz, Cc-Ce); 22.24 (s, Cg').

^{31} P NMR (161.6 MHz, $CDCl_3$): δ +23.43 (s)

Synthesis of OA complex $\boldsymbol{B^{Br}}$[28]

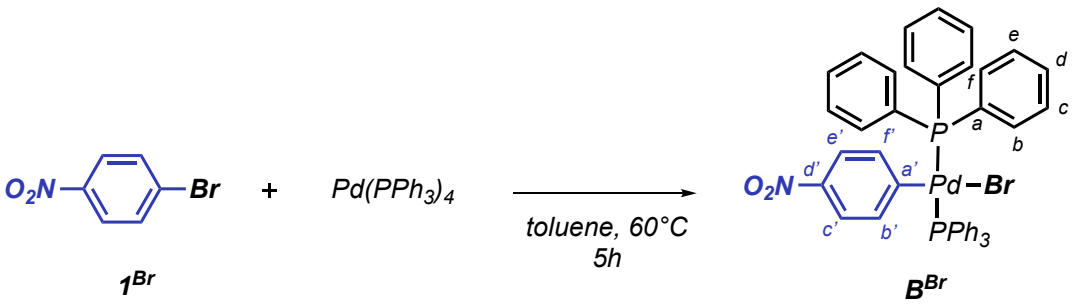

$\boldsymbol{1^{Br}}$ $\boldsymbol{B^{Br}}$

To an oven-dried 20 mL Schlenk purged under argon atmosphere, a mixture of 1-Bromo-4-nitrobenzene $\mathbf{1^{Br}}$ (274 mg, 1.35 mmol, 2.46 eq) and $Pd(PPh_3)_4$ (634 mg, 0.55 mmol, 1.0 eq) was stirred in degassed toluene (13 mL). The reaction mixture was heated to 60°C with an oil bath and stirred for 5 h. The reaction mixture was filtered out and the crude was washed with Et_2O to obtain pure product (411 mg, 90 %) as a white solid.

^{1}H NMR (600 MHz, $CDCl_3$): δ 7.56-7.53 (m, 12H, Hb-Hf); 7.36-7.34 (m, 6H, Hd); 7.28-7.25 (m, 12H, Hc-He); 7.02-7.00 (d, J=12 Hz, 2H, Hc'-He'); 6.87-6.86 (m, 2H, Hb'-Hf')

^{13}C NMR (151.2 MHz, $CDCl_3$): δ 174.27 (s, Cd'); 143.67 (t, J=1.51 Hz, Ca'); 136.06 (t, J=4.54 Hz, Cb'-Cf'), 134.66 (t, 6.05 Hz, Cb-Cf), 130.69 (t, J=24.2 Hz, Ca), 130.26 (s, Cd), 128.07 (t, J=4.54, Cc-Ce), 120.80 (t, Cc'-Ce').

^{31}P NMR (242.4 MHz, $CDCl_3$): δ +24.08 (s)

Synthesis of OA complex ***B^{Cl}***[29]

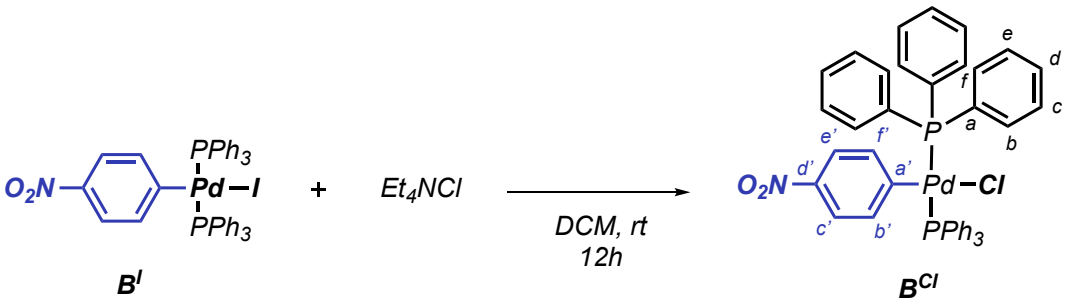

B^{I} ***B^{Cl}***

To an oven-dried 20 mL Schlenk purged under argon atmosphere, a mixture of $Pd(PPh_3)_2(PhNO_2)I$ **B^{I}** (105 mg, 0.12 mmol, 1.0 eq) and Et_4NCl (40 mg, 0.24 mmol, 2.0 eq) was stirred in DCM (1.2 mL) for 12 h at room temperature. The reaction mixture was filtered, washed with toluene (1 mL) and concentrated to 1 mL under reduced pressure. Hexane (1 mL) was added dropwise and the precipitated was filtered. To give the pure product as white solid, the precipitate was washed with hexane and ethanol and dried under vacuum (94 mg, 80%).

^{1}H NMR (600 MHz, $CDCl_3$): δ 7.55-7.52 (m, 12H, Hb-Hf); 7.36-7.34 (m, 6H, Hd); 7.27-7.25 (m, 12H, Hc-He); 7.01-6.99 (d, J=12 Hz, 2H, Hc'-He'); 6.87-6.86 (m, 2H, Hb'-Hf')

^{13}C NMR (151.2 MHz, $CDCl_3$): δ 172.56 (s, Cd'); 143.77 (t, J=1.51 Hz, Ca'); 136.40 (t, J=4.53 Hz, Cb'-Cf'), 134.68 (t, 6.05 Hz, Cb-Cf), 130.52 (t, J=24.2 Hz, Ca), 130.41 (s, Cd), 128.27 (t, J=4.53, Cc-Ce), 120.85 (t, Cc'-Ce').

^{31}P NMR (242.4 MHz, $CDCl_3$): δ +24.18 (s)

Synthesis of OA complex $\boldsymbol{B^{OTf}}$[30]

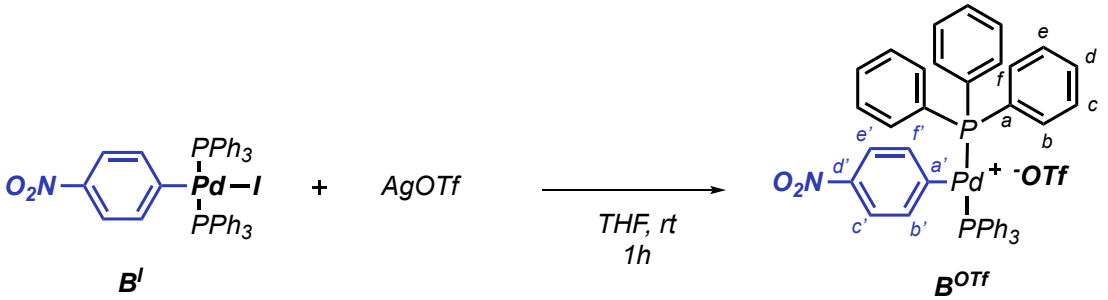

To an oven-dried 20 mL Schlenk purged under argon atmosphere, a mixture of $Pd(PPh_3)_2(PhNO_2)I$ $\mathbf{B^I}$ (60 mg, 0.068 mmol, 1.0 eq) and silver trifluoromethanesulfonate (AgOTf) (18 mg, 0.072 mmol, 1.06 eq) was stirred in THF (2 mL) for 1 h at room temperature in the dark. The reaction mixture was filtered through a pad of celite, washed with THF and concentrated to 0.5 mL of solvent under reduced pressure. The THF solution was layered with hexane and allowed to rest at -24°C overnight. The precipitated was filtered to obtain the pure product as white solid (13 mg, 20%).

^{1}H NMR (400 MHz, DMF-d_7): δ 7.60-7.53 (m, 30H, Hb-Hc-Hd-He-Hf); 7.32-7.30 (m, 6H, Hd); 7.32-7.15 (m, 4H, Hb'-Hc'-He'-Hf').

^{31}P NMR (161.6 MHz, DMF-d_7): δ +22.53 (s).

^{19}F NMR (377 MHz, DMF-d_7): δ -74.37

Synthesis of complex $\boldsymbol{L}$[13]

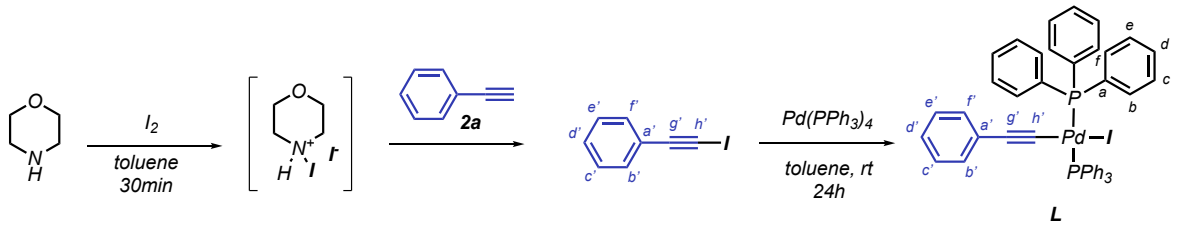

The reaction was performed in presence of I_2 (2.80 g, 11 mmol, 1.1 eq) and morpholine (2.62 mL, 30 mmol, 3 eq) in toluene (12 mL) for 30 min at room temperature. After the formation of an orange solution, phenylacetylene **2a** (1.10 mL, 10 mmol, 1.0 eq) diluted in toluene (18 mL) was added dropwise and the mixture was stirred at 45°C for 24 h. After the filtration and washing with diethyl ether, the organic phase was washed with $NH_4Cl_{(aq)}$, $NaHCO_{3(aq)}$ and water. After drying with Na_2SO_4, the solvent was removed under reduce pressure to obtain **6** (1.35 g, 60%) as a brown oil.

^{1}H NMR (600 MHz, $CDCl_3$): δ 7.47-7.46 (m, 2H, Hb'-Hf'); 7.35-7.32 (m, 3H, Hc'-Hd'-He')

^{13}C NMR (151.2 MHz, $CDCl_3$): δ 132.39 (s, Cb'-Cf'); 128.88 (s, Cd'); 128.32 (s, Cc'-Ce'); 127.48 (s, Ca'), 123.43 (s, Cg'); 94.23 (s, Ch')

To an oven-dried 20 mL Schlenk purged under argon atmosphere, a mixture of **6** (675 mg, 2.96 mmol, 1.1 eq) and $Pd(PPh_3)_4$ (3.11 mg, 2.69 mmol, 1.0 eq) was stirred in degassed toluene (25 mL), in the darkness for 24h at room temperature. The reaction mixture was filtered off and the crude was washed with diethyl ether to obtain pure product (2.15 mg, 80 %) as a white solid.

^{1}H NMR (600 MHz, $CDCl_3$): δ 7.78-7.76 (m, 12H, Hb-Hf); 7.41-7.35 (m, 18H, Hc-Hd-He); 6.91-6.89 (m, 1H, Hd'); 6.86-6.83 (m, 2H, Hc'-He'); 6.09-6.08 (m, 2H, Hb'-Hf')

^{13}C NMR (151.2 MHz, $CDCl_3$): δ 135.16 (t, J= 6.05 Hz, Cb-Cf); 132.79 (t, J=24.2 Hz, Ca); 130.66 (t, J=1.51 Hz, Cb'-Cf'); 130.27 (s, Cd); 127.97 (t, J= 4.53, Cc-Ce); 127.34 (s, Ca'); 127.17 (s, Cc'-Ce'); 125.27 (s, Cd'); 109.67 (t, J=6.05 Hz, Cg'); 101.57 (t, J=13.61 Hz, Ch')

^{31}P NMR (242.4 MHz, $CDCl_3$): δ +23.43 (s)

*Synthesis of complex **M***[13]

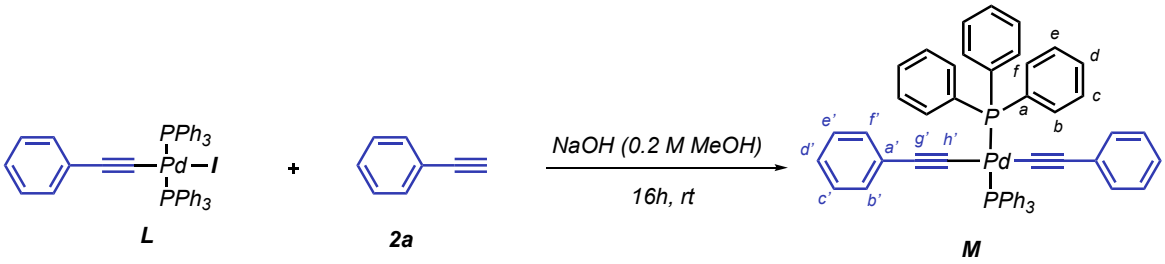

To an oven-dried 20 mL Schlenk purged under argon atmosphere, a mixture of complex **L** (240 mg, 0.28 mmol, 1.0 eq) and phenylacetylene **2a** (396 µL, 3.57 mmol, 12.78 eq) and 0.2 M NaOH in methanol (7 mL) was stirred for 16 h at room temperature. The reaction mixture was filtered out and the crude was washed with water and methanol to obtain pure product (207 mg, 89 %) as a white solid.

^{1}H NMR (600 MHz, $CDCl_3$): δ 7.84-7.81 (m, 12H, Hb-Hf); 7.41-7.38 (m, 6H, Hd); 7.36-7.33 (m, 12H, Hc-He); 6.92-6.91 (m, 6H, Hc'-Hd'-He'); 6.34-6.32 (m, 4H, Hb'-Hf')

^{13}C NMR (151.2 MHz, $CDCl_3$): δ 135.14 (t, J= 6.05 Hz, Cb-Cf); 132.66 (t, J=24.2 Hz, Ca); 130.91 (s, Cb'-Cf'); 130.09 (s, Cd); 128.23 (t, J= 1.51 Hz, Ca'); 128.02 (t, J=4.54 Hz, Cc-Ce); 127.20 (s, Cc'-Ce'); 124.86 (s, Cd'); 114.90 (t, J=4.53 Hz, Cg'); 113.74 (t, J=16.63 Hz, Ch')

^{31}P NMR (242.4 MHz, $CDCl_3$): δ +26.56 (s)

Synthesis of complex ***C***[13]

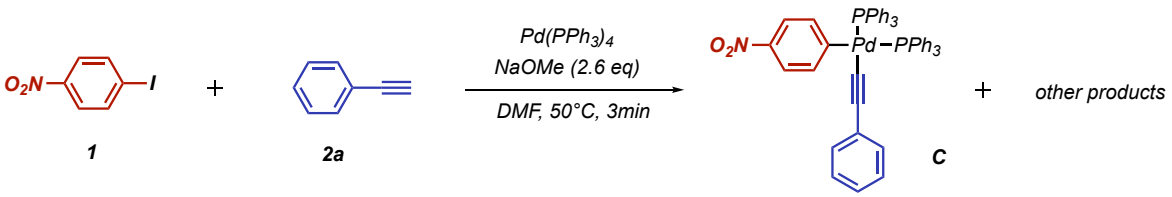

To an oven-dried 20 mL Schlenk purged under argon atmosphere, $Pd(PPh_3)_4$ (578 mg, 0.5 mmol, 1.0 eq) was dissolved in degassed DMF-d_7. The other reagents were added in the following order: 1-Iodo-4-nitrobenzene **1** (249 mg, 1.0 mmol, 2.0 eq), phenylacetylene **2a** (142.8 µL, 1.3 mmol, 2.6 eq) and sodium methoxide (70 mg, 1.3 mmol, 2.6 eq). After 3 minutes, an aliquot was collected and immediately analyzed by ^{31}P NMR.

^{31}P NMR (242.4 MHz, $CDCl_3$): δ +27.56 (s)

Pd^{II} pre-catalyst reduction

Pd^{II}-Pd^0 reduction with base and triphenylphosphine

To an oven-dried 20 mL Schlenk purged under argon atmosphere, the pre-catalyst $PdCl_2(PPh_3)_2$ (9.12 mg, 0.013 mmol, 1.0 eq) was dissolved in the degassed solvent (0.6 mL). The base (0.026 mmol, 2.0 eq), PPh_3 (6.81 mg, 0.026 mmol, 2.0 eq) and triethyl phosphonoacetate as internal standard (0.0065 mmol, 0.5 eq) were added. The reaction was stirred at room temperature and after 10 minutes, the ^{31}P NMR spectra were collected (Yields of the reduction reported in Table 5.1).

Example of the reduction of Pd^{II} with TMG in $CDCl_3$ (Entry 2, Table 5.1)

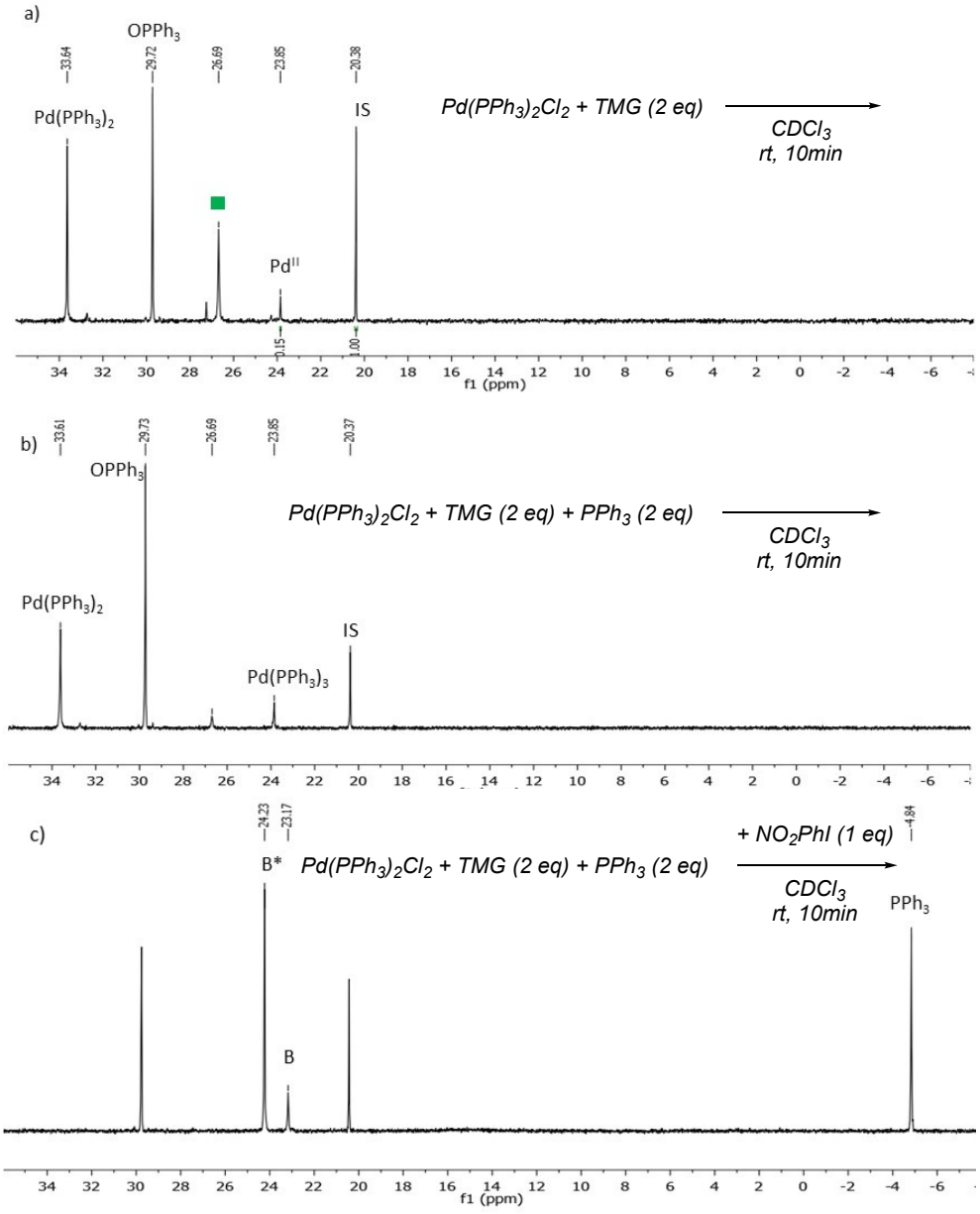

Figure S5.1: *^{31}P NMR spectra of the reduction of $PdCl_2(PPh_3)_2$ in $CDCl_3$ with TMG 2.0 eq. The peak labelled in green represents $(TMG)Pd^0(PPh_3)$ (a); with TMG 2.0 eq and PPh_3 2.0 eq (b); with TMG 2.0 eq, PPh_3 2.0 eq and the reagent 4-NO_2PhI* ***1*** *1.0 eq (c) to show that the reduction of Pd^{II} was complete*

Example of the reduction of Pd^{II} with TMG in DMF-d_7 (Entry 1, Table 5.1)

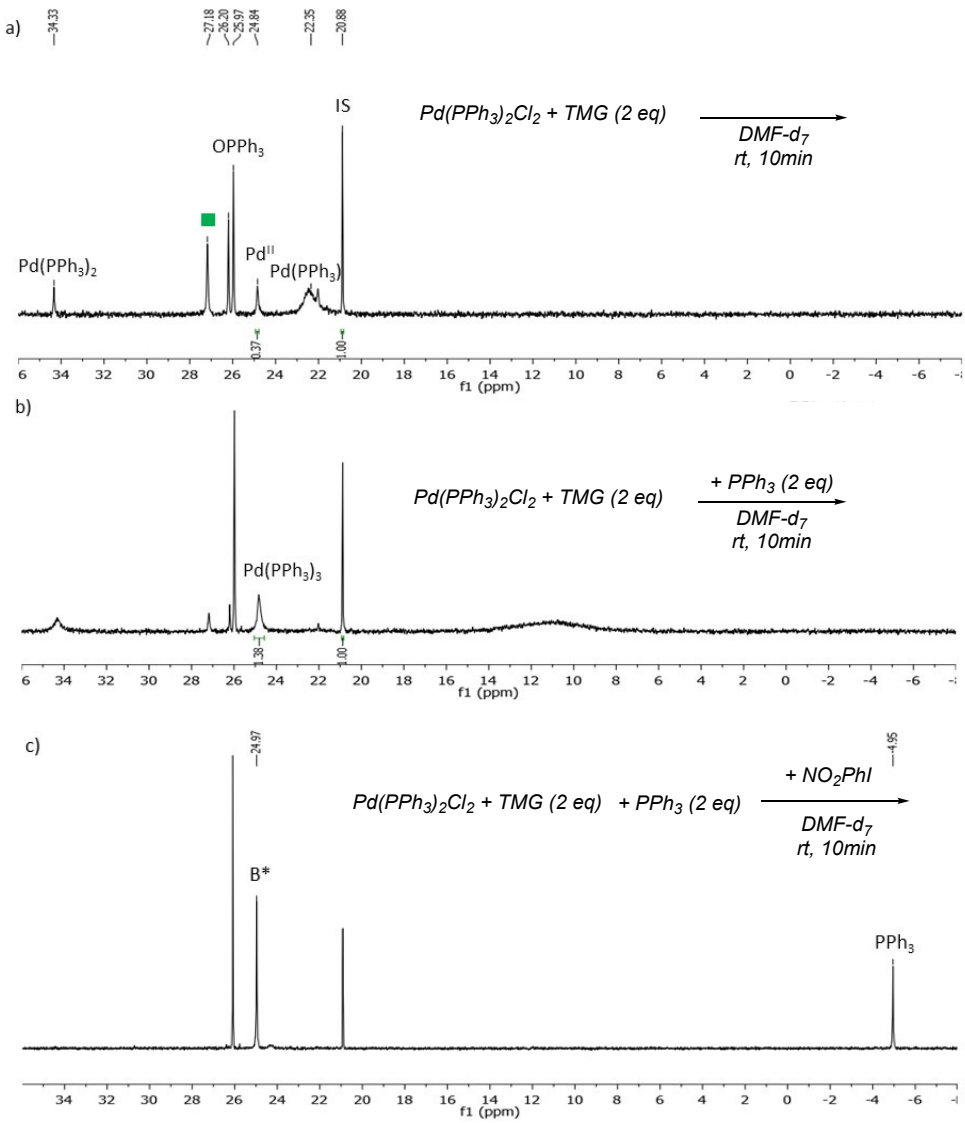

Figure S5.2: *^{31}P NMR spectra of the reduction of $PdCl_2(PPh_3)_2$ in DMF-d_7 with TMG 2.0 eq. The peak labelled in green represents (TMG)$Pd^0(PPh_3)$ (a); with TMG 2.0 eq and PPh_3 2.0 eq (b); with TMG 2.0 eq, PPh_3 2.0 eq and 4-NO_2PhI **1** 1.0 eq (c) to show that the reduction of Pd^{II} was complete.*

Pd^{II}-Pd^0 reduction in the presence of phenylacetylene with or without PPh_3

To an oven-dried 20 mL Schlenk purged under argon atmosphere, the pre-catalyst $PdCl_2(PPh_3)_2$ (9.12 mg, 0.013 mmol, 1.0 eq) was dissolved in the degassed $CDCl_3$ (0.6 mL). Pyrrolidine (53.38 µL, 0.65 mmol, 50 eq), phenylacetylene **2a** (71.38 µL, 0.65 mmol, 50 eq) and PPh_3 (6.81 mg, 0.026 mmol, 2 eq) were added to the solution. Triethyl phosphonoacetate (0.0065 mmol, 0.5 eq) was used as internal standard. The reaction was

stirred at room temperature and ^{31}P NMR spectra were collected after 10 minutes. This experiment was performed to demonstrate that the formation of **M** is achieved only when the reduction is not effective and the alkyne intervenes in the reduction step forming **M** (Figure S5.3a). With the addition of PPh_3 the reduction is efficient and the alkyne doesn't intervene in the reduction and **M** is not formed (Figure S5.3b).

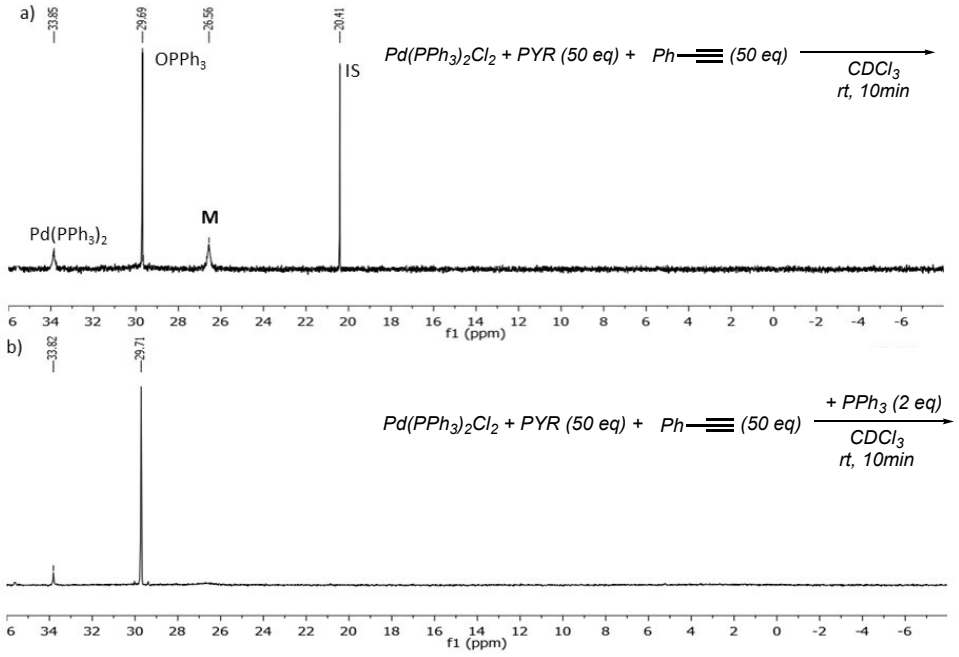

***Figure S5.3**: ^{31}P NMR spectra of $PdCl_2(PPh_3)_2$ in $CDCl_3$ with pyrrolidine 50 eq and **2a** 50 eq (a) and with PPh_3 2.0 eq (b)*

Heck-Cassar reaction with Pd^{II} and Pd^0

General procedure for the HC reaction with Pd^{II}

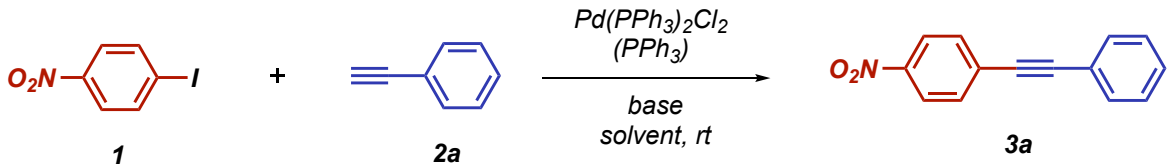

To an oven-dried 10 mL Schlenk purged under N_2 atmosphere, $PdCl_2(PPh_3)_2$ (20% mmol) and PPh_3 (40% mmol) were dissolved in the degassed solvent. After the addition of 1-Iodo-4-nitrobenzene **1** (124.5 mg, 0.5 mmol, 1.0 eq), phenylacetylene **2a** (60 µL, 0.55, 1.1 eq)

and the base (2.0 eq), the reaction mixture was stirred at room temperature. After a given time, the ^{31}P NMR spectra were collected to detect the different species.

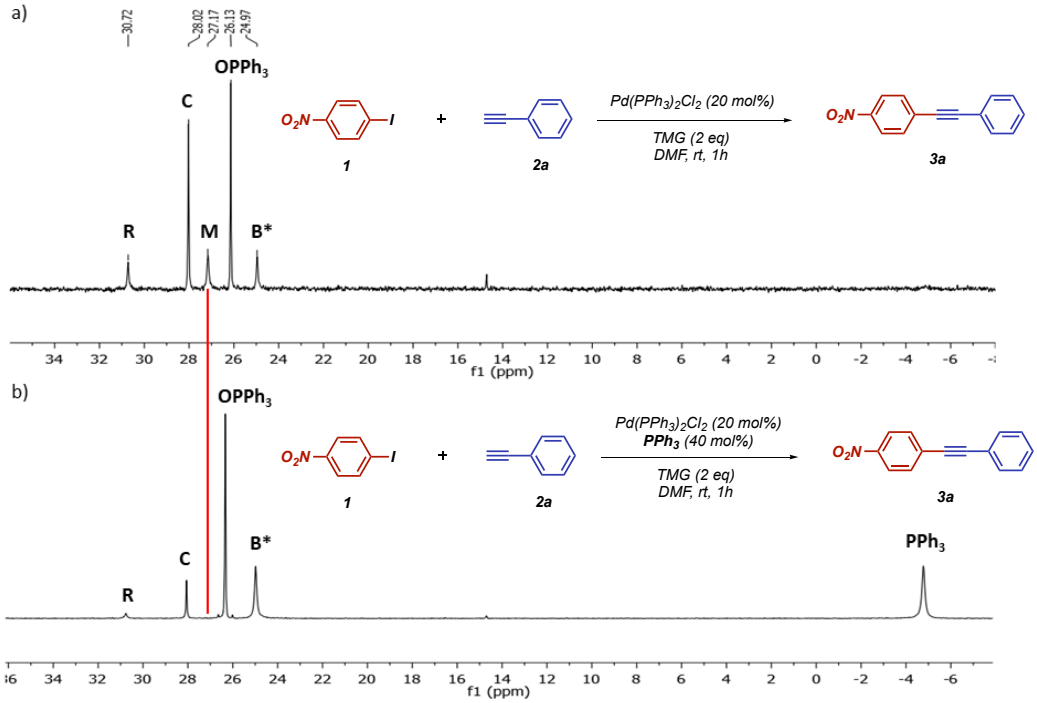

Figure S5.4: *Stacking of ^{31}P NMR spectra after 1 h of the reaction between **1** and **2a** in DMF-d_7, with TMG 2.0 eq (a); with TMG 2.0 eq and 40 mmol% of PPh_3 (b)*

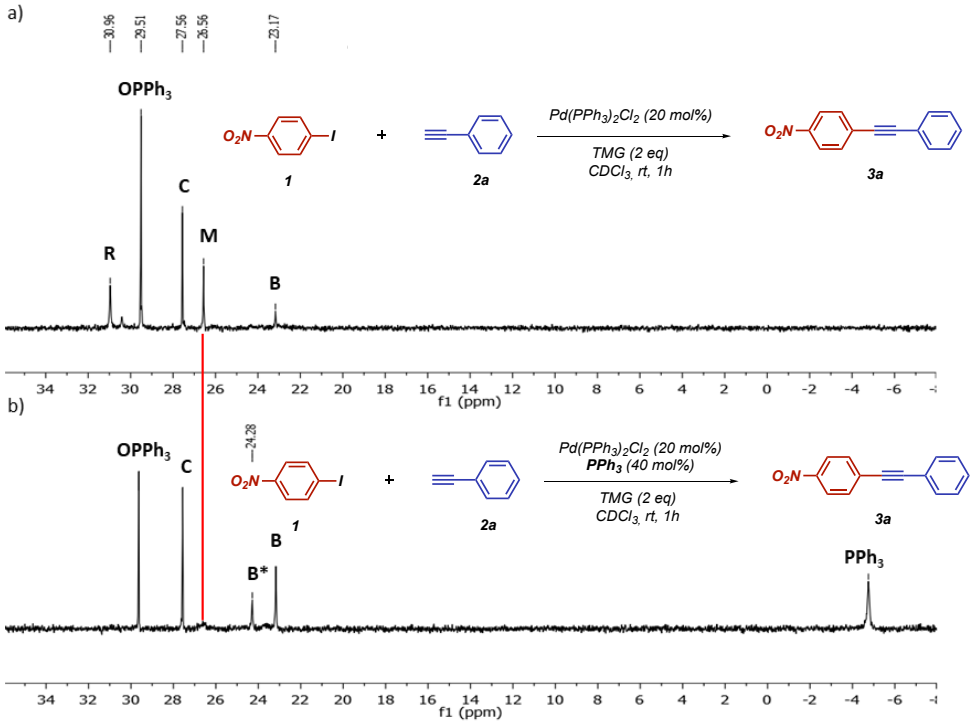

Figure S5.5: *Stacking of ^{31}P NMR spectra after 1 h of the reaction between **1** and **2a** in $CDCl_3$, with TMG 2.0 eq (a); with TMG 2.0 eq and 40 mmol% of PPh_3 (b)*

General procedure for the HC reaction with Pd^0

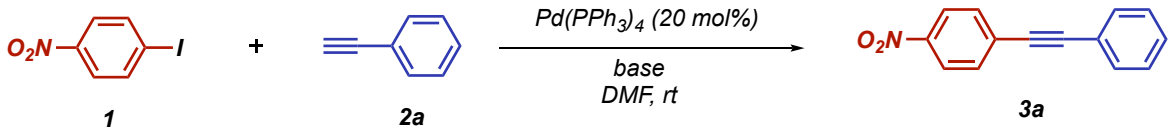

To an oven-dried 10 mL Schlenk purged under N_2 atmosphere, $Pd(PPh_3)_4$ (20% mmol) was dissolved in degassed DMF-d_7. After the addition of 1-Iodo-4-nitrobenzene **1** (124.5 mg, 0.5 mmol, 1.0 eq), phenylacetylene **2a** (60 µL, 0.55, 1.1 eq) and the base (2.0 eq), the reaction mixture was stirred at room temperature. After a given time, the ^{31}P NMR spectra were collected to detect which species were formed.

This experiment was performed to demonstrate that when you use Pd^0, **M** complex is never formed (Figure S5.6). This is the proof that **M** is formed only when the reduction to form the active Pd^0 species from Pd^{II} is not effective and the alkyne intervenes in the reduction.

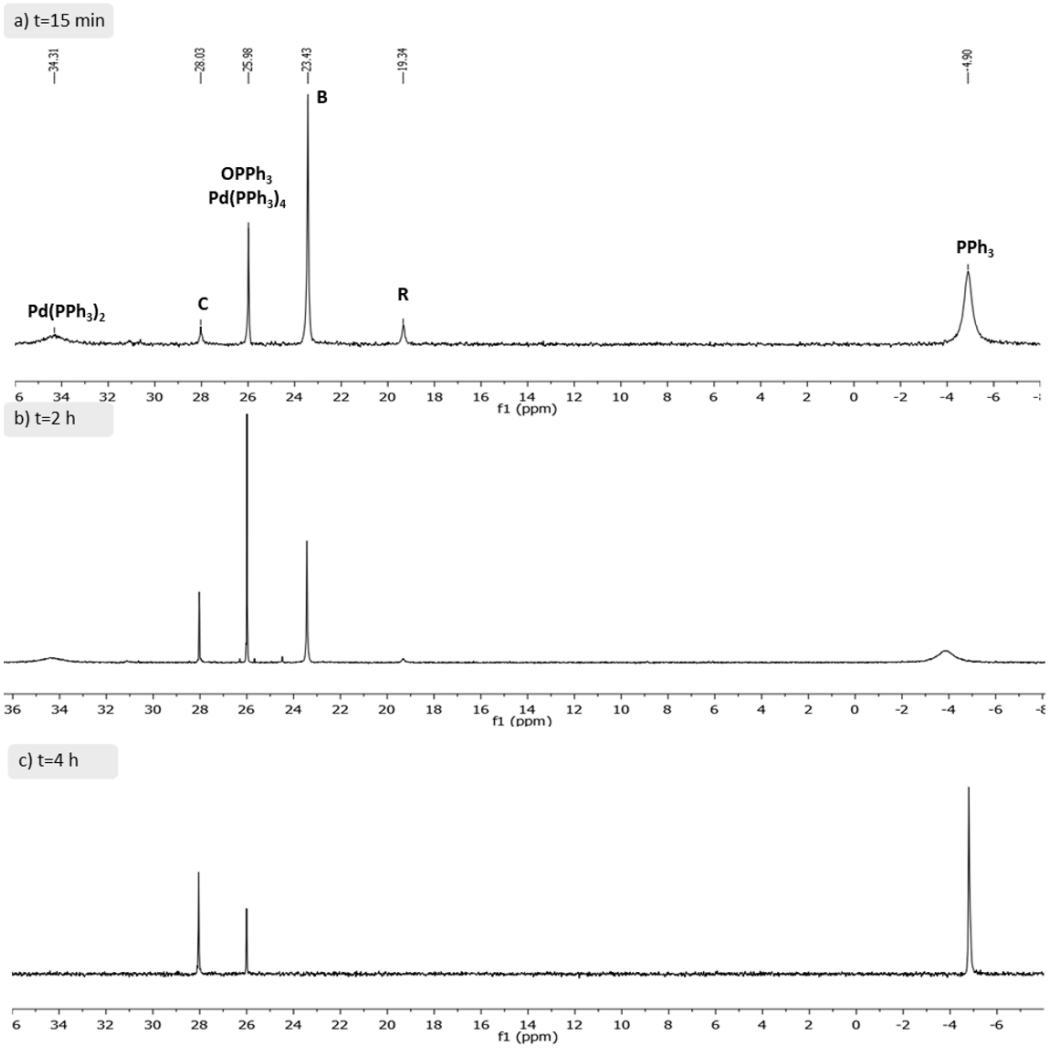

Figure S5.6: *Stacking of ^{31}P NMR spectra of the reaction between **1** and **2a** in DMF-d_7 using TMG after 15 min (a); 1 h (b); 4 h (c).*

Direct coordination versus transmetallation

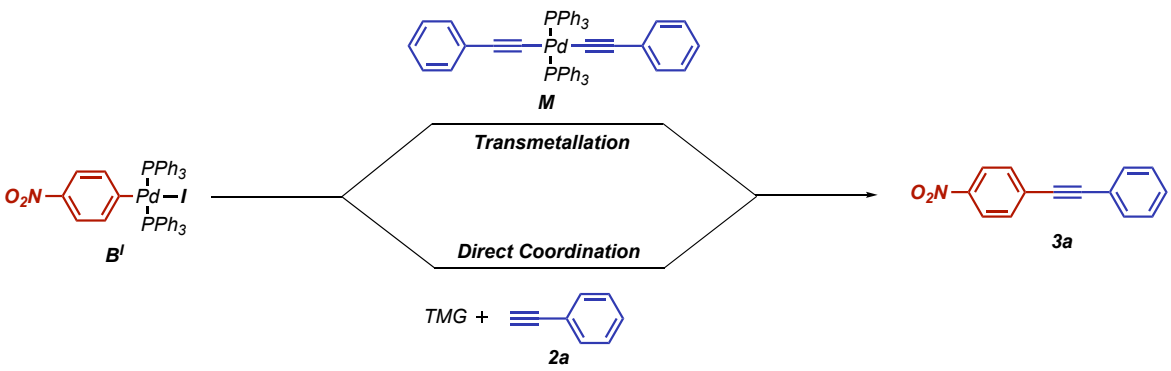

Procedure for the transmetallation step

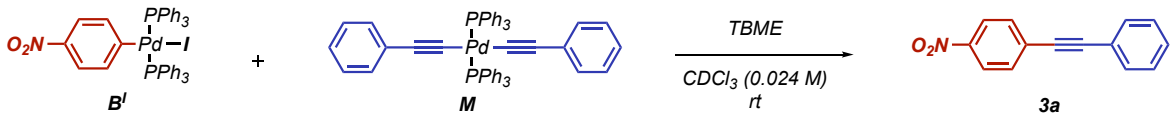

The reaction was performed in an oven-dried glass NMR tube purged under nitrogen atmosphere. The complexes **B**^{I} (15.82 mg, 0.018 mmol, 1.0 eq) and **M** (15 mg, 0.0.18 mmol, 1.0 eq) were dissolved in $CDCl_3$ (0.750 mL). The mixture was let at room temperature and it was monitored by ^{1}H and ^{31}P NMR spectroscopy at intervals of 20 minutes for 7 hours using tert-butyl methyl ether (TBME) as internal standard.

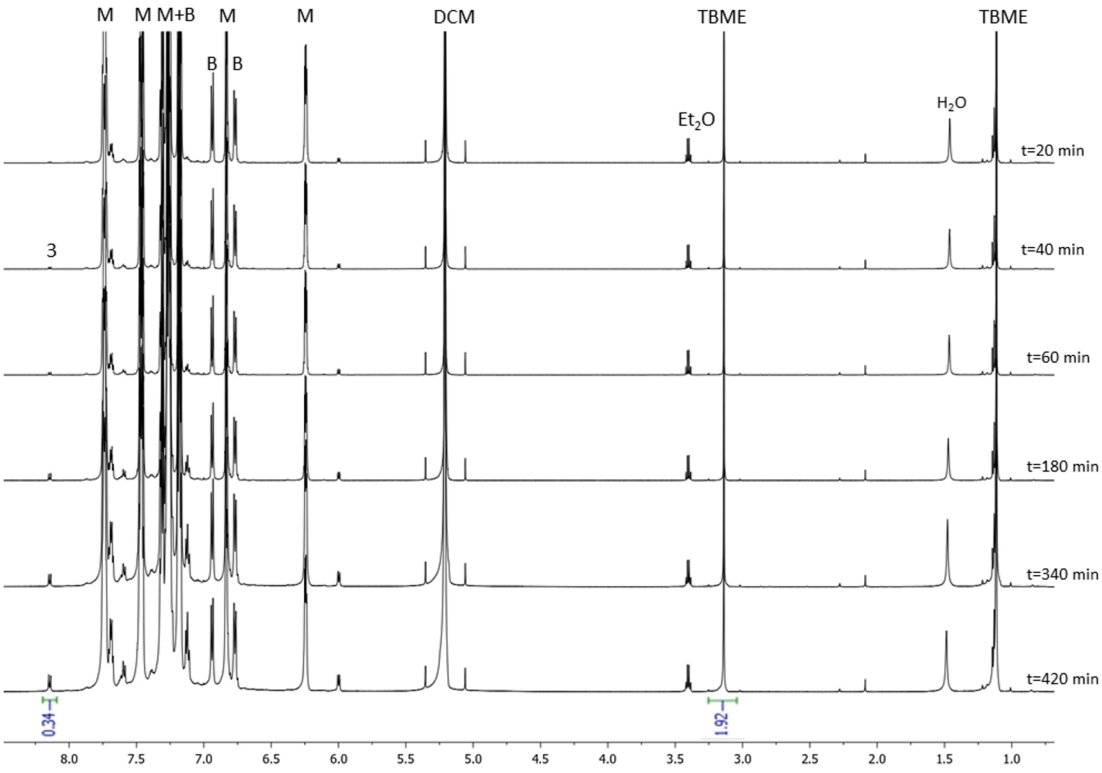

Figure S5.7: *Stacking of ^{1}H NMR spectra of the stoichiometric reaction between **B** and **M** in $CDCl_3$ at several times.*

Procedure for the Direct Coordination step

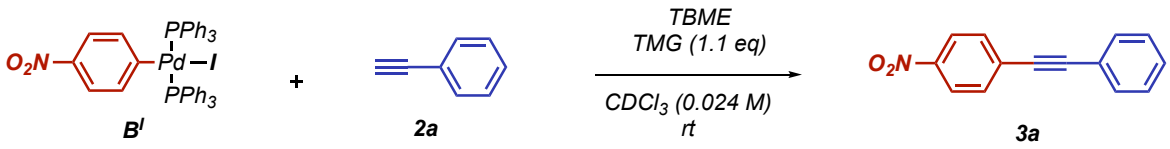

The reaction was performed in an oven-dried glass NMR tube purged under nitrogen atmosphere. The complex **B**^{I} (15.82 mg, 0.018 mmol, 1.0 eq) was dissolved in $CDCl_3$ (0.750 mL), followed by the addition of **2a** (29 µL from a stock solution of 0.66 M, 0.018 mmol, 1.0 eq) and TMG (32.5 µL from a stock solution of 0.66 M, 0.02 mmol, 1.1 eq). TBME (1.0 eq) was used as internal standard. The mixture was let at room temperature and il was monitored by ^{1}H and ^{31}P NMR spectroscopy at intervals of 20 minutes for 7 hours.

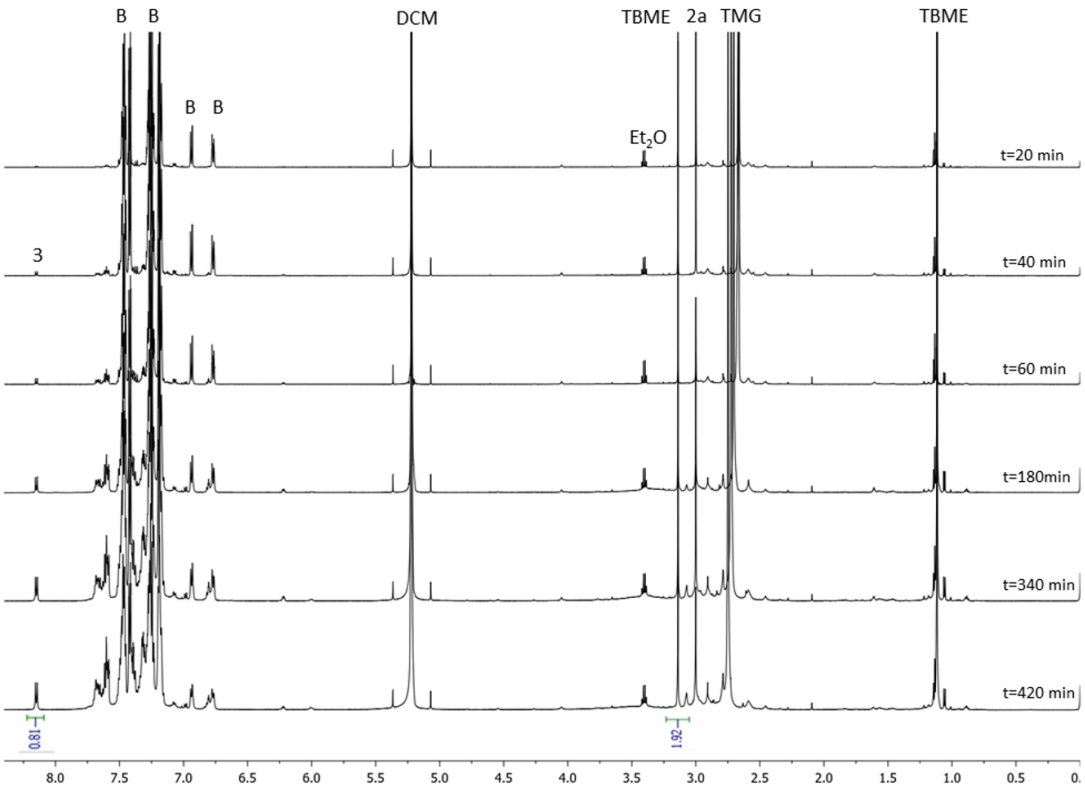

Figure S5.8: *Stacking of ^{1}H NMR spectra of the stoichiometric reaction between **B** and **2a** with TMG in $CDCl_3$ at several times.*

As evidenced by the integrations of the product areas (0.81/1.92 for the direct coordination and 0.34/1.92 for the Pd/Pd transmetallation), the direct insertion of the alkyne to form product **3** is faster than the transmetallation (see the kinetics in Figure 5.4 in the main text).

Parallel side reactions

*Stability of complex **M** (Entries 1-4, Table 5.2)*

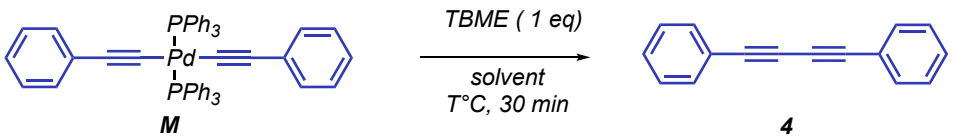

General procedure:

To an oven-dried NMR tube purged under nitrogen atmosphere, complex **M** was dissolved in deuterated solvent (0.75 mL) at room temperature or at 60°C. TBME was used as internal standards. After 30 minutes of stirring, the samples were analyzed using ^{1}H NMR, ^{31}P NMR, HPLC-UV or GC-MS techniques

*Stability of **M** in DMF-d_7 at room temperature (Entry 2, Table 5.2)*

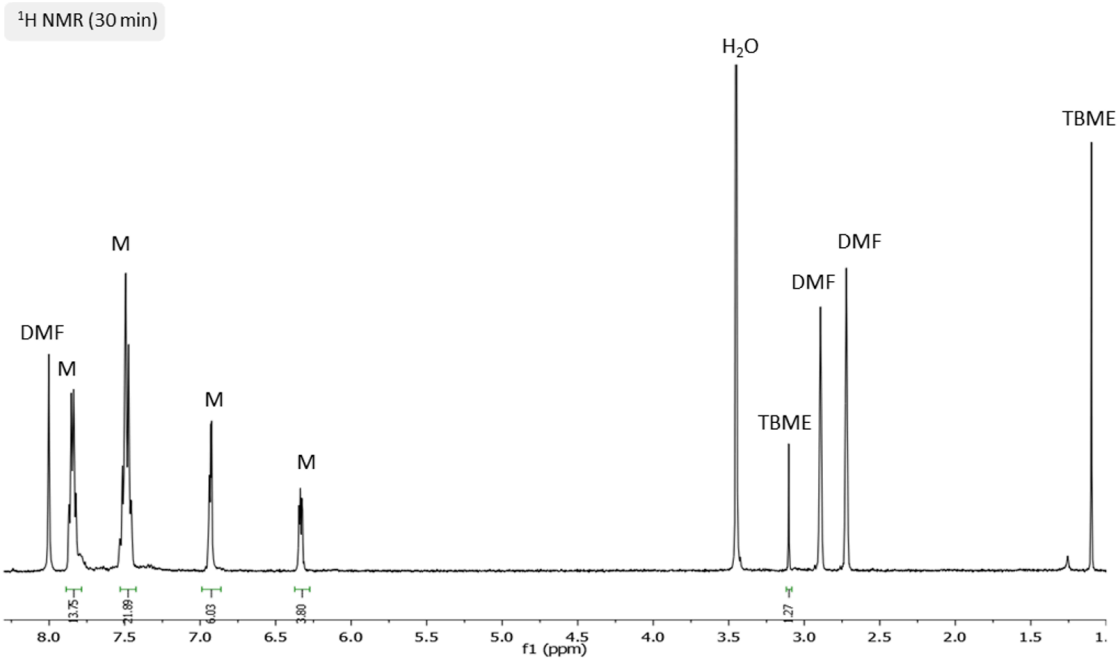

***Figure S5.9**: ^{1}H NMR spectrum of **M** in DMF-d_7 at room temperature after 30 minutes. **M** is stable at room temperature.*

*Stability of **M** in DMF-d_7 at 60°C (Entry 4, Table 5.2)*

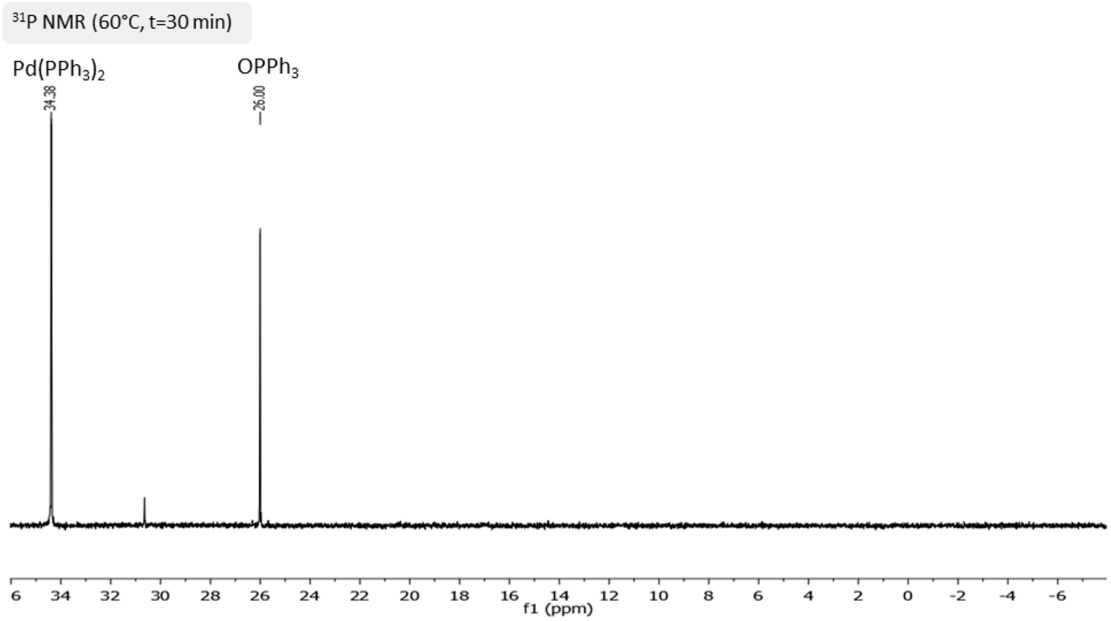

***Figure S5.10**: ^{31}P NMR spectrum of **M** in DMF-d_7 at t=60°C after 30 minutes. **M** completely decomposes in homocoupling byproduct **4** and $Pd(PPh_3)_2$*

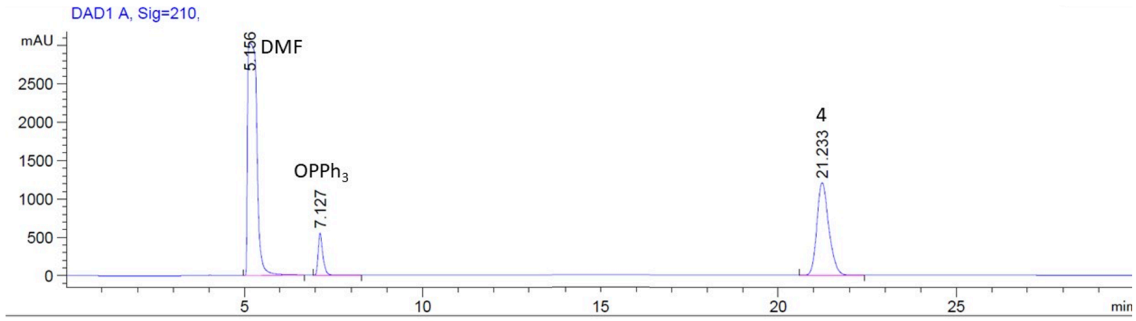

***Figure S5.11**: HPLC chromatogram of complex **M** at 60°C in DMF-d_7 after 30 minutes*

*Reaction between **B**^{I} and **M** (Entries 5-6, Table 5.2)*

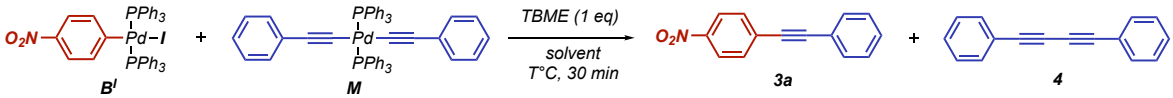

General procedure:

The reaction was performed in an oven-dried NMR tube purged under nitrogen atmosphere. Complexes **B**^{I} (15.82 mg, 0.018 mmol, 1.0 eq) and **M** (15 mg, 0.0.18 mmol, 1.0 eq) were dissolved in solvent (0.750 mL). It was let at room temperature or at 60°C for 30

minutes using TBME as internal standard. The mixture was analyzed with ^{1}H NMR or ^{31}P NMR spectroscopy

*Reaction between **B**^{I} and **M** in $CDCl_3$ at room temperature (Entry 5, Table 5.2)*

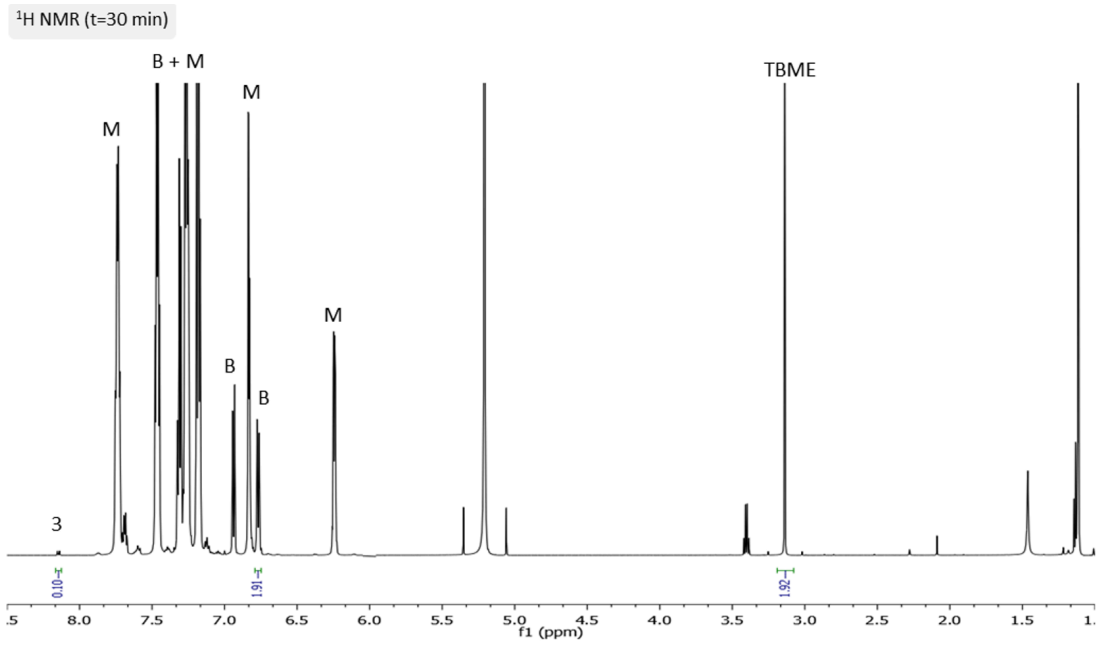

***Figure S5.12**: ^{1}H NMR spectrum of the stoichiometric reaction between **B** and **M** in $CDCl_3$ after 30 minutes at rt.*

*Reaction between **B**^{I} and **M** in DMF-d_7 at 60°C (Entry 6, Table 5.2)*

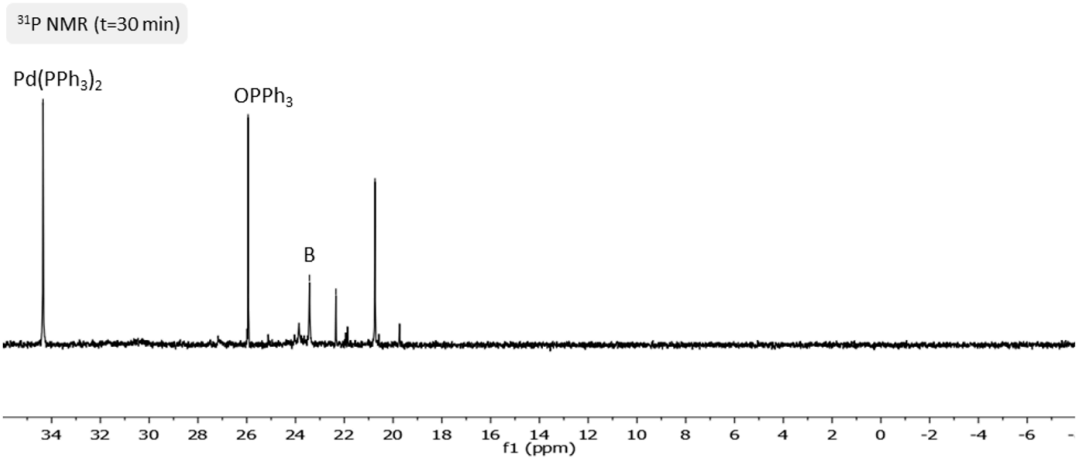

***Figure S5.13**: ^{31}P NMR spectrum of the stoichiometric reaction between **B** and **M** in DMF-d_7 after 30 minutes at 60° C.*

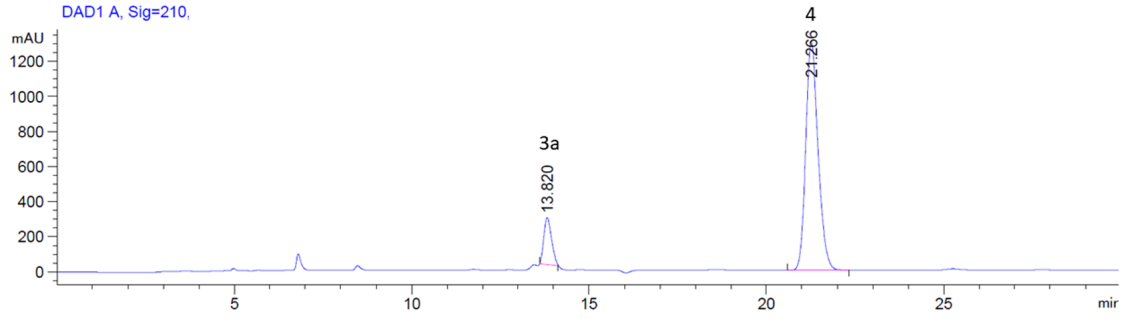

Peak #	RetTime [min]	Type	Width [min]	Area [mAU*s]	Height [mAU]	Area %
1	13.831	MM	0.1830	1747.83301	159.19141	5.2716
2	21.266	BB	0.3668	3.14076e4	1305.00317	94.7284

***Figure S5.14**: HPLC chromatogram of the crude of the reaction between complexes **B** and **M** in DMF at 60°C after 30 minutes. The crude was extracted with cyclohexane. The Relative Response Factor (RRF) between **3a** and **4** is 0.21.*

*Reaction between **B**^{I} and **2a** (Entries 7-8, Table 5.2)*

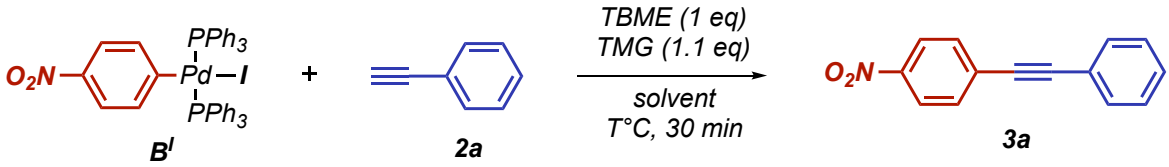

General procedure:

The reaction was performed in an oven-dried NMR tube purged under nitrogen atmosphere. The complex **B**^{I} (15.82 mg, 0.018 mmol, 1.0 eq) was dissolved in solvent (0.750 mL) followed by the addition of **2a** (29 µL from a stock solution of 0.66 M, 0.018 mmol, 1.0 eq) and TMG (32.5 µL from a stock solution of 0.66 M, 0.02 mmol, 1.1 eq). Tert-butyl methyl ether (TBME) was used as internal standard. The mixture was stirred at room temperature and it was monitored by ^{1}H and ^{31}P NMR spectroscopy at several times.

*Reaction between **B**^{I} and **2a** in $CDCl_3$ at room temperature (Entry 7, Table 5.2)*

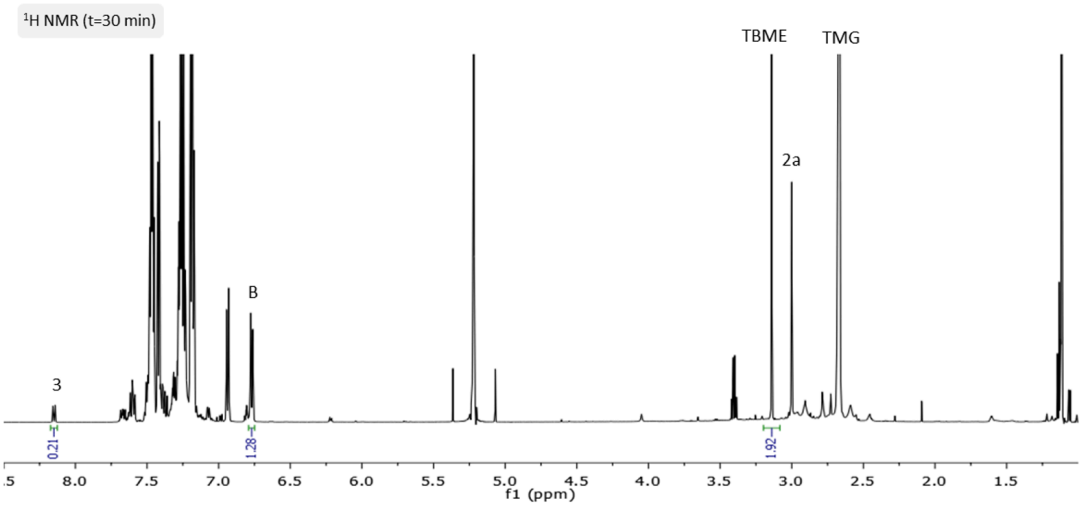

***Figure S5.15**: ^{1}H NMR spectrum of the stoichiometric reaction between **B** and **2a** with TMG in $CDCl_3$ after 30 minutes at rt.*

*Reaction between **B**^{I} and **2a** in DMF-d_7 at 60° (Entry 8, Table 5.2)*

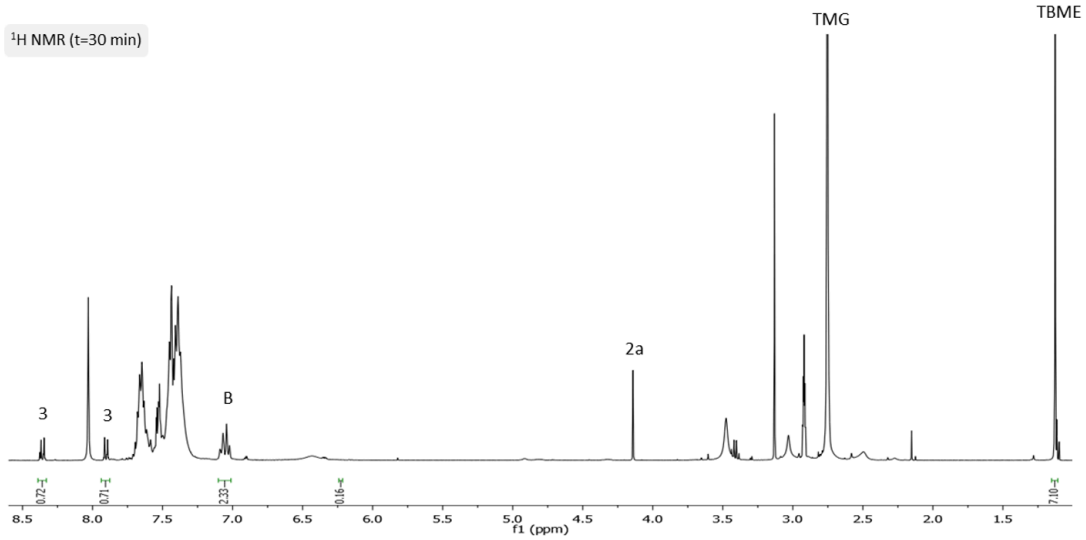

***Figure S5.16**: ^{1}H NMR spectrum of the stoichiometric reaction between **B** and **2a** with TMG in DMF-d_7 after 30 minutes at 60°C*

Simultaneous competition reaction

Procedure:

To an oven-dried 10 mL Schlenk purged under N_2 atmosphere, **B^{I}** (87.9 mg, 0.1 mmol, 1.0 eq), **M** (83 mg, 0.1 mmol, 1.0 eq), and **2b** (13 µL, 0.1 mmol, 1.0 eq) were dissolved in DMF (0.750 mL). After the addition of TMG (14 µL, 0.11 mmol, 1.1 eq), the reaction stirred at 60°C and it was monitored by GC-MS technique.

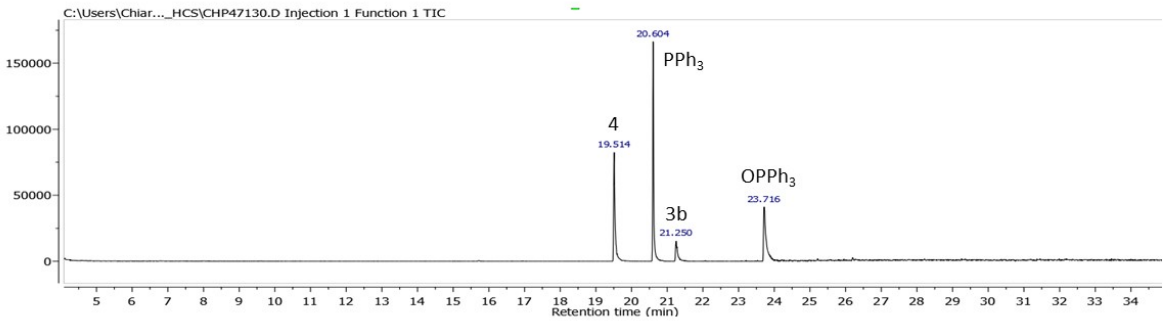

Figure S5.17: *GC-chromatogram of the stoichiometric reaction **B** + **M** + **2b** with TMG, in DMF at 60°C after 30 minutes.*

Base effect on AO-complex B^{x}

General Procedure:

The reaction was performed in an oven-dried glass NMR tube purged under nitrogen atmosphere. The complex **B^{x}** (0.026 mmol, 1.0 eq) was dissolved in DMF-d_7 (0.60 mL) followed by the addition of the base (10-20-50 eq). The base effect was evaluated using ^{31}P NMR technique. The spectra were collected as soon as after the addition and after 30 minutes and provided the same results.

*Example of reaction between **B^{Br}** and TMG (Entry 5, Table 5.3)*

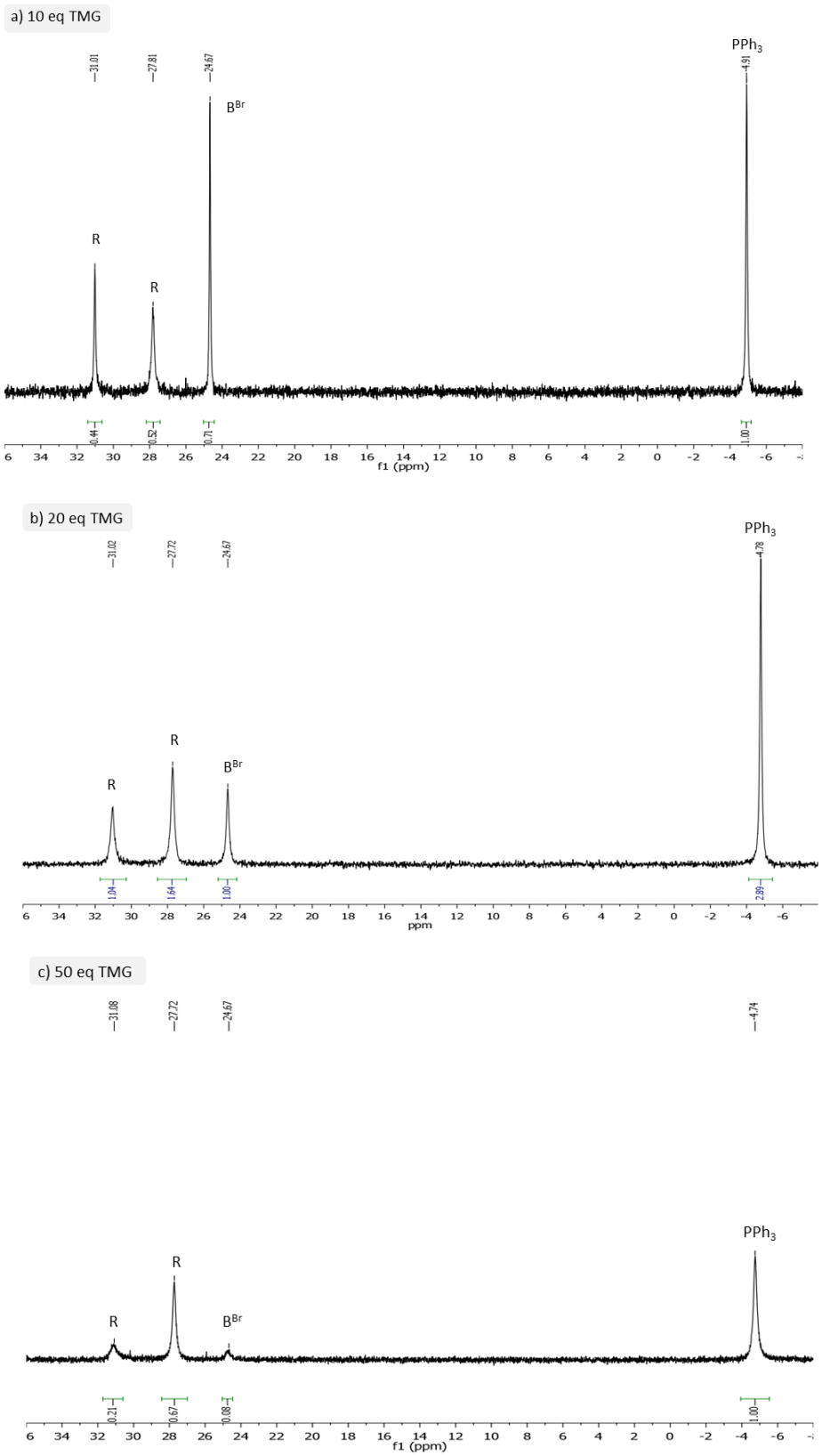

Figure S5.18: *^{31}P NMR spectra in DMF-d_7 of **B^{Br}** with TMG 10 eq (a); TMG 20 eq (b) and TMG 50 eq (c).*

Evaluation of the Kinetic Constant

General procedure[31] *(The results are reported in Table 5.3)*

The equilibrium constant Keq = [Ligand][Σ**R**]/[**B**][base] was determined in DMF-d_7 by ^{31}P NMR spectroscopy.

To evaluate Keq for the compounds $\mathbf{B}^{Br}$ and $\mathbf{B}^{Cl}$**,** the amine was added in the range of 10-50 eq, whereas the amount of base was lowered in case of $\mathbf{B}^{I}$, due to the high tendency to produce **R**. By considering [Ligand] = [Σ**R**], the formula becomes $Keq= x^2/(1-x)(n-x)$ where *n* is the number of equivalents of base added to **B**, *x* is the molar fraction of **R** in the equilibrium $x=2z_L/(z_B + 2z_L)$ and z_L and z_B are the magnitude of the ligand and **B** respectively. Keq was determined from the slope of the straight line obtained by the plot of x^2 versus (1-*x*)(*n*-*x*). All experiments were repeated three times.

Base effect on AO-complex B^{OTf}

General Procedure:

The reaction was performed in an oven-dried glass NMR tube purged under nitrogen atmosphere. The complex $\mathbf{B}^{OTf}$ (11.7 mg mg, 0.013 mmol, 1.0 eq) was dissolved in DMF-d_7 (0.60 mL) followed by the addition of the base. The base effect was evaluated using ^{31}P NMR technique

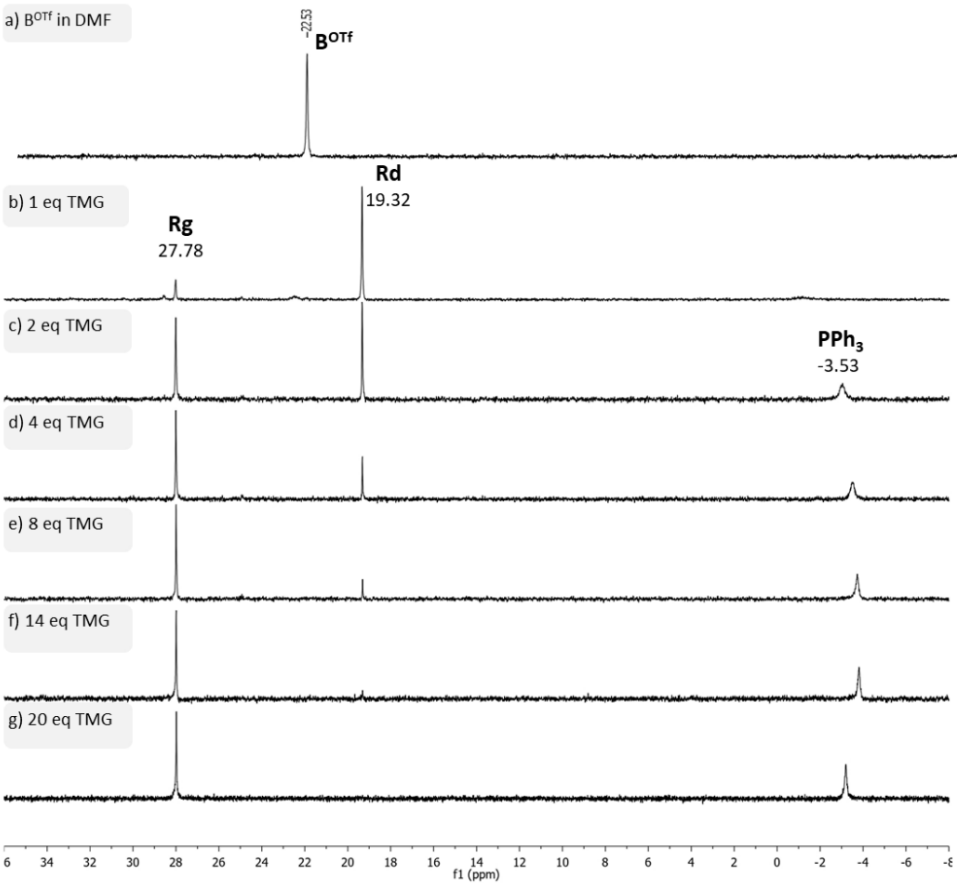

Figure S5.19: *Stacking of ^{31}P NMR spectra in DMF-d$_7$ of* ***B^{OTf}*** *(a); with the addition of TMG 1.0 eq (b); 2.0 eq (c); TMG 4.0 eq (d); TMG 8.0 eq (e); TMG 14 eq (f); TMG 20 eq (g).*

Phenylacetylene addition to B^x complexes

General Procedure:

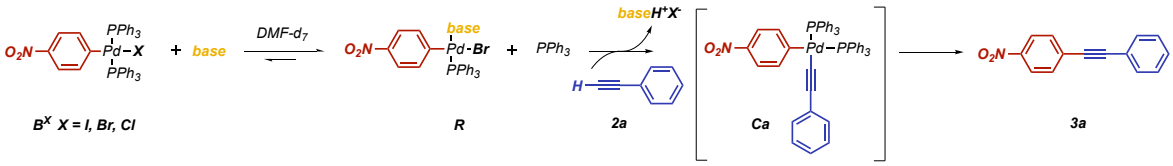

The reaction was performed in an oven-dried glass NMR tube purged under nitrogen atmosphere. The complex **B^x** (0.026 mmol, 1.0 eq) was dissolved in DMF-d$_7$ (0.60 mL) followed by the addition of the base (20-50 eq). The ^{31}P NMR were collected as soon as after the addition of **2a** (20-50eq) and after 10 minutes.

*Example of reaction between **B**^{Br} and **2a** to form **C***

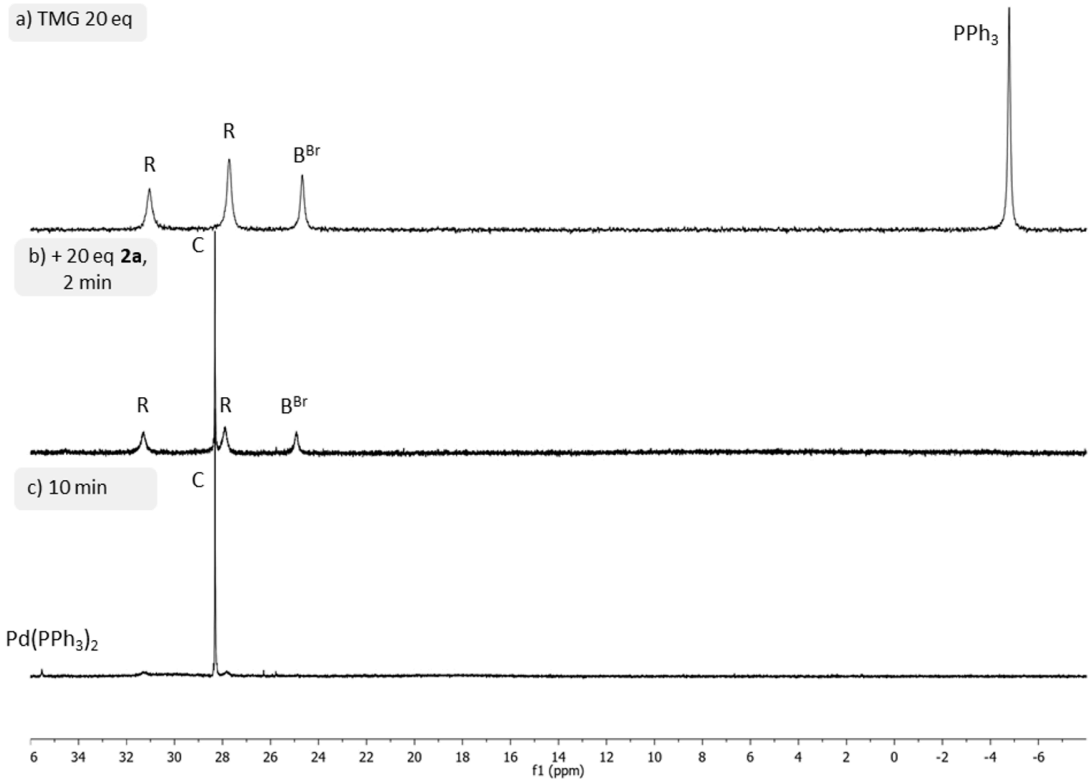

Figure S5.20: *Stacking of ^{31}P NMR spectra in DMF-d_7 of **B**^{Br} after the addition of TMG 20 eq (a), immediately after the following addition of **2a** 20 eq (b) and after 10 minutes (c).*

Scope of alkynes as substrates for the direct coordination step

General Procedure (Figure 5.7):

The reaction was performed in an oven-dried glass NMR tube purged under nitrogen atmosphere. The complex **B**^{Br} (21.6 mg, 0.026 mmol, 1.0 eq) was dissolved in DMF-d_7 (0.60 mL) followed by the addition of TMG (65 µL, 0.52 mmol, 20 eq). The ^{31}P NMR were collected as soon as after the addition of **2a-l** (0.052 mmol, 20 eq). After 24h of stirring, the mixture was quenched with H_2O (1 mL) and extracted with cyclohexane or ethyl acetate (3x1 mL). Then, the collected organic phases were washed with brine, dried over Na_2SO_4 and concentrated under reduced pressure. Finally, the crude was purified by flash chromatography (the eluent is specified below in the Compound characterization section)

Direct coordination step with B^{OTf}

General Procedure:

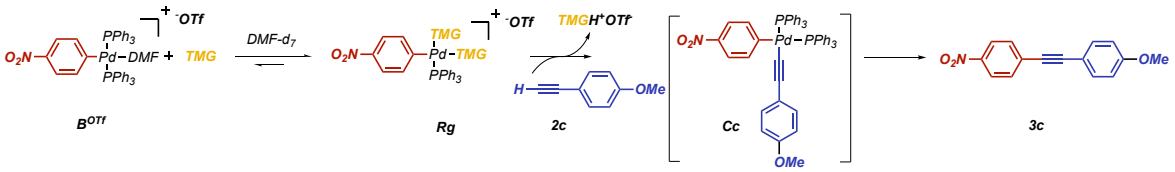

The reaction was performed in an oven-dried glass NMR tube purged under nitrogen atmosphere. The complex **B^{OTf}** (11.7 mg mg, 0.013 mmol, 1.0 eq) was dissolved in DMF-d_7 (0.60 mL) followed by the addition of TMG (33 µL, 0.26 mmol, 20 eq) and the following addition of 4-ethynylanisole **2c** (34 µL, 0.26 mmol, 20 eq). **2c** was chosen in this case, rather than phenylacetylene **2a** as in previous cases, to obtain a better separation between the peaks related to **C** and **Rg**. The ^{31}P NMR were collected immediately after the addition of **2c**.

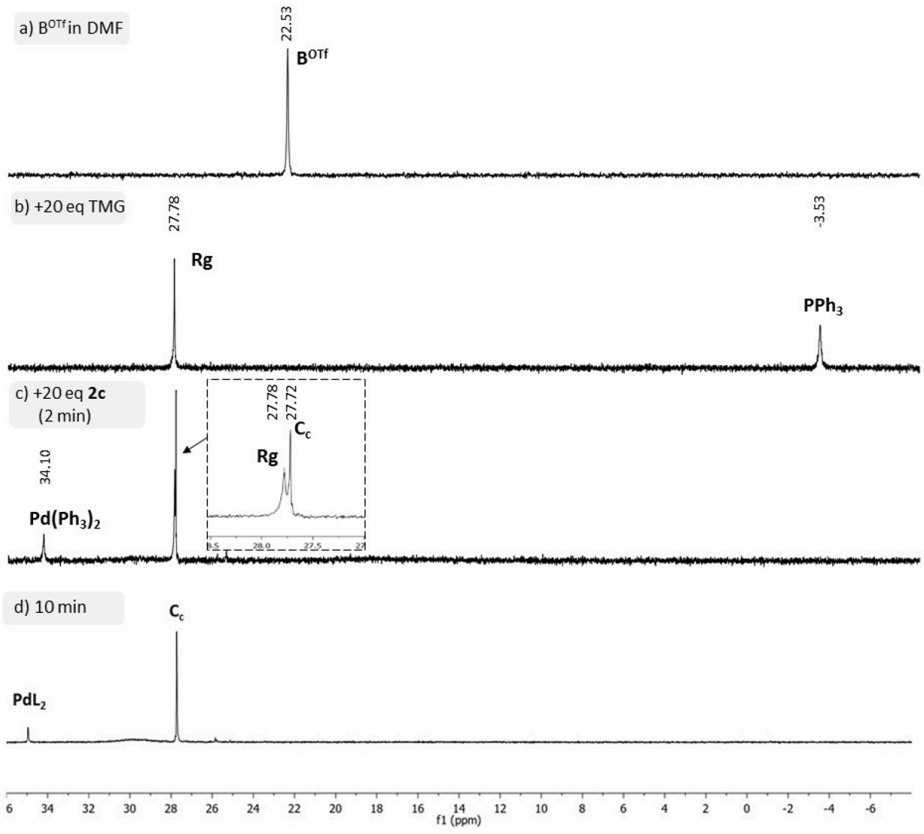

***Figure S5.21**: Stacking of ^{31}P NMR spectra in DMF-d_7 of **B^{OTf}** (a); after the addition of TMG 20 eq, (b); immediately after the following addition of **2c** 20 eq (c) and after 10 minutes (d).*

Compound characterization

*1-nitro-4-(phenylethynyl)benzene (**3a**)*

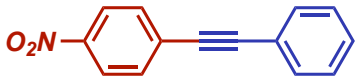

Yellow solid; Purification by flash chromatography (Cy 100%)

^{1}H NMR (400 MHz, $CDCl_3$): δ (ppm) 8.19 – 8.17 (d, J = 9.0 Hz, 2H), 7.64 – 7.62 (d, J = 9.0 Hz, 2H), 7.56 – 7.53 (m, 2H), 7.38 – 7.36 (m, 3H).

^{13}C NMR (100.8 MHz, $CDCl_3$): δ (ppm) 146.95, 132.27, 131.84, 130.22, 129.28, 128.57, 123.58, 122.10, 94.75, 87.59.

*1-methyl-4-((4-nitrophenyl)ethynyl)benzene (**3b**)*

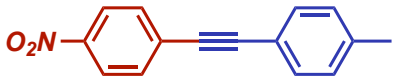

Yellow solid; Purification by flash chromatography (Cy 100%)

^{1}H NMR (400 MHz, $CDCl_3$): δ (ppm) 8.23-8.20 (d, J= 9 Hz, 2H); 7.66-7.64 (d, J= 9 Hz, 2H); 7.39-7.36 (m, 1H); 7.30-7.28 (m, 1H); 7.22-7.20 (m, 1H), 2.38 (s, 3H).

^{13}C NMR (100.8 MHz, $CDCl_3$): δ (ppm)147.02, 138.42, 132.52, 132.36, 130.33, 129.07, 128.57, 125.92, 123.76, 122.54, 122.01, 95.12, 87.38, 21.38.

*1-Methoxy-4-((4-nitrophenyl)ethynyl)benzene (**3c**)*

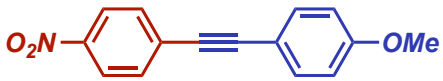

Yellow solid; Purification by flash chromatography (Cy/EtOAc 95/5)

^{1}H NMR (400 MHz, $CDCl_3$): δ (ppm) 8.22-8.20 (d, J= 9 Hz, 2H); 7.64-7.62 (d, J= 9 Hz, 2H); 7.51-7.49 (d, J=8.9 Hz, 2H), 6.92-6.90 (d, J=8.9 Hz, 2H); 3.85 (s, 3H)

^{13}C NMR (100.8 MHz, $CDCl_3$): δ (ppm) 160.54, 146.81, 133.59, 132.13, 130.84, 123.78, 114.35, 95.28, 86.78, 55.52.

*1-Chloro-3-((4-nitrophenyl)ethynyl)benzene (**3d**)*

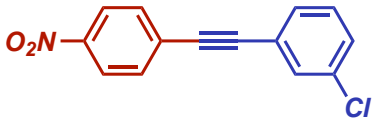

Yellow solid; Purification by flash chromatography (Cy/EtOAc 90/10)

^{1}H NMR (400 MHz, $CDCl_3$): δ (ppm) 8.24-8.22 (d, J= 8.8 Hz, 2H); 7.67-6.65 (d, J= 8.8 Hz, 2H); 7.54 (s, 1H); 7.45-7.43 (m, 2H) 7.38-7.30 (m, 2H).

^{13}C NMR (100.8 MHz, $CDCl_3$): δ (ppm) 147.33, 134.54, 132.51, 131.78, 130.07, 129.91, 129.77, 129.65, 123.92, 123.82, 93.09, 88.61

*3-methyl-1-(4-nitrophenyl)dodec-1-yn-3-ol (**3e**)*

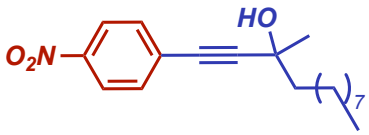

Orange oil; Purification by flash chromatography (Cy/EtOAc 90/10)

^{1}H NMR (400 MHz, $CDCl_3$) δ (ppm) 8.20 – 8.18 (d, J = 9.0 Hz, 2H), 7.57 – 7.55 (d, J = 9.0 Hz, 2H), 1.80 – 2.75 (m, 2H), 1.50 (s, 3H), 1.32 – 1.28 (m, 14H), 0.90 – 0.87 (m, 3H).

^{13}C NMR (100.8 MHz, $CDCl_3$) δ (ppm) 146.99, 132.36, 129.78, 123.50, 98.51, 83.12, 81.49, 68.67, 67.37, 43.53, 29.65, 29.53, 29.42, 29.27, 24.69, 22.64, 14.08

*1-(hept-1-yn-1-yl)-4-nitrobenzene (**3f**)*

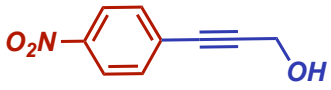

Yellow oil; Purification by flash chromatography (Cy/EtOAc = 95/5).

^{1}H NMR (400 MHz, $CDCl_3$) δ (ppm) 8.21 – 8.18 (d, J = 9.0 Hz, 2H), 7.60 – 7.57 (d, J = 9.0 Hz, 2H), 4.55 (s, 2H).

^{13}C NMR (100.8 MHz, $CDCl_3$) δ (ppm) 147.25, 132.39, 129.41, 123.57, 92.46, 83.81, 51.49.

*2-methyl-4-(4-nitrophenyl)but-3-yn-2-ol (**3g**)*

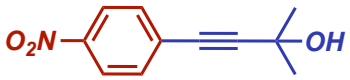

Yellow solid; Purification by flash chromatography (Cy/EtOAc 90/10)

^{1}H NMR (400 MHz, $CDCl_3$) δ (ppm) 8.20 – 8.18 (d, J = 9.0 Hz, 2H), 7.58 – 7.56 (d, J = 9.0 Hz, 2H), 1.65 (s, 3H).

^{13}C NMR (100.8 MHz, $CDCl_3$) δ (ppm) 147.02, 132.34, 129.70, 123.46, 99.08, 80.38, 65.61, 31.20.

*1-((4-nitrophenyl)ethynyl)cyclohexan-1-ol (**3h**)*

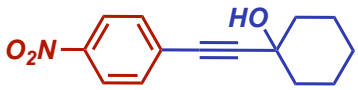

White solid; Purification by flash chromatography (Cy/EtOAc 90/10)

^{1}H NMR (400 MHz, $CDCl_3$) δ (ppm) 8.19 – 8.17 (d, J = 9.0 Hz, 2H), 7.58 – 7.56 (d, J = 9.0 Hz, 2H) 2.19 (s, 1H), 2.04 – 2.03 (m, 2H), 1.78 – 1.55 (m, 8H).

^{13}C NMR (100 MHz, $CDCl_3$) δ (ppm) 147.02, 132.70, 129.81, 123.55, 98.29, 82.54, 69.12, 39.74, 25.04, 23.25

*1-(hept-1-yn-1-yl)-4-nitrobenzene (**3i**)*

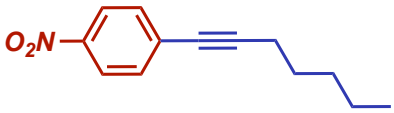

Yellow oil; Purification by flash chromatography (Cy 100%).

^{1}H NMR (400 MHz, $CDCl_3$) δ (ppm) 8.16 – 8.14 (d, J = 9.0 Hz, 2H), 7.52 – 7.50 (d, J = 9.0 Hz, 2H), 2.46 – 2.43 (t, *J* = 12.0 Hz, 2H), 1.66 – 1.60 (m, 2H), 1.48 – 1.34 (m, 4H), 0.95 – 0.91 (t, *J* = 12.0 Hz, 3H).

^{13}C NMR (100.8 MHz, $CDCl_3$) δ (ppm) 146.53, 132.19, 131.20, 123.43, 96.79, 79.25, 31.08, 28.08, 22.16, 19.50, 13.93.

*6-(4-nitrophenyl)hex-5-ynenitrile (**3j**)*

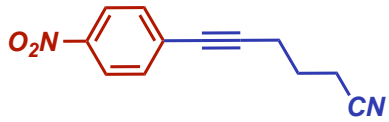

Yellow oil; Purification by flash chromatography (Cy/EtOAc 95/5)

^{1}H NMR (400 MHz, $CDCl_3$) δ (ppm) 8.19 – 8.17 (d, J = 9.0 Hz, 2H), 7.55 – 7.53 (d, J = 9.0 Hz, 2H), 2.69 – 2.66 (t, J = 6.8 Hz, 2H), 2.59 – 2.56 (t, J = 7.1 Hz, 2H), 2.04 – 1.97 (p, J = 7.0 Hz, 2H).

^{13}C NMR (100.8 MHz, $CDCl_3$) δ (ppm) 146.87, 132.32, 130.12, 123.52, 118.88, 92.84, 80.82, 24.21, 18.63, 16.3

*1-(6-chlorohex-1-yn-1-yl)-4-nitrobenzene (**3k**)*

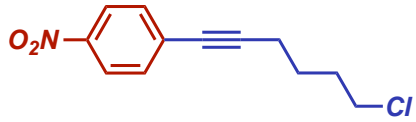

Yellow solid; Purification by flash chromatography (Cy/EtOAc 95/5)

^{1}H NMR (400 MHz, $CDCl_3$): δ (ppm) 8.16-8.14 (d, J= 8.9 Hz, 2H); 7.52-7.50 (d, J= 8.89 Hz, 2H); 3.62-3.59 (J=6.5 Hz, 2H); 2.52-2.49 (7 Hz, 2H); 1.99-1.92 (m, 2H); 1.83-1.76 (m, 2H).

^{13}C NMR (100.8 MHz, $CDCl_3$): δ (ppm) 146.80, 132.39, 130.95, 123.63, 95.61, 44.55, 31.73, 25.71, 19.03

*1-(4-bromobut-1-yn-1-yl)-4-nitrobenzene (**3l**)*

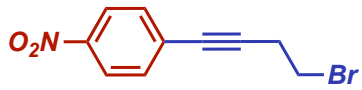

Yellow solid; Purification by flash chromatography (Cy/EtOAc 95/5)

^{1}H NMR (400 MHz, $CDCl_3$) δ (ppm) 8.21 – 8.18 (d, J = 9.0 Hz, 2H), 7.60 – 7.57 (d, J = 9.0 Hz, 2H), 6.08 – 6.01 (dd, J = 17.5, 11.2 Hz, 1H), 5.87 – 5.82 (dd, J = 17.6, 2.0 Hz, 1H), 5.70 – 5.66 (dd, J = 11.2, 2.0 Hz, 1H).

^{13}C NMR (100.8 MHz, $CDCl_3$) δ (ppm) 132.24, 130.06, 129.09, 123.57, 116.45, 93.15, 87.97

Computational studies

Computational Methods

DFT calculations were conducted through the Molecular Graphics and Computation Facility (MGCF) at the University of California, Berkeley using the Gaussian 16 software package.[32] Geometry optimizations for all reported structures were performed using the PBE0 functional (the hybrid functional based on the Perdew-Burke-Ernzerhof functional [PBE])[23,24] with Grimme's D3 dispersion correction with Becke Johnson damping (GD3-BJ)[33] and the basis sets def2-TZVP[25] (with effective core potential) for Pd, I, Br, Cl and def2-SVP for all the other atoms. Frequency calculations were performed on all optimized structures to ensure that each local minimum lacked imaginary frequencies and that each transition state contained exactly one imaginary frequency. Single point energies of all reported structures were calculated using the dispersion corrected PBE0 with def2-TZVP for all atoms. The reported Gibbs free energies were corrected considering the thermal correction computed at 298

Alternative pathways

*Dissociation of PPh_3 from complex **B^I***

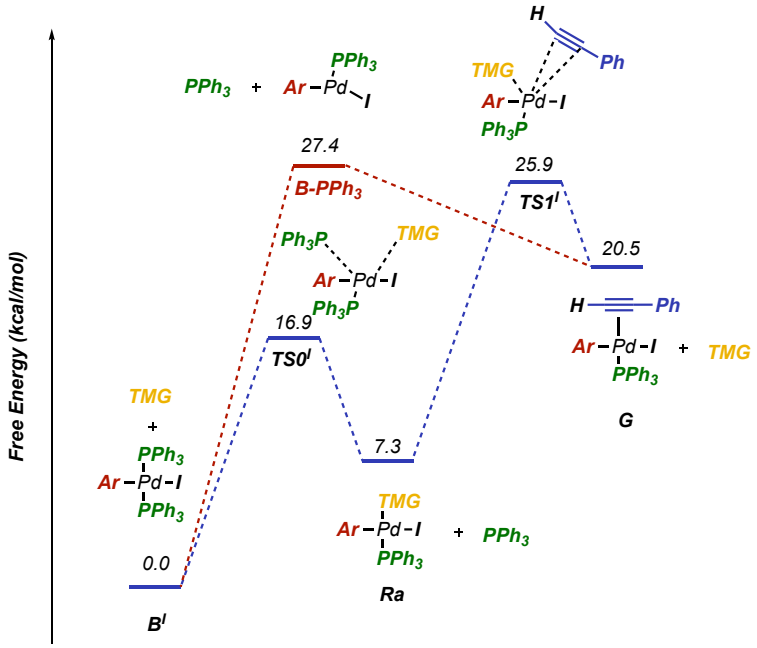

Figure S5.22**: Dissociation of PPh_3 from **B^I** to form complex **B-PPh$_3$** has an energy of 27.4 kcal/mol, therefore unfavored over the formation of **TS0^I** where the TMG displaces the phosphine giving intermediate **Ra

*Reductive elimination from complex **T***

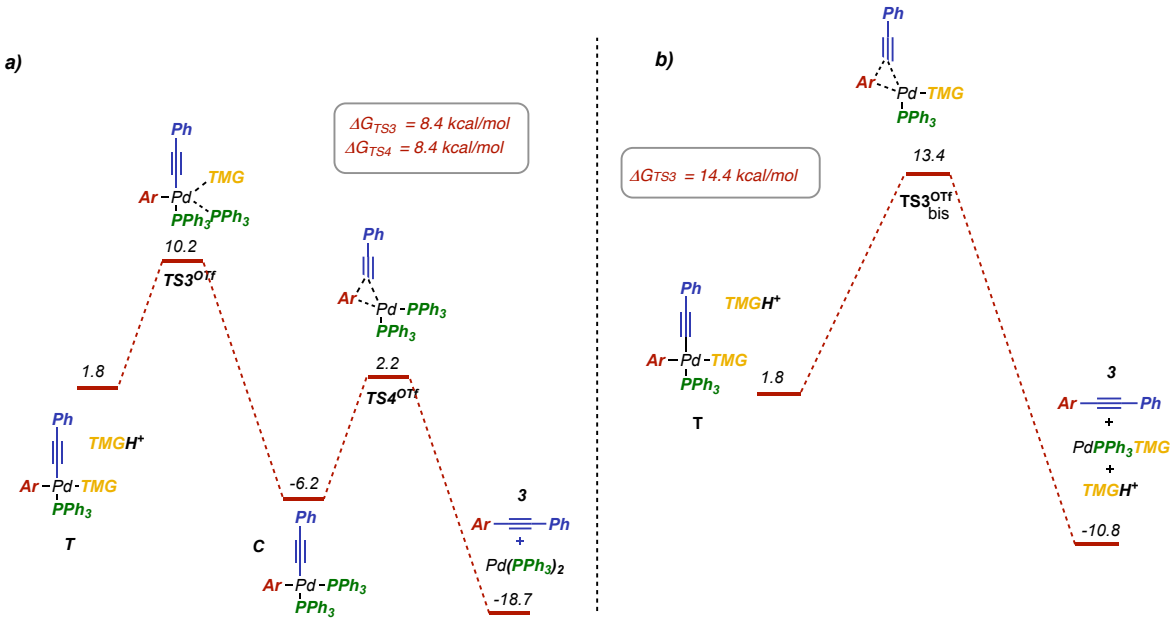

***Figure S5.23**: Reductive elimination from complex **T** to give **C** through **TS3^{OTf}** a) and reductive elimination from **T** to give directly the final product passing through **TS3^{OTf}bis** b).*

5.5 References

(1) McMullin, C. L.; Fey, N.; Harvey, J. N. Computed Ligand Effects on the Oxidative Addition of Phenyl Halides to Phosphine Supported Palladium(0) Catalysts. *Dalton Trans.* **2014**, *43* (36), 13545–13556. https://doi.org/10.1039/C4DT01758G.

(2) Amatore, C.; Azzabi, M.; Jutand, A. Role and Effects of Halide Ions on the Rates and Mechanisms of Oxidative Addition of Iodobenzene to Low-Ligated Zerovalent Palladium Complexes Pd0(PPh3)2. *J. Am. Chem. Soc.* **1991**, *113* (22), 8375–8384. https://doi.org/10.1021/ja00022a026.

(3) Amatore, C.; Carre, E.; Jutand, A.; M'Barki, M. A.; Meyer, G. Evidence for the Ligation of Palladium(0) Complexes by Acetate Ions: Consequences on the Mechanism of Their Oxidative Addition with Phenyl Iodide and PhPd(OAc)(PPh3)2 as Intermediate in the Heck Reaction. *Organometallics* **1995**, *14* (12), 5605–5614. https://doi.org/10.1021/om00012a029.

(4) Liang, H.; Rio, J.; Perrin, L.; Payard, P.-A. Salt-Enhanced Oxidative Addition of Iodobenzene to Pd: An Interplay Between Cation, Anion, and Pd–Pd Cooperative Effects. *Inorg. Chem.* **2022**, *61* (20), 7935–7944. https://doi.org/10.1021/acs.inorgchem.2c00565.

(5) Barrios-Landeros, F.; Carrow, B. P.; Hartwig, J. F. Effect of Ligand Steric Properties and Halide Identity on the Mechanism for Oxidative Addition of Haloarenes to Trialkylphosphine Pd(0) Complexes. *J. Am. Chem. Soc.* **2009**, *131* (23), 8141–8154. https://doi.org/10.1021/ja900798s.

(6) Galardon, E.; Ramdeehul, S.; Brown, J. M.; Cowley, A.; Hii, K. K. (Mimi); Jutand, A. Profound Steric Control of Reactivity in Aryl Halide Addition to Bisphosphane Palladium(0) Complexes. *Angew. Chem., Int. Ed.* **2002**, *41* (10), 1760–1763. https://doi.org/10.1002/1521-3773(20020517)41:10<1760::AID-ANIE1760>3.0.CO;2-3.

(7) Littke, A. F.; Dai, C.; Fu, G. C. Versatile Catalysts for the Suzuki Cross-Coupling of Arylboronic Acids with Aryl and Vinyl Halides and Triflates under Mild Conditions. *J. Am. Chem. Soc.* **2000**, *122* (17), 4020–4028. https://doi.org/10.1021/ja0002058.

(8) Dieck, H. A.; Heck, F. R. Palladium Catalyzed Synthesis of Aryl, Heterocyclic and Vinylic Acetylene Derivatives. *J. Organomet. Chem.* **1975**, *93* (2), 259–263. https://doi.org/10.1016/S0022-328X(00)94049-X.

(9) Soheili, A.; Albaneze-Walker, J.; Murry, J. A.; Dormer, P. G.; Hughes, D. L. Efficient and General Protocol for the Copper-Free Sonogashira Coupling of Aryl Bromides at Room Temperature. *Org. Lett.* **2003**, *5* (22), 4191–4194. https://doi.org/10.1021/ol035632f.

(10) Ljungdahl, T.; Pettersson, K.; Albinsson, B.; Mårtensson, J. Solvent and Base Dependence of Copper-Free Palladium-Catalyzed Cross-Couplings between Terminal Alkynes and Arylic Iodides: Development of Efficient Conditions for the Construction of Gold(III)/Free-Base Porphyrin Dimers. *J. Org. Chem.* **2006**, *71* (4), 1677–1687. https://doi.org/10.1021/jo052423v.

(11) Ljungdahl, T.; Bennur, T.; Dallas, A.; Emtenäs, H.; Mårtensson, J. Two Competing Mechanisms for the Copper-Free Sonogashira Cross-Coupling Reaction. *Organometallics* **2008**, *27* (11), 2490–2498. https://doi.org/10.1021/om800251s.

(12) García-Melchor, M.; Pacheco, M. C.; Nájera, C.; Lledós, A.; Ujaque, G. Mechanistic Exploration of the Pd-Catalyzed Copper-Free Sonogashira Reaction. *ACS Catal.* **2012**, *2* (1), 135–144. https://doi.org/10.1021/cs200526x.

(13) Gazvoda, M.; Virant, M.; Pinter, B.; Košmrlj, J. Mechanism of Copper-Free Sonogashira Reaction Operates through Palladium-Palladium Transmetallation. *Nat. Commun.* **2018**, *9* (1), 4814. https://doi.org/10.1038/s41467-018-07081-5.
(14) Fantoni, T.; Bernardoni, S.; Mattellone, A.; Martelli, G.; Ferrazzano, L.; Cantelmi, P.; Corbisiero, D.; Tolomelli, A.; Cabri, W.; Vacondio, F.; Ferlenghi, F.; Mor, M.; Ricci, A. Palladium Catalyst Recycling for Heck-Cassar-Sonogashira Cross-Coupling Reactions in Green Solvent/Base Blend. *ChemSusChem* **2021**, *14* (12), 2591–2600. https://doi.org/10.1002/cssc.202100623.
(15) Jutand, A.; Mosleh, A. Rate and Mechanism of Oxidative Addition of Aryl Triflates to Zerovalent Palladium Complexes. Evidence for the Formation of Cationic (Sigma-Aryl)Palladium Complexes. *Organometallics* **1995**, *14* (4), 1810–1817. https://doi.org/10.1021/om00004a038.
(16) Cabri, W.; Oldani, E. US5902902, 1998.
(17) Taylor, J. E.; Bull, S. D.; Williams, J. M. J. Amidines, Isothioureas, and Guanidines as Nucleophilic Catalysts. *Chem. Soc. Rev.* **2012**, *41* (6), 2109. https://doi.org/10.1039/c2cs15288f.
(18) Tougerti, A.; Negri, S.; Jutand, A. Mechanism of the Copper-Free Palladium-Catalyzed Sonagashira Reactions: Multiple Role of Amines. *Chem. Eur. J.* **2007**, *13* (2), 666–676. https://doi.org/10.1002/chem.200600574.
(19) Henry, P. *Palladium Catalyzed Oxidation of Hydrocarbons*; Riedel, D., Ed.; Dordrecht, Holland, 1980.
(20) Barnard, C. Palladium-Catalysed C-C Coupling: Then and Now. *Platin. Met. Rev.* **2008**, *52* (1), 38–45. https://doi.org/10.1595/147106708X256634.
(21) Cabri, W.; Candiani, I. Recent Developments and New Perspectives in the Heck Reaction. *Acc. Chem. Res.* **1995**, *28* (1), 2–7. https://doi.org/10.1021/ar00049a001.
(22) Kondrashova, S. A.; Polyancev, F. M.; Latypov, S. K. DFT Calculations of 31P NMR Chemical Shifts in Palladium Complexes. *Molecules* **2022**, *27* (9), 2668. https://doi.org/10.3390/molecules27092668.
(23) Adamo, C.; Barone, V. Toward Reliable Density Functional Methods without Adjustable Parameters: The PBE0 Model. *.J Chem. Phys.* **1999**, *110* (13), 6158–6170. https://doi.org/10.1063/1.478522.
(24) Perdew, J. P.; Burke, K.; Ernzerhof, M. Generalized Gradient Approximation Made Simple [Phys. Rev. Lett. 77, 3865 (1996)]. *Phys. Rev. Lett.* **1997**, *78* (7), 1396–1396. https://doi.org/10.1103/PhysRevLett.78.1396.
(25) Weigend, F.; Ahlrichs, R. Balanced Basis Sets of Split Valence, Triple Zeta Valence and Quadruple Zeta Valence Quality for H to Rn: Design and Assessment of Accuracy. *Phys. Chem. Chem. Phys.* **2005**, *7* (18), 3297. https://doi.org/10.1039/b508541a.
(26) Ahlquist, M.; Fristrup, P.; Tanner, D.; Norrby, P.-O. Theoretical Evidence for Low-Ligated Palladium(0): [Pd−L] as the Active Species in Oxidative Addition Reactions. *Organometallics* **2006**, *25* (8), 2066–2073. https://doi.org/10.1021/om060126q.
(27) Schoenebeck, F.; Houk, K. N. Ligand-Controlled Regioselectivity in Palladium-Catalyzed Cross Coupling Reactions. *J. Am. Chem. Soc.* **2010**, *132* (8), 2496–2497. https://doi.org/10.1021/ja9077528.
(28) Fitton, P.; Rick, E. A. The Addition of Aryl Halides to Tetrakis(Triphenylphosphine)Palladium(0). *J. Organomet. Chem.* **1971**, *28* (2), 287–291. https://doi.org/10.1016/S0022-328X(00)84578-7.

(29) Zhou, T.; Xie, P.-P.; Ji, C.-L.; Hong, X.; Szostak, M. Decarbonylative Suzuki–Miyaura Cross-Coupling of Aroyl Chlorides. *Org. Lett.* **2020**, *22* (16), 6434–6440. https://doi.org/10.1021/acs.orglett.0c02250.
(30) Alcazar-Roman, L. M.; Hartwig, J. F. Mechanistic Studies on Oxidative Addition of Aryl Halides and Triflates to $Pd(BINAP)_2$ and Structural Characterization of the Product from Aryl Triflate Addition in the Presence of Amine. *Organometallics* **2002**, *21* (3), 491–502. https://doi.org/10.1021/om0108088.
(31) Jutand, A.; Négri, S.; Principaud, A. Formation of ArPdXL(Amine) Complexes by Substitution of One Phosphane Ligand by an Amine in Trans-$ArPdX(PPh_3)_2$ Complexes. *Eur. J. Inorg. Chem.* **2005**, *2005* (4), 631–635. https://doi.org/10.1002/ejic.200400413.
(32) Gaussian 16 Rev. A.03 (Wallingford, CT, 2016).
(33) Grimme, S.; Ehrlich, S.; Goerigk, L. Effect of the Damping Function in Dispersion Corrected Density Functional Theory. *J. Comput. Chem.* **2011**, *32* (7), 1456–1465. https://doi.org/10.1002/jcc.21759.

Chapter 6:

Copper-Mediated formation of Aryldifluoronitriles

This project was conducted at the University of California, Berkeley, in the Hartwig Group.

6.1 Introduction

The incorporation of fluorine atoms is a common strategy to improve the physical and biological properties of agrochemicals and drug candidates.[1–4] Aryl fluorides and trifluoromethylarenes are the most common fluorinated motifs present in pharmaceuticals, but there has been increasing interest in the incorporation of other types of fluorine-containing functional groups to tune molecular properties such as metabolic stability, lipophilicity, and binding specificity for an enzymatic target. Many of the desirable effects of incorporating fluorine atoms can be attributed to the combination of fluorine's high electronegativity, small size and its capacity to form strong and highly polarized C-F bonds. Since the van der Waals radius of fluorine (1.47 Å) is intermediate between the one of hydrogen (1.2 Å) and oxygen (1.52 Å),[5] it has often been used to replace both in the drug development process.[6]

In medicinal chemistry, fluorinated compounds often display differences in lipophilicity, metabolic stability, and overall activity relative to their non-fluorinated analogs.[7–10] Modulating the lipophilicity of biological compounds, it is possible to control bioavailability, absorption and membrane permeability. In fact, an average increase in the logP has been observed in the substitution of a hydrogen atom with a fluorine one.[11] The incorporation of fluorine can modulate the pK_a of neighbor functional groups like amines or acids[12–14] and can suppress the metabolic oxidation pathways increasing the half-life of drug candidates and preventing the formation of potentially toxic metabolites.[15–18]

While the installation of CF_3 groups have been extensively studied by several research groups, the incorporation of a benzylic CF_2 motif is less known and has rapidly attracted the scientific community as they serve as bioisostere of carbonyl groups and ethers.[16] In addition, difluoroester, -amide, -nitrile, and -acid groups can be further transformed to generate amines, alcohols, ketones, esters, amides, and acids and represent therefore an advantageous building block in drug development.

Despite the biological and synthetic value of aryldifluorocarbonyl compounds, current methods for their synthesis are limited.

Aryldifluoroesters and -amides can by prepared by deoxyfluorination of the corresponding α-keto amide or ester with diethylaminosulfur trifluoride (DAST) or related aminosulfur trifluorides (Figure 6.1a).[19–21] However, the functional group compatibility of these

reactions is often limited. In addition, DAST and related fluorinating agents release toxic HF upon contact with water and can undergo explosive decomposition by heating. Alternatively, fluorodesulfurization reactions of benzylic thioketals allow the *gem*-difluoronation at the benzylic position (Figure 6.1b).[22] Although the yield of this procedure is often higher than the deoxyfluorination protocol, this strategy requires additional synthetic steps for the synthesis of the 1,3-diothiolane starting material and has therefore a low atom economy.

Fluorination reactions α to esters, amides or nitriles through an electrophilic fluorinating agent have also been reported, but the yields and selectivity for the difluorinated product over monofluorinated byproducts are often low (Figure 6.1c).[23–27]

Similarly, radical-based benzylic fluorinations reactions, requiring high excess of fluorinating reagents, are not so common because of the difficulty to obtain selectivity the difluoroarylarene rather than the corresponding monofluorinated byproduct (Figure 6.1d).[28,29]

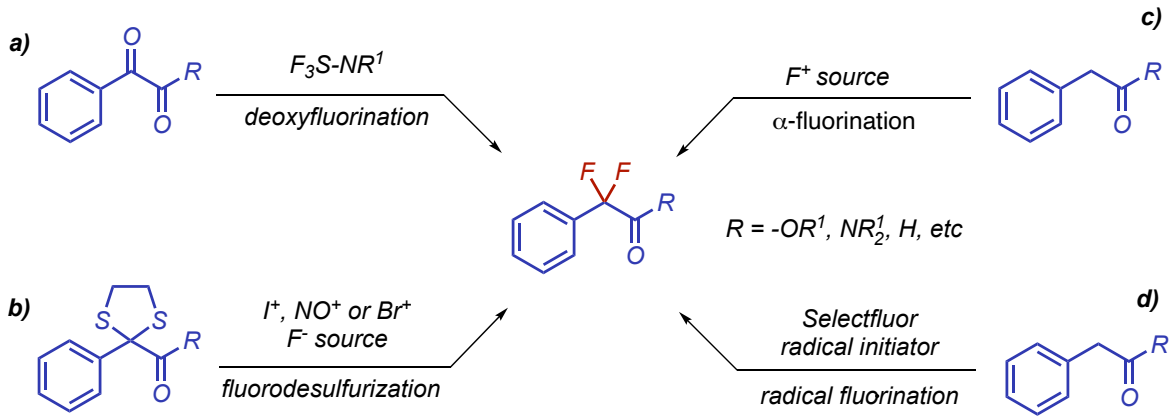

***Figure 6.1**: Methods to prepare $ArCF_2COR$ compounds by C-F bond formation*

Cross-coupling reactions to form aryldifluoromethyl carboxylic acid derivatives are desirable because they can allow variation of both the arene and difluoroenolate coupling partner, thereby enabling access to a wide range of products. The general catalytic cycle for cross-coupling difluorination with aryl halides and boronic acids is depicted in Figure 6.2. While α-arylation reactions of non-fluorinated enolates are well-established synthetic

methods to generate α-aryl carbonyl compounds,[30,31] several challenges are associated with the development of analogous reactions of fluorinated enolates.

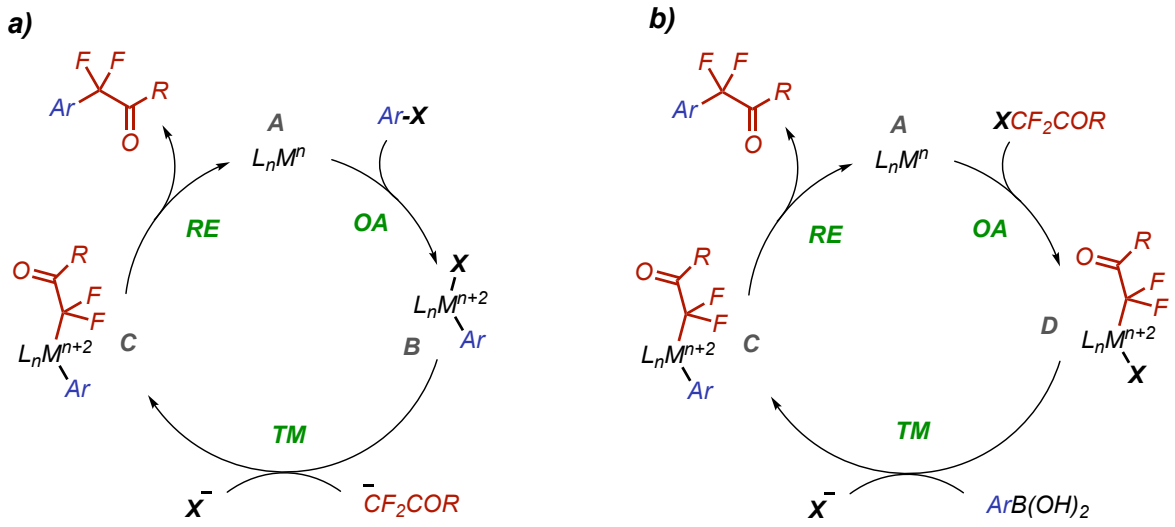

***Figure 6.2**: General catalytic cycles for transition metal-catalyzed syntheses of aryldifluorocarboxylic acid derivatives from aryl halides a) and arylboronic acids b)*

First, the alkali metal enolates of difluorocarbonyl compounds are often unstable at the required reaction conditions of cross-coupling protocols.[32,33] Indeed, the presence of α fluorine motifs enhance the electrophilicity of the carbonyl derivative promoting several decomposition pathways involving the attack of a difluoroenolate on the difluorocarbonyl compound to generate aldol- or Claisen byproducts.[34–36] To address these challenges, sylil-protected difluoroenolates have been introduced in cross-coupling reactions. These reagents can be activated in situ by fluoride or other Lewis bases to facilitate the transmetallation (TM) process. In this way, limiting the presence of difluoroenolate anion in solution can prevent the decomposition side reaction. Alternatively, the cross-coupling reaction employing aryl nucleophiles, such as aryl boronic acids, with halodifluorocarbonyl electrophiles can be performed. This strategy allows the direct generation of a metal difluoroenolate by oxidative addition (OA) (Figure 6.2b), rather than by TM with a potentially unstable difluoroenolate anion (Figure 6.2a).

Usually, the rate determining step of these reactions is the reductive elimination (RE) from an arylmetal difluoroenolate intermediate. This step is likely to be more challenging for complexes containing fluorinated enolates than for those containing the non-fluorinated analogous, as the presence of fluorine on the α-carbon of an arylmetal alkyl intermediate

increases the barrier of the RE step.[37] The rate of the RE can be improved by using appropriates ligands that can decrease the barrier of the process or using metals, such as copper, where the RE may be more accessible.

Cross-coupling reactions of aryl electrophiles with α-iododifluoroacetates mediated by super stoichiometric amounts of copper were first reported by Kobayashi in 1986 (Scheme 6.1a).[38] Subsequently, Sato and coworkers coupled in similar conditions aryl iodides with bromodifluoroacetate[39], which is more stable and readily available, while the first reductive coupling of aryl and vinyl iodides with iododifluoroacetamides were reported by Hu in 2010 (Scheme 6.1a).[40]

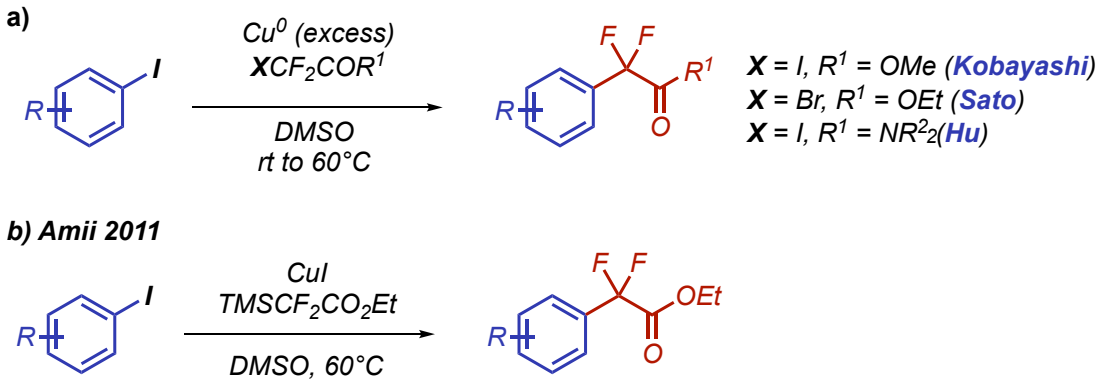

***Scheme 6.1**: Summary of copper-mediated and -catalyzed methods to prepare aryldifluoroesters and -amides.*

In 2011, Amii and coworkers reported a coupling of α- trimethylsilyldifluoroacetates with aryl iodides mediated by catalytic amount of CuI (20 mol%) but with low yields and limited to electron-deficient substrates (Scheme 6.1b).[41]

More recently, Zang reported the coupling of arylboronic acids with halodifluoro esters and amides through palladium- and nickel-catalyzed reactions for the synthesis of aryldifluorocarboxylic acid derivatives.[42,43] The reaction proceeds in high yield with both electron-rich and electron-poor arylboronic acids and tolerates base-sensitive functional groups including esters, ketones, and aldehydes (Scheme 6.2).

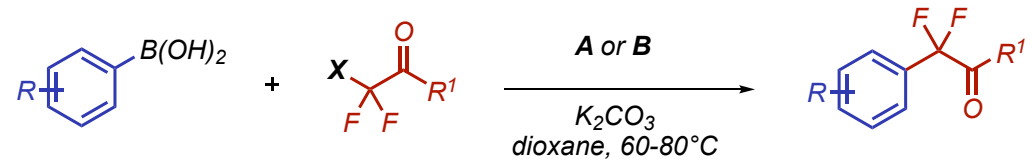

X = Cl, Br; R^1 = OEt, NR_2, Ar

A = $Pd(PPh_3)_4$ (5 mol%), Xantphos (10 mol%) **B** = $Ni(NO_3)_2 \cdot 6H_2O$ (2.5 mol%), bpy (2.5 mol%)

***Scheme 6.2**: Pd- and Ni-catalyzed coupling reactions of arylboronic acids for the synthesis of arylldifluoroesters, -amides, and -ketones*

Cross-coupling reactions of aryl halides with difluoroamide and -ester enolates have also been developed. Hartwig reported a palladium-catalyzed coupling of aryl bromides with α -silyldifluoroacetamides in the presence of a palladacyclic pre-catalyst and P^tBu_2Cy as ligand (Scheme 6.3a)[44] and later a copper mediated reaction of the same nucleophile with both bromo- and iodoaryles (Scheme 6.3b).[45]

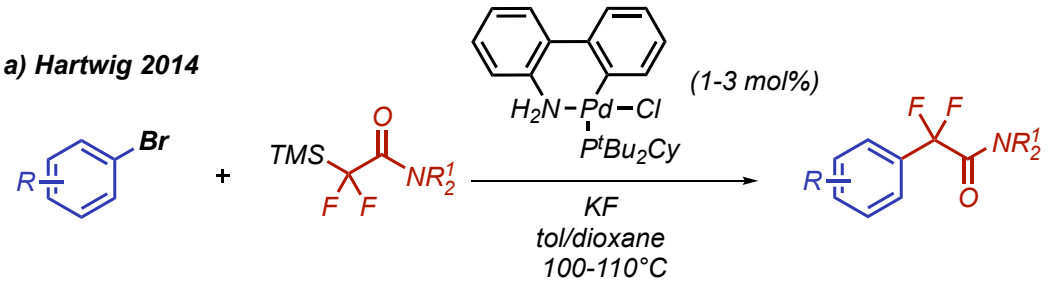

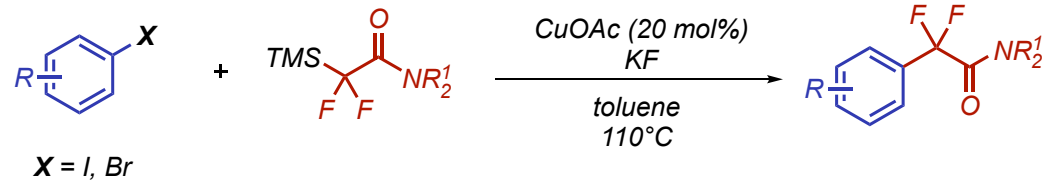

X = I, Br

***Scheme 6.3**: Pd- and Cu-catalyzed methods for the synthesis of aryldifluoroamides*

Although significant developments have been made in the synthesis of aryldifluoro methyl carboxylic acid derivatives, several challenges remain to be address in order to access to a variety of functionalized products. Methods that rely on C-F bond formation (e.g. deoxyfluorination of 1,2-dicarbonyl compounds or radical fluorination) typically suffer from

harsh reaction conditions, poor functional group tolerance and the formation of byproducts. Cross-coupling methods present an attractive alternative because they enable facile variation of both the aryl and difluorocarbonyl coupling partners. Copper and palladium mediated couplings of aryl iodides with XCF_2CO_2Et or $TMSCF_2CO_2Et$ and $TMSCF_2CONR_2$ are well-established, but broadly applicable Cu and Pd catalyzed reaction protocols for the synthesis of aryldifluoroacetonitriles still need to be investigated.

In fact, despite the growing interest in aryldifluoronitrile compounds in materials science and drug discovery, cross-coupling strategies to synthetize this class of derivatives have not been reported.

Aryldifluoronitriles possess interesting biological and physical properties, although relatively few compounds have been reported. For example, compounds containing aryldifluoronitriles have been studied as NSAIDs,[46] prostaglandin D2 receptor antagonists,[47] CHK1 inhibitors,[48] herbicides,[49] and liquid crystals[50] (Figure 6.3).

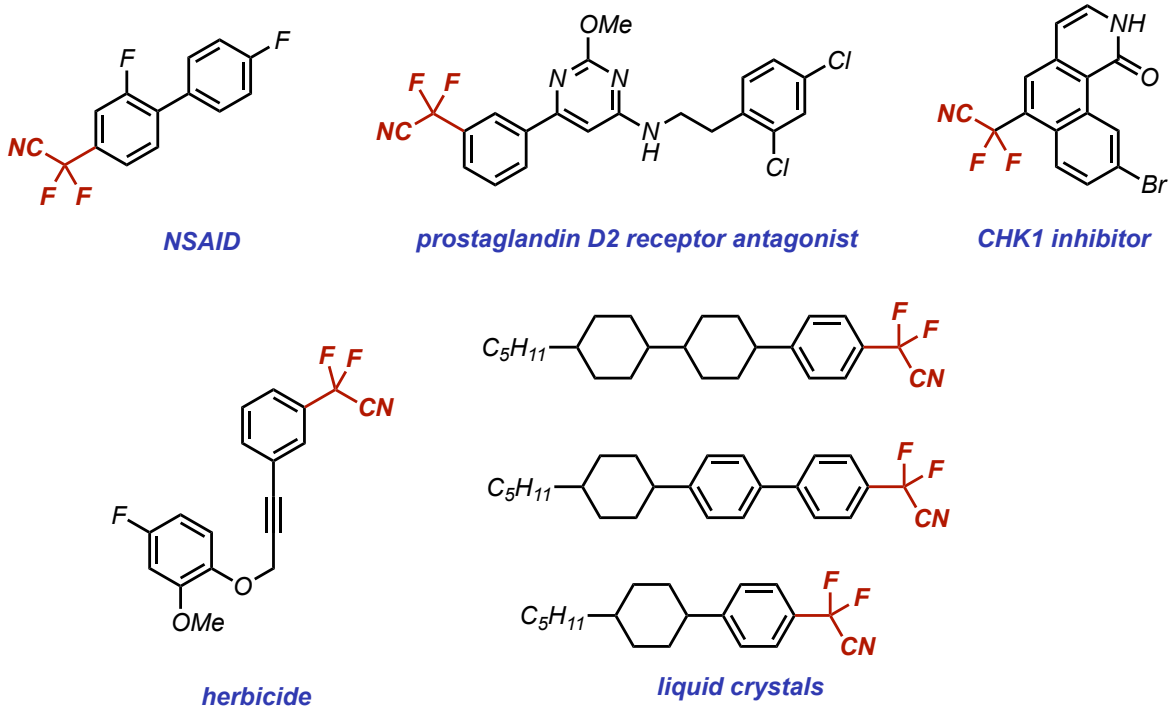

***Figure 6.3**: Examples of compounds containing aryldifluoronitrile groups*

The difluoronitrile group is a strongly electron-withdrawing, relatively small, highly polar and often serve as hydrogen bond acceptors.[51,52] Several crystal structures show hydrogen

bonding interactions between the nitrogen atom of a bioactive nitrile and an amino acid residue or water molecule present in the binding pocket of an enzymatic target.[53,54] The incorporation of fluorine alpha to a nitrile substituent allows to modulate the strength of these hydrogen-bonding interactions, as difluoronitriles are likely to be much weaker hydrogen-bond acceptors than their non-fluorinated analogs (Figure 6.4a).

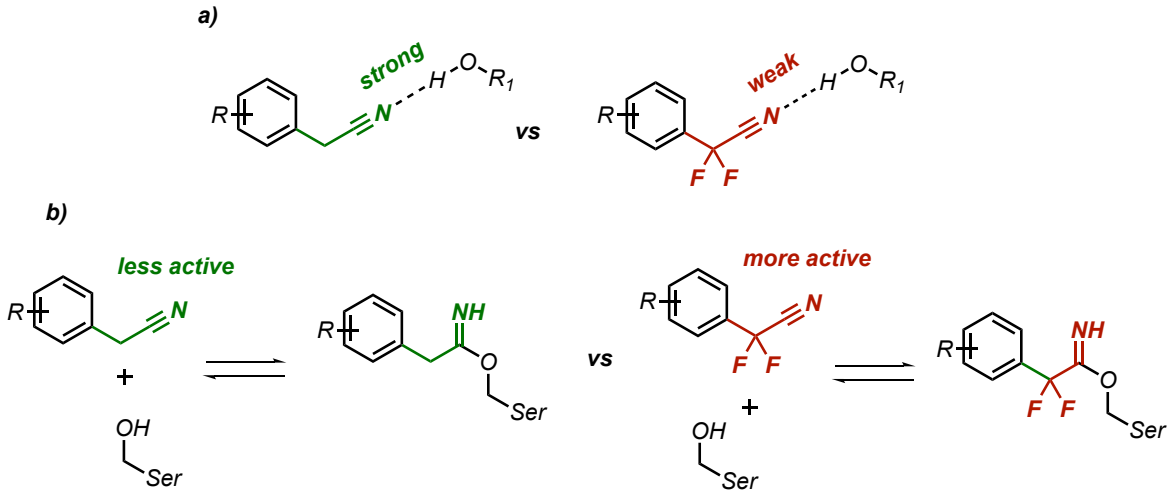

***Figure 6.4**: Comparison between fluorinated and non-fluorinated arylacetonitriles: hydrogen bonding interactions a) and reactivity through nucleophilic attack b)*

Nitrile-containing compounds can serve as reversible covalent inhibitors of serine and cysteine proteases.[55–57] In these compounds, attack of a nucleophilic amino acid side chain on the carbon atom of the nitrile reversibly forms an imidate or thioimidate linkage.[58–60] Relative to their non-fluorinated counterparts, difluoronitriles are likely to be more reactive to nucleophilic attack and may form stronger covalent linkages to amino acid residues in an enzyme active site (Figure 6.4b).

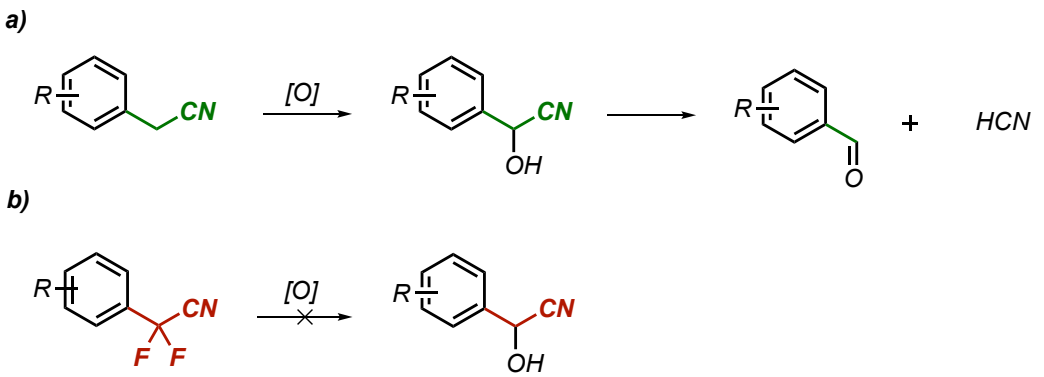

***Figure 6.5**: Modulating the metabolic degradation by incorporation of fluorine atoms*

In addition, incorporating an electron-withdrawing difluoronitrile group onto an aromatic ring would deactivate the ring toward metabolic oxidation, and could also enable new polar interactions, even in sterically congested environments.[61,62] However, alkylnitriles containing α-hydrogen atoms are rare in drugs because α-oxidation to form the corresponding cyanohydrin can occur, followed by the release of toxic cyanide (Figure 6.5a).[51,63] For this reason, benzylic nitriles are particularly problematic in this respect due to the metabolic lability of benzylic C-H bonds. On the other hand, the presence of two fluorine atoms alpha to the nitrile group would block this pathway for metabolic degradation and suppress the cyanide formation (Figure 6.5b).

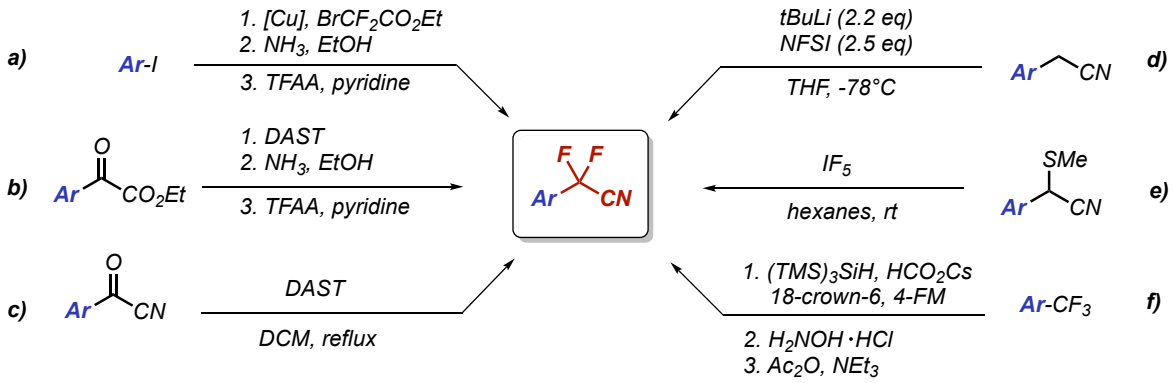

***Figure 6.6**: Reported methods to synthesize aryl-α,α-difluoroacetronitriles*

Traditional routes to aryldifluoronitriles require multi-step syntheses. The most common routes typically begin with either copper-mediated reductive coupling of an aryl iodide with a bromodifluoroester or deoxofluorination of an aryl 2-oxo-acetate to form an aryl-α,α-difluoroester (Figure 6.6a-b). Subsequent addition of ammonia and dehydration of the resulting amide afford the desired aryldifluoromethylacetonitrile.[64,65] These routes are typically low-yielding, intolerant to sensitive functional groups, and are impractical for the rapid diversification of the aryl substituent. Approaches for the synthesis of aryldifluoronitriles by C-F bond formation have also been explored, but suffer from a combination of poor yields, limited scope and functional group tolerance, and the requirement of harsh conditions and dangerous or toxic reagents, such as DAST,[50] N-fluorobenzenesulfonamide (NFSI),[27] or IF_5[66] (Figure 6.6c-e). Recently, Bandar and coworkers reported a base-promoted reductive coupling platform for the

difluorofunctionalization of trifluoromethylarenes.[67] This methodology allows access to diverse benzylic difluorides, but still requires multiple steps to access the corresponding aryldifluoromethylacetonitrile (Figure 6.6f).

To address the lack of a suitable method to rapidly synthesize aryl-α,α-difluoromethylacetonitriles and to provide access to compounds of potential biological interest, we have developed a copper-mediated coupling of (hetero)aryl iodides and electron-poor (hetero)aryl bromides with 2,2-difluoro-2-(trimethylsilyl)acetonitrile ($TMSCF_2CN$). This method delivers several products in high yields while tolerating a wide range of functional groups and complex, drug-like molecules.

6.2 Results and discussion

Copper-mediated and copper-catalyzed fluoroalkylation reactions have been developed for the synthesis of trifluoromethylarenes,[68–73] aryldifluoroesters,[41,74] and aryldifluoroamides.[45] The oxidative addition of electron-poor copper (I) species is known to be challenging, while the reductive elimination of fluoroalkyl ligands from high-valent copper (III) species should be more facile.[75,76]

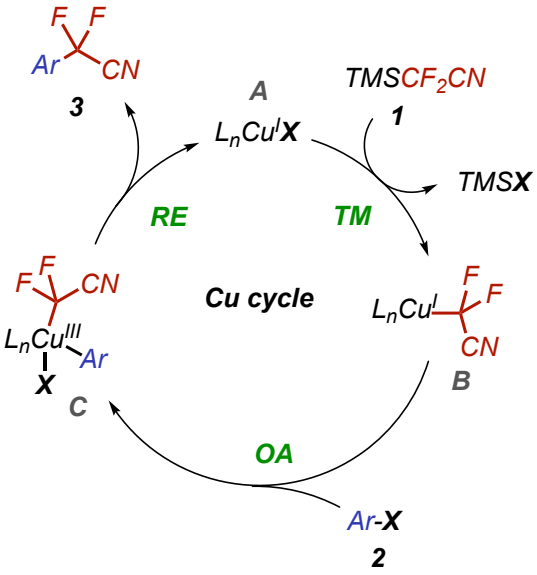

***Figure 6.7**: Proposed catalytic cycle for copper-catalyzed synthesis of aryldifluoronitriles*

In copper-mediated trifluoromethylation reactions, the active copper reagent is often formed by transmetallation of the trifluoromethyl group from $TMSCF_3$.[76] Similarly, 2,2-difluoromethylacetonitrile nucleophiles, such as $TMSCF_2CN$, could undergo transmetallation to copper. The resulting species could then go through an oxidative addition to form a copper (III) intermediate that rapidly undergo the reductive elimination to deliver the desired product (Figure 6.7). To investigate this hypothesis, we selected the model reaction between 1-n-butyl-4-iodobenzene **2a** and $TMSCF_2CN$ **1** and screened several parameters to find the ideal cross-coupling conditions to form product **3a** (Table 6.1).

Table 6.1: *Selected optimization studies for the copper-mediated coupling of aryl iodides and $TMSCF_2CN$ (**1**).*

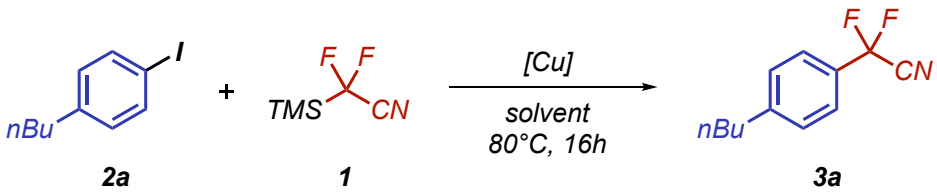

2a **1** **3a**

Entry[a]	[Cu] (equiv)	Equiv **1**	solvent (M)	Yield (%)[b]
1	CuI (2.0)	5.0	DMSO (0.2)	27
2	CuOAc (2.0)	5.0	DMSO (0.2)	65
3	CuDPP (2.0)	5.0	DMSO (0.2)	84
4	CuDPP (2.0)	5.0	DME (0.2)	91
5	CuDPP (1.0)	5.0	DME (0.2)	73
6	CuDPP (1.0)	2.0	DME (0.2)	76
7	CuDPP (1.0)	2.0	NMP (0.2)	96
8	CuDPP (1.0)	2.0	DMF (0.2)	96
9	CuDPP (1.0)	2.0	DMF (0.4)	99
10	CuDPP (0.5)	2.0	DMF (0.4)	48
11	CuDPP (1.0)	2.0	DMF (0.5)	99
12[c]	CuDPP (1.0)	2.0	DMF (0.4)	99
13	CuTC (1.0)	2.0	DMF (0.4)	99

[a]All the reactions were set up in a N_2 glovebox. [b]Determined using ^{19}F NMR spectroscopy with $PhCF_3$ as internal standard; [c]Reaction time = 1h. See Experimental part for complete optimization studies.

After evaluating a variety of copper(I) salts (Table 6.1, entries 1-2 and Experimental section), we found that both copper(I) diphenylphosphinate (CuDPP) and copper(I) thiophenecarboxylate (CuTC) mediated the difluorocyanation reaction (entries 9 and 13). However, CuTC is less expensive than CuDPP ($1,300/kg vs. $12,000/kg, Ambeed), and

reactions with CuTC generally delivered the products in similar or superior yields to those with CuDPP. In addition, CuTC is less air sensitive than CuDPP and can be stored on the benchtop.

When ligands that are common in copper-mediated transformations, such as 1,10-phenanthroholine, bipyridine and oxalamide were explored to render the transformation catalytic in copper, no product was observed (see Experimental section). The addition of various fluoride salts to activate the nucleophile and decrease the amount of copper caused decomposition of the nucleophile **1** under the reaction conditions. In fact, stirring **1** with CsF and no added copper or aryl halide resulted in the complete decomposition of **1** in few minutes (see Experimental section). Further optimization studies on the solvent, concentration and reaction time, with DMF and NMP being equally effective, allowed to decrease the amount of copper and the excess of **1** to 1.0 eq and 2.0 eq, respectively (Entries 3-9). Using 0.5 equivalents of CuDPP decreased the yield to 48%, and addition of product to the reaction mixture was discovered to reduce reaction yield (Entry 10). Reactions conducted at concentrations above 0.4 M occurred in similar yields (Entry 11) but were not considered in further studies because of the poor solubility of CuTC and CuDPP. With the optimized conditions, product **3a** was able to be formed in just 1h instead of 16h as the model reaction (Entry 12).

Table 6.2. *Model reaction under various conditions*

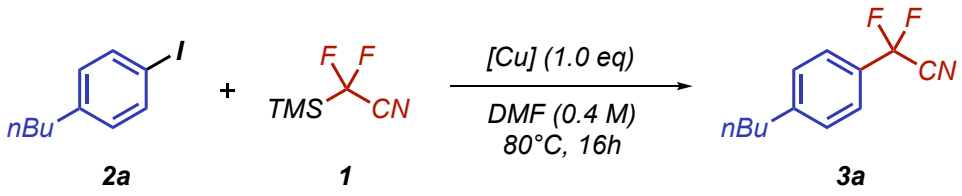

2a **1** **3a**

Entry	Conditions	Yield w/ CuTC	Yield w/ CuDPP
1	*Standard conditions*	99	99
2	under air	25	45
3	Schlenck technique	99	93
4	under Air + N_2 purge	91	36
5	rt, 48 h	99	99
6	rt, 1 equiv **1**, 48 h	96	99

[a]Determined using ^{19}F NMR spectroscopy with $PhCF_3$ as internal standard

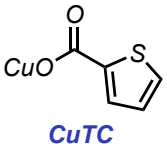

CuTC

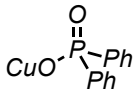

CuDPP

While our studies were conducted in an N_2 glovebox, the reaction also proceeded smoothly when using a Schlenk manifold or when assembled under air and flushed using an N_2-filled balloon (Table 6.2, entries 3-4). However, the reaction is sensitive to air due to the oxidation of the active Cu^I species (Entry 2). The reaction also proceeds at room temperature with both CuTC and CuDPP (Entry 5); no decomposition of the nucleophile was observed by ^{19}F NMR spectroscopy at this temperature allowing the complete conversion in product **3a** also with stoichiometric amount of **1** (Entry 6). The $TMSCF_2CN$ nucleophile (**1**) can be synthesized rapidly on multi-gram scale and stored for extended periods of time in the freezer (see Experimental section for the synthesis of **1**).

Product Functionalization and Bioconjugation. We sought to explore the reactivity of the aryl-α,α-difluoromethylacetonitrile group, especially because they are uncommon in the chemical literature. As mentioned above, fluorination is expected to modulate the electronic effects of the nitrile, possibly enabling reactions uncommon for non-fluorinated nitriles analogs or under more mild conditions. We have found that the aryl-α,α-difluoromethylacetonitrile products are amenable to further reactions to yield biologically relevant molecules containing a benzylic difluoromethylene unit (Figure 6.8). Conversion to the corresponding Boc-protected β,β-difluoromethylamine (**12a**), α,α-difluomethylrtetrazole (**12b**), aryl-α,α-difluoromethylpyridine (**12c**),31 and α,α-difluoromethylamide (**12d**) was accomplished. Dipolar cycloaddition reactions with cysteine (**12e),** and ortho-substituted anilines (**12f-h**) afforded products in high yields, as does the nickel-catalyzed hydrogenative coupling with amines (**12i**) reported by Beller and coworkers.[77] Hydrolysis to form the hydroxyformamide **12j**, which can be further elaborated, proceeds in 75% yield. Finally, reactions with Grignard reagents to form α,α-difluoromethylketones (**12k, 12l**) and synthesis of α,α-difluoromethylimidothioate **12m** also proceed smoothly. The difluoromethylene unit is a known bioisostere for carbonyl units and ethers, and further expanding the synthetic chemist's toolbox for the construction of these privileged motif represents an increasingly interesting research topic.

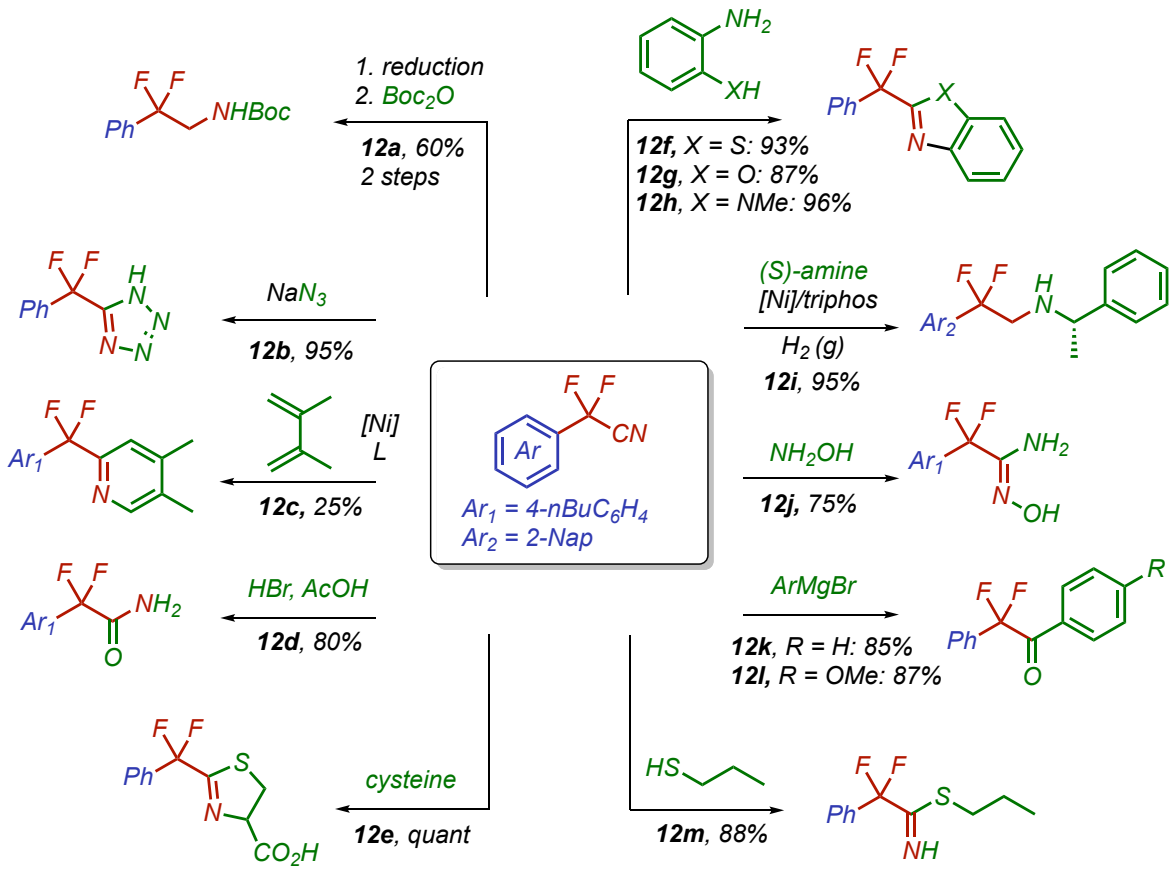

***Figure 6.8**: Functionalization reactions of aryl-α,α-difluoroacetonitriles*

Reaction Scope. Having established conditions to achieve the model reaction in high yield, we explored the scope of the copper-mediated α,α-difluoromethylcyanation reaction with a diverse array of aryl and heteroaryl iodides (Table 6.3 and 6.4) and bromides (Table 6.5). Products of the difluomethylcyanation reaction with low molecular weights were often instable and not able to be isolated; these products were functionalized in a telescoped procedure to more tractable derivatives for purification.

Table 6.3: *Scope of the aryldifluoronitrile cross-coupling between (hetero)aryl iodides and TMSCF₂CN (**1**).*[a,b]

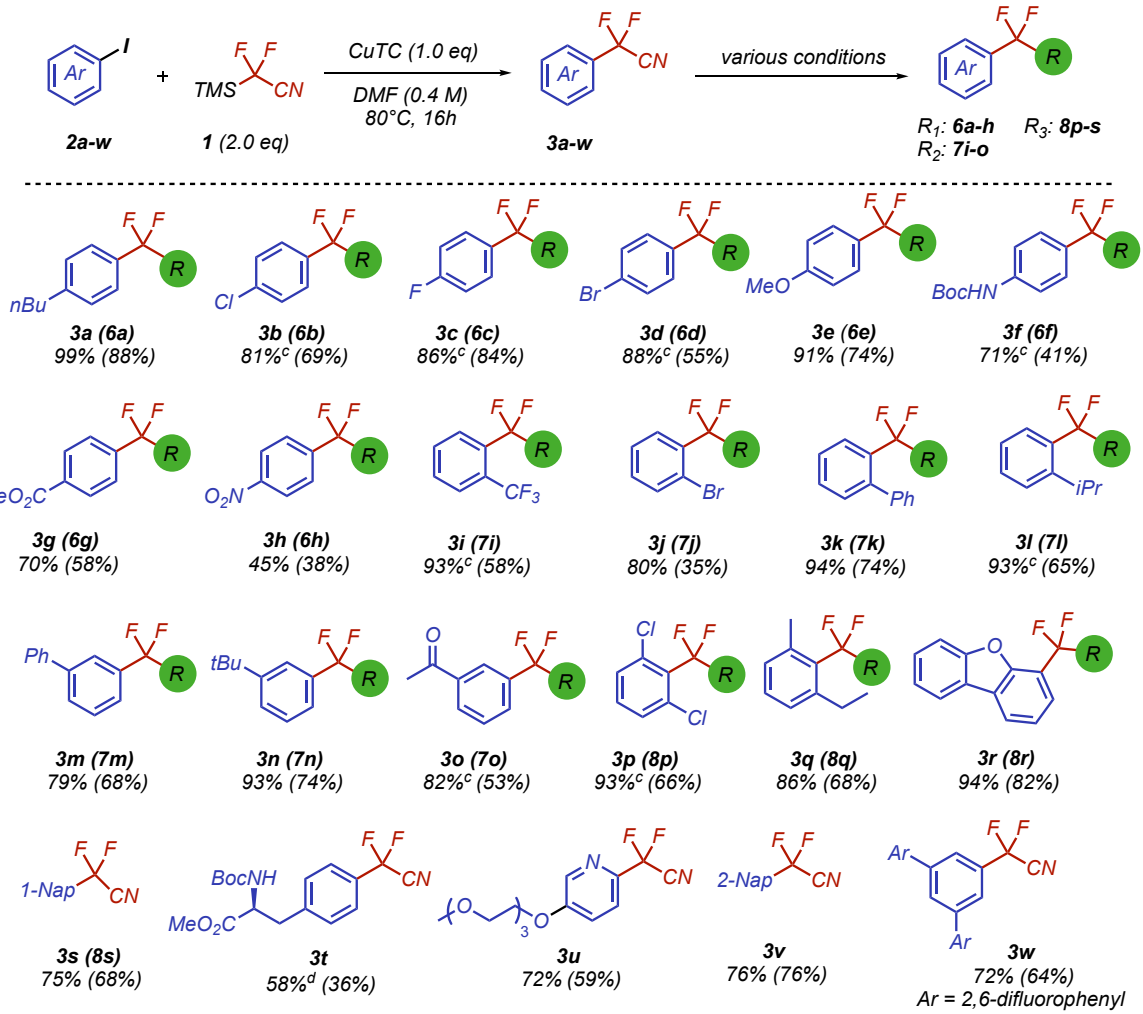

[a]Yields were determined using ^{19}F NMR spectroscopy with $PhCF_3$ as internal standard and yields in parenthesis represent those of the isolated compounds. [b]Compounds in parenthesis were isolated as the denoted difluoromethylene due to stability concerns of the difluoromethylacetonitrile. [c]CuDPP (1.0 eq) used instead of CuTC. [d]2.0 eq CuDPP, 4.0 eq **1** used.

A wide range of aryl iodides are tolerated under the reaction conditions, including electron-neutral (**3a**), electron-poor (**3b-d**) and electron-rich arenes (**3e-f**). Other common functional groups are compatible, including esters (**3g**), nitro groups (**3h**) and trifluoromethyl groups (**3i**). Aryl iodides bearing ortho-bromo (**3j**), phenyl (**3k**), and isopropyl (**3l**) substituents reacted, as did those with 2,6-dichloro (**3p**) and 2-methyl-6-ethyl groups (**3q**). Meta-substituted arenes (**3m-o, 3w)** also reacted. Heterocycles, such as 4-iododibenzofuran (**3r**), naphthalene functional groups (**3s, 3v**) and a water-soluble pyridine

(**3u**), are also compatible with the reaction conditions. Finally, N-boc-4-iodophenylalanine methyl ester underwent the title reaction to give the corresponding aryldifluoromethylacetonitrile in 58% yield (**3t**).

Table 6.4: *Scope of the aryldifluoronitrile cross-coupling between (hetero)aryl iodides and TMSCF₂CN (**1**) for the synthesis of natural products*[a]

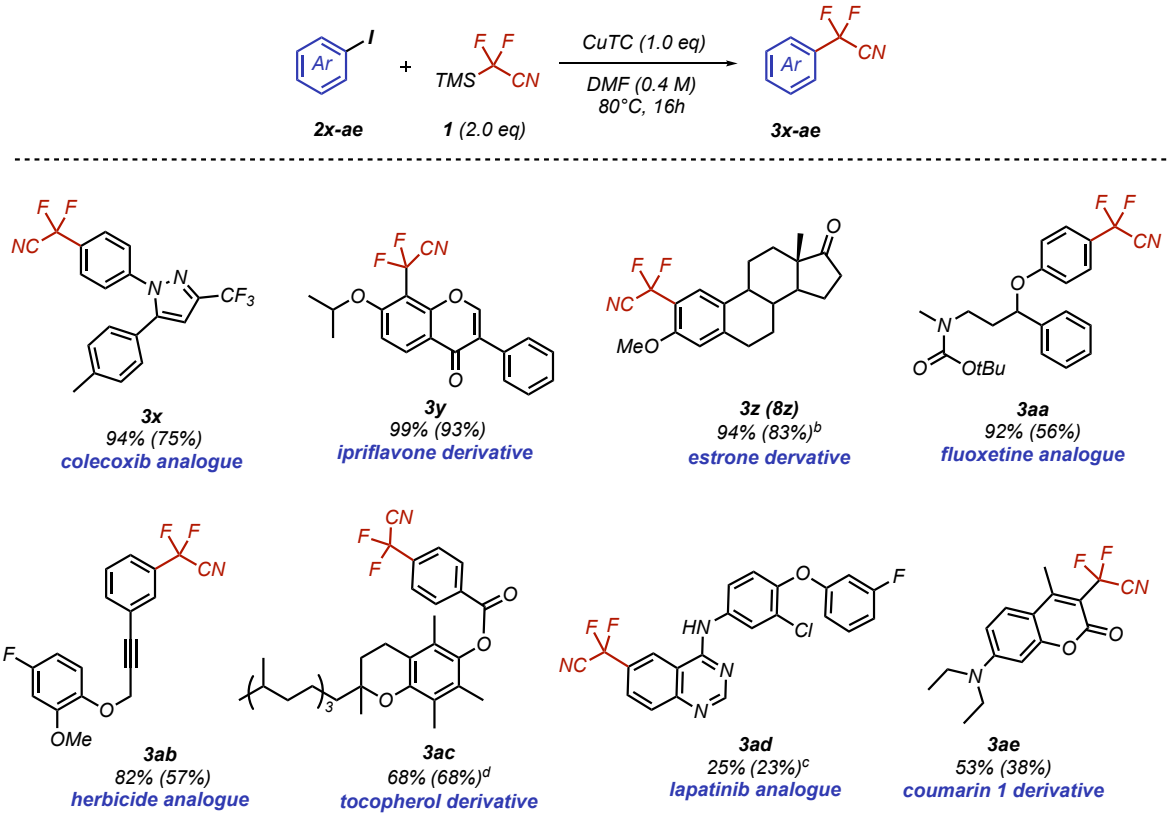

[a]Yields were determined using ^{19}F NMR spectroscopy with $PhCF_3$ as internal standard and yields in parenthesis represent those of the isolated compounds. [b]Yield in parenthesis are of the corresponding derivative **8z**. [c]1.0 eq of CuDPP instead of CuTC. [d]2.0 eq of CuDPP

We observed the difluoromethylcyano group to be susceptible to decomposition on silica or in the presence of water in some cases. In order to isolate these sensible products with high yields, a direct derivatization of product **3** was attempted with some of the protocols described in Figure 6.8 that could give almost complete conversion. The functionalization of the aryldifluoronitrile product with ortho-substituted anilines were performed giving the isolated product **6a-l, 7a-f** and **8a-e** in good yields (Table 6.3). The applicability of this method to late-stage diversification is demonstrated by examples with biologically active and drug-like molecules (Table 6.4). An analogue of the NSAID celecoxib (**3x**), a derivative

of ipriflavone (**3y**), a derivative of estrone methyl ether (**3z**) and an analogue of the SSRI fluoxetine (**3aa**), formed in high yield from their corresponding aryl or heteroaryl iodide. A pesticide bearing an alkyne (**3ab**), a derivative of the kinase inhibitor lapatinib (**3ad**), the laser dye coumarin 1 (**3ae**) and a derivative of vitamin E (**3ac**) also formed from the corresponding iodide. These examples demonstrate the broad functional group compatibility of this method and its suitability for the late-stage diversification of complex molecules.

Table 6.5: *Scope of the aryldifluoronitrile cross-coupling between (hetero)aryl bromides and TMSCF$_2$CN (**1**).*[a,b]

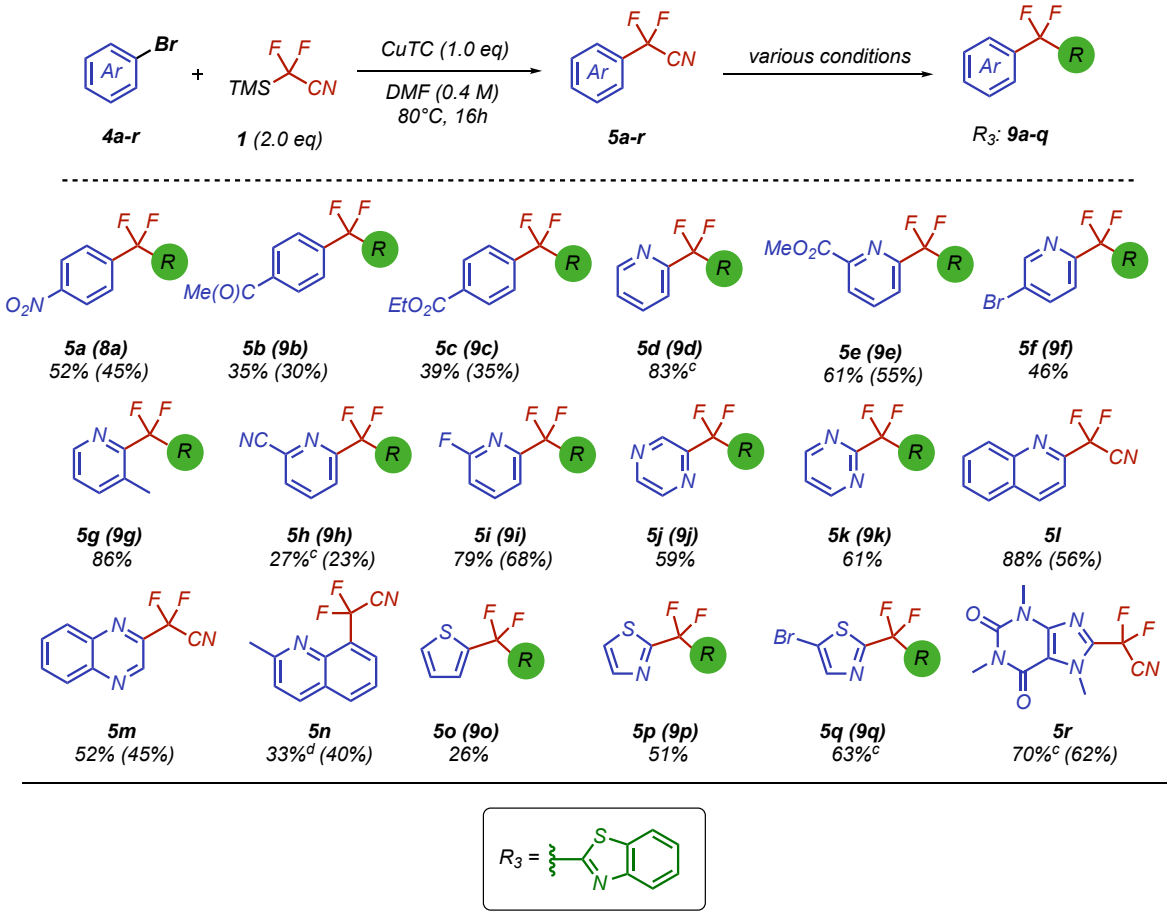

[a]Yields were determined using ^{19}F NMR spectroscopy with PhCF$_3$ as internal standard and yields in parenthesis represent those of the isolated compounds. [b]Compounds in parenthesis were isolated as the denoted difluoromethylene due to stability concerns of the difluoromethylacetonitrile. [c]CuDPP (1.0 eq) used instead of CuTC. [d]2.0 eq CuDPP, 4.0 eq **1** used.

Bromides of electron-poor arenes and heteroarenes also react under the above conditions to furnish aryl and heteroaryl difluoroacetonitriles in good yield (Table 6.5). The reaction tolerates various pyridines (**5d-5i**), as well as pyrazine (**5j**), pyrimidine (**5k**), quinoline (**5l**,

5n), quinoxaline (**5m**), thiophene (**5o**), and methylthiazole (**5p, 5q**) scaffolds. Brominated caffeine provided the difluorocyanated product in 62% isolated yield (**5r**). Again, decomposition-sensitive products were directly functionalized using the protocols previously described to give products **9a-q** in good yields.

DFT Calculations. Density functional theory (DFT) calculations of the reaction coordinate after transmetalation from $TMSCF_2R$ to CuTC to form complexes $[(DMF)CuCF_2R]$ were performed for R = CN, F. Unless otherwise noted, the energies are reported in kcal/mol as Gibbs free energies in DMF. For trifluoromethylation reactions of aryl halides mediated or catalyzed by copper, TM precedes OA. Additionally, computational and experimental studies suggest that complexes of type [(L)Cu(nucleophile)] are more active than those of type $[(L)_2Cu(nucleophile)]$.[78] Therefore, the combined Gibbs free energies of $[(DMF)CuCF_2R]$ and PhI were set as zero. We chose to calculate an associative pathway, wherein DMF does not dissociate from copper. This has been previously shown to be lower in energy throughout the reaction coordinate than a dissociative pathway (wherein DMF can dissociate between elementary steps).[78] Because the Hartwig group has previously investigated trifluoromethylation reactions of aryl halides mediated or catalyzed by copper,[68,76,79,80] we decided to also probe the reaction coordinates for this transformation. The computed reaction coordinate(s) are depicted in Figure 6.9. Our calculations found barriers for the oxidative addition of $[(DMF)CuCF_2R]$ into iodobenzene of 12.9 and 14.1, kcal/mol for R = CN and F, respectively, with R = F having the highest barrier to oxidative addition. This is consistent with previous computational studies where R = F.[78] Subsequently, reductive elimination from the copper species **[Cu] 2** proceeds with a barrier of 3.20 kcal/mol for R = CN and 4.7 kcal/mol for R = F.

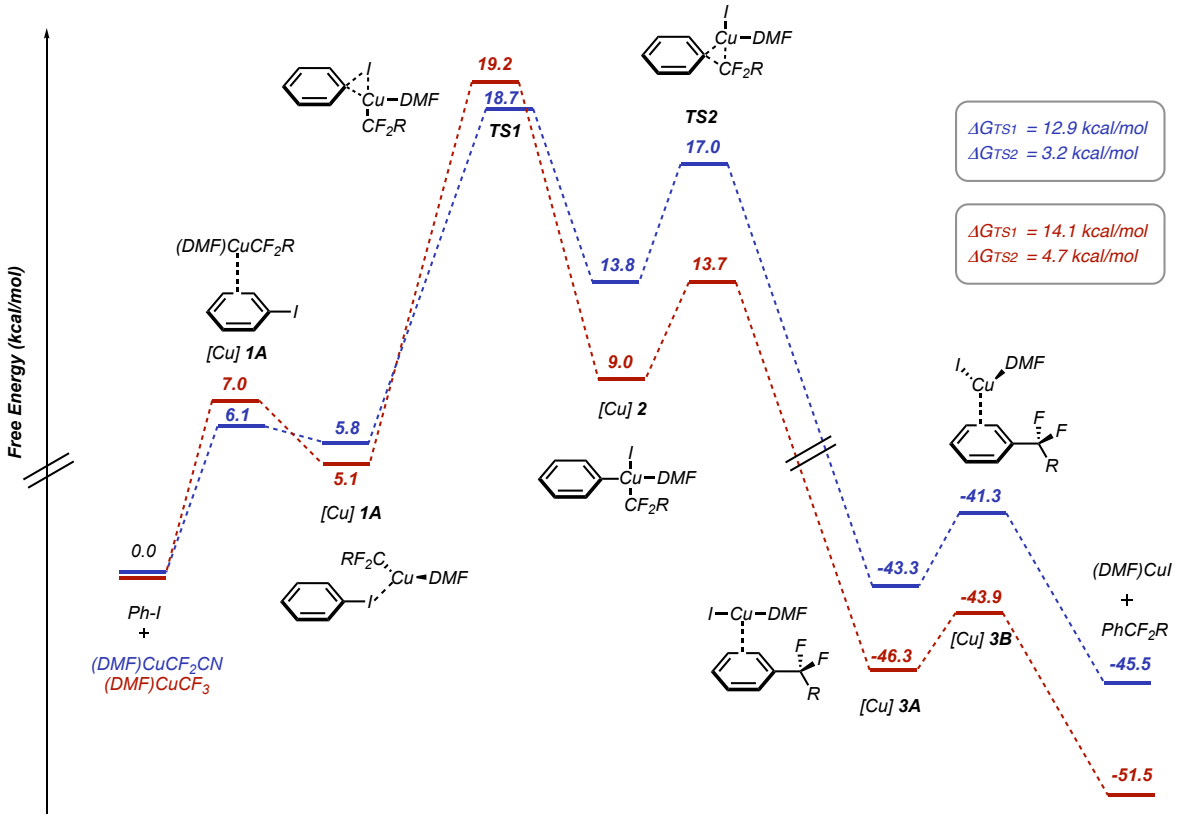

***Figure 6.9**: Computed free energy diagram for the reaction of PhI with [(DMF)CuCF$_2$R], where R = CN and F*

When compared to **TS-1** for R = F, the Cu–Ph bond in **TS-1** for R = CN is predicted to be longer (2.08 Å vs 2.05 Å), and the Ph–I bond shorter (2.31 Å vs. 2.34 Å). Oxidative addition forms complex **[Cu]-2**, which has slightly distorted square-planar geometry at copper, though less so for [(DMF)Cu(I)(Ph)CF$_2$CN] than for [(DMF)Cu(I)(Ph)CF$_3$]. Subsequently, **[Cu]-2** forms product by reductive elimination *via* **TS-2**. In **TS-2**, the forming Ph–CF$_2$CN bond is shorter than the Ph–CF$_3$ bond at 2.11 Å vs 2.14 Å.

As mentioned previously, it is expected that as the fluoroalkyl ligand on copper becomes more electron-withdrawing, the barrier to oxidative addition for [(DMF)CuCF$_2$R] into PhI should increase. However, in this study we find by DFT that the barrier to oxidative addition for [(DMF)CuCF$_2$CN] into PhI is lower than that for [(DMF)CuCF$_3$]. Given that we expect the difluoromethylcyano group to be more electron-withdrawing than the trifluoromethyl group, we attribute this unexpected result to stabilizing non-covalent interactions between the arene and nitrile π-systems in **TS1** that are not present between the arene and trifluoromethyl group (Figure 6.10).

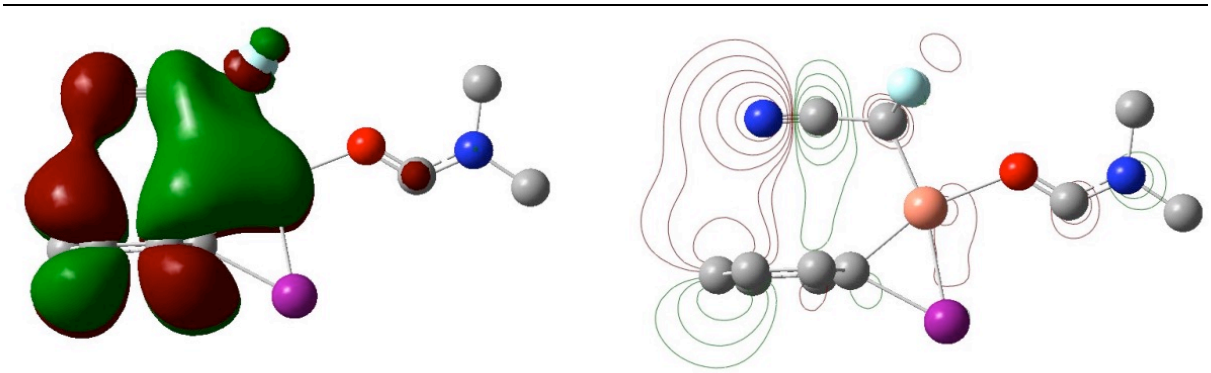

Figure 6.10**: Volume and contour map of non-covalent interactions (NCI) in **TS1

To better understand the effect that α-fluorination has on the adjacent cyano group, we also computed various properties for benzonitrile, α-fluorobenzonitrile, and α,α-difluorobenzonitrile (Table 6.6). Using the software package Vega, we also predicted LogP and total body elimination half-life ($t^{1/2}$). Along this series, the partial charge on the benzylic carbon increases from +0.30 to +1.44 and the partial charge of the nitrogen atom increased from -0.23 to -0.19. Fluorination at the benzylic position causes lengthening of the C(R_2)–CN bond, contraction of the C(R_2)–C–N bond angle, and a decrease in hydrogen bond acceptor ability at nitrogen. The lipophilicity is also predicted to increase with successive fluorination. Therefore, varying the degree of fluorination of such molecules should allow for the tuning of desired physiochemical properties.

***Table 6.6:** Computed and predicted molecular properties for various degrees of α-fluorination of benzonitrile.*[a]

Molecule	$d_{C\text{-}CN}$	$d_{C\text{-}N}$	$\theta_{Ph\text{-}C\text{-}CN}$	$\theta_{C\text{-}C\text{-}N}$	q(CR_2)	q(C)	q(N)	LogP[b]	$t^{1/2}$ (h)[c]
$PhCH_2CN$	1.46	1.16	112.4	179.5	+0.30	+0.07	-0.23	1.75	4.47
PhCH**F**CN	1.47	1.16	112.8	178.7	+0.94	+0.12	-0.22	1.89	4.85
$PhC\mathbf{F_2}CN$	1.49	1.15	112.2	177.8	+1.44	+0.13	-0.19	2.25	9.95

[a]Predictions made using packages in Vega 1.2.0 and with MolInspiration Chemoinformatics v2021.10; [b]average value obtained from Vega and MolInspiration predictions; [c]total body elimination half-life. The experimental LogP value for $PhCH_2CN$ is 1.56

6.3 Conclusions

We report the development of the first cross-coupling reaction for the synthesis of aryldifluoronitriles from reactions of α-silyldifluoroacetronitrile reagents with aryl halides. A copper-mediated coupling of aryl halides with $TMSCF_2CN$ was developed and found to be applicable to the coupling of electron-poor, electron-rich, and sterically hindered aryl iodide and heteroaryl bromide substrates. The reaction proceeds without the addition of an exogenous ligand and employs commercially available and stable copper(I) sources, CuTC and CuDPP, and a difluoronitrile nucleophile, $TMSCF_2CN$, that is available in one step from commercially available starting materials. The copper-mediated coupling reaction offers an alternative to current methods for the synthesis of aryldifluoronitriles, which often require multiple steps, display poor functional group tolerance, require pre-functionalization of substrates, or form mixtures of products. The aryldifluornitrile product proved to be suitable for further functionalization reactions representing therefore an advantageous building block in drug development. Future investigations include the development of alternative difluoronitrile nucleophile sources with increased stability that could allow to optimize the reaction to catalytic amount of copper. In addition, since there is an inescapable necessity for green and sustainable protocols applied to transition-metal catalysis, attempts to perform the reaction with biogenic solvents and sustainable additives would offer notable advantageous in terms of cost and sustainability.

6.4 Experimental

General information

All reactions were conducted under inert atmosphere in a nitrogen-filled glovebox or with standard Schlenk techniques, unless otherwise specified. All reagents and solvents were purchased from commercial sources and used as received, unless otherwise noted. All glassware was flame-dried or dried overnight at 120 °C, allowed to cool under vacuum, and stored in a N_2-atomsphere drybox until use unless otherwise noted. Tetrahydrofuran, toluene, and diethyl ether were purified by passing the degassed solvents (N_2) through a column of activated alumina (solvent purification system purchased from Innovative Technologies, Newburyport, MA). All other solvents were stored over 4 Å molecular sieves

for at least 24 h prior to use. Compounds **2a**-**2g**, **2i**-**2aa**, **2ah**, **2ad**, and **4a**-**4r** are commercially available, were stored on the benchtop, and were used as received. CuDPP was purchased from Ambeed. CuTC was purchased from either ChemScene or AA Blocks. All reagents purchased from commercial suppliers were stored in the glove box and used as received.

Deuterated solvents were purchased from Cambridge Isotope Laboratories and used as received.

^{1}H, ^{13}C, and ^{19}F NMR spectra were recorded on Bruker AV-300, AVQ-400, AVB-400, AV-500, AV-600, NEO-500, and AV-700 spectrometers at the University of California, Berkeley NMR facility. Chemical shifts are reported relative to residual solvent peaks ($CDCl_3$ = 7.26 ppm for ^{1}H NMR spectra and 77.16 ppm for ^{13}C NMR spectra, DMSO-*d6* = 2.50 ppm for ^{1}H NMR spectra and 39.52 ppm for ^{13}C NMR spectra). For ^{19}F NMR spectra, chemical shifts are reported relative to the δ –113.15 resonance of PhF used as an external reference. The following abbreviations are used in reporting NMR data: s, singlet; d, doublet; t, triplet; q, quartet; p, pentet; hept, heptet; m, multiplet.

High-resolution mass spectra were recorded on an Agilent Time of Flight (Q-TOF) mass spectrometer in ESI mode operated by the Catalysis Center at the University of California, Berkeley. Analytical thin layer chromatography (TLC) was performed on Kieselgel 60 F254 glass plates precoated with a 0.25 mm thickness of silica gel. The TLC plates were visualized with UV light and by staining with $KMnO_4$. Column chromatography was generally performed on a Teledyne Isco Combiflash® Rf system with RediSep GoldTM columns.

Optimization studies

Initial investigation of reaction conditions

In a nitrogen-filled glovebox, the copper salt (from 0.2 to 2.0 eq) was added to a 4 mL vial equipped with a stir bar. If applicable, the additive (from 0.0 to 1.2 eq) and the ligand were added, if solid at room temperature (0.11 mmol, 1.1 eq). The solvent (from 0.1 to 1.0 mL) was added, followed by 1-butyl-4-iodobenzene **2a** (17.8 µL, 0.1 mmol, 1.0 eq) and $TMSCF_2CN$ **1** (from 1.2 to 5.0 eq). If applicable, the ligand was added if liquid at room temperature (0.11 mmol, 1.1 eq). The reaction was sealed with a Teflon-lined cap and

heated to 120°C for 16 h. After 16 h, the reaction was allowed to cool to room temperature. The internal standard, α,α,α-trifluorotoluene (12.27 µL, 0.1 mmol, 1.0 eq), was added, and the yield of the reaction was determined by ^{19}F NMR spectroscopy.

Table S6.1: *Full optimization studies for the copper-mediated coupling of aryl iodides and* $TMSCF_2CN$

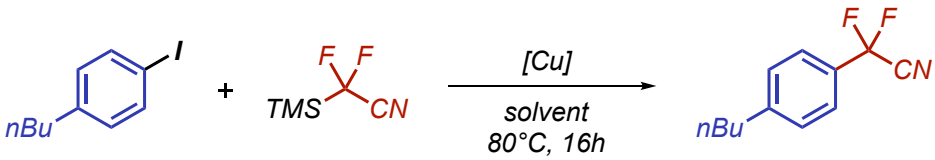

2a **1** **3a**

Entry	[Cu] (eq)	Equiv **1**	solvent (M)	Yield (%)[a]
1[b]	CuI (0.2)	5.0	DMSO (0.2)	0
2[b]	CuI (0.5)	5.0	DMSO (0.2)	6
3[b]	CuI (1.0)	5.0	DMSO (0.2)	19
4[b]	CuI (2.0)	5.0	DMSO (0.2)	27
5[b]	CuI (5.0)	5.0	DMSO (0.2)	48
6[b]	CuCl (2.0)	5.0	DMSO (0.2)	65
7[b]	CuBr (2.0)	5.0	DMSO (0.2)	41
8[b]	$CuBr{\cdot}SMe_2$ (2.0)	5.0	DMSO (0.2)	50
9[b]	CuOAc (2.0)	5.0	DMSO (0.2)	65
10[b]	CuTC (2.0)	5.0	DMSO (0.2)	72
11[b]	CuDPP (2.0)	5.0	DMSO (0.2)	84
12	CuDPP (2.0)	5.0	DME (0.2)	91
13	CuDPP (1.0)	5.0	DME (0.2)	73
14	CuDPP (1.0)	2.5	DME (0.2)	79
15	CuDPP (1.0)	2.0	DME (0.2)	76
16	CuDPP (1.0)	1.2	DME (0.2)	64
17	CuDPP (1.0)	2.0	DCE (0.2)	67
18	CuDPP (1.0)	2.0	THF (0.2)	70
19	CuDPP (1.0)	2.0	NMP (0.2)	96
20	CuDPP (1.0)	2.0	DMF (0.2)	96
21	CuDPP (1.0)	2.0	DMF (0.1)	94
22	CuDPP (1.0)	2.0	DMF (1.0)	93
23[c]	CuDPP (1.0)	2.0	DMF (0.4)	86
24[d]	CuDPP (1.0)	2.0	DMF (0.4)	95
25[e]	CuDPP (1.0)	2.0	DMF (0.4)	99
26	CuDPP (1.0)	2.0	DMF (0.4)	99
27	CuTC (1.0)	2.0	DMF (0.4)	99

[a]Determined using ^{19}F NMR spectroscopy with $PhCF_3$ as internal standard; [b]Reactions conducted with **1** that contained up to 5% TMSCN; [c]Reaction conducted at rt; [d]Reaction conducted at 65 °C; [e]Reaction conducted at 100 °C.

***Table S6.2**: Effect of ligands on the copper-mediated coupling of aryl iodides and $TMSCF_2CN$*

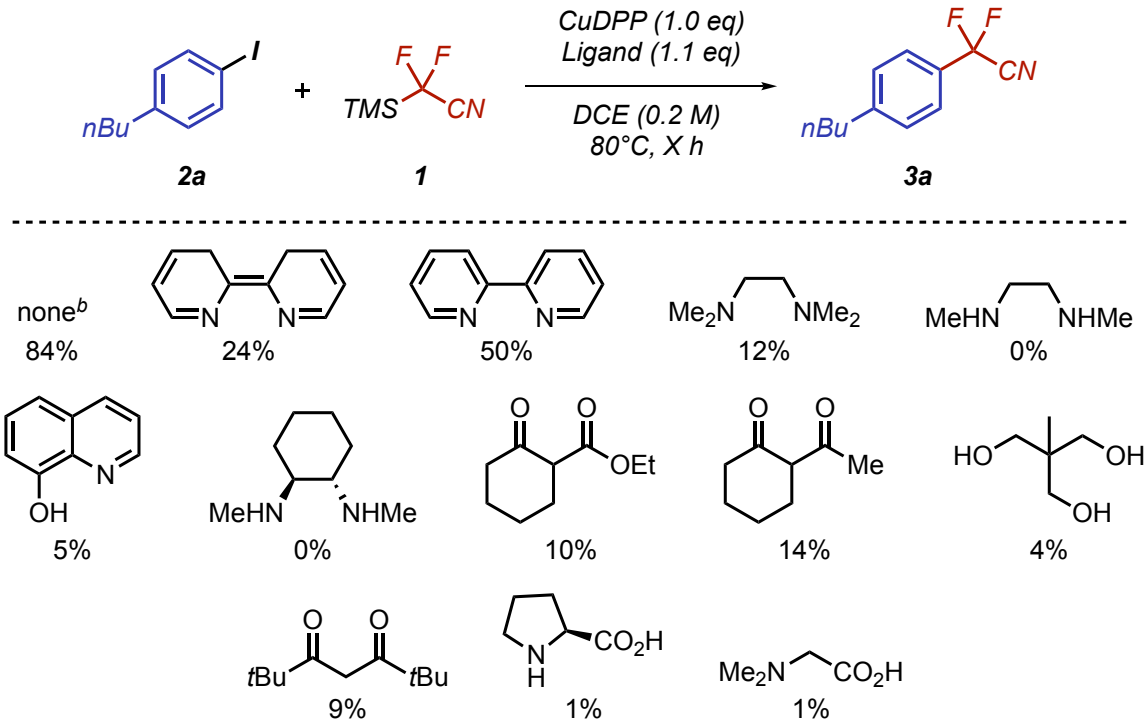

[a]Yield determined by ^{19}F NMR spectroscopy with $PhCF_3$ as internal standard. [b]Reaction conducted with 2 equivalents of CuDPP

***Table S6.3**: Evaluation of additives for the Cu-mediated synthesis of aryldifluoronitriles*

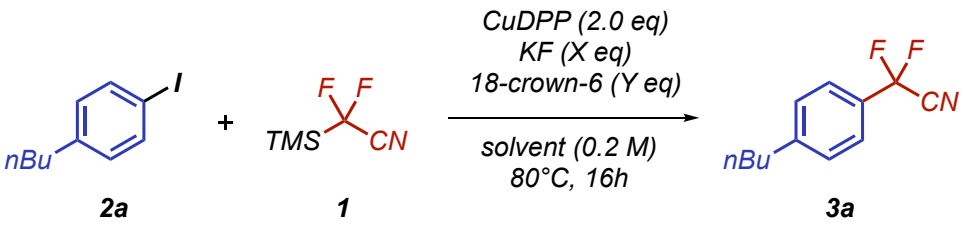

Entry	KF eq	18-crown-6 eq	solvent	Yield (%)[a]
1	-	-	DCE	84
2	0.5	-	DCE	61
3	0.5	0.5	DCE	52
4	1.2	-	DCE	74
5	1.2	1.2	DCE	61
6	5.0	-	DCE	64
7	5.0	5.0	DCE	10
8[b]	1.2	1.2	toluene	56
9[b]	1.2	1.2	dioxane	41
10	1.2	1.2	DMSO	55

[a]Determined using ^{19}F NMR spectroscopy with $PhCF_3$ as internal standard; [b]Reactions conducted at 100°C.

Attempts at catalytic reactivity with various complexes of copper, ligands and additives

***Table S6.4**: Effect of oxalamide or oxalhydrazide ligands on the difluorocyanation reaction*

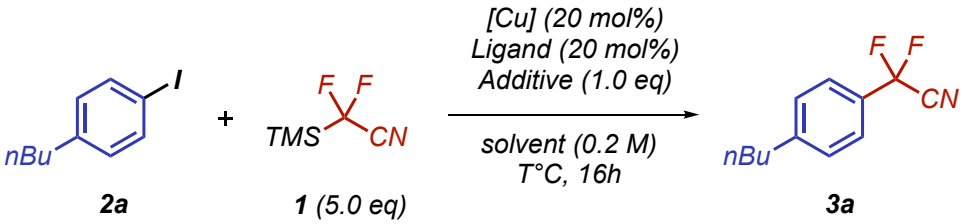

2a **1** *(5.0 eq)* **3a**

Entry	[Cu] / Ligand	Solvent, T°C	Additive	Yield (%)[a]
1	[Cu 1]	DMSO, 100°C	-	0
2	[Cu 1]	DMSO, 100°C	KF	0
3	[Cu 1]	DMSO, 100°C	CsF	0
4	[Cu 2]	DMSO, 100°C	-	0
5	[Cu 2]	DMSO, 100°C	KF	0
6	[Cu 2]	DMSO, 100°C	CsF	0
7	[Cu 3]	DMSO, 100°C	-	0
8	CuDPP	DME, 80°C	KF	12
9	CuDPP	DME, 80°C	CsF	0
10	CuDPP	DME, 80°C	RbF	0
11	[Cu 4]	DME, 80°C	-	0
12	[Cu 4]	DME, 80°C	CsF	0
13	CuDPP + L1	DME, 80°C	-	0
14	CuDPP + L2	DME, 80°C	-	0
15	CuDPP + L3	DME, 80°C	-	0

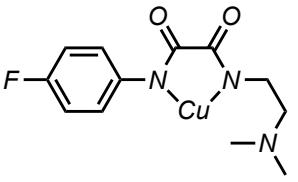

[Cu 1]

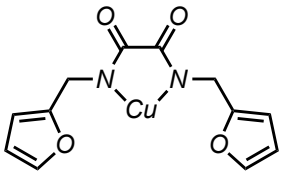

[Cu 2]

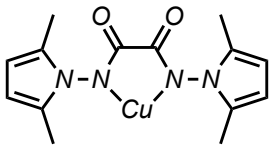

[Cu 3]

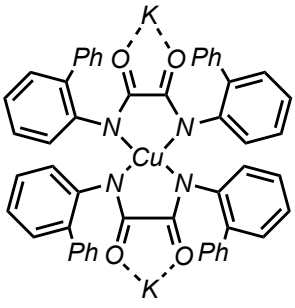

[Cu 4]

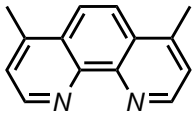

L1

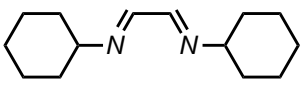

L2

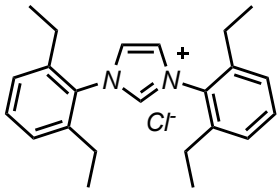

L3

[a]Determined using ^{19}F NMR spectroscopy with $PhCF_3$ as internal standard

General procedures

General Procedure 1: α,α-difluoromethylacetonitriles

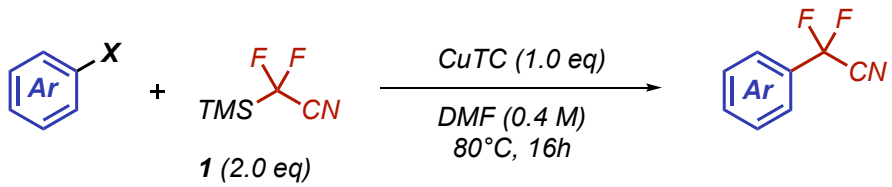

In the glovebox, a dry 4 mL vial equipped with a Teflon stir bar was charged with copper and aryl halide (if solid). Dry DMF was then added, followed by aryl halide (if liquid) and **1** (2.0 eq). The vial was then capped, sealed with electrical tape, and stirred for 16 h at 80 °C. After this time, the crude reaction mixture was directly concentrated and subjected to FCC (SiO_2, 5%-20% EtOAc in Hexanes) to afford pure product. If derivatized, the crude reaction mixture was subjected immediately to general procedures 2-4.

General Procedure 2: α,α-difluoromethylaryl-1-N-methyl-1H-benzoimidazoles

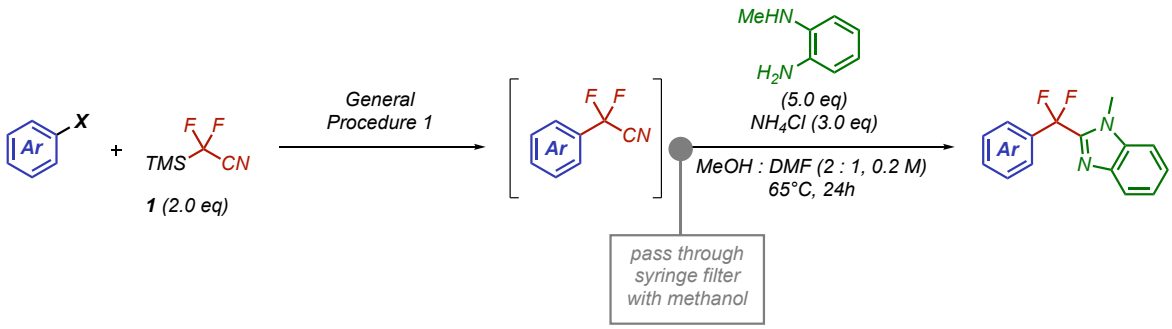

Aryl halide (0.1 mmol) was subjected to General Procedure 1. A dry 4 mL vial was charged with a stir bar and NH_4Cl and, once cooled, the reaction mixture was passed through a syringe filter with dry MeOH as eluent (500 µL) into the vial. Freshly distilled *N*-methylbenzene-1,2-diamine was then added, the headspace was flushed with nitrogen, and the resulting mixture was stirred at 65 C for 24 h. After this time, the reaction mixture was diluted with EtOAc, poured into a separatory funnel containing sat. aq. NH_4Cl, and the aqueous extracted with EtOAc (3x). The combined organics were dried over magnesium sulfate, filtered, and the filtrate concentrated *in vacuo*. The crude residue was purified by column chromatography (SiO_2, 10%-20% EtOAc in pentane) to afford the pure product

General Procedure 3: α,α-difluoromethylaryl-benzooxazoles

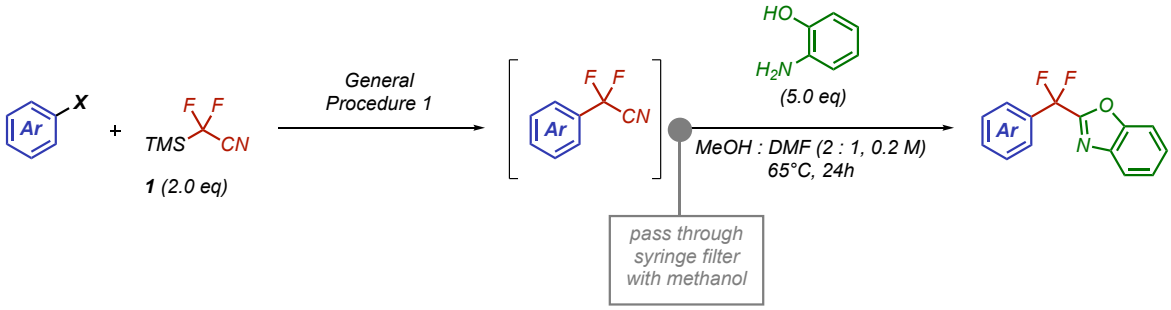

Aryl halide (0.1 mmol) was subjected to General Procedure 1. A dry 4 mL vial was charged with a stir bar and 2-aminophenol and, once cooled, the reaction mixture was passed through a syringe filter with dry MeOH as eluent (500 µL) into the vial. The headspace was flushed with nitrogen, and the resulting mixture was stirred at 65 C for 24 h. After this time, the reaction mixture was diluted with EtOAc, poured into a separatory funnel containing sat. aq. NH_4Cl, and the aqueous extracted with EtOAc (3x). The combined organics were dried over magnesium sulfate, filtered, and the filtrate concentrated *in vacuo*. The crude residue was purified by column chromatography (SiO_2, 10%-20% EtOAc in pentane) to afford pure product.

General Procedure 4: α,α-difluoromethylaryl-benzothiazoles

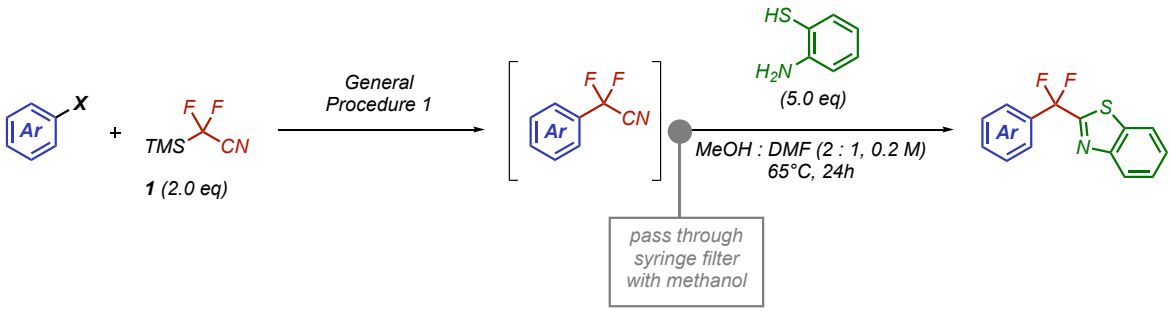

Aryl halide (0.1 mmol) was subjected to General Procedure 1. A dry 4 mL vial was charged with a stir bar and 2-aminobenzenethiol and, once cooled, the reaction mixture was passed through a syringe filter with dry MeOH as eluent (500 µL) into the vial. The headspace was flushed with nitrogen, and the resulting mixture was stirred at rt for 24 h. After this time, the reaction mixture was diluted with EtOAc, poured into a separatory funnel containing sat. aq. NH_4Cl, and the aqueous extracted with EtOAc (3x). The combined organics were dried over magnesium sulfate, filtered, and the filtrate concentrated *in vacuo*. The crude

residue was purified by column chromatography (SiO_2, 5%-15% EtOAc in pentane) to afford pure product.

Synthesis of $TMSCF_2CN$[81]

*2,2-difluoro-2-(trimethylsilyl)acetonitrile (**1**)*

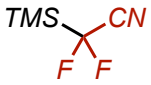

A mixture of TMSCN (3.96 g, 40.0 mmol, 1.0 eq), $TMSCF_2Br$ (8.12 g 40.0 mmol, 1.0 eq), $BnNEt_3Cl$ (372 mg, 2.0 mmol, 5 mol%), and benzonitrile (15 mL) was heated at 110 °C for 80 min. The mixture was cooled to 0 °C, styrene oxide (5.5 mL, 48.0 mmol, 1.2 eq) was added dropwise, and the mixture was stirred for 1 h at room temperature. The reaction flask was immersed into room temperature bath, and volatile components were distilled off under vacuum (1 Torr) collecting into a cold trap (−100°C). The collected liquid was filtered through cotton wool plug and fractionally distilled at atmospheric pressure at 110°C using Vigreux column to provide 2,2-difluoro-2-(trimethylsilyl)acetonitrile **1** as a colorless liquid (3.58 g, 24.0 mmol, 60% yield)

^{1}H NMR (500 MHz, $CDCl_3$) δ 0.41 (s, 9H).

^{13}C NMR (75 MHz, CDCl3) δ 116.44 (t, J = 264.9), 113.32 (t, J = 37.1), −5.79 (t, J = 1.5

^{19}F NMR (565 MHz, $CDCl_3$) δ -115.42

Decomposition of $TMSCF_2CN$

In the glovebox, a dry 4 mL vial equipped with a Teflon stir bar was charged with $TMSCF_2CN$ (14.9 mg, 0.1 mmol, 1.0 eq) and CsF (15.2 mg, 0.1 mmol, 1.0 eq). DMF (0.250 mL) was added and the vial was then capped, sealed with electrical tape, and stirred for 1h at 80°C. The ^{19}F NMR spectrum was acquired with $PhCF_3$ as internal standard to evalueate the decomposition of the nucleophile.

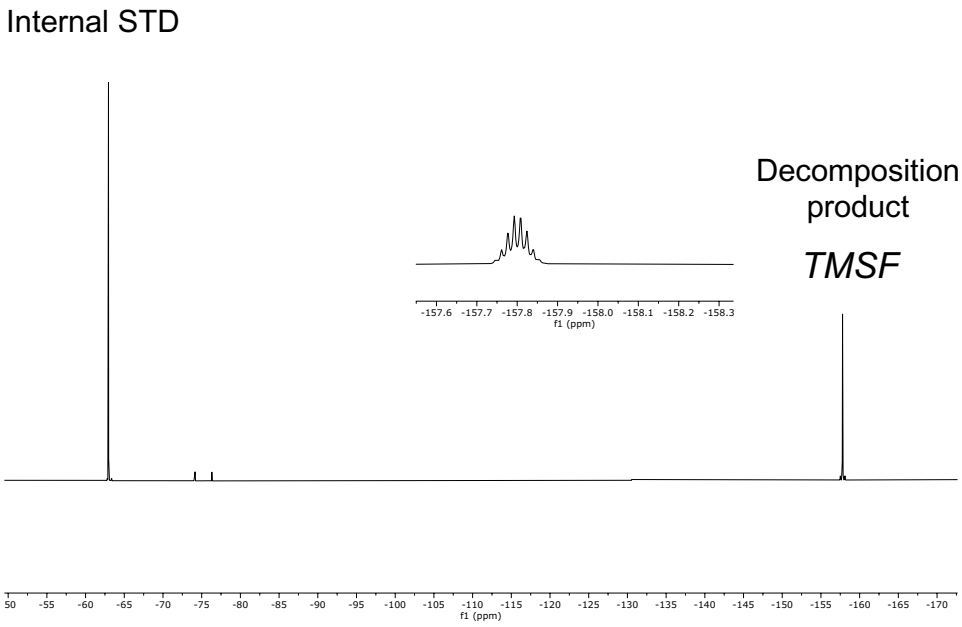

Figure S6.1: *Decomposition of $TMSCF_2CN$ with CsF to give TMSF and $:CF_2$*

Synthesis of aryl iodides

*2-(4-((tert-butyldimethylsilyl)oxy)phenyl)-2,2-difluoromethylacetonitrile (**2h**)*[82]

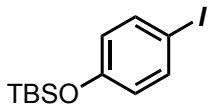

In a 20 mL vial, tert-Butyldimethylchlorosilane (616.5 mg, 4.1 mmol, 1.2 eq) was added to a solution of p-Iodophenol (750.0 mg, 3.4 mmol, 1.0 eq) and triethylamine (570 µL, 4.1 mmol, 1.2 eq) in DCM (7.0 mL). The reaction mixture was stirred at rt for 16 h. The resulting biphasic mixture was poured into water and extracted with EtOAc (3x), the combined organic phases were dried over magnesium sulfate, filtered, and concentrated in vacuo. The crude residue was purified by column chromatography (100% hexanes) to provide tert-butyl(4-iodophenoxy)dimethylsilane **2h** as a colorless liquid (884.5 mg, 78 %).

^{1}H NMR (500 MHz, $CDCl_3$) δ 7.51 (d, J = 8.7 Hz, 2H), 6.63 (d, J = 8.8 Hz, 2H), 0.97 (s, 9H), 0.22 (s, 6H).

^{13}C NMR (126 MHz, $CDCl_3$) δ 155.6, 138.3, 122.5, 83.7, 25.6, 18.2, -4.5

*(R)-2,5,7,8-tetramethyl-2-((4R,8R)-4,8,12-trimethyltridecyl)chroman-6-yl 4-iodobenzoate (**2ac**)*[83]

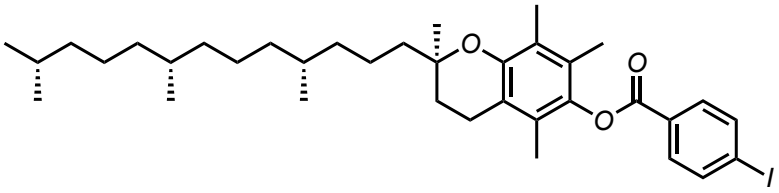

To a solution of (R)-2,5,7,8 tetramethyl-2-((4R,8R)-4,8,12-trimethyltridecyl)chroman-6-ol (250.0 mg, 580.4 µmol, 1.0 eq) and triethylamine (81.0 µL, 580.4 µmol, 1.0 eq) in DCM (2.9 mL) at 0 °C was added 4-iodobenzoyl chloride (154.7 mg, 580.4 µmol, 1.0 eq) in one portion. This was then stirred for 2 h at room temperature. The reaction mixture was then diluted with DCM, washed with 2 M NaOH (3x), and the combined organic phases concentrated in vacuo. The crude residue was purified by column chromatography (20/80 ethyl acetate in hexanes) to provide (R)-2,5,7,8-tetramethyl-2-((4R,8R)-4,8,12-trimethyltridecyl)chroman-6-yl 4-iodobenzoate **2ac** as a viscous yellow oil (77.7 mg, 20% yield).

^{1}H NMR (500 MHz, $CDCl_3$) δ 8.02 – 7.94 (m, 2H), 7.88 (d, J = 8.5 Hz, 2H), 2.58 (t, J = 6.8 Hz, 2H), 2.12 (s, 3H), 2.0 (s, 3H), 2.01 (s, 3H), 1.87 – 1.72 (m, 2H), 1.70 – 1.33 (m, 7H), 1.29 – 1.20 (m, 11H), 1.18 – 1.01 (m, 6H), 0.93 (dd, J = 9.7, 6.5 Hz, 12H).
^{13}C NMR (126 MHz, $CDCl_3$) δ 164.88, 155.27, 149.72, 140.61, 138.12, 131.69, 129.25, 126.92, 125.17, 123.36, 117.68, 101.47, 75.28, 40.63, 39.53, 37.69, 37.54, 37.44, 32.93, 31.38, 29.85, 28.13, 24.97, 24.60, 24.35, 23.83, 22.87, 22.78, 21.20, 20.78, 19.91, 19.84, 19.75, 13.18, 12.34, 12.01.

tert-butyl (3-hydroxy-3-phenylpropyl)(methyl)carbamate

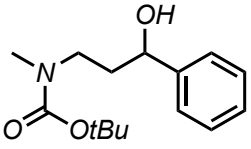

To a solution of 3-(methylamino)-1-phenylpropan-1-ol (500.0 mg, 3.0 mmol, 1.0 eq) and triethylamine (850 µL, 6.1 mmol, 2.0 eq) in DCM, was added Boc_2O (750 µL, 3.3 mmol, 1.1 eq) at room temperature; the resulting solution was stirred for 2 h. The reaction was then

diluted with water, extracted with DCM (3x) and the combined organic phases concentrated in vacuo. The crude residue was purified by column chromatography (25/75 ethyl acetate in hexanes) to provide tert-butyl (3-hydroxy-3-phenylpropyl)(methyl)carbamate as a colorless oil (712.5 mg, 89% yield).

^{1}H NMR (500 MHz, $CDCl_3$) δ 7.44 (dt, J = 15.0, 7.7 Hz, 5H), 4.65 (s, 1H), 3.91 (s, 1H), 3.03 (d, J = 13.2 Hz, 1H), 2.92 (s, 3H), 1.89 (dtd, J = 13.7, 6.2, 3.1 Hz, 1H), 1.80 (s, 1H), 1.47 (s, 9H).
^{13}C NMR (126 MHz, $CDCl_3$) δ 157.2, 144.1, 128.3, 127.0, 125.6, 80.1, 69.9, 45.1, 37.2, 34.3, 28.4.

*tert-butyl (3-(4-iodophenoxy)-3-phenylpropyl)(methyl)carbamate (**2ae**)*[84]

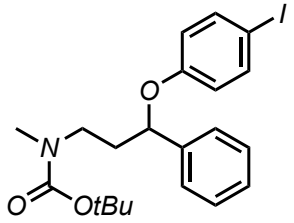

To a flame-dried round-bottom flask flushed with N_2, p-iodophenol (230 µL, 1.9 mmol, 1.0 eq), tert-butyl (3-hydroxy-3-phenylpropyl)(methyl)carbamate (500.0 mg, 1.9 mmol, 1.0 eq), and triphenylphosphine (593.1 mg, 2.3 mmol, 1.2 eq) were added. THF (19 mL) was then added. This solution was cooled to 0 °C and DIAD (488 µL, 1.9 mmol, 1.0 eq) was added dropwise. The resulting mixture was stirred at room temperature overnight. Then, conc. H_3PO_4 was added (3mL) and gas evolution was observed; the resulting mixture was stirred for 3 h before diluting with water and extracting with EtOAc (3x). The combined organic phases were washed with 2M NaOH (3x), dried over magnesium sulfate, filtered, and concentrated in vacuo. The crude residue was purified by column chromatography (20/80 ethyl acetate in hexanes) to provide tert-butyl (3-(4-iodophenoxy)-3-phenylpropyl)(methyl)carbamate **2ae** as a yellow oil (218.9 mg, 25% yield).

^{1}H NMR (500 MHz, DMSO) δ 7.52 (d, J = 8.6 Hz, 2H), 7.43 – 7.31 (m, 4H), 7.29 – 7.21 (m, 1H), 6.74 – 6.68 (m, 2H), 5.31 (dd, J = 8.3, 4.4 Hz, 1H), 2.84 (s, 3H), 2.09 (dt, J = 10.7, 4.1 Hz, 1H), 1.42 – 1.24 (m, 9H).

^{13}C NMR (126 MHz, $CDCl_3$) δ 157.8, 155.7, 141.0, 138.0, 128.7, 127.7, 125.7, 125.6, 118.2, 82.9, 79.3, 45.7, 37.1, 28.4

4-fluoro-2-methoxy-1-(prop-2-yn-1-yloxy)benzene[85]

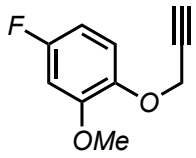

Under an inert atmosphere of nitrogen, 1,2-methoxy-4-fluorophenol (710 mg, 5.0 mmol, 1.0 eq) was dissolved in anhydrous DMF (10 mL), followed by the addition of K_2CO_3 (1.40 g, 10.0 mmol, 2.0 eq), before heating to 55 °C for 30 min. The reaction mixture was allowed to cool to room temperature and propargyl bromide (650 µL, 6.0 mmol, 1.2 eq) was added. The solution was stirred at room temperature for 6 h, monitoring for completion using TLC and then poured into ice-cold water. The aqueous layer was extracted with EtOAc (3 × 10 mL) and the combined organic phases were dried over $MgSO_4$ before removal of the solvent in vacuo. The crude residue was purified by column chromatography (10/90 ethyl acetate in hexanes) to provide 4-fluoro-2-methoxy-1-(prop-2-yn-1-yloxy)benzene as a colorless liquid (765 mg, 85% yield).

^{1}H NMR (500 MHz, $CDCl_3$) δ 7.00-6.97 (dd, J = 8.9, 5.5 Hz, 1H), 6.66 (dd, J = 10.1, 3.0 Hz, 1H), 6.62-6.58 (td, J = 8.4, 2.9 Hz, 1H), 4.72 (d, J = 2.4 Hz, 2H), 3.86 (s, 3H), 2.50 (t, J = 2.4 Hz, 1H).
^{13}C NMR (151 MHz, $CDCl_3$) δ 158.52 (d, J = 240.4 Hz), 151.04 (d, J = 10.1 Hz), 143.06 (d, J = 3.2 Hz), 116.17 (d, J = 10.1 Hz), 106.01 (d, J = 22.5 Hz), 100.55 (d, J = 27.6 Hz), 78.70, 75.94, 57.76, 56.16.
^{19}F NMR (565 MHz, $CDCl_3$) δ -118.74

1-((3-(3-bromophenyl)prop-2-yn-1-yl)oxy)-4-fluoro-2-methoxybenzene[86]

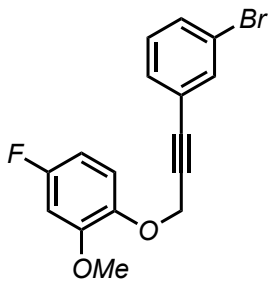

In a nitrogen-filled glovebox, a 20 mL vial equipped with a Teflon magnetic stir bar was charged with $Pd(PPh_3)_2Cl_2$ (0.1 mmol, 70.1 mg, 5 mol%), CuI (0.2 mmol, 38.0 mg, 10 mol%) and 4-fluoro-2-methoxy-1-(prop-2-yn-1-yloxy)benzene (360 mg, 2.0 mmol, 1.0 eq). Triethylamine (10 mL) was added to the vial and the reaction mixture was stirred for 10 min at 65°C. After stirring for 10 minutes, 1-bromo-3-iodobenzene (622 mg, 2.2 mmol, 1.1 eq) was added, and the mixture was stirred overnight. The resulting mixture was then poured into an aqueous saturated solution of NH_4Cl (5 mL) and extracted twice with ethyl acetate (2 × 10 mL). The combined organic layers were washed with brine, dried over anhydrous Na_2SO_4. The crude residue was purified by column chromatography (10/90 ethyl acetate in hexanes) to provide 1-((3-(3-bromophenyl)prop-2-yn-1-yl)oxy)-4-fluoro-2-methoxybenzene as a beige powder (402 mg, 60% yield).

^{1}H NMR (500 MHz, $CDCl_3$) δ 7.56 (m, 1H), 7.46 (m, 1H), 7.34 (m, 1H), 7.17 (t, J = 7.9 Hz, 1H), 7.03 (dd, J = 8.9, 5.5 Hz, 1H), 6.68 (dd, J = 10.2, 2.9 Hz, 1H), 6.62 (td, J = 8.4, 2.9 Hz, 1H), 4.93 (s, 2H), 3.88 (s, 3H).

^{13}C NMR (151 MHz, $CDCl_3$) δ 158.53 (d, J = 240.4 Hz), 151.08 (d, J = 9.9 Hz), 143.18 (d, J = 3.2 Hz) 134.61, 131.98, 130.47, 129.88, 116.19 (d, J = 10.0 Hz), 106.06 (d, J = 22.5 Hz), 100.56 (d, J = 27.5 Hz), 86.04, 85.46, 58.46, 56.18.

^{19}F NMR (565 MHz, $CDCl_3$) δ -118.78

*4-fluoro-1-((3-(3-iodophenyl)prop-2-yn-1-yl)oxy)-2-methoxybenzene (**2af**)*[87]

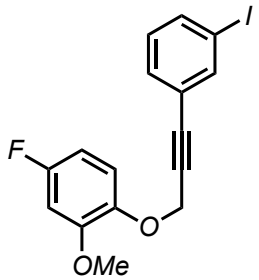

In a nitrogen-filled glovebox, a 20 mL vial equipped with a Teflon magnetic stir bar was charged with CuI (8.0 mg, 0.04 mmol, 5.0 mol%), 1-((3-(3-bromophenyl)prop-2-yn-1-yl)oxy)-4-fluoro-2-methoxybenzene (285 mg, 0.9 mmol, 1.0 eq) and NaI (255 mg, 1.7 mmol, 2.0 eq). Racemic trans-N,N'-dimethyl-1,2-cyclohexanediamine (12.1 mg, 0.08 mmol, 10 mol%) and dioxane (1.0 mL) were added to the vial. The vial was sealed with a Teflon valve

and the reaction mixture was stirred at 110°C for 48 h. The resulting suspension was allowed to reach room temperature, diluted with 30% aq ammonia (5 mL), poured into water (20 mL), and extracted with dichloromethane (3×10 mL). The combined organic layers were washed with brine, dried over anhydrous Na_2SO_4. The crude residue was purified by column chromatography (10/90 ethyl acetate in hexanes) to provide 4-fluoro-1-((3-(3-iodophenyl)prop-2-yn-1-yl)oxy)-2-methoxybenzene **2af** as a yellow oil (273 mg, 84% yield).

^{1}H NMR (500 MHz, $CDCl_3$) δ 7.77 (m, 1H), 7.66 (m, 1H), 7.37 (m, 1H), 7.05-7.01 (m, 2H), 6.68 (dd, J = 10.2, 2.9 Hz, 1H), 6.64-6.60 (td, J = 8.4, 2.9 Hz, 1H), 4.92 (s, 2H), 3.88 (s, 3H).
^{13}C NMR (151 MHz, $CDCl_3$) δ 158.49 (d, J = 240.4 Hz), 151.04 (d, J = 9.8 Hz), 143.17 (d, J = 3.1 Hz) 140.41, 137.81, 131.00, 129.92, 116.15 (d, J = 9.8 Hz), 106.04 (d, J = 22.6 Hz), 100.53 (d, J = 27.3 Hz), 93.67, 85.84, 85.47, 58.44, 56.16.
^{19}F NMR (565 MHz, $CDCl_3$) δ -118.71

*2-iodo-3-Methoxy-1,3,5(10)-estratrien-17-one (**2ag**)*[88]

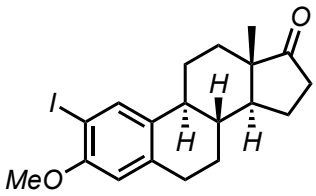

3-Methoxy-1,3,5(10)-estratrien-17-one (300 mg, 1.05 mmol, 1.0 eq) was dissolved in trifluoroacetic acid (10 ml) and N-iodosuccinimide (NIS; 236 mg, 1.05 mmol, 1.0 eq) was added. The mixture was stirred at room temperature for 2 h, and then poured into 100 ml water and extracted with dichloromethane. The organic phase was separated, neutralized with an ammonia solution and washed with a saturated solution of sodium thiosulfate and water. The organic phase was dried over anhydrous sodium sulfate, filtered and evaporated. The crude residue was purified by column chromatography (20/80 ethyl acetate in hexanes) to provide 2-iodo-3-Methoxy-1,3,5(10)-estratrien-17-one **2ag** as a white solid (151 mg, 35% yield).

^{1}H NMR (500 MHz, $CDCl_3$) δ 7.66 (s, 1H), 7.56 (s, 1H), 3.86 (s, 3H), 2.90 (m, 2H), 2.53 (m, 1H), 2.48 (m, 1H), 2.23 (m, 1H), 2.15 (m, 1H), 2.04 (s, 3H), 1.55, (m, 6H), 0.91 (s, 3H).
^{13}C NMR (151 MHz, $CDCl_3$) δ 156.19, 138.25, 136.53, 134.47, 111.48, 82.83, 56.46, 50.40, 48.06, 43.76, 38.74, 35.96, 31.59, 29.70, 26.48, 26.04, 21.69, 13.95.

*1-(4-iodophenyl)-5-phenyl-3-(trifluoromethyl)-1H-pyrazole (**2ai**)*

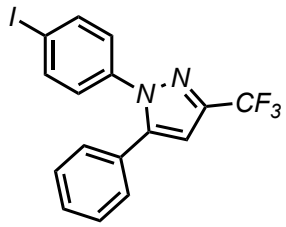

To a solution of 4,4,4-trifluoro-1-phenyl-1,3-butanedione (500.0 mg, 2.3 mmol, 1.0 eq) in DMA (7.7 mL) was added 1-(4-iodophenyl)hydrazine hydrochloride (625.7 mg, 2.3 mmol, 1.0 eq) at room temperature, followed by 6 M hydrogen chloride (1.2 mL). The mixture was stirred at room temperature for 24 h, then cooled to 0°C; at this point, H_2O was slowly added. After diluting with toluene, the organic phases were washed with H_2O (2x), dried over magnesium sulfate, filtered, and the filtrate concentrated in vacuo. The crude residue was purified by column chromatography (15/85 ethyl acetate in hexanes) to provide 1-(4-iodophenyl)-5-phenyl-3-(trifluoromethyl)-1H-pyrazole **2ai** as an off-white solid (620 mg, 65%).

^{1}H NMR (500 MHz, $CDCl_3$) δ 7.71 (d, J = 8.7 Hz, 2H), 7.42 – 7.33 (m, 3H), 7.21 (dd, J = 8.0, 1.7 Hz, 2H), 7.10 (d, J = 8.7 Hz, 2H), 6.71 (s, 1H).

Functionalization Reactions of Aryl-α,α-difluoromethylacetonitriles

*tert-butyl (2,2-difluoro-2-phenylethyl)carbamate (**12a**)*[89]

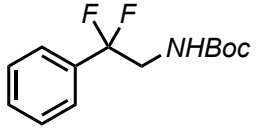

Step 1: In a nitrogen-filled glovebox, a dry 4 mL vial equipped with a Teflon magnetic stir bar was charged with lithium aluminum hydride (94.9 mg, 2.5 mmol, 5.0 eq) and dry and degassed diethyl ether (1.0 mL). The resulting suspension was cooled to –30 °C in the

glovebox freezer. Then, a solution of 2,2-difluoro-2-phenylacetonitrile (76.6 mg, 0.5 mmol, 1.0 eq) in dry, degassed diethyl ether (1.0 mL) was prepared and cooled to –30 °C in the glovebox freezer. The solution containing the nitrile was transferred cold, and dropwise, to the suspension of lithium aluminum hydride with stirring. Diethyl ether (0.5 mL) was used to complete the transfer, the reaction vial was sealed, allowed to warm to room temperature, and stirred vigorously for 2 hours. After this time, the reaction mixture was cooled to 0°C and carefully diluted with water, dropwise. The resulting mixture was extracted with ethyl acetate, dried over sodium sulfate, and concentrated in vacuo in a 20 mL vial.

Step 2: In the 20 mL vial, the crude product was dissolved in dry DCM (2.0 mL) and treated with di-tert-butyl dicarbonate (105.0 mg, 0.5 mmol, 1.0 eq). The reaction vial was sealed and the reaction mixture was stirred at room temperature for 24 hours. After this time, the reaction mixture was concentrated in vacuo and the product was purified by column chromatography (2/98 to 10/90 ethyl acetate in hexanes) to provide tert-butyl (2,2-difluoro-2-phenylethyl)carbamate **12a** as a white powder (113.7 mg, 87% yield). Note: The product exists as a 5.5:1 mixture of amide E/Z isomers that interconvert more slowly than the NMR timescale

^{1}H NMR (600 MHz, $CDCl_3$) δ 7.53 – 7.47 (both isomers, m, 2H), 7.47 – 7.39 (both isomers, m, 3H), 4.87 (major isomer, broad t, J = 6.3 Hz, 1H), 4.58 (minor isomer, broad s, 1H), 3.76 (both isomers, td, J = 14.3, 6.4 Hz, 2H), 1.39 (major isomer, s, 9H), 1.30 (minor isomer, s, 9H).

^{13}C NMR (151 MHz, $CDCl_3$) δ 155.6, 134.9 (t, J = 25.5 Hz), 130.3, 128.6, 125.4 (t, J = 6.1 Hz), 120.7 (t, J = 243.8 Hz), 80.1, 47.0 (t, J = 31.1 Hz), 28.4.

^{19}F NMR (565 MHz, $CDCl_3$) δ -102.8 (major isomer, t, J = 14.3 Hz), -103.0 (minor isomer, broad t, J = 13.3 Hz)

*5-(difluoro(phenyl)methyl)-1H-tetrazole (**12b**)*[90]

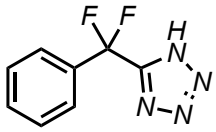

A 20 mL vial equipped with a Teflon magnetic stir bar was charged with 2,2-difluoro-2-phenylacetonitrile (78.5 mg, 0.5 mmol, 1.0 eq) and DMSO (5.0 mL). Then, sodium azide (65.0 mg, 1.0 mmol, 2.0 eq) was added. The headspace was flushed with nitrogen, and the vial was sealed with a Teflon cap and heated at 80°C in a heating block for 20 hours. After this time, the reaction was cooled to room temperature, transferred to a separatory funnel, and diluted with 50 mL ethyl acetate and 40 mL 1.5 M HCl. The aqueous layer was extracted with ethyl acetate (4 x 50 mL), and the combined organic layers were concentrated in vacuo to provide the desired product as a mixture with DMSO. To remove residual DMSO, the product was taken up in ethyl acetate (20 mL) and washed with 1M HCl (8 x 5 mL). The organic layer was dried over sodium sulfate and concentrated in vacuo to provide a thick oil. This oil was stored at –10 °C for 24 hours, after which time it solidified. The resulting solid was crushed to a powder and dried under high vacuum to provide 5-(difluoro(phenyl)methyl)-1H-tetrazole **12b** as a white powder (97.5 mg, 97% yield).

^{1}H NMR (600 MHz, $CDCl_3$) δ 7.66 (d, J = 7.8 Hz, 2H), 7.50 (m, 3H).

^{13}C NMR (151 MHz, $CDCl_3$) δ 166.4 (t, J = 32.2 Hz), 133.5 (t, J = 26.4 Hz), 131.5, 128.9, 125.6 (t, J = 6.0 Hz), 116.7 (t, J = 245.7 Hz).

^{19}F NMR (565 MHz, $CDCl_3$) δ -92.17

*2-((4-butylphenyl)difluoromethyl)-4,5-dimethylpyridine (**12c**)*[91]

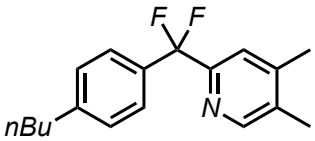

To a solution of $Ni(COD)_2$ (6.6 mg, 23.90 µmol, 10 mol%), tricyclohexylphosphine (26.8 mg, 95.6 µmol, 40 mol%), and 2-(4-butylphenyl)-2,2-difluoromethylacetonitrile (50.0 mg, 239 µmol, 1.0 eq) in toluene (1.2 mL) was added 2,3-dimethyl-1,3-butadiene (108 µL, 956 µmol, 4.0 eq). The vial was then capped, sealed with electrical tape, and heated to 130 °C for 48 h. Upon cooling, the crude reaction mixture was concentrated and subjected directly to

preparatory TLC (20/80 ethyl acetate in hexanes) to afford pure 2-((4-butylphenyl)difluoromethyl)-4,5-dimethylpyridine **12c** as a colorless oil (10.4 mg, 15% yield).

^{1}H NMR (500 MHz, $CDCl_3$) δ 8.4 (s, 1H), 7.54 – 7.42 (m, 3H), 7.21 (d, J = 7.9 Hz, 2H), 2.62 (t, J = 7.8 Hz, 2H), 2.31 (s, 3H), 2.28 (s, 3H), 1.7 (d, J = 13.5 Hz, 2H), 1.32 (h, J = 7.3 Hz, 2H), 0.93 (t, J = 7.4 Hz, 3H).
^{19}F NMR (470 MHz, $CDCl_3$) δ -93.82

*2-(4-butylphenyl)-2,2-difluoroacetamide (**12d**)*[81]

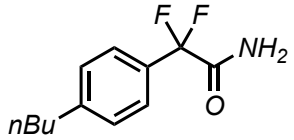

A 4 mL vial equipped with a Teflon magnetic stir bar was charged with 2,2-difluoro-2-phenylacetonitrile (21.0 mg, 0.1 mmol, 1.0 eq) and phenol (19.0 mg, 0.2 mmol) in 33% HBr/AcOH (300 mg) and was stirred for 18 h at room temperature. After this time, the reaction mixture was extracted with diethyl ether, dried over sodium sulfate, and concentrated in vacuo to provide 2,2-difluoro-2-phenylacetamide **12d** as a white solid (18.2 mg, 80% yield).

^{1}H NMR (500 MHz, $CDCl_3$) δ 7.53 (d, J = 8.2 Hz, 2H), 7.27 (d, J = 7.4 Hz, 2H), 6.27 (d, 2H), 2.65 (t, J = 7.7 Hz, 2H), 1.61 (m, 2H), 1.36 (m, 2H), 0.93 (t, J = 7.4 Hz, 3H).
^{13}C NMR (151 MHz, $CDCl_3$) δ 166.67 (t, J = 32.4 Hz), 146.39, 130.01 (t, J = 25.3 Hz), 125.84, 125.53 (t, J = 6.2 Hz), 114.97 (t, J = 252.3 Hz), 35.59, 33.48, 22.42, 14.03.
^{19}F NMR (565 MHz, $CDCl_3$) δ -102.21

*2-(difluoro(phenyl)methyl)-4,5-dihydrothiazole-4-carboxylic acid (**12e**)*[92]

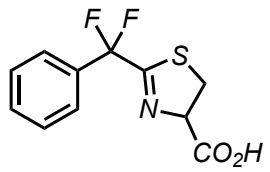

A 20 mL vial equipped with a Teflon magnetic stir bar was charged with 2,2-difluoro-2-phenylacetonitrile (76.6 mg, 0.5 mmol, 1.0 eq) and L-Cysteine (92.0 mg, 0.75 mmol, 1.5 eq). Then methanol (5.0 mL) and the reaction mixture was stirred at 50°C for 15 min. After this time, the solvent was removed in vacuo and the resulting residue was dissolved in dichloromethane. The excess of L-cysteine was filtered out with a syringe to provide 2-(difluoro(phenyl)methyl)-4,5-dihydrothiazole-4-carboxylic acid **12e** as a colorless oil in quantitative yield (128.6 mg, 100% yield).

^{1}H NMR (500 MHz, $CDCl_3$) δ 7.52 (d, J = 9.5 Hz, 2H), 7.34 (m, 3H), 7.05 (s, 1H), 3.50 (m, 2H).
^{13}C NMR (151 MHz, $CDCl_3$) δ 175.35, 166.40 (t, J = 32.2 Hz), 133.90 (t, J = 26.4 Hz), 131.10, 128.82, 125.57 (t, J = 6.0 Hz), 116.67 (t, J = 245.7 Hz), 80.65, 36.74.
^{19}F NMR (565 MHz, $CDCl_3$) δ -93.08.

*2-(difluoro(phenyl)methyl)benzo[d]thiazole (**12f**)*

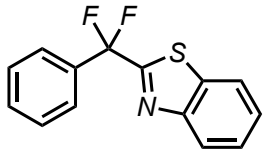

A 20 mL vial was charged with 2,2-difluoro-2-phenylacetonitrile (76.6 mg, 0.5 mmol, 1.0 eq). Then, a solution of 2-aminobenzenethiol (93.9 mg, 0.75 mmol, 1.5 eq) in dry methanol (5.0 mL) was added, and a Teflon stir bar was added. The headspace was flushed with nitrogen, the vial was sealed, and the reaction mixture was stirred at room temperature for 1 hour. After this time, the solvent was removed in vacuo and the resulting residue was purified by column chromatography (1/99 to 10/90 ethyl acetate in hexanes) to provide 2-(difluoro(phenyl)methyl)benzo[d]thiazole **12f** as a colorless viscous liquid (121.6 mg, 93% yield)

^{1}H NMR (600 MHz, $CDCl_3$) δ 8.11 (d, J = 8.2 Hz, 1H), 7.95 (d, J = 8.0 Hz, 1H), 7.75 – 7.70 (m, 2H), 7.53 (ddd, J = 8.3, 7.1, 1.3 Hz, 1H), 7.50 – 7.45 (m, 4H).
^{13}C NMR (151 MHz, $CDCl_3$) δ 165.2 (t, J = 36.5 Hz), 153.0, 135.2, 135.1 (t, J = 26.5 Hz), 130.9 (t, J = 1.5 Hz), 128.7, 126.8, 126.6, 126.0 (t, J = 5.8 Hz), 124.6, 122.0, 117.5 (t, J = 243.6 Hz).
^{19}F NMR (565 MHz, $CDCl_3$) δ -87.01.

*2-(difluoro(phenyl)methyl)benzo[d]oxazole (**12g**)*

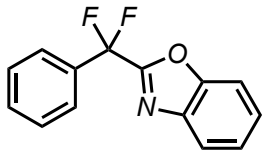

A 20 mL vial was charged with 2,2-difluoro-2-phenylacetonitrile (76.6 mg, 0.5 mmol, 1.0 eq). Then, a solution of 2-aminophenol (81.8 mg, 0.75 mmol, 1.5 eq) in dry methanol (5.0 mL) was added, and a Teflon stir bar was added. The headspace was flushed with nitrogen, the vial was sealed, and the reaction mixture was heated in a heating block at 65 °C for 24 hours. After this time, the solvent was removed in vacuo and the resulting residue was purified by column chromatography (1/99 to 10/90 ethyl acetate in hexanes) to provide 2-(difluoro(phenyl)methyl)benzo[d]oxazole **12g** as a colorless viscous liquid (107.1 mg, 87% yield).

^{1}H NMR (600 MHz, $CDCl_3$) δ 7.82 (d, J = 7.6 Hz, 1H), 7.75 – 7.71 (m, 2H), 7.59 (d, J = 7.9 Hz, 1H), 7.55 – 7.47 (m, 3H), 7.44 (td, J = 7.8, 1.4 Hz, 1H), 7.40 (td, J = 7.6, 1.2 Hz, 1H).
^{13}C NMR (151 MHz, $CDCl_3$) δ 158.6 (t, J = 36.8 Hz), 150.9, 140.2, 133.7 (t, J = 26.0 Hz), 131.3 (t, J = 1.4 Hz), 128.9, 126.9, 125.8 (t, J = 5.8 Hz), 125.4, 121.5, 114.6 (t, J = 243.8 Hz), 111.5.
^{19}F NMR (565 MHz, $CDCl_3$) δ -95.30.

*2-(difluoro(phenyl)methyl)-1-methyl-1H-benzo[d]imidazole (**12h**)*

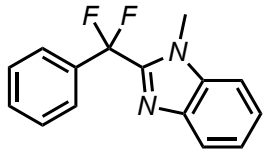

A 20 mL vial was charged with 2,2-difluoro-2-phenylacetonitrile (78.5 mg, 0.5 mmol, 1.0 eq). Then, a solution of freshly vacuum distilled N1-methylbenzene-1,2-diamine (183.3 mg, 1.5 mmol, 3.0 eq) in dry methanol (5.0 mL) was added, followed by ammonium chloride (26.7 mg, 0.5 mmol, 1.0 eq) and a Teflon stir bar. The headspace was flushed with nitrogen, and the vial was sealed with a Teflon cap and heated at 65 °C in a heating block for 24 hours. After this time, the reaction was cooled to room temperature and concentrated in vacuo. The resulting residue was purified by column chromatography (5/95 to 15/85 ethyl

acetate in hexanes) to provide 2-(difluoro(phenyl)methyl)-1-methyl-1H-benzo[d]imidazole **12h** as a colorless oil (124.2 mg, 94% yield).

^{1}H NMR (600 MHz, $CDCl_3$) δ 7.91 (d, J = 8.0 Hz, 1H), 7.67 (d, J = 6.5 Hz, 2H), 7.53 – 7.42 (m, 3H), 7.40 (m, 2H), 7.32 (m, 1H), 3.91 (s, 3H).

^{19}F NMR (470 MHz, $CDCl_3$) δ -89.01

^{13}C NMR (126 MHz, $CDCl_3$) δ 147.2 (t, J = 33.0 Hz), 141.2, 136.4, 134.5 (t, J = 25.6 Hz), 130.7 (t, J = 1.9 Hz), 128.5, 125.9 (t, J = 5.6 Hz), 124.2, 122.7, 121.1, 117.1 (t, J = 240.0 Hz), 109.7, 30.9

*(S)-2,2-difluoro-2-phenyl-N-(1-phenylethyl)ethan-1-amine (**12i**)*[77]

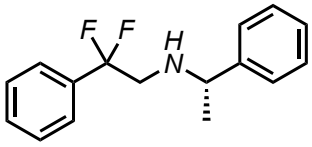

To a flame-dried glass vial in the glovebox equipped with stir bar was added nickel (II) triflate (4.50 mg, 12.5 µmol, 5 mol%), ((Phenylphosphinediyl)bis(ethane-2,1-diyl))bis(diphenylphosphine) (8.0 mg, 15.0 µmol, 6 mol%), and degassed TFE (1.25 mL). This was stirred at rt in the glovebox for 15 minutes; then, 2,2-difluoro-2-phenylacetonitrile (38.3 mg, 0.25 mmol, 1.0 eq) was added followed by (S)-(-)-1-Phenylethylamine (161 µL, 1.25 mmol, 5.0 eq). The vial was fitted with a septum cap and needle, then placed into a parr bomb. The bomb was sealed and the assembly was removed from the glovebox. The bomb was flushed with H_2 (20 bar, 2x) then pressurized to with H_2 (40 bar). This was stirred at 130°C (block temperature) for 16 h. After this time, the reaction mixture was cooled, and the resulting residue was purified by column chromatography (10/90 ethyl acetate in hexanes) to provide (S)-2,2-difluoro-2-phenyl-N-(1-phenylethyl)ethan-1-amine **12i** as a colorless oil (62.1 mg, 95% yield).

^{1}H NMR (500 MHz, $CDCl_3$) δ 7.64 – 7.59 (m, 2H), 7.52 – 7.48 (m, 1H), 7.44 (t, J = 7.5 Hz, 2H), 7.40 – 7.33 (m, 2H), 7.30 – 7.27 (m, 3H), 6.64 (s, 1H), 5.10 (p, J = 7.2 Hz, 1H), 1.66 – 1.58 (m, 5H).

^{19}F NMR (470 MHz, $CDCl_1$) δ -102.32 (d, J = 43.7 Hz).

*(Z)-2-(4-butylphenyl)-2,2-difluoro-N'-hydroxyacetimidamide (**12j**)*[93]

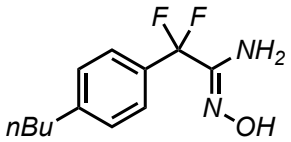

A 4 mL vial equipped with a Teflon magnetic stir bar was charged with 2,2-difluoro-2-phenylacetonitrile (21.0 mg, 0.1 mmol, 1.0 eq) and a 50wt% aqueous hydroxylamine solution (7.92 mg, 0.12 mmol, 1.2 eq). EtOH (0.1 M) was added and the mixture was stirred at room temperature for 18 h. After this time, the reaction mixture was concentrated under reduced pressure and the residue was purified by flash column chromatography (10/90 ethyl acetate in hexanes) to provide (Z)-2-(4-butylphenyl)-2,2-difluoro-N'-hydroxyacetimidamide **12j** as a white powder (18.2 mg, 75% yield).

^{1}H NMR (500 MHz, $CDCl_3$) δ 7.87 (s, 1H), 7.44 (d, J = 8.3 Hz, 2H), 7.24 (d, J = 8.3 Hz, 2H), 4.79 (s, 2H), 2.65 (t, J = 7.7 Hz, 2H), 1.61 (m, 2H), 1.36 (m, 2H), 0.93 (t, J = 7.4 Hz, 3H).
^{13}C NMR (151 MHz, $CDCl_3$) δ 149.75 (t, J = 32.2 Hz), 145.85, 130.88 (t, J = 25.7 Hz), 128.51, 125.90 (t, J = 5.8 Hz), 116.94 (t, J = 242.2 Hz), 35.69, 33.48, 22.40, 14.05.
^{19}F NMR (565 MHz, $CDCl_3$) δ -97.32

*2,2-difluoro-1,2-diphenylethan-1-one (**12k**)*

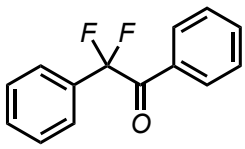

The title compound was prepared according to the following procedure. In a nitrogen-filled glovebox, a 25 mL Schlenk flask with a Teflon plug was charged with 2,2-difluoro-2-phenylacetonitrile (76.6 mg, 0.5 mmol, 1.0 eq) and dry, degassed THF (1.5 mL). The schlenk bomb was sealed and taken out of glovebox, where it was cooled in a dry ice/acetone bath (–78 °C) under nitrogen. Then, a solution of phenyl magnesium bromide (1.0 M, 0.52 mL, 0.52 mmol, 1.05 eq) was added dropwise with a gas-tight syringe with stirring. After complete addition, the reaction mixture was transferred to a water ice bath (0°C) and stirred on ice for 4 h. After this time, 3 M HCl was added on ice dropwise (2 mL). The resulting mixture was heated to 65 °C for 20 hours. After this time, the reaction mixture

was extracted with DCM, dried over sodium sulfate, and concentrated in vacuo. The resulting residue was purified by column chromatography (1/99 to 4/96 ethyl acetate in hexanes) to provide 2,2-difluoro-1,2-diphenylethan-1-one **12k** as a colorless liquid (99.7 mg, 86% yield).

^{1}H NMR (600 MHz, $CDCl_3$) δ 8.04 (d, J = 7.5 Hz, 2H), 7.62 (d, J = 6.6 Hz, 2H), 7.59 (ddt, J = 8.7, 7.2, 1.3 Hz, 1H), 7.51 – 7.42 (m, 5H).
^{13}C NMR (151 MHz, $CDCl_3$) δ 189.1 (t, J = 31.0 Hz), 134.3, 133.3 (t, J = 25.1 Hz), 132.3, 131.1 (t, J = 1.5 Hz), 130.4 (t, J = 2.9 Hz), 129.0, 128.8, 125.8 (t, J = 6.0 Hz), 117.1 (t, J = 253.2 Hz).
^{19}F NMR (565 MHz, $CDCl_3$) δ -97.5.

*2,2-difluoro-1-(4-methoxyphenyl)-2-phenylethan-1-on (**12l**)*

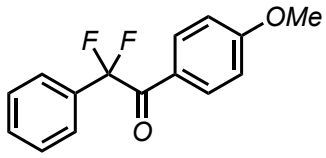

In a nitrogen-filled glovebox, a 25 mL Schlenk flask with a Teflon plug was charged with 2,2-difluoro-2-phenylacetonitrile (76.6 mg, 0.5 mmol, 1.0 eq) and dry, degassed THF (1.5 mL). The Schlenk bomb was sealed and taken out of glovebox, where it was cooled in a dry ice/acetone bath (–78 °C) under nitrogen. Then, a solution of para-methoxy phenyl magnesium bromide (0.5 M, 1.0 mL, 0.52 mmol, 1.05 eq) was added dropwise with stirring. After complete addition, the reaction mixture was transferred to a water ice bath (0 °C) and stirred on ice for 4 h. After this time, 3 M HCl was added on ice dropwise (2 mL). The resulting mixture was heated to 60°C for 18 hours. After this time, the reaction mixture was extracted with diethyl ether, dried over sodium sulfate, and concentrated in vacuo. The resulting residue was purified by column chromatography (1/99 to 8/92 ethyl acetate in hexanes) to provide 2,2-difluoro-1-(4-methoxyphenyl)-2-phenylethan-1-one **12l** as a colorless liquid (113.7 mg, 87% yield).

^{1}H NMR (600 MHz, $CDCl_3$) δ 8.04 (d, J = 9.0 Hz, 2H), 7.64 – 7.59 (m, 2H), 7.50 – 7.42 (m, 3H), 6.91 (d, J = 9.1 Hz, 2H), 3.85 (s, 3H).

^{13}C NMR (151 MHz, $CDCl_3$) δ 187.4 (t, J = 30.4 Hz), 164.5, 133.7 (t, J = 25.1 Hz), 133.0 (t, J = 3.1 Hz), 130.9, 128.9, 125.7 (t, J = 6.0 Hz), 125.1, 117.2 (t, J = 252.9 Hz), 114.1, 55.7.
^{19}F NMR (565 MHz, $CDCl_3$) δ -96.2.

*propyl 2,2-difluoro-2-phenylethanimidothioate (**12m**)*

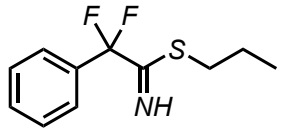

A 50 mL round bottomed flask equipped with a magnetic stir bar was charged with 2,2-difluoro-2-phenylacetonitrile (79.0 mg, 0.52 mmol, 1.0 eq), acetonitrile (4 mL), and water (1 mL). The headspace was flushed with nitrogen and propanethiol (464 µL, 5.0 mmol, 10 eq) was added dropwise. The resulting solution was stirred at room temperature for 2 hours. After this time, the solvent was removed in vacuo through a Schlenk line. The resulting residue was taken up in dichloromethane, dried over sodium sulfate, and concentrated. Purification by column chromatography (2/98 to 20/80 ethyl acetate in hexanes) provided propyl 2,2-difluoro-2-phenylethanimidothioate **12m** as a colorless liquid (101.4 mg, 86% yield).

^{1}H NMR (600 MHz, $CDCl_3$) δ 9.56 (br s, 1H), 7.57 (d, J = 7.4 Hz, 2H), 7.51 – 7.43 (m, 3H), 2.91 (t, J = 7.3 Hz, 2H), 1.68 (h, J = 7.3 Hz, 2H), 1.00 (t, J = 7.4 Hz, 3H).
^{13}C NMR (151 MHz, $CDCl_3$) δ 173.6 (t, J = 32.1 Hz), 133.9 (t, J = 26.6 Hz), 130.9, 128.7, 125.6 (t, J = 6.0 Hz), 116.7 (t, J = 249.1 Hz), 31.7, 21.8, 13.6.
^{19}F NMR (565 MHz, $CDCl_3$) δ -97.0.

Compound characterization

The project is still ongoing and for this reason the characterization of some molecules is not complete.

*2-((4-butylphenyl)difluoromethyl)-1-methyl-1H-benzo[d]imidazole (**6a**)*

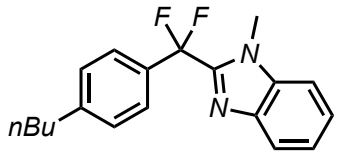

The title compound was prepared by performing General Procedure 1 then General Procedure 2 on the corresponding (hetero)Aryl Iodide: 88% yield (yellow oil).

^{1}H NMR (500 MHz, $CDCl_3$) δ 7.90 (d, J = 8.1 Hz, 1H), 7.52 (d, J = 8.0 Hz, 2H), 7.39 (m, 2H), 7.31 (m, 3H), 3.99 (s, 3H), 2.70 (t, J = 7.8 Hz, 2H), 1.72 – 1.63 (m, 2H), 1.40 (q, J = 7.4 Hz, 2H), 0.94 (t, J = 7.4 Hz, 3H).

^{19}F NMR (470 MHz, $CDCl_3$) δ -88.3.

^{13}C NMR: (126 MHz, $CDCl_3$) δ 146.10, 141.41. 136.52, 128.83, 126.11 (t, J = 6.3 Hz), 124.52, 123.01, 121.40, 109.91, 35.72, 33.41, 31.31, 22.50, 14.14

*2-((4-chlorophenyl)difluoromethyl)-1-methyl-1H-benzo[d]imidazole (**6b**)*

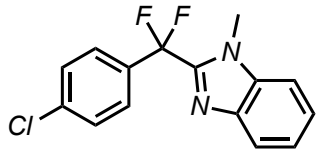

The title compound was prepared by performing General Procedure 1 then General Procedure 2 on the corresponding (hetero)Aryl Iodide: 69% yield (yellow solid)

^{1}H NMR (500 MHz, $CDCl_3$) δ 7.85 (d, J = 8.2 Hz, 1H), 7.61 (d, J = 8.3 Hz, 2H), 7.54 (d, J = 8.3 Hz, 2H), 7.40 (q, J = 8.4 Hz, 2H), 7.31 (m, 1H), 4.0 (s, 3H).

^{19}F NMR (470 MHz, $CDCl_3$) δ -88.41.

^{13}C NMR (126 MHz, $CDCl_3$) δ 146.91 (t, J = 33.2 Hz), 141.32, 137.1 (t, J = 2.5 Hz), 136.40, 133.01 (t, J = 26.0 Hz), 128.94, 127.73 (t, J = 5.8 Hz), 124.61, 123.0, 121.42, 117.09 (t, J = 239.7 Hz), 109.81, 31.18 (t, J = 3.9 Hz).

*2-(difluoro(4-fluorophenyl)methyl)-1-methyl-1H-benzo[d]imidazole (**6c**)*

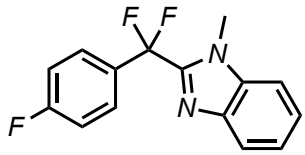

The title compound was prepared by performing General Procedure 1 then General Procedure 2 on the corresponding (hetero)Aryl Iodide: 84% yield (yellow oil)

^{1}H NMR (500 MHz, $CDCl_3$) δ 7.72 (d, J = 8.2 Hz, 1H), 7.60 (d, J = 8.3 Hz, 2H), 7.53 (d, J = 8.4 Hz, 2H), 7.42 (m, 2H), 7.30 (ddd, J = 8.3, 6.6, 1.6 Hz, 1H), 3.98 (t, J = 1.2 Hz, 3H).

^{19}F NMR (470 MHz, $CDCl_3$): δ -89.12.

*2-((4-bromophenyl)difluoromethyl)-1-methyl-1H-benzo[d]imidazole (**6d**)*

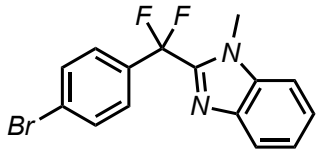

The title compound was prepared by performing General Procedure 1 then General Procedure 2 on the corresponding (hetero)Aryl Iodide: 55% yield (yellow solid)

^{1}H NMR (500 MHz, $CDCl_3$) δ 7.81 (d, J = 8.1 Hz, 1H), 7.65 (d, J = 8.3 Hz, 2H), 7.53 (d, J = 8.4 Hz, 2H), 7.41 (m, 2H), 7.33 (ddd, J = 8.3, 6.6, 1.6 Hz, 1H), 4.01 (t, J = 1.1 Hz, 3H).

^{19}F NMR (470 MHz, $CDCl_3$) δ -88.63.

^{13}C NMR (126 MHz, $CDCl_3$) δ 146.78 (t, J = 33.2 Hz), 141.31, 136.52, 133.47 (t, J = 26.0 Hz), 131.84, 127.88 (t, J = 5.8 Hz), 125.50 (t, J = 2.5 Hz), 124.61, 122.91, 121.43, 117.07 (t, J = 239.7 Hz), 109.80, 31.11 (t, J = 3.9 Hz).

*2-(difluoro(4-methoxyphenyl)methyl)-1-methyl-1H-benzo[d]imidazole (**6e**)*

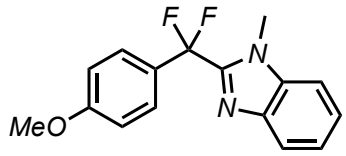

The title compound was prepared by performing General Procedure 1 then General Procedure 2 on the corresponding (hetero)Aryl Iodide: 74% yield (yellow oil)

^{1}H NMR (500 MHz, $CDCl_3$) δ 7.90 (d, J = 8.1 Hz, 1H), 7.61 (d, J = 8.5 Hz, 2H), 7.43 (m, 2H), 7.34 (ddd, J = 8.2, 6.4, 1.9 Hz, 1H), 7.01 (d, J = 8.6 Hz, 2H), 4.02 (s, 3H), 3.94 (s, 3H).

^{19}F NMR (470 MHz, $CDCl_3$) δ -87.23.

^{13}C NMR (126 MHz, $CDCl_3$) δ 161.61, 150.50. 136.49, 127.81 (t, J = 5.1 Hz), 124.48, 123.11, 121.43, 114.13, 109.87, 55.53, 31.35.

*tert-butyl (4-(difluoro(1-methyl-1H-benzo[d]imidazol-2-yl)methyl)phenyl)carbamate (**6f**)*

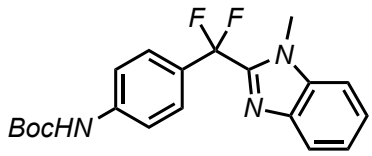

The title compound was prepared by performing General Procedure 1 then General Procedure 2 on the corresponding (hetero)Aryl Iodide: 41% yield (yellow solid).

^{1}H NMR (500 MHz, $CDCl_3$) δ 7.84 (d, J = 8.3 Hz, 1H), 7.62 (d, J = 8.8 Hz, 2H), 7.51 (m, 2H), 7.30 (m, 1H), 7.01 (d, J = 8.6 Hz, 2H), 4.02 (s, 3H), 1.54 (s, 9H).

^{19}F NMR (470 MHz, $CDCl_3$) δ -88.01.

^{13}C NMR: (126 MHz, $CDCl_3$) δ 152.40, 147.55. 141.37, 135.41, 128.74 (t, J = 26.5 Hz), 127.08 (t, J = 6.3 Hz), 124.31, 122.82, 121.30, 118.02, 109.69, 31.10 (t, J = 3.8 Hz), 28.32

*methyl 4-(difluoro(1-methyl-1H-benzo[d]imidazol-2-yl)methyl)benzoate (**6g**)*

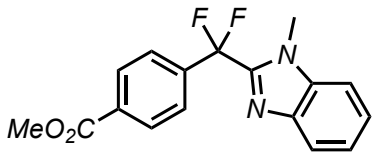

The title compound was prepared by performing General Procedure 1 then General Procedure 2 on the corresponding (hetero)Aryl Iodide: 58% yield (brown solid)

^{1}H NMR (500 MHz, $CDCl_3$) δ 8.21 (d, J = 8.1 Hz, 2H), 7.80 (d, J = 8.2 Hz, 1H), 7.72 (d, J = 8.1 Hz, 2H), 7.53 – 7.41 (m, 2H), 7.31 (t, J = 7.4 Hz, 1H), 3.98 (s, 3H), 3.94 (s, 3H).

^{19}F NMR (470 MHz, $CDCl_3$) δ -89.43.

^{13}C NMR: (126 MHz, $CDCl_3$) δ 165.20, 145.71 (t, J = 27.7 Hz), 140.32, 137.69 (t, J = 21.4 Hz), 135.41, 131.42, 128.87, 125.31 (t, J = 5.0 Hz), 123.60, 121.91, 120.29, 116.01 (t, J = 200.1 Hz), 108.80, 51.41, 30.08 (t, J = 2.5 Hz).

*2-(difluoro(4-nitrophenyl)methyl)-1-methyl-1H-benzo[d]imidazole (**6h**)*

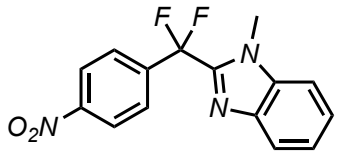

The title compound was prepared by performing General Procedure 1 then General Procedure 2 on the corresponding (hetero)Aryl Iodide: 38% yield (orange solid)

^{1}H NMR (500 MHz, $CDCl_3$) δ 8.44 (d, J = 8.4 Hz, 2H), 7.90 (d, J = 8.4 Hz, 2H), 7.82 (d, J = 8.2 Hz, 1H), 7.44 (dt, J = 15.0, 8.0 Hz, 2H), 7.31 (t, J = 7.6 Hz, 1H), 4.10 (s, 3H).

^{19}F NMR (470 MHz, $CDCl_3$) δ -89.10.

^{13}C NMR: (126 MHz, $CDCl_3$) δ 149.40, 146.11 (t, J = 27.7 Hz), 141.22, 140.55 (t, J = 21.4 Hz), 136.54, 127.77 (t, J = 5.0 Hz), 124.91, 123.62, 123.10, 121.36, 118.41, 116.95 (t, J = 200.3 Hz), 109.91, 31.20 (t, J = 2.5 Hz).

*2-(difluoro(2-(trifluoromethyl)phenyl)methyl)benzo[d]oxazole (**7i**)*

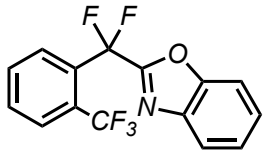

The title compound was prepared by performing General Procedure 1 then General Procedure 3 on the corresponding (hetero)Aryl Iodide: 53% yield (yellow solid)

^{1}H NMR (500 MHz, $CDCl_3$) δ 8.03 (d, J = 7.9 Hz, 1H), 7.91 (d, J = 7.8 Hz, 1H), 7.80 (dt, J = 8.1, 3.9 Hz, 2H), 7.72 (t, J = 7.8 Hz, 1H), 7.61 (d, J = 8.2 Hz, 1H), 7.54 (t, J = 7.8 Hz, 1H), 7.40 (t, J = 7.7 Hz, 1H).

^{19}F NMR (470 MHz, $CDCl_3$) δ -58.21 (t, J = 12.5 Hz), -90.61 (q, J = 12.7 Hz).

^{13}C NMR: 126 MHz, $CDCl_3$) δ 158.21 (t, J = 27.0 Hz), 150.62, 140.00, 132.11, 131.21, 128.37 (t, J = 6.3 Hz), 127.91 (q, J = 5.0 Hz), 127.02, 125.34, 124.18, 122.33, 121.41, 113.68 (t, J = 204.1 Hz), 111.50.

*2-((2-bromophenyl)difluoromethyl)benzo[d]oxazole (**7j**)*

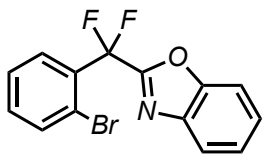

The title compound was prepared by performing General Procedure 1 then General Procedure 3 on the corresponding (hetero)Aryl Iodide: 35% yield (yellow oil)

^{1}H NMR (500 MHz, $CDCl_3$) δ 7.74 (m, 2H), 7.60 (m, 1H), 7.52 (t, J = 7.5 Hz, 1H), 7.51 – 7.40 (m, 2H), 7.39 (m, 1H), 7.31 (m, 1H).

^{19}F NMR (470 MHz, $CDCl_3$) δ -89.10.

^{13}C NMR: (126 MHz, $CDCl_3$) δ 157.7, 150.5, 140.3, 134.6, 132.7, 128.9 (t, J = 7.7 Hz), 127.6, 125.3, 121.5, 111.5.

*2-([1,1'-biphenyl]-2-yldifluoromethyl)benzo[d]oxazole (**7k**)*

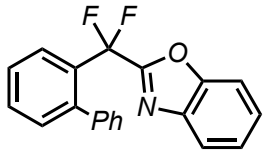

The title compound was prepared by performing General Procedure 1 then General Procedure 3 on the corresponding (hetero)Aryl Iodide: 74% yield (yellow oil)

^{1}H NMR (500 MHz, $CDCl_3$) δ 8.01 – 7.92 (m, 1H), 7.6 (m, 1H), 7.64 – 7.55 (m, 2H), 7.42 – 7.34 (m, 3H), 7.30 (d, J = 4.1 Hz, 1H), 7.11 (tt, J = 8.5, 4.0 Hz, 1H), 7.02 (d, J = 4.5 Hz, 4H).

^{19}F NMR (470 MHz, $CDCl_3$) δ -88.29.

^{13}C NMR (126 MHz, $CDCl_3$) δ 157.9 (t, J = 34.9 Hz), 149.7, 141.5 (t, J = 3.8 Hz), 139.6, 138.6, 131.4 (t, J = 23.8 Hz), 131.2, 130.4, 128.7, 127.1,126.8, 126.8, 126.0, 125.4 (t, J = 7.8 Hz), 124.5, 120.6, 113.8 (t, J = 243.0 Hz), 110.6.

*2-(difluoro(2-isopropylphenyl)methyl)benzo[d]oxazole (**7l**)*

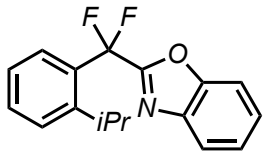

The title compound was prepared by performing General Procedure 1 then General Procedure 3 on the corresponding (hetero)Aryl Iodide: 65% yield (yellow oil)

^{1}H NMR (500 MHz, $CDCl_3$) δ 7.79 (d, J = 7.9 Hz, 1H), 7.70 (dd, J = 7.9, 1.4 Hz, 1H), 7.63 (m, 1H), 7.50 (t, J = 7.5 Hz, 1H), 7.50 – 7.41 (m, 2H), 7.39 (m, 1H), 7.31 (t, J = 7.6 Hz, 1H), 3.11 (p, J = 6.9 Hz, 1H), 1.12 (d, J = 6.8 Hz, 6H).

^{19}F NMR (470 MHz, $CDCl_3$) δ -90.90.

^{13}C NMR: (126 MHz, $CDCl_3$) δ 159.0 (t, J = 29.6 Hz), 150.7, 148.3 (t, J = 2.4 Hz), 140.1, 131.5, 130.2 (t, J = 18.9 Hz), 127.3, 126.8, 125.9, 125.7 (t, J = 7.7 Hz), 125.3, 121.4, 114.9 (t, J = 202.9 Hz), 111.4, 29.8, 24.1.

*2-([1,1'-biphenyl]-3-yldifluoromethyl)benzo[d]oxazole (**7m**)*

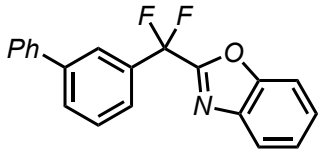

The title compound was prepared by performing General Procedure 1 then General Procedure 3 on the corresponding (hetero)Aryl Iodide: 68% yield (yellow oil).

^{1}H NMR (500 MHz, $CDCl_3$) δ 7.90 (d, J = 1.9 Hz, 1H), 7.81 (m, 1H), 7.73 (d, J = 7.8 Hz, 1H), 7.70 (m, 1H), 7.6 – 7.5 (m, 4H), 7.52 – 7.34 (m, 5H).

^{19}F NMR (470 MHz, $CDCl_3$) δ -95.24.

^{13}C NMR: (126 MHz, $CDCl_3$) δ 158.5 (t, J = 30.2 Hz), 158.8, 142.0, 140.1, 140.0, 134.2 (t, J = 21.4 Hz), 129.9, 129.2, 128.9, 127.9, 127.3, 126.8, 125.3, 124.4, 121.4, 116.3, 114.5 (t, J = 204.1 Hz), 111.4.

*2-((3-(tert-butyl)phenyl)difluoromethyl)benzo[d]oxazole (**7n**)*

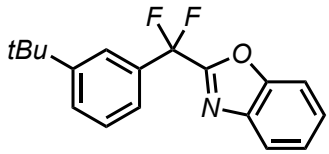

The title compound was prepared by performing General Procedure 1 then General Procedure 3 on the corresponding (hetero)Aryl Iodide: 74% yield (yellow oil)

^{1}H NMR (500 MHz, $CDCl_3$) δ 7.82 (d, J = 7.8 Hz, 1H), 7.70 (s, 1H), 7.61 (d, J = 8.0 Hz, 1H), 7.52 (dd, J = 14.0, 7.8 Hz, 2H), 7.41 (dd, J = 11.7, 7.4 Hz, 3H), 1.32 (s, 9H).

^{19}F NMR (470 MHz, $CDCl_3$) δ -95.02.

^{13}C NMR (126 MHz, $CDCl_3$) δ 158.8 (t, *J* = 37.2 Hz), 152.1, 150.9, 140.3, 133.4 (t, J = 25.6 Hz), 128.6, 128.4, 126.8, 125.4, 123.1 (t, J = 5.8 Hz), 122.4 (t, J = 5.9 Hz), 121.5, 114.8 (t, J = 243.8 Hz), 111.5, 35.1, 31.4.

*1-(3-(benzo[d]oxazol-2-yldifluoromethyl)phenyl)ethan-1-one (**7o**)*

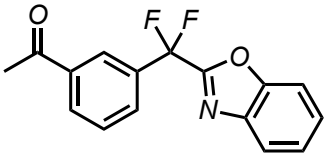

The title compound was prepared by performing General Procedure 1 then General Procedure 3 on the corresponding (hetero)Aryl Iodide: 53% yield (orange solid).

^{1}H NMR (500 MHz, $CDCl_3$) δ 8.30 (s, 1H), 8.13 (d, J = 7.8 Hz, 1H), 7.90 (d, J = 7.9 Hz, 1H), 7.83 (d, J = 8.1 Hz, 1H), 7.59 (dd, J = 13.1, 7.6 Hz, 2H), 7.50 (t, J = 7.7 Hz, 1H), 7.42 (t, J = 7.5 Hz, 1H), 2.71 (s, 3H).

^{19}F NMR (470 MHz, $CDCl_3$) δ -95.22.

^{13}C NMR: (126 MHz, $CDCl_3$) δ 196.9, 158.0 (t, J = 36.5 Hz), 150.8, 140.0, 137.6, 134.3, 130.9, 130.2 (t, J = 5.1 Hz), 129.3, 127.0, 125.7 (t, J = 6.3 Hz), 121.5, 114.0 (t, J = 244.5 Hz), 111.5, 26.7

*2-((2,6-dichlorophenyl)difluoromethyl)benzo[d]thiazolecarboxylate (**8p**)*

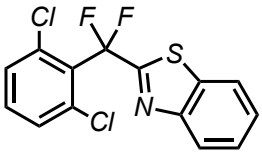

The title compound was prepared by performing General Procedure 1 then General Procedure 4 on the corresponding (hetero)Aryl Iodide: 66% yield (yellow oil).

^{1}H NMR (500 MHz, $CDCl_3$) δ 8.13 – 8.03 (m, 1H), 8.00 (m, 1H), 7.52 (m, 2H), 7.43 (q, J = 0.9 Hz, 1H), 7.40 (d, J = 1.1 Hz, 1H), 7.32 (ddt, J = 8.5, 7.4, 0.9 Hz, 1H).

^{19}F NMR (470 MHz, $CDCl_3$) δ -79.80.

^{13}C NMR (126 MHz, $CDCl_3$) δ 164.3 (t, J = 34.7 Hz), 152.5, 135.6, 135.3 (t, J = 2.6 Hz), 131.7, 130.9, 130.1 (t, J = 23.4 Hz), 126.8 (d, J = 9.7 Hz), 124.9, 122.1, 117.4 (t, J = 246.0 Hz).

*2-((2-ethyl-6-methylphenyl)difluoromethyl)benzo[d]thiazole (**8q**)*

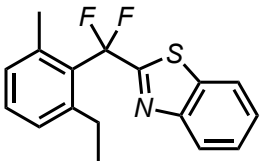

The title compound was prepared by performing General Procedure 1 then General Procedure 4 on the corresponding (hetero)Aryl Iodide: 68% yield (yellow oil).

^{1}H NMR (500 MHz, $CDCl_3$) δ 8.12 (d, J = 8.1 Hz, 1H), 7.94 (d, J = 8.0 Hz, 1H), 7.53 – 7.42 (m, 2H), 7.32 (t, J = 7.6 Hz, 1H), 7.20 (d, J = 7.7 Hz, 1H), 7.12 (d, J = 7.6 Hz, 1H), 2.82 – 2.74 (m, 2H), 2.49 (t, J = 4.6 Hz, 3H), 1.24 (t, J = 7.5 Hz, 3H).

^{19}F NMR (470 MHz, $CDCl_3$) δ -76.84.

^{13}C NMR (126 MHz, $CDCl_3$) δ 165.8 (t, J = 36.1 Hz), 152.8, 144.4 (t, J = 2.8 Hz), 137.8 (t, J = 3.1 Hz), 135.6, 131.3 (t, J = 22.7 Hz), 130.4 (d, J = 10.3 Hz), 129.2, 126.7 (d, J = 7.2 Hz), 124.9, 122.0, 119.9 (t, J = 243.7 Hz), 28.5 (t, J = 5.2 Hz), 22.8 (t, J = 6.3 Hz), 16.9 (d, J = 2.2 Hz).

*2-(dibenzo[b,d]furan-4-yldifluoromethyl)benzo[d]thiazole (**8r**)*

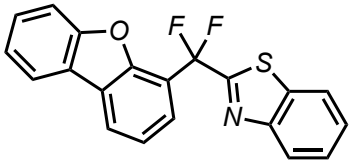

The title compound was prepared by performing General Procedure 1 then General Procedure 4 on the corresponding (hetero)Aryl Iodide: 82% yield (white solid).

^{1}H NMR (500 MHz, $CDCl_3$) δ 8.21 (dd, *J* = 7.7, 1.1 Hz, 1H), 8.01 (d, *J* = 7.8 Hz, 1H), 7.69 (dd, *J* = 11.7, 7.6 Hz, 1H), 7.61 – 7.54 (m, 1H), 7.40 (dt, *J* = 21.4, 7.6 Hz, 2H).

^{19}F NMR (470 MHz, $CDCl_3$) δ -85.10

^{13}C NMR (126 MHz, $CDCl_3$) δ 156.6, 152.1 (t, J = 2.5 Hz), 128.5, 126.4, 125.2 (t, J = 1.3 Hz), 123.7, 123.5 (t, J = 6.3 Hz), 122.8, 122.7, 120.9, 115.4 (t, J = 26.5 Hz), 112.3 (t, J = 244.5 Hz), 107.0.

*2-(difluoro(naphthalen-1-yl)methyl)benzo[d]thiazole (**8s**)*

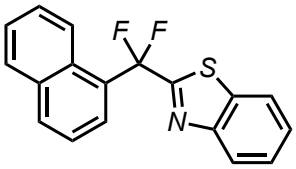

The title compound was prepared by performing General Procedure 1 then General Procedure 4 on the corresponding (hetero)Aryl Iodide: 82% yield (yellow solid).

^{1}H NMR (500 MHz, $CDCl_3$) δ 8.21 (d, *J* = 8.6 Hz, 1H), 8.12 (d, *J* = 8.3 Hz, 1H), 8.04 (d, *J* = 8.2 Hz, 1H), 7.92 (d, *J* = 7.3 Hz, 1H), 7.69 (ddd, *J* = 8.5, 7.0, 1.2 Hz, 1H), 7.63 (dd, *J* = 8.2, 6.8 Hz, 1H), 7.51 (t, *J* = 7.8 Hz, 1H).

^{13}C NMR (151 MHz, $CDCl_3$) δ 134.2, 133.9, 129.3, 128.7, 128.3, 127.2, 126.3 (t, *J* = 23.3 Hz), 125.5 (t, *J* = 8.0 Hz), 124.4, 123.6 (t, *J* = 2.7 Hz), 112.9 (t, *J* = 47.8 Hz), 109.8 (t, *J* = 243.4 Hz).

^{19}F NMR (376 MHz, $CDCl_3$) δ -81.7

*methyl (S)-2-((tert-butoxycarbonyl)amino)-3-(4-(cyanodifluoromethyl)phenyl)propanoate **(3t**)*

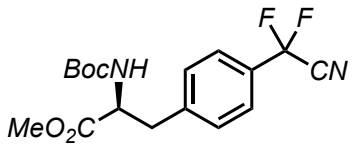

The title compound was prepared by performing General Procedure 1 on the corresponding (hetero)Aryl iodide: 36% (orange solid).

^{1}H NMR (500 MHz, $CDCl_3$) δ 7.61 (t, *J* = 7.7 Hz, 2H), 7.32 (d, *J* = 8.2 Hz, 1H), 6.89 (d, *J* = 8.2 Hz, 1H), 4.92 – 4.61 (m, 1H), 1.44 (s, 3H), 3.31 – 3.02 (m, 2H), 1.42 (s, 9H).

^{19}F NMR (470 MHz, $CDCl_3$) δ -82.73.

^{13}C NMR (126 MHz, CDCl3) δ 171.8, 154.9, 141.5, 137.6, 135.7, 131,3, 130.3, 125.4, 54.1, 52.4, 38.3, 28.2.

*2,2-difluoro-2-(5-(2-(2-(2-methoxyethoxy)ethoxy)ethoxy)pyridin-2-yl)acetonitrile (**3u**)*

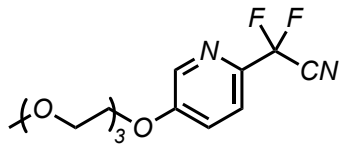

The title compound was prepared by performing General Procedure 1 on the corresponding (hetero)Aryl iodide: 59% (white solid).

^{1}H NMR (500 MHz, $CDCl_3$) δ 8.53 (s, 1H), 7.81 (dd, *J* = 8.7, 2.7 Hz, 1H), 6.90 (d, *J* = 8.9 Hz, 1H), 4.51 (t, J = 5.0 Hz, 2H), 3.92 (t, J = 5.0 Hz, 2H), 3.70 – 3.62 (m, 10H), 3.51 (m, 2H), 3.39 (s, 3H).

^{19}F NMR (470 MHz, $CDCl_3$) δ -82.0.

^{13}C NMR (126 MHz, $CDCl_3$) δ 166.2, 145.2 (t, J = 6.3 Hz), 135.4 (t, J = 3.8 Hz), 120.7 (t, J = 26.5 Hz), 112.1, 108.2 (t, J = 243.2 Hz), 71.9, 70.7 (t, J = 16.4 Hz), 69.3

*2,2-difluoro-2-(naphthalen-2-yl)acetonitrile (**3v**)*

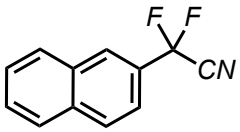

The title compound was prepared by performing General Procedure 1 on the corresponding (hetero)Aryl iodide: 76% (white solid).

^{1}H NMR (500 MHz, $CDCl_3$) δ 8.22 (s, 1H), 7.91-8.04 (m, 3H), 7.63-7.70 (m, 3H).

^{19}F NMR (376 MHz, $CDCl_3$) δ -80.6.

^{13}C NMR (151 MHz, $CDCl_3$) δ 134.77, 132.11, 129.62, 128.86, 128.59, 128.21, 127.89, 127.53, 126.20 (t, J = 6.3 Hz), 120.62 (t, J = 4.1 Hz), 112.59 (t, J = 48.3 Hz), 109.15 (t, J = 242.8 Hz).

*2,2-difluoro-2-(2,2'',6,6''-tetrafluoro-[1,1':3',1''-terphenyl]-5'-yl)acetonitrile (**3w**)*

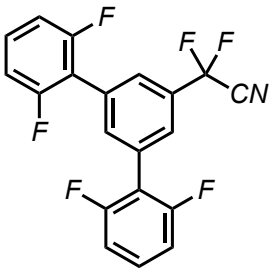

The title compound was prepared by performing General Procedure 1 on the corresponding (hetero)Aryl Iodide: 64% yield (white solid)

^{1}H NMR (500 MHz, $CDCl_3$) δ 7.82 (d, J = 9.2 Hz, 3H), 7.43 (tt, J = 8.4, 6.2 Hz, 2H), 7.00 (t, J = 8.0 Hz, 4H).

^{19}F NMR (470 MHz, $CDCl_3$) δ -83.1, -114.21 (t, J = 6.9 Hz).

^{13}C NMR (126 MHz, $CDCl_3$) δ 160.9 (d, J = 6.3 Hz), 158.9 (t, J = 6.3 Hz), 136.4, 131.6 (t, J = 25.2 Hz), 130.8 (t, J = 10.1 Hz), 130.2, 126.9, 116.4 (t, J = 12.6 Hz), 112.0 (dd, J = 21.4, 5.0 Hz), 108.5 (t, J = 244.5 Hz).

*2,2-difluoro-2-(4-(5-(p-tolyl)-3-(trifluoromethyl)-1H-pyrazol-1-yl)phenyl)acetonitrile (**3x**)*

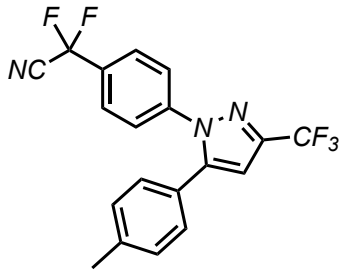

The title compound was prepared by performing General Procedure 1 on the corresponding (hetero)Aryl Iodide: 75% yield (white solid)

^{1}H NMR (500 MHz, $CDCl_3$) δ 7.68 (d, J = 8.4 Hz, 2H), 7.51 (d, J = 8.5 Hz, 2H), 7.19 (d, J = 7.9 Hz, 2H), 7.12 (d, J = 8.2 Hz, 2H), 2.38 (s, 3H).

^{19}F NMR (470 MHz, $CDCl_3$) δ -62.3, -83.11.

^{13}C NMR (126 MHz, $CDCl_3$) δ 145.3, 144.3 (q, J = 38.6 Hz), 142.8 (t, J = 2.0 Hz), 140.0, 130.8 (t, J = 25.6 Hz), 129.9, 128.9, 126.4 (t, J = 5.0 Hz), 125.9, 125.8, 121.2 (q, J = 269.1 Hz), 112.3 (t, J = 48.0 Hz), 108.4, 106.5 (q, J = 2.0 Hz), 21.5.

*2,2-difluoro-2-(7-isopropoxy-4-oxo-3-phenyl-4H-chromen-8-yl)acetonitrile (**3y**)*

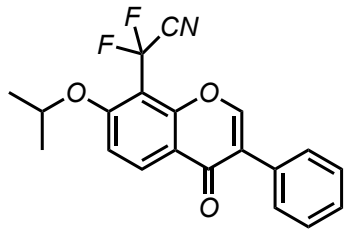

The title compound was prepared by performing General Procedure 1 on the corresponding (hetero)Aryl Iodide: 93% yield (white solid)

^{1}H NMR (500 MHz, CDCl3) δ 8.52 (d, *J* = 11.1 Hz, 1H), 8.01 (s, 1H), 7.56 (dd, *J* = 8.3, 1.4 Hz, 2H), 7.51 – 7.32 (m, 3H), 7.10 (d, *J* = 9.8 Hz, 1H), 4.91 (p, *J* = 6.1 Hz, 1H), 1.51 (d, *J* = 6.1 Hz, 6H).

^{19}F NMR (470 MHz, CDCl3) δ -81.32.

^{13}C NMR (126 MHz, CDCl3) δ 174.6, 160.9 (t, J = 3.8 Hz), 154.9, 152.4, 132.6, 131.0, 128.9, 128.6, 128.5, 125.6, 118.6, 112.9 (t, J = 46.6 Hz), 111.2, 106.9, 106.6, 73.7, 21.6

*2,2-difluoro-2-(3-(3-(4-fluoro-2-methoxyphenoxy)prop-1-yn-1-yl)phenyl)acetonitrile (**3ab**)*

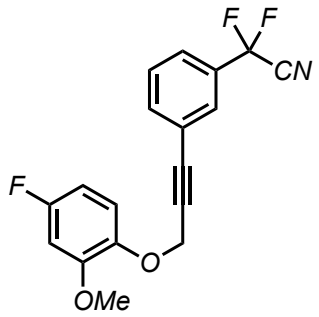

The title compound was prepared by performing General Procedure 1 on the corresponding (hetero)Aryl Iodide: 57% yield (yellow oil)

^{1}H NMR (500 MHz, CDCl3) δ 7.68 (s, 1H), 7.63 – 7.58 (m, 2H), 7.49 (t, J = 7.8 Hz, 1H), 7.01 (dd, J = 8.8, 5.4 Hz, 1H), 6.71 (dd, J = 10.1, 2.9 Hz, 1H), 6.63 (td, J = 8.4, 2.9 Hz, 1H), 4.90 (s, 2H), 3.90 (s, 3H).

^{19}F NMR (470 MHz, CDCl3) δ -83.72, -118.31 (td, J = 9.0, 5.6 Hz).

^{13}C NMR (126 MHz, CDCl3) δ 159.3, 157.7, 151.1 (d, J = 8.8 Hz), 143.0, 135.6, 131.7 (t, J = 21.4 Hz), 129.4, 128.5(t, J = 3.8 Hz), 125.1(t, J = 3.8 Hz), 123.9, 116.3 (d, J = 8.8 Hz), 112.2 (t, J = 40.3 Hz), 108.2 (t, J = 204.1 Hz), 106.0 (d, J = 12.6 Hz), 100.5 (d, J = 22.7 Hz), 86.3, 85.5, 58.3, 56.0.

*(R)-2,5,7,8-tetramethyl-2-((4R,8R)-4,8,12-trimethyltridecyl)chroman-6-yl 4-(cyanodifluoromethyl)benzoate (**3ac**)*

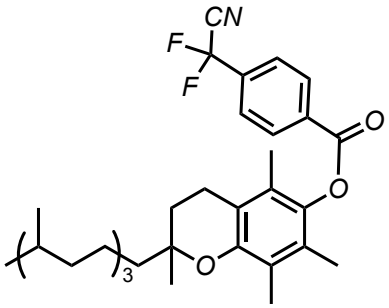

The title compound was prepared by performing General Procedure 1 on the corresponding (hetero)Aryl Iodide: 68% yield (yellow oil)

^{1}H NMR (500 MHz, $CDCl_3$) δ 8.40 (d, *J* = 8.4 Hz, 2H), 7.91 (d, *J* = 8.5 Hz, 2H), 2.62 (t, *J* = 6.9 Hz, 2H), 2.10 (s, 3H), 2.1 (s, 3H), 2.01 (s, 3H), 1.93 – 1.71 (m, 2H), 1.70 – 1.01 (m, 24H), 0.91 – 0.83 (m, 12H).

^{19}F NMR (470 MHz, $CDCl_3$) δ -84.42

^{13}C NMR (126 MHz, $CDCl_3$) δ 163.7, 149.8, 140.4, 135.5 (t, J = 25.2 Hz), 133.7, 131.0, 126.6, 125.7 (t, J = 5.0 Hz), 124.9, 123.4, 117.7, 112.1 (t, J = 47.9 Hz), 108.3 (t, J = 244.4 Hz), 75.2, 39.4, 37.4, 37.3, 32.8, 28.0, 24.8, 24.5, 22.7, 22.6, 21.1, 20.7, 19.7, 13.1, 12.2, 11.9

*2-(4-((3-chloro-4-((3-fluorobenzyl)oxy)phenyl)amino)quinazolin-6-yl)-2,2-difluoromethylacetonitrile (**3ad**)*

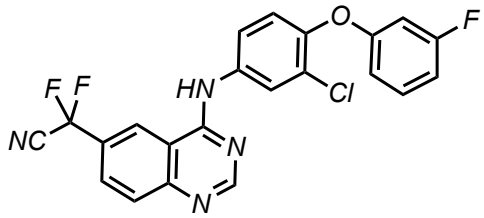

The title compound was prepared by performing General Procedure 1 on the corresponding (hetero)Aryl Iodide: 23% yield (yellow oil)

^{1}H NMR (500 MHz, $CDCl_3$) δ 8.82 (s, 1H), 8.11 (s, 1H), 8.00 (d, *J* = 9.0 Hz, 1H), 7.96 (dd, *J* = 8.8, 2.0 Hz, 1H), 7.82 (d, *J* = 2.7 Hz, 1H), 7.38 (dd, *J* = 8.8, 2.7 Hz, 1H), 7.31 (m, 2H), 7.23 – 7.13 (m, 1H), 6.88 (d, *J* = 8.8 Hz, 2H), 5.12 (s, 2H).

^{19}F NMR (470 MHz, $CDCl_3$) δ -82.72, -112.41.

*2-(7-(diethylamino)-4-methyl-2-oxo-2H-chromen-3-yl)-2,2-difluoroacetonitrile (**3ae**)*

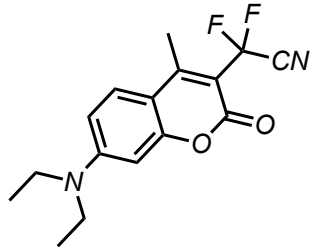

The title compound was prepared by performing General Procedure 1 on the corresponding (hetero)Aryl Iodide: XX% yield (description)

^{1}H NMR (500 MHz, $CDCl_3$) δ 7.62 (d, *J* = 9.3 Hz, 1H), 6.61 (dd, *J* = 9.2, 2.7 Hz, 1H), 6.52 (d, *J* = 2.6 Hz, 1H), 3.43 (q, *J* = 7.2 Hz, 4H), 2.61 (t, *J* = 3.3 Hz, 3H), 1.22 (t, *J* = 7.2 Hz, 6H).

^{19}F NMR (470 MHz, $CDCl_3$) δ -78.31.

^{13}C NMR (126 MHz, $CDCl_3$) δ 158.7, 156.1, 155.7, 152.4, 127.4, 112.6, 110.1, 109.7, 108.2, 108.1, 97.0, 45.0, 14.9, 12.4.

*2-(difluoro(4-nitrophenyl)methyl)benzo[d]thiazole (**9a**)*

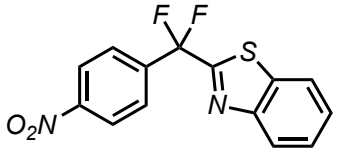

The title compound was prepared by performing General Procedure 1 then General Procedure 4 on the corresponding (hetero)Aryl bromide: 45% yield (yellow solid).

^{1}H NMR (500 MHz, $CDCl_3$) δ 8.31 (d, J = 8.5 Hz, 2H), 7.88 (d, J =8.6 Hz, 2H), 7.82 (d, J = 7.9 Hz, 1H), 7.62 (d, J = 7.9 Hz 1H), 7.49 (t, J = 7.3 Hz, 1H), 7.43 (t, J = 7.60 Hz, 1H).

^{19}F NMR (470 MHz, $CDCl_3$) δ -89.14.

*1-(4-(benzo[d]thiazol-2-yldifluoromethyl)phenyl)ethan-1-one (**9b**)*

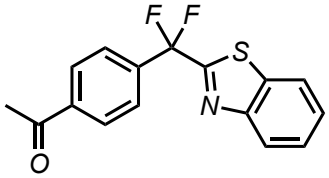

The title compound was prepared by performing General Procedure 1 then General Procedure 4 on the corresponding (hetero)Aryl bromide: 30% yield (Yellow oil)

^{1}H NMR (500 MHz, $CDCl_3$) 8.13 (d, J = 8.2 Hz, 2H), 7.94 (d, J = 8.4 Hz, 2H), 7.85 (d, J = 7.9 Hz, 1H), 7.61 (d, J = 8.0 Hz, 1H), 7.48 (t, J = 7.7 Hz, 1H), 7.42 (t, J = 7.5 Hz, 1H), 2.64 (s, 3H)

^{19}F NMR (470 MHz, $CDCl_3$) δ -88.10.

*ethyl 4-(benzo[d]thiazol-2-yldifluoromethyl)benzoate (**9c**)*

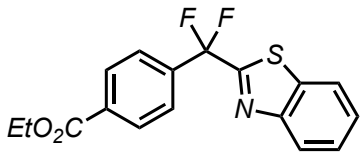

The title compound was prepared by performing General Procedure 1 then General Procedure 4 on the corresponding (hetero)Aryl bromide: 35% yield (Yellow oil)

^{1}H NMR: 8.21 (d, J = 8.7 Hz, 2H), 7.81 (d, J = 8.4 Hz, 3H), 7.64 (dd, J = 7.4 Hz, 1.0 Hz, 1H), 7.53 (td, J = 7.6 Hz, 1.2 Hz, 1H), 7.39 (td, J = 7.6 Hz, 1.3 Hz, 1H), 4.41 (q, J = 7.1 Hz, 2H), 1.38 (t, J = 7.1 Hz, 3H)

^{19}F NMR (470 MHz, $CDCl_3$) δ -87.16.

*methyl 6-(benzo[d]thiazol-2-yldifluoromethyl)picolinate (**9e**)*

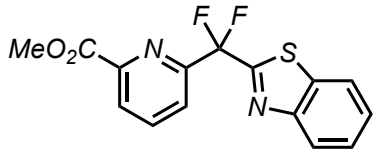

The title compound was prepared by performing General Procedure 1 then General Procedure 4 on the corresponding (hetero)Aryl bromide: 55% yield (Yellow oil)

^{1}H NMR (500 MHz, $CDCl_3$) δ 8.32 (d, J = 7.92 Hz, 1H), 8.02 (t, J = 7.9 Hz, 1H), 7.91 (d, J = 7.8 Hz, 1H), 7.83 (d, J = 8.1 Hz, 1H), 7.38 (m, 3H), 3.98 (s, 3H).

^{19}F NMR (470 MHz, $CDCl_3$) δ -96.75.

*6-(benzo[d]thiazol-2-yldifluoromethyl)picolinonitrile (**9h**)*

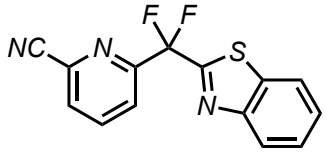

The title compound was prepared by performing General Procedure 1 then General Procedure 4 on the corresponding (hetero)Aryl bromide: 23% yield (Yellow oil)

^{1}H NMR (500 MHz, $CDCl_3$) δ 8.32 – 8.21 (m, 2H), 8.04 (t, J = 7.9 Hz, 1H), 7.91 (d, J = 7.8 Hz, 1H), 7.82 (d, J = 8.1 Hz, 1H), 7.33 (m, 2H).

^{19}F NMR (470 MHz, $CDCl_3$) δ -97.76.

*2-(difluoro(6-fluoropyridin-2-yl)methyl)benzo[d]thiazole **(9i)***

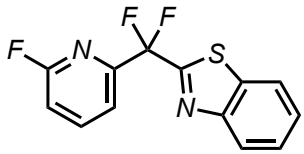

The title compound was prepared by performing General Procedure 1 then General Procedure 4 on the corresponding (hetero)Aryl bromide: 68% yield (yellow oil)

^{1}H NMR (500 MHz, $CDCl_3$) δ 8.10 (d, *J* = 7.7 Hz, 1H), 8.01 – 7.92 (m, 2H), 7.81 (dd, *J* = 6.7, 2.2 Hz, 1H), 7.63 – 7.55 (m, 2H), 7.11 (dd, *J* = 8.2, 2.9 Hz, 1H).

^{19}F NMR (470 MHz, $CDCl_3$) δ -65.02, -92.01.

^{13}C NMR (126 MHz, $CDCl_3$) δ 163.8, 163.4, 162.2, 152.7, 142.4 (d, J = 7.6 Hz), 135.2, 126.6, 124.4, 121.9, 118.3, 114.8, 112.1 (d, J = 30.1 Hz).

*2,2-difluoro-2-(quinolin-2-yl)acetonitrile (**5l**)*

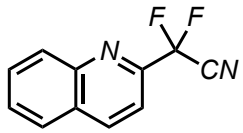

The title compound was prepared by performing General Procedure 1 on the corresponding (hetero)Aryl bromide: 56% yield (Yellow oil)

^{1}H NMR (500 MHz, $CDCl_3$) δ 8.44 (d, J = 8.5 Hz, 1H), 8.31 (d, J = 8.6 Hz, 1H), 7.90 (d, J = 8.2 Hz, 1H), 7.87 (t, J = 7.7 Hz, 1H), 7.82 (d, J = 8.5 Hz, 1H), 7.74 (t, J = 7.6 Hz, 1H).

^{19}F NMR (470 MHz, $CDCl_3$) δ -85.53.

*2,2-difluoro-2-(quinoxalin-2-yl)acetonitrile (**5m**)*

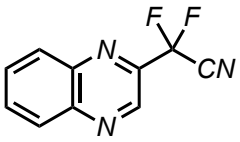

The title compound was prepared by performing General Procedure 1 on the corresponding (hetero)Aryl bromide: 45% yield (Yellow solid)

^{1}H NMR (500 MHz, $CDCl_3$) δ 9.14 (s, 1H), 8.20 (t, J = 9.5 Hz, 2H), 7.92 – 7.81 (m, 2H).

^{19}F NMR (470 MHz, $CDCl_3$) δ -88.51.

*2,2-difluoro-2-(2-methylquinolin-8-yl)acetonitrile **(5n)***

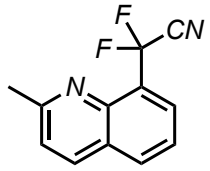

The title compound was prepared by performing General Procedure 1 on the corresponding (hetero)Aryl bromide:40% yield (light yellow solid)

^{1}H NMR (500 MHz, $CDCl_3$) δ 8.11 (d, *J* = 8.5 Hz, 1H), 8.02 (dd, *J* = 7.7, 4.0 Hz, 2H), 7.62 (t, *J* = 7.8 Hz, 1H), 7.41 (d, *J* = 8.5 Hz, 1H), 2.83 (s, 3H).

^{19}F NMR (470 MHz, $CDCl_3$) δ -87.23

^{13}C NMR (126 MHz, $CDCl_3$) δ 160.5, 144.5 (d, *J* = 3.6 Hz), 136.1, 132.4, 127.5 (t, *J* = 23.3 Hz), 127.1 – 126.3 (m), 124.7, 123.5, 113.7 (t, *J* = 46.5 Hz), 107.4 (t, *J* = 242.0 Hz), 29.9, 25.5

*2,2-difluoro-2-(1,3,7-trimethyl-2,6-dioxo-2,3,6,7-tetrahydro-1H-purin-8-yl)acetonitrile (**5r**)*

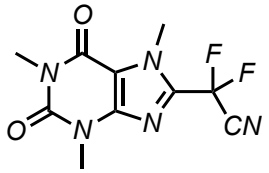

The title compound was prepared by performing General Procedure 1 on the corresponding (hetero)Aryl bromide: 62% yield (White solid)

^{1}H NMR (500 MHz, CDCl3) δ 4.21 (s, 3H), 3.62 (s, 3H), 3.41 (s, 3H)

^{19}F NMR (470 MHz, CDCl3) δ -82.91.

^{13}C NMR (126 MHz, CDCl3) δ 155.4, 151.2, 146.6, 138.8 (t, J = 30.2 Hz), 110.6, 109.9 (t, J = 44.1 Hz), 104.3 (t, J = 243.2 Hz), 33.3, 30.0, 28.3

Computational studies

Computational Methods

DFT calculations were conducted through the Molecular Graphics and Computation Facility (MGCF) at the University of California, Berkeley using the Gaussian 16 software package.[94] Geometry optimizations for all reported structures were performed using the PBE0 functional (the hybrid functional based on the Perdew-Burke-Ernzerhof functional [PBE])[95,96] with Grimme's D3 dispersion correction with Becke Johnson damping (GD3-BJ)[97]in DMF as solvent and the basis sets def2-TZVP[98] (with effective core potential) for Cu and I and def2-SVP for all the other atoms. Frequency calculations were performed on all optimized structures to ensure that each local minimum lacked imaginary frequencies and that each transition state contained exactly one imaginary frequency. The reported Gibbs free energies were corrected considering the thermal correction computed at 298.

6.5 References

(1) Kirk, K. L. Fluorination in Medicinal Chemistry: Methods, Strategies, and Recent Developments. *Org. Process Res. Dev.* **2008**, *12* (2), 305–321. https://doi.org/10.1021/op700134j.

(2) Jeschke, P. The Unique Role of Fluorine in the Design of Active Ingredients for Modern Crop Protection. *ChemBioChem* **2004**, *5* (5), 570–589. https://doi.org/10.1002/cbic.200300833.

(3) Dolbier, W. R. Fluorine Chemistry at the Millennium. *J. Fluor. Chem.* **2005**, *126* (2), 157–163. https://doi.org/10.1016/j.jfluchem.2004.09.033.

(4) Yamazaki, T.; Taguchi, T.; Ojima, I. *Unique Properties of Fluorine and Their Relevance to Medicinal Chemistry and Chemical Biology*, John Wiley & Sons.; 2009.

(5) Bondi, A. Van Der Waals Volumes and Radii. *J. Phys. Chem.* **1964**, *68* (3), 441–451. https://doi.org/10.1021/j100785a001.

(6) O'Hagan, D. Understanding Organofluorine Chemistry. An Introduction to the C–F Bond. *Chem. Soc. Rev.* **2008**, *37* (2), 308–319. https://doi.org/10.1039/B711844A.

(7) Purser, S.; Moore, P. R.; Swallow, S.; Gouverneur, V. Fluorine in Medicinal Chemistry. *Chem. Soc. Rev.* **2008**, *37* (2), 320–330. https://doi.org/10.1039/B610213C.

(8) Müller, K.; Faeh, C.; Diederich, F. Fluorine in Pharmaceuticals: Looking Beyond Intuition. *Science (1979)* **2007**, *317* (5846), 1881–1886. https://doi.org/10.1126/science.1131943.

(9) Hagmann, W. K. The Many Roles for Fluorine in Medicinal Chemistry. *J. Med. Chem.* **2008**, *51* (15), 4359–4369. https://doi.org/10.1021/jm800219f.

(10) Smart, B. E. Fluorine Substituent Effects (on Bioactivity). *J. Fluor. Chem.* **2001**, *109* (1), 3–11. https://doi.org/10.1016/S0022-1139(01)00375-X.

(11) Böhm, H.-J.; Banner, D.; Bendels, S.; Kansy, M.; Kuhn, B.; Müller, K.; Obst-Sander, U.; Stahl, M. Fluorine in Medicinal Chemistry. *ChemBioChem* **2004**, *5* (5), 637–643. https://doi.org/10.1002/cbic.200301023.

(12) Grunewald, G. L.; Seim, M. R.; Lu, J.; Makboul, M.; Criscione, K. R. Application of the Goldilocks Effect to the Design of Potent and Selective Inhibitors of Phenylethanolamine N-Methyltransferase: Balancing PKa and Steric Effects in the Optimization of 3-Methyl-1,2,3,4-Tetrahydroisoquinoline Inhibitors by β-Fluorination. *J. Med. Chem.* **2006**, *49* (10), 2939–2952. https://doi.org/10.1021/jm051262k.

(13) Smyth, M. S.; Ford, H.; Burke, T. R. A General Method for the Preparation of Benzylic α,α-Difluorophosphonic Acids; Non-Hydrolyzable Mimemtics of Phosphotyrosine. *Tetrahedron Lett.* **1992**, *33* (29), 4137–4140. https://doi.org/10.1016/S0040-4039(00)74672-7.

(14) O'Hagan, D.; Wang, Y.; Skibinski, M.; Slawin, A. M. Z. Influence of the Difluoromethylene Group (CF2) on the Conformation and Properties of Selected Organic Compounds. *Pure Appl. Chem.* **2012**, *84* (7), 1587–1595. https://doi.org/10.1351/PAC-CON-11-09-26.

(15) Brown, M. F.; Avery, M.; Brissette, W. H.; Chang, J. H.; Colizza, K.; Conklyn, M.; DiRico, A. P.; Gladue, R. P.; Kath, J. C.; Krueger, S. S.; Lira, P. D.; Lillie, B. M.; Lundquist, G. D.; Mairs, E. N.; McElroy, E. B.; McGlynn, M. A.; Paradis, T. J.; Poss, C. S.; Rossulek, M. I.; Shepard, R. M.; Sims, J.; Strelevitz, T. J.; Truesdell, S.; Tylaska, L. A.; Yoon, K.; Zheng, D. Novel CCR1 Antagonists with Improved Metabolic Stability. *Bioorg. Med. Chem. Lett.* **2004**, *14* (9), 2175–2179. https://doi.org/10.1016/j.bmcl.2004.02.022.

(16) Hunter, T. J.; O'Doherty, G. A. An Enantioselective Synthesis of Benzylidene-Protected *Syn* -3,5-Dihydroxy Carboxylate Esters via Osmium, Palladium, and Base Catalysis. *Org. Lett.* **2001**, *3* (7), 1049–1052. https://doi.org/10.1021/ol0156188.

(17) Ward, S. E.; Harries, M.; Aldegheri, L.; Austin, N. E.; Ballantine, S.; Ballini, E.; Bradley, D. M.; Bax, B. D.; Clarke, B. P.; Harris, A. J.; Harrison, S. A.; Melarange, R. A.; Mookherjee, C.; Mosley, J.; Dal Negro, G.; Oliosi, B.; Smith, K. J.; Thewlis, K. M.; Woollard, P. M.; Yusaf, S. P. Integration of Lead Optimization with Crystallography for a Membrane-Bound Ion Channel Target: Discovery of a New Class of AMPA Receptor Positive Allosteric Modulators. *J. Med. Chem.* **2011**, *54* (1), 78–94. https://doi.org/10.1021/jm100679e.

(18) Lee, L.; Kreutter, K. D.; Pan, W.; Crysler, C.; Spurlino, J.; Player, M. R.; Tomczuk, B.; Lu, T. 2-(2-Chloro-6-Fluorophenyl)Acetamides as Potent Thrombin Inhibitors. *Bioorg. Med. Chem. Lett.* **2007**, *17* (22), 6266–6269. https://doi.org/10.1016/j.bmcl.2007.09.013.

(19) Lal, G. S.; Pez, G. P.; Pesaresi, R. J.; Prozonic, F. M.; Cheng, H. Bis(2-Methoxyethyl)Aminosulfur Trifluoride: A New Broad-Spectrum Deoxofluorinating Agent with Enhanced Thermal Stability. *J. Org. Chem.* **1999**, *64* (19), 7048–7054. https://doi.org/10.1021/jo990566.

(20) Middleton, W. J.; Bingham, E. M. Alpha, Alpha.-Difluoroarylacetic Acids: Preparation from (Diethylamino)Sulfur Trifluoride and Alpha-Oxoarylacetates. *J. Org. Chem.* **1980**, *45* (14), 2883–2887. https://doi.org/10.1021/jo01302a025.

(21) Singh, R. P.; Majumder, U.; Shreeve, J. M. Nucleophilic Di- and Tetrafluorination of Dicarbonyl Compounds. *J. Org. Chem.* **2001**, *66* (19), 6263–6267. https://doi.org/10.1021/jo0157674.

(22) Kuroboshi, M.; Kanie, K.; Hiyama, T. Oxidative Desulfurization-Fluorination: A Facile Entry to a Wide Variety of Organofluorine Compounds Leading to Novel Liquid-Crystalline Materials. *Adv. Synth. Catal.* **2001**, *343* (3), 235–250. https://doi.org/10.1002/1615-4169(20010330)343:3<235::AID-ADSC235>3.0.CO;2-0.

(23) Differding, E.; Rüegg, G. M.; Lang, R. W. Selective Mono- and Difluorination of Enolates. *Tetrahedron Lett.* **1991**, *32* (15), 1779–1782. https://doi.org/10.1016/S0040-4039(00)74328-0.

(24) Peng, W.; Shreeve, J. M. Convenient Fluorination of Nitro and Nitrile Compounds with Selectfluor. *Tetrahedron Lett.* **2005**, *46* (29), 4905–4909. https://doi.org/10.1016/j.tetlet.2005.05.056.

(25) Sadeghi, M. M.; Loghmani-Khouzani, H.; Ranjbar-Karimi, R.; Golding, B. T. Sonochemical Fluorination of Heterocyclic Nitro Compounds with Selectfluor™ (F-TEDA-BF4). *Tetrahedron Lett.* **2006**, *47* (14), 2455–2457. https://doi.org/10.1016/j.tetlet.2006.01.037.

(26) Ward, S. E.; Harries, M.; Aldegheri, L.; Andreotti, D.; Ballantine, S.; Bax, B. D.; Harris, A. J.; Harker, A. J.; Lund, J.; Melarange, R.; Mingardi, A.; Mookherjee, C.; Mosley, J.; Neve, M.; Oliosi, B.; Profeta, R.; Smith, K. J.; Smith, P. W.; Spada, S.; Thewlis, K. M.; Yusaf, S. P. Discovery of N-[(2S)-5-(6-Fluoro-3-Pyridinyl)-2,3-Dihydro-1H-Inden-2-Yl]-2-Propanesulfonamide, a Novel Clinical AMPA Receptor Positive Modulator. *J Med. Chem.* **2010**, *53* (15), 5801–5812. https://doi.org/10.1021/jm1005429.

(27) Kotoris, C. C.; Chen, M.-J.; Taylor, S. D. Preparation of Benzylic α,α-Difluoronitriles, -Tetrazoles, and -Sulfonates via Electrophilic Fluorination. *J. Org. Chem.* **1998**, *63* (22), 8052–8057. https://doi.org/10.1021/jo981163x.

(28) Xu, P.; Guo, S.; Wang, L.; Tang, P. Silver-Catalyzed Oxidative Activation of Benzylic C-H Bonds for the Synthesis of Difluoromethylated Arenes. *Angew. Chem., Int. Ed.* **2014**, *53* (23), 5955–5958. https://doi.org/10.1002/anie.201400225.

(29) Xia, J.-B.; Zhu, C.; Chen, C. Visible Light-Promoted Metal-Free C–H Activation: Diarylketone-Catalyzed Selective Benzylic Mono- and Difluorination. *J. Am. Chem. Soc.* **2013**, *135* (46), 17494–17500. https://doi.org/10.1021/ja410815u.

(30) Johansson Seechurn, C. C. C.; Kitching, M. O.; Colacot, T. J.; Snieckus, V. Palladium-Catalyzed Cross-Coupling: A Historical Contextual Perspective to the 2010 Nobel Prize. *Angew. Chem., Int. Ed.* May 21, 2012, pp 5062–5085. https://doi.org/10.1002/anie.201107017.

(31) Damien, P.; Sylvain, M.; Anne, G.; Jean-Marc, C. *Transition-Metal-Catalyzed α-Arylation of Enolates*, John Wiley & Sons.; 2012; Vol. 76.

(32) Welch, J. T.; Seper, K.; Eswarakrishnan, S.; Samartino, J. Preparation of Alpha-Fluoroenolates and Their Use in the Directed Aldol Reaction. *J. Org. Chem.* **1984**, *49* (24), 4720–4721. https://doi.org/10.1021/jo00198a027.

(33) Welch, J. T.; Seper, K. W. Diastereoselectivity in the Directed Aldol Reactions of 1-Fluoro-3,3-Dimethyl-Butanone Enolates and Enol Silyl Ethers. *Tetrahedron Lett.* **1984**, *25* (46), 5247–5250. https://doi.org/10.1016/S0040-4039(01)81575-6.

(34) McBee, E. T.; Pierce, O. R.; Christman, D. L. The Reformatsky Reaction with Ethyl Bromofluoroacetate. *J. Am. Chem. Soc.* **1955**, *77* (6), 1581–1583. https://doi.org/10.1021/ja01611a053.

(35) Brigaud, T.; Doussot, P.; Portella, C. Synthesis of Difluoroenoxysilanes from Acylsilanes and Trifluoromethyltrimethylsilane (TFMTMS). Dramatic Effect of the Catalytic Fluoride Source. *J. Chem. Soc. Chem. Commun.* **1994**, No. 18, 2117. https://doi.org/10.1039/c39940002117.

(36) Prakash, G. K. S.; Hu, J.; Olah, G. A. *Facile Preparation of Di-and Monofluoromethyl Ketones from Trifluoromethyl Ketones via Fluorinated Enol Silyl Ethers*.

(37) Culkin, D. A.; Hartwig, J. F. Carbon−Carbon Bond-Forming Reductive Elimination from Arylpalladium Complexes Containing Functionalized Alkyl Groups. Influence of Ligand Steric and Electronic Properties on Structure, Stability, and Reactivity. *Organometallics* **2004**, *23* (14), 3398–3416. https://doi.org/10.1021/om049726k.

(38) Taguchi, T.; Kitagawa, O.; Morikawa, T.; Nishiwaki, T.; Uehara, H.; Endo, H.; Kobayashi, Y. Synthesis of 2,2-Difluoroesters by Iododifluoroacetate-Copper with Organic Halides. *Tetrahedron Lett.* **1986**, *27* (50), 6103–6106. https://doi.org/10.1016/S0040-4039(00)85409-X.

(39) Sato, K.; Kawata, R.; Ama, F.; Omote, M.; Ando, A.; Kumadaki, I. Synthesis of Alkenyl- and Aryldifluoroacetate Using a Copper Complex from Ethyl Bromodifluoroacetate. *Chem. Pharm. Bul.l (Tokyo)* **1999**, *47* (7), 1013–1016. https://doi.org/10.1248/cpb.47.1013.

(40) Zhu, J.; Zhang, W.; Zhang, L.; Liu, J.; Zheng, J.; Hu, J. Copper-Mediated Fluoroalkylation Reactions with Iododifluoroacetamides: Controlling the Selectivity among Cross-Coupling, Intramolecular Cyclization, and Homocoupling Reactions. *J. Org. Chem.* **2010**, *75* (16), 5505–5512. https://doi.org/10.1021/jo1005262.

(41) Fujikawa, K.; Fujioka, Y.; Kobayashi, A.; Amii, H. A New Method for Aromatic Difluoromethylation: Copper-Catalyzed Cross-Coupling and Decarboxylation Sequence from Aryl Iodides. *Org. Lett.* **2011**, *13* (20), 5560–5563. https://doi.org/10.1021/ol202289z.

(42) Feng, Z.; Min, Q.-Q.; Xiao, Y.-L.; Zhang, B.; Zhang, X. Palladium-Catalyzed Difluoroalkylation of Aryl Boronic Acids: A New Method for the Synthesis of Aryldifluoromethylated Phosphonates and Carboxylic Acid Derivatives. *Angew. Chem., Int. Ed.* **2014**, *53* (6), 1669–1673. https://doi.org/10.1002/anie.201309535.

(43) Xiao, Y.-L.; Guo, W.-H.; He, G.-Z.; Pan, Q.; Zhang, X. Nickel-Catalyzed Cross-Coupling of Functionalized Difluoromethyl Bromides and Chlorides with Aryl Boronic Acids: A General Method for Difluoroalkylated Arenes. *Angew. Chem., Int. Ed.* **2014**, *53* (37), 9909–9913. https://doi.org/10.1002/anie.201405653.

(44) Ge, S.; Arlow, S. I.; Mormino, M. G.; Hartwig, J. F. Pd-Catalyzed α-Arylation of Trimethylsilyl Enolates of α,α-Difluoroacetamides. *J. Am. Chem. Soc.* **2014**, *136* (41), 14401–14404. https://doi.org/10.1021/ja508590k.

(45) Arlow, S. I.; Hartwig, J. F. Synthesis of Aryldifluoroamides by Copper-Catalyzed Cross-Coupling. *Angew. Chem., Int. Ed.* **2016**, *55* (14), 4567–4572. https://doi.org/10.1002/anie.201600105.

(46) Schiefer, I. T.; Abdul-Hay, S.; Wang, H.; Vanni, M.; Qin, Z.; Thatcher, G. R. J. Inhibition of Amyloidogenesis by Nonsteroidal Anti-Inflammatory Drugs and Their Hybrid Nitrates. *J. Med. Chem.* **2011**, *54* (7), 2293–2306. https://doi.org/10.1021/jm101450p.

(47) Harris, K. J. A Combination of Niacin and a Prostaglandin D2 Receptor Antagonist. WO2008039882, 2008.

(48) Arrington, K. L.; Fraley, M. E.; Garbaccio, R. M.; Hartman, G. D.; Huang, S. Y.; Kreatsoulas, C.; Tasber, E. S. Inhibitors of Checkpoint Kinases. WO2007008502A2, 2001.

(49) Craig, G.; Eberle, M.; Zeller, M.; Bondy, S. S.; Comer, D. D.; Cheng, S.; Penzotti, J. E.; Diederik, P.; Grootenhuis, J.; Ehrler, J. 3-Phenoxy-1-Phenyl Acetylene Derivatives and Their Use as Herbicides. WO2001055066A2, 2001.

(50) Bartmann, E.; Krause, J. Synthesis of α,α-Difluoronitriles from Acyl Cyanides. *J. Fluor. Chem.* **1993**, *61* (1–2), 117–122. https://doi.org/10.1016/S0022-1139(00)80421-2.

(51) Fleming, F. F.; Yao, L.; Ravikumar, P. C.; Funk, L.; Shook, B. C. Nitrile-Containing Pharmaceuticals: Efficacious Roles of the Nitrile Pharmacophore. *J. Med. Chem.* **2010**, *53* (22), 7902–7917. https://doi.org/10.1021/jm100762r.

(52) Laurence, C.; Brameld, K. A.; Graton, J.; le Questel, J.-Y.; Renault, E. The PKBHX Database: Toward a Better Understanding of Hydrogen-Bond Basicity for Medicinal Chemists. *J. Med. Chem.* **2009**, *52* (14), 4073–4086. https://doi.org/10.1021/jm801331y.

(53) Teno, N.; Miyake, T.; Ehara, T.; Irie, O.; Sakaki, J.; Ohmori, O.; Gunji, H.; Matsuura, N.; Masuya, K.; Hitomi, Y.; Nonomura, K.; Horiuchi, M.; Gohda, K.; Iwasaki, A.; Umemura, I.; Tada, S.; Kometani, M.; Iwasaki, G.; Cowan-Jacob, S. W.; Missbach, M.; Lattmann, R.; Betschart, C. Novel Scaffold for Cathepsin K Inhibitors. *Bioorg. Med. Chem. Lett.* **2007**, *17* (22), 6096–6100. https://doi.org/10.1016/j.bmcl.2007.09.047.

(54) le Questel, J.-Y.; Berthelot, M.; Laurence, C. Hydrogen-Bond Acceptor Properties of Nitriles: A Combined Crystallographic and Ab Initio Theoretical Investigation. *J. Phys. Org. Chem.* **2000**, *13* (6), 347–358. https://doi.org/10.1002/1099-1395(200006)13:6<347::AID-POC251>3.0.CO;2-E.

(55) Ward, Y. D.; Thomson, D. S.; Frye, L. L.; Cywin, C. L.; Morwick, T.; Emmanuel, M. J.; Zindell, R.; McNeil, D.; Bekkali, Y.; Marc Girardot; Hrapchak, M.; DeTuri, M.; Crane, K.; White, D.; Pav, S.; Wang, Y.; Hao, M.-H.; Grygon, C. A.; Labadia, M. E.; Freeman, D. M.; Davidson, W.; Hopkins, J. L.; Brown, M. L.; Spero, D. M. Design and Synthesis of Dipeptide Nitriles as

Reversible and Potent Cathepsin S Inhibitors. *J. Med. Chem.* **2002**, *45* (25), 5471–5482. https://doi.org/10.1021/jm020209i.

(56) Li, C. S.; Deschenes, D.; Desmarais, S.; Falgueyret, J.-P.; Gauthier, J. Y.; Kimmel, Donald. B.; Léger, S.; Massé, F.; McGrath, M. E.; McKay, D. J.; Percival, M. D.; Riendeau, D.; Rodan, S. B.; Thérien, M.; Truong, V.-L.; Wesolowski, G.; Zamboni, R.; Black, W. C. Identification of a Potent and Selective Non-Basic Cathepsin K Inhibitor. *Bioorg. Med. Chem. Lett.* **2006**, *16* (7), 1985–1989. https://doi.org/10.1016/j.bmcl.2005.12.071.

(57) Peters, J-U. 11 Years of Cyanopyrrolidines as DPP-IV Inhibitors. *Curr. Top. Med. Chem.* **2007**, *7* (6), 579–595. https://doi.org/10.2174/156802607780091000.

(58) Babine, R. E.; Bender, S. L. Molecular Recognition of Protein−Ligand Complexes: Applications to Drug Design. *Chem. Rev.* **1997**, *97* (5), 1359–1472. https://doi.org/10.1021/cr960370z.

(59) Löser, R.; Schilling, K.; Dimmig, E.; Gütschow, M. Interaction of Papain-like Cysteine Proteases with Dipeptide-Derived Nitriles. *J. Med. Chem.* **2005**, *48* (24), 7688–7707. https://doi.org/10.1021/jm050686b.

(60) Metzler, W. J.; Yanchunas, J.; Weigelt, C.; Kish, K.; Klei, H. E.; Xie, D.; Zhang, Y.; Corbett, M.; Tamura, J. K.; He, B.; Hamann, L. G.; Kirby, M. S.; Marcinkeviciene, J. Involvement of DPP-IV Catalytic Residues in Enzyme-Saxagliptin Complex Formation. *Protein Science* **2008**, *17* (2), 240–250. https://doi.org/10.1110/ps.073253208.

(61) Boyd, M. J.; Crane, S. N.; Robichaud, J.; Scheigetz, J.; Black, W. C.; Chauret, N.; Wang, Q.; Massé, F.; Oballa, R. M. Investigation of Ketone Warheads as Alternatives to the Nitrile for Preparation of Potent and Selective Cathepsin K Inhibitors. *Bioorg. Med. Chem. Lett.* **2009**, *19* (3), 675–679. https://doi.org/10.1016/j.bmcl.2008.12.053.

(62) Patterson, A. W.; Wood, W. J. L.; Hornsby, M.; Lesley, S.; Spraggon, G.; Ellman, J. A. Identification of Selective, Nonpeptidic Nitrile Inhibitors of Cathepsin S Using the Substrate Activity Screening Method. *J. Med. Chem.* **2006**, *49* (21), 6298–6307. https://doi.org/10.1021/jm060701s.

(63) Tanii, H.; Hashimoto, K. Influence of Ethanol on the in Vivo and in Vitro Metabolism of Nitriles in Mice. *Arch. Toxicol.* **1986**, *58* (3), 171–176. https://doi.org/10.1007/BF00340977.

(64) Hagele, G.; Haas, A. Fluorination of 2-Oxo-Ethane Derivatives with Diethylaminosulfur Trifluoride (DAST). *J. Fluor. Chem.* **1996**, *76* (1), 15–19. https://doi.org/10.1016/0022-1139(95)03346-7.

(65) Layton, M. E.; Rodzinak, K. J.; Kelly, M. J.; Sanderson, P. E. 1,3-Disubstituted Heteroaryl NMDA/NR2B Antagonists. WO2006017409, 2016.

(66) Fukuhara, T.; Hara, S. Desulfurizing Difluorination Reaction of Benzyl Sulfides Using IF_5. *Synlett* **2009**, *2009* (02), 198–200. https://doi.org/10.1055/s-0028-1087511.

(67) Wright, S. E.; Bandar, J. S. A Base-Promoted Reductive Coupling Platform for the Divergent Defluorofunctionalization of Trifluoromethylarenes. *J. Am. Chem. Soc.* **2022**, *144* (29), 13032–13038. https://doi.org/10.1021/jacs.2c05044.

(68) Morimoto, H.; Tsubogo, T.; Litvinas, N. D.; Hartwig, J. F. A Broadly Applicable Copper Reagent for Trifluoromethylations and Perfluoroalkylations of Aryl Iodides and Bromides. *Angew. Chem., Int. Ed.* **2011**, *50* (16), 3793–3798. https://doi.org/10.1002/anie.201100633.

(69) Oishi, M.; Kondo, H.; Amii, H. Aromatic Trifluoromethylation Catalytic in Copper. *Chem. Comm.* **2009**, No. 14, 1909. https://doi.org/10.1039/b823249k.

(70) Kondo, H.; Oishi, M.; Fujikawa, K.; Amii, H. Copper-Catalyzed Aromatic Trifluoromethylation via Group Transfer from Fluoral Derivatives. *Adv. Synth. Catal.* **2011**, *353* (8), 1247–1252. https://doi.org/10.1002/adsc.201000825.

(71) Knauber, T.; Arikan, F.; Röschenthaler, G.-V.; Gooßen, L. J. Copper-Catalyzed Trifluoromethylation of Aryl Iodides with Potassium (Trifluoromethyl)Trimethoxyborate. *Chem. Eur. J.* **2011**, *17* (9), 2689–2697. https://doi.org/10.1002/chem.201002749.

(72) Gonda, Z.; Kovács, S.; Wéber, C.; Gáti, T.; Mészáros, A.; Kotschy, A.; Novák, Z. Efficient Copper-Catalyzed Trifluoromethylation of Aromatic and Heteroaromatic Iodides: The Beneficial Anchoring Effect of Borates. *Org. Lett.* **2014**, *16* (16), 4268–4271. https://doi.org/10.1021/ol501967c.

(73) Urata, H.; Fuchikami, T. A Novel and Convenient Method for Trifluoromethylation of Organic Halides Using $CF_3SiR'_3$/KF/Cu(I) System. *Tetrahedron Let.t* **1991**, *32* (1), 91–94. https://doi.org/10.1016/S0040-4039(00)71226-3.

(74) Levitre, G.; Granados, A.; Cabrera-Afonso, M. J.; Molander, G. A. Synthesis of α-Fluorinated Areneacetates through Photoredox/Copper Dual Catalysis. *Org. Lett.* **2022**, *24* (17), 3194–3198. https://doi.org/10.1021/acs.orglett.2c00969.

(75) Kieltsch, I.; Dubinina, G. G.; Hamacher, C.; Kaiser, A.; Torres-Nieto, J.; Hutchison, J. M.; Klein, A.; Budnikova, Y.; Vicic, D. A. Magnitudes of Electron-Withdrawing Effects of the Trifluoromethyl Ligand in Organometallic Complexes of Copper and Nickel. *Organometallics* **2010**, *29* (6), 1451–1456. https://doi.org/10.1021/om901122z.

(76) Mormino, M. G.; Fier, P. S.; Hartwig, J. F. Copper-Mediated Perfluoroalkylation of Heteroaryl Bromides with (Phen)CuR. *Org. Lett.* **2014**, *16* (6), 1744–1747. https://doi.org/10.1021/ol500422t.

(77) Chandrashekhar, V. G.; Baumann, W.; Beller, M.; Jagadeesh, R. Nickel-Catalyzed Hydrogenative Coupling of Nitriles and Amines for General Amine Synthesis. *Science (1979)* **2022**, *376* (6600), 1433–1441. https://doi.org/10.1126/science.abn7565.

(78) Konovalov, A. I.; Lishchynskyi, A.; Grushin, V. v. Mechanism of Trifluoromethylation of Aryl Halides with $CuCF_3$ and the Ortho Effect. *J. Am. Chem. Soc.* **2014**, *136* (38), 13410–13425. https://doi.org/10.1021/ja507564p.

(79) Litvinas, N. D.; Fier, P. S.; Hartwig, J. F. A General Strategy for the Perfluoroalkylation of Arenes and Arylbromides by Using Arylboronate Esters and [(Phen)CuRF]. *Angew. Chem. Int. Ed.* **2012**, *124* (2), 551–554. https://doi.org/10.1002/ange.201106668.

(80) Morstein, J.; Hou, H.; Cheng, C.; Hartwig, J. F. Trifluoromethylation of Arylsilanes with [(Phen)$CuCF_3$]. *Angew. Chem. Int. Ed.* **2016**, *55* (28), 8054–8057. https://doi.org/10.1002/anie.201601163.

(81) Kosobokov, M. D.; Dilman, A. D.; Levin, V.; Struchkova, M. I. Difluoro(Trimethylsilyl)Acetonitrile: Synthesis and Fluoroalkylation Reactions. *J. Org. Chem.* **2012**, *77* (13), 5850–5855. https://doi.org/10.1021/jo301094b.

(82) Ogawa, T.; Ohta, K.; Iijima, T.; Suzuki, T.; Ohta, S.; Endo, Y. Synthesis and Biological Evaluation of P-Carborane Bisphenols and Their Derivatives: Structure–Activity Relationship for Estrogenic Activity. *Bioorg. Med. Chem.* **2009**, *17* (3), 1109–1117. https://doi.org/10.1016/j.bmc.2008.12.044.

(83) Kwon, E.-M.; Kim, C.-G.; Goh, A.-R.; Park, J.-S.; Jun, J.-G. Preparation of Benzoyloxy Benzophenone Derivatives and Their Inhibitory Effects of ICAM-1 Expression. *Bull. Korean Chem. Soc.* **2012**, *33* (6), 1939–1944. https://doi.org/10.5012/bkcs.2012.33.6.1939.

(84) Wang, J.; Zhang, X.; Wan, Z.; Ren, F. TCDA: Practical Synthesis and Application in the Trifluoromethylation of Arenes and Heteroarenes. *Org. Process Res. Dev.* **2016**, *20* (4), 836–839. https://doi.org/10.1021/acs.oprd.6b00079.

(85) Chetty, S.; Armstrong, T.; Sharma Kharkwal, S.; Drewe, W. C.; de Matteis, C. I.; Evangelopoulos, D.; Bhakta, S.; Thomas, N. R. New InhA Inhibitors Based on Expanded Triclosan and Di-Triclosan Analogues to Develop a New Treatment for Tuberculosis. *Pharmaceuticals* **2021**, *14* (4), 361. https://doi.org/10.3390/ph14040361.

(86) Fang, J.; Yan, X.; Zhou, L.; Wang, Y.; Liu, X. Synthesis of 3-Organoselenyl-2H-Coumarins from Propargylic Aryl Ethers via Oxidative Radical Cyclization. *Adv. Synth. Catal.* **2019**, *361* (9), 1985–1990. https://doi.org/10.1002/adsc.201801565.

(87) Klapars, A.; Buchwald, S. L. Copper-Catalyzed Halogen Exchange in Aryl Halides: An Aromatic Finkelstein Reaction. *J. Am. Chem. Soc.* **2002**, *124* (50), 14844–14845. https://doi.org/10.1021/ja028865v.

(88) Bacsa, I.; Jójárt, R.; Schneider, G.; Wölfling, J.; Maróti, P.; Herman, B. E.; Szécsi, M.; Mernyák, E. Synthesis of A-Ring Halogenated 13α-Estrone Derivatives as Potential 17β-HSD1 Inhibitors. *Steroids* **2015**, *104*, 230–236. https://doi.org/10.1016/j.steroids.2015.10.008.

(89) Pevarello, P. Fluorinated Arylalkylaminocarboxamide Derivatives. US2014088074A1, 2014.

(90) Harris, K. J. A Combination of Niacin and Prostaglandin D2 Receptor Antagonist. WO2008039882A1, 2008.

(91) Ohashi, M.; Takeda, I.; Ikawa, M.; Ogoshi, S. Nickel-Catalyzed Dehydrogenative [4 + 2] Cycloaddition of 1,3-Dienes with Nitriles. *J. Am. Chem. Soc.* **2011**, *133* (45), 18018–18021. https://doi.org/10.1021/ja208162w.

(92) Shalayel, I.; Coulibaly, S.; Ly, K.; Milet, A.; Vallée, Y. The Reaction of Aminonitriles with Aminothiols: A Way to Thiol-Containing Peptides and Nitrogen Heterocycles in the Primitive Earth Ocean. *Life* **2018**, *8* (4), 47. https://doi.org/10.3390/life8040047.

(93) Lin, C.-C.; Hsieh, T.-H.; Liao, P.-Y.; Liao, Z.-Y.; Chang, C.-W.; Shih, Y.-C.; Yeh, W.-H.; Chien, T.-C. Practical Synthesis of N-Substituted Cyanamides via Tiemann Rearrangement of Amidoximes. *Org. Lett.* **2014**, *16* (3), 892–895. https://doi.org/10.1021/ol403645y.

(94) Gaussian 16 Rev. A.03 (Wallingford, CT, 2016).

(95) Adamo, C.; Barone, V. Toward Reliable Density Functional Methods without Adjustable Parameters: The PBE0 Model. *J. Chem. Phys.* **1999**, *110* (13), 6158–6170. https://doi.org/10.1063/1.478522.

(96) Perdew, J. P.; Burke, K.; Ernzerhof, M. Generalized Gradient Approximation Made Simple [Phys. Rev. Lett. 77, 3865 (1996)]. *Phys. Rev. Lett.* **1997**, *78* (7), 1396–1396. https://doi.org/10.1103/PhysRevLett.78.1396.

(97) Grimme, S.; Ehrlich, S.; Goerigk, L. Effect of the Damping Function in Dispersion Corrected Density Functional Theory. *J. Comput. Chem.* **2011**, *32* (7), 1456–1465. https://doi.org/10.1002/jcc.21759.

(98) Weigend, F.; Ahlrichs, R. Balanced Basis Sets of Split Valence, Triple Zeta Valence and Quadruple Zeta Valence Quality for H to Rn: Design and Assessment of Accuracy. *Phys. Chem. Chem. Phys.* **2005**, *7* (18), 3297. https://doi.org/10.1039/b508541a.